

Welcome to the ICM12  
Karlsruhe, Germany

ICM<sup>12</sup>  
Karlsruhe

Conference Center  
May 10-14 2015

# Book of Abstracts

PLENARIES  
TALKS  
POSTERS

## Topics

- A Multiscale phenomena in plasticity
- B Residual stresses
- C Cyclic deformation behavior, crack initiation & crack growth of metals
- D In-situ microscopy and diffraction
- E Size effects and small-scale mechanical behavior of materials
- F Advanced steels and steel composite materials
- G Fracture mechanics
- H Materials for fission and fusion
- I High temperature materials
- K Polymer based composites
- L Lightweight alloys and structures
- M Ultrastrong metallic and non-metallic glasses
- X General mechanical behavior

## Supporting Organizations



Karlsruhe Institute of Technology · Institut für Angewandte Materialien  
Engelbert-Arnold-Str. 4 · 76131 Karlsruhe · Germany  
phone: +49 (0) 721 608-24815  
mail: info@icm12.com

# CONTENTS

---

## Plenary Talks

The treatment of residual stresses in fracture mechanics calculations: BOB AINSWORTH .....	25
X-Mechanics for Metal Plasticity: W. A. CURTIN .....	25
Materials for ultra high-temperature applications: HARUYUKI INUI, KYOSUKE KISHIDA, NORIHIKO L. OKAMOTO .....	26
Materials Innovation for Nuclear Energy - Super ODS Steels R&D: AKIHIKO KIMURA, WENTUO HAN, HWANIL JE, YOOSUNG HA, HIROYUKI NOTO, DONGSHENG CHEN, NORIYUKI IWATA, RYUTA KASADA, TAKANARI OKUDA, SHIHEHARU UKAI, MASAYUKI INOUE, PENG DOU, SANGHOON NOH .....	27
Tensile and fatigue behavior of steels in high pressure hydrogen gas atmospheres: HISAO MATSUNAG, JUNICHIRO YAM, SABURO MATSUOKA .....	28
Deformation, Fatigue, and Fracture of Ultrafine Grained and Nanocrystalline Materials: A. HOHENWARTER, T. LEITNER, O. RENK, C. B. YANG, M. KAPP, L. KRÄMER, P. GUPTA, V. MAIER, R. PIPPA .....	28
Damage Tolerance in Natural and Bioinspired Structural Materials: ROBERT O. RITCHI .....	29

## Talks

### Topic A1: Multiscale phenomena in plasticity

#### Talks Topic A1

Atomistic Simulations as Bridge between Experiments and Mesoscale Models: a Case-Study on Dislocation-Precipitate Interactions in Ni-base Superalloys: ERIK BITZEK .....	32
Accelerated molecular dynamics study of grain boundary motion and dislocation nucleation from grain boundary: SHIGENOBU OGATA, AKIO ISHII, YUNJIANG WANG, JUNPING DU.....	33
Ab initio-based atomistic model simulation of deformation and fracture in SiC power device: YOSHITAKA UMENO, ATSUSHI KUBO, SHIJO NAGAO .....	33
Research on constitutive model of nickel-based superalloy and the numerical simulation during superalloy blade cold rolling process: XIANGWEI KONG, WENRAN GENG, CHUNLIN QIU .....	34
Development of Mechanism-Based and Microstructure-Sensitive Modeling Approach to Plastic Deformation in Multi- Phase Alloys: DUCHAO LV, PENGYANG ZHAO, DON MCALLISTER, STEPHEN NIEZGODA, MICHAEL MILLS, <u>YUNZHI WANG</u> .....	35

#### Talks Topic A2

Size-Dependent Mechanical Properties of Crystalline Nanoparticles: DAN MORDEHAI .....	37
Molecular dynamics study of the response of a nanowire containing defects to a uni-axial strain: case of nickel: KAHINA LOUNIS, EL HOCINE MEGCHICHE, ZENIA HAND .....	37
Tension/compression anisotropy in yield stress and Bauschinger effect in ultrafine-grained metals: TOMOHITO TSURU, YOSHITERU AOYAGI, YOSHIYUKI KAJI, TOMOTSUGU SHIMOKAWA .....	38
Particle and solid solution strengthening. Part 1: experiments to control microstructure: PHILIPP SCHUMACHER, STEFAN POGATSCHER, MARCO J STARINK, CHRISTOPH SCHICK, OLAF KESSLER, VOLKER MOHLES, BENJAMIN MILKEREIT .....	39
Particle and solid solution strengthening. Part 2: modelling plastic behaviour: VOLKER MOHLES, VOLKER PANKOKE, PHILIPP SCHUMACHER, BENJAMIN MILKEREIT .....	40

#### Talks Topic A3

Comparison of statistical descriptors for the construction of Statistically Similar RVEs: LISA SCHEUNEMANN, DANIEL BALZANI, DOMINIK BRANDS, JÖRG SCHRÖDER .....	42
Phase transitions' energies and activation energies from nothing else than indentation loading curves: GERD KAUPP .....	43

Rate effects in finite element modeling of transformation induced visco-plasticity: MAHER EL HAJ KACEM, FABRICE BARBE, NICOLAS LECOQ..... 44

**Talks Topic A4**

Size effects in void growth from nano- to microscale: JAVIER SEGURADO, HYUNG-JUN CHANG, JAVIER LLORCA..... 46

Dislocation interaction across grain boundaries and grain boundary yielding in a discrete dislocation dynamics framework: MARKUS STRICKER, DANIEL WEYGAND ..... 46

Dislocation alignment tensors: their conservation laws and how to determine them from discrete dislocation configurations: THOMAS HOCHRAINER ..... 47

Representation of Dislocation Interactions in a Dislocation Density Field Theory for Crystal Plasticity: SEVERIN SCHMITT, PETER GUMBSCH, KATRIN SCHULZ ..... 47

Microstructural comparison of continuum models for dislocation plasticity: MEHRAN MONAVARI, MICHAEL ZAISER, STEFAN SANDFELD ..... 49

**Talks Topic A5**

The «Cauchystat»: accurate control of the true stress in molecular dynamics simulations of martensitic phase transformations: RONALD E. MILLER, ELLAD B. TADMOR, NOAM BERNSTEIN, FABIO PAVIA, JOSH GIBSON ..... 51

Multiscale modeling of solute atom effect on critical resolved shear stress of Fe: MASATO WAKEDA, SHIGENOBU OGATA..... 51

Multi-scale modeling of dislocation-precipitate interactions in Fe: from molecular dynamics to discrete dislocations: A. LEHTINEN, F. GRANBERG, L. LAURSON, K. NORDLUND, M. ALAVA..... 52

Detailed description of the screw dislocation motion in iron revealed by atomistic simulations: GHIATH MONNET, AKIYOSHI NOMOTO ..... 53

Depinning-Controlled Plastic Deformation during Nanoindentation of BCC Iron Thin Films and Nanoparticles: ROMAN KOSITSKI, DAN MORDEHAI ..... 53

**Talks Topic A6**

Gradient enhanced modeling of fcc and bcc nanocrystalline materials: BENJAMIN KLUSEMANN, SWANTJE BARGMANN, YURI ESTRIN ..... 56

A consistent homogenization theory for a higher order plasticity model from meso to macro scale: PHAN VAN TUNG, POH LEONG HIEN ..... 57

Spectral Method Simulations of High Phase-Contrast Materials: A Joint Numerical–Experimental Study: M. DIEHL, P. SHANTHRAJ, P. EISENLOHR, C.C. TASAN, F. ROTERS, D. RAABE ..... 58

Influence of the microstructure of Al-components on the life time of integrated circuits: F. MEIER, C. SCHWARZ, E. WERNER ..... 59

Deformation behavior of gradient materials with nanostructured near surface regions: FLORIAN RIEGER, ANDREY MOLOTNIKOV, XIAOLEI L. WU, YUNTIAN T. ZHU, THOMAS BÖHLKE, YURI ESTRIN ..... 59

**Talks Topic A7**

Modelling the thermomechanical behaviour of the polycrystalline microstructure of dual phase steels during sheet bulk metal forming: STEFAN LOEHNERT, SEBASTIAN ZELLER, PETER WRIGGERS..... 62

Computational assessment of the microstructure-dependent plasticity of lamellar gray cast iron: MARIO METZGER, THOMAS SEIFERT ..... 62

A Multiscale approach for thermo-mechanical simulations of loading courses in cast iron brake discs: CHRISTOPH HERRMANN, STEFAN SCHMID, DANIEL SCHNEIDER, MICHAEL SELZER, BRITTA NESTLER ..... 63

Multi-physics, Multiscale Modeling of Plastic Deformation in Plasma-Facing Components: N.M. GHONIEM, J. BLANCHARD, D. RIVERA, E. GAO, M. WASFY, C. MARTIN ..... 64

## Talks Topic A8

A Continuum Model for Dislocation Dynamics in Three Dimensions using the Dislocation Density Potential Functions: YANG XIANG, YICHAO ZHU .....	66
A Minimalistic Continuum Approach to Formation of Dislocation Patterns Under Multislip Conditions: DOMINIK STEINBERGER, STEFAN SANDFELD, MICHAEL ZAISER .....	66
Orientation Dependence of the Forest Strengthening Studied with Dislocation Dynamics Simulations: VANESSA VERBEKE, STEFAN SANDFELD, BENOIT DEVINCRE .....	67
Formation of Persistent Dislocation Patterns in the Similitude Regime: STEFAN SANDFELD, MICHAEL ZAISER .....	68
Structural model of dislocation plasticity and twinning for high-rate deformation of metals: ALEXANDER MAYER, VASILYI KRASNIKOV, ELIJAH BORODIN .....	68

## Talks Topic A9

Stress and Strain Fluctuations in Plastic Deformation of Crystals with Disordered Microstructure: OLGA KAPETANOOU, MARKUS STRICKER, DANIEL WEYGAND, MICHAEL ZAISER .....	71
Strain localization and surface effects in 2D and 3D stochastic models of amorphous plasticity: DAVID FERNANDEZ CASTELLANOS, STEFAN SANDFELD .....	72
Numerical investigation of welding residual stress field in tubular joints considering the effects of solid-state phase transformation: KIMIYA HEMMESI, MAJID FARAJIAN, DIETER SIEGELE .....	72
The influence of GP and GDP precipitates on the viscoplastic material behaviour of Inconel 718: ANDREAS DREXLER, HERMANN MADERBACHE, HANS-PETER GÄNSER, WERNER ECKER, ANDREAS FISCHERSWORRING-BUNK, BERND OBERWINKLER .....	73
A representative volume element based multiscale modeling of fish scale: A.M. RAJENDRAN, M.P. NELMS .....	74
Multiscale crystal plasticity simulation on anisotropic yielding behavior of ultrafine-grained metal: YOSHITERU AOYAGI .....	75

## Topic B: Residual stresses

### Talks Topic B1

Fatigue Strength of Anodized Al 7050-T7451. HERMAN JACOBUS CORNELIS VOORWALD, JOSÉ ANDRÉ MARIN DE CAMARGO, MARIA ODILA HILÁRIO CIOFFI, MIDORI YOSHIKAWA PITANGA COSTA .....	77
The Influence of Residual Stress on the Failure Modes in a Thermal Barrier Coating System: DONG LIU, CLAUDIA RINALDI, PETER E J FLEWITT .....	78
Overloads on cracks: using Barkhausen microscope and SEM-based digital image correlation to evaluate mechanisms and effects on local (residual) stress fields: MATTHIAS THIELEN, MEISAM SHEIKH-AMIRI, MICHAEL MARX, CHRISTIAN BOLLER, CHRISTIAN MOTZ .....	78
Assessment of shot-peening on fatigue life prediction: microstructural effects. LOUISE TOUALBI, PASCALE KANOUTÉ, SERGE KRUCH, ARNAUD LONGUET, ALEXANDRE SEROR, JEAN-PATRICK GOULMY, QUENTIN PUYDT .....	79
Thermal Stability of Residual Stresses in Ti-6Al-4V components. ALEKSANDAR STANOJEVIC, HERMANN MADERBACHER, PAUL ANGERER, BERND OBERWINKLER .....	80
Development of residual stresses during cyclic loading in the very high cycle fatigue regime: HONGWANG FU, BENJAMIN DÖNGES, HANS-JÜRGEN CHRIST .....	81

### Talks Topic B 2

3DXRD microscopy applied to study stress-induced martensitic transformation over one hundred individual grains in a shape-memory alloy polycrystal: SOPHIE BERVEILLER, BENOIT MALARD, YOUNES EL-HACHI, JONATHAN WRIGHT .....	83
Measuring Residual Stresses in Monolithic Fuel Foils using Neutron Diffraction: BJØRN CLAUSEN, DONALD W. BROWN, MARIA A. OKUNIEWSKI, LEVENTE BALOGH, THOMAS A. SISNEROS .....	83

Characterization of microscopic stress and strain evolved in polycrystalline Fe-Ga alloys using synchrotron radiation: SHIGERU SUZUKI, YUSUKE ONUKI, SHIGEO SATO, SHUN FUJIEDA, KOZO SHINODA, KENTARO KAJIWARA, MASUGU SATO .....	84
Analysis and Assessment of Residual Stresses in Ground Steels and Ceramics: A. LIEHR, W. ZINN, B. SCHOLTES ...	85
Assessing material properties with Neutron and Synchrotron radiation - Two complementary tools: T. BUSLAPS, V. HONKIMÄKI, M. DIMICHIEL, J. WRIGHT, A. FITCH, C. CURFS, T. PIRLING .....	85

### Talks Topic B 3

Estimation of residual stress distribution in polyethylene pipes. JAN PODUŠKA, PAVEL HUTAŘ, JIŘÍ SADÍLEK, JAROSLAV KUČERA, MARTIN ŠEVČÍK, LUBOŠ NÁHLÍK .....	88
A combined experimental and numerical approach to the investigation of the influence of geometry on residual stresses in structural glass: MITHILA ACHINTHA, BOGDAN BALAN .....	89
Benefits of Whole Powder Pattern Decomposition in the Determination of Residual Stress in Multiphase Materials: HUGUES GUÉRAULT, JENS BRECHBUEHL.....	90
Simulation-based optimization of the multiple incremental hole-drilling method for the simultaneous analysis of residual stresses and the measurement accuracy: FRANK SCHWEIZER, MELANIE SENN, WULF PFEIFFER .....	90
Analysis of residual stress gradients by X-ray diffraction with five-axis diffractometer: ALEX ULYANENKOV, ANDREI BENEDEKTOVITCH, TATIANA ULYANENKOVA, JOSEF KECKES.....	91
Comparison of the residual stress distributions in conventional and stationary shoulder friction stir welding: TIANZHU SUN, YINGCHUN CHEN, PHILIP B. PRANGNELL, MATTHEW J. ROY, PHILIP J. WITHERS.....	92

### Talks Topic B 4

Nitriding stress due to nitrogen diffusion and nitride formation: TATSUO INOUE.....	94
Influence of rotational speed in friction stir welding on heat generating behavior of MPS analysis: HISASHI SERIZAWA, TAKU HAYAMI, FUMIKAZU MIYASAKA .....	94
Failure analysis and optimization of welding process for 347H boiler tube of thermal power plant: HAN-SANG LEE, JINE-SUNG JUNG, DOO-SOO KIM, KEUN-BONG YOO .....	95
Evaluation of the interfacial shear stress between FeCrAl coating and Zircaloy-4 fuel cladding: YANG LIU, IMRAN BHAMJI, PHILIP J. WITHERS, WEICHENG ZHONG, PETER MOUCHE, BRENT J. HEUSER, MICHAEL PREUSS .....	96
Mechanical property and Residual Stress in Type304 stainless steel repaired partially by HVOF sprayed technique: MASAYUKI ARAI, SHO TANAKA, TATSUO SUIDZU .....	97
Comparative residual stress measurements on shot peened spring steel by XRD and PRISM hole drilling method: THEO RICKERT, DOMINIK DAPPRICH, CARLO SCHEER.....	98

### Talks Topic B 5

Combined machining/burnishing process optimization for alloy steel 42CrMo4 using Taguchi technique: ANIS RAMI, SALEM SGHAIER, HEDI HAMDI, SAMIR LAHOUAR.....	100
The residual stress homogeneity state induced by gear manufacturing processes: FRITZ KLOCKE, JEFFERSON GOMES, CHRISTOPH LÖPENHAUS, <u>RONNIE REGO</u> .....	100
Influence of specimen size on the residual stress formation after heat treatment of hot-work tool steel components: M. SCHEMMEL, P. PREVEDEL, R. SCHÖNGRUNDNER, W. ECKER, T. ANTRETTER.....	101
Effect of different surface treatments on A7N01S-T5 aluminum alloy butt joints fatigue properties: CHUANPING MA, HUI CHEN, QIMENG ZHU, YUANMING MA, XU ZHAO.....	102
Thermomechanical behaviour and microstructural evolution of high temperature forged Ti-6Al-4V during heat treatment quenching: RENAUD JULIEN, VINCENT VELAY, VANESSA VIDAL, MEHDI SALEM, YOANN DAHAN, ROMAIN FORESTIER, FARHAD REZAI-ARIA .....	102
Development of ProCast® Models to Predict Residual Stress within Femoral Implant Castings: BRIAN CONROY, ALAN KAVANAGH, DAVID TANNER .....	103

## Talks Topic B 6

Evolution of residual stresses and work hardening during cycling loading and their impact on fatigue behavior of a single crystal nickel based superalloy: AMÉLIE MORANÇAIS, PASCALE KANOUTÉ, MANUEL FRANÇOIS, MATHIEU FÈVRE, ANAÏS GAUBERT .....	106
Numerical and Experimental Description of the Surface and Subsurface Residual Stresses in Metallic Components after Mechanical Surface Treatment : MAJID FARAJIAN, MIRKO BOIN, ROBERT C. WIMPORY, MICHAEL HOFMANN, ALEXANDRU D. STOICA, KE AN.....	107
Evaluation of stress determination methods for a 2D x-ray diffraction portable apparatus using in-situ measurements during tensile testing: JOAQUIN RAMIREZ RICO, JINJING LI, SEUNG YUB LEE, ISMAIL CEVDET NOYAN .....	108
Laboratory Micro-focus X-ray Sources for Stress Measurements: BERND HASSE, ANDREAS KLEINE, JÖRG WIESMANN, CARSTEN MICHAELSEN .....	109
Phase-Field Model for Solid-Solid Phase Transformation Driven by Elasticity. OLEG TSCHUKIN, DANIEL SCHNEIDER, BRITTA NESTLER .....	109

## Talks Topic B 7

Experimental and Numerical Investigation of Residual Stress Relaxation in Shot-Peened Notch Geometries under Low-Cycle Fatigue: CHAO YOU, MITHILA ACHINTHA, KATHERINE SOADY, PHILIPPA REED .....	111
Analysis of compositionally ungraded FGM analogues: Neutron diffraction measurements of residual stress and mechanical testing of pressure sintered Mo-Y <sub>2</sub> O <sub>3</sub> and Mo-Al <sub>2</sub> O <sub>3</sub> systems: MICHAEL SALEH, DORJI CHAVARA, KARL TOPPLER, JAMES ALEXANDER, ANDREW RUYS, KAVEH KABIR, VLADIMIR LUZIN .....	112
The distribution laws of residual stress of high speed trains by statistical method: GUOQING GOU, HUI CHEN, YUPING YANG, JIA CHEN.....	113
How to depict measured data and results in the matrix method: BALDER ORTNER .....	113
Finite Element modeling and investigation of the process parameters in Deep Rolling of a plane geometry: NATALIYA LYUBENOVA, DIRK BAEHRE .....	114

## Topic C: Cyclic deformation behavior, crack initiation & crack growth of metals

### Talks Topic C 1

Effect of chemical heterogeneity on the low-cycle-fatigue behavior of austenitic Cr–Ni stainless steels: JIŘÍ MAN, MAREK SMAGA, IVO KUBĚNA, ALICE CHLUPOVÁ, JAROSLAV POLÁK.....	117
The distribution of local plastic deformation during VHCF loading of duplex stainless steel and martensitic steel: ALEXANDER GIERTLER, RUDOLF DENK, ULRICH KRUPP .....	118
Fatigue mechanisms of an austenitic-ferritic duplex stainless steel at loading conditions close to the conventional fatigue limit: BENJAMIN DÖNGES, CLAUS-PETER FRITZEN, HANS-JÜRGEN CHRIST .....	118
Material Development for Precision Steel Tubes for Stabilizer Bars: MARIO MÜCHER, ROBERT BRANDT .....	119
Effect of Cementite Morphology on Fatigue Crack Propagation in Smooth Steel Specimen: ZHOU-JIA XI, MOTOMICHI KOYAMA, YUICHI YOSHIDA, NOBUYUKI YOSHIMURA, KOHSAKU USHIODA, HIROSHI NOGUCHI .....	120

### Talks Topic C 2

The role of corrosion pit in corrosion fatigue crack initiation process of 12Cr stainless steel: RYUICHIRO EBARA.....	122
Characterization of the fatigue behavior of the metastable austenitic steel X6CrNiNb1810 from LCF to VHCF at 300°C: ANDREAS SORICH, MAREK SMAGA, DIETMAR EIFLER, TILMANN BECK .....	122
Influence of the surface morphology on the cyclic deformation behaviour of cryogenic turned metastable austenitic steel X6CrNiNb1810: ROBERT SKORUPSKI, MAREK SMAGA, DIETMAR EIFLER, TILMANN BECK .....	123
Hybrid surface treatment on austenitic stainless steel JIS SUS316 to improve fretting fatigue strength: TOSHIHIRO Omori, TATSURO MORITA, KOHEI OKADA, HIDEAKI MAEDA .....	124

Low cycle fatigue behaviors of hot-bent 347 Stainless Steels in a simulated PWR water: JUNHO LEE, JONG-DAE HONG, <u>CHANGHEUI JANG</u> .....	125
Effect of Cold-Drawing on High-Cycle Fatigue Properties of Austenitic TWIP and Fully Pearlitic Steels: SEOK WEON SONG, JEONG HUN LEE, HYONG JIK LEE, CHUL MIN BAE, CHONG SOO LEE.....	126

### Talks Topic C 3

Influence of characteristics of inclusion on rolling contact fatigue of bearing steel: EIICHI TAMURA, YUSUKE SANDAIJI, TAKEHIRO TSUCHIDA .....	128
Evaluation of the fatigue behavior of damage tolerant TRIP-modified SAE 52100 steels using the short-time-procedures PHYBAL <sub>CHT</sub> - and PHYBAL <sub>LT</sub> : MARCUS KLEIN, HENDRIK S. KRAMER, TILMANN BECK, DIETMAR EIFLER.....	129
The development of the indirect method for estimation of strain life fatigue parameters: ROBERT BASAN, DOMAGOJ RUBEŠA, MARINA FRANULović .....	130
Fatigue Properties of DLC Coated Steel AISI1045 with Cr Diffusion Layer on the Substrate Surface by AIH-FPP Process: KENTA UEYAMA, KOJI KOBAYASHI, HIROYUKI AKEBONO, JUN KOMOTORI, ATSUSHI SUGETA .....	131
Low cycle fatigue properties of the Fe-28Mn-5Cr-6Si-0.5NbC alloy: NOBUO NAGASHIMA, TAKAHIRO SAWAUCHI, KAZUYUKI OGAWA .....	132

### Talks Topic C 4

Effects of nitriding temperature on the fatigue properties of Ti-6Al-4V alloy and in-situ observation of fatigue cracks in 4-points bending: SHOICHI KIKUCHI, SHO YOSHIDA, YUTA NAKAMURA, AKIRA UENO, YOSHIKAZU NAKAI .....	134
The influences of foreign object damage on the high cycle fatigue behavior of titanium alloy TC11: ZHAO ZHENHUA, CHEN WEI, WU TIEYING .....	135
Effect of forging condition on fatigue behavior in AZ61 bulk nanostructured metal fabricated by multi-directional forging: YOSHIHIKO UEMATSU, TOSHIFUMI KAKIUCHI, TAISHI NOZAKI, HIROMI MIURA .....	135
Variable-Amplitude of Aluminum Alloy 7075 in the VHCF Regime under Superimposed Loading Conditions: S.E. STANZL-TSCHEGG, M. MEISCHEL, N. IYER, A. ARCARI, N. PHAN .....	136

### Talk Topic C 5

Assessment of fatigue crack closure under in-phase, out-of-phase and phase-shift thermomechanical fatigue loading using a temperature dependent strip yield model: CARL FISCHER, CHRISTOPH SCHWEIZER, THOMAS SEIFERT.....	138
Dwell time effects on the Thermo-Mechanical Fatigue Behaviour of a Wrought Ni-base Alloy: STEFAN GUTH, JONAS MÜLLER, KARL-HEINZ LANG .....	139
Biaxial fatigue behavior of a hot-pressed metastable austenitic steel: STEPHANIE ACKERMANN, TIM LIPPMANN, SEBASTIAN HENKEL, HORST BIERMANN.....	140
High temperature low cycle fatigue behavior of cast superalloy Inconel 713LC coated with ZrO <sub>2</sub> -SiO <sub>2</sub> -Al <sub>2</sub> O <sub>3</sub> nanocrystalline thermal barrier coating: KAREL OBRTLIK, LADISLAV ČELKO, TOMÁŠ CHRÁSKA, IVO ŠULÁK, LENKA KLAKURKOVÁ, DAVID JECH, VIKTOR ŠKORÍK, JIŘÍ ŠVEJCAR .....	141
Optimal Design of Skirt Supporting Structure of Coke Drum for Thermal-Mechanical Cyclic Loading: EDWARD WANG, ZIHUI XIA .....	142
Numerical and experimental analysis of the influence of process parameters on the damage of hot rolling rolls: LUIZ GUSTAVO DEL BIANCHI DA SILVA LIMA, ALEXANDRE GONÇALVES, ANA PAOLA VILLALVA BRAGA, IZABEL FERNANDA MACHADO, ROBERTO MARTINS DE SOUZA, MÁRIO BOCCALINI JR.....	143

### Talks Topic C 6

Rolling Contact Fatigue Strength of Ceramic Coated Steel Laser-Quenched after Coating Process: HIROTAKA TANABE, YUKI NAKAMURA, YUI IZUMI, TOHRU TAKAMATSU .....	145
---	-----

Crack propagation behavior in titanium alloy under combined axial-torsional cyclic loading modes: TOSHIHIKO HOSHIDE, TETSUYA TOKUHARA, MASASHI NAGAOKA .....	145
The AA2124/SiC metal matrix composites under fatigue, creep and monotonic loading conditions: AGNIESZKA RUTECKA, PAWEŁ GRZYWNA, LECH DIETRICH .....	146
Fatigue crack growth behavior of Ti-6Al-4V ELI alloy under constant amplitude loading with different single overloads: CHUANYONG CHEN, DUYI YE, XUMIN HU, JIANZHONG LIU, LINA ZHANG .....	147
Prestrain memory on subsequent cyclic behavior of FCC metallic materials presenting different dislocation slip tendencies: GAEL MARNIER, CLEMENT KELLER, LAKDHAR TALEB .....	148

### Talks Topic C 7

The effects of periodic overloads and high/low loading blocks on fatigue crack growth of aluminum alloy: HAIFENG XU, DUYI YE, LEI XIAO, JIANZHONG LIU, LINA ZHANG .....	150
Multiaxial fatigue damage in fibrous composites: an approach based on micromechanical crack growth: ROBERTO BRIGHENTI, ANDREA CARPINTERI, DANIELA SCORZA .....	150
Predicting the fatigue life at crack initiation in cruciform welded joints by using the effective cyclic J-integral ( $\Delta J_{eff}$ ): DESIRE TCHOFFO NGOULA, HEINZ THOMAS BEIER, MICHAEL VORMWALD .....	151
Fatigue behavior of Al/Steel dissimilar resistance spot welds fabricated using Al-Mg insert film: REN ITO, ISHAK IBRAHIM, YOSHIHIKO UEMATSU, TOSHIFUMI KAKIUCHI, YUN KYOUL, CHIHIRO MATSUDA .....	152
High cycle fatigue strength of pure lead: MASAHIRO ENDO, KEIKO MORITA, AKIRA YASUNAGA .....	153

### Talks Topic C 8

Accuracy improvement of fatigue damage evaluation based on phase analysis of dissipated energy: DAIKI SHIOZAWA, TSUYOSHI INAGAWA, ATSUSHI AKAI†, TAKAHIDE SAKAGAMI .....	155
Fatigue damage evaluation of polycrystalline alloy by diffraction contrast tomography using ultra-bright synchrotron radiation: YOSHIKAZU NAKAI, DAIKI SHIOZAWA, SHOICHI KIKUCHI, SHOTA MATSUDA, RYOTA NAKAO .....	156
Dislocation-based modelling of low cycle fatigue in FCC single and polycrystals: NICOLÒ GRILLI, KOENRAAD G. F. JANSSENS, HELENA VAN SWYGENHOVEN .....	156
3D dislocation dynamics simulation of crack shielding and blunting in FCC metals: LAURENT KORZECZEK, BENOIT DEVINCRE, RICCARDO GATTI, ARJEN ROOS .....	157
Analysis of the cyclic plastic response of materials based on the hysteresis loop shape: ROMAN PETRÁŠ, JIŘÍ TOBIÁŠ, JAROSLAV POLÁK .....	158

### Talks Topic C 9

The role of graphite in fatigue crack growth of ductile cast iron under the presence of internal and external hydrogen: TAKASHI MATSUO, KOSEI YAMADA, HISAO MATSUNAGA, MASAHIRO ENDO, SABURO MATSUOKA .....	160
Shear mode crack propagation along with plastic flow of small area SHUTO FUKUDOME, SIGERU HAMADA, MASAHARU UEDA, HIROSHI NOGUCHI .....	161
A Continuum Damage Mechanics Approach For Prediction of Fatigue Crack Initiation Life: SHIVA KUMAR CHITTA, M.M.MAYURAM .....	161
Generalized critical fatigue crack length for transition from microstructure-driven to mechanics-driven propagation: YASUAKI HAMANO, MOTOMICHI KOYAMA, KANEAKI TSUZAKI, HIROSHI NOGUCHI .....	162
Fatigue crack growth characteristic under hydrogen atmosphere in an ultra-low frequency region in Low Carbon and Interstitial Free Steels: YOUSUKE ONISHI, MOTOMICHI KOYAMA, ATSUSHI NISHIMOTO, DAISUKE SASAKI, YASUJI ODA, HIROSHI NOGUCHI .....	162
Short crack growth kinetics in heat resistant austenitic stainless steel Sanicro 25: VERONIKA MAZÁNOVÁ, JAROSLAV POLÁK, GUOCAI CHAI .....	163

## Talks Topic C 10

Application of $\sqrt{\text{area}}$ parameter for estimation of threshold stress intensity factor range $\Delta K_{th}$ of small shear-mode cracks SABURO OKAZAKI, HISAO MATSUNAGA, MASAHIRO ENDO .....	166
Fatigue crack initiation near inclusions in Ni superalloys – a SEM based study with high resolution EBSD: JUN JIANG, JIE YANG, TIAN TIAN ZHANG, MAKI KUWABARA, FIONN DUNNE, BEN BRITTON .....	167
Non-destructive evaluation of multiple-site small cracks in high-temperature low cycle fatigue of an austenitic stainless steel by using multipoint probe DC potential difference measuring system: SHIO NAKANISHI, TAKAYUKI SUZUKI, YUJI NAKASONE .....	167
Crack detection by Sonic-IR method using ultrasonic wave inputted through water: YUI IZUMI, HIROTAKA TANABE, TOHRU TAKMATSU1, TAKAHIDE SAKAGAMI.....	168
Low-cycle fatigue Simulation in micro-scale to obtain fatigue behavior of bimodal AL alloys: H. HOSSEINI-TOUDESHPY, M. JAMALIAN.....	169
Fatigue of automotive engine cylinder heads – A new model based on crack propagation and micro-structure interaction: GUILLAUME MORIN, ROMAIN DEJEAN, <u>JEAN-MICHEL FIARD</u> , MATHIEU BERANGER.....	169

## Topic D: In-situ microscopy and diffraction

### Talks topic D 1

In-situ TEM deformation of lightweight alloys and local strain measurements with diffraction imaging: ANDREW M. MINOR .....	172
CSL $\Sigma 3$ and $\Sigma 9$ activity as a deformation pathway in nanocrystalline Pd and AuPd: AARON KOBLER, <u>CHRISTIAN KÜBEL</u> 1, HORST HAHN .....	172
In-situ characterization of martensite plasticity by high resolution microstructure and strain mapping: C.C. TASAN, L. MORS DORF, M-M. WANG, D. BARBIER, O. JEANNIN, D. RAABE.....	173
Complex analyses of mechanical and electrical performance of metallic thin films on flexible substrates combined with in-situ Reflectance Anisotropy Spectroscopy: ANDREAS WYSS, MATTHIAS SCHAMEL, RICHARD DENK, MICHAEL HOHAGE, ALLA S. SOLOGUBENKO, RALPH SPOLENAK .....	174
Crystallographic and mechanical characterization of micro-bicrystal cantilevers: S. ZAEFFERER, N. BOZZOLO, S. KLEINDIEK, A. J. SMITH.....	174

### Talks Topic D 2

In-situ micro-mechanical testing at the synchrotron: STEVEN VAN PETGEM .....	176
Optimizing Single Crystal Growth for Detector Applications using Energy-dispersive Neutron Imaging: H. MATTHIAS REICHE, SVEN C. VOGEL, EDITH D. BOURRET, ADRIAN LOSKO, ANTON TREMSIN, GREGORY A. BIZARRI, MARTIN M. GASCON, DIDIER PERRODIN, ERIC C. SAMULON .....	176
Time-resolved (4D) in situ x-ray tomographic microscopy at TOMCAT: Understanding the dynamics of materials: J.L.FIFE, F. MARONE, R. MOKSO, M. STAMPANONI.....	177
Grain and subgrain high resolution diffraction from polycrystalline bulk materials: ULRICH LIENERT, WOLFGANG PANTLEON, GÁBOR RIBÁRIK, TAMÁS UNGÁR.....	178
Advanced Laboratory X-ray Microscopy : In Situ Materials Characterization and Diffraction Contrast Tomography: ARNO MERKLE, CHRISTIAN HOLZNER, BENJAMIN HORNBERGER, HRISHIKESH BALE, WILLIAM HARRIS, LEAH LAVERY .....	179

## Topic E: Size effects and small-scale mechanical behavior of materials

### Talks Topic E 1

Size dependent strength and its exploitation for length-scale engineered material systems: ANDY BUSHBY, DAVID DUNSTAN .....	181
---	-----

Three-dimensional modeling of size effects in micromechanical testing: EDGAR HUSSER, ERICA LILLEODDEN, SWANTJE BARGMANN.....	182
Dislocation grain boundary interaction in bi-crystalline micro pillars studied by in situ SEM and in situ $\mu$ Laue diffraction. NATALIYA MALYAR, CHRISTOPH KIRCHLECHNER, GERHARD DEHM.....	182
Size effects and dislocation structure under torsion loading of single crystalline wires: a discrete dislocation dynamics study: DANIEL WEYGAND, PETER GUMBSCH .....	183
Investigation of crystal plasticity of single crystal copper by using micro scale torsion test: KOZO KOIWA, CHUANTONG CHEN, NOBUYUKI SHISHIDO, MASAKI OMIYA, SHOJI KAMIYA, HISASHI SATO, MASAHIRO NISHIDA, TAKASHI SUZUKI, TOMOJI NAKAMURA, TOSHIAKI SUZUKI, TAKESHI NOKUO .....	184

## Talk Topic E 2

Study of fatigue damage evolution in micron sized bending beams by in situ $\mu$ Laue diffraction: C. KIRCHLECHNER, P.J. IMRICH, J.-S. MICHA, O. ULRICH, C. MOTZ .....	186
A comparative study of fatigue properties of nanoscale Cu films on a flexible substrate: BIN ZHANG, YING ZHANG, XIAO-FEI ZHU, XUE-MEI LUO, GUANG-PING ZHANG .....	187
Strain-dependent fatigue damage of nanocrystalline 930-nm-thick Au films: XUE-MEI LUO, GUANG-PING ZHANG .....	188
Influence of surface energy and dislocation pile-up on the size dependent strength of single-crystalline micro-pillars BO PAN, YOJI SHIBUTANI.....	189
In situ fracture tests of brittle materials at the microscale: GIORGIO SERNICOLA, TOMMASO GIOVANNINI, RUI HAO, T. BEN BRITTON, FINN GIULIANI .....	190

## Talks Topic E 3

Smaller is not always stronger – inverse scale effect on metal- ceramics interface strength observed in LSI interconnect structures : HOJI KAMIYA, NOBUYUKI SHISHIDO, KOZO KOIWA, MASAKI OMIYA, HISASHI SATO, MASAHIRO NISHIDA, TAKASHI SUZUKI, TOMOJI NAKAMURA, TOSHIAKI SUZUKI, TAKESHI NOKUO.....	192
Characterisation and Mechanical Properties of the Boundary Layers of Soft Magnetic Composites: TABEA SCHWARK, RUTH SCHWAIGER, OLIVER KRAFT.....	193
Multiscale Modelling of Damage and Failure in a Biological Hierarchical Material: INGO SCHEIDER, SONGYUN MA, EZGI YILMAZ, SWANTJE BARGMAN .....	193
Surface properties of biopolymer films - Morphology, adhesion and friction: MAURICE BROGLY, AHMAD FAHS, SOPHIE BISTAC.....	194
Microstructure evolution of Cu/Au and Cu/Cr multilayers under cyclic sliding: ZHAO-PING LUO, GUANG-PING ZHANG, RUTH SCHWAIGER.....	195
Toward the modulation of interface barrier strength of Cu/Au nanolayered composites: XI LI, GUANG-PING ZHANG .....	196

## Talks Topic E 4

Probing thermally activated properties on a local scale: DANIEL KIENER, ALEXANDER LEITNER, VERENA MAIER.....	198
Micro- and Macro-mechanical Testing of Grain Boundary Sliding (GBS): JUNNAN JIANG, ANGUS WILKINSON, RICAHRD TODD .....	198
Nanoindentation at Room and Elevated Temperatures of Au/Cu-Multilayers: THOMAS KREUTER, GUANG-PING ZHANG, OLIVER KRAFT, RUTH SCHWAIGER .....	199
Mechanical behavior of the MAX-phase Nb <sub>2</sub> AlC at the nanometer and micrometer scale by means of in situ indentation: NADINE SCHRENKER, YONNES KABIRI, MIRZA MAČKOVIĆ, JULIAN MÜLLER, PETER SCHWEIZER, FLORIAN NIEKIEL, BJÖRN HOFFMANN, SILKE CHRISTIANSEN, ERDMANN SPIECKER.....	200
Deformation behavior of copper thin films indented with patterned nanoindenter tips: ANKE SCHACHTSIEK, OLIVER KRAFT, RUTH SCHWAIGER .....	201

## Talks Topic E 5

Using high temperature micromechanical testing to inform microstructure based models: application to IN718: J. MOLINA-ALDAREGUIA, B. GAN, A. CRUZADO, M. JIMÉNEZ, J. SEGURADO, J. LLORCA .....	203
Multi-scale Fracture Behaviour of Tungsten Alloys for Nuclear Fusion: BO-SHIUAN LI, DAVID ARMSTRONG, JAMES MARROW, STEVE ROBERTS .....	203
Effect of composition and morphology on the mechanical and electrical behavior of Cu-Cr thin films: ALLA. S. SOLOGUBENKO, WILHELM HÜTTENES, HUAN MA, RALPH SPOLENAK.....	204
Thermomechanical influence grinding of electrodeposited chrome coated on a 300M substrate: BENJAMIN WEISS, ANDRÉ LEFEBVRE, OLIVIER SINOT, ALBERT TIDU.....	205
Orthogonal machining of a Cu-1.8wt%Be-0.1wt%Co alloy: influence of the microstructure: ALBAN DE SAEVER, ALBERT TIDU .....	206

## Talks Topic E 6

Grain size gradient-induced work hardening and extraordinary ductilization: XIAOLEI WU, YUNTIAN ZHU .....	208
Mechanical properties and microstructural changes of high strength AA7075 alloy during low temperature ECAP: SEBASTIAN FRITSCH, MARIO SCHOLZE, MARTIN F.-X. WAGNER .....	208
Effect of creep and aging on the precipitation kinetics of an Al-Cu-Alloy after ECAP: MARKUS HÄRTEL, KEVIN G. ABSTOSS, SWETLANA WAGNER, PHILIPP FRINT, PETER MAYR, MARTIN F.-X. WAGNER.....	209
On shear localization in an SPD-processed Aluminum Alloy – Part 1: Microstructures and local mechanical properties: PHILIPP FRINT, STEFFEN PFEIFFER, MARTIN F.-X. WAGNER .....	209
On shear localization in an SPD-processed Aluminum Alloy– Part 2: A simple model concept and FE simulation of the formation of alternating bands: STEFFEN PFEIFFER, PHILIPP FRINT, MARTIN F.-X. WAGNER.....	210

## Talks Topic E 7

Bio-inspired, self-assembled functionalized Fe <sub>3</sub> O <sub>4</sub> nanoparticles with tunable mechanical properties: GEROLD A. SCHNEIDER, AXEL DREYER, ARTUR FELD, EZGI YILMAZ, ANDREAS KORNOWSKI, TOBIAS KREKELER, HESHMAT NOEI, MARTIN RITTER, ANDREAS STIERLE, HOSRT WELLER.....	212
In situ SEM compression tests of layered crystals : PETER SCHWEIZER, FLORIAN NIEKIEL, ERDMANN SPIECKER .....	212
Material development for high-strength nanocomposites: ALMUT SCHROER, JENS BAUER, OLIVER KRAFT.....	213
Mechanical behavior of ultrathin aluminum oxide films: Influence of open or closed porosity: A. VAN DER REST, F. HENRY, A. FAVACHE, J. PROOST, Q. VAN OVERMEERE, T. PARDOEN .....	214
Influences of vacancy defects on compressive behaviors of open-tip carbon nanocones: MING-LIANG LIAO .....	215

## TalksTopic E 8

Size Effect of Single Crystalline Noble FCC Metal Nanowires: IN-SUK CHOI.....	217
Mechanical Behavior of Fivefold Twinned Nanowires understood from Anisotropic Elasticity: FLORIAN NIEKIEL, ERDMANN SPIECKER, ERIK BITZEK.....	217
Mechanical properties of nano-twinned Ag wires: AARON KOBLER, THORSTEN BEUTH, TOBIAS KLÖFFEL, MARKUS MOOSMANN, HORST HAHN, CHRISTIAN KÜBEL, BERND MEYER, ERIK BITZEK, THOMAS SCHIMMEL.....	218
Influence of artificial defects on the mechanical behavior of Au nanowires: CHARLOTTE ENSSLEN, CHRISTIAN BRANDL, GUNTHER RICHTER, OLIVER KRAFT.....	219
In-Situ Electromechanical Properties of ZnO Nanowires: SANJIT BHOWMICK, UDE HANGEN, DOUGLAS STAUFFER, SYED ASIF.....	219

## Topic F: Advanced steels and steel composite materials

### Talks Topic F 1

Mechanical Properties of a 0.2%C–1.5%Si–5%Mn TRIP-aided Annealed Martensitic Steels: KOHICHI SUGIMOTO, HIKARU TANINO .....	221
Nano-laminate TRIP-TWIP steel with dynamic strain partitioning and enhanced damage resistance: C. C. TASAN, M-M. WANG, D. PONGE, D. RAABE .....	221
Characterization of strain localizations during plastic deformation of TRIP/TWIP steels: ANJA WEIDNER, CHRISTIAN SEGEL, HORST BIERMANN .....	222
Temperature evolution during tensile straining of high Mn twinning induced plasticity (TWIP) steels: JEEHYUN KANG, TOBIAS INGENDAHL, WOLFGANG BLECK .....	222
Microstructure as well as mechanical and magnetic properties of Fe-based alloys with different contents of metastable austenite: MAREK SMAGA, DIETMAR EIFLER, TILMANN BECK .....	223
Microstructural Evolution of TRIP-aided Medium Mn Steel During Warm Deformation: YONGMOON LEE, CHONG SOO LEE .....	224

### Talks Topic F 2

Influence of temperature on fatigue-induced martensitic phase transformation in a metastable CrMnNi-steel: HORST BIERMANN, MATTHIAS DROSTE, ALEXANDER GLAGE.....	226
Importance of $\epsilon$ -martensite on embrittlement and fatigue crack growth in Fe-Mn-based austenitic steels: MOTOMICHI KOYAMA, HUICHAO LI, TAKAHIRO SAWAGUCHI, KANEAKI TSUZAKI, HIROSHI NOGUCHI.....	226
Importance of strain aging on fatigue limit in austenitic TWIP steels: YUUSUKE YAMAMURA, MOTOMICHI KOYAMA, RENQING CHE, TAKAHIRO SAWAGUCHI, KANEAKI TSUZAKI, HIROSHI NOGUCHI.....	227
Influence of Si addition on deformation and fracture behaviors of aging treated cast Fe-Mn-Al-C lightweight steel: SOON IL KWON, JE HYUN LEE, SEONG JUN PARK, HYUN UK HONG.....	228
Effect of shot peening on microstructure of steels exhibiting a TRIP effect – Experimental and modeling approaches: ROMAIN GUIHEUX, SOPHIE BERVEILLER, DENIS BOUSCAUD, RÉGIS KUBLER, ETIENNE PATOOR, QUENTIN PUYDT .....	229
Study of Lüders band propagation using IR thermography and DIC method in the wide range of strain rates: MICHAL MAJ .....	230

### Talks Topic F 3

Homogenization of TRIP steel behaviour using a strain gradient plasticity model: M.K. HATAMI, T. PARDOEN, P. BERKE, P.J. JACQUES, T.J. MASSART .....	232
A crystal plasticity model for advanced high strength steels including both TRIP and TWIP effect: FRANZ ROTERS, SU LEEN WONG .....	232
Multiscale Modelling of Damage and Fracture in High Mn TWIP Steels: MANJUNATHA MADIVALA, CHRISTIAN SEGEL, ANJA WEIDNER, HORST BIERMANN, WOLFGANG BLECK, ULRICH PRAHL .....	233
Artificial microstructure model and its applications on plasticity and damage of the dual phase steels: NAPAT VAJRAGUPTA, MOHAMED SHARAF, JUNHE LIAN, SEBASTIAN MÜNSTERMANN, WOLFGANG BLECK .....	234
Dislocation plasticity in precipitate hardened advanced austenitic lightweight high-Mn steels by coupled TEM and DDD simulations: Strengthening and dislocation-based mechanisms: E. WELSCH, S.M. HAFEZ HAGHIGHAT, I. GUTIERREZ-URRUTIA, D. RAABE .....	235
Phase-field modeling of solid-solid phase transformations: DANIEL SCHNEIDER, OLEG TSCHUKIN, MICHAEL SELZER, BRITTA NESTLER.....	236

## Talks Topic F 4

Z phase strengthened steels for ultra-supercritical power plants: DANIEL F. URBAN, CHRISTIAN ELSÄSSER, HERMANN RIEDEL.....	238
Different mechanical behavior of MA957 ODS and Eurofer'97 steels exposed to flowing helium of 720°C: ANNA HOJNA, HYNEK HADRABA, JANA KALIVODOVA, ROMAN HUSAK.....	238
Characterization of the weldability of different AHS steel and aluminium alloy grades using thermo-mechanical physical simulation: JÁNOS LUKÁCS, LÁSZLÓ KUZSELLA, ZSUZSANNA KONCSIK, ÁDÁM DOBOSSY, DÓRA PÓSZALAKY.....	239
The microstructure characterization of the HAZ and welding CCT diagram of API X100 steel: CHUNLIN QIU, LIANGYUN LAN, XIANGWEI KONG.....	240
Weldability of modern high strength bainitic steel: LIANGYUN LAN, XIANGWEI KONG, CHUNLIN QIU.....	241

## Topic G 1: Fracture mechanics

### Talks Topic G 1

Numerical Simulation of ZrO <sub>2</sub> (Y <sub>2</sub> O <sub>3</sub> ) Ceramic Plate Penetration by Cylindrical Plunger: VLADIMIR BRATOV, NIKITA KAZAIRNOV, YURI PETROV.....	243
Temporal Peculiarities of Fracture Caused by Threshold Pulses in Spallation: GRIGORY VOLKOV, YURI PETROV, YURI MESCHERYAKOV, NATALIA MIHAYLOVA.....	243
Dynamic fracture of concrete: Experimental and numerical studies on compact tension and L- specimen: JOŠKO OŽBOLT, UWE MAYER, NATALIJA BEDE, AKANSHU SHARMA.....	244
Multiscale model of the dynamic tensile fracture of solid and molten metals: molecular dynamics and continuum mechanics: ALEXANDER MAYER, VASILIJ KRASNIKOV, POLINA MAYER.....	245
Stage I fatigue crack studies in order to validate the dislocation-free zone model of fracture for bulk materials: FLORIAN SCHÄFER, MICHAEL MARX, HORST VEHOFF.....	246

### Talks Topic G 2

The Mechanics of Bridged Fatigue Cracks: JAMIE J. KRIZIC.....	248
On the need to reconsider fatigue crack growth at negative stress ratios: CHRISTOPER BENZ, MANUELA SANDER.....	248
Effect of adjacent small defects on fatigue limit of steels: MARI ÅMAN, SABURO OKAZAKI, HISAO MATSUNAGA, GARY MARQUIS.....	249
Comparison between three fatigue damage models and experimental results for composite materials submitted to spectrum loading: MOHAMMED BOUSFIA, M. ABOUSSALEH, B. OUHBI, R. BOUKHILI.....	250
Experimental and numerical analysis of damage in random fibrous networks: E. SOZUMERT, E. DEMIRCI, M. ACAR, B. POURDEYHIMI, V. V. SILBERSCHMIDT.....	251

### Talks Topic G 3

A boundary finite element for anisotropic/piezoelectric materials containing multiple cracks: CHYANBIN HWU, SHAO-TZU HUANG.....	253
Effect of micromorphology on crack growth in cortical bone tissue: X-FEM study: MAYAO WANG, XING GAO, ADEL ABDEL-WAHAB, SIMIN LI, ELIZABETH A. ZIMMERMANN, CHRISTOPH RIEDEL, BJÖRN BUSSE, VADIM V. SILBERSCHMIDT.....	254
Extended damage modelling for fracture control in modern line pipe steels: AIDA NONN.....	254

### Talks Topic G 4

Cleavage Initiation Angle for High Strength Steels under Mixed-Mode Conditions: ZEFENG ZHANG, XUDONG QIAN.....	257
--	-----

Experimental and numerical investigations on the crack growth stage of crane runway girders subjected to cyclic loading: PHILIPP RETTENMEIER, EBERHARD ROOS, STEFAN WEIHE, XAVER SCHULER .....	258
Crack Path in connection with the Two-Parameter Fracture Mechanics Approach on X52 steel pipe repairing: M. HADJ MELIANI, G. PLUVINAGE, Y.G. MATVIENKO .....	259
A modified Sih criterion for crack deflection in dipolar gradient elasticity: IOANNIS D. GAVARDINAS, ANTONIOS E. GIANNAKOPOULOS.....	259
Cohesive laws for adhesive layers loaded in a state close to pure shear: ULF STIGH, ANDERS BIEL .....	260
The role of Geometrically Necessary Dislocations in the fracture process of metallic materials: EMILIO MARTÍNEZ-PAÑEDA, CHRISTIAN NIORDSON .....	261

## Talk Topic G 5

On the fracture toughness of bulk-metallic glasses: BERND GLUDOVATZ, JAMIE J. KRIZIC, MARIOS D. DEMETRIOU, WILLIAM L. JOHNSON, ROBERT O. RITCHIE.....	263
Damage & Fracture Toughness of Fibrous Dual-Phase Steels for Automotive Applications: KARIM ISMAIL, THOMAS PARDOEN, PASCAL J. JACQUES, LAURENCE BRASSART, ASTRID PERLADE .....	263
New insights on the physically correct application of the J-integral for characterizing fatigue crack growth in elastic–plastic materials: WALTER OCHENSBERGER, OTMAR KOLEDNIK .....	264
Grain Boundary Precipitation and Creep Crack Growth in polycrystalline Ni-base superalloys: H. SOMMER, C. SOMSEN, F. MUELLER, V. KNEZEVIC, N. DE BOER, J. KLÖWER, G. EGGELER.....	265
Examination of Evaluation Method for Static Strength of Casting Materials by Regarding Shrinkage Porosity as Cracks: Example of AZX912 Mg Cast Alloy: YU-KI HIGUCHI, NAOYA OCHI, HIROSHI NOGUCHI .....	265
Insight into MAG welding under constructive constraint conditions by means of high energy synchrotron X-ray diffraction: FLORIAN VOLLERT, JENS GIBMEIER, JONNY DIXNEIT, THORBEN FISCHER, P.STARON, ARNE KROMM, THOMAS KANNENGIESSER .....	266

## Talks Topic G 6

Testing fracture toughness of brittle materials via chevron- notched bend bars of microscopic length-scale: GORAN ZAGAR, MARTIN MUELLER, VACLAV PEJCHAL, LIONEL MICHELET, MARCO CANTONI, ANDREAS MORTENSEN ....	268
Micro-fracture testing of tungsten single crystals: CHRISTOPH BOHNERT, NICOLA SCHMITT, <u>SABINE M. WEYGAND</u> , RUTH SCHWAIGER, OLIVER KRAFT .....	268
An Improved Micromechanical Method for Investigating the Statistical Strength of Poly-Silicon Membranes: JOHN BRÜCKNER, HOLGER PFAFF , ALFONS DEHÉ, SVEN RZEPKA .....	269
How Crystals Break – Crack speed dependent environmental effect and surface instabilities ANNA GLEIZER, LIRON BEN-BASHAT BERGMAN, <u>DOV SHERMAN</u> .....	270

## Talks Topic G 7

Influences of hydrogen-affected yielding and work hardening on plastic zone evolution studied by Finite Element Method: DAISUKE SASAKI, MOTOMICHI KOYAMA, KENJI HIGASHIDA, KANEAKI TSUZAKI, HIROSHI NOGUCHI .	272
On the fracture toughness of fcc medium- and high-entropy alloys at ambient to cryogenic temperatures: BERND GLUDOVATZ, KELI V. S. THURSTON, ANTON HOHENWARTER, DHIRAJ CATOOR, HAO BEI, EASO P. GEORGE, ROBERT O. RITCHIE .....	273
Stress corrosion cracking in sensitized austenitic stainless steel type 304 under tetrathionate solution environment: TOMOYUKI FUJII, KEIICHIRO TOHGO, YUTARO MIURA, YOSHINOBU SHIMAMURA .....	273
Effect of post weld heat treatment on the long-term reliability of austenitic stainless steel 347H: JINE-SUNG JUNG, HAN-SANG LEE, DOO-SOO KIM, KEUN-BONG YOO .....	274
Interaction between torsion damage and toughness anisotropy in a drawn pearlitic steel wire: AURÉLIE JAMONEAU, JEAN-HUBERT SCHMITT, DENIS SOLAS.....	275

## Topic H 1: Materials for fission and fusion

### Talks Topic H 1

Effects of helium and irradiation damage on microstructure and mechanical properties of Fe base alloys for fusion applications: RICHARD KURTZ .....	277
New Material Developments for Applications in Fusion Reactors: J.W. COENEN, J. ENGELS, S. HEUER, A. HOUBEN, B. JASPER <sup>1</sup> , A. LITNOVSKY, TH. WEBER, T. WEGENER, W. BIEL, T. HOESCHEN, F. KOCH, R. NEU, J. RIESCH, M. RASINSKI, B. UNTERBERG, CH. LINSMEIER .....	277
Functional graded tungsten/EUROFER coating systems for First Wall application: D. D. QU, W.W. BASUKI, J. GIBMEIER, R. VASSEN, J. AKTAA .....	279
CuCrZr alloys reinforced by Tungsten as structural Divertor applications for DEMO: JAN HOFFMANN, STEFFEN ANTUSCH, JENS REISER, MICHAEL RIETH, VERENA WIDAK, SOEREN MUELLER, HOHE JOERG .....	279
Lithium evaporation and redeposition experiments under high density linear plasma dumping: X. CAO, W. OU, Z. CAO, Y. XIA, W. ZHANG, X. XUE, C. WANG, J. WANG, D. YANG, S. CHEN, F. GOU.....	280

### Talks Topic H 2

Analyzing the ions radiation-induced defects and cavity swelling evolution in representative PWR internal austenitic steels: BERTRAND MICHAUT, JOËL MALAPLATE, ALEXANDRA RENAULT LABORNE, FAIZA SEFTA, DANIEL BRIMBAL, LIONEL FOURNIER, BRIGITTE DÉCAMPS .....	282
Insights in microstructure of austenitic ods steels: TIM GRAENING, MICHAEL RIETH, ANTON MOESLANG .....	282
Studies of high dpa ion beam irradiation effects on fcc AA-6061 and fcc-bcc duplex steel 2205: micromechanical modelling and nano-indentation examination of hardness variations: MICHAEL SALEH, PAUL MUNROE, LYNDON EDWARDS.....	283
Mechanical Behavior of Unalloyed Plutonium: ADAM FARROW, TARIK SALEH, DENIECE KORZEKWA, JEREMY MITCHELL .....	284
Temperature dependent X-ray adsorption spectroscopy studies of Fe, Cr, and Ni local atomic structure for ferritic and austenitic ODS steels: ANDRIS ANSPOKS, JURIS PURĀNS, ALEKSEJS KUZMINS, PAVEL VLADIMIROV, TIM GRÄNING, JAN HOFFMANN, KĀRLIS LAZDIŅŠ <sup>1</sup> , ARTURS CINTIŅŠ, ANTON MÖSLANG, MICHAEL RIETH .....	284

### Talks Topic H 3

Mechanical Properties of a PM2000 ODS alloy tested at temperatures up to 700°C: UDE D. HANGEN, ASTA RICHTER.....	287
High temperature investigation of the fusion relevant material EUROFER by instrumented indentation: JULIAN BREDL, MANUEL DANY, HANS-CHRISTIAN SCHNEIDER, OLIVER KRAFT .....	287
Study of irradiation creep based on nanomechanical lab-on-chip testing: PIERRE LAPOUGE, FABIEN ONIMUS, YVES BRÉCHET, THOMAS PARDOEN, JEAN-PIERRE RASKIN, RENAUD VAYRETTE .....	288
Atom probe tomography of nanoscale precipitates in 13% Cr ODS steels with Ti variation: S. ROGOZHKIN, N. ORLOV, A. ALEEV, A. BOGACHEV, A. NIKITIN, A. ZALUZHNYI, R. LINDAU, A. MÖSLANG, P. VLADIMIROV .....	289
Identification of Cr-Y-O Nano-Cluster in a 14Cr Oxide Dispersion Strengthened Steel: XUE HU, WEI YAN, WEI WANG, YIYIN SHAN, KE YANG .....	290
Deuterium retention in reduced-activation ODS steels irradiated with 20 MeV W ions : O.V. OGORODNIKOVA, K. SUGIYAMA, Z. ZHOU, YU. GASPARYAN, V. EFIMOV .....	290

### Talks Topic H 4

Combined effect of radiation damage and helium on the hardening and embrittlement of ferritic / martensitic steels: YONG DAI, KUN WANG, CHRISTIANE VIEH, VLADIMIR KRŠJAK .....	293
Mechanical Properties of Irradiated Ferritic/Martensitic Steels: TARIK A. SALEH, STUART A. MALOY, TOBIAS ROMERO, MATTHEW E. QUINTANA .....	293

Influence of neutron irradiation on precipitate microstructure in EUROFER97: CHRISTIAN DETHLOFF, ERMILE GAGANIDZE, JARIR AKTAA .....	294
Atomic scale investigation of phase decomposition of Fe-22%Cr during thermal aging and subsequent heavy ion irradiation: O. KORCUGANOVA, A. ALEEV, S. ROGOZHNIKIN .....	295
Comparison of mechanical properties between the HT9 and Gr.92 steel with various heat treatment conditions in a viewpoint of microstructure: SANGGYU PARK, HYEONGMIN HEO, JUNHWAN KIM, SUNGHO KIM ...	295
Creep rupture behavior of the China Low Activation Martensitic steel at 600°C: XUE HU, LIXIN HUANG, WEI YAN, WEI WANG, YIYIN SHAN, KE YANG.....	296

## Talks Topic H 5

Positron annihilation research on ferritic/martensitic steels irradiated under mixed spectrum of high energy protons and spallation neutrons: VLADIMIR KRŠJAK, <u>YONG DAI</u> .....	298
Loss of strength and embrittlement of neutron irradiated beryllium: V. CHAKIN, A. MOESLANG .....	298
Modeling Hydrogen Ad- and Desorption on Beryllium-(0001)-Surface: CHRISTOPHER STIHL, DMITRY BACHURIN, PAVEL VLADIMIROV .....	299
Dislocation microstructure evolution in tungsten due to indentation loading simulated by discrete dislocation dynamics: KINSHUK SRIVASTAVA, DANIEL WEYGAND, PETER GUMBSCH.....	300
Characterization and modelling of the mechanical behaviour of Nb <sub>3</sub> Sn: GILLES LENOIR, VERONIQUE AUBIN.....	300
Characterisation and modelling of nuclear graphite : from micrometres to metres: DONG LIU, PETER HEARD, GILLIAN SMITH, BRANKO SAVIJ2 ERICK SCHELANGEN, PETER FLEWITT .....	301

## Talks Topic I 1

Development of a novel microstructure highly resistant to grain boundary damage during creep at 950°C in Alloy 617: JI-WON LEE, HYUN-HWA PARK, TAE-HO LEE, HYUN-UK HONG .....	303
Numerical multi-criterion optimization method for developing Ni-based superalloys: Development of a software tool and experimental validation: RALF RETTIG, NILSS C. RITTER, ALEXANDER MÜLLER, HARALD E. HELMER, ROBERT F. SINGER.....	304
On the importance of the matrix for the creep properties of single crystal nickel based superalloys: R. VÖLKL, E. FLEISCHMANN, E. AFFELDT, U. GLATZEL .....	304
Influence of misfit stresses on dislocation glide in single crystal superalloys: A three-dimensional discrete dislocation dynamics study: SIWEN GAO, MARC FIVEL, ANXIN MA, ALEXANDER HARTMAIER .....	305
TEM analysis of localized, planar deformation events which govern creep of single crystalline CoNi-super alloys with $\gamma/\gamma'$ -microstructures: YOLITA M. EGGELER, JULIAN MÜLLER, MICHAEL S. TITUS, AKANE SUZUKI, TRESA M. POLLOCK, ERDMANN SPIECKER .....	305

## Talks Topic I 2

On the Formation of Ledges and Grooves at $\gamma/\gamma'$ Interfaces of Single Crystal Superalloys: ALIREZA B. PARSA, PHILIP WOLLGRAMM, HINRICH BUCK, ALEKSANDER KOSTKA, CHRISTOPH SOMSEN, ANTONIN DLOUHÝ, GUNTHER EGGELER .....	308
The influence of Re and Ru on the high-temperature creep strength and phase stability of Ni-based superalloys: KAMIL MATUSZEWSKI, RALF RETTIG, ROBERT F. SINGER.....	308
Super-Solvus Heat Treatments of Ni-Based Superalloys in a Hot Isostatic Press/Quench Unit: LAIS MUJICA RONCERY, INMACULADA LOPEZ-GALILEA, BENJAMIN RUTTERT, WERNER THEISEN .....	309
Crystal plasticity modeling of porosity reduction in an as-cast Ni-base single crystal superalloy during hot isostatic pressing: SIWEN GAO, INMACULADA LOPEZ-GALILEA, <u>ANXIN MA</u> , STEPHAN HUTH, WERNER THEISEN, ALEXANDER HARTMAIER.....	310
Characterization of <100> superdislocations and the $\gamma/\gamma'$ interface by an advanced FIB lamella lift out technique: JULIAN MÜLLER, MICHAEL J. MILLS, <u>ERDMANN SPIECKER</u> .....	311
New Experimental Results on Atomistic and Microstructural Aspects of Creep of Ni-Base Single Crystal Superalloys (SXs): H. BUCK, A. KOSTKA, P. NÖRTERSCHÄUSER, A.B. PARSA, P. WOLLGRAMM, <u>G. EGGELER</u> .....	311

### Talks Topic I 3

Mechanical properties and microstructures of new polycrystalline $\gamma/\gamma'$ Co-base superalloys: STEFFEN NEUMEIER, LISA FREUND <sup>1</sup> , MATHIAS GÖKEN .....	314
Investigation of the quaternary system Co-Al-W-Ta in the range of Co <sub>9</sub> Al <sub>10</sub> W <sub>2</sub> Ta: ALEXANDER EPISHIN, THOMAS LINK, JAN MIDTLYNG, NIKOLAY PETRUSHIN, GERT NOLZE .....	314
Influence of rhenium on the local mechanical properties of the $\gamma$ and $\gamma'$ phase in cobalt-base superalloys: M. KOLB, C. ZENK, S. NEUMEIER, M. GÖKEN.....	315
Radiation stability of ZrSiN system under the Xe ions irradiation: VLADIMIR UGLOV, VITALI SHYMANSKI, GREGORY ABADIAS, GENNAGY REMNEV <sup>2</sup> , ANDREY SUVALOV .....	316
Effect of casting defects on high cycle fatigue behavior of nickel-based superalloy MAR-M 247: MIROSLAV ŠMÍD, STANISLAVA FINTOVÁ, LUDVÍK KUNZ, PAVEL HUTAŘ, KAREL HRBÁČEK .....	317
Finite Element Simulation of the creep behavior of directionally solidified NiAl-9Mo: JÜRGEN ALBIEZ, IOANNIS SPRENGER, MARTIN HEILMAIER, THOMAS BÖHLKE.....	317

### Talks Topic I 4

On the nucleation of Mo-rich Laves phase particles in 12% Cr tempered martensite ferritic steels: ALEKSANDER KOSTKA, MEHMET IKBAL ISIK, GUNTHER EGGELER .....	320
Temperature dependent solid solution strengthening of Nickel by transition metal solutes: HAMAD UR REHMAN, KARSTEN DURST, STEFFEN NEUMEIER, ROGER REED, MATHIAS GÖKEN .....	320
Effect of the Stress Multi-Axiality on the Creep Damage in Fine Grained HAZ of Mod. 9Cr-1Mo Steels: KIMIYAKI YOSHIDA, MASATAKA YATOMI, MASAOKI TABUCHI, KEN-ICHI KOBAYASHI.....	321
Thermal stability of ferritic and austenitic nanocluster containing ODS steels: SASCHA SEILS, DANIEL SCHLIEPHAKE, DANIEL JANDA, ALEXANDER KAUFFMANN, JULIA N. WAGNER, MARTIN HEILMAIER .....	321
Microstructure and micromechanics of directionally solidified eutectic alloys: AMRITESH KUMAR, RUTH SCHWAIGER, OLIVER KRAFT .....	322

### Talks Topic I 5

Tungsten (W) laminate pipes made of ultrafine-grained (UFG) W foil: JENS REISER, SIMON BONK, JAN HOFFMANN, MICHAEL RIETH.....	325
Internal Friction and Shear Modulus Temperature Dependence of 9%Cr Ferritic Steel P92 in 25 ÷750°C Temperature Range: ELGUJA KUTELIA, GEORGE DARSVELIDZE, TENGIZ KUKAVA, TEMUR DZIGRASHVILI, IA KURASHVILI, FRANCISCO J. PEREZ TRUJILLO .....	325
Bayesian approach to determine optimum inspection intervals for structural components of high temperature materials subjected to creep: Kyoko Nakamura, YUJI NAKASONE .....	326
Microstructural study on the intermetallic compound NiAl-Cr: ANTJE KRUEGER, MICHAEL KLIMENKOV, ANTON MOESLANG .....	327
The crystallographic template effect preceding the formation of stable $\alpha$ -Al <sub>2</sub> O <sub>3</sub> during low temperature oxidation of Fe-Al alloys: PEDRO BRITO, HAROLDO PINTO, ANKE KAYSSER-PYZALLA .....	327

## Topic K 1: Polymer based composites

### Talks Topic K 1

Integrative simulation of short glass fibers reinforced polyamides: methodology followed to identify polymer matrix constitutive models on a wide range of solicitations, temperature, moisture and strain rate: GILLES ROBERT, OLIVIER MOULINJEUNE.....	330
X-ray microtomography and finite element modelling of the failure mechanism in epoxy syntactic foams under compressive loads: PEIFENG LI, RUOXUAN HUANG .....	331

Mechanical Properties of CFRTP Made from CF/PA Composite Yarn Sutured with PA Fiber: YUJI TAKUBO, HIROAKI KIMURA, TAKASHI MATSUOKA, TOMOKO HIRAYAMA1 HIROYUKI FUJITA, YASUJI MIYATA, KUNIO FUJII.....	331
Overall mechanical properties of composites with complex orientationally distributed microstructures: OLESYA I. ZHUPANSKA, PAVLO KROKHMAL.....	332
Estimataion of Dispersion Condition for PP/CNT Nano Composite by Using the New Segments with Extensional Flow for Co-Rotating Twin ScREW Extruder: KOKI MATSUMOTO, TAKAYUKI MORITA, YOSHIHIKO ARAO, TATSUYA TANAKA.....	333
Characterisation of graphene-reinforced nanocomposites: optical-microscopy analysis of spatial non-uniformity: OSMAN BAYRAK, MARIANA IONITA, EMRAH DEMIRCI, VADIM V. SILBERSCHMIDT.....	334

## Talks Topic K 2

Progressive damage evaluation of Glass-Epoxy laminated composites under fatigue loading: SORAN HASSANIFARD, MOHSEN FEYZI.....	336
Experimental Investigation of Cold Forming of PC-Films and tensile bars using Optical Measurements: KAI-UWE WIDANY, CHRISTIAN DAMMANN, ROLF MAHNKEN.....	337
Failure processes of fiber reinforced composites under off-axis loading: CHRISTIAN MAROTZKE, TITUS FELDMANN.....	337
Analysis and Simulation of the Fatigue Behaviour of CFRP Laminates: JANKO KREIKEMEIER, LUKAS GEIGER.....	338
Inline metrology of carbon fiber preforms as an indicator of mechanical properties of consolidated CFRP parts: DANIEL BRABANDT, GISELA LANZA.....	339
Characterization of complexly warped components made from locally reinforced UD-tape laminates: BENJAMIN HANGS, TOBIAS LINK, FRANK HENNING.....	340

## Talks Topic K 3

RVE modeling of fibre-reinforced-polymer curing coupled to visco-elasticity: CHRISTIAN DAMMANN, ROLF MAHNKEN.....	342
Characterization and simulation of the time-dependent anisotropic deformation behaviour of continuously reinforced PA6 material: ANDREAS ROESNER, LUISE KAERGER, FRANK HENNING.....	342
Topological Interlocking Materials - Towards New Polymeric Hybrid Materials: LEE DJUMAS, ANDREY MOLOTNIKOV, GEORGE P.SIMON, YURI ESTRIN.....	343
Homogenisation of thermoelastic properties of short-fibre reinforced polymers and validation based on experimental characterisation: L. KEHRER, V. MÜLLER, B. BRYLKA, T. BÖHLKE.....	344
Phenomenological characterization and macromechanical modeling of anisotropic, non-linear behavior of sheet molding compounds (SMC): MARINA MRKONJIĆ, UTE RAYLING, KAY ANDRÉ WEIDENMANN, LUISE KÄRGER, FRANK HENNING.....	345

## Topic L 1: Lightweight alloys and structures

### Talks Topic L 1

Mechanical properties and microstructure of Ti6Al4V fabricated by selective laser melting: RADOMILA KONECNA, GIANNI NICOLETTO, ADRIAN BACA, LUDVIK KUNZ.....	347
Formation of Twin Bands and Inhomogeneous Deformation in Mg-wrought Alloy AZ31 During Tension-Compression or Bending Loading: K. ANTEN, A. LIEHR, B. SCHOLTES.....	348
Electrochemical-based characterization of the corrosion fatigue behavior of creep-resistant magnesium alloy DieMag422: MARTIN KLEIN, PHILIPP WITTKER, FRANK WALTHER.....	348
Very High Cycle Fatigue (VHCF) Assessment of Selective Laser Melted (SLMed) AlSi12 Alloy: SHAFQAAT SIDDIQUE, FRANK WALTHER.....	
Formability Enhancement of 7075 Al Sheet with Two Step Forming: YONG-NAM KWON, YOUNG SEON LEE.....	349

## Talks Topic L 2

Effect of Missing Cells on the Initial Stiffness and Plastic Yielding Surface of Three-Dimensional Micro-Lattice Structures: KUNIHARU USHIJIMA <sup>1</sup> DAI-HENG CHEN, WESLEY JAMES CANTWELL .....	351
High-strength microarchitected cellular materials: The interplay of design and size-dependent strengthening: JENS BAUER, OLIVER KRAFT .....	351
Self-assembled ultra high strength, ultra stiff mechanical metamaterials based on inverse opals: GEROLD A. SCHNEIDER, JEFFERSON J. DO ROSÁRIO, ERICA T. LILLEODDEN, MARTIN WALECZEK, ROMAN KUBRIN, ALEXANDER YU. PETROV, PAVEL N. DYACHENKO, JULIAN E.C. SABISCH, KORNELIUS NIELSCH, NORBERT HUBER, MANFRED EICH.....	352
An efficient analysis model for the stresses in arbitrary adhesive lap joints with flat laminated adherends: NICOLAS STEIN, PHILIPP WEISSGRAEBER, WILFRIED BECKER .....	352
Optimization of fatigue behaviour of metallic shear joints: TAHA BENHADDOU, ALAIN DAIDIE, PIERRE STEPHAN, CLEMENT CHIROL, JEAN-BAPTISTE TUERY.....	353
Microstructure evolution and deformation texture during rolling of TIMETAL407. GAURAV SINGH, J. QUINTA DA FONSECACA, M. THOMAS, M. PREUSS .....	354

## Topic X 1: General mechanical behavior

### Talks Topic X 1

Wedge indentation studies of Zr-Cu-based bulk metallic glass: V. NEKOUIE, A. ROY, V.V. SILBERSCHMIDT .....	356
Mechanics Behavior of Protein Material: INCHUL BAEK, MYEONGSANG LEE, HYUN JOON CHANG, JAE IN KIM, SUNGSOO NA .....	356
Rigidity characterization and fracture analysis of the solar-grade multi-crystalline silicon plates at low temperature: LV ZHAO, ANNE MAYNADIER, DANIEL NELIAS .....	357
Quantum field theory approach in mechanics of polycrystalline materials: VYACHESLAV SHAVSHUKOV, ANATOLY TASHKINOV .....	358
Axial Crash and Crush Response of Novel Nested Tubes: ZANA EREN, FATİH USTA, ZAFER KAZANCI , HALİT S. TKMEN, ZAHİT MECTOĞLU .....	359
Neutron diffraction and imaging for industrial and engineering applications: ANNA PARADOWSKA .....	359

### Talks Topic X 2

Preparation and Characterization of Neat and Thermally- treated Silicon Carbide Fibers-reinforced Gypsum Cements: Y. E. GREISH, H. F. EL MAGHRABY, O. GEDEON, O. ALNUAIMI, M. S. KATSIOTIS, K. POLYCHRONOPOULOU....	361
Phase-field modeling for microstructure formation of metal foam materials: TAKUYA UEHARA .....	362
Fiber-reinforced Calcium Sulfate Bone Cement Composites with Enhanced Bioactivity, Mechanical Properties and Controlled Biodegradability: YASER E. GREISH <sup>1</sup> ABDEL HAMID I. MOURAD, NUHA F. ATTIA.....	362
Mixed Elastic Variational Formulation of Composite Plates Based on Dimension Reduction Method: MOHAMMAD JAVAD KHOSHGOFTAR, MOHAMMAD MIRZAALI.....	363
Effect of Friction on Material Mechanical Behaviour in Non-equal Channel Multi Angular Extrusion (NECMAE): MOHAMED S. EL-ASFOURY, MOHAMED N. A. NASR, AHMED ABDEL-MONEIM .....	364

## Poster

### Poster Topic A: Multiscale phenomena in plasticity

The effect of hydrogen on the macroscopic strain localization of steels: SVETLANA BARANNIKOVA, ANATOLY MALINOVSKY, DMITRII PESTSOV .....	367
Atomistic analyses of nucleation and propagation behavior of ridge shaped kink band in long-period-stacking-ordered phase: RYOSUKE MATSUMOTO, MASAYUKI URANAGASE.....	368

Microtension behavior of hydrogen-containing metastable austenitic stainless steel: RYO MATSUOKA, KAORU KOGA, YOJI MINE, KAZUKI TAKASHIMA .....	368
Microtension behaviour of dual-phase steel subjected to pre-straining: SHINYA OGATA, YOJI MINE, KAZUKI TAKASHIMA, HIROSHI SHUTO, TATSUO YOKOI .....	369
Adaptive boost molecular dynamics method for study of rare events in plastic deformation: NAOMCHI TSUJI, AKIO ISHII, JUNPING DU, SHIGENOBU OGATA .....	370
Quantitative evaluation of dislocation nucleation as thermal activation process via atomistic simulations: MASAYUKI URANAGASE, RYOSUKE MATSUMOTO .....	371

### Poster Topic B: Mechanical behavior

Residual stress evaluation of shot peened Ag-based contact materials via diffraction technique: SEUNG-YUB LEE, JINGJING LING, HYO-SOO LEE, MIN-HA LEE .....	373
Structural phase states and residual stresses in the Ta/TiNi surface layers before and after high-current pulsed electron beam impact. L.L.MEISNER, M.G.OSTAPENKO, M.A.ZAKHAROVA, E.YU.GUDIMOVA .....	373
The effect of residual stresses on the change of the B2 phase lattice parameter in the NiTi with Tantalum coating after pulsed electron-beam treatment: M.G. OSTAPENKO, L.L. MEISNER, M.A. ZAKHAROVA, E.YU. GUDIMOVA.....	374
Laser assisted residual stress determination in ceramic coatings: PETER WEIDMANN, GIANCARLO PEDRINI, VENANCIO MARTÍNEZ-GARCÍA, ULRICH WEBER, ANDREAS KILLINGER, MARTIN WENZELBURGER, SIEGFRIED SCHMAUDER, RAINER GADOW, WOLFGANG OSTEN .....	375

### Poster Topic C: Cyclic deformation behavior, crack initiation & crack growth of metals

Fatigue crack initiation from notches and mean stress effect in 2024 T351 Al-alloy: MUSTAPHA BENACHOUR, NADJIA BENACHOUR, MOHAMED BENGUEDJAB .....	377
Resonant acoustic for nondestructive inspection of accumulated damage assessment in austenitic stainless steel subjected to fatigue tests in rotating bending: RICARDO A. CASALI, MARIA A. CARAVACA, CESAR G. VEROLI, GABRIEL VALLEJOS, JORGE FORTE .....	377
Determination of the Critical Resolved Shear Stress in a NiAl-Cr composite by Discrete Dislocation Dynamics: HERVE GAKAM, DANIEL WEYGAND .....	378
Cyclic softening in the MA956 ODS steel:IVO KUBENA,JAROSLAV POLÁK, TOMÁŠ KRUML .....	378
Influence of pre-strain on fatigue crack growth behavior in rolled AZ31 magnesium alloy: RYOICHI MOMOE, SHIGEKI MORITA, TSUYOSHI MAYAMA, NOBUSUKE HATTORI .....	379
Anisotropy of cyclic deformation and fatigue properties in rolled AZ31 magnesium alloy: SHIGEKI MORITA, RYOTA IKEDA, TSUYOSHI MAYAMA, NOBUSUKE HATTORI.....	380
Fatigue properties of fine-grained AZ31 magnesium alloy: YUJI OKAMOTO, TAKAHITO HORI,SHIGEKI MORITA, HIDETOSHI SOMEKAWA, TSUYOSHI MAYAMA, NOBUSUKE HATTORI.....	381
Dwell effects on low cycle fatigue behaviour of diffusion coated nickel base superalloy IN 713LC at temperature of 800°C: IVO ŠULÁK, KAREL OBRTLÍK, SIMONA HUTAŘOVÁ, MARTIN JULIŠ, TOMÁŠ PODRÁBSKÝ, LADISLAV ČEKLKO .....	382

### Poster Topic D: In-situ microscopy and diffraction

Strain induced martensitic Transformation in Austempered Ductile Iron (ADI): XIAOHU LI, PATRICK SAAL, MICHAEL HOFMANN , MARKUS HÖLZEL.....	384
An in situ experimental method for evaluating the tensile property of single crystalline gold nanorod: YABIN YAN, XIAOYUAN WANG, TAKASHI SUMIGAWA, TAKUYA NAKANO, TAKAYUKI KITAMURA.....	384

### Poster Topic E: Size effects and small-scale mechanical behavior of materials

Indentation Size Effect of Nanoporous Gold: Correlated by Unique Structure and its Size-Dependent Mechanical Behavior: SEUNG-MIN AHN, YOUNG-CHEON KIM, AND JU-YOUNG KIM .....	387
---	-----

High temperature nanoindentation - Dynamic measurements for thin film analysis: DENNIS BEDORF, MARTIN KNEIPS, WOLFGANG STEIN.....	387
Ductility in cold-rolled ultrafine-grained (UFG) tungsten (W): Correlation between microstructure and mechanical properties: SIMON BONK, JENS REISER, JAN HOFFMANN, MICHAEL RIETH .....	388
Fabrication of Al-Cu Composite Reinforced with BN by Powder Liquid-Phase Forging: CUNGUANG CHEN, LEICHEN GUO, WENWEN WANG, JI LUO, ZHIMENG GUO .....	389
Mechanical response of nanoporous gold made from Au-Ag precursor alloys with different initial microstructure: EUN-JI GWAK, YOUNG-CHEON KIM, JU-YOUNG KIM .....	389
Simulation of mechanical properties of nanotwin-strengthened metals: H. HOSSEINI-TOUDESHPY, M. YADOLLAPOUR.....	390
Nanotubular ZnO for flexible gas sensor: NA-RI KANG, JU-YOUNG KIM.....	391
Improved elasticity of bilayer graphene cantilevers with interlayer shear and in-plane extension effects: ABED MOHEB SHAH DIN, AMIN FARROKHABADI .....	391
Fracture of brittle spheres in compression: testing microscopic fused quartz: VACLAV PEJCHAL, GORAN ŽAGAR, DENIS LANG, MARTA FORNABAIO, ANDREAS MORTENSEN .....	392
How to optimize the fatigue properties of bimodal microstructures of nanocrystalline (nc) and ultrafine grained (ufg) Nickel?: DOMINIC RATHMANN, MICHAEL MARX, CHRISTIAN MOTZ.....	393
Surface oxidation of metallic glass surfaces and its effect on nanotribology: K. RITTGEN, A. CARON, R. BENNEWITZ .....	393
Investigation of mechanical anisotropy in Mg using Berkovich indentation. JULIAN E. C. SABISCH, ERICA T. LILLEODDEN.....	394
Size- and phase-dependent mechanical properties of ultra- thin silicon and Ge <sub>2</sub> Sb <sub>2</sub> Te <sub>5</sub> films: FRANZISKA SCHLICH, RALPH SPOLENAK.....	395
Compression-shear behavior of a strongly textured Magnesium alloy AZ31 under different strain rates: SEBASTIAN SEIPP, SHIBAYAN ROY, BENJAMIN ZILLMANN, MARTIN F.-X. WAGNER .....	395
Roughness behaviour of nanomaterials: SAYAH TAHAR, BOUTI SAMIR .....	396
Electronic properties and mechanical stability of ZnO in the bulk and nanowire structures under large uniaxial stresses: LUCY A. VALDEZ, RICARDO A.CASALI.....	397
First-principles study on ferroelectricity and its coupling behavior with mechanical deformation of ultrathin PbTiO <sub>3</sub> nanotube: XIAOYUAN WANG, TAKAHIRO SHIMADA, TAKAYUKI KITAMURA.....	398
Thickness-dependent tensile properties of PEDOT:PSS: O BAE WOO, JU-YOUNG KIM .....	398

## Poster Topic F: Advanced steels and steel composite materials

Effect of filler metal on micro-structural, mechanical and corrosion behavior of austenitic stainless steel weldment 316L: A. SRIBA, K. M. REHOUMA, S.E. AMARA, N. MADAOUI.....	400
---	-----

## Poster Topic G: Fracture mechanics

Estimation of Fracture Toughness of Metallic Materials Using Instrumented Indentation Test: JUN-YEONG KIM, WOJOO KIM, SEUNG-HUN CHOI, DONGIL KWON .....	402
The experimental study of stress-strain states in stress concentrators with the use of the method of digital image correlation: ELENA M. SPASKOVA, EVGENIY V. LOMAKIN .....	402
Methods of Stochastic Mechanics for Characterisation of Microstructural Failure in Heterogeneous Materials: MIKHAIL TASHKINOV, NATALIA MIKHAILOVA.....	403
The complex experimental studies of the mechanical properties of reinforcing elements: MARIA S. TEMEROVA, VALERIY E. VILDEMAN, EVGENIY V. LOMAKIN .....	404
Shock loading direction effects on ejection mass and particle sizes of micro-jet from a grooved metal surface: SHI YI-NA, QIN CHENG-SEN .....	404

## Poster Topic H: Materials for fission and fusion

XRD examination of oxide dispersion strengthened steels irradiated by swift heavy ions: ANDREI BENEDIKTOVITCH, VLADIMIR UGLOV, SVETLANA VLASENKO, TATIANA ULYANENKOVA, ALEXANDER SOHATSKY, JACQUES O'CONNELL, VLADIMIR SKURATOV .....	407
Creep and anelasticity of ferritic ODS steel MA956: JOSÉ RODOLPHO DE OLIVEIRA LEO, AMIR SHIRZADI, JAN KOWAL, MICHAEL E. FITZPATRICK.....	407
Application of Automated Ball Indentation Innovative Technique on the Determination of Mechanical Properties of Nuclear Structural Materials: JAN ŠTEFAN, RADIM KOPŘIVA, JAN SIEGL .....	408
Radiation stability of ZrSiN system under the Xe ions irradiation: VLADIMIR UGLOV, VITALI SHYMANSKI, GREGORY ABADIAS, GENNAGY REMNEV, ANDREY SUVALOV .....	409

## Poster Topic I: High temperature materials

Atomistic Simulations of Dislocation-Interface Interactions in the $\gamma/\gamma'$ Microstructure in Ni-base Superalloys: FREDERIC HOULLE, JUAN WANG, JULIEN GUENOLE, JOHANNES J. MÖLLER, ARUNA PRAKASH, ERIK BITZEK .....	411
Internal Friction and Shear Modulus Temperature Dependence of 9%Cr Ferritic Steel P92 in 25 ÷750°C Temperature Range: ELGUJA KUTELIA, GEORGE DARSVELIDZE, TENGIZ KUKAVA, TEMUR DZIGRASHVILI, IA KURASHVILI, FRANCISCO J. PEREZ TRUJILLO .....	412

## Poster Topic K: Polymer based composites

Research of the Processing Parameters of Three-dimensional Printer and the Product: KUNIHIRO ARAKI, GOSHI HAMABE, TATSUYA TANAKA, YOSHIHIKO ARAO .....	414
Supervised Estimation of the Local Glass Fiber Content from 2D X-ray Imaging of Plate-like Parts made from Sheet Molding Compounds: BENJAMIN BERTRAM, KAY ANDRÉ WEIDENMANN .....	414
Deformation and fracture of aircraft fibrous polymer composites in external actuating factors and high temperature mechanical tests: DMITRII S. LOBANOV, VALERIY E. WILDEMAN, EVGENIY V. LOMAKIN.....	415
Numerical simulation for developing grounds in support of application of fiber optic sensors for monitoring of composite materials: VALERY P. MATVEENKO, GRIGORIY S. SEROVAEV, VALERY, V. KOREPANOV, NATALIA A. YURLOVA, ALEKSANDR N. ANOSHKIN, ANATOLIY A. TASHKINOV, GLEB S. SHIPUNOV, VALERIY Y. ZUYKO .....	416

## Poster Topic L: Lightweight alloys and structures

Ab-initio coarse-grained approach for modeling the two-dimensional packing structure of solute nanoclusters in Mg-based LPSO phases: HAJIME KIMIZUKA, SHIGENOBU OGATA.....	419
Surface Nitriding of Titanium Using Atmospheric-controlled IH-FPP Treatment. OTA SHUMPEI, MURAI KAZUE, OMIYA MSAKI, KOMOTORI JUN, FUKAZAWA KENGO, MISAKA YOSHITAKA, KAWASAKI KAZUHIRO .....	420

## Poster Topic X: General mechanical behavior

Thermal ageing effect on mechanical behavior of polycarbonate: HAMID BBABOU, FERHOUM RABAH, MEZIANE ABERKANE .....	422
Effect of Ultra-violet radiation on the mechanical behavior of PMMA (polymethyl methacrylate): AMIRAT BOUKHALFA, FERHOUM RABAH .....	422
Dynamic Mechanical Properties of Cortical Bone Depend on Bone Mineral Content: ZUDE FENG, TING WANG.....	423
Study of concretes and mortars made with metallic fibers: SOUAD KHERBACHE, KARIM MOUSSACEB, NEDJIMA BOUZIDI, A. KADER TAHAKOURT .....	424
Effect of Strain-Rate on Tensile Properties of Nuclear Piping Materials at RT and 316oC. JIN WEON KIM, MYUNG RAK CHOI .....	424

Variation of Mechanical Properties in the Pipe Bends Fabricated by High-frequency Induction Bending:  
JIN WEON KIM, MI YEON LEE, YOUNG JIN OH, HEUNG BAE PARK, KYUNG SU KIM, TAE SOON KIM..... 425

Modeling and observation of compressive behaviors of anisotropic aluminum cellular structures based  
on the Voronoi tessellation concept: SANG-YOUN PARK, BYOUNG-HO CHOI, SEUNG KI MOON, IL-HYUK AHN ..... 426

Influence of the addition of cooked and crushed clay on the mechanical strength of a self-compacting  
concrete: FATIHA SOUDI, NASSER CHELOUAH, TIZIRI BEZZI ..... 427

Retained Austenite: Non Destructive Analysis by using X-Ray according to ASTM 975-03: M. MICHIEL  
VAN DER MEY ..... 428

# Plenary Talks

---

# The treatment of residual stresses in fracture mechanics calculations

BOB AINSWORTH

The University of Manchester, Manchester, UK

Fitness-for-purpose assessments of engineering components are required in order to demonstrate defect tolerance and the ability to continue to operate safely (Zerbst et al 2003). Such assessments are particularly required for welded regions as these are susceptible to flaws and contain residual stresses which may contribute to structural failure (Zerbst et al 2014). The assessments need inputs from both stress analysis and materials properties.

For the stress analysis, loadings can be both primary, such as pressure and dead-weight, and secondary, such as the residual stresses at weldments. In the elastic region, primary and secondary stresses are simply added linearly to calculate the total stress intensity factor. However, the relative contributions of the primary and secondary loads to the total crack driving force change during the loading sequence as plasticity develops. In particular, the secondary stress becomes much less significant when gross yielding occurs (Ainsworth 1986a). However, if the crack tip plastic zone remains surrounded by elastic material at high remote stresses this can lead to an increase in the contribution of the secondary stresses to the crack driving force (Ainsworth 2012). Such cases are referred to as exhibiting elastic follow-up. This paper describes how the contribution of secondary stresses can be included in fitness-for-purpose assessments, including recent developments which allow the treatment of cases exhibiting elastic follow-up.

Weldments are not only regions of high residual stresses but are also often regions of low fracture toughness properties. The paper therefore also addresses the fracture toughness input to fitness-for-purpose assessments and specifically how this may be influenced by

the prior plastic straining which occurs either during the welding process or as a result of subsequent loading, such as during pre-service proof loading. Consideration is limited to the influence of prestrain on ductile fracture. Both uniform plastic straining (Ainsworth 1986b) and recent studies on highly non-uniform straining, such as occurs if a defect is present during the proof loading for example, are addressed. It is shown that non-uniform prestrain may significantly complicate the measurement of representative fracture toughness values.

## References

- Ainsworth, R. A. (1986a): The treatment of thermal and residual stresses in fracture assessments. *Engng Fract Mech* 24, 65-76.
- Ainsworth, R. A. (1986b): An assessment of the effects of prestrain on upper shelf fracture toughness. *J Strain Analysis* 21, 219-223.
- Zerbst, U., Schwalbe, K.-H. & Ainsworth, R. A. (2003): An overview of failure assessment methods in codes and standards. Chapter 7.01 in *Comprehensive Structural Integrity* (Eds I Milne, R O Ritchie, B Karihaloo), Elsevier, Oxford.
- Ainsworth, R. A. (2012): Consideration of elastic follow-up in the treatment of combined primary and secondary stresses in fracture assessments. *Engng Fract Mech* 96, 558-569.
- Zerbst, U., Ainsworth, R. A., Beier, H.-TH., Pisarski, H., Zhang, Z.L., Nikbin, K., Nitschke-Pagel, T., Münstermann, S., Kucharczyk, P. & Klingbeil, D. (2014): Review on fracture and crack propagation in weldments – a fracture mechanics perspective. *Engng Fract Mech* 132, 200-276.

## X-Mechanics for Metal Plasticity

W. A. CURTIN

Institute of Mechanical Engineering, Ecole Polytechnique Federale de Lausanne, Switzerland

The application of X-Mechanics (X= quantum, atomistic, statistical, dislocation, mesoscale, and continuum) to elucidate the mechanistic origins of plasticity phenomena is emerging as a powerful paradigm for predictive metallurgy. In particular, the structure of dislocations and the interactions of dislocations with solutes, precipitates, other dislocations, and grain boundaries,

requires application of X-Mechanics for both qualitative and quantitative models of plastic flow as a function of alloying, temperature, strain-rate, grain size, and including size effects in plasticity.

Here, we start with a brief overview of recent work at the quantum, atomistic, and statistical scales aimed at quantitative prediction of yield strength in Al and Mg

alloys. The onset of macroscopic plastic flow can be predicted without recourse to higher-level modeling. Such studies also provide “inputs” to higher-level models, and can guide the formal structure of such models. We then move to mesoscale dislocation dynamics in 2d plane strain, but in the presence of pinning obstacles typical of metal alloys. We present a new concept, “stress gradient plasticity”, that emerges naturally from the analysis of dislocation pile-ups under a spatial stress gradient.<sup>1</sup> The analysis shows that the spacing between pinning obstacles is a material length scale that can give rise to size-scale effects in the presence of stress gradients. Discrete dislocation models clearly demonstrate the stress gradient plasticity phenomenon and the role of obstacle spacing. “Stress gradient plasticity” is then implanted within a low-order continuum plasticity framework and is shown to predict size effects in bending, torsion, indentation, and void expansion. The model is applied to explain experimental size effects – both strengthening and hardening – in recent bending and torsion experiments in pure polycrystalline metals.

We have recently extended the 2d mesoscale dislocation dynamics models to include elements of 3d “forest hardening” and, thus, strain hardening phenomena. This yields model systems with tunable yield strength and work-hardening, to enable study of the interplay of these mechanisms in mesoscale deformation. However, this method will not be discussed in detail in this talk.

We conclude with discussion on how to bridge between the smaller- and larger-scale X-Mechanics methods. The key issue is whether smaller-scale X-Mechanics simply provides inputs into existing higher-scale X-Mechanics models or provides guidance for entirely new higher-scale X-Mechanics models.

#### References

Chakravarthy, S.S. & Curtin, W. A. (2011): Proc. Natl. Acad. Sci. 108, 15716-15720.

## Materials for ultra high-temperature applications

HARUYUKI INUI, KYOSUKE KISHIDA, NORIHIKO L. OKAMOTO

Kyoto University, Kyoto, Japan

There are various applications for structural materials used at high and ultra-high temperatures. Of these applications, turbines for land-based power generation and aircraft jet engines may be one of the typical examples. For these applications, there is an ever-increasing demand for efficiency improvement, in order to reduce fuel consumption and CO<sub>2</sub> gas emission. The efficiency of a gas turbine combined cycle power plant can be improved by increasing the turbine inlet temperature. There is, therefore, a very strong demand for structural materials that can withstand for these very high temperatures. The turbine inlet temperature has increased year by year so that gas inlet temperature is always higher than the temperature capability of material, indicating that the materials cooling is essential. Material cooling usually leads to the efficiency loss of a combined cycle engines by a few to several %. So, materials that can be used without cooling is badly desired. New high-temperature materials that can withstand very high temperatures exceeding the upper limit of Ni-base superalloys are strongly demanded. Generally speaking, high strength and high toughness is a primary concern as the properties required for high-temperature structural materials, although these two are in the pay-off relation. Light weight is sometimes very important especially when used in a rotating part, since the centrifugal force is proportional to the weight. High oxidation resistance is another pri-

mary concern. The material should not lose the body by oxidation in a severe oxidizing environment at very high temperatures. That means the material should form protective oxide scales during oxidation. When judged from the so-called Ellingham diagram, Al and Si are known to readily form thermodynamically very stable oxides with a slow growth rate. This means that alumina and silica can be a protective oxide scale and that the material of our concern should contain either Al or Si in a good quantity for better oxidation resistance. On top of that, the material should have some dislocation activity to achieve some allowable value of toughness. Dislocation properties are obviously influenced by the lattice periodicity, as Peierls evaluated the stress required for dislocation to overcome the potential barrier a long time ago. The lower Peierls stress may lead to a higher dislocation mobility, and hence the higher fracture toughness. Then, simple crystal structures are naturally beneficial to high dislocation mobility, and hence the higher fracture toughness. In that sense, intermetallics with superlattices based on either FCC, BCC or HCP structures, especially aluminides and silicides formed with transition-metal can be strong candidates.

In the presentation, the current status for the development of high-temperature structural silicide and aluminides will be reviewed, after the introduction to high-temperature structural materials.

# Materials Innovation for Nuclear Energy - Super ODS Steels R&D

AKIHIKO KIMURA<sup>1\*</sup>, WENTUO HAN<sup>1</sup>, HWANIL JE<sup>2</sup>, YOOSUNG HA<sup>2</sup>, HIROYUKI NOTO<sup>2</sup>, DONGSHENG CHEN<sup>2</sup>, NORIYUKI IWATA<sup>1</sup>, RYUTA KASADA<sup>1</sup>, TAKANARI OKUDA<sup>3</sup>, SHIHEHARU UKAI<sup>4</sup>, MASAYUKI INOUE<sup>5</sup>, PENG DOU<sup>6</sup>, SANGHOON NOH<sup>7</sup>

<sup>1</sup> Institute of Advanced Energy, Kyoto University, Kyoto, Japan

<sup>2</sup> Graduate School of Energy Science, Kyoto University, Kyoto, Japan

<sup>3</sup> KOBELCO Research Institute, Kobe, Japan

<sup>4</sup> Hokkaido University, Sapporo, Japan

<sup>5</sup> Japan Atomic Energy Agency, Tokaimura, Ibaragi, Japan

<sup>6</sup> Chongqing University, Chongqing, China

<sup>7</sup> Korea Atomic Energy Research Institute, Daejeon, Korea

Materials development is essential for realization of advanced nuclear fission reactors as well as fusion DEMO reactors and beyond. High performance structural materials R&D has been conducted for the last several decades and there have been made some remarkable technology innovations of nuclear structural materials [1].

Among the candidate nuclear and blanket structural materials, oxide dispersion strengthened (ODS) steels, which have been produced by means of “mechanical alloying”, are considered to be promising for advanced nuclear systems with high thermal efficiency, because the ODS steels have high-strength at elevated temperatures and good resistance to corrosion and irradiation degradation. The operation temperature can be elevated up to 700 °C. Radiation tolerance was considerably improved by a dispersion of nano-scaled oxide particles.

There are several sorts of ODS steels with different Cr contents: (9-12)Cr-ODS ferritic/martensitic steels [2] and (14-16)Cr-ODS ferritic steels with and without Al addition [3]. The former two groups of ODS steels were developed for application to sodium cooled fast reactors and fusion reactors, and the last group of ODS steels were for so-called Generation IV fission nuclear reactors. More recently, accident tolerant fuel R&D is progressing to apply high Cr-high Al ferritic steels to fuel cladding of light water reactor because of “Fukushima Incident”. It has been considered that the replacement of Zirconium alloys cladding with high-performance ferritic steels cladding may retard the hydrogen generation at a severer accident (SA) of nuclear reactors, resulting in a large time lag up to hydrogen explosion. High performance of ODS steels stems from the fine nano-scaled oxide particle dispersion. Dispersion morphology of the oxide particles, such as size, number density, chemical compositions and coherency between matrix and particles, are characterized by FE-

TEM/EDS observations, high temperature XRD measurements and analyses by FE-EPMA and FE-AES. Chemical compositions of the main particles in Al-added ODS steel were influenced by addition of small amount of Zr, which resulted in the formation of (Y, Zr) oxide particles rather than (Y, Al) oxide particles. The size and the number density of Zr-added steel was reduced and increased, respectively. The coherency of the (Zr, Y) oxide particles depended on the size of the particle. Characteristic features of the oxide particles in strengthening mechanism is summarized for the ODS steels.

In this presentation, current status of ODS steels R&D in Japan is also summarized and the impacts of some material innovations on the safety issue of nuclear technologies are addressed. Radiation tolerance mechanism of advanced ferritic steels is introduced in terms of trapping capacity for radiation defects caused by nano-scaled ultra-fine oxide particles dispersion. Furthermore, the recent experimental results on mechanical properties at elevated temperatures, corrosion behavior in SCW and LBE and phase stability under ion irradiation of ODS steel are shown to demonstrate that the ODS steels with nano-scaled oxide particles in high number density are promising for the fuel cladding material of next generation nuclear systems.

## References

- [1] A. Kimura, R. Kasada, N. Iwata, H. Kishimoto, T. Okuda, M. Inoue, S. Ukai, T. Fujisawa, T.F. Abe et al., (2011): *J. Nucl. Mater.* 417, p176-179.
- [2] S. Ukai, T. Nishida, H. Okada, T. Okuda, M. Fujiwara and K. Asabe, (1997): *J. Nucl. Sci. Technol.*, 34[3], p256.
- [3] A. Kimura, S. Ukai and M. Fujiwara, (2003): *Proc. Int. Conf. On Global Environment and Advanced Nuclear Power Plants, (GENES4/ ANP2003)* ISBN: 4-901332-01-5, CD-ROM file, p. 1198.

## Tensile and fatigue behavior of steels in high pressure hydrogen gas atmospheres

HISAO MATSUNAGA<sup>1, 2, 3</sup>, JUNICHIRO YAMABE<sup>2, 3, 4</sup>, SABURO MATSUOKA<sup>2</sup>

<sup>1</sup>Department of Mechanical Engineering, Kyushu University, Fukuoka, Japan

<sup>2</sup>Research Center for Hydrogen Industrial Use and Storage (HYDROGENIUS), Kyushu University, Fukuoka, Japan

<sup>3</sup>International Institute for Carbon-Neutral Energy Research (I2CNER), Kyushu University, Fukuoka, Japan

<sup>4</sup>International Research Center for Hydrogen Energy, Kyushu University, Fukuoka, Japan

In preparation for the forthcoming commercialization and subsequent world-wide adoption of fuel-cell vehicles and hydrogen stations, a specialized set of components (e.g., vessels, valves, regulators and metering devices) is being developed for the handling of high-pressure hydrogen gas. The degree of susceptibility of materials to hydrogen embrittlement (HE) greatly influences their possible selection and qualification for use with high-pressure hydrogen gas. This is because HE is a potentially dangerous phenomenon known to be dependent on various factors such as material type, hydrogen gas pressure, temperature and loading conditions.

NASA categorized numerous metallic materials into four specific grades according to their individual susceptibility to high-pressure hydrogen (NASA 2005). For instance, austenitic stainless steels with FCC structure (e.g., types 316, 310 and 304ELC) are categorized in the guidelines as being “negligibly-embrittled” or “slightly-embrittled” and, therefore, are widely used for various components exposed to hydrogen gas. On the other hand, martensitic and ferrite-pearlite steels with BCT/BCC structure (e.g., AISI 1042 and AISI 1020) are categorized as being “severely-embrittled” or “extremely-embrittled”, due to such a high degree of susceptibility. Therefore, the use of BCT/BCC steels in high-pressure hydrogen gas environments is highly restricted under current regulations and standards. However, with the widespread commercialization of hydrogen energy systems, BCT/BCC steels are also likely to be used extensively for hydrogen service so as to reduce production costs.

In this study, the following tests were conducted on a variety of steels; austenitic stainless steels with various austenitic stabilities, a quenched-and-tempered Cr-Mo steel and an annealed carbon steel, in high-pressure hydrogen gas up to 115 MPa.

1. Slow strain rate tensile (SSRT) tests
2. Tension-compression fatigue tests using smooth specimens
3. Fatigue crack growth tests using compact tension (CT) specimens

The experimental results manifest the susceptibility of the strength properties of these steels to high-pressure hydrogen gas, as well as the microscopic mechanism of degradation associated with hydrogen-enhanced crack growth. Finally, simple requirements are proposed for the qualification of metallic materials used under *design by rule* (fatigue limit design) and *design by analysis* (fatigue life design) for hydrogen service.

### Reference

National Aeronautics and Space Administration. (2005): Safety standard for hydrogen and hydrogen systems, NSS 1740.16.

### Acknowledgements

This work was supported by the New Energy and Industrial Technology Development Organization (NEDO), Fundamental Research Project on Advanced Hydrogen Science (2006 ~ 2012) and Hydrogen Utilization Technology (2013 ~ 2018).

## Deformation, Fatigue, and Fracture of Ultrafine Grained and Nanocrystalline Materials

A. HOHENWARTER<sup>2</sup>, T. LEITNER<sup>2</sup>, O. RENK<sup>1</sup>, C. B. YANG, M. KAPP<sup>1</sup>, L. KRÄMER<sup>1</sup>, P. GUPTA<sup>1</sup>, V. MAIER<sup>1</sup>, R. PIPPAN<sup>1,2</sup>,

<sup>1</sup> Erich Schmid Institute of Austrian Academy of Sciences and

<sup>2</sup> Department of Material Physics University Leoben, Austria

Tensile, fatigue and fracture mechanics properties of nanocrystalline materials are rare, because the available material volume is usually very small. Severe plastic deformation (SPD) is a new method to produce ultrafine grained or nanocrystalline materials in larger

quantities. This enables us to determine the fatigue properties, ductility and fracture toughness of these types of materials. High pressure torsion allows SPD of most metallic materials. Hence, it allows to transform the typical microcrystalline materials to an ultrafine or

nanocrystalline state. The large HPT equipment at our institute permits now to determine standard tension and fracture mechanic tests on a large variety of metals and alloys. The paper will give an overview of the ob-

tained results in pure metals, alloys, and nanocomposites. Special attention will be devoted to the developed anisotropy of the fracture toughness, which is in some materials extremely pronounced.

## Damage Tolerance in Natural and Bioinspired Structural Materials

ROBERT O. RITCHIE<sup>1,2</sup>

<sup>1</sup>University of California, Berkeley, CA, USA

<sup>2</sup>Lawrence Berkeley National Laboratory, CA, USA

The attainment of both strength and toughness, *i.e.*, damage tolerance, is invariably a vital requirement for structural materials; unfortunately in many material classes these properties can be mutually exclusive (Ritchie 2011). Accordingly, the development of damage-tolerant engineering materials has traditionally been a compromise between hardness vs. ductility.

Natural materials often display excellent strength and toughness (in relative terms) even though they are synthesized at ambient temperatures from a fairly limited palette of constituents, often with relatively meagre properties. Nature's structures, however, usually comprise both hard and soft phases arranged in complex hierarchical composite architectures, with characteristic dimensions spanning from the nanoscale to the macroscale. The result can be materials that are lightweight and often multi-functional, which can display unique combinations of mechanical properties that are generally far superior to those of their constituents, but are difficult to replicate synthetically (Wegst et al. 2015).

In this work, we seek the inspiration of biology to discern strategies for the development of new engineering structural materials with enhanced damage tolerance. We focus on the interplay between the individual nano/micro-mechanisms that contribute to strength and toughness, that of plasticity and crack-tip shielding, noting that these phenomena originate at very different structural length-scales – strength at the nano to micro scales, toughness primarily at the micro to macro scales. The lessons from Nature are particularly relevant as natural materials can display unusual combinations of properties that derive from these differing length-scales because of their multi-dimensional hierarchical architectures with precisely engineered interfaces. Our objective is that by mimicking these natural structural architectures, identifying the salient strengthening and toughening mechanisms over multiple length-scales, and most importantly finding ways to actually make these bioinspired materials in bulk form, that we can develop new lightweight structural materials where the strength vs. toughness “conflict” has been solved to achieve exceptional levels of damage-tolerance.

Here we focus on the mechanistic basis for the mechanical properties of several natural materials, namely bone, tooth dentin and nacre in seashells which are prime examples of natural materials that are truly damage-tolerant (Launey et al. 2011), fish scales which are designed as natural flexible dermal armors combining hard surface layers with a tough (and adaptable) subsurface region (Yang et al. 2013), and skin with its remarkable resistance to tearing and fracture. (Yang et al. 2015).

We further examine attempts to make synthetic composites in the image of such natural materials, though in general the large span in length-scales and overall complexity of most biological materials impose combinations of requirements and design motifs that make the development of new biomimetic materials generally well beyond the reach of present technologies. We do describe, however, several examples where one technique, freeze-casting has been used to make “compliant-phase” ceramic composites in the image of nacre with exceptional damage tolerance (Munch et al. 2008), although this and most of the other current processing techniques are still not feasible for large-scale materials production.

### References

- Launey M.E., Buehler M.J. & Ritchie R.O. (2011): On the mechanistic origins of toughness in bone. *Ann. Rev. Mater. Res.*, 40: 25-53.
- Munch E., Launey M.E., Asem D.H., Saiz E., Tomsia A.P. & Ritchie R.O. (2008): Tough bio-inspired hybrid materials. *Science*, 322: 1516-1520.
- Ritchie R.O. (2011): The conflicts between strength and toughness. *Nature Materials*, 10: 817-822.
- Wegst U.G.K., Bai H., Saiz E., Tomsia A.P. & Ritchie R.O. (2015): Bioinspired structural materials. *Nature Materials*, 14: 23-36.
- Yang W., Chen I.H., Gludovatz B., Zimmermann E., Ritchie R.O. & Meyers M.A. (2013): Natural flexible dermal armor. *Adv. Mater.*, 25: 31-48.
- Yang W., Sherman V.R., Gludovatz B., Schiavone E., Stewart P., Ritchie R.O. & Meyers M.A. (2015): Extraordinary tear resistance of skin. *Nature Comm.*, in press.

# TALKS

---

Talks Topic A1:

***Multiscale phenomena in plasticity***

# Atomistic Simulations as Bridge between Experiments and Mesoscale Models: a Case-Study on Dislocation-Precipitate Interactions in Ni-base Superalloys

ERIK BITZEK

Friedrich-Alexander-Universität Erlangen-Nürnberg (FAU), Department of Materials Science and Engineering, Germany

To study the mechanical properties of a specific material or class of materials, mesoscale models like dislocation dynamics (DD) or phase field simulations require quantitative information on the properties of the defects of interest. While some information like the shape and arrangement of precipitates are readily obtained by experiments, other properties like dislocation mobilities or interface energies require more involved experiments and analysis. Some material parameters like unstable stacking fault energies, however, can not be determined experimentally. Atomistic simulations, either based on density functional theory (DFT) or on semi-empirical potentials, are ideally suited to calculate many of these material parameters. Yet, the simulation setups used to study atomic scale deformation processes are in most cases highly idealized. While this is often necessary in order to quantitatively determine certain material properties, overly simplified or constricted setups might artificially suppress important deformation mechanisms.

Here we present an example of how using atom probe tomography (APT) data can lead to more realistic atomistic samples which show significantly different properties and deformation processes compared to the usually used simulation setups. The atom probe informed atomistic simulations in turn provide important insights and material parameters for DD models. The present example is centered on the study of dislocation processes in the  $\gamma/\gamma'$  microstructure of single crystalline Ni-base superalloys. The superior high-temperature mechanical properties of these superalloys is a direct consequence of this microstructure which consists of a high volume fraction of the cuboidal  $L1_2$  ordered  $\gamma'$ -phase that is precipitated in a disordered face-centered cubic  $\gamma$ -matrix. Such precipitate strengthened alloys are much stronger than the individual phases, and the strengthening effect is believed to mainly arise from the difficulty of channel dislocations in the  $\gamma$ -phase to cut into the  $\gamma'$ -precipitate.

A novel technique was developed to reconstruct an atomistic sample from an APT experiment on the alloy ERBO/1. The curvature of the reconstructed precipitate leads to the formation of a misfit dislocation network (MFDN), which is significantly different from the MFDN obtained for a planar interface. Unlike the constricted misfit dislocation cores obtained in the usual 2D setups, the misfit dislocations can dissociate, and the overall network structure is reminiscent of the interfacial dislocation network formed during the initial stages of creep, see e.g. (Agudo Jacome et al. 2013), and contains the same Burgers vectors and line directions. Simulations of the interaction of one and two  $60^\circ$  channel dislocations with the MFDN reveal typical processes also observed in experiments like the knitting out of dislocations from the MFDN and the cutting of the precipitate by a pair of channel dislocations. These results cannot be obtained with simulation setups that were previously used in the literature. As APT does not only provide information on the sample morphology but also on its chemical composition, the simulations were performed using stoichiometric Ni/Ni<sub>3</sub>Al as well as with representative local concentrations of Ni, Al and Re, thus allowing to assess the role of chemical composition on the dislocation – precipitate interactions. In addition to the qualitative information gleaned from the simulation on the reconstructed APT sample, quantitative information on dislocation mobility and the critical cutting stress necessary for dislocations to penetrate the  $\gamma'$ -phase was obtained on 2D samples with representative local chemical compositions and passed on to DD simulations.

## References

Agudo Jácome, L. et al. (2013) High-temperature and low-stress creep anisotropy of single-crystal superalloys. *Acta Mater.* 61, 2926–2943.

## Accelerated molecular dynamics study of grain boundary motion and dislocation nucleation from grain boundary

SHIGENOBU OGATA<sup>1,2</sup>, AKIO ISHII<sup>1</sup>, YUNJIANG WANG<sup>3</sup>, JUNPING DU<sup>1</sup>

<sup>1</sup>Osaka University, Osaka, Japan

<sup>2</sup>Kyoto University, Kyoto, Japan

<sup>3</sup>Chinese Academy of Sciences, Beijing, China

Grain boundary motion and dislocation nucleation from grain boundary are key deformation units to understand plastic deformation properties of nano-crystalline metals because of the less intra-grain dislocation activities in the nano-grains. Since these deformation units are atomistic scale events and consist of thermally-activated processes at finite temperature, we need to perform an atomistic simulation, like molecular dynamics (MD) simulation, at finite temperature to obtain atomistic, kinetic and energetic details of these events. However, it is difficult to find and analyze them at finite temperature and at usual experimental strain rates using conventional MD simulation method, because these are rare events in a typical MD time-scale. Recently, we have developed an accelerated MD simulation method (Ishii et al. 2012), that is called adaptive boost MD method, and we have applied this method to investigate a carbon diffusion (Ishii et al. 2012) and dislocation motion with solute atom (Ishii et al. 2013) in iron, and demonstrated that the adaptive boost MD method can successfully accelerate these rare events and provide atomistic event details, kinetics and energetics.

In this study, we applied this method to investigate the grain boundary motion and dislocation nucleation from a grain boundary. First we analyzed a behavior of several grain boundaries in copper crystal under shear strain along the grain boundaries. Actually grain boundary

motion was successfully accelerated, and we found a sharp mechanism transition from displacive to diffusive motions with increasing temperature in several grain boundaries, such as a sliding and migration coupled grain boundary motion at low temperatures less than ~500K and a decoupled motion above ~500K. The latter was mainly driven by local atomic diffusion in the grain boundary. We estimated temperature dependent activation volume of the grain boundary motion and found that the activation volume sharply changed at the mechanism transition temperature. Next, we applied this method to dislocation nucleation from grain boundary. Again, dislocation nucleation event from grain boundaries was successfully accelerated and observed in the MD simulation. Then, we analyzed temperature and stress dependent activation free energy and activation volume, and based on them, we also studied temperature and strain rate dependencies of a critical stress of the dislocation nucleation.

### References

- Ishii, A., Ogata, S., Kimizuka, H. & Li, J. (2012): Adaptive boost molecular dynamics simulation of carbon diffusion in iron, *Physical Review B*, 85-6, 064303.  
 Ishii, A., Li, J. & Ogata, S. (2013): "Conjugate channeling" effect in dislocation core diffusion: carbon transport in dislocated BCC iron, *PLoS ONE*, 8-4 (2013), e60586.

## Ab initio-based atomistic model simulation of deformation and fracture in SiC power device

YOSHITAKA UMENO<sup>1</sup>, ATSUSHI KUBO<sup>1</sup>, SHIJO NAGAO<sup>2</sup>

<sup>1</sup>Institute of Industrial Science, The University of Tokyo, Japan

<sup>2</sup>The Institute of Scientific and Industrial Research, Osaka University, Japan

SiC, which is semiconducting crystal having wider bandgap than that of Si, is one of the most promising materials for power semiconductor device. Major challenges toward application include cracking during manufacturing process due to thermal stress and stacking fault growth brought by migration of Shockley partial dislocations around PN junction in operation. It is therefore required to perform atomistic model sim-

ulations to reveal the mechanism behind such deformation.

In fact, there have been some studies on the deformation in SiC using atomistic model simulation such as molecular dynamics. However, interatomic potentials suggested thus far for SiC were constructed without taking into account the strong anisotropy of the crystal strength and the effect of multiaxial loading condi-

tions. To perform reliable atomistic-model simulations, it is necessary to construct an interatomic potential that can describe such aspects.

In this study, we firstly performed ab initio density functional theory (DFT) calculations to obtain ideal shear and tensile strength of SiC to develop an interatomic potential function based on the obtained DFT data. Then, we carried out molecular dynamics simulations of deformation of SiC crystal under mechanical loading using the developed interatomic potential.

We employed the Angular-Dependent Potential (ADP) model for the interatomic potential function. An additional term for pairwise interaction is included in the model to describe the Coulomb interaction, which should play an important role in SiC. Potential parameters are fitted using the Force-Matching method for better transferability. The developed potential can successfully reproduce the ideal strength, the effect of superimposed multiaxial loading on the strength and phase transition under compression.

Our molecular dynamics simulations of tension of thin film models of 3C-SiC and 4H-SiC showed that different deformation modes appear in the two models because the crystallographic plane that possesses the lowest strength against tension, (0001) in 4H and (111)

in 3C, has different arrangement according to the crystal structure. Our simulations also demonstrated that both cleavage and slip can occur at the atomistic scale although SiC is macroscopically brittle.

An analysis of shear deformation of a model containing Shockley partial dislocations revealed that electric environment can alter the mobility of the two kinds of dislocation core (Si- and C-cores). When negatively charged, the order of their mobilities can be reversed. This result explains the contradiction between a calculation with the Tight-Binding method (where C-core moved) and an experimental observation (where Si-core moved) and provides an important insight to the mechanism of expansion of stacking faults under electric current.

This work was supported in part by the Network Joint Research Center for Materials and Devices.

#### References

- Y. Mishin *et al.*, *Acta Mater.* **53**.15 4029 (2005).  
 F. Ercolessi *et al.*, *Europhys. Lett.* **26**.8 583 (1994).  
 A. T. Blumenau *et al.*, *J. Phys.: Condens. Matter* **14**.48 12741 (2002).  
 M. Skowronski and S. Ha, *J. Appl. Phys.* **99**.1 011101 (2006).

## Research on constitutive model of nickel-based superalloy and the numerical simulation during superalloy blade cold rolling process

XIANGWEI KONG<sup>1</sup>, WENRAN GENG<sup>2</sup>, CHUNLIN QIU<sup>3</sup>

<sup>1</sup> School of Mechanical Engineering and Automation, Northeastern University, Shenyang, China

<sup>2</sup> CFHI Dalian International Tech & Trade Co. Ltd., Dalian, Liaoning Province, China

<sup>3</sup> State Key of Laboratory of Rolling Technology and Automation, Northeastern University, Shenyang, China

In recent years, cold rolling as a new technology has been widely applied in the field of aviation blade manufacture because it has many advantages, such as stable working process, small equipment tonnage, fine work-piece mechanical properties and high production efficiency (Chaboche 2008). However, very few researches are focused on the blade rolling process because of the complexity of blade shape and the difficult-to-deformation of blade superalloys. The control of technical schedule and mould shape of blade rolling process is totally dependence on the experiences. The blade polishing method and mould adjustment also mainly depend on the manual operation. Under such condition the production efficiency and the product quality are not guaranteed. Therefore, the material flow behavior and forming mechanism of blade rolling process should be further investigated to optimize the design of mould and the selection of technical parameters. In this working, the constitutive model of superalloy was established according to the flow stress of materials.

Then, the numerical simulation of blade rolling process was implemented using the software DEFORM-3D embedded with the established constitutive model.

In order to describe severe plastic deformation accurately, the Yoshida-Uemori constitutive model (Yoshida 2002 and 2003) was employed in our study. The mechanical properties of nickel-based superalloy GH4169 was performed under different conditions at ambient temperature to obtain the material parameters of the constitutive model. The secondary development of DEFORM is carried out using the established constitutive model of GH4169. Comparing the numerical simulation results with the results of cuboid compression test, the maximum error is lower than 1.1% for the GH4169. This verifies that the new constitutive model for GH4169 is suitable for simulating the blade rolling process. The flow rule of blade metal during the process is that the forward and back slip zones is not homogeneous along the transverse direction of blade.

This work exhibits a new idea for the study on the form-

ing law, the optimization of moulds and the selection of technique parameters during variable cross-section rolling process.

#### References

Chacoche J.L. (2008): A Review of Some Plasticity and Viscoplasticity Constitutive Theories, *International Journal of Plasticity*, 24: 1642-1693; Troyes.

Yoshida F., Uemori, T.(2002): A model of large-strain cyclic plasticity describing the Bauschinger effect and workhardening stagnation, *International Journal of Plasticity*, 18: 661-686; Hiroshima  
Yoshida F, Uemori T. (2003): A model of large-strain cyclic plasticity and its application to springback simulation, *International Journal of Mechanical Sciences*, 45:1687-1702; Hiroshima.

## Development of Mechanism-Based and Microstructure-Sensitive Modeling Approach to Plastic Deformation in Multi-Phase Alloys

DUCHAO LV, PENGYANG ZHAO, DON MCALLISTER, STEPHEN NIEZGODA, MICHAEL MILLS, YUNZHI WANG

Department of Materials Science and Engineering, The Ohio State University, Columbus, Ohio, USA

The key to predicting, and therefore optimizing, properties of materials is the knowledge of the state of microstructure. Figure 1 shows a typical example of dramatic change in creep mechanism from dislocation-based creep in the bore region to the remarkable microtwinning process in the rim region observed in an ME3 turbine disk for identical deformation conditions (Kovarik2009). The sensitivity of creep response to subtle changes in microstructure and the need for location-specific microstructure optimization in a turbine disk are quite obvious.

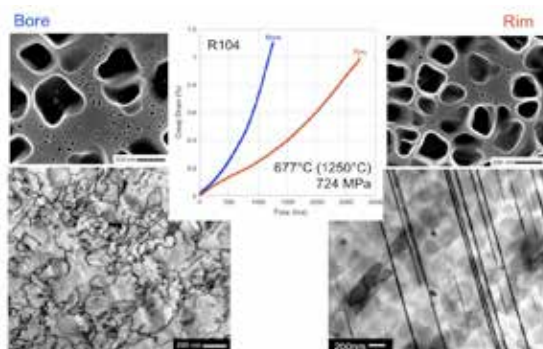


**Fig. 1:** Strong dependence of monotonic creep response as a function a subtle microstructure differences between the bore and rim of an actual disk forging for ME3.

In the past decade, unprecedented methods to quantify, use and explore grain- and precipitate-scale microstructures have been developed. However, most modeling approaches to microstructure-property relationship utilize highly simplistic descriptors of microstructures (such as average particle size and volume fraction) that are empirically correlated to the properties (e.g., cutting vs. looping). Such approaches are utterly inadequate for addressing the design needs. To enable location-specific design where the designers strive to move away from using a uniform (usually the

most conservative) property set over an entire component, next generation modeling tools that incorporate specific deformation mechanisms operating in specific alloy systems under a given set of processing parameters, microstructure states and service conditions are desperately needed.

In this presentation, using plastic deformation in Ni-base superalloys as an example, we show how to integrate mesoscale modeling (phase field (Wang2010)) with experimental characterization to bridge *ab initio* calculations and image-based crystal plasticity (CP) simulations to (a) identify deformation mechanisms, quantify activation pathways, and provide deformation mechanism maps (DMMs) as function of alloy composition, processing, microstructure and loading condition (Unocic2011; Zhou2011), (b) develop a fully integrated phase-field + FFT-CP modeling approach to simultaneous polycrystalline and precipitate microstructure evolution and dislocation density evolution during creep, which incorporates the DMMs obtained from (a), and (c) develop a continuum level FEM for macroscopic response, which incorporates the deformation behavior of individual RVEs obtained from (b).

#### References

Kovarik, L. (2009): Microtwinning and Other Shearing Mechanisms at Intermediate Temperatures in Ni-Base Superalloys – In *Prog. Mat. Sci.* **54**: 839-873.  
Wang, Y. and J. Li (2010): Acta Materialia Overview 150: Phase Field Modeling of Defects and Deformation in *Acta Mater.* **58**: 1212-1235.  
Unocic, R, N. Zhou, L. Kovarik, C. Shen, Y. Wang, and M.J. Mills (2011): Evolution of Deformation Microtwins during Creep of a  $\gamma'$  Precipitate Strengthened Ni-Base Superalloy in *Acta Mater.* **59**:7325-7339.  
Zhou, N., C. Shen, M.J. Mills, J. Li and Y. Wang (2011): Modeling Displacive-Diffusional Coupled Dislocation Shearing of  $\gamma'$  Precipitates in Ni-Base Superalloys in *Acta Mater.* **59**:3484-3497.

Talks Topic A2:

***Multiscale phenomena in plasticity***

## Size-Dependent Mechanical Properties of Crystalline Nanoparticles

DAN MORDEHAI

Department of Mechanical Engineering, Technion, Haifa, Israel

It is well established that materials can drastically change mechanical properties when their size is reduced to the nanoscale, mainly because of an increase in surface to volume ratio and of lowering the amount of defects in the lattice. In particular, defect-free crystalline nanostructures reach strengths which are close to their ultimate shear strength, since their deformation is controlled by dislocation nucleation from the surfaces. In this talk we examine how the size and shape of defect-free nanoparticles affect the mechanical response to compression and indentation.

Earlier experiments on Au nanoparticles showed that they become easier to indent as they are smaller, but a reduction of their size increases their strength under compression. With large scale Molecular Dynamics (MD) simulations, we show how the lateral dimensions give rise to size effect in indentation through the competition between dislocation storage and depletion on free surfaces. On the other hand, under compression, the size effect arises from a size-dependent dislocation nucleation threshold at the nanoparticle's vertices. A dislocation nucleation model is employed to study how stress at which FCC nanoparticles yield depends on ma-

terial properties, such as the stacking fault energy and elastic constants.

In contrast, Fe nanoparticles (BCC) exhibit a much less profound size effect due to strong dislocation pinning at their nucleation sites. We denote this type of deformation as depinning-controlled mechanisms. Under compression, the deformation of Fe nanoparticles exhibit a size effect, similarly to FCC nanoparticles. However, they differ in the governing dislocation mechanism. While dislocations are nucleated at the vertices of both Fe and FCC nanoparticles, these are accumulated within the Fe nanoparticle instead of escaping from the free surfaces, as in the FCC nanoparticles.

Furthermore, the size effect is shown to be suppressed in Ni<sub>3</sub>Al intermetallic nanocubes under compression, since the stress concentration vanishes in this geometry. An analysis of the dislocation evolution in Ni<sub>3</sub>Al nanoparticles shows that partial dislocations are nucleated at the vertices, shearing the nanoparticle with large complex stacking faults planes.

This combined computational-experimental study provides us with insights on how to model dislocation-nucleation controlled deformation at the nanoscale.

## Molecular dynamics study of the response of a nanowire containing defects to a uni-axial strain: case of nickel

KAHINA LOUNIS<sup>1</sup>, EL HOCINE MEGCHICHE<sup>1</sup>, ZENIA HAND<sup>2</sup>

<sup>1</sup>Laboratoire de Physique et Chimie Quantique (LPCQ), Université Mouloud Mammeri, Tizi-Ouzou, Algérie

<sup>2</sup>Laboratoire de Physique Théorique, Université Abderrahmane Mira, Béjaia, Algérie

Nanostructures hold very important potential technological applications nowadays. Besides their reduced dimensionality (spatial dimensions) these structures exhibit peculiar electronic, optical and mechanical properties. Recent experiments conducted on nickel nanowires have revealed elastic limits many orders of magnitude greater than their corresponding values in bulk nickel [1]. This disparity has been attributed to differing concentrations of defects (point or extended) present in both systems: nanowire and bulk. To simulate these systems care must be taken in tuning parameters structure size, temperature, strain/stress rate, presence of defects to ensure that the simulation conditions are as close as possible to the experimental setup. Although many researchers [2, 3] have studied the influence of the system size, temperature as well as

strain rate on the elastic limit of nickel nanowires, the role of defects has not yet been explored to our knowledge. In this work we will present the results of our simulations of nickel nanowires with defects in them. The calculations have been carried out using molecular dynamics as implemented in the Lammmps[4] code, where Ni-Ni interactions are modeled by an embedded atom model (EAM) kind of semi-empirical potential. Our results show that the elastic limit decreases with increasing temperature and/or increasing strain rate (frequency). We have found that the elastic limit (yield strain) decreases by a half when the strain rate (frequency) varies from  $10^{10} \text{ S}^{-1}$  to  $10^{08} \text{ S}^{-1}$ .

Moreover, we have found that presence of a small cluster of defects (three, six or thirteen monovacancies) in the nanowire leads to a substantial decrease in

the elastic limit. Additionally, our results point to the important role played by the initial location, of the defect cluster, in the occurrence of the yield point in the nanowire.

#### References

Celik, E. Guven, I & Madenci, E. (2011): *Nanotechnology* 22, 155702.

Setoodeh, A, R. Attariani, H & Khosrownejad, M (2008): *Computational Materials Science* 44, 378.  
 Peng, C. Ganesan, Y. Lu, Y & Lou, J. (2012): *Journal of Applied Physics*. 111, 063524.  
 Plimpton, S. (1995): *Journal of computational Physics*, 117, 1-19.

## Tension/compression anisotropy in yield stress and Bauschinger effect in ultrafine-grained metals

TOMOHIITO TSURU<sup>1</sup>, YOSHITERU AOYAGI<sup>2</sup>, YOSHIYUKI KAJI<sup>1</sup>, TOMOTSUGU SHIMOKAWA<sup>3</sup>

<sup>1</sup>Japan Atomic Energy Agency, Tokai-mura, Ibaraki, Japan

<sup>2</sup>Tohoku University, Sendai, Miyagi, Japan

<sup>3</sup>Kanazawa University, Kanazawa, Ishikawa, Japan

While the plastic deformation characteristics of coarse-grained metals is generally determined by the average quantity of collective motion of dislocations, the mechanical properties of nanocrystalline metals ( $d < 100$  nm,  $d$  is the grain size) cannot be simply predicted based on assumptions of the average quantity of collective motion of dislocations. Recently, it has been possible to produce ultrafine-grained metals ( $100$  nm  $< d < 1$   $\mu$ m) in bulk by severe plastic deformation process<sup>1-2)</sup> and it has been known these UFG metals achieve unique and excellent mechanical properties.<sup>3-4)</sup> As well as this strengthening mechanism, the anomalous tension/compression deformation characteristics and the Bauschinger effect have been observed in UFG metals<sup>5)</sup>. Dislocation emission from grain boundaries becomes more important deformation mechanism to describe the plastic deformation because it is difficult to construct any intragranular dislocation source due to the very limited individual grain's space in UFG metals. However it is difficult to express these unique mechanical properties in UFG metals using conventional theories.

In this study, the plastic deformation characteristics of UFG metals were investigated by huge scale atomistic simulations. Some polycrystalline models with intragranular Frank-Read sources were constructed to elucidate the relationship between the inter- and intra-granular plastic deformation processes and the mechanical properties. Then the uniaxial tension and compression were applied to the polycrystalline aluminum and copper models. It is found that yield stress is strongly influenced by the number of intragranular dislocation sources, i.e., dislocation density. Frank-Read sources were activated prior to intergranular dislocation emission, and the yield event of the whole

system seems to occur when some dislocation sources activated. The Bauschinger effect of UFG metals is caused by the change in dislocation density in the process of forwarding and backwarding deformation. Additionally, the yield stresses of tensile and compressive deformation have some sort of plastic anisotropy. UFG aluminum shows more significant anisotropy than UFG copper. It would be illustrated well by comparing two materials that the intergranular dislocation nucleation plays more important role in tension/compression anisotropy.

#### References

Y. Iwahashi, Z. Horita, M. Nemoto, J. Wang and T. G. Langdon (1996): Principle of equal-channel angular pressing for the processing of ultra-fine grained materials, *Scripta Mater.* 35: 143-146.  
 Y. Saito, H. Utsunomiya, N. Tsuji and T. Sakai (1999): Novel ultra-high straining process for bulk materials—development of the accumulative roll-bonding (ARB) process, *Acta Mater.* 47: 579-583.  
 X. Huang, N. Hansen and N. Tsuji (2006): Hardening by Annealing and Softening by Deformation in Nanostructured Metals, *Science* 312: 249-251.  
 Y. M. Wang and E. Ma (2004): Three strategies to achieve uniform tensile deformation in a nanostructured metal, *Acta Mater.* 52: 1699-1709.  
 M. Haouaoui, I. Karaman and H. J. Maier (2006): Flow stress anisotropy and Bauschinger effect in ultrafine grained copper, *Acta Mater.* 54, 5477-5488.  
 J. Rajagopalan, C. Rentenberger, H. P. Karnthaler, G. Dehm and M. T. A. Saif (2010): In situ TEM study of microplasticity and Bauschinger effect in nanocrystalline metals, *Acta Mater.* 58, 4772-4782.

## Particle and solid solution strengthening.

### Part 1: experiments to control microstructure

PHILIPP SCHUMACHER<sup>1,2</sup>, STEFAN POGATSCHER<sup>3</sup>, MARCO J STARINK<sup>4</sup>, CHRISTOPH SCHICK<sup>2</sup>, OLAF KESSLER<sup>1</sup>, VOLKER MOHLES<sup>5</sup>, BENJAMIN MILKEREIT<sup>1,2,4</sup>

<sup>1</sup>University of Rostock, Chair of Materials Science, Rostock, Germany

<sup>2</sup>University of Rostock, Polymer Physics Group, Rostock, Germany

<sup>3</sup>ETH Zurich, Department of Materials, Laboratory of Metal Physics and Technology Zurich, Switzerland

<sup>4</sup>University of Southampton, Engineering Materials Group, Engineering and the Environment, Southampton, UK

<sup>5</sup>RWTH Aachen, Institute of Physical Metallurgy and Metal Physics, Aachen, Germany

During quenching of age-hardenable aluminium alloys thermal gradients can occur, which generate residual stresses and distortion. Heat treatment simulation is a powerful tool for the prediction of their extent. However, mechanical properties of the simulated alloy are required depending on temperature, strain rate and its microstructure, which is strongly affected by the cooling condition. Approaches to model flow curves with appropriate state variables have therefore been developed in the past, but influences of microstructural elements such as solutes and second-phase particles need further investigation. This study presents an approach to generate reliable experimental data on mechanical properties of well-defined microstructural states for the calibration and validation of a simulation model.

Pure binary Al-Si alloys were analysed as Al-Si is an ideal model system and Si is an important alloying element in commercial age-hardenable 6xxx alloys. During cooling from solution annealing of Al-Si alloys two different types of precipitates occur in certain cooling rate and temperature ranges. Their microstructure was investigated by light optical, scanning electron, and transmission electron microscopy, as well as by atom probe tomography. The precipitation enthalpy during cooling was investigated with advanced DSC techniques in a wide cooling rate range of 0.0001 K/s to 2 K/s. Hence, the whole range of physical interest – from slow cooling close to thermodynamic equilibrium up to faster

cooling than the upper critical cooling rate – is covered. To analyse this wide dynamic range three different types of DSC devices were utilised. The dependence of formation enthalpy on cooling rate and temperature is modelled, providing a consistent physical description of precipitated volume fraction and amount of Si remaining in solid solution during cooling. This allows the generation of well-defined microstructural states with application of controlled heat treatments. Compression tests in a quenching and deformation dilatometer were carried out on specific states to investigate the strengthening effect of Si in solid solution and different types of coarse quench-induced precipitates. Thereby, samples possessing an equal amount of Si in solution but different types of precipitates with same precipitate volume fractions were produced and tested. The flow characteristics of these states were compared to precipitate-free conditions having the same amount of solute Si. A big advantage of this method is that the strengthening contribution of precipitates can be determined without the need to assume any - potentially inaccurate - superposition law between particle and solute strengthening. The fundamental ideas of this technique can be transferred to other precipitation hardening alloys. The flow behaviour was modelled. The modelling will be presented in part two of this work.

## Particle and solid solution strengthening.

### Part 2: modelling plastic behaviour

VOLKER MOHLES<sup>1</sup>, VOLKER PANKOKE<sup>1</sup>, PHILIPP SCHUMACHER<sup>2</sup>, BENJAMIN MILKEREIT<sup>2</sup>

<sup>1</sup>RWTH Aachen University, Institute of Physical Metallurgy and Metal Physics, Aachen, Germany

<sup>2</sup>University of Rostock, Chair of Materials Science, Rostock, Germany

Through-process modelling (TPM) has been established in recent years to simulate and predict the microstructure and the resulting material properties in the production of aluminium sheet. One core ingredient of such a simulation set-up is a statistical work hardening and recovery model that predicts the evolution of dislocation densities and the subgrain sizes during hot and cold rolling. These quantities affect the material strength and thereby the rolling forces immediately, and they influence texture evolution significantly. Furthermore, they are also important in subsequent processing because they form the driving force for recrystallisation. One such work hardening model that had been integrated in a full TPM set-up is 3IVM+ (3 Internal Variables Model). As designed, it allows successful TPM for all rolling and annealing steps in many cases. However, 3IVM+ fails to model those annealing steps well in which only recovery takes place. The main reason for this lies in the state variables chosen for modelling. They enforced that during recovery simulation, the state variables of the model approached the same values as for a fully recrystallised material, making a distinction between recovered and recrystallized states impossible. Moreover, only in a few cases 3IVM+ offers good predictions for the impacts of variations in alloy composition even though direct strengthening contributions by particles and by solute atoms had been considered.

Therefore, a new statistical work hardening and recovery model called 4IVM has been developed recently. Since this model is expected to cover many more aspects of plasticity than 3IVM+, the new model should

be considered as a work in progress until all new aspects can be validated by corresponding experiments. 4IVM describes the material state by the densities,  $\rho_x$ , of four dislocation classes with distinctly different properties: mobile dislocations ( $\rho_{mob}$ ), dislocation dipoles ( $\rho_{dip}$ ), dislocation locks ( $\rho_{ock}$ ), and subgrain boundary dislocations ( $\rho_{ub}$ ). While the mobile dislocations facilitate plasticity, the dipole dislocations do not contribute to slip even though they can move in response to internal stress gradients. Lock and subgrain boundary dislocations are considered entirely immobile for now. For all dislocation densities  $\rho_x$ , generation and annihilation rates are defined in dependence of all other variables as well as the initial grain size (and eventually other influences like solute concentrations). By integration over time, these rates determine the coupled evolution of all  $\rho_x$ . From these, the work hardening stress is derived by application of the Taylor formula. The total flow stress is calculated as a superposition of this Taylor stress and models for precipitate and solute strengthening.

The new model is validated by comparing simulated flow curves to measured ones. For this, binary Al-Si and Al-Mg alloys have been prepared and compression tested in varying precipitation states as described. This is described in the accompanying paper titled "Particle and solid solution strengthening. Part 1: experiments to control microstructure" by Schumacher, Pogatscher, Starink, Schick, Keßler, Mohles, and Milkereit. Compared to its predecessor, 4IVM offers improved flow curve predictions.

Talks Topic A3:

***Multiscale phenomena in plasticity***

# Comparison of statistical descriptors for the construction of Statistically Similar RVEs

LISA SCHEUNEMANN<sup>1</sup>, DANIEL BALZANI<sup>2</sup>, DOMINIK BRANDS<sup>1</sup>, JÖRG SCHRÖDER<sup>1</sup>

<sup>1</sup>Universität Duisburg-Essen, Institut für Mechanik, Abteilung Bauwissenschaften, Fakultät für Ingenieurwissenschaften, Essen, Germany

<sup>2</sup>TU Dresden, Institut für Mechanik und Flächentragwerke, Fakultät für Bauingenieurwesen, Germany

In microheterogeneous materials, the effective material response is influenced by the underlying microstructure morphology, the behavior of the individual phases and the interaction at the interface. In order to take into account these microstructural effects, homogenization approaches, such as the FE<sup>2</sup>-method, see e. g. Smit et al. (1998), Miehe et al. (1999) & Schröder (2014) are suitable tools. Herein, at every macroscopic Gauss point, an additional microscopic boundary value problem is solved, which typically incorporates a representative volume element (RVE) to represent the microstructure. As the microstructure of a real material is governed by a highly complex morphology, the consideration of such structures involves large computational efforts which pose a serious drawback to the homogenization method. The use of statistically similar RVEs (SSRVEs) is an alternative which involves much lower computational costs. SSRVEs have a statistically similar artificial inclusion morphology as well as a similar mechanical behavior as the real microstructure. SSRVEs are constructed by minimizing a least-square functional taking into account the difference of statistical measures computed for the real microstructure and the SSRVE. This approach was proposed by Balzani et al. (2009) for two-dimensional SSRVEs and extended to 3D in Balzani et al. (2014). For the construction of SSRVEs, the statistical measures used play a crucial role. Balzani et al. (2010) showed the importance of considering statistical measures of higher order, such as spectral density, Yeong & Torquato (1998) point out that hybrid approaches lead to improved results when reconstructing microstructures based on statistical measures. Statistical descriptors based on Minkowski functionals, a class of integral measures which can be used to describe geometrical objects, cf. Schröder-Turk et al. (2013), offer a possibility to increase the efficiency of construction compared with the lineal-path function. This contribution focusses on the comparison of SSRVEs obtained from different sets of statistical measures. Namely, SSRVEs based on volume fraction, spectral density and lineal-path function will be compared

to ones constructed using probability density functions based on Minkowski functionals to replace the lineal-path function.

## References

- Balzani, D., Schröder, J. & Brands, D. (2009): FE<sup>2</sup> simulation of microheterogeneous steels based on statistically similar RVEs. Proc. IUTAM Symp. Variational Concepts with application to mechanics of materials, September 22-26, Bochum, Germany.
- Balzani, D., Brands, D. & Schröder, J. (2010): Sensitivity analysis of statistical measures for the reconstruction of microstructures based on the minimization of generalized least-square functionals. Tech. Mech. Vol. 30, 297-315.
- Balzani, D., Scheunemann, L., Brands, D. & Schröder, J., (2014): Construction of Two- and Three-Dimensional Statistically Similar RVEs for Coupled Micro-Macro Simulations. Comp. Mech., doi: 10.1007/s00466-014-1057-6.
- Miehe, C., Schröder, J. & Schotte, J. (1999): Computational homogenization analysis in finite plasticity. Simulation of texture development in polycrystalline materials. Comp. Meth. Appl. Mech. Eng., Vol. 171, 387-418.
- Schröder, J.: A numerical two-scale homogenization scheme: the FE<sup>2</sup> method. In: Plasticity and Beyond – Microstructures, Crystal Plasticity and Phase Transitions, CISM Lecture notes 550, Editors: K. Hackl & J. Schröder, Springer 2014
- Schröder-Turk, G.E., Mickel, W., Kapfer, Schaller, S., Breidenbach, B., Hug, D. & Mecke, K. (2013): Minkowski Tensors of Anisotropic Spatial Structures. New Journal of Physics. Vol. 15 083028
- Smit, R., Brekelmans, W. & Meijer, H. (1998): Prediction of the mechanical behavior of nonlinear heterogeneous systems by multi-level finite element modeling. Comp. Meth. Appl. Mech. and Eng., Vol. 155, 181-192.
- Yeong, C.L.Y. & Torquato, S. (1998): Reconstructing random media. Phys. Rev. E., Vol. 57, 495-506.

# Phase transitions' energies and activation energies from nothing else than indentation loading curves

GERD KAUPP

University of Oldenburg, Faculty 5 Natural Sciences, Oldenburg, Germany

Pyramidal and conical (as do spherical) indentation loading curves strictly follow the  $F_N = k h^{3/2}$  law for all uniform materials under all thinkable conditions of constant normal force increase. This has been shown by analysis of experimental loading curves from all over the world, giving linear correlation coefficients of  $r > 0.999$  and often  $r > 0.9999$ . It does not matter whether the materials are elastic, plastic, hard, ductile, brittle, viscous, adhesive, soft, etc. Undeniable surface effects are revealed and directly corrected. The penetration resistance  $k$  has the dimension  $[N/m^{3/2}]$ . Elementary mathematics derives the applied work ( $W_{\text{applied}}$ ) and the indentation work ( $W_{\text{indent}}$ ) relating with 5 : 4 for all uniform materials. The  $F_N = k h^{3/2}$  parabola enables the simplest determination of the **indentation work** that is precisely 80% of the applied work. The remaining 20% produce all long range processes away from the indentation volume, be these reversible or irreversible, including local phase transitions, if they occur.

This quantitative analysis of indentations is of importance for the identification and energetic of pressure induced **phase transitions** ( $W_{\text{trans}}$ ). When these occur the  $F_N-h^{3/2}$ -plot yields a linear branch *before* (slope  $k_1$ ) and *after* the onset of the phase transition (slope  $k_2$ ) with sharp intersection at a kink point, both with the above correlation coefficients. Clearly, the transformed material exhibits different mechanical properties including the penetration resistance  $k$ . This is observed for structural transitions and all other types of phase transformation, simply by the energy balance:  $W_{\text{trans}} = \text{full } W_{\text{applied}} - (W_{1\text{applied}} + W_{2\text{applied}})$ . **Phase transformation energies** can thus be positive (endothermic) or negative (exothermic). Basic arithmetic using the  $F_N = k h^{3/2}$  law allows for their calculation at freely chosen

loading ranges. Examples with Berkovich pyramid are compared for different types of materials.

The precision of the new analytic technique without approximations and without iterations allows also for the determination of the **activation energy of phase transitions** by indentations at variable temperatures. These are available with reliable temperature control by various commercial nanoindentation instruments. But activation energy for pressure induced phase transformations is unprecedented in materials research. Its measurement under the Berkovich pyramid will be exemplified with the phase transition of NaCl (001), where the B1 and B2 states are most precisely known, and where the transition is used as a pressure standard. The  $k_1$  and  $k_2$  values change with indentation temperature, here from room temperature to 400°C, with correlation coefficients of  $r > 0.9999$ . The normalized transition work ( $W_{\text{trans}}/mN$ ) rises with temperature, due to deeper immersion  $h$ . The semi-logarithmic plot of  $W_{\text{trans}}/mN$  against temperature is linear and the slope provides the normalized **phase transition activation energy** ( $E_a/mN$ ) for the calculation of the transition work for all interesting temperatures and pressures.  $E_a/mN$  proves insensitive to creep-on-load. It yields valuable new material's property of practical importance for adjustments of compatibility within composite materials under mechanical impact, or for the interpretation of shearing interactions at elevated temperatures, etc.

## References

- Kaupp, G. (2014): Activation energy of the low-load NaCl transition from nanoindentation loading curves – Scanning, DOI: 10.1002/sca.21158; 8 pages; Wiley.

## Rate effects in finite element modeling of transformation induced visco-plasticity

MAHER EL HAJ KACEM<sup>1</sup>, FABRICE BARBE<sup>1</sup>, NICOLAS LECOQ<sup>1,2</sup>

<sup>1</sup>INSA de Rouen, Groupe de Physique des Matériaux, Saint Etienne du Rouvray, France

<sup>2</sup>Université de Rouen, Morphodynamique Continentale et Côtière, Mont-Saint-Aignan, France

The TRansformation Induced Plasticity (TRIP) in steels is a permanent strain which is achieved under the combination of a phase transformation at elevated temperature and small external loading. This phenomenon can be interpreted from the elastoplastic interactions that occur locally between the growing particles and a parent matrix and which preferentially develop in the loading direction. This model mechanism enables to obtain a first-order agreement on TRIP, as shown by the model of [Leblond, 89] or by numerical simulations [Tahimi et al., 2012] for displacive as well as diffusive transformations.

However, in most modelling approaches (e.g. Leblond, Taleb-Sidoroff, Fischer et al. ; see [Barbe & Quey, 2011] for references), viscous strains are neglected. By contrast, on an experimental basis, for 100C6 steel at 700°C, both phases show high strain-rate sensitivity [Tahimi et al., 2012]. The analytical model presented in [Vincent et al., 2003] is one of the few accounting for viscous effects but relies on strong hypotheses concerning the distribution of plasticity between phases. In this work, the problem of viscoplastic interactions between diffusively growing phases is introduced explicitly in the constitutive laws of a phase transforming RVE; the mechanical problem is solved by means of the finite element method [Tahimi et al, 2012, Barbe and Quey, 2011]. A particular processing of the total inelastic deformation induced during a classical TRIP test (consisting in imposing a small constant stress imposed during the phase transformation) enables to distin-

guish between creep deformation and transformation plasticity.

It is found that not only viscosity can be very influential on the prediction of the transformation induced plasticity, but also the final properties of the product phase could be considerably affected due to the phase transformation history. The FE Modelling is also used for other objectives: (i) to evaluate the contribution of viscosity to predict Transformation visco-plasticity at different strain-rate sensitivities and (ii) to analyse particular cases of model TRIP tests which could help improving a simple rate-sensitive analytical model.

### References

- [Leblond, 89] Leblond, J.B., Mathematical modelling of transformation plasticity in steels II: coupling with strain hardening phenomena *Int J Plasticity* 5:573–591, 1989.
- [Tahimi et al., 2012] A. Tahimi, F. Barbe, L. Taleb, R. Quey, A. Guillet, Evaluation of microstructure-based transformation plasticity models from experiments on 100C6 steel. *Comput Mater Sci* 52:55–60, 2012.
- [Barbe & Quey, 2011] F. Barbe, R. Quey. *International Journal of Plasticity*. 27 (2011) 823-840.
- [Vincent et al., 2003] Yannick Vincent, Jean-Michel Bergheau, Jean-Batiste Leblond. Viscoplastic behaviour of steels during phase transformations. *C.R. Mecanique* 331(2003) 587-594.

Talks Topic A4:

***Multiscale phenomena in plasticity***

## Size effects in void growth from nano- to microscale

JAVIER SEGURADO<sup>1,2</sup>, HYUNG-JUN CHANG<sup>1</sup>, JAVIER LLORCA<sup>1,2</sup>

<sup>1</sup>Department of Materials Science, Polytechnic University of Madrid, Spain

<sup>2</sup>Madrid Institute for Advanced Studies of Materials (IMDEA Materials Institute), Spain

The ductility of metallic materials is determined to large extent by the kinetics of void growth. The growth mechanisms depend on the size of the initial voids. In the case of very small voids (<100 nm), void growth is triggered by the emission of shear dislocation loops from the void surface when the stress approaches the strength of the perfect crystal. For voids with sizes >1 μm, void growth is controlled by dislocations nucleated in the bulk, that shear the void upon slip.

For a correct description of nano-sized void growth, the discrete nature of the crystal has to be accounted to accurately represent the nucleation process [1]. However, for micron-sized voids the volume of material and the number of dislocations involved prevents the use of a pure discrete study. In this case, Discrete Dislocation Dynamics (DDD) arises as an ideal technique because it allows the use of larger simulation volumes by considering a continuum framework with an explicit representation of the individual dislocations and their interactions. Moreover, size effects are naturally reproduced by DDD simulations [2-3]

In this work, simulation of the void growth process at different length scales (from 1 nm to microns) will be presented for an ideal FCC material with special emphasis on void size effects.

At the nano-scale, the void growth process has been studied first by means of a 2D model of a periodic array of circular voids [1]. The simplicity of the model allowed to cover a wide range of void sizes (<0.1microns). In addition, 3D models with cylindrical holes were used at smaller sizes to confirm the similarity of the mechanisms in the two cases : dislocation nucleation at the void surface. The level of stresses necessary

to nucleate the dislocations were in the order of GPa, much larger than typical yield of these materials.

For micron sized voids, DDD simulations were performed. In this case both 2D models representing cylindrical holes [2,3] and 3D models [4] with spherical voids were employed. The interaction of the dislocations with the void surface was accounted coupling the DDD simulations with finite element models using the Needleman and Van-der-Giessen approach.

This study using different models and covering a void size range of several orders of magnitude allow to have a general picture of the mechanisms at each scale and the size effects in void growth process.

### References

- [1] H-J. Chang, J. Segurado, O. Rodríguez de la Fuente, B. M. Pabón, J. Llorca (2013), "Molecular dynamics modeling and simulation of void growth in two dimensions" *Modelling Simulation in Materials Science and Engineering* 21 075010
- [2] J. Segurado, J. Llorca (2010) Discrete dislocation dynamics analysis of the effect of lattice orientation on void growth in single crystals. *International Journal of Plasticity* 26, 806-819,
- [3] J. Segurado, J. Llorca, (2009) An analysis of the size effect on void growth in single crystals using discrete dislocation dynamics *Acta Materialia*, 57, 1427-1436
- [4] H-J Chang, J. Segurado, J. Llorca (2015), Three-dimensional dislocation dynamics analysis of size effects on void growth, *Scripta Materialia* 95,1-14

## Dislocation interaction across grain boundaries and grain boundary yielding in a discrete dislocation dynamics framework

MARKUS STRICKER, DANIEL WEYGAND

Institute for Applied Materials IAM, Karlsruhe Institute of Technology, Germany

The plasticity of polycrystalline samples is strongly related to the effective resistance of grain boundaries (GBs) against plastic flow. Depending on the crystallographic misorientation of adjacent grains, a dislocation from one grain is either blocked by the GB, transmitted completely into the next grain or transmitted leaving

a residual Burgers vector<sup>1</sup>. Recent strain gradient plasticity models describe this process phenomenologically<sup>2</sup>, but the underlying physical picture is unclear. This work revisits GB yielding from a DDD point of view, focusing on the elastic interaction of discrete dislocations across GBs modelled as impenetrable for dislocations

and addresses the question how the effective resistance to plastic slip of a GB can be quantified within this framework. A systematic study of bicrystalline samples containing tilt GBs is done, where the misorientation between the grains is varied between  $0^\circ$  to  $45^\circ$ . A simple shear loading is applied and the strain profiles perpendicular to the GB and the strain gradients at the GB are evaluated: Although the GBs are physically impenetrable for dislocations within this framework<sup>3</sup>, yielding of the GB is observed due to transparency of the GB to the corresponding stress and strain fields. The results show that with an increasing misorientation angle, the effective transmission of plastic slip across a GB decreases due to the effective residual Burgers vector left at the GB and the strain gradients reflect

the mismatch between otherwise cancelling stress and displacement fields of dislocations in the vicinity of the GB. This work discusses the (continuum) definition of GB yielding and shows insights from DDD to bridge the gap between molecular dynamics findings<sup>4</sup> to continuum level frameworks.

#### References

- [1] Sutton, A. P. & Balluffi, R. W. (1996): Interfaces in crystalline materials, Clarendon Press
- [2] Zhang, X. et al. (2014): J. Mater. Res., 29: 2116
- [3] Weygand, D. et al (2002): Model. Simul. Mater. Sc., 10:437
- [4] Jin, Z.-H. et al. (2006): Scripta Mater., 54:1163

## Dislocation alignment tensors: their conservation laws and how to determine them from discrete dislocation configurations

THOMAS HOCHRAINER

Universität Bremen, BIME, Germany

Alignment tensors are well known measures for the characterization of directional distributions of line like structures. They have recently been introduced to dislocation theory (Hochrainer 2015). The series of alignment tensors of increasing order recovers the total dislocation density as zeroth order tensor and the dislocation density tensor is connected to the alignment tensor of first order. The second order dislocation density tensor is a tensorial generalization of the occasionally used decomposition of the total dislocation density in edge and screw character (e.g., Reuber et al. 2014). Besides the dislocation alignment tensors we also introduce density measures of dislocation curvature, the scalar measure of which is closely related to the number of dislocations. In the current talk we show how the alignment tensors and the curvature tensors may

be obtained from DD simulations or from TEM pictures of dislocations. In light of these discrete definitions we also review the evolution equations of the alignment tensors, as introduced in Hochrainer 2015, and clarify their interpretation as conservation laws.

#### References

- Hochrainer, T. (2015): Multipole expansion of continuum dislocation dynamics in terms of alignment tensors, ArXiv e-prints.
- Reuber, C., Eisenlohr, P., Roters, F., Raabe, D., 2014. Dislocation density distribution around an indent in single-crystalline nickel: Comparing nonlocal crystal plasticity finite-element predictions with experiments. Acta Materialia 71 (0), 333-348

## Representation of Dislocation Interactions in a Dislocation Density Field Theory for Crystal Plasticity

SEVERIN SCHMITT<sup>1</sup>, PETER GUMBSCH<sup>1,2</sup>, KATRIN SCHULZ<sup>1</sup>

<sup>1</sup>Institute of Applied Materials, Karlsruhe Institute of Technology, Germany

<sup>2</sup>Fraunhofer Institute for Mechanics of Materials, Freiburg, Germany

Even though many phenomenological models have been developed for the description of dislocation based plasticity incorporating the underlying effects due to the internal length scale, there has always been

a drive to derive models containing physically motivated formulations. Multiscale material modeling is inevitable to bring the effect of length and time scales of smaller scales to regimes where they are relevant

for the prediction of macroscopic material properties. Multiscale material modeling aims to either couple the simulation of different scales at the prize of high computational costs or to reduce the number of unknowns of a system by incorporating information about the physical behavior gained on small scales onto larger scales. The latter approach presumes a deep understanding of the underlying physical effects and the application of homogenization techniques to translate discrete phenomena to a continuous representations. In recent years, different approaches for physically based continuum theories have been introduced. Allowing for different dislocation orientations, the Continuum Dislocation Dynamics Theory was formulated in order to introduce a kinematic description of the evolution of dislocations displayed in a density field theory [1]. Based on this theory, we focus on developing methods for incorporating the physical behavior of dislocations and their stress interactions into the dislocation density field theory. The understanding of these processes is gained on the scale of discrete dislocation dynamics and analytical descriptions available for simplified 2d systems [2]. By homogenizing the ef-

fects of the discrete scale, we derive a formulation of the internal stress caused by plastic distortion due to dislocation motion and the interaction of dislocations on a slip system.

We discuss the method for the computation of the internal stresses derived for a 2d dislocation configuration and compare our results with discrete dislocation dynamics and results from statistical physics [3]. Furthermore we demonstrate how these results can be generalized and applied to a 3d dislocation density field theory.

#### References

- [1] Hochrainer et al., Continuum dislocation dynamics: Towards a physical theory of crystal plasticity. *JMPS*, 63:167-178,2014.
- [2] Schulz et al., Analysis of dislocation pile-ups using a dislocation-based continuum theory. *MSMSE*, 22:025008, 2014.
- [3] Groma et al., Spatial correlations and higher-order gradient terms in a continuum description of dislocation dynamics. *Acta Materialia*, 51:1271-1281, 2003.

# Microstructural comparison of continuum models for dislocation plasticity

MEHRAN MONAVARI, MICHAEL ZAISER, STEFAN SANDFELD

Friedrich-Alexander-Universität Erlangen-Nürnberg, Fürth, Germany

Continuum modeling of dislocation microstructures started with the early works of Kröner and Nye [1]. They envisaged the geometrically necessary dislocation (GND) density tensor ( $\alpha$ ) as the curl of the plastic distortion in the crystal. The Kröner-Nye tensor, however, cannot represent the statistically stored dislocations (SSD) which become relevant when the plastic distortion is resolved on a larger scale than the scale of single dislocations. Various continuum dislocation models have approached this problem from different perspectives: (I) complementing the evolution equation of  $\alpha$  by semi-phenomenological terms (A. Acharya [2]); (II) representing fluxes of positive and negative edge dislocations which automatically can represent GNDs and SSDs and their mutual conversion (I. Groma [3]); generalizing this approach one step further by distinguishing edge and screw dislocations forming systems of rectangular loops as done by A. Arsenlis [4]. Recently, also theory that allows for arbitrary dislocation orientations was proposed in the form of the *higher-dimensional continuum dislocation dynamics theory* (hdCDD) introduced by T. Hochrainer [5]. Subsequently, Hochrainer et al. derived a systematic framework for constructing numerically efficient models based on Fourier expansions of the hdCDD density tensor [5,6] which, however, require closure assumptions in order to arrive at finite systems of continuum dislocation dynamics (CDD) equations.

In this paper we use the maximum entropy principle to derive closure assumptions for the two lowest order

CDD models, CDD<sup>(1)</sup> and CDD<sup>(2)</sup> [7]. We then discuss in detail the advantages and the deficiencies of the two CDD variants in comparison with the initially mentioned models of Acharya, Groma and Arsenlis. As a benchmark test we compare the performance of these models by studying the evolution of dislocation microstructure in a velocity field which idealizes the situation found in persistent slip bands (PSB). This is a very challenging model system because a continuum theory needs to be able to represent the formation of edge dipoles in regions of low velocity and the threading screw dislocations in the channels – a complex interaction of two types of SSDs and their (partial) conversion into GND fields all of which has been directly observed in experiments.

## References

- [1] E. Kröner, Springer-Verlag, 1958.
- [2] A. Acharya, J. Mech. and Phys. Solids 52 (2) (2004)301–316.
- [3] I. Groma, Phys. Rev. B 56 (10) (1997)
- [4] A. Arsenlis, et al., J. Mech. and Phys. Solids 52 (6) (2004)
- [5] T. Hochrainer, et al., J. Mech. and Phys. Solids 63 (2014)
- [6] T. Hochrainer, submitted to Phil. Mag. (arXiv: 1409.8461)
- [7] M. Monavari, et al., Mater. Res. Soc. Symp. Proc. 1651 (2014)

Talks Topic A5:

***Multiscale phenomena in plasticity***

## The «Cauchystat»: accurate control of the true stress in molecular dynamics simulations of martensitic phase transformations

RONALD E. MILLER<sup>1</sup>, ELLAD B. TADMOR<sup>2</sup>, NOAM BERNSTEIN<sup>3</sup>, FABIO PAVIA<sup>4</sup>, JOSH GIBSON<sup>1</sup>

<sup>1</sup>Carleton University, Ottawa, Canada

<sup>2</sup>University of Minnesota, St. Paul, MN, USA

<sup>3</sup>NRL, Washington, DC, USA

<sup>4</sup>EPFL, Lausanne, Switzerland

When using molecular dynamics (MD) to study, for example, soft materials or stress-induced phase transformations of crystals, we are confronted with the need to describe the material behaviour from the perspective of finite deformation mechanics. Perhaps the most important consequence of this is the correct definition and interpretation of what we nominally refer to as the “stress” on a system.

It is common in MD simulations to want to control the applied stress. In some MD codes, this control is limited to control of only the hydrostatic pressure, or only the direct (axial) stresses. In order to control the full stress tensor including shear stress, MD codes almost universally use the Parrinello-Rahman technique (Parrinello & Rahman 1981) or some related variation (e.g. Martyna et al. 1994, Wentzcovitch 1991). However, none of these techniques are able to control the true (Cauchy) stress applied to the system. Instead, they apply an approximation to the second Piola-Kirchhoff stress (related to the “engineering” stress). The true Cauchy stress that results during such a simulation is dependent on the deformation of the simulation cell, and it cannot be known a priori. In fact, it can be significantly different from the nominally applied stress when the deformation is large.

In this presentation, I will discuss an alternative MD algorithm that controls the true Cauchy stress applied

to the system. The “Cauchystat” is based on the constant stress ensemble presented by Tadmor and Miller (2011), but with modified equations of motion that update the system boundary conditions in response to the resulting deformation of the simulation cell. As a clear example of the method’s usefulness, we show that the correct stress control is important in the case of martensitic phase transformations, where the predicted martensitic start temperature and austenitic finish temperature are significantly altered as compared to the Parrinello-Rahman result. We also examine the effects of shear stress on the mechanism of the phase transformation.

### References

- Parrinello, M. and A. Rahman (1981): Polymorphic transitions in single crystals: A new molecular dynamics method. *J. Appl. Phys.*, 52(12):7182–7190.
- Martyna, G.L., D.J. Tobias and M.L. Klein (1994): Constant-pressure molecular dynamics algorithms. *J. Chem. Phys.*, 101(5) pp. 4177-4189.
- Wentzcovitch, R.M. (1991): Invariant molecular-dynamics approach to structural phase transitions. *Phys. Rev. B*, 44(5):2358–2361.
- Tadmor, E.B. and R.E. Miller (2011): *Modeling Materials: Continuum, Atomistic and Multiscale Techniques*. Cambridge: Cambridge University Press.

## Multiscale modeling of solute atom effect on critical resolved shear stress of Fe

MASATO WAKEDA<sup>1</sup>, SHIGENOBU OGATA<sup>1,2</sup>

<sup>1</sup>Osaka University, Japan

<sup>2</sup>Kyoto University, Japan

Solute atom changes mechanical properties of bcc Fe; critical resolved shear stress (CRSS) and work hardening coefficient increase with increasing solute atom concentration at room temperature [1]. In bcc Fe alloys, screw dislocation is a dominant plastic deformation unit, since the energy barrier for screw dislocation motion is much higher than that of edge dislocation. Therefore, understanding of the effect of solute atom

on screw dislocation is a key to design and control plastic properties of Fe alloys. In this study, we predict CRSS of Fe-Si alloys using a multiscale modelling framework, which includes from density functional theories (DFT) calculation of atomistic scale to kinetic Monte Carlo model for screw dislocation dynamics.

First we investigated the interaction between solute Si and screw dislocation in bcc Fe using DFT calcula-

tion method [2]. In the calculation models, of which crystal structure is bcc Fe, there are substitutional Si atoms and two screw dislocations with opposite helicities. It is found that the substitutional Si atoms change the stable screw dislocation core structure, which is a six-fold symmetry in the case of pure Fe [3]. Moreover, interaction between screw dislocation and solute Si is found to be attractive, and the interaction becomes larger if the screw dislocation approaches to the solute Si. Based on charge density distribution, we show origin of the interaction from an electronic viewpoint. Using empirical Fe-Fe [4] and Fe-Si [5] interatomic potentials, which can quantitatively reproduce attractive interaction between solute Si and screw dislocation, we next evaluated the energy barriers for screw dislocation motion. In this calculation, we use a larger scale atomic model with more than 100,000 atoms, and there is one screw dislocation in the model. The energy barriers for screw dislocation motion via kink mechanism are evaluated for a pure Fe model and Fe-Si alloy models. It is observed that energy barrier for kink nucleation decreases if the screw dislocation approaches to solute Si, while increases if the screw dislocation moves away from solute Si because of attractive interaction between solute Si and screw dislocation. Moreover, it is found that solute Si increases energy barrier for kink migration. We finally evaluated the CRSS at give temperature, Si concentration and strain rate using the calculated energy barriers and kinetic Mote Carl model for screw dis-

location motion. The kinetic Mote Carl model can evaluate the screw dislocation dynamics with considering kink nucleation and migration and cross-kink mechanism. Based on the obtained screw dislocation velocity, we evaluated CRSS using a relationship between plastic strain rate and dislocation velocity, so called Orowan's equation. The CRSS of Fe-Si alloys is smaller than that of pure Fe at low temperature because of the reduction of energy barrier for kink nucleation due to solute Si. In contrast CRSS of Fe-Si alloys is larger than that of Pure Fe at high temperature because of the increase of energy barrier for kink migration due to solute Si. These results agree well with experimental reports of Fe-Si alloys, where solute softening at low temperature and solute strengthening at high temperature are observed.

#### References

- [1] *Advanced Steels: The Recent Scenario in Steel Science and Technology*, Y. Weng, H. Dong, Y. Gan. Springer, Berlin (2011) pp.229-240.
- [2] <http://www.openmx-square.org/>
- [3] M. Itakura, H. Kaburaki, M. Yamaguchi, *Acta Mater.*, **60** (2012) pp.3698-3710.
- [4] G. J. Ackland, M. I. Mendelev, D. J. Srolovitz, S. Han and A. V. Barashev, *J. Phys.: Condens. Matter.*, **16** (2004) pp. S2629-S2642.
- [5] M. Wakeda, H. Kimizuka and S. Ogata, *J. Japan Inst. Met. Mater.*, **77** (2013) pp. 409-414.

## Multi-scale modeling of dislocation-precipitate interactions in Fe: from molecular dynamics to discrete dislocations

A. LEHTINEN,<sup>1</sup> F. GRANBERG,<sup>2</sup> L. LAURSON,<sup>1</sup> K. NORDLUND,<sup>2</sup> M. ALAVA<sup>1</sup>

<sup>1</sup>Department of Applied Physics, Aalto University School of Science, Aalto, Espoo, Finland

<sup>2</sup>Department of Physics, University of Helsinki, Finland

Plasticity in crystalline materials is due to the motion of crystal defects known as dislocations. Dislocations create an anisotropic stress field around themselves which can be quite complex, giving rise to a rich variety of possible interactions. Discrete Dislocation Dynamics (DDD) is a method where the dislocation lines are taken to consist of straight segments. The dislocation stress fields are obtained from linear elasticity theory. Reactions related to the dislocation core, such as junction formation and pinning to defects, are beyond the reach of linear elasticity theory and thus require input from more microscopic approaches.

Here we combine molecular dynamics (MD) with DDD in order to model carbide precipitate interactions with edge dislocations in BCC-iron. We have implemented immobile spherical precipitates into the ParaDis[1] simulation code, interacting with the dislocations via a Gaussian potential which generates a normal force to the dislocation segments. The parameters for the pre-

cipitate potential and the dislocation mobility are obtained from a molecular dynamics simulations. When dislocation encounters an impenetrable obstacle, eg. precipitate, it will become pinned. If the external stress is high enough, the dislocation bypasses the obstacle by bending around it, leaving behind an Orowan loop. New dislocations need more stress to get depinned because they must overcome the old loop in addition to the obstacle. This leads to work hardening of the metal which is an important phenomenon to understand eg. in the context of building structural parts for nuclear reactors.

#### References

- Athanasios Arsenlis *et al.* (2007): Enabling strain hardening simulations with dislocation dynamics. *Modelling and Simulation in Materials Science and Engineering*.

## Detailed description of the screw dislocation motion in iron revealed by atomistic simulations

GHIATH MONNET<sup>1</sup>, AKIYOSHI NOMOTO<sup>2</sup>

<sup>1</sup>EDF – R&D, MMC, Moret sur Loins, France

<sup>2</sup>CRIEPI, Tokyo, Japan

It is well known that the motion of screw dislocations is the key feature of plastic deformation in body-centered-cubic materials at low temperature. In spite of the large number of associated investigations reported in the literature, some important issues are still unclear.

One of the most important of these issues is the ability of screw and other dislocations to move on specific crystallographic planes, which determines their availability as active slip planes.

In this work, we first present new molecular dynamics results of dislocation motion in iron. Simulations conditions were varied in order to cover a large spectrum of factors affecting the dislocation motion, such as the dislocation length, temperature, strain rate and the state of the applied stress.

Then, simulation results are stochastically analyzed following a recently reported theory [Monnet 2011]. The analysis results allow for the determination of parameters of thermal activation, such as the activation energy and volume. The identification of these parameters allows for the establishment of constitutive equations, necessary for the description of the dislocation mobility over the different slip planes at the continuum scale.

### References

Monnet, G., 2011. Determination of the activation energy by stochastic analyses of molecular dynamics simulations of dislocation processes. *Philosophical Magazine*, 91(29), pp.3810–3829.

## Depinning-Controlled Plastic Deformation during Nanoindentation of BCC Iron Thin Films and Nanoparticles

ROMAN KOSITSKI, DAN MORDEHAI

Department of Mechanical Engineering, Technion – Israel Institute of Technology, Haifa, Israel

The strength of a dislocation-free specimen at the sub-micrometer scale focuses great attention in recent years. One of the techniques commonly employed to study mechanical properties at this scale is nanoindentation. Nanoindentation of Au (FCC structure) nanoparticles revealed that the indentation forces decrease as the particle size increases and that thin-films of the same height are substantially harder [1]. Based on Molecular Dynamics (MD) simulations, it was suggested that the deformation commences with dislocation nucleation and that the size effect arises from the competition between accumulating the nucleated dislocations and the efficiency of depleting them on the lateral surfaces.

In this work we present MD simulations of nanoindentation  $\alpha$ -Fe (BCC phase) thin films and nanoparticles in order to better understand how dimensionality effect their mechanical response and the effect of size on the strength of BCC samples. After an elastic regime, which corresponded well to a Hertzian curve, plastic deformation was accompanied with small load drops. A detailed analysis revealed that  $\frac{1}{2}\langle 111 \rangle (110)$  edge dislocations are nucleated beneath the top facet

on the periphery of the indenter. The dislocations are nucleated on six possible slip systems: 4 in-plane and 2 out-of-plane directions. However, as opposed to FCC metals, the dislocations remain pinned after nucleation on both ends to the contact area with the indenter. A drop in the load, which in turn corresponds to strain bursts, is observed only when these dislocations depin from around the indent and not with the nucleation of a new dislocation [2]. Thus, we denote this type of deformation as depinning-controlled.

Two depinning mechanisms are identified in thin films. The out-of-plane dislocations detaches from the indent by turning into prismatic loops via double cross-slip and annihilation of their screw components. The in-plane dislocations, which are half prismatic loops, depin from their nucleation site on both ends and glided away from the indenter.

Indentation of faceted nanoparticles demonstrates similar dislocation mechanism. In addition to the mechanisms found in thin-films, the in-plane dislocations depin only on one end at a time, resulting in pure screw dislocation that reaches the lateral surfaces. Glide of these screw dislocations to upper facets pro-

vides an additional route for dislocations to escape the crystal, as well as depinning of the second end. Due to the locality of the depinning-controlled deformation, an indentation size effect was not identified in the simulations, nor was a difference found between thin films and nanoparticles of the same height, in contrast with the observations in FCC metals. Finally, we relate the dislocation mechanisms during the depinning-controlled deformation to the frequency and extent of strain bursts during nanoindentation of BCC specimens.

#### References

- Mordehai, D., Kazakevich, M., Srolovitz, D. J., & Rabkin, E. (2011). Nanoindentation size effect in single-crystal nanoparticles and thin films: A comparative experimental and simulation study. *Acta Materialia*, 59(6), 2309-2321.
- Li, J., Van Vliet, K. J., Zhu, T., Yip, S., & Suresh, S. (2002). Atomistic mechanisms governing elastic limit and incipient plasticity in crystals. *Nature*, 418(6895), 307-310.

Talks Topic A6:

***Multiscale phenomena in plasticity***

# Gradient enhanced modeling of fcc and bcc nanocrystalline materials

BENJAMIN KLUSEMANN<sup>1</sup>, SWANTJE BARGMANN<sup>1,2</sup>, YURI ESTRIN<sup>3</sup>

<sup>1</sup>Institute of Continuum Mechanics and Materials Mechanics, Hamburg University of Technology, Germany

<sup>2</sup>Institute of Materials Research, Helmholtz-Zentrum Geesthacht, Germany

<sup>3</sup>Centre for Advanced Hybrid Materials, Monash University, Clayton, Australia

Nanocrystalline materials are polycrystalline materials with an average grain size below 100 nm. Their mechanical properties are distinctly different from those of coarse grained materials. Therefore, bulk nanocrystalline materials have received great attention of the materials research community.

A modeling approach for nanocrystalline materials adopted here is based on the phase-mixture model introduced by Kim et al. (2000a). In this model, different deformation mechanisms are assumed to operate in the grain interior and the grain boundaries. It is further assumed that the strain and the strain rate are the same in both phases. For simplicity, the nanocrystalline grain shape is approximated as cube-shaped. The stress is determined additively by a rule of mixtures. The deformation mechanism in the grain boundaries is associated with the diffusional mass transport along the boundaries; the maximum stress that can be supported by the boundary phase is set to be equal to the yield strength of the amorphous state (Kim et al., 2000b). As the model should be valid over several length scales, from coarse grained material to nanometer grain sizes, Kim et al. (2000a) considered in the grain interior dislocation glide mechanism as well as diffusion mechanisms, namely Nabarro-Herring creep and Coble creep. The studies by Kim and Estrin (Kim and Estrin, 2005, 2008) showed that the model is capable of correctly predicting the transition of the flow stress from the Hall-Petch behavior in the conventional grain size range to an inverse Hall-Petch relation for nanocrystalline materials. Especially for small grain size and low strain rates, the material behavior is controlled by diffusion mechanisms. Additionally, their studies showed an increase of the strain rate sensitivity with decreasing grain size. However, this type of behavior is only observed in face-centered cubic (fcc) materials.

By contrast, nanocrystalline body-centered cubic (bcc) materials show a decrease of the strain rate sensitivity with decreasing grain size. To account for experimental observations for bcc materials, we have modified the original phase-mixture model to capture this inverse strain rate dependency. We assume that plastic deformation in bcc materials is governed by the Peierls mechanism, while the constraints put on the dislocation kink formation by the small grain size are considered to be responsible for a decrease of the strain rate sensitivity with grain refinement. The model for dislocation glide is modified accordingly.

Additionally, we look into the effect of strain gradients on the mechanical response of nanocrystalline materials. The phase mixture model is augmented with gradient terms. Differences in the mechanical behavior of fcc and bcc nanomaterials will be discussed in terms of the numerical results obtained with this gradient enhanced model.

## References

- Kim, H. & Estrin, Y. & Bush, M. (2000a): Plastic deformation behaviour of fine-grained materials. *Acta Materialia*, 48 (2), 493 - 504.
- Kim, H. S. & Bush, M. B. & Estrin, Y. (2000b): A phase mixture model of a particle reinforced composite with fine microstructure. *Materials Science and Engineering: A*, 276 (12), 175 - 185.
- Kim, H. S. & Estrin, Y. (2005): Phase mixture modeling of the strain rate dependent mechanical behavior of nanostructured materials. *Acta Materialia*, 53 (3), 765 - 772.
- Kim, H. S. & Estrin, Y. (2008): Strength and strain hardening of nanocrystalline materials. *Materials Science and Engineering: A*, 483-484 (0), 127 - 130.

# A consistent homogenization theory for a higher order plasticity model from meso to macro scale

PHAN VAN TUNG, POH LEONG HIEN

National University of Singapore, Singapore

Classical plasticity models, being scale independent, cannot capture any size dependent behavior. A remedy is to adopt a gradient plasticity model at the sub-granular (meso) scale to account for the different micro-processes leading to the various size effects. In this contribution, we adopt, at the meso scale, an isotropic gradient plasticity model (Gurtin, 2004) which incorporated the plasticity rotation effect to mimic the behavior of an analogous crystal plasticity model with multiple slip systems (Bardella and Giacomini, 2008).

For a generic problem, the interaction and competition between the different processes are captured through three length scale parameters: a microstructural length scale characterizing the rapid intra-granular fluctuations, the grain size describing the direct grain boundary effect, and a structural length scale accounting for the overall structural effect (Poh et al., 2013). Such a high resolution approach, however, is computationally expensive for a large problem since the FE discretization has to be done at a sub-granular level.

This motivates a novel homogenization theory (Poh, 2013) that translates the isotropic plasticity model from meso to macro. First, we introduce an additional kinematic field that characterizes the average surface deformation of a unit grain. Next the Hill-Mandel condition is applied to extract the homogenized governing equations at the macro scale. Departing from most homogenization approaches, we furthermore impose the equivalence of energy and dissipation across the two scales in order to determine the macroscopic constitutive relations and plasticity flow rules. The scale translation framework is thus thermodynamically consistent, with the three length scale parameters – the microstructural length scale, the grain size and the characteristic structural length scale – manifesting themselves in the homogenized solutions. This allows for a direct study on the interaction and competition between the different micro-processes, with a lower computational cost compared to a detailed crystal plasticity model.

Considering an idealized bending problem, we illustrate the excellent match between the homogenized solutions and meso solutions for the two limiting cases – microfree and microhard conditions at the grain boundaries. It is also highlighted that through the homogenization framework, the strain gradient plasticity model at the meso scale translates into a *micromorphic* continuum at the macro scale.

The homogenized plasticity model is next implemented numerically, and its predictive capabilities further demonstrated through a plane indentation problem. For the aforementioned two limiting cases, the homogenized solutions resemble closely the reference meso solutions, both in terms of the load displacement graphs and the plastic strain profiles. It is noteworthy that the excellent predictions are obtained with a significantly lower computational cost.

## References

- Gurtin, M.E. (2004): A gradient theory of small-deformation isotropic plasticity that accounts for the Burgers vector and for dissipation due to plastic spin – *Journal of the Mechanics and Physics of Solids*, 52: 2545-2568.
- Bardella, L. & Giacomini, A. (2008): Influence of material parameters and crystallography on the size effects describable by means of strain gradient plasticity – *Journal of the Mechanics and Physics of Solids*, 56: 2906-2934.
- Poh, L.H., Peerlings, R.H.J, Geers, M.G.D. & Swaddiwudhipong, S. (2013): Towards a homogenized plasticity theory which predicts structural and microstructural size effects – *Journal of the Mechanics and Physics of Solids*, 61: 2240-2259.
- Poh, L.H. (2013): Scale transition of a higher order plasticity model – A consistent homogenization theory from meso to macro – *Journal of the Mechanics and Physics of Solids*, 61: 2692-2710.

# Spectral Method Simulations of High Phase-Contrast Materials: A Joint Numerical–Experimental Study

M. DIEHL<sup>1</sup>, P. SHANTHRAJ<sup>1</sup>, P. EISENLOHR<sup>2</sup>, C.C. TASAN<sup>1</sup>, F. ROTERS<sup>1</sup>, D. RAABE<sup>1</sup>

<sup>1</sup>Max Planck-Institut für Eisenforschung, Düsseldorf, Germany

<sup>2</sup>CHEMS, Michigan State University, East Lansing, MI, USA

The spectral method has emerged as a powerful numerical tool to predict the mechanical response of polycrystalline materials (Lebensohn et al. 2011) and its efficiency over finite element methods has been demonstrated (Eisenlohr et al. 2013). Applications to heterogeneous materials with a large stiffness are, however, limited by the slow convergence of the iterative scheme. Various ideas have been proposed to overcome this issue, and we recently formulated direct and mixed variational conditions for mechanical equilibrium and strain compatibility in a framework that couples them to a general class of non-linear solution methods (Shanthraj et al. 2014). These formulations are implemented in DAMASK, the Düsseldorf Advanced Material Simulation Kit (Roters et al. 2012). A comparison on benchmark examples show, that the solution method has a dominant influence on performance and stability at large material heterogeneities, and improvements are obtained when higher-order solution methods are employed over the conventional approach.

Optimal solution strategies are devised based on this and applied to a dual phase (DP) steel microstructure, created from an electron backscatter diffraction (EBSD) based phase and orientation map. DP steels are used as an application example to show, how the mechanical response of multi-phase alloys is governed by the microscopic strain and stress partitioning behavior among the various phases, crystals and subgrains. Due to the limitations that are inherent in the experimental characterization of the stress-strain partitioning that takes place at the microscale, microstructure optimization of such alloys is typically based on the averaged macroscale response (e.g. engineering stress-strain curve). To strengthen the connection between microstructure and mechanical properties, a novel methodology is presented, that enables the joint experimental and simulation-based analysis of the deformation-induced evolution of heterogeneous materials with multiphase microstructures.

This is achieved through a combined experimental-numerical approach, i.e. relying on in-situ deformation experiments and crystal plasticity simulations both initiated from the same microstructural area of interest. For the experiments, deformation induced microstructure evolution is tracked to increasing strain levels. To map local strains free of surface roughening effects, a recently developed, digital image correlatiobased,

high-resolution, 2D strain mapping methodology is employed, in which 3D effects are considered by a post-mortem serial sectioning procedure. A promising correlation between the experiments and simulations is achieved, despite the complex micro-mechanics of this material. Obtained strain maps reveal significant strain heterogeneity arising from martensite dispersion, ferrite grain size, and defect densities effects; and early damage nucleation at notch-like irregularities in martensitic zones that cause high stress triaxiality. Deviations between experiments and simulations can be explained in terms of limitations of the involved techniques.

The presented integrated engineering approach provides a high dimensional set of micro-mechanical output information that can enhance the understanding and further development of complex bulk multiphase alloys (Tasan et al. 2014, Tasan et al. 2014).

## References

- Lebensohn, R. A., Rollett, A. D., & Suquet, P. (2011). Fast fourier transform-based modeling for the determination of micromechanical fields in polycrystals. *JOM*, 63(3), 13–18.
- Eisenlohr, P., Diehl, M., Lebensohn, R. A., & Roters, F. (2013). A spectral method solution to crystal elasto-viscoplasticity at finite strains. *Int. J. Plast.*, 46, 37–53.
- Shanthraj, P., Eisenlohr, P., Diehl, M., & Roters, F. (2014). Numerically robust spectral methods for crystal plasticity simulations of heterogeneous materials. *Int. J. Plast.*, in press.
- Roters, F., Eisenlohr, P., Kords, C., Tjahjanto, D. D., Diehl, M., & Raabe, D. (2012). DAMASK: the Düsseldorf Advanced Material Simulation Kit for studying crystal plasticity using an FE based or a spectral numerical solver. In O. Cazacu (Ed.), *Procedia IUTAM* (Vol. 3, pp. 3–10).
- Tasan, C. C., Diehl, M., Yan, D., Zambaldi, C., Shanthraj, P., Roters, F., et al. (2014). Integrated experimental-numerical analysis of stress and strain partitioning in multi-phase alloys. *Acta Mat.*, 81, 386–400.
- Tasan, C. C., Hoefnagels, J. P. M., Diehl, M., Yan, D., Roters, F., & Raabe, D. (2014). Strain localization and damage in dual phase steels investigated by coupled in-situ deformation experiments-crystal plasticity simulations. *Int. J. Plast.*, 63, 198–210.

## Influence of the microstructure of Al-components on the life time of integrated circuits

F. Meier<sup>1</sup>, C. SCHWARZ, E. WERNER

<sup>1</sup>Institute of Materials Science and Mechanics of Materials, Technische Universität München, Germany

Growing demands on performance and durability of integrated circuits (ICs) require an understanding of possible failure mechanisms. One main cause for damage of ICs arises from thermo-mechanical loads of the involved materials as a result of current pulses. The mismatch in thermal expansion leads to stresses which cause crack initiation and, in consequence, short circuits and the loss of functionality of the assembly.

This study presents a series of numerical simulations using a three dimensional model considering aluminium conductor paths sputtered on a silicon substrate and surrounded by a passivation layer. The thermo-mechanical problem is solved utilizing the *Abaqus/Standard* solver in combination with an user-defined material subroutine which takes into account the microstructure, the grain orientation and size and the temperature dependent anisotropic visco-plastic material behaviour of aluminium. Voronoi tessellation is used to model a realistic microstructure. The passiva-

tion layer and the silicon substrate are supposed to behave elastically and temperature dependent.

We investigate the influence of the microstructure on the stress and strain distribution within the model by changing the grains' orientation, distribution and especially size. Where possible, the simulation results are compared with experimental results taken from literature. Observations like surface roughening, crack initiation and life extension when decreasing the aluminium film thickness can be predicted qualitatively correct.

### Acknowledgements

This work has been conducted in the context of the research project SCHW 1347/3-1, funded by the DFG (Deutsche Forschungsgemeinschaft). We thank the Max Planck Institut für Eisenforschung in Düsseldorf for providing the simulation kit *DAMASK* and for the open and constructive collaboration.

## Deformation behavior of gradient materials with nanostructured near surface regions

FLORIAN RIEGER<sup>1</sup>, ANDREY MOLOTNIKOV<sup>2,3</sup>, XIAOLEI L. WU<sup>4</sup>, YUNTIAN T. ZHU<sup>5,6</sup>, THOMAS BÖHLKE<sup>1</sup>, YURI ESTRIN<sup>2,3</sup>

<sup>1</sup>Chair for Continuum Mechanics, Institute of Engineering Mechanics, Karlsruhe Institute of Technology (KIT), Germany

<sup>2</sup>Department of Materials Engineering, Monash University, Clayton, Australia

<sup>3</sup>National University of Science & Technology "MISIS" Leninskii pr.4, 119049, Russia, Moscow

<sup>4</sup>State Key Laboratory of Nonlinear Mechanics, Institute of Mechanics, Chinese Academy of Sciences, Beijing, China

<sup>5</sup>Department of Materials Science & Engineering, North Carolina State University, Raleigh, USA

<sup>6</sup>School of Materials Science and Engineering, Nanjing University of Science and Technology, Nanjing, China

Materials processed by surface mechanical attrition treatment (SMAT) are attracting considerable interest. They possess extremely fine grain structure in a near-surface layer, while retaining a coarse grained (CG) interior. The experimental observations by various groups (Wu et. al 2014, Lu 2014) have demonstrated that such materials exhibit a favorable combination of strength and ductility. Computational models are required to accelerate the design of such materials with microstructure architected for better performance. This study aims at investigating the deformation behav-

ior of IF steel with a gradient microstructure produced by SMAT through use of computational modelling.

The proposed model is based on a microstructure-related constitutive description in which the dislocation density is considered as a scalar internal variable (Estrin, 1996). The model accounts for the grain size dependent dislocation density evolution and also incorporates the Kachanov-type damage model to predict failure. The model parameters were obtained using uniaxial tensile test data for CG material and a nanostructured strip as the two extremes.

The average grain size variation with the distance from the surface was used as input for one-dimensional calculations of different SMAT-processed IF steels. Under the Taylor (iso-strain) assumption, calculations were carried out and validated against experimental uniaxial tension data for different SMAT processing times. A good predictive capability of the model was thus demonstrated.

#### References

- Wu X, Jiang P, Chen L, Yuan F, Zhu YT (2014) Extraordinary strain hardening by gradient structure. Proceedings of the National Academy of Sciences. 111:7197-201.
- Lu K. (2014) Making strong nanomaterials ductile with gradients. Science. 345:1455-6.
- Estrin Y. (1996) Dislocation-Density-Related Constitutive Modeling. In: Krausz AS, Krausz K, editors. Unified Constitutive Laws of Plastic Deformation. San Diego: Academic Press; p. 69.

Talks Topic A7:

***Multiscale phenomena in plasticity***

## Modelling the thermomechanical behaviour of the polycrystalline microstructure of dual phase steels during sheet bulk metal forming

STEFAN LOEHNERT, SEBASTIAN ZELLER, PETER WRIGGERS

Institute of Continuum Mechanics, Leibniz Universität Hannover, Germany

During the forming process of metals, heat is released due to the dissipative nature of plastic deformations. This heat leads to an increase of the temperature within the material. Depending on the speed of the forming process the rising temperature can be significant and may cause undesired effects such as residual stresses or additional distortions. Depending on the speed of the forming process the heat conduction may lead to larger or smaller increase of the temperature. Thermal strains may also lead to a loss of geometrical accuracy of the formed part. It is thus essential to consider temperature effects and the strong coupling between the mechanical and the thermal part of the metal forming process.

To motivate the development of an effective, homogenized macroscopic material model that can be used in macroscopic metal forming simulations, the polycrystalline microstructure of the material is considered. This necessitates the thermo-mechanical extension of the available purely mechanical crystal plasticity models. This extension of this crystal plasticity model helps to explain macroscopically observable effects like a temperature dependent yield stress or a storage of energy that cannot be retrieved by mechanical unloading. In this contribution we focus on dual phase steels like the DP600. For the different constituents of the microstructure different thermal effects can be observed leading to the requirement of different thermo-mechanical crystal plasticity models for each constituent. The evolution of the dislocation density in the ferritic part of the microstructure is temperature dependent

which leads to a significant temperature dependence of the hardening.

The three dimensional geometry of the polycrystalline microstructure is modelled by means of randomly generated Voronoi-cells of different sizes. To each cell a random crystal orientation is assigned. The fully coupled initial boundary value problem is solved for different boundary conditions applied on the outer boundary of a representative volume element of the polycrystal. In contrast to the commonly used staggered schemes here the coupled problem is solved directly leading to a more robust numerical behaviour and faster convergence.

From the results of the microstructural simulations eventually the effective material behaviour can be computed by means of a homogenization procedure.

### References

- Anand, L. & Gurtin, M.E. & Reddy, B.D. (2015): The stored energy of cold work, thermal annealing, and other thermodynamic issues in single crystal plasticity at small length scales. – *International Journal of Plasticity*, 64, 1-25
- Zaiser, M. (2013): The energetics and interaction of random dislocation walls. – *Philosophical Magazine Letters*, 93, 387-394
- Stainier, L. & Cuitino, A.M. & Ortiz, M. (2002): A micro-mechanical model of hardening, rate sensitivity and thermal softening in BCC single crystals. – *Journal of the Mechanics and Physics of Solids*, 50, 1511-1545

## Computational assessment of the microstructure-dependent plasticity of lamellar gray cast iron

MARIO METZGER<sup>1,2</sup>, THOMAS SEIFERT<sup>1</sup>

<sup>1</sup>Offenburg University of Applied Sciences, Germany

<sup>2</sup>Fraunhofer Institute for Mechanics of Materials IWM, Freiburg, Germany

This work focuses on the microstructure-dependent inelastic behavior of lamellar gray cast iron. It comprises the reconstruction of three dimensional volume elements by use of the serial sectioning method for the materials GJL-150, GJL-250 and GJL-350. The obtained volume elements are prepared for the numeri-

cal analyses by means of finite-element method. In the finite-element analysis, the metallic matrix is modeled with an elastic-plastic deformation law. The graphite inclusions are modeled nonlinear elastic in order to describe the typical tension-compression asymmetry for this material class. The stress-strain curves obtained

with the microstructure-based finite-element models agree well with experimental curves of tension and compression tests. Besides the analysis of the whole volume element, the scatter of the stress-strain response in smaller statistical volume elements is investigated. Numerical studies are performed to reduce computational costs.

Furthermore, the initial multiaxial yield behavior is analyzed. Therefore, the reconstructed volume elements are loaded bi- and triaxially beyond macroscopic yield. The shape of the obtained yield surfaces are compared to the surfaces of four continuum models which, amongst others, are proposed in literature to describe the inelastic behavior of gray cast iron with lamellar shaped graphite inclusions. It is found that none of these models is able to describe all features of the macroscopic yield surfaces obtained with the

microstructure-based finite-element models correctly. The initial inelastic flow direction is also computed at the onset of macroscopic yielding. The analysis shows that the inelastic flow is not normal to the yield surface. Therefore, a new yield function is proposed that is able to recompute the microstructure-dependent yield surfaces properly.

Besides the monotonic loading of the volume elements, also cyclic loading conditions are applied. Therefore, the isotropic elastic-plastic deformation law of the matrix material is substituted with a kinematic hardening law.

The obtained stress-strain hysteresis of the microstructure-dependent volume elements describes the experimental data very well.

Subsequently the macroscopic yield surfaces of the volume elements are analyzed after cyclic preloading.

## A Multiscale approach for thermo-mechanical simulations of loading courses in cast iron brake discs

CHRISTOPH HERRMANN<sup>1</sup>, STEFAN SCHMID<sup>1</sup>, DANIEL SCHNEIDER<sup>2</sup>, MICHAEL SELZER<sup>1,2</sup>, BRITTA NESTLER<sup>1,2</sup>

<sup>1</sup>Hochschule Karlsruhe, Institute of Materials and Processes, Germany

<sup>2</sup>Karlsruhe Institute of Technology, IAM - CMS, Germany

This talk presents a multiscale approach for the simulation of coupled heat and stress evolution induced by different loading courses in grey cast iron brake discs. The concept integrates the microstructural properties as homogenized material laws into the macroscopic computations. Extensive experimental testing is required to establish a complete set of material parameters required to conduct thermo-mechanical simulations on a macroscopic length scale. In addition, the microstructure can vary within the disc due to differences in wall thicknesses and cooling rates.

In order to reduce the experimental effort and to estimate the influence of microstructure characteristics on macroscopic heat and stress distributions, simulations on the mesoscopic scale resolving the heterogeneous microstructure with graphite flakes in a cast iron matrix are conducted. The workflow to derive the elasto-plastic properties according to its microstructure is demonstrated for a typical cast iron material. Geometrical parameters of the graphite phase distributions and shape

factors composed from micrographic analysis are used to generate three-dimensional representative volume elements (RVE) and to define the metallographic constituents. The information serves as input parameters to algorithmically construct cast iron microstructure.

The elastic and elasto-plastic material models of the constituents are briefly elucidated. In order to simulate the different material behaviour in tension and compression, a crack opening and crack closure mechanism is included. The potential of complementing and substituting experimental testing is shown by a quantitative comparison of the simulation results with experimental data at ambient temperature. Both, virtual tension and compression tests are executed as well as a tension-compression cycle. The presented approach provides a first step into a versatile range of applications and illustrates a broad potential for future challenges of multiscale modelling in the field of thermo-mechanical failure analysis.

# Multi-physics, Multiscale Modeling of Plastic Deformation in Plasma-Facing Components

N.M. GHONIEM,<sup>1</sup> J. BLANCHARD,<sup>2</sup> D. RIVERA<sup>1</sup>, E. GAO<sup>1</sup>, M. WASFY<sup>3</sup>, C. MARTIN<sup>2</sup>

<sup>1</sup> Mechanical & Aerospace Engineering Department, UCLA, Los Angeles, USA

<sup>2</sup> Department of Eng Physics and Nuclear Engineering, University of Wisconsin, Madison, USA

Plasma-facing components (PFCs) are exposed to unprecedented operational environments, thus requiring extraordinary research and development efforts. Physics-based models of material behavior are urgently needed to design new alloys or material architectures that can withstand the challenging and punishing conditions of high heat flux, neutron irradiation, plasma ion bombardment and thermomechanical transients. Advances in fundamental research on structural material degradation in a fusion environment serve two distinct purposes: (1) enable a rational process of alloy design and optimization for service life and performance, and (2) have a connection with mechanical design of fusion components. We present here a “Multiscale Modeling” strategy for determination of plastic deformation and damage in large-scale plasma-facing components. We focus on two main components: (1) the blanket and first wall structure of a fusion energy system (the ACT-2 Tokamak design), and (2) a test article representative of an element of a plasma divertor facing high heat flux. The method relies on the creation of successive coarse-grained elasto-plasticity models, with increased levels of spatial resolution and accuracy. At the largest scale, an elastic model with several millions degrees of freedom is used to determine the global stress and deformation, where the structural model is coupled with heat transfer and fluid flow models. Critical Regions (CRs), where failure is likely to occur are identified. Each CR is then modeled with a dislocation-density based, viscoplastic model that describes the evolution of plastic strain and associated dislocation densities, where the polycrystalline nature of the structure is smeared out. A region of the

structure is then represented as a polycrystal, and the viscoplasticity model is used to describe plastic flow and reveal damage accumulation at grain boundaries. Experimental results will also be presented for the dependence of the thermomechanical damage in tungsten test articles on the intensity and duration of the plasma heat flux, from plasma exposure experiments in an arcjet facility at UCLA. These results are presented in the context of an advanced Tokamak design with aggressive physics assumptions. The paper will conclude with an assessment of the viability of these structures in a typical Fusion Nuclear Science Facility (FNSF).

a) This material is based upon work supported by the U.S. Department of Energy, Office of Science, Office of Fusion Energy Sciences, under Award Number DE-FG02-03ER54708 with UCLA, and DE-FG02-98ER-54462 with the University of Wisconsin, Madison.

## References

- Shahram Sharafat, Aaron Aoyama, Nasr Ghoniem, Brian Williams, “Design and Fabrication of a Flat-Plate Multichannel He-Cooled Refractory HX for Divertor Applications,” *Fusion Science And Technology*, 60 (1), 203-207 (2011).
- S Sharafat, AT Aoyama, N Ghoniem, „Assessment of the DCLL TBM Thermostructural Response Based on ITER Design Criteria,” *Fusion Science & Technology* 60 (1), 264-271 (2011)
- T Crosby, NM Ghoniem, „Thermo-mechanical damage of tungsten surfaces exposed to rapid transient plasma heat loads, „*Interaction and Multiscale Mechanics* 4 (3), 207-217 (2011).

Talks Topic A8:

***Multiscale phenomena in plasticity***

## A Continuum Model for Dislocation Dynamics in Three Dimensions using the Dislocation Density Potential Functions

YANG XIANG, YICHAO ZHU

Department of Mathematics, the Hong Kong University of Science and Technology, Hong Kong

With the development of the micro-technology, an effective model, which properly describes the mechanical properties of crystals of size from the order of microns to sub-millimeters is highly expected. This is because for crystals at such physical length scales, there is still limitation in applying the existing plasticity theories, such as the discrete dislocation dynamical (DDD) models or the phenomenological continuum plasticity theories. Here a three-dimensional continuum model homogenized from the underlying dynamics of the dislocation substructures is derived by representing the existing dislocation ensembles with two dislocation density potential functions (DDPFs), denoted by  $\psi$  and  $\phi$  as shown in the figure. This piece of work is generalized from the continuum model for dislocation dynamics in a single slip plane [1-3].

With the DDPFs defined, the slip planes of dislocations are characterized by the contour surfaces of  $\psi$ , while the dislocation curves on each slip plane are identified by the contours of  $\phi$  on that plane. Some advantages in adopting such way in representing the dislocation substructures are straightforward: the geometries and the density distribution of the dislocation ensembles can be simply expressed in terms of the spatial derivatives of the two DDPFs. More importantly, one is able to summarize the underlying dislocation dynamics to explicitly write down an evolutionary system of constitutive equations, which include i) a stress rule, which describes how the internal stress field is determined in the presence of dislocation networks and applied loads; ii) a plastic flow rule, which describes how exist-

ing stress field drives the motion of the dislocation ensembles. The derived continuum model using the DDPFs are validated through comparisons with the DDD simulation and experimental observation. As an application of the derived continuum model, the "smaller-being-stronger" size effect on crystal strength observed in the uniaxial compression tests of micropillars is studied and an explicit formula between the yield stress  $\sigma_{\text{flow}}$  and the pillar size  $D$  is derived. The obtained formula shows excellent agreement with the experimental observations and it is found that  $\sigma_{\text{flow}}$  scales with  $\log(D)/D$ , which is not far from the empirical power law  $\sigma_{\text{flow}} \sim D^m$  with  $0 < m < 1$ .

### Acknowledgement

This work was partially supported by the Hong Kong Research Grants Council General Research Fund grants 606313.

### References

- Xiang, Y. (2009): Continuum approximation of the Peach-Koelher force on dislocations in a slip plane, *J. Mech. Phys. Solids*, 57:728-743.
- Zhu, X. H. and Xiang, Y. (2010): Continuum model for dislocation dynamics in a slip plane, *Philos. Mag.*, 90:4409-4428.
- Zhu, Y. C., Wang, H. Q., Zhu, X. H. and Xiang, Y. (2014): A continuum model for dislocation dynamics incorporating Frank-Read sources and Hall-Petch relation in two dimensions, *Int. J. Plast.*, 61:1835-1853.

## A Minimalistic Continuum Approach to Formation of Dislocation Patterns Under Multislip Conditions

DOMINIK STEINBERGER, STEFAN SANDFELD, MICHAEL ZAISER

Friedrich-Alexander-Universität Erlangen-Nürnberg, Institut für Werkstoffsimulation, Fürth, Germany

Failure in fatigue experiments is linked to the emergence of meta-stable dislocation patterns. Up to now the underlying mechanisms of their formation have not been understood entirely. Besides the desire to unravel these mechanisms from a materials research point of view, their knowledge would enable the development of countermeasures prolonging the lifetime of materials subjected to cyclic strain.

A prominent dislocation pattern is the so-called vein structure that arises during the initial cycles in fatigue experiments. It is characterized by bundles of edge dislocations that are separated by quasi dislocation free channels and is able to accommodate large plastic strains. Due to the limits of modern computers discrete simulations are not sufficient for the description of the formation of these patterns that involve the interaction

of a lot of dislocations in a large sample over long time spans. A remedy to those limitations are continuum models representing ensemble averages of dislocations.

In the present study, the formation of dislocation patterns during the first cycles of deformation under multislip conditions is investigated using a minimalistic quasi-2D continuum model [1] that a priori complies with the “similitude principle”. Instead of describing individual edge dislocations the model represents continuous ensemble averages of discrete edge dislocation systems. The driving force for the system of a positive and a negative edge dislocation density is an externally applied stress. A linear velocity law with a flow stress

is employed in order to take short-range interactions into account.

Using this model we analyze the underlying mechanisms of the dislocation structure formation under monotonic and under cyclic deformation. The influence of the stress amplitude and in the latter case the frequency on the evolution and shape of the patterns is investigated.

#### References

- [1] M. Zaiser and S. Sandfeld: Scaling properties of dislocation simulations in the similitude regime. *Modell. Simul. Mater. Sci. Eng.* 22, 065012 (2014)

## Orientation Dependence of the Forest Strengthening Studied with Dislocation Dynamics Simulations

VANESSA VERBEKE<sup>1</sup>, STEFAN SANDFELD<sup>2</sup>, BENOIT DEVINCRE<sup>1</sup>

<sup>1</sup>Laboratoire d’Etude des Microstructures, Châtillon, France

<sup>2</sup>Institute for Materials Simulation (WW8), Friedrich-Alexander-University Erlangen-Nürnberg, Germany

In the long march that leads from dislocation theory to the mechanical response of real materials, one finds collective dislocation processes and the formation of dislocation-patterned microstructures. Despite many years of investigations, dislocation patterning is an unsolved problem and a challenging issue since heterogeneities of the dislocation density cause strain incompatibilities in deformed crystals and therefore control kinematic hardening.

Dislocation-dislocation forest interactions are known to control plastic strengthening in FCC crystals. For this reason, details investigations have been made in the past years with Dislocation Dynamics (DD) simulations to improve the equation initially proposed by Taylor and linking the plastic critical resolved shear stress to the dislocation density accumulated in a material [1]. Today, tensorial forms of the “forest” or “Taylor” equation exist and provide to the continuous models (like crystal plasticity codes) the possibility to account for different strength level in the slip systems interactions. Nevertheless, such equations are physically justified only for simple loading conditions since they suppose a homogeneous distribution of the dislocation density [2-3].

In the present study, the concept of slip system interaction coefficients is now extended to calculate the ef-

fect of the dislocation density orientation (character) on the forest mechanism. From 3D-DD simulations, direction-dependent strengthening coefficients are determined. These new forest coefficients are thought to be essential parameters of the continuum dislocation dynamics (CDD) theory recently proposed by Hochrainer et al. [4-5] since they represent short range and orientation dependent driving forces for the formation of dislocation patterns.

#### References

- [1] B. Devincré, L. Kubin, and T. Hoc. (2006) Physical analyses of crystal plasticity by DD simulations. *Scripta Materialia*, 54:741–746, 2006.
- [2] B. Devincré, T. Hoc, and L. Kubin. (2008) Dislocation mean free paths and strain hardening of crystals. *Science*, 320:1745–1748.
- [3] L. Kubin, B. Devincré, and T. Hoc. (2008) Modeling dislocation storage rates and mean free paths in face-centered cubic crystals. *Acta Materialia*, 56(20):6040–6049.
- [4] T. Hochrainer, M. Zaiser, and P. Gumbsch. (2007) *Phil. Mag.*, 87(8-9):1261–1282.
- [5] S. Sandfeld, T. Hochrainer, P. Gumbsch, and M. Zaiser. (2010) *Phil. Mag.*, 90:3697–3728.

## Formation of Persistent Dislocation Patterns in the Similitude Regime

STEFAN SANDFELD, MICHAEL ZAISER

Institute for Materials Simulation (WW8), Friedrich-Alexander-University Erlangen-Nürnberg, Germany

Work hardening during plastic deformation of crystalline solids is associated with significant changes in dislocation microstructure. The increase in dislocation density on the specimen scale is accompanied by the quasi spontaneous emergence of regions of low dislocation density and clusters of high dislocation density which to a large extent persist upon unloading. These metastable structures are denoted as “dislocation patterns”. Despite a significant degree of morphological variation depending on slip geometry and loading mode (e.g. cell or labyrinth structures, dislocation accumulation in veins or walls), these patterns are characterized by some fairly universal scaling relationships. These relationships are commonly referred to as ‘law of similitude’ or ‘similitude principle’ [1]. They relate the characteristic length of deformation-induced dislocation patterns to the applied stress at which they have formed, and to their average dislocation density - which is interesting and also a useful fact that can be applied to expose models that generate ‘unphysical’ patterns, i.e. patterns that can not possibly be formed by dislocations. Despite long-standing efforts in the materials science and physics of defect communities, there is no general consensus regarding the physical mechanism which leads to the formation of dislocation patterns.

We present for the first time dislocation patterning results from a continuum theory that (i) captures the coupled dynamics of statistically stored and geometrically necessary dislocations while accounting for the specific kinematics of curved dislocation lines and (ii)

produces patterns that are consistent with the similitude principle. We show that already a minimum set of ‘ingredients’ is sufficient to create patterns - given that our set of continuum evolution equations are indeed able to represent fluxes of curved dislocations [2]. We start with a minimal model of dislocation patterning in a single slip configuration, which allows to comprehend the basic mechanisms that leads to pattern formation [3]. We then turn to more elaborate and realistic 3D models with multislip systems where latent hardening terms couple the dislocation densities on different slip systems through short-range interaction stresses. Our simulations explain how complex dislocation cell structures form which match those experimentally observed. Furthermore, we discuss which types of dislocation interactions are indispensable and which are not - explaining why some materials seem to form patterns more easily than others.

### References

- [1] M. Zaiser, and S. Sandfeld (2014) : Scaling Properties of Dislocation Simulations in the Similitude Regime. *Modelling Simul. Mat. Sci. Eng.*, 22(06).
- [2] T. Hochrainer, S. Sandfeld, M. Zaiser, and P. Gumbsch (2014) : Continuum dislocation dynamics: Towards a physical theory of crystal plasticity. *J. Mech. Phys. Solids*, 63:167-178.
- [3] S. Sandfeld, and M. Zaiser (2015) : Pattern formation in a minimal model of continuum dislocation plasticity. *arXiv preprint*, arXiv:1501.03527.

## Structural model of dislocation plasticity and twinning for high-rate deformation of metals

ALEXANDER MAYER<sup>1</sup>, VASILIIY KRASNIKOV<sup>1</sup>, ELIJAH BORODIN<sup>2</sup>

<sup>1</sup>Chelyabinsk State University, Chelyabinsk, Russia

<sup>2</sup>Institute of Problems of Mechanical Engineering RAS, St. Petersburg, Russia

We present a structural model of plasticity describing the coupled evolution of dislocations and microtwins in metals. The model is intended for the high-rate deformation conditions, including the high speed impact, the intensive electron or laser irradiation. It is based on our theoretical results for the dislocation plasticity (Krasnikov et al. 2010; Krasnikov et al. 2011; Mayer et al. 2013; Yanilkin et al. 2014) and twinning (Borodin et

al. 2014; Borodin & Mayer 2014). We propose the constitutive equation based on the dynamics and kinetics of defects (dislocations and microtwins), which seems to be the most natural way of the plasticity description. It is especially important for the dynamical problems, where this approach allows one to take into account the inertness of the plastic relaxation in deformed substance.

The model includes equations of the mechanics of continua for elastic-plastic medium, where the plastic deformation tensor is determined as a result of the structural defects evolution in the material. The next processes are accounted: a) motion, generation and immobilization of dislocations; b) formation, growth and immobilization of twins. Interaction of the defect subsystems is accounted through their barrier stresses. All possible crystallographic orientations of dislocations and twins are considered in the general model, while only active ones are accounted in the simplified version of the model.

The structural approach demands a little bit more parameters than the empirical model, but this disadvantage can be overcome, partially due to involvement of the molecular dynamics simulation results (Krasnikov et al. 2010; Yanilkin et al. 2014), and partially due to an appropriate theoretical consideration. Resulting model is a self-consistent and allows one to determine the mechanical properties in a wide range of strain rates and thermodynamic conditions and investigate the defect subsystems modification.

Complete equations system and numerical method for its solution are developed for 1D and 2D cases. Verification of the model on the basis of experimental data from literature is presented. Attenuation of the elastic precursor in thin metal foils, change of shape of samples in the Taylor impact tests, modification of the defects density in the course of deformation, and localization of plastic deformation are discussed on the basis of our structural model.

Work is supported by the Ministry of Education and Science of the Russian Federation (state task No. 3.1334.2014/K) and grant of the President of Russian Federation (MD-286.2014.1)

#### References

- Krasnikov, V.S., Kuksin, A.Yu., Mayer, A.E. & Yanilkin, A.V. 2010: Plastic deformation under high-rate loading: the multiscale approach. – *Phys. Solid State*, 52: 1386–1396.
- Krasnikov, V.S., Mayer, A.E. & Yalovets, A.P. 2011: Dislocation based high-rate plasticity model and its application to plate-impact and ultra short electron irradiation simulations – *Int. J. Plast.*, 27: 1294–1308.
- Mayer, A.E., Khishchenko, K.V., Levashov P.R. & Mayer, P.N. (2013): Modeling of plasticity and fracture of metals at shock loading. – *J. Appl. Phys*, 113: 193508.
- Yanilkin, A.V., Krasnikov, V.S., Kuksin, A.Yu. & Mayer, A.E. 2014: Dynamics and kinetics of dislocations in Al and Al–Cu alloy under dynamic loading. – *Int. J. Plast.*, 55: 94–107.
- Borodin, E.N., Atroshenko, S.A. & Mayer, A.E. 2014: Distribution of dislocations and twins in copper and 18Cr–10Ni–Ti steel under shock-wave loading. – *Techn. Phys.*, 59: 1163–1170.
- Borodin, E.N. & Mayer, A.E. 2014: Localization of plastic deformation and mechanical twinning in dynamical channel angular pressing. – *IOP Conf. Series: Mat. Sci. Engng*, 63: P. 012034.

Talks Topic A9:

***Multiscale phenomena in plasticity***

# Stress and Strain Fluctuations in Plastic Deformation of Crystals with Disordered Microstructure

OLGA KAPETANO<sup>1,2</sup>, MARKUS STRICKER<sup>3</sup>, DANIEL WEYGAND<sup>3</sup>, MICHAEL ZAISER<sup>1,2</sup>

<sup>1</sup>Institute for Materials Simulation (WW8), Friedrich-Alexander-University Erlangen-Nuremberg, Germany

<sup>2</sup>School of Engineering, Institute for Materials and Processes, The University of Edinburgh, UK

<sup>3</sup>IAM-ZBS, Karlsruhe Institute of Technology, Karlsruhe, Germany

In this study we investigate spatial fluctuations of stress and strain in plastic deformation of crystals with disordered (dislocation) microstructure. For this purpose we combine theoretical arguments with plasticity simulation results. More specifically we obtain results from three different models and subsequently we investigate the statistical properties of these fluctuations.

The first model is a 2D generic model of bulk crystal plasticity with stochastic evolution of the local microstructure which was used, proposed by Zaiser and Morreti [1]. Internal stresses in a system with periodic boundary conditions are calculated using a Greens function method. Space is discretized into a lattice and local flow stresses in the lattice cells evolve randomly with local strain according to a stationary stochastic process. The second model is a 2D discrete dislocation simulation in a bulk crystal with periodic boundary conditions [2] where dislocations are initially distributed at random on a grid and then move under the combined action of a remotely applied stress and of their mutual interactions. In this case dislocations are allowed to move to a neighbouring grid point if such a move decreases the elastic energy of the system. Both models consider deformation to occur on a single slip system. To reduce artefacts associated with the periodic boundary conditions, the simulation lattice is tilted by a generic angle  $\phi$  with respect to the slip direction such as to avoid wrapping slip planes onto themselves. The last model is a 3D discrete dislocation dynamics model which simulates micro pillars with free side surfaces under strain controlled compression. The method superimposes a finite element method to evaluate the stresses due to surface tractions and boundary constrains with a nodal representation of dislocation lines to simulate the evolution and interactions of the dislocations [3].

For all three models we investigate the scale-dependent magnitude of local fluctuations of internal stress and plastic strain. We determine the fluctuations of internal stress and plastic strain as the differences between the local values of the resolved shear stress and the plastic slip, and their system-scale averages, then we coarse grain these variables by averaging over different box sizes and different simulations to investigate the scale dependency. Finally, we determine the spatial structure of the respective auto and cross-correlation functions for the 2D models.

We demonstrate that the spatial structure of stress and strain fluctuations as well as the respective cross correlation functions can be evaluated from a single correlation function which characterizes the pattern of geometrically necessary dislocations in the deforming crystal. The investigations show that, after an initial transient characterized by uncorrelated initiation of plasticity in different sample locations, nontrivial long range correlations emerge in this pattern. We investigate the influence of boundary conditions on the observed spatial patterns of stress and strain and discuss implications of our findings for larger-scale plasticity models.

## References

1. Zaiser, M. and P. Moretti, *Fluctuation phenomena in crystal plasticity - a continuum model*. 2005.
2. Ispánovity, P.D., et al., *Average yielding and weakest link statistics in micron-scale plasticity*. Acta Materialia, 2013. **61**(16): p. 6234-6245.
3. Weygand, D., et al., *Aspects of boundary-value problem solutions with three-dimensional dislocation dynamics*. 2002.

## Strain localization and surface effects in 2D and 3D stochastic models of amorphous plasticity

DAVID FERNANDEZ CASTELLANOS, STEFAN SANDFELD

Institute of Materials Simulation, FAU, Fürth, Germany

A key challenge for understanding plasticity in amorphous materials is the link between microscopic (i.e., atomistic) and macro-scale behaviour (i.e., the scale of the sample). To establish this link, it is useful to coarse-grain the microscopic details and construct a mesoscopic model that captures important aspects from the atomistic scale without fully resolving the atomic motions, being thus computationally more efficient. The common approach taken in mesoscale descriptions of amorphous plasticity is to consider plastic activity as a sequence of spatially and temporally localized events, known as shear transformations (Argon 1983), which correspond to local rearrangements of atoms within the bulk material in response to the locally acting shear stress. Amorphous plasticity arises then as a stochastic phenomenon, consequence of the elastic interaction of a big number of such individual plastic events, whose self-organization leads to the emergent plastic deformation on the specimen scale. Additionally, this process is dependent on the system geometry and material loading conditions.

Using a finite element-based approach (Sandfeld 2015), we can account for different boundary conditions and simulate the deformation process of the sample in a

‘bottom-top’ approach. We present results for different 2D and 3D loading scenarios such as pure shear, simple shear or bending. Depending on the applied load, the (average) plastic strain patterns are found to have a shape that resembles the external stress field, with some additional non-trivial characteristic features. We characterize the plastic yield transition of each loading scenario with statistical measures, such as critical exponents (Budrikis 2013). We will study the effects of softening in the localization of the deformation and failure of the samples, and will find that the presence of surfaces naturally introduces a position dependent hardening.

### References

- Sandfeld, S. (2015): Avalanches, loading and finite size effects in 2D amorphous plasticity. ArXiv:1411.2473. Submitted to J. Stat.
- A.S. Argon and L.T. Shi. (1983): Development of visco-plastic deformation in metallic glasses. *Acta Metallurgica*, 31(4):499 – 507
- Zoe Budrikis and Stefano Zapperi (2013). Avalanche localization and crossover scaling in amorphous plasticity. *Phys. Rev. E*, 88:062403.

## Numerical investigation of welding residual stress field in tubular joints considering the effects of solid-state phase transformation

KIMIYA HEMMESI<sup>1</sup>, MAJID FARAJIAN<sup>2</sup>, DIETER SIEGELE<sup>2</sup>

<sup>1</sup> Institute of Applied Materials - Computational Materials Science IAM-CMS, Karlsruhe Institute of Technology, Germany

<sup>2</sup> Fraunhofer Institute for Mechanics of Materials IWM, Freiburg, Germany

In order to achieve fatigue resistant welded structures, it is necessary to manage and control welding process related factors which affect the fatigue strength. These factors are sometimes present as welding defects and sometimes as inevitable residual stresses which are unwanted byproducts of welding processes. This subject has been treated in welding research communities since the 50s. The earliest evidence of detrimental effect of welding residual stress on fatigue was reported in 1956 (Kudryavtsev 1956, Trufyakov 1958). The extent of this effect was however unclear and is still matter of debate. Having advanced predictive tools for determin-

ing accurately welding residual stresses will not only lead to the possibility of considering precise welding residual stress effects during life estimation, but also can be useful to have effective measures for the subsequent mitigation or modification processes on the welding residual stress fields.

Circumferential butt weld is one of the most common type of joints in tubular welded structures. Complicated welding residual stress field and specially the through thickness stress variation can be a threat to the structural integrity. Beside the complexity of the tubular welded joints, there exists also a number of key

problems which have not completely solved. For example, in the context of carbon steel weld, it has been recognized that solid-state phase transformation should be taken into account in the welding simulation (Leblond & Devaux 1984). During welding, the thermal stress caused by the non-uniform plastic deformation field leads to the formation of welding residual stresses. In the materials with solid-state phase transformations during cooling, other factors like phase volume changes, mechanical properties variation due to microstructure change and transformation induced plasticity, also influence the development of welding residual stresses. However, limited studies have been conducted in the field of welding residual stresses in steel pipes considering the metallurgical transformations. Chin-Hyung and Kyong-Ho have simulated the residual stresses in tubular welded joints of high strength carbon steels, considering the effects of phase transformation (Chin-Hyung & Kyong-Ho 2011). Deng and Murakawa have studied the different factors related to the solid-state phase transformations in formation of residual stresses in carbon steel welded joints. Based on the results, transformation plasticity has the minor effect rather than the other parameters in Austenite-Martensite phase transformation of medium carbon steels (Deng & Murakawa 2013).

The objective of this study is to investigate the effects of phase transformations on the residual stress field in welded tubular joints made of structural steel S355J2. SYSWELD software is used to calculate the welding re-

sidual stresses by integrating the metallurgical transformation effects in order to compute the link between material microstructure and residual stresses. Thermal and metallurgical calculations, couple temperatures and phase Proportions by considering the latent heat of fusion/solidification and the transformations in the transient heat conduction equation. Obtained results from this early stage which include both thermal and metallurgical history, are used as input data for mechanical calculations afterward.

#### References

- Kudryavtsev, I. V. (1956): The influence of internal stresses on the fatigue endurance of steel, *Int. Conf. on Fatigue*, I. Mech. E, 317.
- Trufyakov, V. I. (1958): Welded joints and residual stresses, *Br. Weld. J*, Vol. 5, 11: 491-498.
- Leblond, J. B. & Devaux, J. A. (1984): new kinetic model for anisothermal metallurgical transformations in steels including effect of austenite grain size, *Acta Metallurgica*, Vol. 32, 137-146.
- Chin-Hyung, L. & Kyong-Ho, C. (2011): Prediction of residual stresses in high strength carbon steel pipe weld considering solid-state phase transformation effects, *Computers & Structures*, Vol. 89, 256-265.
- Deng, D. & Murakawa, H. (2013): Influence of transformation induced plasticity on simulated results of welding residual stress in low temperature transformation steel, *Computational Materials Science*, Vol. 78, 55-62.

## The influence of GP and GDP precipitates on the viscoplastic material behaviour of Inconel 718

ANDREAS DREXLER<sup>1</sup>, HERMANN MADERBACHE<sup>2</sup>, HANS-PETER GÄNSER<sup>1</sup>, WERNER ECKER<sup>1</sup>, ANDREAS FISCHER-SWORRING-BUNK<sup>3</sup>, BERND OBERWINKLER<sup>4</sup>

<sup>1</sup>Materials Center Leoben Forschung GmbH, Austria

<sup>2</sup>Department Product Engineering, Chair of Mechanical Engineering, Montanuniversität Leoben, Austria

<sup>3</sup>MTU Aero Engines AG, Munich, Germany

<sup>4</sup>Böhler Schmiedetechnik GmbH & Co KG, Kapfenberg, Austria

The standard heat treatment process of turbine disks from Inconel 718 starts with air cooling from the forging temperature of approximately 1000 °C to room temperature. Afterwards the turbine disks are reheated in a furnace for the two-step ageing sequence at the temperatures 720 °C and 620 °C for 8 hours each. The viscoplastic deformation of the turbine disks during the full heat treatment process is caused by the inhomogeneous initial temperature field and the thermal gradients during air cooling and heating. In the end there are considerable residual stresses inside the disks, which may influence the lifetime markedly.

The main aim of the present work is to study the viscoplastic material behaviour in the relevant temperature

range of the heat treatment process. This includes also the temperature regime below 900°C, in which precipitates are formed. Viscoplastic material behaviour in the high temperature regime includes climb controlled and glide controlled deformation. Climb and glide as well as the transition between these two mechanisms are described by a phenomenological sinhyp function. The transition stress depends on the volumes and radii of GP and GDP precipitates. This dependence is incorporated into the sinhyp function.

For the mechanical characterisation of the viscoplastic material behaviour, creep tests are performed at different stresses and temperatures. Stress and temperature ranges are estimated in advance using finite element

simulations. The measured time-temperature curve of each specimen is linearly fitted and used as an input for the precipitation kinetics simulation software MatCalc. The MatCalc software provides information about the evolution of the mean radius and volume fraction of the GP and GDP precipitates during the creep measurements. For this purpose a user-written MatCalc software routine is provided by Böhler Schmiedetechnik. The MatCalc predictions are validated with the results of tensile tests and neutron measurements. The understanding of the influence of GP and GDP precipitates on the viscoplastic material behaviour is used to develop a material model. The model can be used for time and cost efficient and yet accurate finite element simulations of the residual stress evolution in turbine disks from Inconel 718 during the heat treatment process.

#### References

- Arzt, E., "Creep of Dispersion Strengthened Materials: A Critical Assessment", *Res Mechanica*, Vol. 31 (1991), pp. 399 - 453
- Charturvedi, M.C. and Han, Y., "Strengthening mechanisms in Inconel 718 superalloy", *Metal Science*, Vol. 17 (1983), pp. 145 – 149
- Oblak, J.M. *et al.*, "Coherency Strengthening in Ni Base Alloys Hardened by DO22 GDP Precipitates", *Metallurgical Transactions*, Vol. 5 (1974), pp. 143 - 153
- Han, Y. and Charturvedi, M.C., "A Study of Back Stress During Creep Deformation of a Superalloy Inconel 718", *Materials Science and Engineering*, Vol. 85 (1987), pp. 59 - 65
- Han, Y. and Charturvedi, M.C., "Steady State Creep Rate Equation of Inconel 718 Superalloy", *Chin. Journal Metallurgy Science Technology*, Vol. 5 (1989), pp. 79 - 84
- Han, Y. *et al.*, "Coarsening behaviour of GP- and GDP-particles in Inconel alloy 718", *Metal Science*, Vol. 16 (1982), pp. 555 - 561
- Frost, H.J. and Ashby, M.F, *Deformation Mechanism Maps – The Plasticity and Creep of Metals and Ceramics*, 1<sup>st</sup> ed., Pergamon Press GmbH (Kronberg-Taunus, 1982)
- Heilmaier, M. and Reppich, B., "Particle threshold stresses in high temperature yielding and creep: a critical review", *Creep Behavior of Advanced Materials for the 21<sup>st</sup> Century*, pp. 267 - 281

## A representative volume element based multiscale modeling of fish scale

A.M. RAJENDRAN, M.P. NELMS

Department of Mechanical Engineering, University of Mississippi, Oxford, USA

Biological materials (biomaterials) often contain a more structured hierarchy from macro- to nanoscale (Gao & Ji 2004) that is not currently possible with today's engineering composites. The robust mechanical behavior has caused an increasing interest in biomaterial modeling and bio-inspired design of advanced material systems (Wu 2011). With this comes a need for the development of theoretical mechanics and the computational methods that aid in the understanding of such diverse biomaterials that otherwise cannot be determined from physical experiments.

*Atractosteus spatulas* (Alligator gar) possess a flexible dermal armor consisting of overlapping ganoid scales. Each scale is a bilayer hydroxyapatite and collagen-based biocomposite for defense against predation. The fish scale is defined by a stiff outer ganoine layer, a characteristic "sawtooth" pattern at the interface and a soft bone inner layer with all materials exhibiting a decreasing elastic modulus, yield strength and density through the thickness. Experimental testing of the fish scales display properties such as damage localization, tortuous crack path propagation and energy dissipation that are unique to biological dermal armor. The

main objective of this investigation is to quantify the effects of the material grading as a function of depth as well as the influence of the geometrically anisotropic interface between the ganoine and inner bone layers on the elastic properties. The fish scale was modeled with a high resolution (over one million elements) representative volume element (RVE) using the ABAQUS<sup>®</sup> finite element software. The effective properties of the RVE have been determined for both kinematics and periodic boundary conditions. Preliminary results with an idealized elastic-perfectly plastic description has revealed that the effect of microscopic archistructure and the nonlinear material response on the dissipative energy and stress redistribution is to significantly to reduce von-Mises stresses (84-91% of effective stress) at the bone interfaces.

The main objective of this investigation is to quantify the effects of the material grading as a function of depth as well as the influence of the geometrically anisotropic interface between the ganoine and bone layers on the elastic properties. The fish scale interface was modeled using the finite element method. The results were based on an idealized elastic-perfectly plas-

tic mathematical model. The mathematical model was used to infer the effects of the nonlinear material response in terms of energy dissipation and stress redistribution at the ganoine-bone interfaces. The fish scale was modeled with a high resolution (over one million elements) representative volume element (RVE) using the ABAQUS<sup>®</sup> finite element software. The effective properties of the RVE have been determined for both kinematics and periodic boundary conditions. Preliminary results with an idealized elastic-perfectly plastic description has revealed that the effect of microscopic archistructure and the nonlinear material response on the dissipative energy and stress redistribution is to

significantly to reduce von-Mises stresses (84-91% of effective stress) at the bone interfaces.

#### References

- Gao, H. & Ji, B. (2004): Modeling fracture in nano materials - In: IUTAM Symposium on Asymptotics, Singularities and Homogenisation in Problems of Mechanics (307-316). Springer Netherlands.
- Wu, M. S. (2011). Strategies and challenges for the mechanical modeling of biological and bio-inspired materials. *Materials Science and Engineering: C*, 31(6), 1209-1220.

## Multiscale crystal plasticity simulation on anisotropic yielding behavior of ultrafine-grained metal

YOSHITERU AOYAGI

Department of Nanomechanics, Tohoku University, Japan

High-strength, light-weight metal materials are required to improve safety and reduce transportation cost. Ultrafine-grained (UFG) metals produced by severe plastic deformation have attracted interest as high-strength materials. UFG metals with a grain size of less than 1  $\mu\text{m}$  exhibit remarkable mechanical properties (e.g., increased yield stress, decreased hardening ratio, yield point drop of FCC metal, temperature dependency, tension-compression asymmetry, and increased strain-rate sensitivity). A computational model predicting these properties is desired in the field of materials science and engineering. Multiscale crystal plasticity models expressing a size effect on grain size have been proposed by introducing information on grain size as a material parameter (Ohashi, Kawamukai & Zbib 2007, Ohno & Okumura 2007). However, conventional theory cannot express the effect of the grain boundary precisely and directly. It is assumed that such unusual mechanical properties originate from the enormous volume fraction of the grain boundary. Grain boundaries play important roles in dislocation dynamics. Recently, the effect of the grain boundary has attracted the attention of many researchers as an important factor determining the mechanical properties of UFGM. The authors propose a reaction-diffusion system expressing dislocation patterning in order to

reproduce the fine graining caused by severe plastic deformation (Aoyagi, Tsuru & Shimokawa).

In our previous work, we proposed a crystal plasticity model considering the behavior of the dislocation source and the grain boundary as a dislocation source. In order to predict the variation of critical resolved shear stress due to grain boundaries, mobile dislocations, or dislocation sources, information on these crystal defects is introduced into a hardening law of crystal plasticity. In this study, information on crystal orientation and shape are introduced into a computational model for multiscale crystal plasticity simulation considering the effects of grain boundaries and dislocation sources. We perform FE simulation for Al polycrystal to investigate the effects of dislocation behavior and crystal orientation on anisotropic yielding behavior of the UFG material. The validity of this model is investigated by comparing experimental and numerical data.

#### References

- Ohashi, T., Kawamukai & M., Zbib, H. M. (2007): *International Journal of Plasticity* 23: 897-914.
- Ohno, N. & Okumura, D. (2007): *Journal of the Mechanics and Physics of Solids* 55: 1879-1898.
- Aoyagi, Y., Tsuru, T. & Shimokawa, T. (2014): *International Journal of Plasticity* 56: 43-57.

Talks Topic B 1:

## ***Residual stresses***

---

## Fatigue Strength of Anodized Al 7050-T7451

HERMAN JACOBUS CORNELIS VOORWALD, JOSÉ ANDRÉ MARIN DE CAMARGO, MARIA ODILA HILÁRIO CIOFFI, MIDORI YOSHIKAWA PITANGA COSTA

Department of Materials and Technology, Guaratinguetá, Brazil

In aircraft design, each component presents a group of mechanical properties according to the application. As an example, for landing gear considering these characteristics and cyclic loadings, high strength and fatigue resistance are fundamental design criteria. In aluminum alloys, the 7xxx series are predominating alloys when strength is the primary requirement.

Several corrosive environmental friction forces imposed to structural components usually reduce the service life. Therefore wear and corrosion control of several components is accomplished by surface treatments. In the case of aluminum alloys, sealed anodic layers confers protective efficiency against corrosion which; on the other hand, degrade the fatigue life performance of the base material.

Tensile residual stresses and cracks noticed at the interface coating/substrate are associated to reduction in the fatigue strength of anodized base material. In the case of tensile residual stresses, the initiation and propagation phases of the fatigue process are accelerated; whereas compressive stresses close to the surface may increase fatigue life.

The technique to improve the coated materials fatigue strength, is the shot peening process, which induce compressive residual stresses on the surface, in order to delay or even avoid nucleation and propagation phases.

The objective of this research is to evaluate the influence of anodic films grown on Al 7050-T7451 aluminum alloy, by sulfuric acid anodizing, chromic acid anodizing and hard anodizing, on the rotating bending fatigue strength. As already mentioned, the influence of anodic films grown on Al 7050-T7451 aluminum alloy is to degrade the stress life fatigue performance of base material. A significant improvement in the fatigue life in comparison to anodic surface coated and base material was obtained for shot peened coated specimens. The base material used in the investigation was the Al7050-T7451 aluminum alloy. Mechanical properties

are: elastic modulus 65GPa, yield strength 429MPa ultimate tensile strength. 502MPa and elongation 10%. Specimens were prepared from a  $19 \times 10^{-3}$ m thick Al7050-T7451 aluminum alloy rolled plate with the rolling axis parallel and perpendicular to the loading axis. Aluminum alloy specimens were obtained by grind machining, which represents surface roughness  $R_a = 0,89 \pm 0,32 \mu\text{m}$ . S-N curves were obtained for the aluminum alloy treated with shot peening intensity of 0,013N (30psi), using glass shot ( $\varnothing$  0,4mm) with coverage of 120%, carried out on an air-blast machine according to standard MIL-13165. The residual stress field induced by shot peening and anodizing, was determined by X-Ray diffraction method. Coating thickness for chromic acid anodizing, sulfuric acid anodizing and hard anodizing was, respectively,  $3,8 \mu\text{m}$ ;  $14,2 \mu\text{m}$  and  $65,0 \mu\text{m}$ . Rotating bending fatigue test parameters were: stress ratio equal -1,0; frequency of 50Hz and room temperature.

Scanning electron microscopy technique and optical microscopy were used to observe crack origin sites thickness and coating/substrate adhesion.

### References

1. José André Marin de Camargo, Herman Jacobus Cornelis Voorwald, Maria Odila Hilário Cioffi, Midori Yoshikawa Pitanga Costa, Coating Residual Stress Effects on Fatigue Performance of 7050-T7451 Aluminum Alloy. *Surface & Coatings Technology* 201 (2007) 9448-9455.
2. A.L.M. Carvalho, H.J.C. Voorwald, Influence of Shot Peening and Hard Chromium Electroplating on the Fatigue Strength of 7050-T7451 Aluminum Alloy. *International Journal of Fatigue*, vol.29, p.1282-1291, 2007.
3. J.A.M. Camargo, H.J.C. Voorwald, Influence of Anodization on the Fatigue Strength of 7050-T7451 Aluminum Alloy. *Fatigue & Fracture of Engineering Materials & Structures*, vol.30, p.993-1007, 2007.

## The Influence of Residual Stress on the Failure Modes in a Thermal Barrier Coating System

DONG LIU<sup>1</sup>, CLAUDIA RINALDI<sup>2</sup>, PETER E J FLEWITT<sup>2</sup>

<sup>1</sup>School of Physics, HH Wills Physics Laboratory, University of Bristol, UK

<sup>2</sup>RSE - Ricerca sul Sistema Elettrico SpA, Milan, Italy

Thermal barrier coatings (TBC) are applied to components working at elevated temperatures. These are applied in combination with the internal cooling, so that a thermal gradient is generated through the thickness of the ceramic layer to sustain an appreciable temperature difference between the hot working media and the surface of the superalloy component. A thermal barrier coating system normally consists of three layers: (i) an outer ceramic coating, the TBC, to insulate the superalloy substrate from the high temperature gas flow; (ii) a metallic bond coat (BC) to provide good adherence for the TBC to the substrate as well as oxidation and/or corrosion protection for the underlying superalloy, and (iii) a thermally grown oxide (TGO) layer predominately  $\alpha$ -Al<sub>2</sub>O<sub>3</sub> that is formed at the TBC/BC interface at temperature during service. The durability, stability and integrity of the coatings are of significant importance, yet the failure of TBC systems in-service is a complex and not fully-understood process (Evans et al 2001). Failure normally occurs in the form of local detachment and spallation of the TBC layer (Miller et al 1982). The stored strain energy in the system is recognised as a main driving force for the failure (Padture et al 2002). Hence, residual stresses are acknowledged to contribute to potential failure in this multi-layer system. These stresses arise from mainly the growth of the TGO, and the mismatch stresses due to the different expansion coefficients between the constituent layers (Padture et al 2002). The failure of these multi-layered systems is also dependent on component geometry.

In the present work, a typical thermal barrier coating produced by electron physical vapour deposition (EPBVD) that usually applied on rotatory components such

as turbine blades in jet engines is studied. This EPBVD TBC is applied to a Ni-based single crystal superalloy aero-blade substrate with changing curvature, and the intermediate coating is platinum aluminate BC. The residual stresses generated in the outer ceramic thermal barrier coating (TBC) and the thermally grown oxides (TGO) have been evaluated non-destructively by Raman spectroscopy (RS) and photo-stimulated luminescence piezo-spectroscopy (PLPS) respectively. It has been found that there were tensile residual stresses in the as-fabricated TBCs, and these stresses became compressive with extended thermal exposure. For the TGO, the residual stresses were measured using a Renishaw Raman system, model 2000 (Bristol University) and an in-house built PLPS system developed at RSE, Italy which has automatic mapping for large areas. These residual stresses are analysed as a function of the thermal exposure and the substrate curvature. The discussion focuses on understanding the role of substrate curvature on microstructural degradation of the TBCs, and the magnitudes/distribution of the residual stresses in the TBCs and TGO. The results are considered with respect to overall coating integrity.

### References

- Evans, A.G., Mumm, D.R., Hutchinson, J.W., Meier, G.H., Pettit, F.S.: (2001) *Prog. Mater. Sci.*, 46, 505-553.  
 Miller, R.A., Lowell, C.E. (1982) *Thin. Solid. Films.*, 95, 265-273.  
 Padture, N.P., Gell, M., Jordan, E.H.: (2002) *Science*, 296, 280-284.

## Overloads on cracks: using Barkhausen microscope and SEM-based digital image correlation to evaluate mechanisms and effects on local (residual) stress fields

MATTHIAS THIELEN<sup>1</sup>, MEISAM SHEIKH-AMIRI<sup>2</sup>, MICHAEL MARX<sup>1</sup>, CHRISTIAN BOLLER<sup>2</sup>, CHRISTIAN MOTZ<sup>1</sup>

<sup>1</sup>Saarland University, Chair of Materials Science and Methods, Saarbrücken, Germany

<sup>2</sup>Saarland University, Chair of Nondestructive Testing and Quality Control, Saarbrücken, Germany

Most models that describe or predict fatigue failure and fatigue crack propagation are based on the simplification that materials are subjected to constant amplitude loadings. However, in-service loadings usually

do not fulfill this assumption which causes the calculations and predictions to become complex or even wrong. One important effect which is responsible for some divergences in the models is the so called over-

load effect. This well known phenomenon describes the behaviour of a growing fatigue crack that was subjected to an overload at least for one cycle: the resulting effect is a strong crack growth deceleration.

Although the phenomenon of the overload effect has been known for many years now, it has been the subject of multiple discussions regarding the underlying mechanisms. Actually, two reasons have been discussed: Plasticity induced crack closure (PICC) behind the crack tip or residual stresses (RS) in front of it. Whereas PICC is said to delay the crack opening to higher loads and therefore to a reduced  $\Delta K$  due to a reduced  $K_{min}$ , RS prevent the crack to open completely which causes a  $\Delta K$  reduction through  $K_{max}$ .

One major point which hindered the solution of the discussion, was the lack of possibilities to measure local RS fields and strain fields resulting from applied forces. However, last year's developments of high resolution synchrotron XRD strain field mapping have lead to several publications regarding this topic. Nevertheless, as the requirements for these measurements are high, results have so far been obtained by third generation synchrotron radiation with quite limited availability. Accordingly, there are hardly any extensive studies on this topic that allow a proper model development. Starting from this point, we chose two different tech-

niques to investigate the aforementioned effects. The induced RS fields in front of and behind the crack tip were analyzed using a Barkhausen Noise and Eddy Current Microscope (BEMI). It was also analysed how they change with the overload and with the crack growth through the stress field. After a custom calibration based on the application of defined plastified samples in situ under well known loading states we have been able to measure the residual stresses quantitatively and with a spatial resolution of  $10\mu\text{m}$ . The RS distribution showed a strong correlation with the local crack grow rate.

The second technique, high resolution Digital Image Correlation in the scanning electron microscope was used to investigate the strain field in situ due to applied forces and crack tip opening displacement and its change with changing RS. We were able to measure the strain fields up to elastic strains that could be assigned to the RS effect, whereas the opening behaviour (PICC) did not show a significant contribution.

The good accessibility of these techniques allows further studies of different loading cases to develop a model to improve the description of variable amplitude loading effects. Furthermore it can be used to measure local RS and its influence on fatigue crack growth.

## Assessment of shot-peening on fatigue life prediction: microstructural effects

LOUISE TOUALBI<sup>1</sup>, PASCALE KANOUTÉ<sup>1</sup>, SERGE KRUCH<sup>1</sup>, ARNAUD LONGUET<sup>2</sup>, ALEXANDRE SEROR<sup>2</sup>, JEAN-PATRICK GOULMY, QUENTIN PUYDT<sup>3</sup>

<sup>1</sup>Onera – The French Aerospace Lab, Châtillon, France

<sup>2</sup>Snecma, Groupe Safran, Moissy-Cramayel, France

<sup>3</sup>IRT-M2P, Metz, France

Surface enhancement methods, such as shot peening, are widely used in the aerospace industry to improve the fatigue life of critical component. Such process generates residual compression stresses which tend to delay fatigue crack initiation and prevent small crack propagation.

However, surface enhancement methods are efficient only if the thermo-mechanical relaxation of residual stresses at operating temperatures is moderate.

In order to assess the benefit of shot peening on the fatigue life of IN718 turbine disk, a whole understanding of the microstructure modifications induced by shot peening is needed. The critical point is to evaluate how fast the residual stresses relax at high temperature.

As detailed in [1], the effect of work hardening is preponderant. There is a strong dependence of the degree of work hardening induced by creation of the compres-

sive layer on the amount of relaxation during thermal loadings.

Furthermore, work hardening is strongly related to the microstructure. The microstructural state of the component part before shot peening can then significantly modify the effect of this surface enhancement method. This study aims to investigate the impact of the initial microstructure on the residual stresses and the work hardening induced by shot peening. Assessment of initial hardening, grain size and strengthening precipitates, which are specific parameters of the turbine disk, is needed.

Different initial hardening states are obtained by taking samples from different parts of the disk (bore, rime and web samples). Effect of grain size and strengthening precipitates are specifically investigated through model microstructures. These extreme microstruc-

tures, which are achieved by performing specific heat treatments, make it possible to discriminate the impact of relevant microstructural parameters. Two grain sizes and two strengthening precipitate sizes are considered.

Microstructure evolution is followed by SEM observations and Backscatter analysis. The X-ray diffraction method is both used to assess the residual stresses by measuring the peak shift and to evaluate the work hardening through diffraction peak width determination [2]-[4]. This method requires calibration measurements, which are performed on tensile specimens in which a specific amount of work hardening is introduced.

Finally, the impact on the shot peening efficiency is evaluated by comparing the thermal relaxation of a variety of initial microstructures.

## References

- [1] Prev y, P. S. (2000): The effect of cold work on the thermal stability of residual compression in surface enhanced IN718. – In: 20<sup>th</sup> ASM Materials Solutions Conference & Exposition Proceedings, St. Louis, Missouri, October 10-12, 2000.
- [2] Moore, M. G. and Evans, W. P. (1958): Mathematical correction for stress in removal layers in X-ray diffraction residual stress analysis. – In: SAE Trans. 66, pp. 340-345.
- [3] Prev y, P. S. (1987): The measurement of subsurface residual stress and cold work distributions in nickel base alloys. – In: Residual Stress in Design, Process and Materials Selection, ed. W. B. Young, ASM, Metals Park, OH, pp. 11-19.
- [4] Francois, M., Convert, F. and Lu, J. (1996) : ‘X-ray diffraction method’ Handbook of measurement of residual stresses. – In: Society of Experimental Mechanics, Fairmont Press, Lilburn, GA, pp. 71-132.

## Thermal Stability of Residual Stresses in Ti-6Al-4V components

ALEKSANDAR STANOJEVIC<sup>1</sup>, HERMANN MADERBACHER<sup>1</sup>, PAUL ANGERER<sup>2</sup>, BERND OBERWINKLER<sup>3</sup>

<sup>1</sup>Montanuniversit t Leoben, Chair of Mechanical Engineering, Leoben, Austria

<sup>2</sup>Material Center Leoben, Austria

<sup>3</sup>Bohler Forging, Business Development, Kapfenberg, Austria

The need for light weight design while maintaining a high safety is essential for many components, especially in the aircraft industry. Therefore, it’s of utmost importance to consider every aspect to reduce weight, improve fatigue life and maintain safety of crucial components. Residual stresses are an important factor which can positively influence components and fulfil all three requirements. However, due to the inconstancy of the behaviour of residual stresses during the life time of a component, residual stresses are often neglected.

If the behaviour of residual stresses could be described reliably over the entire life time of a component, residual stresses could be taken into account and components could be optimized even further. Mechanical and thermal loads are the main reason for relaxation of residual stresses.

This work covers the thermal stability of residual stresses in Ti-6Al-4V components. Therefore, exposure tests at raised temperatures were performed on specimens with different surface conditions. The residual stresses were measured by x-ray diffraction before and after testing. Creep tests were also carried out to describe the creep behaviour and thereby the ability for residual stress relaxation. A correlation between the creep rate and amount of relaxed stress was found.

The creep behaviour of the material was described by using a combination of the Norton Power law and the Arrhenius equation. The Zener-Wert-Avrami model was used to describe the residual stress relaxation. With these models a satisfying correlation between measured and calculated data was found. Hence, the relaxation of residual stresses due to thermal load was described reliably.

# Development of residual stresses during cyclic loading in the very high cycle fatigue regime

HONGWANG FU, BENJAMIN DÖNGES, HANS-JÜRGEN CHRIST

Universität Siegen, Institut für Werkstofftechnik, Germany

In a jointed project, which is carried out in the framework of the priority programme *Life*<sup>∞</sup> (SPP 1466), the fatigue behavior of an austenitic-ferritic duplex steel is investigated in detail in the very high cycle fatigue regime. A variety of factors, such as crystallographic grain orientations, slip band formation, barrier strength of grain and/or phase boundaries against slip band expansion and microcrack propagation, and residual stress distribution are considered, in order to develop a mechanism-based model representing the relevant crack initiation and propagation mechanisms. The study presented is focusing on the determination of the residual stresses and their evolution caused by the heat treatment prior to cyclic loading and the fatigue process, respectively. The measurements were performed by means of in-situ ultrasonic fatigue testing applying high energy synchrotron radiation in PETRAIII Hamburg. It was observed that the initial micro residual stress in austenite is approximately 186 MPa in the longitudinal direction (parallel to the stress axis) and 137 MPa in the transversal direction. The ferritic phase contains very similar absolute values of internal stresses, however as negative values, i.e., compressive stresses, fulfilling the mechanical equilibrium condition. A redistribution of the residual stresses in terms of an increase of the tensile micro residual stresses in the austenitic phase and a decrease of the compressive residual stresses in the ferritic phase was found after 107 cycles under symmetric push-pull condition at an external stress amplitude of 380 MPa. At 5·10<sup>7</sup> cycles, the micro residual stresses were observed to reach a maximum and a minimum in austenite and ferrite, respectively. Further fatigue loading seems to lead to an internal stress relaxation. The development of the residual stresses can be understood by the localized plastic deformation caused by dislocation motion and

multiplication. The evolution of slip markings provides a clear indication of such changes, taking place despite the very low stress amplitude typical of the very high cycle fatigue conditions. A separate experiment to investigate the change of slip markings was executed at a stress amplitude of 350 MPa. Due to this low stress amplitude, only few austenitic grains undergo noticeable plastic deformation. The growth of slip markings (width and length) in all plastically deforming grains was monitored up to 2·10<sup>9</sup> cycles. The results showed that the slip markings exhibit similar growth characteristics. All slip markings become continuously broader up to 10<sup>8</sup> cycles and subsequently stay stable, indicating working hardening which occurs in these grains because of dislocation motion and multiplication. TEM examination showed that the dislocations in austenite pile up against the phase boundary, which form obviously strong obstacles, leading to local residual stress concentrations. As a consequence, a high dislocation density forms in the adjacent ferritic grains. When cyclic plasticity proceeds into the neighboring grain, the localized residual stress can release, and a second stage of an increase of the width and length of the slip markings was experimentally observed in the regime between 10<sup>8</sup> and 2·10<sup>8</sup> cycles. The modified Williamson plot of the dislocation density also presents the two transition stages, during which the dislocation density increases/decreases. In the final part of fatigue life (more than 90% of the number of cycles until failure), the dislocation density increases steadily until crack nuclei can exceed the barrier strength of grain and phase boundaries. FEM simulation showed that residual stress changes not only strongly affect the stress distribution but also play a significant role for the crack initiation and propagation processes.

Talks Topic B 2:

## ***Residual stresses***

---

## 3DXRD microscopy applied to study stress-induced martensitic transformation over one hundred individual grains in a shape-memory alloy polycrystal

SOPHIE BERVEILLER<sup>1</sup>, BENOIT MALARD<sup>2</sup>, YOUNES EL-HACHI<sup>2</sup>, JONATHAN WRIGHT<sup>3</sup>

<sup>1</sup>Arts et Métiers ParisTech, Metz, France

<sup>2</sup>CIRIMAT, Toulouse, France

<sup>3</sup>ESRF, Grenoble, France

Specific properties of the so-called shape memory alloys are based on the martensitic transformation that can occur in the austenite phase. This stress-induced transformation is reversible during unloading, the reversible strain being around 3%; this phenomenon is known as superelasticity. At the microstructure scale, during loading, austenite grains rotate and deform; when martensite appears, a stress redistribution occurs between both phases.

The bulk properties of Shape Memory Alloys (SMA) such as the macroscopic stress-strain and the superelasticity depend strongly on the orientation of the embedded grains and their interactions within the polycrystal. Therefore experimental data obtained on single crystals can not be easily extended to polycrystals. So it is necessary to perform measurements at different scales directly in the polycrystal. The Three-dimensional X-Ray diffraction technique (3DXRD), developed with synchrotron radiation, allows determination of strain tensor and crystallographic orientation distribution in individual embedded grains of a polycrystal (Margulies 2002). We had applied this technique previously to study the behaviour of four grains of 1 mm<sup>3</sup> in a Cu-Al-Be SMA alloy (Berveiller et al. 2011).

In this work, in-situ 3DXRD technique was used to study about one hundred grains of 10<sup>-3</sup> mm<sup>3</sup> during a superelastic loading test on a Cu-Al-Be alloy. 3DXRD was performed on the ESRF ID11 beamline and the resulting data were analyzed using the software ImageD11. The improvements made on the software to

process a large number of micrometric grains lead to more efficient quantification of intra/inter granular rotations and internal stress. The stress tensor of 101 grains were then determined as well as their crystallographic orientation and their spatial localization inside the sample. Due to the high anisotropy of the Cu-Al-Be alloy ( $a = 13$ ), a strong heterogeneity was obtained in the stress state of the grains, depending on their orientation. A factor higher than 3 was measured between the minimum and the maximum value. During loading and unloading, a reversible rotation of each austenite grain is observed, the magnitude of the rotation being also dependant on the grain orientation. Last, we observe that for a given orientation, the stress state of the grains is not the same if it is located at the surface or in the bulk material, pointing out the effect of intergranular interactions on local behaviour.

### References

- Berveiller S., Malard B., Wright J., Geandier G. & Pattoor E. (2011): In-situ synchrotron analysis of lattice rotations in individual grains during stress-induced martensitic transformations in a polycrystalline CuAlBe shape memory alloy, *Acta Materialia*, 59, 3636–3645
- Margulies, L., Lorentzen, T., Poulsen, H.F. & Leffers, T. (2002): Strain tensor development in a single crystal in the bulk of a polycrystal under loading. *Acta. Mat.*, 50, 1771-1779

## Measuring Residual Stresses in Monolithic Fuel Foils using Neutron Diffraction

BJØRN CLAUSEN<sup>1</sup>, DONALD W. BROWN<sup>1</sup>, MARIA A. OKUNIEWSKI<sup>2</sup>, LEVENTE BALOGH<sup>3</sup>, THOMAS A. SISNEROS<sup>1</sup>

<sup>1</sup>Los Alamos National Laboratory, Los Alamos, USA

<sup>2</sup>Idaho National Laboratory, Idaho Falls, USA

<sup>3</sup>Queen's University, Kingston, Canada

Residual stresses are expected in monolithic, aluminum clad uranium 10 weight percent molybdenum (U-10Mo) nuclear fuel plates because of the large mismatch in thermal expansion between the bonded materials.

Previous high energy x-ray diffraction measurements successfully profiled the residual stresses in the U-10Mo (Brown et al. 2013), but were unable to probe either the Al cladding or the 15 micron Zr diffusion prevention barrier due to poor grain statistics. Neutron

diffraction, with its inherently more divergent incident beam alleviates this problem and, moreover, allowed for the determination of the dislocation density and texture in all three phases.

Measurements of thin foil samples using neutron diffraction is not straight forward due to partially filled gauge volumes which can give rise to significant geometrical pseudo-strains if not addressed properly (Fitzpatrick & Lodini 2003). In the present case we used annealed copper foils attached to both sides of the fuel foils as an ‘on-board’ calibrant. By using multiple sequential measurements of the same strain components in both banks of the SMARTS instrument it was possible to validate the approach and determine an effective error bar for the technique.

Several samples were examined as a function of pro-

cessing step and the phase stresses, dislocation density and texture are monitored with respect to the processing conditions.

#### References

- Brown, D.W., Okuniewski, M.A., Almer, J.D., Balogh, L., Clausen, B., Okasinski, J.S. & Rabin, B.H. (2013), “High Energy X-ray Diffraction Measurement of Residual Stresses in a Monolithic Aluminum Clad Uranium–10 wt% Molybdenum Fuel Plate Assembly”, *J. Nucl. Mater.*, 441(1-3), 252-261. DOI
- Fitzpatrick, M.E & Lodini, A. (2003), “Analysis of residual Stress by Diffraction using Neutron and Synchrotron Radiation”, Taylor & Francis, New York, 233-248.

## Characterization of microscopic stress and strain evolved in polycrystalline Fe-Ga alloys using synchrotron radiation

SHIGERU SUZUKI<sup>1</sup>, YUSUKE ONUKI<sup>1</sup>, SHIGEO SATO<sup>2</sup>, SHUN FUJIEDA<sup>1</sup>, KOZO SHINODA<sup>1</sup>, KENTARO KAJIWARA<sup>1</sup>, MASUGU SATO<sup>3</sup>

<sup>1</sup>Institute of Multidisciplinary Research for Advanced Materials Tohoku University, Sendai, Japan

<sup>2</sup>Graduate School of Science and Engineering, Ibaraki University, Hitachi, Japan

<sup>3</sup>Japan Synchrotron Radiation Research Institute, Hyogo, Japan

Fe-Ga alloys reveal the large magnetostriction, compared to that of pure metals, such as Fe and Ni (Summers, 2007). Although the magnetostriction of the alloys is smaller than those of TbFe<sub>2</sub> and CoFe<sub>2</sub>O<sub>4</sub>, the Fe-Ga alloys can be machined into desired shapes because of the relatively good mechanical property. Thus, the Fe-Ga alloys are considered to be candidate materials for application to vibration power generators and actuators (Ueno, 2011). On the other hand, it has been known that magnetostrictive and elastic properties of the Fe-Ga alloy strongly depend on crystal orientation (Clark, 2003; Kellogg, 2004). If the polycrystalline Fe-Ga alloys are used for the magnetostrictive materials, this anisotropy of these properties is important in their application(). Therefore, the elastic properties of the Fe-Ga alloys are essential in their application. The objective of this study is to investigate the microscopic stress evolved in the polycrystalline Fe-Ga alloys by the external elastic stress.

In order to analyze the microscopic stresses in crystalline materials, an analytical method using white X-ray diffraction with micro-beam synchrotron radiation has been developed (Kajiwara, 2009). In this study, this method was applied to obtain information on microscopic stress evolved in coarse grains of the Fe-Ga alloys. Besides this technique, electron backscatter diffraction (EBSD) was also used to determine the crystal orientation of grains in the polycrystalline Fe-Ga alloys. Based on these orientation data, the stress and strain distribution in the microstructure of the steel under

loading and unloading was estimated using an FEM simulation where the elastic anisotropy or the crystal orientation dependence of the elasticity was taken into account.

The results by micro-beam synchrotron radiation showed that the microscopic stresses are distributed to the polycrystalline Fe-Ga alloys, which may play important role in the magnetostrictive properties of the polycrystalline Fe-Ga alloys. The FEM simulation showed that the strain distribution in the microstructure depends on the crystal orientation of each grain and is influenced by grain boundaries. In addition, the stress analysis by the white X-ray diffraction indicated that the direction of the maximum principal stresses at measured points in the steel under tensile loading are mostly oriented to the tensile direction. This is qualitatively consistent with the results of by the FEM simulation, although absolute values of the principal stresses may contain the effect of heterogeneous plastic deformation on the stress distribution. In this presentation, the characteristic stress distribution in Fe-Ga alloys with large anisotropic elasticity will be discussed in the basis of these different results.

#### References

- Clark, A. E., Hathaway, K. B., Wun-Fogle, M., Restorff, J. B., Lograsso, T. A., Keppens, V. M., Petculescu G. & Taylor R. A. (2003): *J. Appl. Phys.* 93, 8621.
- Kajiwara, K., Sato, M., Hashimoto, T., Hirotsawa, I., Yamada, T., Terachi, T., Fukumura, T. & Arioka, K.

- (2009): Phys. Status Solidi A, 206, 1838.
- Kellogg, R. A., Russell, A. M., Lograsso, T. A., Flatau, A. B., Clark, A. E. & Wun-Fogle, M. (2004): Acta Materialia. 52, 5043.
- Sato, S., Kwon, E.P, Imafuku, M., Wagatsuma, K. & Suzuki, S. (2011): Mater. Character., 62, 781.
- Summers, E. M., T. A. Lograsso, T. A., & Wun-Fogle, M. (2007): J. Mater. Sci. 42, 9582.
- Ueno, T. & Yamada, S. (2011): IEEE Trans. Magn. 47, 2407.

## Analysis and Assessment of Residual Stresses in Ground Steels and Ceramics

A. LIEHR, W. ZINN, B. SCHOLTES

University of Kassel, Institute of Materials Engineering – Metallic Materials, Kassel, Germany

Near surface alterations of the materials microstructure and induced residual stress states are very important consequences of grinding processes, which may have a pronounced impact on the behavior of the manufactured components. As a consequence, there is a great interest in the potential of existing methods for the quantitative analysis of residual stress depth distributions. Due to the steep microstructural and residual stress gradients in ground surface layers, this is a challenging task. Preferably X-ray methods are applied and different strategies are pursued.

In this paper, first characteristic depth distributions of grinding residual stresses are presented and discussed for a quenched and tempered steel SAE 52100 as well as for a  $Al_2O_3$ -ceramic. These results were achieved applying the conventional  $\sin^2\psi$ -method. Then results

of further measurements are outlined where special methods were applied for the nondestructive analysis of the steep residual stress gradients. Different types of radiations including white X-rays were used. The results of these measurements are presented and the potentials and the limitations of the methods are discussed.

### References

- Manns, Th.; Scholtes, B. (2012), Diffraction Residual Stress Analysis in Technical Components - Status and Prospects, Thin Solid Films 530, pp.. 53 – 61.
- Genzel, Ch.; Denks, I. A.; Klaus, M. (2013) Residual Stress Analysis by X-ray Diffraction Methods. In: E. J. Mittemeijer, U. Welzel (Eds.), Modern Diffraction Methods, Wiley-VCH.

## Assessing material properties with Neutron and Synchrotron radiation - Two complementary tools

T. BUSLAPS<sup>1</sup>, V. HONKIMÄKI<sup>1</sup>, M. DIMICHIEL<sup>1</sup>, J. WRIGHT<sup>1</sup>, A. FITCH<sup>1</sup>, C. CURFS<sup>1</sup>, T. PIRLING<sup>2</sup>

<sup>1</sup>ESRF, Grenoble, France

<sup>2</sup> ILL, Grenoble, France

Technical progress in many areas critically depends on knowing how complex materials behave in - often extreme - service conditions combining high temperatures with strong mechanical forces.

Facilities like ESRF and ILL, located on the European Photon and Neutron campus (EPN) in Grenoble, provide high energy synchrotron X-rays and neutron beams of high intensity and high penetration power enabling non-destructive diffraction studies to assess material properties over different time and length scales. Especially the non-destructive character of these diffraction methods turns them into powerful and unique tools for residual stress determination and in-situ studies. The combination of synchrotron X-ray and neutron experiments provides comprehensive analyses from micrometre to metre scales and time resolution from

10ms to minutes.

Dedicated instrumentation is regularly improved extending experimental conditions for a maximum range of applications responding to the demand of materials and engineering science. On the ILL side SALSA (Stress Analyzer for Large scaled Engineering Applications) has recently been upgraded with a larger and more efficient detector, providing three times faster acquisition. New beam optics allow in-situ studies with time resolution of 1 s or measurements in very large samples. At the same time near-surface/interface measurements with 40 $\mu$ m resolution are possible.

At the ESRF several experimental stations (ID11, ID15, ID22, BM32) with specialized instrumentation are made available to respond to a wide range of quite different materials science problems.

Both institutes share sample environments, such as dedicated stress rigs and high temperature furnaces providing unique experimental conditions to evaluate physical properties of matter in situ while varying the thermo-mechanical parameters.

This equipment is delivered by the Materials Science Support Laboratory (MSSL) on site, which also provides tools for sample preparation.

The paper presents new developments on the EPN campus, with an outlook on future projects. Examples, comprising microstructural analysis, solidification studies on in-situ casting, and imaging techniques, demonstrate the potential of the photon and neutron techniques especially when taking advantage of their complementarity.

Talks Topic B 3:

## ***Residual stresses***

---

## Estimation of residual stress distribution in polyethylene pipes

JAN PODUŠKA<sup>1,2</sup>, PAVEL HUTAŘ<sup>2</sup>, JIŘÍ SADÍLEK<sup>3</sup>, JAROSLAV KUČERA<sup>3</sup>, MARTIN ŠEVČÍK<sup>2</sup>, LUBOŠ NÁHLÍK<sup>4</sup>

<sup>1</sup>Brno University of Technology, Faculty of Mechanical Engineering, Czech Republic

<sup>2</sup>Institute of Physics of Materials, Academy of Sciences of the Czech Republic, Brno, Czech Republic

<sup>3</sup>Polymer Institute Brno, Czech Republic

<sup>4</sup>CEITEC IPM, Institute of Physics of Materials, Brno, Czech Republic

Polyethylene is one of the most frequently used materials for piping applications. Polyethylene pipes, thanks to their qualities such as durability, simple and quick production and installation and also their significantly long lifetime, have been replacing the conventional pipes in various fields of use in the last couple of decades. (Janson 1999)

With that, a correct estimation of the lifetime of polyethylene pressure pipes has become important and several methods has been designed for the purpose. A common method is to measure the time to failure of a pipe segment under the load of hydrostatic pressure – the so called hydrostatic pressure test. By extrapolation of the results of such tests, lifetime of an actual pipe can be calculated. However, it is not the most effective test, because with the increasing quality of the material the lifetime of the pipe also rises and the tests can take a very long time to achieve the desired failure. Based on the fact, that most of the failures in working conditions is the result of a slow crack growth mechanism or quasi-brittle fracture, tests like PENT, FNCT and CRB test have been developed, that measure the crack growth rate on notched specimens and the lifetime can then be calculated using these data and the linear elastic fracture mechanics approach (Hutař et al. 2011).

There are several factors that influence the crack growth and have to be included in the mentioned lifetime calculations. Besides the hoop stress that is caused by the internal pressure inside the pipe, it is the residual hoop and axial stress that influence the lifetime negatively, because, due to the character of their distribution, they help the cracks grow (Hutař et al. 2013). In this contribution, an experimental procedure of obtaining the residual hoop and axial stress in a polyethylene pipes is described. For the experiment a simple ring slitting method is used, where ring specimen

are cut off of the pipe, their wall thickness is modified on a lathe and then they are axially slit, which causes the relaxation of residual hoop stress, and change in their diameter that is measured. Further evaluation of the results then shows, that the residual hoop stress is independent on dimensions and one general equation, that describes the distribution of residual stress in polypropylene and polyethylene pipes is derived. The number of specimen, that has to be made for the experiment to be successful, is still quite high. That's why, the method of evaluating the experiment is altered, so that just one specimen is needed for a satisfactory estimation of the residual stress distribution. This allows us then to revisit older data and compare results of similar measurements from different sources (e.g. Clutton & Williams 1995) and see, if the magnitudes of residual stress are really similar for different pipes. Also, the magnitude and distribution of the axial residual stress in the pipe wall is covered in this contribution and the influence on the total residual stress in an actual polyethylene pipe is studied.

### References

- Janson, L. E. (1999): Plastic pipes for water supply and sewage disposal, Borealis; Stockholm.
- Hutař, P., et al. (2011): A numerical methodology for lifetime estimation of HDPE pressure pipes, Engineering Fracture Mechanics 2011; vol. 78, pp. 3049-3058.
- Hutař, P., et al. (2013): The effect of residual stress on polymer pipe lifetime, Engineering Fracture Mechanics 2013; vol. 108, pp. 98-108.
- Clutton, E. Q. & Williams, J. G. (1995): On the measurement of residual stress in plastic pipes, Polymer Engineering & Science, vol. 35, issue 17, pp. 1381 – 1386.

# A combined experimental and numerical approach to the investigation of the influence of geometry on residual stresses in structural glass

MITHILA ACHINTHA, BOGDAN BALAN

Faculty of Engineering and the Environment, University of Southampton, United Kingdom

This paper reports selected findings from a combined experimental and numerical analyses of the influence of geometry on residual stresses in commercially-available float and tempered glass. The effect of residual stresses is critical for the performance of structures; unexpected premature failure may occur because residual stresses can critically combined with applied stresses [1]. Despite the potential consequences of ignoring the effects of residual stresses, the current design guidelines of glass structures [2] do not explicitly take into account the effect of residual stresses.

The misfit strains (i.e. eigenstrains) developed due to the cooling of glass during the manufacturing process generate residual stresses. The authors have previously [3] developed a contour method–eigenstrains hybrid model to predict the residual stresses present in commercially available float glass. This paper extends the hybrid model to investigate the interaction between the geometry and residual stress in both float and tempered glasses.

Contour method experiments have been used to construct the residual stress depth profile, and then the results validated using scattered-light-polariscopic experiments are used to devise eigenstrains – i.e. the misfit strains that generated due to differential cooling during the manufacturing process. The full 3D residual stress distribution is then devised by incorporating the eigenstrain as a misfit strain in an appropriate finite element (FE) model. The results show that in both float and tempered glass, the residual stress depth profile has a parabolic distribution with ~20 % of thickness surface compression zone on each side balanced by a mid-thickness tension zone. The model predictions agree well with residual stresses measured using scattered-light-polariscopic experiments. Surface compressive stress of ~100 MPa has been determined in tempered glass, while that in float glass is ~8 MPa.

Once the underlying eigenstrain depth profile has been determined residual stress in new geometries (e.g. stress concentrations features) and/or during subse-

quent loading applications, are determined from FE models by simply using the knowledge of eigenstrain depth profile. For instance, results of a glass plate with a central hole shows that the presence of the hole affects the stress distribution, and the results also suggest that change in stress is not proportional to the magnitude of applied stresses. Furthermore, investigations have shown that the negligence of the effect of residual stress can significantly underestimate critical design stresses.

A further application of the eigenstrain method has been explored. Eigenstrains generated in float glass depends on differential cooling that takes place during manufacturing, and this means that eigenstrain depth profiles in glass of different thickness are different. The results show that by combining the knowledge of eigenstrain depth profile in float glass of known thickness and a “thickness effect”, which indirectly takes into account of different rates of cooling experienced by glasses of different thicknesses, eigenstrains in other thicknesses and subsequently the stress distributions can be determined.

The study suggests that the hybrid contour method/eigenstrain approach is particularly effective in predicting residual stress distribution in different glass geometries. The approach has been used to model the interaction between the geometry and the residual stresses.

## References

- [1] Withers, PJ. (2007): Residual stress and its role in failure. – Reports on progress in physics, 70: 2211-2264.
- [2] IStructE. (2014): Structural use of glass in buildings, (2<sup>nd</sup> ed.). – Institution of Structural Engineers. London, UK.
- [3] Balan, B. & Achintha, M. (2014): hybrid contour method/eigenstrain model to predict residual stress in glass. Proceedings of ICCM2014, Cambridge, UK.

## Benefits of Whole Powder Pattern Decomposition in the Determination of Residual Stress in Multiphase Materials

HUGUES GUÉRAULT, JENS BRECHBUEHL

BRUKER AXS GmbH, Karlsruhe, Germany

In multiphase materials or multilayer coatings, the determination of residual stress may become unworkable due to strong overlap between the diffraction patterns originating from the different crystalline phases. Whole powder pattern decomposition is an efficient method for resolving the convolution of diffraction peaks and gives the opportunity to use all (hkl) reflections during evaluation. It offers in particular a chance to simultaneously refine structural parameters (i.e. stress free lattice parameter) together with additional peak shifts due to the presence of residual stress.

Wide diffraction patterns (up to 150°) have been collected on different types of materials (single and mul-

tiphase) using fixed angles of incidence. For a given penetration depth, the depth averaged residual stresses (Laplace space) of each crystalline phase could be evaluated using the grazing incident  $\sin^2(\psi)$  method. Further angles of incidence have been used in order to investigate individual stress gradients. The whole set of diffraction patterns were treated either sequentially or using a parametric refinement through an analytical function for the real space residual stress profile. An approach based on spherical harmonics is also proposed for the accounting of the anisotropic elastic behavior for the different (hkl) planes.

## Simulation-based optimization of the multiple incremental hole-drilling method for the simultaneous analysis of residual stresses and the measurement accuracy

FRANK SCHWEIZER<sup>1</sup>, MELANIE SENN<sup>1</sup>, WULF PFEIFFER<sup>1</sup>

<sup>1</sup>Fraunhofer Institute for the Mechanics of Materials IWM, Freiburg, Germany

For the analysis of residual stresses in the outer layers of components the incremental hole-drilling method is often used in industrial applications. This standardized mechanical measurement method is partial destructive because a small hole has to be drilled into the material. The evaluation of the strains surrounding the hole allows to calculate the residual stresses. By subdividing the depth of the hole into different substeps the analysis of the residual stresses can be applied at every depth step. This information leads to the evaluation of stress gradients arising from various manufacturing processes.

One of the shortcomings of the method is that no further information about the measurement process and its accuracy can be acquired from the measurement data. This can be achieved if the hole-drilling is also subdivided into different steps in radial direction of the hole. From this extended data basis a statistical interpretation of the process and a quantitative evaluation of the measurement accuracy can be obtained.

The additional subdivision of the measurement steps in both depth and radial direction leads to a large number of required drilling steps and very long measurement times. Therefore the drilling procedure has to be optimized.

It will be shown that with the use of an optimization framework coupled with a Finite Element Simulation of the drilling process the sizes of drilling steps into depth and radial direction can be optimized.

The Finite Element model is also used to determine calibration functions for the inverse calculation of residual stresses from the measured strains surrounding the hole. These have to be adapted, because the subdivision of drilling steps does not meet the standard drilling case and also these functions have to be interpolated in the optimization procedure.

The method of multiple incremental hole-drilling with and without optimization is experimentally evaluated by using real components with known stress states. As a result the residual stresses in the material and the measurement accuracy for every depth step of the measurement can be assessed simultaneously. Thus different shortcomings and failures in the measurement procedure can be evaluated from the extended measurement data.

An outlook will be derived which focusses on further simulation capabilities which may lead to an in-situ optimization of drilling steps using the standard as well as the multiple incremental hole-drilling method.

## References

E837 – Standard Test Method for Determining residual stresses by the hole-drilling strain-gage method  
 Pfeiffer W.; Wenzel J. (2008): The Multiple-Incremental Hole Drilling Method. *MP Materials testing* 50, pp 495-499  
 Schwarz, T.; Kockelmann. H. (1993): Die Bohrlochmethode – Ein für viele Anwendungsbereiche optimales Verfahren zur experimentellen Ermittlung von Eigenspannungen. *Messtechnische Briefe* 29 (2), pp 33-38

Schajer, G.S.; Prime, M.B. (2006): Use of inverse solutions for residual stress measurement. *Journal of Engineering Materials and Technology* 128 (3), pp 375-382  
 Schajer, G.S. (1981): Application of finite element calculations to residual stress measurements. *Journal of Engineering Materials and Technology* 103, pp. 157-163

## Analysis of residual stress gradients by X-ray diffraction with five-axis diffractometer

ALEX ULYANENKOV<sup>1</sup>, ANDREI BENEDIKTOVITCH<sup>2</sup>, TATIANA ULYANENKOVA<sup>3</sup>, JOSEF KECKES<sup>4</sup>

<sup>1</sup>Atomicus GmbH, Karlsruhe, Germany

<sup>2</sup>Belarusian State University, Minsk, Belarus

<sup>3</sup>Rigaku Europe SE, Ettlingen, Germany

<sup>4</sup>Department of materials Physics, Montanuniversitaet Leoben, Leoben, Austria

Residual stress gradients occur in thin films and protective coatings during deposition process or as result of intended treatment, e.g. blasting. The resulting distribution of residual stress has significant influence on the physical properties of the film and on the performance of the coated tool.

The depth profile of the residual stress can be analysed by the X-ray diffraction methods, and a number of approaches to do this exists. Each approach has its pros and cons and applicability range. In this contribution we propose a new method (Benediktovitch 2014a) that takes the advantage of the in-plane arm rotation provided by several modern diffractometers and facilities. The basic idea of the method is to perform the  $\sin^2\psi$  plots, i.e. to measure the Bragg peak position at changed angle  $\psi$  between sample normal and transferred wavevector, by means of combination of source and detector arm movements keeping the penetration depth constant. Compared to a similar method applied to conventional four-circle diffractometers (Kumar 2006), the additional degree of movement provided by in-plane detector arm rotations enables to get  $\sin^2\psi$  plots at fixed penetration depth without sample tilting, which may be advantageous at the conditions when sample movement is undesirable, e.g. like during in-situ high temperature studies.

The explicit analytical expressions were derived that enable to calculate the position of source and detectors arms corresponding to given hkl,  $\sin^2\psi$ , and penetration depth. In this way, the series of  $\sin^2\psi$  plots at a number of fixed penetration depth values can be measured. Traditional processing of these  $\sin^2\psi$  plots directly gives the values of residual stress tensor versus the information depth. We have also found that it is advantageous to combine the results from several hkl

values to broaden the available  $\sin^2\psi$  range at given penetration depth. The results of residual stress analysis are sensitive to a number of corrections and to peak search methods. The most important correction in considered case was found to be the refraction correction which was considered in detail for the investigated experimental geometry (Benediktovitch 2014c). The peak position was obtained by peak fitting accounting for instrumental function profile specific for considered experimental geometry (Benediktovitch 2014b). The method was applied to characterize the residual stress gradient in wet blasted TiN coating on WC-Co substrate. The obtained residual stress depth profile was in good agreement with synchrotron data.

## References

Benediktovitch, A. Ulyanenkova, T., Keckes, J. & Ulyanenkov, A. (2014a): Sample tilt-free characterization of residual stress gradients in thin coatings using an in-plane arm-equipped laboratory X-ray diffractometer. - *J. Appl. Cryst.*, 47: 1931-1938.  
 Kumar, A., Welzel, U. & Mittemeijer, E.J. (2006): A method for the non-destructive analysis of gradients of mechanical stresses by X-ray diffraction measurements at fixed penetration/information depths. - *J. Appl. Cryst.*, 39: 633-646.  
 Benediktovitch, A. Ulyanenkova, T. & Ulyanenkov, A. (2014b): Resolution function for X-ray powder diffraction in a noncoplanar measurement geometry with the detector arm having two degree of freedom. - *J. Appl. Cryst.*, 47: 1298-1303.  
 Benediktovitch, A. Ulyanenkova, T., Keckes, J. & Ulyanenkov, A. (2014c): Stress gradient analysis by noncoplanar x-ray diffraction and corresponding refraction correction. - *Adv. Mater. Res.*, 996: 162-168.

## Comparison of the residual stress distributions in conventional and stationary shoulder friction stir welding

TIANZHU SUN, YINGCHUN CHEN, PHILIP B. PRANGNELL, MATTHEW J. ROY, PHILIP J. WITHERS

School of Materials, The University of Manchester, UK

Friction stir welding (FSW) is especially well suited to joining aluminium alloys, as it produces welds with excellent mechanical properties and avoids issues such as solidification and liquation cracking. However, despite the solid-state nature of the process, the weld members are heated to close to their melting point and as a result distortion and considerable levels of residual stress still occur, as has been noted in a number of studies (e.g. [1, 2]). Although a range of methods, such as thermal and mechanical tensioning, have been developed to control the residual stresses in FSW they are often difficult to apply in practice and it would be desirable to engineer the welding process itself to reduce their level [3-4].

Recently, a variant to the conventional friction stir welding technique has been proposed that shows considerable promise in this regard. In stationary shoulder (SS) FSW, instead of using an integrated tool where the pin and shoulder both turn at the same rotational speed, the shoulder is fixed to the welding head so that only the pin rotates. With the SS-FSW process the amount of heat generated by the tool shoulder is thus greatly reduced and virtually all the welding power is controlled by the action of the pin. Consequently, a more uniform through-thickness heat distribution is achieved. It has recently been shown that this allows welds to be produced with a lower net heat input that have better mechanical properties and lower levels of distortion than those made by conventional FSW [5]. Furthermore, the sliding shoulder contact also contributes to better surface quality [5].

To our knowledge no residual stress measurements have been made on SS-FSW. In this paper we will explore whether the reduction in heat input and more uniform temperature distribution seen in SS-FSW also leads to lower levels of residual stresses compared to in the conventional FSW process. The residual stress

measurements have been made using the newly developed contour technique [6]. In contrast to neutron and synchrotron stress measurement methods, this technique is much more cost effective as it can be readily applied using advanced workshop tools, requiring only electro-discharge machining and a coordinate measurement machine. The residual stresses produced in the two processes will be compared using welds made with identical tool geometries and optimum welding conditions. Further, we will address an important question; can the downforce from the cold shoulder be exploited to modify the residual stress field?

The magnitude and the location of the peak residual stresses will be discussed, as a function of the welding parameters for each process variant, and in relation to the observed variation of material properties across the weld zones and the observed levels of distortion. Finally the corresponding relative microstructural variation will be also be presented across the parent, heat affected (HAZ), thermomechanically affected (TMAZ) and nugget zones for each set of welds.

### References

- [1] P.L. Threadgill, A.J. Leonard, H.R. Shercliff, P.J. Withers, *International Materials Reviews*, 54 (2009) 50-93.
- [2] M. Peel, A. Steuwer, M. Preuss, P.J. Withers, *Acta Mater.*, 51 (2003) 4791-4801.
- [3] D.G. Richards, P.B. Prangnell, P.J. Withers, S.W. Williams, *Mat Sci Eng A*, 489, (2008) 351-36.
- [4] D.G. Richards, P.B. Prangnell, P.J. Withers, S.W. Williams, T. Nagy and S. Morgan, *Sci. & Tech. of Welding and Joining*, 15 (2010) 156-165.
- [5] H. Wu, Y-C. Chen, D. Strong, and P.B. Prangnell, *Mat Sci Forum Vols. 783-786* (2014) pp 1770-1775.
- [6] M. Prime, in: G.A. Webster (Ed.) *Int. Conf Res. Stress 6*, Inst. of Mat., Oxford, 2000, pp. 617-624.

Talks Topic B 4:

## ***Residual stresses***

---

## Nitriding stress due to nitrogen diffusion and nitrides formation

TATSUO INOUE

Saitama Institute of Technology, Fukaya, Japan

Strategy based on stoichiometry is presented, in the first part of the present paper on gas nitriding process under non-equilibrium thermodynamic condition, to simulate diffused nitrogen, nitrides formation and volumetric dilatation [1-2]. Considering the fact that the process is limited in the very thin layer near substrate surface, one dimensional diffusion equation is solved to know the nitrogen concentration after some incubation time, where nitrogen atoms diffuse as interstitials in  $\alpha$ -iron followed by the compound formation process. Some part of diffused nitrogen above the solute limit produce  $\gamma'$ -Fe<sub>4</sub>N phase, where molar volume of Fe atoms is possible to be evaluated since the number of Fe atoms in an fcc unit cell is 4 instead of 2 in bcc  $\alpha$ -phase. Similar situation is seen when forming  $\epsilon$ -Fe<sub>3</sub>N phase with 6 Fe number in hcp crystal from  $\gamma'$ -Fe<sub>4</sub>N phase as is seen in Fe-N phase diagram. Thus the volume dilatation ratios of progressing step of initial to  $\alpha$ -phase,  $\gamma'$ -Fe<sub>4</sub>N and  $\epsilon$ -Fe<sub>3</sub>N with 0.3, 10.0 and 19.5 are successively evaluated, and one third of which gives the intrinsic or initial strain.

In the second part, a conventional stress estimation method is employed in the framework of incremental plastic strain theory under the consideration that stress equilibrium equation and strain compatibility condition lead to the non-zero stress and strain in plane without shear stress and strain. If simple elastic-plastic stress-strain constitutive relation is assumed by introducing the intrinsic strain derived in the first part, successive profile along the depth direction is easily obtained to

avoid complicated numerical calculation.

Both results of nitrogen concentration and stress (residual stress) for some kinds of operating condition are compared with the experimental data with qualitative agreement.

More sophisticated discussions will be available [3-4] considering mixed two phases regions of  $\alpha$ -Fe $\sim\gamma'$ -Fe<sub>4</sub>N and  $\gamma'$ -Fe<sub>4</sub>N  $\sim\epsilon$ -Fe<sub>2</sub>N, which will be presented during the conference.

### References

- Inoue, T., (2014): Nitrogen concentration, nitride formation and volume dilatation in nitriding process – 1<sup>st</sup> report: Simulation of nitriding and induced stress, Journal of Materials Science, Japan, Vol.62, No.10, pp.735-740.
- Inoue, T., (2014): Simulation of strain and residual stress in nitriding process – 2<sup>nd</sup> report: Simulation of nitriding and induced stress, Journal of Materials Science, Japan, Vol.62, No.10, pp.741-745.
- Sumida, M. & Inoue, T. (2013): Nitrogen concentration distribution based on successive diffusion into each phase during gas nitriding, Preprints of 76<sup>th</sup> Annual Meeting, Japan Society for Heat Treatment, pp.47-48,
- Inoue, T. & Sumida, M. (2013) : Strain and residual stress during gas nitriding due to nitrides formation Preprints of 76<sup>th</sup> Annual Meeting, Japan Society for Heat Treatment, pp.49-50,

## Influence of rotational speed in friction stir welding on heat generating behavior of MPS analysis

HISASHI SERIZAWA<sup>1</sup>, TAKU HAYAMI<sup>2</sup>, FUMIKAZU MIYASAKA<sup>2</sup>

<sup>1</sup>Joining and Welding Research Institute, Osaka University, Japan

<sup>2</sup>Graduate School of Engineering, Osaka University, Japan

As one of the solid state joining methods, the friction stir welding (FSW) has been employed for joining the light materials such as aluminum and magnesium alloys industrially and it has many advantages in comparison with the fused junctions. Although a large amount of researches and developments has been conducted about this process in order to reveal its mechanism and to expand its applicability to other materials, there have been several papers regarding the distortion and

the residual stress.

The finite element method (FEM) is one of the most powerful tools for predicting the welding distortion and the residual stress. Since the welding process is transient behavior thermally and mechanically, both the thermal and mechanical analyses should be conducted alternately with increasing the time step. Generally, however, the transient thermal distributions are computed at first and then the elastic-plastic analyses

are conducted using the temperature distributions obtained. So, the transient thermal distributions have to be accurately computed in order to predict the welding distortion and the residual stress precisely. As for FSW, in addition to the thermal stress, the plastic flow caused by the stir of FSW tool also seems to affect the distortion and the residual stress. However, there have been no detailed reports about the influence of plastic flow on the distortion and the residual stress.

Recently, Yoshikawa *et al.* developed a new numerical simulation model based on the moving particle semi-implicit (MPS) method, which is one of the particle methods, and demonstrated the effectivity of this method for FSW simulation (Yoshikawa 2012). However, it is unreasonable to calculate a whole model by MPS method because the structures are modeled by the aggregate of particles and the deformations are represented by the movement of particles. So, the authors has been developed a combined method of MPS and FEM (Serizawa 2014), where the inhomogeneous volumetric heat source employing in the thermal analysis of FEM is defined from the quasi-static temperature distributions near the tool of FSW computed by MPS. By using this combined method, the inhomogeneous temperature distributions through the thickness

near the joint line could be simulated and the maximum temperature distributions computed had a good agreement with the experiments. However, the method for defining the volumetric heat source for FEM have not been clearly identified.

Then, in this study, as one of the parameters in FSW, the rotational speed of FSW were varied during the butt joining process of Al plates and the influence of rotational speed on the determination method was examined. The computational results suggested that the area for determining the total heat input for FEM should become larger with increasing the rotational speed. Also, it was revealed that the diameter of the heating area might linearly increase with increasing the rotational speed.

#### References

- Yoshikawa G. et al. (2012): Development of Numerical Simulation Model for FSW employing Particle Method, Science and Technology of Welding and Joining, Vol.17, No.4 (2012) pp.255-263.
- Serizawa H. et al. (2014): Development of A Combined Method between MPS and FEM for Simulating Friction Stir Welding", Materials Science Forum, Vols.783-786 (2014), pp.2531-2536.

## Failure analysis and optimization of welding process for 347H boiler tube of thermal power plant

HAN-SANG LEE, JINE-SUNG JUNG, DOO-SOO KIM, KEUN-BONG YOO

Power Generation Lab., Research Institute of Korea Electric Power Corporation, Korea

Increasing operating temperatures in fossil power plants require better oxidation and corrosion resistances as well as higher creep strength. Especially, the welded joints in steam boiler tube can be a weak point for long operating hours. The failed welded joints of austenitic stainless steel, TP347H were prepared from the operating facilities. A microstructural investigation for the welded joints was carried out to find the root causes. Modeling and experiments for optimization of welding procedure were also performed in the present study.

The welded joints of a boiler tube, TP347H were exposed to the steam temperature of 590°C for 3,600hrs. The cracks were detected at boundaries between fusion and heat affected zone by non-destructive tests. The chemical compositions of TP347H tube were 0.072C - 0.32Si - 1.99Mn - 0.03P - 0.012S - 10.1Ni - 18.02Cr - 0.97Nb - Fe(wt.%) and microhardness was measured along boundaries at heat affected zone using a vickers hardness tester under 200 g load. Residual stress and strain analysis for failure analysis and optimization of welding procedure were performed using by SYSWELD. Crack initiated and propagated along grain boundaries

very next to interface between fusion and heat affected zone. Oxidized layer was found around crack and its thickness decrease from 50um at inner steam-side to 20um at outer fire-side. Therefore, it can be thought that crack initiated steam-side and propagated to fire-side.

At the opposite heat affected zone, narrow bands were found especially at steam-side. These bands are determined as a b.c.t phase by EBSD (Electron Back-Scattered Diffraction) analysis. Heat affected zone next to fusion zone can be deformed during welding process and strain-induced martensite can be formed [1]. It can be assumed that narrow bands were formed in the accommodation process of plastic deformation during welding process [2].

Cr-rich carbides are seen along grain-boundaries of heat affected zone and its density was higher than grain-boundaries of substrate. On the other hand, Nb-rich carbides are not seen at grain interior of heat affected zone. Nb-rich carbides next to fusion zone can be disappeared by the heating and cooling of welding process. These findings and grain-boundary oxidation are known as 'knife line attack' [3].

By modeling residual stress, biggest tensile residual stress occurred in inner side at heat affected zone and its location and direction was same with crack initiation site and propagation direction. Also, residual stress increased greatly after 2nd pass of welding procedure. To reduce residual stress, preheat, high interpass temperature, low Ar gas flow and narrow gap were tested.

The welded joints of a boiler tube, TP347H were failed by intergranular cracking at heat affected zone. Based on microstructural investigation and stress analysis, this phenomenon can be thought as a stress relaxation cracking. Reduction of residual stress and strain after

welding is important to optimize welding procedure.

#### References

- H. Lee et al, "Influence of peening on the corrosion properties of AISI 304 stainless steel", *Corrosion science*, vol.51 (2009), pp. 2826-2830.
- Mitsuhiro Okayasu et al, "Strain-induced martensite formation in austenitic stainless steel", *J. Mater. Sci*, vol. 48 (2013), pp. 6157-6166.
- S.A. Jenabali Jahromi et al, "Failure analysis of welded joints in a power plant exhaust flue", *Eng. Failure analysis*, vol. 13 (2006), pp. 527-536.

## Evaluation of the interfacial shear stress between FeCrAl coating and Zircaloy-4 fuel cladding

YANG LIU<sup>1</sup>, IMRAN BHAMJI<sup>1</sup>, PHILIP J. WITHERS<sup>1</sup>, WEICHENG ZHONG<sup>2</sup>, PETER MOUCHE<sup>2</sup>, BRENT J. HEUSER<sup>2</sup>, MICHAEL PREUSS<sup>1</sup>

<sup>1</sup>Materials Performance Centre, School of Materials, The University of Manchester, UK

<sup>2</sup>Department of Nuclear, Plasma, and Radiological Engineering, University of Illinois, Urbana-Champaign, USA

The Fukushima Daiichi nuclear disaster has raised significant awareness in the nuclear industry of the capability to cope with extreme operation conditions such as loss of coolant (LOCA) events. One way to enhance safety is through the application of accident tolerant coatings onto the surface of the existing fuel cladding. For a coating/substrate system, it is crucial to produce a sound bond at the interface. Hence it is important to characterise the interfacial shear strength (ISS) between the coating and the substrate.

One way of analysing the adhesion and fracture behaviour between a coating and a ductile substrate is to employ a model based on a shear-lag approximation [1-5] to predict the transfer of load between substrate and coating.

In this paper, a modified shear-lag model has been proposed to estimate the distribution and maximum value of the interfacial shear strength and the in-plane tensile stress of a potential protective coating (FeCrAl) on a zirconium alloy (Zircaloy-4) substrate. This model is based on the approximation previously used for fiber/matrix composites [6], but it is physically transformed and mathematically reformulated to be appropriate for the coating-substrate system.

This model was employed for the FeCrAl/Zircaloy-4 system through the utilisation of uniaxial tensile loading experiments, giving parallel cracks transverse to the straining direction (transverse cracks) in the coating. The fracture strength of the coating was also estimated using the strain at which transverse cracks first start to appear. With continued tensile straining the crack frequency reaches a maximum value, i.e. the number and spacing of transverse cracks in the oxide saturates. The interfacial shear strength was then evaluated by measuring the average crack spacing.

The parameters critical to this analysis were measured experimentally; namely, the residual stress in the coating (~ 800 MPa) was determined by X-ray diffraction; the elastic modulus of the FeCrAl coating and the Zircaloy-4 substrate were measured using nano-indentation, and the fracture strength of the coating (~ 2 GPa) was inferred from the onset of transverse cracking at 1.0% strain using in-situ loading experiments. From these input parameters the interfacial shear strength between the coating and zirconium substrate was inferred to be around 500 MPa. This bond strength is benchmarked against the interfacial shear strength measured previously for the thermally grown zirconium oxide and zirconium alloy system (~ 100 MPa). It is concluded that after deposition, the newly developed FeCrAl coating exhibits a 4-5 times higher bonding strength than the thermally grown ZrO<sub>2</sub> on a Zircaloy-4 substrate. Our modified shear-lag measurement is easy to undertake and has the potential to be used as an assessment tool for other coating/cladding systems.

#### References

- [1] D.C. Agrawal, R. Raj, *Acta Metallurgica*, 37 (1989) 1265-1270.
- [2] M.S. Hu, A.G. Evans, *Acta Metallurgica*, 37 (1989) 917-925.
- [3] M. Yanaka, Y. Tsukahara, N. Nakaso, N. Takeda, *J Mater Sci*, 33 (1998) 2111-2119.
- [4] B.F. Chen, J. Hwang, G.P. Yu, J.H. Huang, *Thin Solid Films*, 352 (1999) 173-178.
- [5] U.A. Handge, *J Mater Sci*, 37 (2002) 4775-4782.
- [6] T.W. Clyne, P.J. Withers, *An introduction to metal matrix composites*, Cambridge University Press, Cambridge, 1993.

## Mechanical property and Residual Stress in Type304 stainless steel repaired partially by HVOF sprayed technique

MASAYUKI ARAI<sup>1</sup>, SHO TANAKA<sup>2</sup>, TATSUO SUIDZU<sup>2</sup>

<sup>1</sup> Department of Mechanical Engineering, Tokyo University of Science, Japan

<sup>2</sup> Department of Mechanical Engineering, Tokyo University of Science, Japan

<sup>3</sup> Thermal Spray Laboratory, TOCALO, Hyogo, Japan

In large-sized pipes installed in a power generation plant, the surface is often cracked by subjecting to bending loading and cyclic loading. When such cracks are detected by a non-destructive inspection and its depth of crack is less than 20% of wall thickness, the cracked part is shaved off. After that the repairing treatment is done by a welding process for instance. Although weldment-based repair technique has a reliability as we know, because the adhesion strength between weld part and base material is very high, the residual stress could be as high as hundreds of MPa order. Such a high tensile residual stress brings about a large distortion in the pipe structure. Thus a post weld heat treatment has to be performed in order to reduce such distortion if possible, which eventually makes a maintenance cost and a maintenance period increase. We have interested in a plasma spraying process as one of advanced repairing technique replaced with weldment technique. As first step in our project, we tried to repair the notched plate-sample removed the damage part to the crack depth direction by an atmospheric plasma spraying process (APS) with CoNiCrAlY alloy powder. Then we conducted a tensile test for those repaired samples at room temperature in order to examine about deformation behaviour of the whole sample and a critical strain up to the repaired part being spalled completely off. The results revealed that the repair process can perform on the spot, which is one of a merit of thermal spray technique, and residual stress after the repair is quite low, which can reduce a distortion generated in the pipe structure without post-heat treatment. On the other hand, it also turned out that the further improvement of the adhesion strength of a repair part is desired.

In this report, we pay attention to the HVOF thermal spraying technology in which an improvement of adhesion strength might be expectable compared with atmospheric plasma thermal spray technology. As following the previous report, tensile test was conducted for the plate-shaped sample Type 304 stainless steel

repaired by HVOF in order to investigate improvement of mechanical property after the HVOF repair. Herein, supposing that the elliptical crack was detected on the pipe surface by UT, the sample surface was shaved off in the shape of an elliptical cone. In this study, CoNiCrAlY alloy powder was also sprayed for that removed area as the same as the previous work. Furthermore, during tensile loading, strain distribution in the repair part based on image processing was measured in addition to three dimensional finite element analysis. The result obtained by this study is as follows. It was found that the stress-strain curve of the specimen repaired in the shape of an elliptical cone is not affected by the aspect (a/b) identified at the bottom of an elliptical cone. While the residual stress in the repair part was in compression side, the critical strain up to delamination of the repairing part increases with amount of residual stress. The critical strain also increased as an aspect ratio changes, however the aspect ratio in case (a/b)=1.0 brought about lowest critical strain, which means the weakest strength. Finally, it can be recommended that the slender shape as surrounding the crack face is desired to improve effectively the adhesion strength at the repairing part/base metal.

### References

- Chowdhury, S.G., Mukhopadhyay, H.K., Das, G. & Das, S.K. (1998): Failure Analysis of a Weld Repaired Steam Turbine Casting, *Engineering Failure Analysis*, Vol.5, No.3: 205-218.
- Kumar, A., Boy, J., Zatorski, R. & Stephenson, L.D. (2005): Thermal Spray and Weld Repair Alloys for the Repair of Cavitation Damage in Turbines and Pumps, *Journal of Thermal Spray Technology*, Vol.14, No.2: 177-182.
- Sakamoto, K., Arai, M. & Suidzu, T. (2013): Study on Strength Properties of 2-D Material Repaired by Thermal Spraying under Tensile Load, *Proceedings of The 15th IUMRS International Conference in Asia (Fukuoka, Japan)*.

# Comparative residual stress measurements on shot peened spring steel by XRD and PRISM hole drilling method

THEO RICKERT<sup>1</sup>, DOMINIK DAPPRICH<sup>2</sup>, CARLO SCHEER<sup>2</sup>

<sup>1</sup>American Stress Technologies, Inc.

<sup>2</sup>Stresstech GmbH,

The effect of shot-peening is characterized in much detail by residual stress depth profiles. They are frequently measured by XRD. Hole-drilling is an alternative, though usually considered less accurate than XRD. Instead of the traditional hole-drilling method with strain-gages an optical method, ESPI (Electronic Speckle Pattern Interferometry) is used here for the stress relief analysis. No strain-gages have to be applied and the whole process is quicker than XRD and strain-gage hole-drilling. This paper compares residual stress depth profile measurements made by ESPI hole-drilling with XRD on shot-peened leaf spring sections and discusses differences between the two methods.

## References

- V.Hauk, H. Hougardy, E. Macherauch; Residual Stress – Measurement, Calculation, Evaluation; 1991 by DGM Informationsgesellschaft mbH, Adenauerallee 2, 6370 Oberursel
- Lothar Spieß, Robert Schwarzer, Herfried Behnken, Gerd Teichert(2005); Moderne Röntgenbeugung; B.G Teubner Verlag, GWV Fachverlag GmbH Wiesbaden 2005
- Dr. Jian Lu (1996); Handbook of Measurement of Residual Stresses; Faimont Press Inc. 700 Indian Trail, Lilburn, GA 30247

Talks Topic B 5:

## ***Residual stresses***

---

## Combined machining/burnishing process optimization for alloy steel 42CrMo4 using Taguchi technique

ANIS RAMI<sup>1</sup>, SALEM SGHAIER<sup>1</sup>, HEDI HAMDI<sup>2</sup>, SAMIR LAHOUAR<sup>1</sup>

<sup>1</sup>National School of Engineering, Laboratory of Mechanical Engineering, Monastir, Tunisia

<sup>2</sup>National School of Engineering, Laboratory of Tribology and System Dynamics, St Etienne, France

Burnishing is a cold working surface treatment process without removal of metal, in which plastic deformation of surface irregularities occurs by exerting pressure through a very hard and smooth ball surface with adequate pressure. As a result all pre-machined peaks gets compressed into valleys thus giving a finish surface, also a compressive residual stress is induced during the process, in order to have a long life (Sirinivasa 2008). This treatment occurs generally after the machining process.

In this study, a new combined machining/burnishing tool is designed, fabricated and used. It allows simultaneous turning and ball burnishing of the surface revolution using a CN turning machine.

The goal is to take advantage of the cutting temperature when the burnishing process is done, in order to promote crushing peaks and to generate a compressive residual stress (Bouزيد Saï 2005) that reaches the depth of the workpiece.

The combined cutting/burnishing parameters considered for this study are the common turning/burnishing

parameters (speed, feed rate), burnishing parameters (burnishing force, burnishing ball dimension), and the machining parameters (penetration depth). A design of experiments based on Taguchi technique is employed in this present investigation in order to identify the optimal machining/burnishing parameters, and to find a compromise between the optimal arithmetic surface roughness ( $R_a$ ), the compressive residual stress in the feed direction ( $\sigma_{xx}$ ), and the micro-hardness ( $H_v$ ) applied to low alloy steel **42CrMo4**.

### References

- Bouزيد Sai W & Sai K., (2005): Finite element modeling of burnishing of AISI 1042 steel, *Int J Adv Manuf Technol*, 460-465; Tunisia.
- Srinivasa D., (2008): Investigations on the Effect Ball Burnishing Process Parameters on the Surface Hardness and Wear Resistance of HSLA Dual-Phase Steels, *Materials and Manufacturing processes*, 23-3, 295-302.

## The residual stress homogeneity state induced by gear manufacturing processes

FRITZ KLOCKE<sup>1</sup>, JEFFERSON GOMES<sup>2</sup>, CHRISTOPH LÖPENHAUS<sup>1</sup>, RONNIE REGO<sup>1,2</sup>

<sup>1</sup>Rheinisch-Westfälische Technische Hochschule (RWTH), Aachen, Germany

<sup>2</sup>Aeronautics Institute of Technology (ITA), São José dos Campos, Brazil

Gear fatigue failures are widespread in most part of the machinery industry. The well-established benefits of compressive residual stresses over the fatigue performance constantly motivate research efforts on manufacturing processes optimization. Most part of these studies approach the surface states only through residual macrostresses assessment. The diffraction measurement methods are limited to the evaluation of a small area, hugely reducing the feasibility of the surface homogeneity analysis. The state uniformity is often not considered, and an incomplete picture of the fatigue life prediction is resultant.

But the residual stress state is classified from macro to microstresses into three levels, depending on the domain size of analysis. The importance of the microstrain to the fatigue performance was highlighted

earlier by Delhez, Keijser and Mittemeijer (1987). Recently, the uniformity of the residual stress level and its influence over fatigue was approached for shot peened surfaces (Zhan, Jiang & Li, 2013). The importance of a better stress distribution is emphasized, but an analysis of microstresses is not considered. And starting from a macro level, the subsequent microstress levels are considered a mean deviation from the respective previous level (Hauk & Nikolin, 1988). Therefore, the residual stress homogeneity state could be simply assessed through the micro intensity level: This approach of linking the residual macrostress heterogeneity and the intensity of the microstresses is however not explored. The objective of this study is to define a methodology for evaluating the homogeneity state of the residual stresses induced by processes of the gear manufactur-

ing chain. The main goal is to characterize this uniformity through the microstresses assessed from XRD line profile analysis.

The proposed methodology validation starts with the analysis of spur gears' flank surfaces after the shot peening process. Different levels of plastic deformation homogeneity were produced. The specimens analysed were dual peened and shot peened with different coverage levels. Residual macrostresses were evaluated along the depth profile with XRD. The first micro level was assessed through stress measurements of each phase from the 16MnCr5 steel studied. The single line profile analysis, by means of the Voigt deconvolution method, was used to evaluate the peak broadening effects of the diffracted curves.

The intensity of the micro residual stresses was correlated with two direct results from the surface macrostress homogeneity. The measurement of a macrostress matrix was applied for the correlation on the surface. The results were reinforced by topography maps, through three-dimensional roughness measurements. Together with the surface macrostress matrix, the functional roughness parameters found a coherent relationship with the strain contribution value of the

diffracted profiles. The result was complying with the objective, but the methodology was additionally correlated to results from fatigue tests. For this case, surfaces ground with different process parameters were evaluated. The comparison shows that the residual macrostresses must be complemented by the micro levels for a more precise understanding of the contact fatigue mechanism.

#### References

- Delhez, R.; Keijsers, T.H. & Mittemeijer, E.J. (1987): Role Of X-Ray Diffraction Analysis In Surface Engineering: Investigation Of Microstructure Of Nitrided Iron And Steels. In: Surface Engineering Vol. 3. The Institute of Metals and the Wolfson Institute for Surface Engineering, p. 331-342.
- Hauk, V. & Nikolin, H.-J. (1988): The Evaluation of the Distribution of Residual Stresses of the I. Kind (RS I) and of the II. Kind (RS II) in Textured Materials. Textures and Microstructures Vol. 8&9. Gordon and Breach Science Publishers Inc., 693-716.
- Zhan, K.; Jiang, C.H. & Li, V. (2013): Uniformity Of Residual Stress Distribution On The Surface Of S30432 Austenitic Stainless Steel By Different Shot Peening

## Influence of specimen size on the residual stress formation after heat treatment of hot-work tool steel components

M. SCHEMMELE<sup>1</sup>, P. PREVEDEL<sup>1</sup>, R. SCHÖNGRUNDNER<sup>1</sup>, W. ECKER<sup>1</sup>, T. ANTRETTNER<sup>2</sup>

<sup>1</sup>Materials Center Leoben Forschung GmbH, Austria

<sup>2</sup>Institute of Mechanics, Montanuniversität Leoben, Austria

The heat treatment process is one of the most crucial steps in the production chain of steel components. A wide variety of tailored technologies exists in order to adjust the desired material properties for the respective application.

In the field of hot-work tool steel components high pressure gas quenching is the state-of-the-art technology delivering final products with homogeneous hardness distributions, clean surfaces, reduced distortion and lower residual stress values compared to using liquid quenchants. A high level of tensile residual stresses may lead to surface cracks during the heat treatment process or may have a negative impact on the lifetime of tools.

Therefore, a finite element modelling scheme has been developed to predict the formation of residual stresses for given tool geometries. The multi-phase transformation kinetics of a hot-work tool steel grade X38CrMoV5-1 is modelled following an approach by Mahnken (2012), where the austenite-to-bainite transformation and the austenite-to-martensite transformation are taken into account. The focus lies on the diffusional bainitic phase transformation model which considers

the incomplete reaction of bainite resulting from the carbon enrichment of the retained austenite. Additionally, a micromechanical approach is included dealing with the phenomenon of transformation induced plasticity (Fischer, 2000) and the determination of the plastic behaviour of a mixture of phases with different yield strengths. Eventually, the overall material model is implemented in the finite element package ABAQUS (Abaqus 2013).

Large components require longer process time intervals to compensate for temperature differences between the core and surface regions. In order to calibrate the material model, test geometries of different sizes and shapes are heat treated. Thermal boundary conditions are determined by an inverse optimization routine and are applied to surface sets. In the FE model multiple layers of continuum shell elements are used in the surface regions to ensure a sufficiently fine discretization normal to the surface for resolving the residual stress distribution without causing excessively high computational costs. Residual stress profiles are measured by X-ray diffraction up to a depth of 1500 µm. The influence of the component size on the residual stress

formation is then investigated by simulations and compared with the experiments.

#### References

Mahnken, R., Wolff, M., Schneidt, A., Böhm, M. (2012): Multi-phase transformations at large strains – Thermodynamic framework and simulation. – International Journal of Plasticity, 39: 1-26

Fischer, F.-D., Reisner, G., Werner, E., Tanaka, K., Cailletaud, G., Antretter, T. (2000): A new view on transformation induced plasticity (TRIP). – International Journal of Plasticity, 16: 723-748  
 ABAQUS/Standard User's Manual, Version 6.13

## Effect of different surface treatments on A7N01S-T5 aluminum alloy butt joints fatigue properties

CHUANPING MA, HUI CHEN, QIMENG ZHU, YUANMING MA, XU ZHAO

School of Materials Science and Engineering, Southwest Jiaotong University, Chengdu, China

A7N01S-T5 aluminum alloy is used widely on some components of high speed train body, such as corbel, traction beam and so on. Welding residual stress of aluminum alloy is inevitable to be produced due to uneven heat input in the welding process. The fatigue properties of welded joints are affected by the welding residual stress, especially the tensile residual stress, while the compressive residual stress is useful to improve the fatigue properties of welded joints.

This paper is focused on the residual stress distribution and the fatigue properties of the A7N01S-T5 aluminum alloy butt joints were treated by the fine particle steel shot, glass balls, and corundum. The X-ray diffraction method was used to measure welding residual stress and the S-N curves were compared of the treated butt joints of different surface treatments. The results showed that: the maximum compressive residual

stress of the fine particle steel shot treated butt joints is -236MPa, that is large than the other two treated butt joints, corundum treatment and glass balls treatment which are -203MPa and -191MPa. The conditions fatigue limit of  $10^7$  of fine particle steel shot treated butt joints is 120MPa, and the corundum and glass balls treated butt joints are the same of 110MPa, while the untreated butt joints is 100MPa. The fine particle steel shot treatment can be considered for high speed train body surface treatment.

#### Reference

Mutoh Y, Fair G H, Nuble B, et al. The effect of residual stresses induced by shot peening on fatigue crack propagation in two high strength aluminum alloys[J]. Fatigue and Fracture Engineering Materials and Structure, 1987, 10( 4): 261 ~ 272

## Thermomechanical behaviour and microstructural evolution of high temperature forged Ti-6Al-4V during heat treatment quenching

RENAUD JULIEN<sup>1</sup>, VINCENT VELAY<sup>1</sup>, VANESSA VIDAL<sup>1</sup>, MEHDI SALEM<sup>1</sup>, YOANN DAHAN<sup>2</sup>, ROMAIN FORESTIER<sup>2</sup>, FARHAD REZAÏ-ARIA<sup>1</sup>

<sup>1</sup>Université de Toulouse, ICA (Institut Clément Ader), Albi, France

<sup>2</sup>Aubert & Duval, Pamiers, France

Ti-6Al-4V is a titanium alloy widely used for aircraft components (Banerjee & Williams 2013). Its manufacturing processes comprise thermo-mechanical treatments including cooling steps during which residual stresses can be generated and can thus make more difficult the machining steps (Gunnberg et al. 2006).

This contribution deals with a global approach undertaken to get better insight into the thermomechanical

behaviour and the microstructural evolution during heat treatments, and particularly during the cooling operations from the ( $\alpha + \beta$ ) phase field, of the high temperature forged Ti-6Al-4V titanium alloys.

A new experimental facility using conventional hydraulic testing machine and induction heating was developed to investigate different temperature-time histories representatives of the conditions undergone in

parts during quenching. Specific thermo-mechanical tests of the Ti-6Al-4V titanium alloy were then carried out as a function of the temperature, the strain rate and the cooling rate.

Tensile mechanical tests performed on Ti-6Al-4V alloy exhibits a predominant viscosity at high temperature whereas a significant hardening mechanism occurs at low temperature. Tensile tests with strain dwell time allow to determine the effect of both viscous and non viscous stress levels whatever the temperature and the cooling rate considered.

Moreover, as the mechanical properties, at a specific temperature, can be strongly related to the microstructure (phase transformation) (Roy & Suwas 2013), post-mortem optical and scanning electron microscope observations was carried out to study the metallurgical evolution (fraction, size and morphologies of the  $\alpha$  and  $\beta$  phases).

Hence, an image analysis protocol was developed to study the surface fraction of phases and grain sizes. It shows that they mainly evolve in a particular domain of temperature (950 to 700 °C) and for a specific range of cooling rate (5 to 60 °C/min). The grains belonging to

the high temperature  $\beta$  phase transform progressively into lamellar grains ( $\beta + \alpha_{||}$ ) where the surface fraction of  $\beta$  evolves linearly with the cooling rate.

Furthermore, a high cooling rate may favors the nucleation of  $\alpha_{||}$  lamellae which can lead to a large population of thin lamellae. It is shown that cooling rate effect induce a material hardening due to a wide number of interfaces.

#### References

- Banerjee, D. & Williams, J.C. (2013): Perspectives on Titanium Science and Technology. - In: Acta Materialia, 61: 844–879.
- Gunnberg, F., Escursell, M. & Jacobson, M. (2006): The influence of cutting parameters on residual stresses and surface topography during hard turning of 18MnCr5 case carburised steel. - In: Journal of Materials Processing Technology, 174: 82–90.
- Roy, S. & Suwas, S. (2013): The influence of temperature and strain rate on the deformation response and microstructural evolution during hot compression of a titanium alloy Ti–6Al–4V–0.1B. - In: Journal of Alloys and Compounds, 548: 110–125.

## Development of ProCast® Models to Predict Residual Stress within Femoral Implant Castings

BRIAN CONROY<sup>1</sup>, ALAN KAVANAGH<sup>2</sup>, DAVID TANNER<sup>1</sup>

<sup>1</sup>Department of Design and Manufacturing Technology and Materials and Surface Science Institute, University of Limerick, Ireland

<sup>2</sup>DePuy(Ireland), Cork, Ireland

Manufacturers of Cobalt Chrome (ASTM F75) femoral knee implants experience scrap resulting from out-of-tolerance parts. Femoral implants are “C”-shaped and the dimension across the open end of the “C”, the Anterior-Posterior (A-P) feature, can vary, requiring high levels of control and dimensional inspection. The A-P dimension is considered critical in order to ensure optimum fit to the patient’s bone. Parts which fall out of specification are rejected at significant business cost. Femoral implants are investment cast and moving-contact surfaces are machine ground and polished to achieve high surface finish requirements. There are two main points of identification of dimensional problems: **post-casting and post-grinding**.

**Post Casting:** Changes in dimensions between a wax-pattern and the cast part are expected, but are inconsistent. Complex geometries also cause unexpected movements during casting which are problematic when specifying wax-pattern dimensions and tolerances.

**Post Grinding:** Castings which are within specification can experience A-P “flowering”, or spread, resulting in

out of specification parts post machine grinding. Dimensional off-sets are frequently used, but parts can still move out-of-specification dimensionally. The cause of this movement is the result of the redistribution of Residual Stress (RS). RS can result from elastic stresses remaining in parts following non-uniform plastic deformation<sup>1</sup> which can arise from differential cooling during casting.

ProCast® models of the investment casting process have been developed to further understand distortion and predict RS. The development of the models has involved significant effort in the determination of temperature dependent material properties and the specification of realistic boundary conditions. Material properties required for both the metal & the mould are as follows: specific-heat, thermal-conductivity, density, Young’s modulus, Poisson’s ratio, yield-stress and expansion coefficients. Additional properties required for the metal are: latent-heat, fraction-solid, viscosity, plastic data (two possible models: Isotropic / Kinematic-to include the Bauschinger effect), visco-plastic data (to include strain-hardening creep). Material proper-

ties for the metal have been collected from various published sources and ASTM F75 specific data was calculated utilising JMatPro<sup>®</sup> material property calculation software. However, mould strength material properties have proven difficult to identify in the public domain.

In order to create a model which reliably predicts RS states there needs to be validation of three aspects; **thermal, RS** and **dimensional**. The final dimensions and RS of cast part will be affected by the amount of plasticity experienced during cooling which is directly affected by both the mould strength<sup>2</sup> and differential cooling-rates<sup>3</sup>. Therefore it is important that the models include mould strength properties and that the model accurately predicts the thermal state of the casting process.

Dimensional validation has involved the comparison of measured parts with predicted final dimensions. RS validation will be completed using neutron diffraction, centre-hole drilling and the contour method. The main body of work to date has been related to thermal validation.

Two casting trials have been conducted in a production Foundry with thermocouples (TCs) mounted in the

casting shell at various locations. Significant variation in the shell pre-heat temperature (differences of 150°C at the time of pouring) and casting cooling-rates were observed depending on the position of the casting on the mould.

Broad alignment with ProCast<sup>®</sup> was observed for a number of TC locations. However, simplifications of the casting set-up need to be addressed in order to truly reflect the process. Simplifications include; the absence of insulation effects as a result a sand-bed and the absence of thermal interface conditions between the TCs and the shell.

#### References

- <sup>1</sup>Prevéy, P.S. (1986) 'XRD RS Techniques', in Mills, K., ed., Metals H.book, 9<sup>th</sup> ed., 10, Ohio, ASM.
- <sup>2</sup>Sadrossadat, S.M. and Johansson, S. (2008) 'The effects of casting param. on RS and microstructure variations of an Al-Si cast alloy', Denver X-Ray Conf., Colorado, ICDD.
- <sup>3</sup>Farhangi, H., Norouzi, S. and Nili-Ahmadabadi, M. (2004) 'Eff. of casting proc. variables on the RS in Ni-base superalloys', Mat. Proc. Tech., Nov.

Talks Topic B 6:

## ***Residual stresses***

---

# Evolution of residual stresses and work hardening during cycling loading and their impact on fatigue behavior of a single crystal nickel based superalloy

AMÉLIE MORANÇAIS<sup>1&2&4</sup>, PASCALE KANOUTÉ<sup>2&1</sup>, MANUEL FRANÇOIS<sup>2</sup>, MATHIEU FÈVRE<sup>3</sup>, ANAÏS GAUBERT<sup>4</sup>

<sup>1</sup>ONERA – The French Aerospace Lab, Châtillon, France

<sup>2</sup>ICD-LASMIS, UMR CNRS 6281 Université de Technologie de Troyes, France

<sup>3</sup>LEM UMR 104 CNRS-ONERA, Châtillon, France

<sup>4</sup>SAFRAN Snecma Villaroche, Réau, France

High pressure turbine blades of aircraft engines are made of single crystal nickel-based superalloys. They are submitted to thermomechanical stresses, high temperatures and vibrations. The root of the turbine blade is a sensitive area because of the presence of stress concentrations due to its shape. In order to postpone the appearance of cracks, this area is shot-peened. This pre-stressing introduces compressive residual stresses (RS) and work hardening in a surface layer which evolve during service loadings. The knowledge of this initial mechanical state and its evolution under cyclic loads are required to improve the lifetime analysis.

The determination of residual stresses in single crystal using X-ray diffraction involve the use of a specific method developed by (Ortner 1983) and (François 1987). To our knowledge, this approach has not been used to measure stress profiles in shot-peened single crystal superalloys. The fatigue behaviour of the AM1 superalloy is usually modelled with the constitutive equations derived by (Chaboche 2012) and the lifetime analysis is described with the model developed by (Gallerneau 2007). This approach take into account the thermomechanical loading, the anisotropy of the material and the specific shape of the sample. However, the evolution of the stress and work hardening distribution associated with the shot-peening process is not yet implemented.

The aim of this study is to investigate the influence of residual stresses and work hardening introduced by shot-peening on the lifetime of the AM1 superalloy.

The experimental work is devoted to the determination of the initial mechanical state introduced by shot-peened. Ortner's method is used to determine an initial profile of macro-RS on shot-peened samples with simple and complex geometries. Experimental procedures are suggested to overcome the problems

linked to the mosaic structure (lattice fragmentation) of the crystal and to determine the stress levels with the maximum of accuracy and the minimum of acquisition time. Work hardening is then characterised from the diffraction peaks widths, Vickers hardness tests and electron microscopy with the electron backscatter diffraction technique.

The RS depth profiles are then introduced as an input in the finite element code Zset/Zebulon. Different methods are assessed in this study. The viscoplastic constitutive equations are then used and improved to reproduce the stress and the work hardening evolution during the fatigue loadings. To validate this model, measurements of residual stresses and work hardening are carried out on specimens loaded with different number of cycles. The fatigue lifetime analysis is performed with a macroscopic damage model, written in cycles. Finally, the results of modeling are compared with fatigue tests on shot peened samples exhibiting a stress concentration area.

## References

- Ortner, B. (1983): «Röntgenographische Spannungsmessung an Einkristallinen Proben», *Eigenstressungen*, Karlsruhe, Bd2, p46-68
- François, M. (1987): «Analyse des contraintes résiduelles dans le monocristaux et les matériaux à gros grains par diffraction des rayons X», mémoire de DEA, ENSCP-Univ. Paris VI.
- Chaboche, J.-L., Kanouté, P. and Azzouz, F. (2012): «Cyclic inelastic constitutive equations and their impact on the fatigue life prediction», *Int. J. of Plasticity*, vol 35, 44-66.
- Gallerneau, F. (1995) : «Etude et modélisation de l'endommagement d'un superalliage monocristallin revêtu pour aube de turbine», PhD thesis, ENSMP.

# Numerical and Experimental Description of the Surface and Subsurface Residual Stresses in Metallic Components after Mechanical Surface Treatment

MAJID FARAJIAN<sup>1</sup>, MIRKO BOIN<sup>2</sup>, ROBERT C. WIMPORY<sup>2</sup>, MICHAEL HOFMANN<sup>3</sup>, ALEXANDRU D. STOICA<sup>4</sup>, KE AN<sup>4</sup>

<sup>1</sup>Fraunhofer Institute for Mechanics of Materials IWM, Freiburg, Germany

<sup>2</sup>Helmholtz Centre Berlin for Materials and Energy (HZB), Berlin, Germany

<sup>3</sup>Forschungsneutronenquelle Heinz Maier-Leibnitz (FRM II), Munich, Germany

<sup>4</sup>Oak Ridge National Laboratory ORNL, Spallation Neutron Source, Oak Ridge, USA

It is a frequent practice to perform mechanical surface treatment e.g. shot peening, deep rolling and hammer peening in different industrial disciplines in order to improve the surface integrity of components and structures. These treatments invariably change the material properties and the residual stress state in the surface and subsurface and induce beneficial surface conditions; compressive residual stresses and cold working which in turn increase the performance of materials against fatigue, wear and corrosion.

Determination of the surface and sub-surface material states is a critical point for quantitative consideration of the beneficial induced surface conditions in structural integrity assessments. Most research work has focused on experimentally determining the residual stress and its depth profile by means of x-ray diffraction and corresponding electro-polishing the surface layers or hole drilling method. This valuable body of knowledge has led to development of phenomenological-models [1,2] which could describe the material behavior during treatment qualitatively. Since there are quite a number of parameters which could influence the residual stress field after mechanical surface treatment, covering the whole possible process parameters combinations with the purpose of experimentally determining the residual stress profiles would be an impossible task. Taking into account the development of new alloys, complex geometries, mechanical surface treatment in higher temperatures and under pre-strained conditions, relaxation of residual stresses under thermal and mechanical loadings, one would conclude that the application of numerical analysis as an effective tool to treat different issues of residual stress field and its influence on the structural integrity with lower experimental costs and time is indispensable. A literature study showed that, in the numerical works, a shortcoming in gener-

al is that a quantitative description of the surface and subsurface conditions by material modelling and process simulation has not kept pace with the rapid developments in the field of characterization of polycrystalline materials by means of combination of the available diffraction techniques.

In this paper some issues in simulation and modelling of shot peening, deep rolling and hammer peening will be discussed first. The corresponding calculations are then compared with the complementary experimental analysis [3] by means of x-ray, synchrotron and neutron diffraction methods.

Further the necessity of the development of the concept **residual stress engineering** for metallic components in which wanted residual stress states are tailored for specific cases by appropriate means will be discussed. The possibilities of the quantitative consideration of the benefits into the structural integrity assessments will be presented in some practical examples.

## References

- Wohlfahrt W., in Residual stress and stress relaxation, Sagamore Army Mat. Res. Conf. Vol. 28, Editor: Kula E., Weiss V., Plenum Press, 1982, pp. 71-92
- Vöhringer O., Changes in the state of the material by shot peening, Proceedings of the 3rd International Conference on Shot Peening, Garmisch-Partenkirchen, 1987.
- Farajian M., Nitschke-Pagel Th., Wimpory R.C., Hofmann M., Klaus M., Residual Stress Field Measurements in Welds by Means of X-ray, Synchrotron and Neutron Diffraction, Journal of Materials Science and Engineering Technology, Vol. 42, No. 11, pp. 996-1001, 2011.

# Evaluation of stress determination methods for a 2D x-ray diffraction portable apparatus using in-situ measurements during tensile testing

JOAQUIN RAMIREZ RICO<sup>1</sup>, JINJING LI<sup>2</sup>, SEUNG YUB LEE<sup>2</sup>, ISMAIL CEVDET NOYAN<sup>2</sup>

<sup>1</sup>Dpto. Física de la Materia Condensada-ICMS, Universidad de Sevilla-CSIC, Spain

<sup>2</sup>Dept. App. Physics & App. Math, Columbia University, New York, USA

Two-dimensional x-ray detectors allow the recording of residual strain in a material along a set of scattering vectors in a single measurement, so that the number of sample rotations required for determination of the residual stress state is significantly reduced and, in some cases, completely unneeded. In contrast to the conventional  $\sin^2\psi$  technique used with point detectors, which requires the measurement of strain in at least two distinct sample orientations for plane stress states (Noyan 1987), with area detectors the residual stress can in principle be determined in a single exposure. This advantage, combined with the miniaturization of image plates, x-ray sources and associated reading electronics, have resulted in commercial portable apparatus designed for in-line and field measurement applications, especially for ferrous metals (Ling 2014). Different approaches for the determination of the stress state from the information contained in a single Debye exposure exist, such as the  $\cos\alpha$  method introduced by Sasaki *et. al* (1997) or the direct least squares fitting of the measured strain (Kampfe 2000). Despite the attractiveness of these portable devices in both industrial and scientific applications, there no consensus on what the most efficient and precise calculation method.

In this work, we perform a comparison of the three proposed methods both from a theoretical as well as an experimental point of view. A code for the generation of synthetic 2D x-ray diffraction patterns was implemented and used to study the different methods' sensitivity to misalignment, detector calibration parameters as well as scatter in the data. For the experimental assesment we have used a portable x-ray residual stress measurement apparatus ( $\mu$ -X360 residual stress analyzer from Pulstec Industrial Co., Ltd.) to determine the residual stress in 1010 Carbon Steel cylindrical tubes in-situ during tensile loading. The meas-

urement conditions, with tight space constraints for the detector, as well as the use of a non-flat specimen, were chosen to approach those of actual applications. Several samples were tested up to yield and the residual stress at various loads was determined from single x-ray exposures, using both the  $\cos\alpha$  and the direct least squares fitting methods. Measurements were performed at different sample orientations with respect to the incoming beam to both asses its effect on the calculated stress, as well as to allow us to use the  $\sin^2\psi$  technique for comparison. Macroscopic strain was in all cases recorded using a clip-on extensometer. Results show that  $\cos\alpha$  and the direct least squares fitting methods give similar results, although both underestimate the axial stress and overestimate transversal stresses, while giving zero shear stress values as expected. The  $\sin^2\psi$  method yields results closer to the actual values for the axial stress, although using data from exposures at three different orientations.

## References

- Noyan, I. C., and Cohen, J. B. (1987). *Residual Stress* (Springer-Verlag, New York, NY).
- Ling, J., and Lee, S.-Y. (2014). "Characterization of a portable x-ray device for residual stress measurements" (Submitted to the J. Powder Diffraction).
- Sasaki, T., Hirose, Y., Sasaki, K., and Yasukawa, S. (1997). "Influence of Image Processing Conditions of Debye Scherrer Ring Images in X-Ray Stress Measurement Using an Imaging Plate," *Advances in X-ray Analysis*, 40, 588-594.
- Kampfe, A., Kampfe, B., Goldenbogen, S., Eigenmann, B., Macherauch, E., and Lohe, D. (2000). "X-Ray Stress Analysis on Polycrystalline Materials Using Two-Dimensional Detectors," *Advances in X-ray Analysis*, 43, 54-65.

## Laboratory Micro-focus X-ray Sources for Stress Measurements

BERND HASSE, ANDREAS KLEINE, JÖRG WIESMANN, CARSTEN MICHAELSEN

Incoatec GmbH, Geesthacht, Germany

In this contribution, we give an overview on current developments of multilayer optics for diffractometry in the lab as well as of new X-ray sources for laboratory applications. We explain the manufacturing process of the optics, summarize the different types of optics and give some examples of typical applications which benefit from the new possibilities, especially in combination with modern microfocus X-ray sources.

The optics consist of bent substrates with shape tolerances below 100 nm, upon which multilayers are deposited with single layer thicknesses in the nanometer range and up to several hundreds of layer pairs. The multilayers were designed with lateral thickness gradients within  $\pm 1\%$  deviation of the ideal shape. We use sputtering technology for deposition, optical profilometry in order to characterize the shape and X-ray reflectometry in order to characterize the multilayer thickness distribution both laterally and as in-depth. Beam parameters like monochromaticity, flux, brilliance and divergence demonstrate the quality of the multilayer optics.

We will present actual results of a combination of our microfocus source  $\mu\text{S}$  with two-dimensional beam shaping multilayer optics. These so called Quasar Optics are used for all common wavelengths like Cu, Mo, Ag, Cr, and Co. Our optics shape a focused or a collimated beam with a very high flux density as well as an adequate divergence directly at the sample position. In the field of stress measurements on iron containing samples especially Co and Cr sources are of interest, fluorescence radiation is not excited with these sources.

Examples of measurements using a microfocus source in combination with a two-dimensional beam shaping multilayer mirror with linear and position sensitive detectors are shown. Phase identification on iron containing samples is possible even at difficult accessible locations. Measurements of residual stresses are shown in a weld seam as well as in a steel spring and with high local resolution in different sections of a turbo-charger.

## Phase-Field Model for Solid-Solid Phase Transformation Driven by Elasticity

OLEG TSCHUKIN<sup>1,2</sup>, DANIEL SCHNEIDER<sup>1</sup>, BRITTA NESTLER<sup>1,2</sup>

<sup>1</sup>KIT, Institute of Applied Materials -Computational Materials Science, Karlsruhe, Germany

<sup>2</sup>University of Applied Science, Institute of Materials and Processes, Karlsruhe, Germany

In the last decades the phase field model has developed to an excellent simulation tool which allows the elegant mathematical description and efficient numerical calculation of different physical, thermodynamical or mechanical processes in the systems with locally different material properties and with time changing morphology. It is based on an optimisation of the Lyapunov functional of Ginzburg-Landau type, where the system variables are the intensive or extensive thermodynamical and/or mechanical quantities. An additional field on variables is introduced to describe different bulk volumes with uniform material properties. The evolution equations for the system variables are derived by the variational approach. A mathematically constructed diffuse interface between two different phases is of the length scale much higher compared to the real atomistic interface width of some angstroms. This model offers an elegant and efficient method for numerical simulations.

We present a new potential for the formulation of the optimised Lyapunov functional. The derivation is based

on the mechanical jump conditions on the two-phase boundary surface in equilibrium. The stress components of the traction vector and the strain components, due to the Hadamard jump condition, define the homogeneous variables of new potential. By the variational approach we derive (1) new formulation of the driving force for the solid solid phase transformation, (2) the new prescription for the stress calculation and (3) consequently the interpolation type and form of bulk material properties in the diffuse interface.

We validate our model on the analytical calculations in a two phase system with different isotropic stiffness tensors and compare the results with models based on a Voigt/Taylor and Reuss/Sachs approaches.

### Reference

Schneider, D., et al. (2015): Phase-field elasticity model based on mechanical jump conditions: Schneider, D., Tschukin, O., Choudhury, A., Selzer, M., Böhlke, T., Nestler, B.: submitted to Computational Mechanics

Talks Topic B 7:

## ***Residual stresses***

---

# Experimental and Numerical Investigation of Residual Stress Relaxation in Shot-Peened Notch Geometries under Low-Cycle Fatigue

CHAO YOU<sup>1</sup>, MITHILA ACHINTHA<sup>1</sup>, KATHERINE SOADY<sup>2</sup>, PHILIPPA REED<sup>1</sup>

<sup>1</sup>University of Southampton, Southampton, UK

<sup>2</sup>E.ON New Build and Technology Ltd., Nottingham, UK

In service, turbine components are subjected to low-cycle fatigue (LCF) during start-up and shut-down operations, especially at the fir tree root blade-disc connection which has a complex geometry and corresponding high stress concentration. Shot peening generates compressive residual stress and strain hardening which can improve fatigue life [1]. However, prediction of the fatigue life of shot-peened components under LCF is challenging due to difficulties associated with predicting residual stress relaxation, especially in regions of high stress concentration. The current study aims to develop a validated 3-D eigenstrain-based modelling tool to model residual stress relaxation under LCF in shot-peened notch geometries. The residual stress and strain hardening profiles caused by shot peening have been first evaluated by experiments and then incorporated into the finite element (FE) model separately.

The material under investigation is FV448 - a ferritic heat resistant steel representative of those used for steam turbine blades. An industrially applied shot peening treatment (intensity: 13A, coverage: 200%) for steam turbine blades has been applied to U-notched samples ( $K_t = 1.58$ ) representative of the real fir tree geometry. The LCF behaviour of the shot-peened sample has been evaluated by three-point bend tests with a load ratio  $R = 0.1$  [2].

Residual stress variation with depth at the notch root of shot-peened samples was measured before and after fatigue load cycles, using an X-ray diffraction (XRD) device and an incremental layer removal approach achieved by electropolishing. In addition, an EBSD-based approach [3] has been used to measure the plastic strain caused by shot peening, which was then used to determine the local strain hardening levels in peened samples.

In the FE model, a combined isotropic-kinematic hardening material model has been applied, considering both the monotonic and cyclic mechanical properties of FV448 which have been determined experimentally [2]. The residual stress distribution in peened samples was simulated as an elastic response of the whole com-

ponent to the predicted misfit strain (i.e. eigenstrain) caused by shot peening [4]. In order to incorporate the effects of strain hardening into the FE model, varying local yield stresses were defined at different depths within the surface layer affected by shot peening. Residual stress relaxation after 1 cycle and 50% life (about 15000 cycles) was then simulated by applying a similar load as in the real experiment to the FE model; the applied nominal strain range  $\Delta\epsilon$  in the loading direction was 0.68%.

The results show that the full residual stress distribution has been accurately modelled in the peened notched sample. The modelling results of residual stress relaxation after cyclic loading ( $\Delta\epsilon = 0.68\%$ ) match well with experimental data; a 20% relaxation was observed after the first cycle but with no further relaxation during subsequent fatigue cycles.

This study suggests that the hybrid eigenstrain/FE approach is particularly effective in modelling residual stresses in shot-peened components with notch geometry. This approach is helpful in evaluating the benefit of shot peening by effectively predicting residual stress relaxation after fatigue loading.

## Acknowledgements

Financial support from the China Scholarship Council (CSC) and E.ON New Build and Technology Ltd. is gratefully acknowledged. Thanks must also be extended to Gary Harrison at the University of Manchester, for his assistance in collecting residual stress data.

## References

- E.R. de los Rios et al. (1995): International Journal of Fatigue, 17, pp. 493-499.
- K.A. Soady (2013): University of Southampton (EngD Thesis).
- K.A. Soady et al. (2013): International Journal of Fatigue, 54, pp. 106-117.
- M. Achintha et al. (2013): Surface and Coatings Technology, 216, pp. 68-77.

# Analysis of compositionally ungraded FGM analogues: Neutron diffraction measurements of residual stress and mechanical testing of pressure sintered Mo-Y<sub>2</sub>O<sub>3</sub> and Mo-Al<sub>2</sub>O<sub>3</sub> systems

MICHAEL SALEH<sup>1\*</sup>, DORJI CHAVARA<sup>1</sup>, KARL TOPPLER<sup>1</sup>, JAMES ALEXANDER<sup>1</sup>, ANDREW RUYS<sup>2</sup>, KAVEH KABIR<sup>3</sup>, VLADIMIR LUZIN<sup>4</sup>

<sup>1</sup> Institute of Materials Engineering, Australian Nuclear Science and Technology Organisation, Kirrawee DC, Australia

<sup>2</sup> School of Aerospace, Mechanical and Mechatronic Engineering, University of Sydney, Australia

<sup>3</sup> School of Mechanical and Manufacturing Engineering, University of New South Wales, Sydney, Australia

<sup>4</sup> The Bragg Institute, Australian Nuclear Science and Technology Organisation, Kirrawee DC, Australia

Functionally graded materials (FGMs) are a type of naturally inspired composite materials whose properties (e.g. microstructure, chemical or phase composition) vary over one or more dimensions. The FGMs were first proposed as an advanced engineering material in 1972 and research into application for Biomaterials, Aerospace, Chemical Plants, Mining, and Building material commodities [1, 2] is ever present. Within the nuclear industry FGMs can be engineered to effectively resist corrosion, radiation and are a potential choice for nuclear reactor components e.g. first wall for fusion reactors and fuel pellets. Additionally FGM's have been proposed as potential plasma facing components (PFC) whereby the PFC would gradually vary from a refractory material (tungsten, plasma face) to a heat sink material (copper, coolant side). In the case of a metal-ceramic FGM, the composite mates the strength and ductility of a metal with the hardness and toughness of a ceramic [3-5].

The authors have sought to elucidate the development of residual stress in FGMs using neutron measurements on the Kowari Strain Scanner, ANSTO for the Mo-Y<sub>2</sub>O<sub>3</sub> and Mo-Al<sub>2</sub>O<sub>3</sub> system. Due to their extreme gradients FGM's are not optimal for fast neutron measurements due to the high spatial resolution requirements and long measurement times. An alternative approach was employed to examine compositionally ungraded analogues of varying metal-ceramic ratios. All sample were manufactured using constituent powders, mixed and subsequently sintered using a hot press with close monitoring of the sintering curve. Optical microscopy and scanning electron microscopy were used to look at the resultant samples to observe the grain growth and the defect-like cracks attributable to the thermally induced stresses. Relaxation due to micro cracking and micro-fracturing are evaluated in light of the neutron

residual stress measurements and mechanical strength measurements of : (a) bending stiffness using a three point bend tests, (b) bulk modulus through GrindoSonic techniques and (c) statistically averaged micro-hardness.

Further evaluation of the residual stress is done through comparison between established analytical models, neutron diffraction and preliminary FEA. The major contribution of residual stress are further realised and evaluated in light of the interfacial instabilities present and the appropriate ways to optimise the thermal protection characteristics of a compositional gradient.

## References

1. Miyamoto, Y., et al., Functionally graded materials: Design, processing and applications. Other Information: PBD: Sep 19991999. Medium: X; Size: 352 pages.
2. Kieback, B., A. Neubrand, and H. Riedel, Processing techniques for functionally graded materials. MATERIALS SCIENCE AND ENGINEERING A, 2003. 362(1-2): p. 81-106.
3. Chavara, D.T., Synthesis and Testing of Metal-Ceramic Functionally Graded Materials, in School of Aerospace, Mechanical and Mechatronic Engineering, 2009, University of Sydney: Sydney.
4. Nawka, S., et al. Synthesis, Characterization and FEM-Simulation of W/CuCrZr-Composites for Extreme Thermal Applications. in PM2010 Powder Metallurgy World Congress. 2010. Florence, Italy: European Powder Metallurgy Association
5. Ling, Y.-H., et al., Fabrication and evaluation of SiC/Cu functionally graded material used for plasma facing components in a fusion reactor. Journal of Nuclear Materials, 2002. 303(2-3): p. 188-195.

## The distribution laws of residual stress of high speed trains by statistical method

GUOQING GOU<sup>1</sup>, HUI CHEN<sup>1</sup>, YUPING YANG<sup>2</sup>, JIA CHEN<sup>3</sup>

<sup>1</sup> School of Materials Science and Engineering, Southwest Jiaotong University, Chengdu, China

<sup>2</sup> EWI, Columbus, Ohio, USA

<sup>3</sup> Chengdu Technician College, Chengdu, China

Residual stress (RS) have significant influence on the performance of high speed trains. The research group members of this paper have accured many test and research data from many types of CRH2 high speed trains.

This paper is focused on the distribution laws of RS by statistical method. The research objects are A5083P-O aluminum alloys welded joints, A6N01S-T5 aluminum alloys welded joints and A7N01S-T5 aluminum alloys welded joints of high speed train bodies. The RS of butt welded joints, angle joints are also discussed. Finally the peak RS in different structure and interval of high speed trains are discussed too. The results showed that the RS of A5083P-O joints that welded with the same materials is manily distributed between -100MPa and 100MPa and the probability is 92.93%. The RS of A6N01S-T5 joints that welded with the same materials is manily distributed between -150MPa and 150MPa and the probability is 92.27%. The RS of joints that welded with A5083P-O materials and A7N01S-T5 materials is mainly distributed between -100MPa and

150MPa and the probability is 94.06%. The RS of joints that welded with A6N01S-T5 materials and A7N01S-T5 materials is mainly distributed between -100MPa and 150MPa and the probability is 88.89%. The RS of butt welded joints is mainly distributed between -100MPa and 150MPa and the probability is 88.44%. And the RS of angle welded joints is mainly distributed between -100MPa and 150MPa and the probability is 95.28%. The peak RS is mainly distributed on the weld zone and the probability is 50%.

With the statistical distribution laws, the researchers, designers, maintenance personnel can reference to improve and protect the safety of high speed trains.

### References

- G. Totten, M. Howes, T. Inoue. Handbook of Residual Stress and Deformation of Steel. The Materials Information Society, 2002.
- Zhili Feng. Processes and Mechanisms of Welding Residual Stress and distortion. Woodhead Publishing and Maney Publishing, 2005.

## How to depict measured data and results in the matrix method

BALDER ORTNER

University Leoben, Austria

The matrix method (Ortner 2011), also called  $g\text{-}\sin^2\psi$  method (Skrzypek et al. 2001, Haase et al. 2014) which is based on Hooke's law in the form of Dölle-Hauk's equation (Dölle & Hauk 1978, Dölle 1979) or a derivation of it (Ortner 2011) has a lot of advantages over all other methods used for data evaluation in x-ray and neutron stress measurements. Yet there is some resistance to its introduction. One of the reasons for this resistance seems to be the problem of how to visualize measured data and results. When using the  $\sin^2\psi$  method or any other method based on a line of best fit, the corresponding diagram provides us with an immediate impression about the stress and the accuracy of all single measurements. For the matrix method the question is: can the data also be represented in a way which is similarly meaningful as the usual diagram in the  $\sin^2\psi$  method is? To give an answer to this question

we adapted the  $\sin^2\psi$  plot and developed some new types for the graphic representation of the results. The plotting methods can be subdivided into two categories.

A) Diagrams in which only measured / recalculated values with the same azimuth  $\phi$  are plotted.

A1) The  $\sin^2\psi$ -plot

Here the measured and the recalculated lattice constants  $a(\phi, \psi, hkl)$  are plotted versus  $\sin^2\psi$ .

With  $a(\phi, \psi, hkl)$  we mean a fictitious lattice parameter, calculated from the measured lattice plane distance.  $\phi$  and  $(hkl)$  must be the same in one plot, but plots can be done for any constant  $\phi$  and  $(hkl)$ , provided that there are enough data with different  $\psi$ s. Such a plot is virtually the same as we are used to from the  $\sin^2\psi$  method.

A2) The  $F_{\phi}$  plot

Instead of  $\sin^2\psi$  one can also use  $F_{\phi}(\phi, \psi, hkl)$  for the abscissa, where  $F_{\phi}(\phi, \psi, hkl)$  means the longitudinal effect [Haussühl 2007] of the tensor  $F_{ij}(\phi, \psi, hkl)$  in the direction given by  $\phi$ . In this plot the recalculated data always lie on a straight line, not only if the material is quasi-isotropic but also if it has significant texture.

B) Diagrams in which all data are shown, independent of their  $\phi$ -values and also independent of their Miller indices.

B1) The  $a'_{\phi}(\phi, \psi, hkl)$  versus  $F_{\phi}(\phi, \psi, hkl)$  plot  $a'$  is another fictitious lattice parameter.

In the  $a'$ -plot the recalculated values of  $a'$  lie on a straight line. The slope of this line is proportional to  $\sigma_{\phi}$ , ( $\phi=0^{\circ}, 90^{\circ}, 60^{\circ}, \dots$ ) the distances of  $a'$ -measured to that line provides us with the wanted impression about the accuracy of all measurements. But the greatest ad-

vantage of this representation lies in the fact that all measured and recalculated values can be shown in one diagram with one single regression line. This is especially helpful in thin film or single crystal stress measurements, because in the general case one must make use of different (hkl)s and all values of  $\phi$  can be different from each other.

## References

- Ortner B. (2011) Materials Science Forum Vol. 681 pp 7-12, Trans Tech Publications, Switzerland  
 Skrzypek et al. (2001), J. Appl. Cryst. 34, 427-435  
 Haase et al. (2014), Adv. In X-Ray Analysis, 57  
 Dölle H., Hauk V., (1978) Z. Metallkunde 69, 410  
 Dölle H. (1979) J. Appl. Cryst. 12, 48  
 Haussühl S. (2007), Physical Properties of Crystals, 80f, Wiley-VCH, Weinheim

## Finite Element modeling and investigation of the process parameters in Deep Rolling of a plane geometry

NATALIYA LYUBENOVA, DIRK BAEHRE

Saarland University, Institute of Production Engineering, Saarbruecken, Germany

In the modern industry the targeted application of compressive (negative) residual stresses in highly stressed components is gaining great importance. Compressive residual stresses are often used as design instrument in order to increase the fatigue life of the components and to improve their resistance to Foreign Object Damage (Mader 2005). It is well known that parts, which are exposed to tensile (positive) static as well as dynamic loads, are prone to crack formations. When compressive residual stresses are superimposed to the operating tensile loads they reduce the total loading, thus retarding the surface cracking and preventing the initiation of new cracks.

There are numerous production processes which are able to introduce pronounced compressive residual stresses differing in the depth profile. Typical examples are Shot Peening, Autofrettage, Laser Shock Peening, Ultrasonic Impact Treatment and Deep Rolling.

Well-recognized is the Deep Rolling (DR) process that has attracted the interest of the scientific community initially in the thirties of the last century (Thum 1935). Investigations of the process in the seventies and eighties led to the clear consideration that it is able to improve the fatigue life of the treated components. According to the VDI guideline 3177 (VDI 1983), DR is classified as fine surface rolling method, next to finishing and size rolling. In the available literature different terms, like Deep Rolling, Deep Cold Rolling, Roller Burnishing, Low Plasticity Burnishing and others, are used to describe processes similar in mechanism and

results. The main advantage of DR is the high amount and depth of achieved compressive residual stresses which in some materials can exceed 1 mm (Jung 1996). Another advantage is the reduction of the surface roughness which prevents the crack formation and -propagation. In steel the roughness after treatment with DR can be well below  $1 \mu\text{m}$  (Rz). A deep layer of strain hardening and plastic deformation also belongs to the properties of the treated component, thus contributing to its longer life time.

Although well-known, DR is still investigated due to the large amount of input parameters which leads to great differences in the results. Schulze (Schulze 2006) offers a comprehensive classification of the DR parameters by dividing them into work piece-, tool-, process- and device parameters. Some of them, like the applied force or pressure, the number of overturns, the percentage of overlapping, the properties and geometry of the work piece, etc., directly influence the quality of the surface as well as the depth and amount of the achieved residual stresses.

Finite Element (FE) Modelling is a powerful instrument to model complex processes, e.g. DR, and offers a good opportunity to vary and investigate numerous input- and output parameters. In this paper the Explicit module of the FE-Code ABAQUS 6.13 is applied to model the DR process on a plane geometry. The input parameters applied force, number of overturns and percentage of overlapping are varied and their influence on the induced residual stresses is commented.

Along with this the geometrical deformations due to the process are investigated.

#### References

Jung, U., Kaiser, B., Kloos, K. H. & Berger, C. (1996): Festwalz-Eigenstressen per Computer Simulation bestimmen – In: Mat.-wiss., u. Werkstofftech. 27, 159-164.  
Mader, S. & Klocke, F. (2005): Fundamentals of the deep rolling of compressor blades for turbo aircraft

– In: Conf. Proc.: ICSP-9, 125-130; Paris.  
Oberflächen-Feinwalzen (1983) – In: VDI-Richtlinie 3177; Düsseldorf  
Schulze, V. (2006): Surface Layer States after Mechanical Surface Treatments – In: Schulze, V. (ed.): Modern Mechanical Surface Treatment – States, Stability, Effects. WILEY-VCH Verlag GmbH & Co. KGaA, 95; Weinheim  
Thum, A. & Bautz, W. (1935) – In: Forsch. Ing. Wesen 6: 121.

Talks Topic C 1:

***Cyclic deformation behavior, crack initiation & crack growth of metals***

---

# Effect of chemical heterogeneity on the low-cycle-fatigue behavior of austenitic Cr–Ni stainless steels

JIŘÍ MAN<sup>1</sup>, MAREK SMAGA<sup>2</sup>, IVO KUBĚNA<sup>1</sup>, ALICE CHLUPOVÁ<sup>1</sup>, JAROSLAV POLÁK<sup>1,3</sup>

<sup>1</sup>Institute of Physics of Materials AS CR, Brno, Czech Republic

<sup>2</sup>Institute of Materials Science and Engineering, University of Kaiserslautern, Germany

<sup>3</sup>CEITEC, Institute of Physics of Materials AS CR, Brno, Czech Republic

The AISI type 300 (Cr–Ni) austenitic stainless steels represents an important class of materials widely used in engineering practice at room, elevated (Marshall, 1984) and as well as at cryogenic temperatures (Tobler et al., 1997). The austenitic structure of these alloys is metastable, i.e. martensitic transformation  $\gamma \rightarrow \alpha'$  can occur during cooling and/or plastic straining. The stability of austenite depends primarily on the chemical composition (see two threshold temperatures designated  $M_s$  and  $M_{d30}$  (Pickering, 1978)). Further important factors influencing martensite formation in fatigued austenitic steels are: initial thermo-mechanical state prior fatiguing (solution treatment vs. cold working), type of cycling (stress or strain control), frequency of cycling and grain size.

In all studies performed so far only nominal chemical composition of steels was considered. However, as will be shown in the present work characteristic chemical banding occurs in divers steel semi-products used for machining of cylindrical low-cycle-fatigue specimens, i.e. plates and bars. The extent of chemical heterogeneity was visualized via color etching (see Fig. 1) and quantified using EDS spectroscopy in SEM. Its origin is discussed in terms of particular manufacturing steps in the production of steels, i.e. continuous casting followed by subsequent thermo-mechanical treatment (hot and cold working).

The aim of the present work is to point out the importance of chemical heterogeneity on the destabilization of austenite during cyclic straining of two most used representatives of the AISI 300-grade steels, namely 304 and 316L steels. For this purpose the steels in solution-annealed state were subjected to low-cycle fatigue under well controlled conditions with constant plastic strain amplitudes at room temperature and in the case of 316L steel also at depressed temperatures.

Electron channeling contrast imaging (ECCI) technique and color etching were adopted to characterize microstructural changes after completion of fatigue tests. Distribution of deformation induced martensite in the volume of material is correlated with the presence of long fatigue cracks and with the characteristic variations of chemical composition corresponding to areas with reduced nickel content.

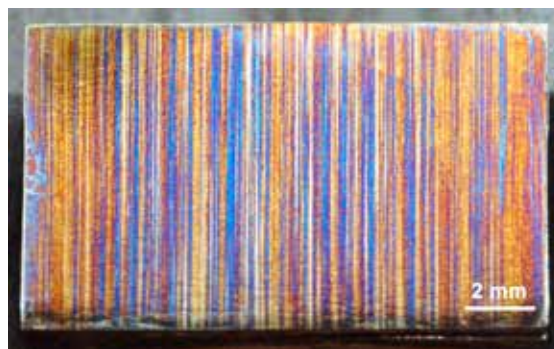


**Fig. 1.** Chemical heterogeneity revealed on the longitudinal section of cylindrical rod of 304 austenitic steel using color etching technique.

## References

- Marshall, P. (1984): *Austenitic Stainless Steels: Microstructure and Mechanical Properties*. Elsevier Applied Science Publ.; London.
- Tobler, R.L., Nishimura, A. & Yamamoto, J. (1997): Design-relevant mechanical properties of 316-type steels for superconducting magnets. *Cryogenics*, Vol. 37:533-350.
- Pickering, F.B. (1978): *Physical Metallurgy and The Design of Steels*. Applied Science Publishers; London.

## The distribution of local plastic deformation during VHCF loading of duplex stainless steel and martensitic steel

ALEXANDER GIERTLER, RUDOLF DENK, ULRICH KRUPP

University of Applied Sciences Osnabrück, Faculty of Engineering and Computer Science, Osnabrück, Germany

Due to the anisotropy of polycrystalline metallic materials a substantial scatter of microstrains is observed during uniaxial cyclic loading conditions. Generally, fatigue cracks initiate at sites where the microstrains reach maximum values within the plastic regime. Very high cycle fatigue (VHCF) loading manifests itself by a low macroscopic strain amplitude; however on a microscopic scale, crack initiation is caused by the crystallographic misorientation of neighboring grains which give rise to stress and microstrain concentration leading to the development and growth of slip bands. Eventually, the local microstructure has to be taken into account as a barrier for slip transmission in the following stage of VHCF damage evolution, and later also for crack initiation and propagation.

Experimental results on the VHCF damage of grade 1.4462 austenitic-ferritic duplex stainless steel and a grade 1.7227 tempering steel reveal the relationship between the crystallographic orientation of individual grains, grain patches and local strains within the grains on the one hand, and slip band formation, fatigue crack initiation and growth on the other hand. For this purpose, electrolytically polished small bending specimens have been fatigued under pure bending in a resonance fatigue testing machine. The specimens were investigated by means of scanning electron microscopy (SEM) in combination with automated electron back-scatter diffraction (EBSD). Digital image correlation (DIC) within the SEM in combination with EBSD was used to link the local crystal orientations with the microstrain distribution.

Under VHCF loading conditions, it was found that in case of the duplex stainless steel, slip band formation is limited to the softer austenite phase. The slip

bands generate high stresses at the austenite-ferrite ( $\gamma$ - $\alpha$ ) phase boundaries, where they eventually lead to intergranular or transgranular crack initiation. Crack initiation in the tempering steel can be attributed to shear band formation between the martensitic laths structure. Earlier investigations regarding the microcrack propagation process show that in both materials microcracks are sensitive to changing crystallographic orientations when crossing a grain or phase boundary. In particular, phase boundaries in the case of the duplex steel, and prior austenite grain boundaries in the case of the tempering steel, were identified as effective barriers to slow down or even to stop the microcrack propagation process (Zhai et al.).

The results are discussed by means of a Finite Element Modelling (FEM) approach that accounts for elastic anisotropy and crystal plasticity, following the work of Huang. The model (implemented in the commercial FE software ABAQUS) shall be capable to calculate the distribution of the microstrains within the microstructure and to explain the local occurrence of slip bands depending on the crystallographic orientation.

### References

- Zhai, T., et al. (2005): The grain boundary geometry for optimum resistance to growth of short fatigue cracks in high strength Al-alloys, *Int. J. Fatigue*, 27: 1202.
- Huang, Y. (1991): A User-Material Subroutine Incorporating Single Crystal Plasticity in the ABAQUS Finite Element Program, Mech. Report 178, Division of Engineering and Applied Sciences, Harvard University, Cambridge.

## Fatigue mechanisms of an austenitic-ferritic duplex stainless steel at loading conditions close to the conventional fatigue limit

BENJAMIN DÖNGES<sup>1,2</sup>, CLAUS-PETER FRITZEN<sup>2</sup>, HANS-JÜRGEN CHRIST<sup>1</sup>

<sup>1</sup>Universität Siegen, Institut für Werkstofftechnik, Germany

<sup>2</sup>Universität Siegen, Institut für Mechanik und Regelungstechnik - Mechatronik, Germany

Recent results obtained by experiments in the very high cycle fatigue regime are questioning the former assumption that all bcc materials have a fatigue limit,

whereas fcc materials do not. It was shown by numerous authors that bcc materials can fail even after two million load cycles and more due to crack initiation

at subsurface defects. In order to investigate the very high cycle fatigue mechanisms of a material that contains both lattice structures (bcc and fcc), cyclic deformation experiments close to the conventional fatigue limit were executed on the austenitic-ferritic duplex stainless steel 318LN (X2CrNiMoN22-5-3) up to one billion load cycles. The ultrasonic fatigue testing technique from BOKU Vienna was applied to conduct the experiments in symmetric push-pull-mode in a reasonable testing time ( $10^9$  load cycles in about one week) on electrolytically polished hourglass-shaped samples. After testing, the samples were investigated by means of TEM and high resolution SEM in combination with focused ion beam (FIB) cutting. The cyclic damage evolution on the sample surface was investigated by means of far field microscopy (in-situ) and by means of confocal laser scanning microscopy. The cyclic evolution of residual stresses and dislocation densities was investigated by means of high energy X-ray diffraction experiments. These results will be presented in the session "residual stresses" of this conference. Fractographic investigations showed that all fatal cracks initiated at the sample surface. Only very few samples failed in the very high cycle fatigue regime. Cyclic irreversible plastic deformation predominantly takes place in the austenitic phase, whereas crack nucleation occurs in the ferritic phase starting from intersection points between phase boundaries and austenite slip traces as documented by means of FIB cutting in combination with high resolution SEM. TEM investigations

showed significantly higher dislocation densities in ferrite grains close to intersection points between phase boundaries and austenite slip bands in contrast to other sites. The experiments revealed that the stages of fatigue crack nucleation and short fatigue crack propagation through the first grain determine significantly the lifetime of the material. Numerous fatigue samples which endured one billion load cycles without fracture (run-out samples) contained several microcracks in the order of less than one grain diameter. It was observed rarely that run-out samples contained microcracks which reached or overcame the first microstructural barrier (phase or grain boundary). The present study documents that the experimentally identified fatigue mechanisms can be represented in mesoscopic finite element simulations. Such simulations enable the determination of the fatigue limit and fatigue life of both real and synthetic microstructures by considering the effects of anisotropic elasticity, crystal plasticity, macro and micro residual stresses, plastic strain concentration in form of slip bands, fatigue crack nucleation and short fatigue crack propagation. By means of real microstructures, containing slip traces and microcracks, the calculations can be verified and the required microstructural parameters can be determined. Based on synthetic microstructures, parameters, which hardly or not at all can be varied in an experimental investigation (such as the misorientation between adjacent grains), can systematically be analyzed.

## Material Development for Precision Steel Tubes for Stabilizer Bars

MARIO MÜCHER, ROBERT BRANDT

Universität Siegen, Germany

Modern lightweight stabilizer bars for mass production are made by use of precision steel tubes. Thus the mass can be reduced by 50% compared to solid stabilizer bars. Tubular stabilizer bars provide the same function, which is characterized by a spring rate. However the stress level of a tubular stabilizer bar is rising compared to a solid stabilizer bar, especially at the inner surface. Furthermore, the stress profile of stabilizer bars under loading is rather inhomogeneous and complex. Maximum stress is localized in a few spots and the material is hardly utilized.

The use of tailored tubes can reduce this shortcoming. The wall thickness is adapted along the routing of the stabilizer bar in order to homogenize the stress distribution: The wall thickness in a lowly stressed section has to be reduced, in a highly stressed section the wall thickness has to be increased. The design optimization is done by numerical methods. For a further mass reduction of tubular stabilizer bars a high carbon steel

with increased tensile strength is evaluated.

Precision steel tubes are manufactured by means of an induweld-process. An axial weld seam is formed in the tube. The high carbon boron steel material of the tube exhibits inhomogeneities in the weld seam area and the heat affected zone (HAZ), which has a detrimental impact on the fatigue strength of the stabilizer bar.

The complex state of stress near the weld seam is characterized by the value and the orientation of the main principal stresses. Up to now no in-depth analysis of the fatigue strength of the weld seam has been done. Hence, the investigation of the orientation sensitivity of the stress in the weld seam area is done. Small pieces of material are cut out of the weld seam areas such, that three different orientations of the weld seam with respect to the uniaxial loading direction can be realized. Standard fatigue specimen are prepared according to ASTM E 466-07, which are tested with alternating stress (stress factor  $R=-1$ ). The resulting S-N curves

are discussed. The orientation dependency of the fatigue strength of the weld seam is a key information for a further mass reduction by choosing an optimum

position of the weld seam. Furthermore this method is used to evaluate new high strength tube material and its weld seam.

## Effect of Cementite Morphology on Fatigue Crack Propagation in Smooth Steel Specimen

ZHOU-JIA XI<sup>1</sup>, MOTOMICHI KOYAMA<sup>1</sup>, YUICHI YOSHIDA<sup>2</sup>, NOBUYUKI YOSHIMURA<sup>2</sup>, KOHSAKU USHIODA<sup>2</sup>, HIROSHI NOGUCHI<sup>1</sup>

<sup>1</sup>Faculty of Engineering, Kyushu University, Fukuoka, Japan

<sup>2</sup>NIPPON STEEL & SUMITOMO METAL, Tokyo, Japan

Since fatigue is the most important cause of accidental failure in structure parts, prediction of fatigue lives has been required to safely use structure materials. A factor affecting fatigue lives associated with short fatigue crack growth is microstructure, dominating a crack propagation life. Therefore, including the microstructural factors, we have to separately investigate the fatigue crack growth consisting of three periods: crack initiation, short crack propagation, and long crack propagation. Then, the focused propagation process, short crack propagation regime, dominates at least 90% of fatigue lives of high cycle fatigue in smooth specimens. Thus, the microstructure dependence of short crack propagation behaviour is noticed in this study.

In terms of precipitates in steels, effects of carbide should be noted, since general steels contain a significant amount of carbon. More specifically, we focus on influences of cementite morphology on short crack propagation. To our best knowledge, roles of the cementite morphology on the short crack propagation have never been revealed yet, although some simple relationships between cementite formation and fatigue limit have been studied. Hence, the novelty of this paper is placed on clarifying some roles of the cementite morphology on the short crack propagation in smooth specimens.

We prepared two types of low carbon steels with the same chemical composition and different cementite morphologies by the different heat treatment. The undeformed microstructures after the two different heat treatments show that cementite precipitates along grain boundaries or in grain interior. Hereafter, the former and latter cementite morpholo-

gies are called as intergranular cementite precipitation (ICP) and transgranular cementite precipitation (TCP) steels, respectively.

These steels do not contain solute carbon and second phase except for cementite. The ICP and TCP steels showed 248 and 270 MPa tensile strengths, respectively.

Thanks to the present study, the cementite morphology could be concluded to affect the fatigue properties as follows.

- 1) The crack initiation site was a grain boundary in both the ICP and TCP steels.
- 2) The ratios of fatigue limit to tensile strength of the ICP and TCP steels were 0.52 and 0.63, respectively. Namely, the fatigue strength is effectively enhanced by transgranular precipitation.
- 3) In the same stress amplitude/tensile strength ratio, the crack propagation rate of the ICP steel is lower than that of the TCP steel.
- 4) Intergranular cementite as well as transgranular cementite acts as obstacle against short fatigue crack propagation, resulting in crack propagation interception and branching.

### References

- T. Svensson, *Fatigue and Fracture of Engineering Materials and Structures*. 27 (2004) 981-990.
- C. Laird, in: J.C. Grosskreutz (Eds.), *Fatigue crack propagation*, American Society for Testing and Materials, Philadelphia, 1967, pp. 131-180.
- Wolburg, M. Herbig, A. King, P. Reischig, H. Proudhon, E.M. Lauridsen, J. Marrow, J.-Y. Buffière, W. Ludwig, *Acta Mater.* 59 (2011) 590-601.

Talks Topic C 2:

***Cyclic deformation behavior, crack initiation & crack growth of metals***

---

## The role of corrosion pit in corrosion fatigue crack initiation process of 12Cr stainless steel

RYUICHIRO EBARA

Institute of Materials Science and Technology, Fukuoka University, Japan

Although corrosion fatigue crack initiation mechanism of structural materials is not fully understood well, failure analyses for various machine components revealed that corrosion fatigue cracks most frequently initiate from corrosion pits (Ebara 1985). In fact corrosion fatigue cracks in association with corrosion pits are frequently observed on failed steam turbine blade (Ebara, Kai, Mihara, Kino, Katayama & Shiota 1983).

In this presentation characteristics of corrosion pit 12Cr stainless steel is briefly summarized mainly on the basis of author's corrosion fatigue testing results (Ebara, Kai & Inoue 1978, Ebara, Kai, Inoue & Masumoto 1978). Then corrosion fatigue crack initiation and propagation process in association with corrosion pits is demonstrated on the basis of the continuous surface observation results on 12Cr stainless steel specimen in 3% NaCl aqueous solution with 318K (Ebara, Yamada & Kawano 1990). It can be concluded that the most of the corrosion fatigue life of 12 Cr stainless steel in 3% NaCl aqueous solution is controlled by initiation and growth of corrosion pit. Three dimensional electrochemical measurement method is also available to detect initiation of corrosion pit in corrosion fatigue crack initiation process of 12 Cr stainless steel (Kim, Miyazawa, Ebara & Ohtsu 2006). Finally recommended studies on corrosion pit initiation are touched on briefly.

### References

- Ebara, R (1985): Environmental Crack Initiation Behavior under Repeated Stress (in Japanese)-Fushoku Boshoku 85, 221-225.
- Ebara, R, Kai, T, Mihara, M, Kino, H, Katayama, K & Shiota, K(1983): Corrosion Fatigue Behavior of 13Cr Stainless Steel for Turbine Moving Blades-In Jaffee, R.I editor, Pergamon Press, 4-150-4-167.
- Ebara, R, Kai, T & Inoue, K(1978): Corrosion- Fatigue Behavior of 13Cr Stainless Steel in Sodium-Chloride Aqueous Solution and Steam Environment - In Craig Jr. H.L, Crooker, T.W, & Hoepfner, D.W, Corrosion-Fatigue Technology, ASTM STP642, ASTM, 155-168.
- Ebara, R, Kai, T, Inoue, K & Masumoto, I (1978): Fractographic Analysis of Corrosion Fatigue Cracking of 13Cr Stainless Steel in NaCl Aqueous Solution (in Japanese), J. JSMS, 27, 64-68.
- Ebara, R, Yamada, T & Kawano, H (1990): Corrosion Fatigue Process of 12Cr Stainless Steel, ISIJ Intern. 30, 7, 535-539.
- Kim, S, Miyazawa, M, Ebara, R & Ohtsu, T (2006): Analysis of Corrosion Fatigue Crack Initiation Process of 12Cr Stainless Steel in 3%NaCl Aqueous Solution by Electrochemical Noise Measurement Method (in Japanese). J. JSSFM, 40, 2, 35-45.

## Characterization of the fatigue behavior of the metastable austenitic steel X6CrNiNb1810 from LCF to VHCF at 300°C

ANDREAS SORICH, MAREK SMAGA, DIETMAR EIFLER, TILMANN BECK

Institut of Materials Science and Engineering, University of Kaiserslautern, Germany

In addition to loadings in the Low Cycle Fatigue (LCF) regime due to start up and shut down procedures of power plants, in some components also high-frequency loading in the High Cycle Fatigue (HCF)- and Very High Cycle Fatigue (VHCF) regime occurs. These loadings are induced e.g. by stresses due to thermal cyclic fluctuations and fluid dynamic processes. Therefore it is necessary to characterize experimentally the cyclic deformation behavior of metastable austenitic steels at operating temperatures, particularly in the HCF- and VHCF regime. The austenitic stainless steel X6CrNiNb1810 (AISI 347, 1.4550) was fatigued on servo-hydraulic testing systems in isothermal, total strain-controlled tests in the LCF regime with a frequency of

0.01 Hz and in stress-controlled tests with 20 Hz in the HCF- and 980 Hz in the VHCF regime. All tests were conducted at  $T = 300\text{ }^{\circ}\text{C}$ . The fatigue related changes in microstructure and phase transformation were analyzed by scanning and transmission electron microscopy as well as by x-ray diffraction. The cyclic deformation behavior in the LCF-regime at  $300\text{ }^{\circ}\text{C}$  is characterized by initial cyclic hardening, followed by cyclic softening until the stress amplitude drops before final failure, associated with the propagation of a fatigue crack. In the LCF-regime no formation of ferromagnetic  $\alpha'$ -martensite could be detected by a Feritscope<sup>®</sup> magnetic sensor and the reached stress amplitudes for total strain amplitudes  $0.8\% \leq e_{a,t} \leq 1.6\%$  are in the range

of  $275 \text{ MPa} \leq s_a \leq 375 \text{ MPa}$  (Altpeter et al. 2012). The cyclic deformation behavior in the HCF-range (Sorich 2014) is characterized by cyclic softening for stress amplitudes  $s_a > 160 \text{ MPa}$  until specimen failure. At the stress amplitude  $s_a = 160 \text{ MPa}$  cyclic softening is followed by cyclic hardening due to martensite formation, which results in a significant increase in life time, up to the ultimate number of cycles of  $N_u = 10^7$  in HCF-regime (Fig. 1, white squares). In the VHCFrange also deformation induced martensite formation is observed. This transformation results in an endurance limit before the ultimate number of cycles  $N_u = 5 \cdot 10^8$  is reached (Fig. 1, black circles). The cyclic hardening is driven by a deformation induced phase transformation from face-centered cubic austenite to body-centered cubic  $\alpha'$ -martensite and/or hexagonal  $\epsilon$ -martensite. The fatigue-related material behavior in the HCF- and VHCF-regime is characterized by microstructural investigations with scanning and transmission electron microscopy as well as x-ray diffraction. The focus of these studies is the deformation induced martensite formation, which significantly affects the cyclic deformation behavior and increases life time.

#### Acknowledgements

The authors thank the Ministry of Economy and Energy (BMWi), Germany as well as the German Research Foundation (DFG) for the financial support within the SFB 926 "Microscale Morphology of Component Surfaces".

## Influence of the surface morphology on the cyclic deformation behaviour of cryogenic turned metastable austenitic steel X6CrNiNb1810

ROBERT SKORUPSKI, MAREK SMAGA, DIETMAR EIFLER, TILMANN BECK

Institut of Materials Science and Engineering, University of Kaiserslautern, Germany

In this investigation deformation induced  $\alpha'$ -martensite formation in the near surface microstructure was realized using a low temperature turning process with carbon dioxide cooling in the cutting zone. Via variation of the cutting parameters different near surface morphologies can be formed. With optical micrographs of the near surface microstructure and additional micro hardness measurements it was proved that a surface layer with a thickness of about  $300 \mu\text{m}$  during the cryogenic turning process develops. Quantitative x-ray analysis of the cryogenic turned surface layers showed that the feed  $f$  has a great influence on the resulting phase distribution. In addition to the paramagnetic fcc  $\gamma$ -austenite and ferromagnetic bcc  $\alpha'$ -martensite a third phase, the paramagnetic hexagonal  $\epsilon$ -martensite, exists. Furthermore, for the small feed a continuous decrease of

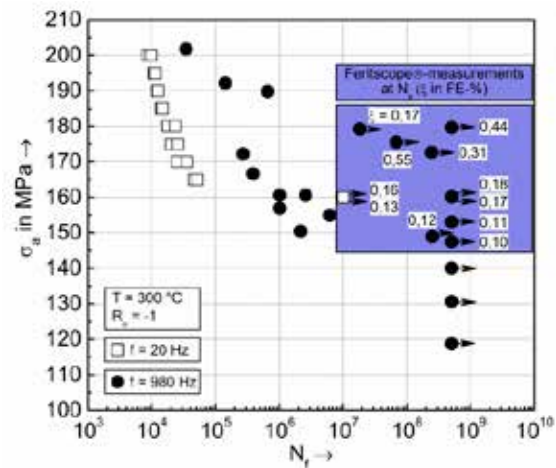


Fig. 1: HCF- and VHCF-Woehler curve at 300 °C

#### References

- Altpeter, I., et al. (2012): Early detection of damage in thermo-cyclically loaded austenitic materials – in Electromagnetic Nondestructive Evaluation (XV), Vol. 36, Rao, B.P.C., Jayakumar, T. and Balasubramanian, K., Eds., IOS, Amsterdam, pp. 130139.
- Sorich, A., Smaga, M. and Eifler, D. (2014): Influence of cyclic deformation induced phase transformation on the fatigue behavior of the austenitic steel X6CrNiNb1810, Advanced Materials Research, Vols. 891-892, pp 12311236.

the  $\alpha'$ -martensite fraction from the maximum value of 25 vol.-% at a distance of  $12 \mu\text{m}$  from the surface down to 0 vol.-% at  $285 \mu\text{m}$  was measured. At higher feed, first an increase of the  $\alpha'$ -martensite fraction from 9 vol.-% at the surface to 37 vol.-% at  $72 \mu\text{m}$  below the surface and a following continuous decrease to zero was measured. For both feeds, at the surface only the two phases  $\gamma$ -austenite and  $\alpha'$ -martensite exist. The  $\epsilon$ -martensite was detected only below the surface (Aurich, J., et al. 2014). The feed also influences the surface topography, which affects significantly the fatigue strength in the high cycle fatigue regime. With increasing feed rate the surface roughness increases and the surface defects trough chip replacement decreases. The fatigue tests were performed on a servo-hydraulic testing system using a triangular load-time function at

ambient (AT) and elevated temperatures ( $T = 300^{\circ}\text{C}$ ) in HCF range by stress control and a load frequency  $f = 5$  Hz with the load ratio of  $R = -1$ . The benefit of the martensitic surface layer on fatigue life can be clearly seen by the comparison of the fatigue life of a specimen loaded at AT after electrolytic polishing. The specimens with the martensitic layer reach the ultimate number of  $2 \cdot 10^6$  cycles without failure whereas the specimens with austenitic surface layer fail ten times earlier. The plastic strain amplitude is significantly reduced by the deformation induced martensitic layer caused by the restriction of dislocation mobility. Despite their larger roughness specimens with turned surface morphologies reach the same number of cycles to failure as specimens with a polished austenitic surface. In analogy to results at AT the highest plastic strain amplitudes and consequently the shortest fatigue life at  $T = 300^{\circ}\text{C}$  are observed in specimens with an austenitic surface layer after polishing. In fatigue tests at elevated temperatures specimens with a martensitic surface layer reach, independent of the surface roughness, higher fatigue limits than specimens with austenitic surfaces (Skorupski, R., et al. 2014).

#### Acknowledgements

The authors thank the German Research Foundation (DFG) for the financial support within the SFB 926 “Microscale Morphology of Component Surfaces”. The fatigue specimens were turned at the Institute for Manufacturing Technology and Production Systems (FBK), University of Kaiserslautern, Germany. We thank Prof. J.C. Aurich, Dr. B. Kirsch and P. Mayer for their support.

## Hybrid surface treatment on austenitic stainless steel JIS SUS316 to improve fretting fatigue strength

TOSHIHIRO Omori<sup>1</sup>, TATSURO MORITA<sup>2</sup>, KOHEI OKADA<sup>2</sup>, HIDEAKI MAEDA<sup>1</sup>

<sup>1</sup>Torishima Pump Manufacturing Co., Ltd., Osaka, Japan

<sup>2</sup>Kyoto Institute of Technology, Kyoto, Japan

Fretting is special wear which is induced by repeated relative surface motion. This phenomenon often occurs on the contact surfaces of combined machine parts and causes marked wear damage. If fretting was induced under applied cyclic stress, it facilitates crack initiation and greatly decreases fatigue strength (Endo & Goto 1976). Accordingly, the above phenomenon, called fretting fatigue, has to be adequately prevented to assure the safety of the rotating machine products such as turbines and water pumps.

The fretting fatigue is complicated because it is related to many factors such as friction-wear, metal fatigue, complex stress condition at contact surfaces and their interaction (Waterhouse 1992, Hoepfner 1994). However, it is expected that the fretting fatigue is prevent-

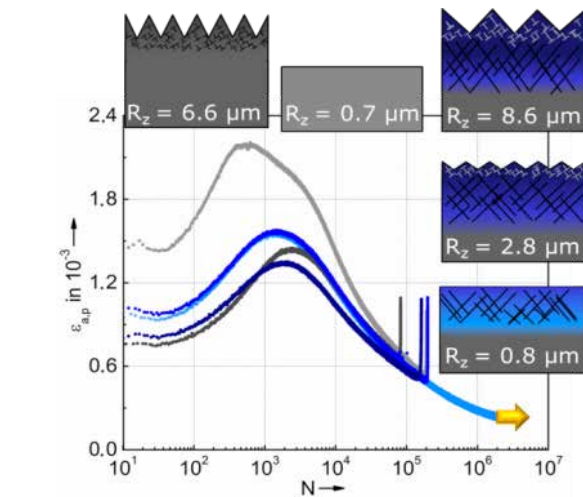


**Fig. 1:** Cyclic deformation curves of specimens with different near surface morphologies, loaded with  $\sigma_a = 270$  MPa at ambient temperature

#### References

- Skorupski, R., et al. (2014): Influence of Surface Morphology on the Fatigue Behavior of Metastable Austenitic Steel. – Adv. Mat. Res. Vols. 891-892, pp. 464-469.
- Aurich, J., et al. (2014): Characterization of deformation induced surface hardening. – CIRP Annals - Manufacturing Technology, Bd. 63: 65-68.

ed by simultaneous improvement in the friction-wear properties and the fatigue strength of metals. The above improvement can be achieved by appropriate surface treatments. Moreover, the surface treatments have an engineering advantage that there is no necessity of correcting the shapes of machine parts.

In recent years, one of the authors has investigated the effect of various surface treatments such as plasma hardening treatments, fine-particle bombarding (hereafter, FPB), diamond-like carbon coating and their hybrid surface treatments (Morita 2012, 2013). The results showed that the hybrid surface treatments were more effective to improve the friction-wear properties and the fatigue strength than individual treatments. From the above background, this study was systemati-

cally conducted to investigate the effect of hybrid surface treatment on the fretting fatigue strength of typical austenitic stainless steel JIS SUS316. In this study, the hybrid surface treatment was composed of plasma nitriding and FPB (hereafter, PN/FPB).

The fretting fatigue test was performed under the condition in which two contact pads were pressed onto both sides of one fatigue specimen. The combinations of fatigue specimen and contact pads are: 1. PN/FPBed specimen and contact pads; 2. PN/FPBed specimen and untreated contact pads; 3. untreated specimen and contact pads for comparison.

The PN/FPB treatment formed a hardened layer. It gave no influence on the mechanical properties. The results of the fretting fatigue test showed that the PN/FPB treatment was very effective to improve the fret-

ting fatigue strength. In the combination cases 1 and 2, the fretting fatigue strength reached the same level and the improvement ratio was about 50 %. It was thought that the above improvement resulted from the simultaneous improvement in the wear resistance and the fatigue strength.

#### References

- Endo, K. & Goto, H. (1976): *Wear* 38, 311-24.  
 Waterhouse, R.-B. (1992): *Inter. Mater. Rev.* 37, 77-97.  
 Hoepfner, D.-W. (1994): *Fretting Fatigue* -in: Waterhouse, R.-B. & Lindley, T.-C. (eds.): *Mech. Eng. Publications*, 3-19; London.  
 Morita, T. et al. (2012): *Mater. Sci. Eng. A* 558, 349-55.  
 Morita, T. et al. (2013): *Mater. Trans.* 54, 732-37.

## Low cycle fatigue behaviors of hot-bent 347 Stainless Steels in a simulated PWR water

JUNHO LEE, JONG-DAE HONG, CHANGHEUI JANG

KAIST, Daejeon, Republic of Korea

An austenitic stainless steel, SS347 is used for the pressurizer surge line pipes in a pressurized water reactor (PWR). However, if the environmental fatigue is considered per NRC Regulatory Guide 1.207 and NUREG/CR-6909 (Chopra, 2014), fatigue design criteria would be difficult to be satisfied. To reduce the stress indices as well as number of weld joints, hot-bending of SS347 surge line pipes is considered. Previously, there have been some efforts to quantify the effects of several factors considered in environmental fatigue, such as temperature, strain rate, and water environments (Solin, 2013a; Solin 2013b).

In this study, the effects of hot-bending on the low cycle fatigue (LCF) in air and simulated PWR environments are investigated by tests and analysis. In the completed hot-bent pipes, the amount of deformation and thermal cycle were different depending on the location of the pipes, which in turn showed different LCF behaviors. The LCF of hot-bent SS347 is similar to or greater than that of the as-received one in room temperature air and PWR environments, though the scatter is large for the intrados and extrados where extensive deformation was accumulated during the process. The fatigue tested specimens were sectioned and analyzed to observe crack morphology, secondary cracks, and effects of microstructure.

In general, cyclic hardening response of SS347 was greater at room temperature and lower in PWR environment, which is consistent with that of 316LN (Cho, 2008). Unlike 316LN, a clear secondary hardening was observed at room temperature for the as-received and hot-bent SS347 irrespective of the position. However,

secondary hardening was not observed for the specimen tested in a PWR environment. Also, the cyclic hardening behaviors showed some orientation dependence, which was usually not observed for the as-received pipes. The different cyclic hardening behaviors were discussed in view of the microstructure and associated hot-bending process. The correlation between the LCF life and cyclic hardening behaviors was discussed also. In summary, the LCF behaviors of SS347 in both air and PWR environments were not significantly affected by the hot-bending.

#### References

- Chopra, O.K. & Stevens, G.L. (2014): *Effect of LWR Coolant Environments on the Fatigue Life of Reactor Materials – NUREG/CR-6909(Rev. 1)*, Argon National Laboratory; USA.  
 Solin, J. & Reese, S. & Karabaki, H.E. & Mayinger, W. (2013a): *Environmental Fatigue Factors (NUREG/CR-6909) and Strain Controlled Data for Stabilized Austenitic Stainless Steel – Proceedings of the ASME 2013 Pressure Vessels and Piping Conference*, PVP2013-97500; France.  
 Solin, J. & Reese, S. & Mayinger, W. (2013b): *Long Life Fatigue Performance of Stainless Steel – Proceedings of the ASME 2013 Pressure Vessels and Piping Conference*, PVP2013-57942; France.  
 Cho, H. & Kim, B.K. & Kim, I.S. & Jang, C. (2008): *Low cycle fatigue behaviors of Type 316LN austenitic stainless steel in 310°C deaerated water – fatigue life and dislocation structure development – Materials Science & Engineering-A*, 476: 248-256.

## Effect of Cold-Drawing on High-Cycle Fatigue Properties of Austenitic TWIP and Fully Pearlitic Steels

SEOK WEON SONG<sup>1</sup>, JEONG HUN LEE<sup>2</sup>, HYONG JIK LEE<sup>3</sup>, CHUL MIN BAE<sup>3</sup>, CHONG SOO LEE<sup>1,2</sup>

<sup>1</sup>Graduate Institute of Ferrous Technology, Pohang University of Science and Technology, Republic of Korea

<sup>2</sup>Department of Materials Science and Engineering, Pohang University of Science and Technology, Republic of Korea

<sup>3</sup>POSCO Technical Research Lab., Pohang, Republic of Korea

This study aims to investigate the effect of cold-drawing on fatigue properties of austenitic twinning-induced-plasticity (TWIP) and fully pearlitic (FP) wire steels. High cycle fatigue tests were carried out on two different alloys, both of which were drawn to have similar tensile strength of ~1500 MPa. Fatigue crack propagation behavior and fracture mode were clearly different in two alloys. The FP steel exhibited higher value of fatigue strength revealing well-developed and

fine striations on its ductile fracture-surface, while that of TWIP steel showed irregularly formed striations and brittle fracture-surface. The different behavior in fatigue crack propagation behavior was considered due to the difference in the amounts of dislocations accumulated near the grain boundaries or twin boundaries. By applying an appropriate heat-treatment, fatigue strength of TWIP steel was greatly increased without sacrifice of tensile strength.

Talks Topic C 3:

***Cyclic deformation behavior, crack initiation & crack growth of metals***

---

## Influence of characteristics of inclusion on rolling contact fatigue of bearing steel

EIICHI TAMURA, YUSUKE SANDAIJI, TAKEHIRO TSUCHIDA

Kobe Steel Ltd., Japan

For the compact design of the bearing, higher fatigue strength steel is expected to apply. In the bearing, fatigue crack is initiated from non-metallic inclusion due to the cyclic shear stress caused by rolling contact. So this rolling contact fatigue strength is thought to be influenced on by the characteristics of inclusions. However the effect factor of each characteristic is not clear, because, with conventional rolling contact test, crack initiating inclusion cannot be found on the fracture surface.

In this research, to clarify the effect factor on the rolling contact fatigue, the analytical method was developed, which is based on simple 2D FEM but can evaluate the crack initiated area and the growth direction with concerning the influence of cyclic loading.

In 2D FEM analysis, repeatedly static loading was substituted for the 3 cycle continuous rolling contact loading. During 1st cycle, the effect of compressive loading was strong and the behavior was relatively unstable. But, after 2nd cycle, the effect of compressive loading becomes so weak and the effect of cyclic shear deformation becomes stronger and the strain behavior becomes stable. And by analyzing strain behavior after 2nd cycle around internal inclusion simulated part, maximum strain range ( $\Delta\varepsilon_{\max}$ ) distribution was evaluated and the location of maximum  $\Delta\varepsilon_{\max}$ , that is to say, the location where the crack is the easiest to initiate, was determined. Furthermore the direction of the crack initiation and propagation was also determined. Comparing the measurement result of the crack growth around the inclusion to analysis result, the location of the crack initiation and the direction of the crack growth are similar in both results.

Furthermore by the comparison of the effect of inclusion type on crack initiation life between UT measure-

ment results and analytical estimated results, analysis was found to be able to estimate that effect. From these comparisons, this 2D FEM analysis was found to simulate the actual crack initiation and growth behavior.

Using this developed analytical method, the mechanism of crack initiation from inclusion and the effect of some inclusion's characteristics were discussed. Although It is easy to find that strain becomes lower when the Young's modulus of the inclusion becomes closer to that of the matrix around inclusion and the size of the inclusion becomes smaller, furthermore, it was found that, when the strength of the interface between inclusion and matrix is zero, then the strain around inclusion becomes much higher. That is, the interfacial peeling of inclusion was indicated to give stronger influence to the fatigue life of the bearing than the inclusion's size and Young's modulus. By controlling the strength of interface between inclusion and matrix, it is expected that rolling contact fatigue strength of bearing steel becomes higher.

### References

- Yaguchi, H. (2001): Effect of Non-Metallic Inclusions of Rolling Contact Fatigue Life of Bearing Steels - Epilogue: Further Research Subjects – In: Journal of Japanese Society of Tribologists, 46-9: 702-705.
- Yamakawa, K., Kizawa, K., Oguma, N. & Kida, K. (2004): The Influence of Subsurface Defect on Stress Distributions under Rolling Contact Fatigue Conditions – In: Koyo Engineering Journal, 166 : 24-28.
- Nagao, M., Hiraoka, K. & Unigame, Y. (2005): Influence of nonmetallic inclusion size on rolling contact fatigue life in bearing steel – In: Sanyo Technical Report, 12: 38-45.

# Evaluation of the fatigue behavior of damage tolerant TRIP-modified SAE 52100 steels using the short-time-procedures PHYBAL<sub>CHT</sub>- and PHYBAL<sub>LIT</sub>

MARCUS KLEIN, HENDRIK S. KRAMER, TILMANN BECK, DIETMAR EIFLER

TU Kaiserslautern, Institute of Materials Science and Engineering, Kaiserslautern, Germany

Different modules of the physically based fatigue life calculation (PHYBAL) method for metallic materials were developed in the last decade at the Institute of Materials Science and Engineering at the University of Kaiserslautern.

Enormous benefits of the "PHYBAL"-method are high reliability and cost effectiveness as a result of the reduction of the number of experiments in comparison to the conventional determination of fatigue data. The application of the "PHYBAL"-method requires a very limited number of high-precision fatigue experiments. In addition to conventional mechanical stress-strain hysteresis measurements supplementary temperature and electrical measurements are used to characterize the fatigue behavior. All measured quantities are directly influenced by deformation-induced changes of the microstructure of the bulk material and provide a high potential to estimate the endurance limit, to calculate woehler curves including consideration of mean stress as well as scatter bands, even for loading and material conditions leading to very limited cyclic plastic deformation.

Recently the new short-time procedure PHYBAL<sub>CHT</sub> was developed. This module requires only a planar material surface to perform cyclic force-controlled hardness indentation tests. To characterize fatigue properties of metallic materials the change of the width of the force-indentation-depth-hysteresis  $h_{a,p}$  has to be plotted versus the number of indentation cycles  $N$ . The slope of the  $h_{a,p}$ - $N$ -curves and thus cyclic hardening can be described by the exponent  $e_{II}$ . Consequently,  $e_{II}$  is defined as hardening-exponent<sub>CHT</sub>.

In this study PHYBAL<sub>CHT</sub> is used to identify promising heat-treatment-parameters and alloying compositions of SAE 52100-TRIP steels. Fatigue cracks in SAE 52100 components quite often initiate at microstructural imperfections like nonmetallic inclusions. Due to the wide spectrum of their size, microstructure, elastic and adhesion properties, a high scatter in fatigue life is observed. The strategy in this investigation was to induce local hardening and compressive residual stresses around imperfections by activating the TRIP-effect to achieve an improved damage tolerance.

One TRIP-modified SAE 52100 steel was selected for detailed investigations: Woehler curves of this TRIP-modi-

fied and two standard SAE 52100 - batches were compared to the estimations from the PHYBAL<sub>LIT</sub> method. An increase of the ferromagnetic phase in constant amplitude tests above the fatigue limit indicates the TRIP-effect. No phase transformation was observed at and below the fatigue limit. It can be concluded that the TRIP-effect will not be activated in a component loaded below the fatigue limit.

Type and size of the nonmetallic inclusions leading to crack initiation have minor influence on fatigue life of the TRIP-modified SAE 52100 compared to the standard batches. The reduced scatter in fatigue life confirms the enhanced damage tolerance of the TRIP - modified matrix.

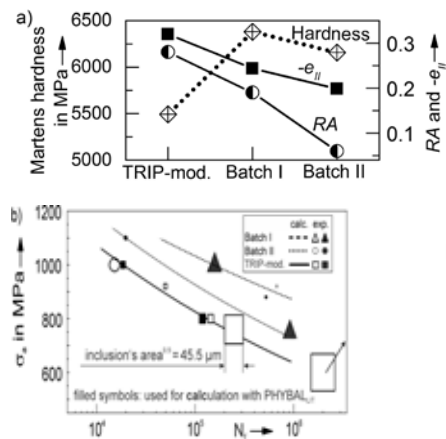


**Fig. 1.** a) Hardness, retained austenite RA, hardening-exponent<sub>CHT</sub>  $e_{II}$  of TRIP-modified SAE 52100, SAE 52100 - Batch I and - Batch II

b) Comparison of the woehler curves. The size of the symbols represents the dimension of the nonmetallic inclusions, which caused failure.

## References

- Kramer, H.; Starke, P.; Klein, M.; Eifler, D.: Cyclic Hardness Test PHYBAL<sub>CHT</sub> - short-time procedure to evaluate fatigue properties of metallic materials, *Int. J. Fatigue*, 78-84 (2014)
- Starke, P.; Eifler, D.: Fatigue Assessment and Fatigue Life Calculation of Metals on the Basis of Mechanical Hysteresis, Temperature, and Resistance Data, *MP Materials Testing*, 261-268 (2009)

# The development of the indirect method for estimation of strain life fatigue parameters

ROBERT BASAN<sup>1</sup>, DOMAGOJ RUBEŠA<sup>2</sup>, MARINA FRANULović<sup>1</sup>

<sup>1</sup>Faculty of Engineering, University of Rijeka, Rijeka, Croatia

<sup>2</sup>FH Joanneum GmbH, Graz, Austria

Experiment-based determination of strain life fatigue parameters  $\sigma'_f$ ,  $b$ ,  $\epsilon'_f$  and  $c$  although most accurate, quickly becomes prohibitive due to the complexity and high costs of cyclic experiments (ASTM Standard E606). Monotonic tensile tests are simple and inexpensive, and their results are usually readily available, so that one of the methods for estimation of fatigue parameters from material's monotonic properties (Muralidharan, Manson 1988, Bäuml, Seeger 1990, Ong 1993, Roessle, Fatemi 2000) is often used, especially during early phases of product development.

Most of the existing methods for the estimation of strain life parameters were developed by correlating experimentally determined strain life parameters independently of each other and directly with one or more monotonic tensile material properties. In some cases, this resulted in relatively complicated expressions for the calculation of fatigue parameters, while in others, because of the poor correlation between certain fatigue and monotonic parameters, constant values were assigned to some of these fatigue parameters.

Based on the previously proposed approach (Basan 2009, Basan et al. 2010) new, indirect method for estimation of strain life fatigue parameters from materials monotonic properties is proposed. Unlike the existing methods, proposed method is based on the identification and establishment of functional relationships between selected monotonic property and  $\Delta\epsilon/2-2N_f$  relations which is achieved by correlating ultimate strength  $R_m$  and individual points on strain life curves. From these established relationships, new values of fatigue parameters  $\sigma'_f$ ,  $b$ ,  $\epsilon'_f$  and  $c$  were then determined for each value of the ultimate strength  $R_m$  so that new functions  $\sigma'_f=f_1(R_m)$ ,  $b=f_2(R_m)$ ,  $\epsilon'_f=f_3(R_m)$  and  $c=f_4(R_m)$  could be derived. Main advantage of the new approach and proposed method is that fatigue parameters ( $\sigma'_f$ ,  $b$ ) and ( $\epsilon'_f$ ,  $c$ ) are not estimated individually, i.e. independently from one another.

For the development and a validation of the proposed approach to the estimation of fatigue parameters, nec-

essary data were gathered for a set of differently heat treated high-strength low-alloy 42CrMo4 steels tested at room temperature.

Performance of proposed indirect estimation method was evaluated using criteria which have been extensively used in different comparisons and verifications of estimation methods reported in literature. Fatigue lives calculated using estimated values of fatigue parameters are found to be in very good agreement with those calculated using experimentally obtained fatigue parameters. Furthermore, determined values of comparison criteria are significantly higher for proposed method than those calculated for other estimation methods. Proposed method will be extended and adapted for estimation of fatigue parameters of unalloyed, low- and high-alloy steels as well as aluminium and titanium alloys in an extended paper.

## References

- ASTM Standard E606, 1992 (1998). West Conshohocken (PA): ASTM International.
- Muralidharan, U., Manson, S.S. (1988): A modified universal slopes equation for estimation of fatigue characteristics of metals. *J Engng Mater Techn* 1988;110:55–58.
- Bäumel, A., Seeger, T. (1990): *Materials data for cyclic loading – Supplement 1*. Amsterdam: Elsevier; 1990.
- Ong, J.H.: (1993): An improved technique for the prediction of axial fatigue life from tensile data. *Int J Fatigue* 1993;15:213–219.
- Roessle, M.L., Fatemi, A. (2000): Strain-controlled fatigue properties of steels and some simple approximations. *Int J Fatigue* 2000;22:495–511.
- Basan, R. (2009): *Fatigue and damage of the gear tooth flank*. Dissertation (in Croatian). Rijeka: Faculty of Engineering, University of Rijeka
- Basan, R., Rubeša, D., Franulović, M., Križan, B. (2010): A novel approach to the estimation of strain life fatigue parameters. *Procedia Engineering* 2010;2:417-426.

# Fatigue Properties of DLC Coated Steel AISI1045 with Cr Diffusion Layer on the Substrate Surface by AIH-FPP Process

KENTA UYAMA<sup>1</sup>, KOJI KOBAYASHI<sup>2</sup>, HIROYUKI AKEBONO<sup>1</sup>, JUN KOMOTORI<sup>2</sup>, ATSUSHI SUGETA<sup>1</sup>

<sup>1</sup>Department of Mechanical Science and Engineering, Hiroshima University, Hiroshima, Japan

<sup>2</sup>Department of Mechanical Engineering, Keio University, Kanagawa, Japan

In recent years, diamond-like carbon (DLC) films have attracted much attention in many industrial fields because of their properties, high hardness, chemical inertness, biocompatibility. Especially, DLC films are well known for their excellent tribological properties, so DLC films are attractive coating processes to achieve energy savings and CO<sub>2</sub> emissions reduction. However, achieving higher adhesion of DLC films is an important task because poor adhesion between the films and the substrate limits the practical applications of DLC films. In this study, we focused on Atmospheric-controlled Induction Heating Fine Particle Peening (AIH-FPP) treatment system as a pretreatment to improve the adhesion between the DLC films and the substrate. AIH-FPP system has possibility to achieve the high adhesion strength compared with practical coating process by applying the Cr particle which indicates high chemical affinity to carbon which constitutes the DLC films as shot material because AIH-FPP system can generate a shot particle diffusion layer on the substrate surface. The aim of this study is to examine the effects of Cr diffusion layer generated by AIH-FPP process on the fatigue properties and fracture mechanism of DLC coated steel.

The material (substrate) used in this study was a medium carbon steel (AISI1045) having a carbon content of 0.45%. After being machined into an hourglass-shaped specimen for fatigue tests, the specimen surface was polished using SiC paper and alumina powder.

These specimens were modified AIH-FPP process in the chamber replaced by Ar gas. Shot particle was Cr shot (30-50 μm in diameter), processing temperature was 1473 K, peening time was 30 sec. In addition, for comparison specimens, we prepared substrates which had not been performed AIH-FPP process. After AIH-FPP process, all specimens were coated with DLC films using unbalanced magnetron sputtering (UBMS) to a thickness of 2 μm (Cr interlayer 1 μm + DLC layer 1 μm). Fatigue tests were carried out by using an electro-magnetic type bending fatigue testing machine in ambient air without any controls of the temperature and the moisture at a frequency of 20 Hz under the stress ratio  $R = -0.8$ . The fatigue crack was observed continuously by using a plastic replicas technique.

From the fatigue tests, it indicated that fatigue strength makes no difference regardless of Cr diffusion layer. So it was found that Cr diffusion layer hardly affected fatigue strength. On the other hand, fatigue strength of DLC coated specimen with Cr diffusion layer was higher than it of other specimen. So DLC films can improve the fatigue strength of steel. Finally, in order to examine the reason for that, fatigue crack initiation behavior was observed by replicas technique. From this observation, fatigue crack initiation life of DLC coated specimen was longer than other specimen. Therefore, it was clear that DLC films increased the fatigue crack initiation resistance caused by the high compressive residual stress and high hardness.

# Low cycle fatigue properties of the Fe-28Mn-5Cr-6Si-0.5NbC alloy

NOBUO NAGASHIMA, TAKAHIRO SAWAUCHI AND KAZUYUKI OGAWA  
National Institute for Materials Science (NIMS), Japan

Since the shape memory effect (SME) was discovered in Fe-30Mn-1Si (hereafter all compositions are in mass %) single crystals by Sato et al. [1], which was followed by the development of polycrystalline Fe-30Mn-6Si alloys by Murakami et al., the Fe-Mn-Si alloys undergoing face-centered cubic (fcc) ( $\gamma$  austenite) / hexagonal close-packed (hcp) ( $\epsilon$  martensite) martensitic transformation have attracted much attention. Aiming to further develop these shape memory alloys (SMAs), considerable efforts were made to induce corrosion resistance by alloying with Cr and Ni [3], and to improve the SME by microalloying. In this way, SMAs with good workability and reasonable cost have been developed.

Recently, some of the present authors reported that an Fe-28Mn-6Si-5Cr-0.5NbC SMA showed significant damping capacity when subjected to cyclic tension-compression loading with strain amplitudes larger than 10<sup>-3</sup>. Quantitative X-ray diffraction analysis and atomic force microscopy (AFM) performed in our previous report [4] proved that reverse martensitic transformation of tensile-stress-induced martensite took place when the specimen was compressed back to zero strain. In this study, we conducted a low-cycle fatigue testing in the Fe-28Mn-6Si-5Cr-0.5NbC (FMS) alloy and the SUS304 steel.

The FMS alloy was prepared by vacuum induction melting followed by hot-forging and rolling. A solution treatment was carried out at 1470 K for 10 h. Then a thermomechanical treatment, consisting of 14% warm-rolling at 870 K and subsequent aging at 1070 K for 10 min was performed to produce fine precipitates of NbC carbides. The choice of the above mentioned alloy composition and the thermomechanical treatment refers to our earlier study [5].

The fatigue tests were made using a servo hydraulic fatigue testing machine of capacity 50kN, at maximum total strain amplitudes ( $\epsilon_{ta}$ ) of 2.0%, 1.4%, 0.9%, 0.6%. Deformation microstructure after fatigue testing, were analyzed using ferrite meter and X-ray diffraction analysis.

In the SUS304 steel, with decrease in applied strain amplitude, stress-strain hysteresis loop is reduced. On the other hand, the stress response of the FMS alloy is almost unchanged, irrespective of the applied

strain amplitude. The rupture life of the FMS alloy is 4 times higher at  $\epsilon_{ta}=0.6\%$ , and twice at  $\epsilon_{ta}=0.9\%$  and at  $\epsilon_{ta}=1.4\%$  than the SUS304 steel. In addition, the stress amplitude of the FMS alloy is 1.5 times higher at  $\epsilon_{ta}=0.9\%$ , and twice at  $\epsilon_{ta}=0.6\%$  than the SUS304 steel. Deformation-induced  $\alpha'$  martensite in low cycle fatigue test specimen of SUS304 has been detected with ferrite meter, but was not detected in the FMS alloy. The low cycle fatigue test specimen of FMS alloy  $\epsilon$  martensite (hcp) has been detected with X-ray diffraction analysis. Therefore the prolonged fatigue life of the FMS alloy is attributable to the reversible deformation associated with the transformation pseudo-elasticity that can reduce the accumulated strain.

## References

- [1] A. Sato, E. Chishima, K. Soma, T. Mori, Acta Metall. 30(1982) 1177.
- [2] M. Murakami, H. Otsuka, H.G. Suzuki, S. Matsuda, in: Proc. Int. Conf. Martensitic Transformation, Japan Institute of Metals, 1986, pp. 985–990.
- [3] L.J. Rong, Y.Y. Li, C.X. Shi, Scripta Metall. Mater. 34(6) (1996) 993.
- [4] T. Sawaguchi, P. Sahu, T. Kikuchi, K. Ogawa, S. Kajiwara, A. Kushibe, M. Higashino, T. Ogawa, Scripta Materialia, 54(2006), 1885
- [5] Baruj A, Kikuchi T, Kajiwara S, Shinya N. Mater Sci Eng A 378(2004):333.

**Tab. 1:** Low-cycle fatigue test results

	Nf	$\sigma_a$	$\epsilon_{ta}$	$\epsilon_{pa}$	$\epsilon_{ea}$
SUS	164	607	0.020	0.0157	0.0043
304	304	524	0.014	0.0106	0.0034
Steel	1600	413	0.009	0.0065	0.0025
	5250	317	0.006	0.0042	0.0018
FMS alloy	157	722	0.020	0.0140	0.006
	631	711	0.014	0.0082	0.0058
	3315	679	0.009	0.0041	0.0049
	18290	618	0.006	0.0016	0.0046

Talks Topic C 4:

***Cyclic deformation behavior, crack initiation & crack growth of metals***

---

# Effects of nitriding temperature on the fatigue properties of Ti-6Al-4V alloy and in-situ observation of fatigue cracks in 4-points bending

SHOICHI KIKUCHI<sup>1</sup>, SHO YOSHIDA<sup>2</sup>, YUTA NAKAMURA<sup>2</sup>, AKIRA UENO<sup>2</sup>, YOSHIKAZU NAKAI<sup>1</sup>

<sup>1</sup>Department of Mechanical Engineering, Kobe University, Japan

<sup>2</sup>Department of Mechanical Engineering, Ritsumeikan University, Kusatsu, Shiga, Japan

Nitriding has been widely applied in various fields of engineering to improve wear resistance of material because nitriding can form high hardness layers; a nitrogen compound layer and a nitrogen diffusion layer (Morita et. al 1997 and Shibata et. al 1994). The aim of this study is to examine the effects of nitriding on the fatigue properties and fatigue crack propagation behavior of Ti-6Al-4V alloy in 4-points bending.

The material used in this study was the  $\alpha + \beta$  titanium alloy (Ti-6Al-4V). Titanium plates were machined into the specimens with 4 mm in width and 40 mm in length using a wire-electrical discharge machine. These specimens were polished with emery papers (#320 to #4000) to 3 mm in thickness and mirror-finished using SiO<sub>2</sub> suspension. Nitriding was performed at 550 °C, 600 °C and 850 °C for 5 h on the basis of the previous study (Kikuchi et. al 2014). Surface hardness of the nitrided specimens was measured using a micro-Vickers hardness tester. The surface microstructures of the specimens were characterized using an optical microscope, scanning electron microscopy (SEM), X-ray photoelectron spectroscopy (XPS), X-ray diffraction (XRD) with CuK $\alpha$  radiation and electron backscatter diffraction technique (EBSD).

4-points bending fatigue tests were performed in ambient air without any controls of the temperature and the moisture at a frequency of 20 Hz under the stress ratio  $R = 0.1$  and  $0.5$ . For some specimens, in-situ observation of fatigue cracks was conducted using a microscope and digital video camera. After testing, the fracture surfaces were observed using SEM. Moreover,  $K$ -decreasing tests were conducted for the un-nitrided DC(T) specimen.

Surface hardness of titanium alloy was increased with nitriding temperature. Specimens nitrided at 600 °C and 850 °C exhibited the X-ray diffraction peaks of substrate and nitrogen compounds. In contrast, the XRD and XPS analyses indicate that a nitrogen diffusion layer without nitrogen compounds is formed on the specimen nitrided at 550 °C. It was found that nitrogen

compound layer was formed on Ti-6Al-4V alloy nitrided at the temperature higher than 600 °C.

The fatigue strength of the nitrided specimens was increased with decreasing nitriding temperature. Especially, the specimens nitrided at 550 °C without nitride compounds showed higher compared to the un-nitrided specimen. On the other hand, fatigue strength of the specimens nitrided at 850 °C was much lower than that of the un-nitrided specimen. These results imply that nitrogen compound layer reduces the fatigue strength of Ti-6Al-4V alloy.

Fatigue fracture mechanism of the nitrided specimen was discussed from viewpoints of fractography. In this study, every specimen exhibited the surface fracture modes. Characteristic flat area; corresponding to the thickness of compound layer, was clearly observed at the nitrided specimen. As results of in-situ observations of fatigue cracks, life of fatigue crack initiation was short due to the existence of surface compound layer. Nitrogen compound layer shows brittle fracture during fatigue tests and adversely affects the fatigue properties of titanium alloy.

## References

- Morita, T., Takahashi, H., Shimizu, M., & Kawasaki, K. (1997): Factors controlling the fatigue strength of nitride titanium – *Fatigue & Fracture of Engineering Materials & Structures*. 20: 85-92.
- Shibata, H., Tokaji, K., Ogawa, T., & Hori, C. (1994): The effect of gas nitriding on fatigue behavior in titanium alloys – *International Journal of Fatigue*. 16: 370-376.
- Kikuchi, S., Nakamura, Y., Ueno, A., & Ameyama, K. (2014): Development of low temperature nitriding process and its effects on the 4-points bending fatigue properties of commercially pure titanium – *Advanced Materials Research*. 891-892: 656-661.

## The influences of foreign object damage on the high cycle fatigue behavior of titanium alloy TC11

ZHAO ZHENHUA<sup>1</sup>, CHEN WEI<sup>1,2</sup>, WU TIEYING<sup>1</sup>

<sup>1</sup>College of Energy and Power Engineering, Nanjing University of Aeronautics and Astronautics, Jiangsu Province Key Laboratory of Aerospace Power System, Nanjing, China

<sup>2</sup>Collaborative Innovation Center of Advanced Aero-Engine, Nanjing, China

When the plane takeoff and landing, the foreign objects, including stones and gravels of different sizes and shapes, can be ingested into the aero-engine and cause damages on the fan or compressor component (Nicholas 2006). The damage, commonly referred to as Foreign Object Damage (FOD), is typically in the form of notching, including a wide range of notch depth, radius, and possible cracking at the root of the notching. FOD can reduce the fatigue life of those components subjected to vibratory loading. Peters (2000) investigated the influence of FOD on the high cycle fatigue performance of Ti-6Al-4V and analyzed the effect of micro-cracking caused by impact on the process of fatigue crack initiation. Mall (2010) discovered the distinctly different damage mechanisms caused by different damage simulated methods.

In this paper, the effect of FOD on fatigue performance of aircraft engine fan/compressor blade material TC11 titanium alloy were investigated. Foreign object damage (FOD) test on TC11 titanium alloy plate specimens were conducted using gas gun test system. The steel spheres of 2 mm and 3 mm diameter were employed and the launching velocity was in the range of 250~400 m/s. The macroscopical and microscopical characteristics of specimen damage were observed by three-dimensional digital microscope and scanning electron microscope (SEM) respectively. It is found that the macroscopical damage mainly involves the material extrusion deformation, shear loss and plastic deformation, while the microscopical damage mainly involve the micro cracks, plastic deformation, micro notches and etc.

With the same size of foreign objects, the damage area enlarges with the increasing of impact velocity, and more micro cracks and lamellar structures emerge. The high cycle fatigue strength of damaged TC11 specimens after impact was determined by fatigue tests employing step loading test method. The results indicate that there is obviously descend in the fatigue strength of damaged specimens. And the fatigue strength decreases with the depth of damage increasing.

The SEM observations on the fatigue fracture surface indicate that the fatigue source locates in the surface of damage area, and initiates from the micro cracks or micro notches caused by impact. Under similar conditions of macroscopic damage, the fatigue strength of specimen impacted with higher impact velocity is inferior to that impacted with lower impact velocity.

### References

- Nicholas, T. (2006): High Cycle Fatigue: A Mechanics Of Materials Perspective[M]. Elsevier Ltd.
- Peters, J.O., Roder, O., Boyce, B.L., Thomson, A.W. & Ritchie, R.O. (2000): Role of Foreign Object Damage on Thresholds for High-Cycle Fatigue in Ti-6Al-4V. Metallurgical and Materials Transactions., 31A: 1571-83
- Mall, S. Hamrick, II. Joseph, L & Nicholas, T. (2001): High Cycle Fatigue Behavior of Ti-6Al-4V with Simulated Foreign Object Damage. Mechanics of Materials., 33: 679-92.

## Effect of forging condition on fatigue behavior in AZ61 bulk nanostructured metal fabricated by multi-directional forging

YOSHIHIKO UEMATSU<sup>1</sup>, TOSHIFUMI KAKIUCHI<sup>1</sup>, TAISHI NOZAKI<sup>1</sup>, HIROMI MIURA<sup>2</sup>

<sup>1</sup>Gifu University, Gifu, Japan

<sup>2</sup>Toyohashi University of Technology, Toyohashi, Japan

Magnesium (Mg) alloys are attractive as structural materials due to their light weight and high specific strengths. But 0.2% proof stress and tensile strengths are still lower than conventional light weight alloys such as Ti and Al alloys. It is well known that grain refinement is effective to improve mechanical properties

of materials. Recently, many severe plastic deformation (SPD) methods, such as multi-directional forging (MDF), equal channel angular pressing (ECAP), high-pressure torsion (HPT), accumulative roll bonding (ARB) and so on, are proposed to achieve very fine grains by SPD. In MDF technique, the material is forged with chang-

ing forging direction 90 degrees pass-by-pass. In the present study, MDF was applied to AZ61 magnesium alloy to achieve bulk nanostructured metal. Fully reversed axial fatigue tests were conducted using MDFed AZ61. The number of forging path was changed as 1, 3, 6 and 8, and the effect of forging condition on fatigue behavior was investigated.

The microstructural observation revealed that the average grain size becomes smaller with increasing forging paths. The minimum grain size was about 0.3 $\mu\text{m}$ , while that of the as-received material was 21.6 $\mu\text{m}$ . The average grain size was 21.6 $\mu\text{m}$ , 19 $\mu\text{m}$ , 0.6 $\mu\text{m}$  and 0.3 $\mu\text{m}$  for the as-received, 1path, 6path and 8path materials, respectively. The hardness and tensile strength increased with decreasing average grain size, and the mechanical properties corresponded to Hall-Petch relationship.

Subsequently, fully reversed axial fatigue tests had been performed. It was found that the fatigue strengths increased with increasing forging path number up to 3 times. However, when the forging path number was 6 and 8, the fatigue strengths of are nearly the same with

or slightly decreased compared with 3path specimen. Consequently, fatigue limits, which are defined as fatigue strengths at  $10^7$  cycles, are not in accordance with Hall-Petch relationship.

As mentioned above, the fatigue strength was not further increased by the 6<sup>th</sup> and 8<sup>th</sup> paths forging process. Thus the surface morphologies after fatigue loading were examined in detail by a scanning electron microscope (SEM). After fatigue loading, the surface roughness was increased in 6path and 8path specimens. The peak-to-peak distances on the fatigue-loaded samples were nearly the same with the average grain sizes in both specimens. It indicates that grain boundary slipping might have occurred. In fine-grained Mg alloys, grain boundary slipping could easily occur. Consequently, it is considered that 6path and 8path materials had very fine grains resulting in grain boundary slipping during fatigue loading, and thus fatigue strengths were not further improved by 6<sup>th</sup> and 8<sup>th</sup> path because the operation of grain boundary slipping had detrimental effect on fatigue strength.

## Variable-Amplitude of Aluminum Alloy 7075 in the VHCF Regime under Superimposed Loading Conditions

S.E. STANZL-TSCHEGG, M. MEISCHEL, N. IYER, A. ARCARI, N. PHAN

BOKU, Vienna, Austria

Characterizing the material behaviour below the traditional endurance limit, the threshold between high-cycle-fatigue (HCF) and very-high-cycle-fatigue (VHCF), is an important step towards understanding the significance of a fatigue limit usage in life calculation with the strain life methods. The aim of this study is to quantify the influence of VHCF cycles on fatigue life of 7075-T6 Al-alloys using both constant and variable amplitude loading. Constant amplitude loading tests with and without superimposed mean levels were performed to characterize the material behaviour in fatigue with minimal effect of load interactions. These tests helped advancing hypothesis, elucidating the role of mean stresses and understanding the scatter of fatigue data. The effects of combined cycle fatigue (CCF) loadings

were studied by using a spectrum composed by a low frequency carrier wave at 0.01, 2 and 5 Hz and a superimposed high-frequency wave at 20 kHz. The low frequency wave is assumed sinusoidal or rectangular shaped, the high-frequency wave has constant and variable amplitudes and the effects of different loading sequences are investigated. For a better understanding of the relevant mechanisms, the initiation and growth of small and long cracks were measured. Correlating the measurement results with microscopic surface observations and SEM fracture surface studies allowed identification of surface and interior fatigue crack initiation and propagation. Predictions based of the obtained data and appropriate modeling of the different mechanical processes are detailed.

Talk Topic C 5:

***Cyclic deformation behavior, crack initiation & crack growth of metals***

---

# Assessment of fatigue crack closure under in-phase, out-of-phase and phase-shift thermomechanical fatigue loading using a temperature dependent strip yield model

CARL FISCHER<sup>1,2</sup>, CHRISTOPH SCHWEIZER<sup>1</sup>, THOMAS SEIFERT<sup>2</sup>

<sup>1</sup>Fraunhofer Institute for Mechanics of Materials IWM, Freiburg, Germany

<sup>2</sup>Offenburg University of Applied Sciences, Offenburg, Germany

In high temperature components mechanical and thermal loads are acting at the same time during start-up and shut-down cycles resulting in thermomechanical fatigue (TMF) of the materials. Gas turbines are classical examples of such components where nickel-base alloys are used in the hot parts. Above 750 °C the yield stress of nickel-base superalloys becomes strongly temperature dependent.

As a consequence of the temperature dependent yield stress, the mean stress strongly changes with the applied phasing of thermal strains and mechanical strains. Typically, tensile mean stresses arise during out-of-phase (OP) TMF loading, while in-phase (IP) TMF loading usually leads to compressive mean stresses.

For isothermal loading it is known, that the mean stress affects fatigue crack growth and fatigue lives. Higher mean stresses lead to faster fatigue crack growth and thus to shorter fatigue lives. However, under TMF loading, IP TMF tests with negative mean stresses often show shorter fatigue lives than OP TMF tests at high mechanical loadings. At low mechanical loadings this trend can be reversed (see Guth et al. (2014)).

In mechanism based lifetime approaches the mean stress effect is accounted for by fatigue crack closure models. Since fatigue crack growth in ductile metallic materials involves irreversible plastic deformations at least in a small zone around the crack-tip, plasticity induced fatigue crack closure, which is the dominant mechanism for the explanation of mean stress effects, immediately becomes history dependent, too. The strip yield model from Newman (1981) has proven to be a powerful tool to examine load history effects such

as fatigue crack retardation after overloads.

In this paper fatigue crack closure under in-phase, out-of-phase and phase-shift thermomechanical fatigue loading is studied using a temperature dependent strip yield model. It is shown that fatigue crack closure is strongly influenced by the phase relation between mechanical loading and temperature, if the temperature difference goes along with a temperature dependence of the yield stress. In order to demonstrate the effect of the temperature dependent yield stress, the influence of in-phase, out-of-phase and phase-shift TMF loading is studied for a polycrystalline nickel-base superalloy. By using a mechanism based lifetime model, implications for fatigue lives are demonstrated. It is shown, that fatigue crack closure can explain that in-phase thermomechanical fatigue tests show lower lifetimes at high mechanical loadings than out-of-phase tests and that the lifetime curves cross each other at lower mechanical loadings.

## References

- Guth, S. et al. (2014): Lifetime, cyclic deformation and damage behaviour of MAR-M247 LC under thermo-mechanical fatigue loading with 0°, 180°, -90° and +90° phase shift between strain and temperature. – *Procedia Engineering* 74 (2014) 269-272.
- Newman, J. C. (1981): A crack-closure model for predicting fatigue crack growth under aircraft spectrum loading – In: J. B. Chang, C. M. Hudson (eds.): *Methods and Models for Predicting Fatigue Crack Growth under Random Loading*. ASTM STP 748, American Society for Testing of Materials, 1981, 53-84.

## Dwell time effects on the Thermo-Mechanical Fatigue Behaviour of a Wrought Ni-base Alloy

STEFAN GUTH, JONAS MÜLLER, KARL-HEINZ LANG

Karlsruhe Institute of Technology, Germany

The influence of dwell times on lifetime, cyclic deformation and damage behaviour of the wrought Ni-base alloy NiCr22Co12Mo (comparable to Inconel Alloy 617) under thermo-mechanical fatigue (TMF) loading was studied. Strain controlled TMF tests with a temperature range of 100 – 850 °C and dwell times of 0, 2, 5 or 30 min at 850 °C were conducted in air. Mechanical strain amplitudes varied from 0.3 to 0.7 %. Phase angles between mechanical strain and temperature were 0° (in-phase, IP), 180° (out-of-phase, OP), +90° (clockwise diamond, CD) and -90° (counterclockwise diamond, CCD). Light microscopy was used to observe damage on longitudinal sections of cycled specimens. Microstructural evolution was studied using transmission electron microscopy (TEM).

The introduction of a dwell time in IP and CCD tests resulted in a prolonged lifetime compared to tests without dwells although the plastic strain amplitude increased. With increasing dwell duration the lifetime decreased. However, shortest life was found in continuous tests. Lifetimes under OP and CD phasing were not significantly influenced by dwells. The saturated stress amplitudes in dwell tests were in general about 30 % lower than in comparable continuous tests. TEM investigations indicate that the reason for this is a re-

duced amount of secondary carbides precipitating in dwell tests. Cracks propagate mainly intergranular in IP and CCD tests for both dwell times and continuous tests. Damage occurs in form of wedge type cracks at grain boundary triple junctions. The cracks show a high angle to the stress axis and tend to interconnect when growing. In dwell time tested specimens additional round type cavities could be found. Crack propagation in OP and CD tests was predominantly transgranular and similar for continuous and dwell time tests. Some specimens showed internal wedge type cracks under a low angle to the stress axis that remain relatively small. The occurrence of wedge type cracks with direction dependent on the phase angle indicates that grain boundary sliding accumulates during testing (Fujino 1979). The somewhat unexpected effects of dwell times on lifetime are discussed on the basis of the observed deformation and damage behaviour.

### Reference

Fujino, M. and Taira, S. (1979): Effect of thermal cycle on low cycle fatigue life of steels and grain boundary sliding characteristics. – In: ICM 3, Cambridge, England, Volume 2, 49 - 58

## Biaxial fatigue behavior of a hot-pressed metastable austenitic steel

STEPHANIE ACKERMANN, TIM LIPPMANN<sup>1</sup>, SEBASTIAN HENKEL, HORST BIERMANN

Technische Universität Bergakademie Freiberg, Institute of Materials Engineering, Freiberg, Germany

Biaxial fatigue is an important load state occurring in structural components. Higher fatigue lives under shear loading were reported in literature for several materials (Doquet 1997). Pure shear fatigue can be studied by using biaxial-planar tests with cruciform specimens. In the present study cyclic deformation tests were carried out at room temperature under total strain control. A variety of biaxial states of strain were set by varying strain ratio between the axial strain amplitudes from -1 to 1. Straining with a strain ratio of -1 correspond to pure shear as well as pure torsion.

The investigated material is a high alloy metastable austenitic stainless CrMnNi steel which was produced by hot-pressing. The steel exhibits martensitic transformation from austenite via  $\epsilon$ -martensite into  $\alpha'$ -martensite during cyclic deformation. The  $\alpha'$ -martensite formation causes cyclic hardening and depends on the plastic strain amplitude as well as on the accumulated plastic strain. The dominating deformation structures are stacking faults and deformation bands wherein  $\alpha'$ -martensite is formed.

Cyclic shear deformation (strain ratio = -1) caused the earliest beginning of martensite formation and the highest volume fractions of  $\alpha'$ -martensite at fatigue failure in comparison to uniaxial and other biaxial states of strain. The maximum  $\alpha'$ -martensite contents were 25-50 % higher under shear than under equibiaxial loading (strain ratio = 1).

In accordance to the literature using von Mises equivalent strain amplitude (Doquet 1997, Itoh et al. 1994), cyclic shearing caused higher fatigue lives after fatigue failure than other biaxial and uniaxial conditions. The Basquin and Manson-Coffin assessment is appropriate to correlate the fatigue life of uniaxial and biaxial loading conditions, but is too conservative for shear fatigue. It is assumed that the period of crack initiation is much longer under shear fatigue in comparison to other studied biaxial conditions. Moreover, the uncritical

crack type A according to (Brown & Miller 1973) and the absence of crack opening normal stress (Doquet 1997) are possible reasons.

Thus, surface cracks were investigated at different states of fatigue life and after fatigue failure in order to clarify the higher fatigue lives under shear fatigue. Different techniques were used such as electron beam universal system, replica technique, light optical microscopy, backscatter electron contrast and electron backscatter diffraction in a high-resolution field emission scanning electron microscope.

Different types of macro cracks on the sample surface which caused fatigue failure were observed. Cracks after shear fatigue were oriented 45° to the loading axes. This direction corresponds to maximum shear strain direction which is mode II (Itoh et al. 1994). In addition, crack branching was observed. Crack directions perpendicular to the loading axes which corresponds to mode I were observed after biaxial cyclic deformation with strain ratios of 1, 0.5, -0.1 and -0.5 as well. These results confirm the findings in literature (Itoh et al. 1994, Parsons & Pascoe 1976).

### References

- Doquet, M. (1997): Crack initiation mechanisms in torsional fatigue. – *Fatigue Fract. Eng. Mater. Struct.*, 20: 227-35.
- Itoh, T. & Sakane, M. & Ohnami, M. (1994): High Temperature Multiaxial Low Cycle Fatigue of Cruciform Specimen. – *Trans. ASME*, 116: 90-98.
- Brown, M.W. & Miller, K.J. (1973): A Theory for Fatigue Failure under Multiaxial Stress-Strain Conditions. – *Proc. Inst. Mech. Eng.*, 187: 745-55.
- Parsons, M.W. & Pascoe, K.J. (1976): Observations of Surface Deformation, Crack Initiation and Crack Growth in Low-cycle Fatigue under Biaxial Stress. – *Mater. Sci. Eng.*, 22: 31-50.

## High temperature low cycle fatigue behavior of cast superalloy Inconel 713LC coated with $ZrO_2-SiO_2-Al_2O_3$ nanocrystalline thermal barrier coating

KAREL OBRTLIK<sup>1</sup>, LADISLAV ČELKO<sup>2</sup>, TOMÁŠ CHRÁSKA<sup>3</sup>, IVO ŠULÁK<sup>1</sup>, LENKA KLAKURKOVÁ<sup>2</sup>, DAVID JECH<sup>2</sup>, VIKTOR ŠKORÍK<sup>1</sup>, JIŘÍ ŠVEJCAR<sup>2</sup>

<sup>1</sup>Institute of Physics of Materials, AS CR, Brno, Czech Republic

<sup>2</sup>Brno University of Technology, CEITEC, Brno, Czech Republic

<sup>3</sup>Institute of Plasma Physics, ASCR, Praha, Czech Republic

Cast polycrystalline nickel base superalloy Inconel 713LC is used for production of blades and discs of gas turbine engines that are subjected to repeated elastic-plastic loading in aggressive environments at variable temperatures. Thermal barrier coatings (TBCs) consist of thermally insulating ceramic top coat and of a metallic oxidation/corrosion-protective bond coat. They can prolong the component life particularly by a reduction of temperature gradient during heating and cooling.

In the present work, the high temperature low cycle fatigue behavior of cast nickel-based superalloy Inconel 713LC in as-received state and coated with novel  $Al_2O_3-SiO_2-ZrO_2/CoNiCrAlY$  TBC system was studied at the temperature of 900 °C. The microstructure of the substrate material consisted of dendritic grains with carbides and shrinkage pores. The average grain size was 0.66 mm.

The novel TBC system consists of a (inter)metallic CoNiCrAlY bond coat and a eutectic ceramic, i.e. zirconia ( $ZrO_2$ ), alumina ( $Al_2O_3$ ) and silica ( $SiO_2$ ) top coat deposited on the gauge section of cylindrical specimens using atmospheric gas stabilized plasma and water stabilized plasma, respectively. Due to the system of eutectic ceramic coupled with high temperature developed by

using water stabilized plasma the top coat was formed in partially crystalline phase. Its subsequent heat treatment enabled to produce the nanocrystalline mullite phase in the remaining mostly  $ZrO_2$  and  $Al_2O_3$  coating matrix.

Button-end samples with dimensions close to the final specimens were manufactured using investment-casting. Cylindrical specimens of Inconel 713LC in as-received condition and with TBC surface treatment were cyclically strained under strain control with constant total strain amplitude in symmetrical cycle at 900 °C in air.

The microstructure of the surface treated layer was documented and the hardness of the layers was evaluated. Hardening/softening curves, cyclic stress-strain curve and fatigue life data of coated and uncoated material were obtained. The fracture surface, surface relief and polished sections parallel to the specimen axis were examined using optical microscopy and SEM to study damage mechanisms in cyclic loading at high temperature. The microstructural and degradation mechanisms data help to discuss the differences in the stress-strain response and fatigue life of both materials.

# Optimal Design of Skirt Supporting Structure of Coke Drum for Thermal-Mechanical Cyclic Loading

EDWARD WANG, ZIHUI XIA

Department of Mechanical Engineering, University of Alberta, Edmonton, Canada

Coke drums are vertical clad pressure vessels used in petroleum refineries to facilitate the delayed coking process. The drums are operated under severe thermal-mechanical conditions due to cyclic heating and cooling of the drums. Most existing coke drums are supported by a continuous cylindrical shell commonly referred to as the skirt. They are often joined tangentially to the vertical portion of the vessel by a continuous fillet weld. Stresses in this junction are very high due to the combination of physical constraints and thermal-mechanical loading of the vessel. Under cyclic loading, these stresses may induce fatigue failure. In a previous study, it was found by means of an analytical solution that slotting the skirt, and thereby reducing its overall stiffness near the junction, can reduce junction stress (Cheng and Weil). However, the effect of slotting the skirt can be studied in more detail by using finite element analysis.

To determine the effect of the slot dimensions on junction stress, an existing coke drum with a slotted skirt is modelled and solved using finite element analysis. Properties of base material SA387 steel and clad material TP410S stainless steel are used for the determination of stresses (Yan et al.). Temperature-dependent Bilinear kinematic hardening plasticity model is used to capture the deformation and stress/strain of the structure under cyclic thermal-mechanical loading. A convection boundary condition is applied to the faces of the model corresponding to the interior of the drum. The ambient temperature and convection coefficient are then ramped to simulate two full cycles of thermal-mechanical loading (Xia et al.). The outer surfaces of the model are fully insulated, as is the case

with the actual drum. Due to large radial expansion of the shell that may cause contact of the shell and the skirt surfaces, contact elements are specified near the junction corner.

In this study, slot dimensions are manipulated to optimize the slot dimensions for minimal junction stress. The slots currently used are typically narrow in relation to their circumferential spacing, representing a decrease of only about 3% in the moment of inertia compared to a solid skirt. Contrary to earlier findings, no significant difference is found in the average and maximum junction stress between the solid (without slots) and current slotted skirt designs. In addition, it is found that the junction stress shows no significant response to the distance between the slot and junction based on the current slot size. Furthermore, it is found that slots which are significantly wider than the current slots result in a significant decrease in junction stress. Using finite element analysis, the slot design of the skirt support structure can be efficiently and accurately optimized.

## References

- Cheng, D. H. and N. A. Weil. "The Junction Problem of Solid-Slotted Cylindrical Shells." *Journal of Applied Mechanics* (1960): 343-349. Document.
- Yan Z. et al., Statistical method for the fatigue life estimation of coke drums. *Eng Fail Anal* (2014), <http://dx.doi.org/10.1016/j.engfailanal.2014.11.007>
- Xia, Z., Ju, F., and Plessis, P. D., 2010, "Heat transfer and stress analysis of coke drum for a complete operating cycle." *Journal of Pressure Vessel Technology*, 132: 051205

## Numerical and experimental analysis of the influence of process parameters on the damage of hot rolling rolls

LUIZ GUSTAVO DEL BIANCHI DA SILVA LIMA<sup>1</sup>, ALEXANDRE GONÇALVES<sup>2</sup>, ANA PAOLA VILLALVA BRAGA<sup>2</sup>, IZABEL FERNANDA MACHADO<sup>1</sup>, ROBERTO MARTINS DE SOUZA<sup>1</sup>, MÁRIO BOCCALINI JR.<sup>2</sup>

<sup>1</sup>Surface Phenomena Laboratory, Department of Mechanical Engineering, Polytechnic School, University of São Paulo, Brazil

<sup>2</sup>Institute for Technological Research, São Paulo, Brazil

Thermal fatigue is one of the main phenomena that lead to loss of rolling quality or failure in hot rolling rolls, mainly in the roughing stands but also in finishing passes (Stevens et al, 1971). This phenomenon is caused by the heating of the roll surface when in contact with the slab, followed by the cooling imposed in this surface to keep its temperature under control during successive rolling passes. The amount and rate of damage is influenced by several variables of the hot rolling process, such as slab temperatures, thickness reduction, roll and slab velocities and many others. In fact, such dependency on process variables makes the study of thermal fatigue a complex subject, which include the difficulty in instrumentating an actual working roll and the inherent cost of periodically removing it from operation to conduct surface inspection.

The main alternatives to actual roll instrumentation and inspection are: (i) To work in a reduced scale mill and (ii) to study the subject using numerical tools. Both scenarios have limited scope when uncoupled, since reduced scale models are costly and time-consuming, while numerical modeling needs calibration and validation from actual processes. Thus, a more powerful strategy is to couple both approaches – that is, to perform a limited number of reduced scale experiments and use the results to calibrate and validate a wider series of numerical models. This strategy was applied successfully by other authors (e.g. Tseng et al, 1989; Mercado-Solis et al, 2007), although these works either focus only in general subjects of hot rolling or approach the rolling process and the thermal fatigue involved in a simplified manner.

In this work, the methodology described above was applied. A reduced scale mill was assembled, and several AISI 1045 slabs were hot-rolled by a pair of AISI H13 rolls. Rolling was performed in an alternate fashion - 5 passes for slab, each pass with a thickness reduction of 15% - and cooling was applied to the surface of the rolls after each pass. The rolls were instrumented to retrieve roll temperature and rolling forces in each pass. Additionally, the roll was unmounted periodically for wear and thermal fatigue crack inspection. The data obtained in this mill was analyzed and then used to validate and calibrate a three-dimensional numerical model of the process, developed in finite-element commercial package ABAQUS/Explicit. Once the model was validated, different scenarios could be studied, by changing three rolling parameters: initial temperature distribution in the slab, thickness reduction at each pass and roll cooling regime. The results for each group of scenarios were then compared, in terms of axial and circumferential stresses in the roll, which are the main parameters that control thermal fatigue cracking throughout the rolling process.

### References

- Mercado-Solis, R.D., Talamantes-Silva, J., Beynon, J.H., Hernandez-Rodriguez, M.A.L. (2007): Modelling surface thermal damage to hot mill rolls – *Wear*, 263: 1560-1567.
- Stevens, P.G., Ivens, K.P., Harper, P. (1971): Increasing work-roll life by improved roll-cooling practice – *Journal of The Iron and Steel Institute*, 209: 1-11.
- Tseng, A.A., Lin, F.H., Gunderia, A.S., Ni, D.S. (1989): Roll cooling and its relationship to roll life – *Metallurgical Transactions*, 20A: 2306-2320.

Talks Topic C 6:

***Cyclic deformation behavior, crack initiation & crack growth of metals***

---

## Rolling Contact Fatigue Strength of Ceramic Coated Steel Laser-Quenched after Coating Process

HIROTAKE TANABE<sup>1</sup>, YUKI NAKAMURA<sup>2</sup>, YUI IZUMI<sup>1</sup>, TOHRU TAKAMATSU<sup>1</sup>

<sup>1</sup>The University of Shiga Prefecture, Hassaka, Hikone, Japan

<sup>2</sup>Engineering Graduate School, The University of Shiga Prefecture, Hassaka, Hikone, Japan

In our previous studies, a new surface modification method by combination of ceramic coating and laser heat treatment, “laser quenching after coating”, was developed. In this method, a steel substrate is first coated with a ceramic thin film by PVD or CVD method, and then the substrate is quenched by laser irradiation to the ceramic coated surface. By applying this method, it was possible to improve the adhesive strength and substrate hardness of ceramic coated steels effectively without compromising the film hardness and the toughness. From these results, it was considered that the raceway of ball bearing would be one of the good applications of this method.

In this study, to investigate the effects of “laser quenching after coating” on the rolling contact fatigue strength of ceramic coated steels, the thrust type rolling contact fatigue tests were carried out for ceramic coated steels processed by laser quenching after coating. For the substrate, carbon tool steel JIS-SK105 was used. CrAlN film was coated on this substrate by arc ion plating. The film thickness was 2.5 μm. For laser quenching process, a high power diode laser system was used. Laser power was changed from 800W to 900W. For the comparison, the rolling contact fatigue tests were also carried out for the specimens furnace-quenched after coating.

The delamination initiation life of the laser quenched specimens and the furnace quenched specimens were compared. The delamination initiation life of the laser quenched specimens was longer than that of the furnace quenched specimens. After the initiation, the delamination of the furnace quenched specimen grew much faster than that of laser quenched specimen. These reasons could be explained by the difference of the process time of the furnace quenching and the la-

ser quenching. The process time, in which the ceramic coating of the specimen was exposed to an elevated temperature, of the furnace quenching was much longer than that of laser quenching.

The effects of laser power on the delamination initiation life of laser quenched specimens were investigated. From 800W to 880W, the delamination initiation life was increased with laser power. The delamination initiation life of the specimen laser-quenched at 900W was quite short. A good correlation was recognized between the delamination initiation life and the adhesive strength of CrAlN film of laser-quenched specimens.

It is considered that laser quenching after coating with the suitable laser power could be an effective way to improve the delamination initiation life and to reduce the delamination growth rate under rolling contact fatigue.

### References

- H. Tanabe, et al. (2014): Effects of laser heat treatment on mechanical properties of ceramic coated steels Part 1 – Laser irradiation conditions and mechanical properties of ceramic coated steels, *Materials Research Innovations*, 18, S12 – S16, Maney Publishing.
- H. Tanabe, et al. (2014): Effects of laser heat treatment on mechanical properties of ceramic coated steels Part 2 – Fracture strength of laser heat treated ceramic thin film, *Materials Research Innovations*, 18, S17 – S21, Maney Publishing.

### Acknowledgements

This work was supported by JSPS Grants-in-Aid for Scientific Research (C) (No. 25420025).

## Crack propagation behavior in titanium alloy under combined axial-torsional cyclic loading modes

TOSHIHIKO HOSHIDE<sup>1</sup>, TETSUYA TOKUHARA<sup>2</sup>, MASASHI NAGAOKA<sup>2</sup>

<sup>1</sup> Department of Energy Conversion Science, Kyoto University, Kyoto, Japan

<sup>2</sup> Graduate School of Energy Science, Kyoto University, Kyoto, Japan

Titanium (Ti) alloys are expected to be a candidate of light materials having higher strength. To guarantee long-term integrities of Ti alloy components in their services, it is important to clarify the behavior of fatigue crack propagation in Ti alloy under biaxial stress

state which is anticipated being generated in actual components.

In this work, the behavior of fatigue cracks in Ti alloy under biaxial stress state was investigated by using thin tubular specimens of Ti-6Al-4V titanium alloy.

Force-controlled fatigue tests were executed under axial, torsional and combined axial-torsional loading modes. Fatigue tests in the aforementioned three loading modes were conducted under a stress ratio  $R$  of -1 or -1.2 (especially in axial loading mode), while tests under axial and torsional loading modes were also carried out under  $R = 0$ . By interrupting a fatigue test several times, the behavior of fatigue cracks was observed by using a plastic replication technique, and deformation in a cracked tube was also examined by monitoring crack-center opening displacement (CCOD) versus force curves.

Fatigue crack propagation rate is quantitatively analyzed in the framework of fracture mechanics, and usually by using stress intensity factor (Paris 1961, ASTM E-647 2007). It was seen that relations between crack propagation rate and stress intensity factor range in eight distinct testing conditions were different from each other. Effective stress intensity factor was evaluated by taking account of crack closure (Elber 1970), and a crack opening point was determined from CCOD vs. force curve. The effective stress intensity factor was correlated with crack propagation rate, and almost good correlation was found. However, the propagation rate under large scale yielding state shifted toward higher rate region compared with the crack growth relation under small scale yielding state. A simple method of J-integral evaluation (Rice, Paris & Merkle 1973, Hoshide, Yamada & Tanaka 1983) was developed for

thin-walled tubular specimens with inclined cracks. The range of J-integral was estimated by using the developed procedure, and correlated with the crack growth rate. The crack growth rate in the Ti alloy under all testing conditions was almost uniquely expressed by a power function of J-integral range, independently of testing condition.

Furthermore, in the correlation with the crack growth rate, availabilities of J-integral range based parameters, i.e., J-integral range divided by yield strength or Young's modulus, were also discussed.

#### References

- Paris, P.C., Gomez, R.E. & Anderson, W.E. (1961): A rational analytic theory of fatigue, *The Trend in Engineering*, Vol. 13, No. 1, 9-14.
- ASTM Designation E647-05 (2007): Standard test method for measurement of fatigue crack growth rates, *Annual Book of ASTM Standards*, Vol. 03.01.
- Elber, W. (1970): Fatigue crack closure under cyclic tension, *Eng. Fract. Mech.*, 2, 37-45.
- Rice, R.J., Paris, P.C., & Merkle, J.G. (1973): Some further results of J-Integral analysis and estimates, *ASTM STP 536*, 231-245.
- Hoshide, T., Yamada A. & Tanaka, K. (1983): Elastic-plastic finite-element analysis of cracked plate under biaxial stress and its application to fatigue crack propagation, *J. Soc. Mater. Sci., Japan*, 32(356), 528-534.

## The AA2124/SiC metal matrix composites under fatigue, creep and monotonic loading conditions

AGNIESZKA RUTECKA, PAWEŁ GRZYWNA, LECH DIETRICH

Institute of Fundamental Technological Research, Polish Academy of Sciences (IPPT PAN), Warsaw, Poland

Metal matrix composites (MMCs) are well known as materials lighter and simultaneously more durable than traditional ones [1-3]. Recently they are more often used in aerospace and automotive industries. Engine components such as pistons, connecting rods, brake callipers and cylinder liners as well as chassis components can be manufactured from the MMCs. During exploitation they are often subjected to fatigue, creep or monotonic loadings. Therefore AA2124/SiC MMCs were investigated under aforementioned conditions.

During the MMCs production aluminium alloy AA2124 powders (matrix) and SiC particles (reinforcement) were mixed and subjected to hot isostatic compaction, forging and CWQ T6 heat treatment. The MMCs were reinforced with 17 and 25% of SiC. The size of SiC particles was equal to 3  $\mu\text{m}$ .

Strain controlled tensile tests were performed at ambient temperature with strain rate equal to  $2 \cdot 10^{-4}$  1/s.

The first aim of the investigations was to obtain materials parameters such as elastic modulus, yield stress, ultimate tensile strength and strain to failure. Moreover, during tensile tests several unloadings were performed to evaluate degradation of elastic modulus of the MMCs during tension. Thus, damage evolution of the MMCs under tensile conditions was obtained. Additionally, the unloadings for engineering strain equal to 1, 2, 3 and 4% were repeated twice and two hysteresis loops for each aforementioned unloading strain values were obtained. It is worth to notice that the widths of the second loops for each unloading were smaller and the elastic moduli during unloading were higher in comparison to the same parameters for the first loops. Thus, strain hardening was observed for the MMCs from the first to the second cycles.

Force controlled fatigue tests were carried out at ambient temperature. Sine shape symmetric tension-compression cycles were applied with frequency equal to

10 Hz. Constant stress amplitudes ranged from 300 to 350 MPa for AA2124+17%SiC and from 330 to 380 MPa for AA2124+25%SiC. Both MMCs under aforementioned stress amplitudes behaved similarly. Hysteresis loops width enlarged significantly during compression and first cycles, and decreased during subsequent cycles. Thus, inelastic strain amplitudes obtained high values at the beginning of tests and decreased during subsequent cycles, which indicated strain hardening. Mean inelastic strain remained negative during fatigue tests.

Tensile creep tests under constant loading were performed at 300°C. The material investigated was AA2124+17%SiC. The MMC subjected to stress equal to 50 MPa did not reach tertiary creep and the test was stopped after about 1200 hours. Two specimens subjected to stress equal to 55 MPa reached tertiary creep after about 200 hours while a specimen under stress equal to 60 MPa (with 39 MPa preloading) reached tertiary creep after about 2 hours. Hence, small range of stress values between long-term and short-term creep was observed. Additionally, minimum creep rates were

calculated for each specimen. They obey Norton's law of secondary creep.

#### Acknowledgements

The results presented in this abstract have been obtained within the project "KosDeKom" (project no. 1576/B/T02/2011/40) with the National Science Center, Poland.

#### References

- Clyne, T.W. & Withers, P.J. (2003): An introduction to Metal Matrix Composites, Cambridge University Press.
- Chawla N. & Shen Y.L. (2001): Mechanical Behavior of Particle Reinforced Metal Matrix Composites, *Advanced Engineering Materials*, 3, No. 6; 357-370.
- Rutecka, A., Kowalewski, Z.L., Pietrzak, K., Dietrich, L., Makowska, K., Woźniak, J., Kostecki, M., Bochniak, W., Olszyna, A. (2011): Damage development of Al/SiC metal matrix composite under fatigue, creep and monotonic loading conditions, *Procedia Engineering*, 10, 1420-1425.

## Fatigue crack growth behavior of Ti-6Al-4V ELI alloy under constant amplitude loading with different single overloads

CHUANYONG CHEN<sup>1</sup>, DUYI YE<sup>1</sup>, XUMIN HU<sup>1</sup>, JIANZHONG LIU<sup>2</sup>, LINA ZHANG<sup>2</sup>

<sup>1</sup>Institute for Process Equipments, Zhejiang University, Hangzhou, China

<sup>2</sup>Division of Mechanical Properties, Beijing Institute of Aeronautical Materials, Beijing, China

Aviation components widely made of titanium alloy are usually suffered to variable amplitude loading in the process of service. Many researches have been carried out attempting to obtain clear crack propagation behavior under variable amplitude loading to predict the residual life of a component with detectable cracks accurately (Skorupa 1998), but few these investigations for titanium alloy especially for the Ti-6Al-4V ELI were conducted.

The aim of this study is to investigate effects of different single overloads (i.e., single tensile overload, single compressive overload, tensile-compressive overload and compressive-tensile overload) on the fatigue crack growth behavior and in Ti-6Al-4V ELI alloys. The crack growth rate under constant amplitude loading and that interspersed with different single overloads at the same crack length were examined systematically in laboratory environment. Three overload ratios were applied for each overload form, thus a total of 12 crack propagation tests were conducted using M(T) specimens according to ASTM E647-08. Fractography and crack morphology such as branching, deflection and blunting were inspected using SEM and optical microscope respectively. The measurements of crack

rate showed that different degrees of retardation effects occurred after all single overloads except single compressive overload. The intensity of retardation effect diminished dramatically with the decreasing of overload ratios and almost disappeared at the minimum overload ratio  $R_{oi}=1.375$ . There did not appear pronounced acceleration effect in the single compressive overload condition. Transient acceleration phenomena immediately after single overloads were also obtained in some situations.

Quite a lot of models were proposed to interpret crack growth rates under variable amplitude loading including yield zone models and crack closure models (Schijve 2008). In this study, the mechanism of overload effect was discussed based on the crack propagation behavior and crack profiles evolution. Here, it was thought that the interaction effects of the plastic zone containing compressive residual stress ahead of crack tip and the crack closure in crack wake played a dominated role in influencing the crack growth behavior under variable amplitude loading. The crack profile would be changed dramatically with the arising of large overload and there were interactions between crack growth behavior after overload and these crack profile

changes. The transient acceleration after overloads was due to the combination of lack of closure induced by crack blunting and more slip bands and secondary cracks at crack tip.

#### References

Skorupa, M. (1998). Load interaction effects during fatigue crack growth under variable amplitude load-

ing—a literature review. Part I: empirical trends. *Fatigue & Fracture of Engineering Materials & Structures*, 21(8), 987-1006.

Schijve, J. (2008): Interaction models for prediction of fatigue crack growth under VA loading. – In: *Fatigue of Structures and Materials*(pp.353-361). Springer Netherlands.

## Prestrain memory on subsequent cyclic behavior of FCC metallic materials presenting different dislocation slip tendencies

GAEL MARNIER, CLEMENT KELLER, LAKDHAR TALEB

Groupe de Physique des Matériaux, INSA Rouen, Université de Rouen, St. Etienne du Rouvray, France

The forming process of metallic industrial parts often involves steps of strong plastic strains which are susceptible to modify subsequent fatigue properties (fatigue life, stress-strain level ...) in service compared to the well-known cyclic behavior of the equivalent fully annealed material. Such modification, henceforth called “memory effect”, is related to the prehardening inherent to predeformation and has been widely studied during the past decades. Nonetheless, the deep understanding of this phenomenon is still a work in progress.

In the case of FCC metallic materials, several researchers argued about the influence of dislocations slip planarity. On one hand, wavy slip materials such as pure copper have been presented as independent, or at least weakly dependent, to prestrain history [1,2]. On the other hand, investigated purely planar slip materials were reported as strongly sensible to memory effect [1,3]. Anyway, this prestrain history dependence deserves further discussion and this work intends to cartography the domain of existence of memory effect as a function of stacking fault energy by studying three different materials: pure Copper as a wavy slip material, Nickel-Chromium alloy as a mainly planar slip material, and a 316L stainless steel which presents a mixed behavior.

In order to do so, Cyclic Stress-Strain Curves (CSSCs) were acquired for all materials by incremental step tests in total strain control. Both monotonic and cyclic prestrains were used for this study. The tensile prestrains were chosen accordingly to the strain-hardening

stages of each material and the cyclic ones were selected in order to study the influence of prehardening due to each of the typical dislocations structure in fatigue (i.e. veins, persistent slip bands and cells). All tests have been carried out under tension-compression at room temperature.

The CSSCs of prestrained specimens and virgin ones were compared. Firstly, the existence of a prestrain threshold implying a memory effect was thus highlighted. Then, cyclic plastic strain thresholds required to erase prestrain memories were also identified. Finally, stress partition has been applied on fatigue tests and it results that memory effect is mainly related to the memory of the internal stress value inherited from prestrain.

In the past, memory effect was reported to be a consequence of the stability of the prehardening dislocations structures [1-3] and this statement is also confirmed here by the role of internal stress in memory. As a consequence, TEM investigations were carried out on each material with the objective of discussing the evolution of the fraction of grains still presenting the prestrain structure after different amount of cycling.

#### References

[1] C.E. Feltner and C. Laird, *Acta Met.*, 15 (1967), 1612-1653.

[2] H.-J. Christ, G. Hoffmann, O. Öttinger, *Mater. Sci. Eng. A201* (1995), 1–12.

[3] K. Schoeler, H.-J. Christ, *Int. J. of Fatigue* 23 (2001), 767-775.

Talks Topic C 7:

***Cyclic deformation behavior, crack initiation & crack growth of metals***

---

## The effects of periodic overloads and high/low loading blocks on fatigue crack growth of aluminum alloy

HAIFENG XU<sup>1</sup>, DUYI YE<sup>1</sup>, LEI XIAO<sup>1</sup>, JIANZHONG LIU<sup>2</sup>, LINA ZHANG<sup>2</sup>

<sup>1</sup>Institute for Process Equipments, Zhejiang University, Hangzhou, China

<sup>2</sup>Division of Mechanical Properties, Beijing Institute of Aeronautical Materials, Beijing, China

Aluminum alloy is widely used in aircraft manufacturing for its lightweight, but working in extreme conditions. As an example, the tension wing skin which is made of aluminum alloy subject to variation of loads in its lifetime and is well recognized as a fatigue critical part (Schijve 2008). Therefore it is important to figure out the generalization of damage tolerance to variable amplitude fatigue (Romeiro 2009).

This paper presents an analysis of fatigue crack growth on M(T) specimens made of 2524-T3 aluminum alloy. The specimens were subjected to repeated blocks of cycles made up of a single overload (i.e. tensile, compressive, tensile-compressive or compressive-tensile) or a block (10000 cycles) of high ratio loads separated by a number (10000 or 20000 cycles) of baseline cycles. Crack opening displacement (COD) extensometer and optical microscope were used to measure the crack length and investigate the crack profiles respectively. The retardation and delay retardation have been found after overloads of tensile, tensile-compressive and compressive-tensile, but acceleration effect were found after compressive overloads. An interesting phenomenon was that, the stable crack propagation rate was reduced gradually after every single tensile overload ( $R_{ol} = 1.685$ ), and nearly stopped to grow under baseline cycles after several single tensile overloads.

The same phenomenon was found in high/low and low/high loading tests, while the high ratio load ( $R = 1.375$ ) is smaller, but the crack propagation rate is equal to 0 after a high ratio loading block.

At last, fracture surfaces were examined with stereomicroscope, black spots have been found between shear lips of a fatigue crack where tensile overload or high ratio loads took place. That indicates severe friction or squeeze exists at the front of crack tip after overload or high loads that cause black fretting products. The results have shown that the retardation effects in fatigue crack growth are closely related to the residual stress around crack tip and the plasticity induced crack closure, and the later could play the dominated roles in influencing the crack growth behavior under variable amplitude loading.

### References

- Schijve, J. (2008): Different types of loads on a structure in service. – In: *Fatigue of Structures and Materials*(pp.261-267). Springer Netherlands.
- Romeiro, F. De Freitas, M, De Fonte. (2009) Fatigue crack growth with overloads/underloads: Interaction effects and surface roughness. – In: *International Journal of Fatigue*, 31(11-12), 1889-1894.

## Multiaxial fatigue damage in fibrous composites: an approach based on micromechanical crack growth

ROBERTO BRIGHENTI, ANDREA CARPINTERI, DANIELA SCORZA

Dept. of Civil-Environmental Engng & Architecture, Univ. of Parma, Parma, Italy

Fibre reinforced composite elements are frequently used in severe structural applications involving repeated loading responsible for progressive deterioration and damage. Fibre reinforced composites are multiphase materials characterized by complex mechanical phenomena due to the different mechanical properties of the constituents and their reciprocal interactions [1-2]. In presence of fatigue loading, the safety assessment of fibrous composites requires to describe and quantify the degradation phenomena taking place mainly in the matrix material and at the fibre-matrix interface. The possibility to apply damage mechanics and fracture mechanics concepts to this class of problems al-

lows to easily describe their behaviour under fatigue loading.

Damage degradation can thus be applied to the matrix mechanical characteristics, and – by assuming a 3-D mixed Mode fracture description of the fibre-matrix detachment – fracture mechanics and crack growth rate concepts can be conveniently used to determine the progressive fibre debonding responsible for the loss of effectiveness of the reinforcing phase [3].

In the present paper a micromechanical model for unidirectional or random distributed fibre reinforced elements is developed and applied to the evaluation of the fatigue behaviour under uniaxial and multiaxial

fatigue stress states. Damage in the bulk material is accounted for through a Wöhler based damage parameter,  $D_c(\sigma^*, R^*, N)$ , suitable for the reduction of a generic mechanical property of the material  $P_m(N)$  with the number of loading cycles:

$$P_m(N) = P_{m,0} \cdot [1 - D_c(\sigma^*, R^*, N)]$$

On the other hand the 3D crack, representing the fibre-matrix detached region (Fig. 1), can be assumed to present a crack growth velocity  $v_g$  given by:

$$v_g = \frac{d}{dN} = C_i \cdot \Delta K_i^{m_i}, \Delta K_h < \Delta K_i \leq K_{LC}$$

where  $\Delta K_i$  represents the equivalent SIF range at the crack front interface region:

$$K_i = \begin{cases} \sqrt{K_I^2(\sigma_r^\infty) + [K_I(\sigma_r^\infty) + K_I(\sigma_z^\infty)]^2} & \sigma_r^\infty > 0 \\ K_I(\sigma_r^\infty) & \sigma_r^\infty \leq 0 \end{cases}$$

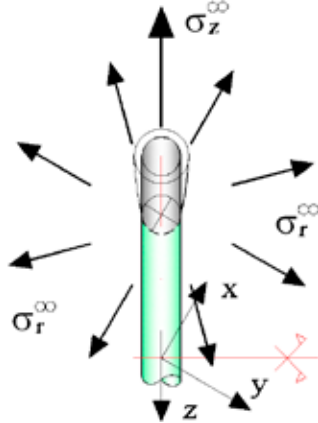


**Fig. 1.** Debonded extremity (3D cylindrical crack) of a fibre under remote radial ( $\sigma_r^\infty$ ) and axial ( $\sigma_z^\infty$ ) stresses.

expressed through the SIFs related to the radial and axial stress field of the fibre (Fig. 1).

The above degrading effects are finally taken into account in a proper homogenisation procedure in order to determine the averaged macroscopic properties of one equivalent locally homogeneous material that can be simply used in practical FE numerical analyses of real structural components.

Some applications related to the fatigue behavior of polymeric fibre-reinforced composite are presented for both uniaxial as well as biaxial in phase and out of phase fatigue stresses; the obtained results are compared with experimental data found in the literature.

#### References

- [1] Cheng, QG. (2012) Fiber Reinforced Composites. Nova Science Publishers, Inc., Hauppauge, NY.
- [2] Brighenti, R, Carpinteri A, Scorza D. (2012) A computational approach to evaluate the mechanical influence of fibres on brittle-matrix composite materials. *Comput. Mat. Sci.* 64: 212-215.
- [3] Brighenti, R., Carpinteri, A., Scorza, D. (2013) Fracture mechanics approach for partially debonded cylindrical fibre. *Comp Part B* 53: 169–178.

## Predicting the fatigue life at crack initiation in cruciform welded joints by using the effective cyclic $J$ -integral ( $\Delta J_{eff}$ )

DESIRE TCHOFFO NGOULA, HEINZ THOMAS BEIER, MICHAEL VORMWALD

Institute of Steel Construction and Materials Mechanics, Technische Universität Darmstadt, Germany

In this paper, recent results of the Institute of Steel Construction and Materials Mechanics (IFSW) of TU Darmstadt inside a project called IBESS („Integrale Bruchmechanische Ermittlung der Schwingfestigkeit von Schweißverbindungen“) are presented. The aim of IBESS is the fracture mechanics based simulation of Wöhler curves (S-N curves) in welded joints, see [4]. IBESS is divided into 8 subprojects and the IFSW is working on the subproject titled: “Modelling of fatigue crack growth in welded joints under consideration of the transient plastic deformation behaviour.” In this

work numerical analyses using two dimensional plane strain models and elastic-plastic materials behaviour of steel are performed in order to predict the fatigue life at crack initiation of cruciform welded joints. Fatigue crack growth analyses are performed by using the node release technique together with the finite element program Abaqus. The element size used in the crack domain is about 0.025 mm which is small comparing to the Dugdale’s plastic zone size . is commonly used as reference. The plasticity-induced crack closure (see, [1]) effects are taken into account by de-

termining the time at which the crack remains close/open and by using the effective cyclic  $J$ -integral ( $\Delta J_{\text{eff}}$ ) instead of the cyclic  $J$ -integral ( $\Delta J$ ) in a relation similar to the Paris equation. For this purpose, a python code was written in order to determine  $\Delta J_{\text{eff}}$  at every crack length phase. It is also shown in this contribution that the plasticity-induced crack closure and consequently  $\Delta J_{\text{eff}}$  depend on the elastic-plastic material law to be used. This is done by using the Döring's (see, [2]) and the Chaboche's material models. The predicted fatigue lives are compared with experimental data and a good accordance between both results was achieved. Due to the importance of residual stresses in the integrity assessment of welded joints, their influence on  $\Delta J_{\text{eff}}$  as well as on the fatigue life during short crack growth is investigated. Specific structure calculations are used in order to introduce the measured welding residual stress field in finite element model, see [5]. The calculated residual stress field match the measured one especially in the weld notch area. Results show that a tensile residual stress field is unfavourable to fatigue life while a compressive residual stress field is favourable to fatigue life. Furthermore, it is shown that calculations using the initial welding residual stress field and those using the redistributed residual stress field lead only to slightly different results in fatigue life.

## References

- E. Herz, O. Hertel, M. Vormwald: Numerical simulation of plasticity induced fatigue crack closure for autofrettaged intersecting holes. *Engineering Fracture Mechanics*, 78, S. 559-572, 2011
- R. Döring, J. Hoffmeyer, T. Seeger, M. Vormwald: A Plasticity Model for Calculating Stress-Strain Sequences Under Multiaxial Nonproportional Cyclic Loading. *Computational Materials Science*, 28, S. 587-596, 2003
- R. Thumser, J.W. Bergmann, M. Vormwald: Residual stress fields and fatigue analysis of autofrettaged parts. *International Journal of Pressure Vessels and Piping*, 79, S 113-117, 2002
- U. Zerbst: Assessment of welded joints by fracture mechanics. IBESS – The development of a procedure. *Proceedings of the 4<sup>th</sup> Symposium on Structural Durability in Darmstadt*, ISBN 978-3-8396-0734-3, S. 49-65, 2014
- H. Th. Beier, B. Schork, J. Bernhard, D. Tchoffo Ngoula, T. Melz, M. Oechsner, M. Vormwald: Simulation of fatigue crack growth in welded joints. *Proceedings of the 4<sup>th</sup> Symposium on Structural Durability in Darmstadt*, ISBN 978-3-8396-0734-3, S. 1-17, 2014

## Fatigue behavior of Al/Steel dissimilar resistance spot welds fabricated using Al-Mg insert film

REN ITO, ISHAK IBRAHIM, YOSHIHIKO UEMATSU, TOSHIFUMI KAKIUCHI, YUN KYOUL, CHIHIRO MATSUDA

Gifu University, Japan

Recently, reducing weight is one of very important topics in automobile industries to improve fuel efficiency. Conventional steels are still widely used as automobile structural components because of its advantages such as lower price and higher strength than aluminum (Al) alloys, recyclability and so on. But the major disadvantage is the heavier weigh than Al alloys. Thus, it is important to develop joining method between steel and Al to use steel for load-bearing parts and Al for the others. For example, Japanese automobile company MAZDA has applied a friction stir spot welding (FSSW) technique to join steel and aluminum alloy to reduce the weight of components. But the processing time of FSSW is longer than that of conventional resistance spot welding (RSW), and they have to integrate new and expensive FSSW equipment into their production line. If RSW technique could be efficiently used for the joining between steel and Al, processing time is much shorter than FSSW and the current equipment could be used. Furthermore, applying Al/steel dissimilar welds to the actual components, it is very important to understand fatigue behavior of joint. In this work, RSW

was applied for the joining between Al and steel using Al-Mg insert film. The film is aiming at the reduction of electric resistance between Al and steel sheets. Al-Mg insert film exhibits lower melting point than Al alloy. Consequently, melted film at lower voltage would fill the gap between two sheets and reduce the electric resistance, resulting in the effective joining at lower voltage. Subsequently, lap-shear fatigue tests had been conducted to evaluate fatigue strength and figure out fatigue fracture mechanism.

Materials used are Type304 stainless steel and A6061-T6 sheets with the thickness of 2mm. Thin Al-Mg file was inserted between two sheets and lap-shear type specimen was fabricated by an RSW technique. Fatigue tests were conducted using electro-hydraulic fatigue testing machine at a load ratio,  $R$ , of 0.1. The  $S-N$  diagram revealed that the RSW joints exhibited higher lap-shear fatigue strengths than Al/steel dissimilar welds fabricated by an FSSW method. Fatigue fracture modes were dependent on the load levels, where pull-out fracture occurred at high load levels, shear fracture in the nugget at medium load levels, and through-

thickness fatigue crack propagation in Al sheet at low load levels.

The fractographic analysis revealed that the pull-out fracture occurred due to the crack initiation at the edge of the nugget followed by the crack propagation

around the nugget. By lowering the load level, the initiated crack tended to propagate along the interface, resulting in the shear-type fracture. Further decrease of load level led to the through-thickness crack propagation into Al sheet.

## High cycle fatigue strength of pure lead

MASAHIRO ENDO<sup>1,2</sup>, KEIKO MORITA<sup>3</sup>, AKIRA YASUNAGA<sup>4</sup>

<sup>1</sup>Department of Mechanical Engineering, Fukuoka University, Japan

<sup>2</sup>Institute of Materials Science and Technology, Fukuoka University, Japan

<sup>4</sup>Sumitomo Metal Mining Siporex Co., Ltd., Tokyo, Japan

Pure lead is a typical hysteretic damping material that has a high energy dissipation capability by plastic deformation because of its almost perfect rigid-plastic behavior with little strain rate dependence. The lead damper, which can absorb effectively a large amount of the kinetic energy during an earthquake, has been used as a component of a base isolation system of modern buildings.

In recent year, it has been reported that cracking is observed on the surface of in-service lead dampers that have never experienced a major earthquake. These cracks could lead to degradation of the damping performance. The principal cause of the cracking is a large number of small oscillations due to wind and traffic-induced excitations. This problem is exactly a high cycle fatigue (HCF) problem. There are very few researches on the HCF of lead because the strength of lead is smaller than 1% of that of steels.

On the other hand, Snowden (1964), Morita et al. (2010) and Maruta et al. (2013) reported that the fatigue life of lead can be increased by a grease-coating. However, its effect has yet to be understood quantitatively and qualitatively. In this study, therefore, to tackle the underlying problems, we conducted a series of rotating-bending and tension-compression fatigue tests with pure lead round-bar specimens. To investigate the influence of a large number of small oscillations, the fatigue tests were conducted mainly in the HCF regime.

The S-N curves obtained in the rotating-bending fatigue tests for specimens with and without grease-coating on the surface demonstrated that the grease-coating

on the surface of lead had a favorable effect in enhancing the fatigue life and the fatigue limit (defined at  $3 \times 10^7$  cycles). Gough and Sopwish (1935) and Snowden (1964) inferred that fatigue strength in air was influenced by the interacting effect between oxygen and cyclic loading. In addition, the tension-compression tests of specimens containing a slit performed in this study revealed that a crack closure induced by grease-coating affected significantly the arrest and deceleration of propagation of a crack emanating from the slit.

### References

- Snowden, K.U. (1964): The effect of atmosphere on the fatigue of lead. *Acta Metallurgica*, 12, 295-303.
- Morita, K., Takayama, M., Yasunaga, A. (2010): Experimental Study on Fatigue Properties of Lead Damper for Seismic Isolation System (in Japanese). Summaries of technical papers of Annual Meeting Architectural Institute of Japan, No. 21168: 335-336
- Maruta, S., Takayama, M., Morita, K., Yanase, K., Endo, M. (2013): A study on high cycle fatigue behavior in Lead, 9th Int. Conf. Fracture & Strength of Solids.
- Gough, H.J., Sopwish, D.G. (1935): Some further experiments on atmospheric action in fatigue, *J. Inst. Met.* 56, 55-89.

### Acknowledgement

The authors gratefully acknowledge the contributions made by Mr. S. Maruta, Master student of Department of Mechanical Engineering, Fukuoka University, in the experimental works.

Talks Topic C 8:

***Cyclic deformation behavior, crack initiation & crack growth of metals***

---

# Accuracy improvement of fatigue damage evaluation based on phase analysis of dissipated energy

DAIKI SHIOZAWA, TSUYOSHI INAGAWA, ATSUSHI AKAI<sup>†</sup>, TAKAHIDE SAKAGAMI

Department of mechanical engineering, Kobe University, Kobe, Hyogo, Japan

<sup>†</sup>Present affiliation: Toyota Central R&D Labs. INC, Nagakute, Aichi, Japan

Fatigue limit estimation based on the dissipated energy measurement using infrared thermography has been getting an increasing attention in various industries. Mechanism of energy dissipation in relation to fatigue damage initiation has not been investigated yet. The present author's group has investigated the mechanism of energy dissipation through AFM observation at crack initiation and dissipated energy investigation under shot peening treatment. It was found from these results that energy dissipation was related to activity of slip band and estimated fatigue limit is corresponding to crack initiation stress level of the material. Most of study on dissipated energy has been discussed based on the mean temperature rise or irreversible component of heat generation due to energy dissipation. In this study, phase information of energy dissipation was investigated and was applied to the accuracy improvement of dissipated energy measurement for fatigue damage estimation.

Temperature rise is observed under compressive stress, and temperature fall is observed under tensile stress. This phenomenon is called as thermoelastic effect. Thermoelastic temperature change  $\Delta T_E$  is formulated by thermoelastic coefficient  $k$ , absolute temperature  $T$ , and sum of principal stresses  $\Delta\sigma$ .

$$\Delta T_E = -k T \Delta\sigma$$

The thermo-elastic temperature change  $\Delta T_E$  is a reversible phenomenon. However, in the actual case under cyclic loading, temperature rise due to irreversible energy dissipation  $\Delta T_D$  is observed in addition to thermoelastic temperature change  $\Delta T_E$ . This kind of heat generation is considered to be caused by local plastic deformation, so it occurs at the maximum tensile stress and at the maximum compressive stress. Therefore, temperature change due to dissipated energy  $\Delta T_D$  can be obtained as double frequency component for the load frequency  $f$ . In this study, the phase difference  $\Delta\theta$  between temperature change due to dissipated energy  $\Delta T_D$  and thermo-elastic temperature change  $\Delta T_E$ , which was signal with opposite phase for load signal, was obtained.  $\Delta T_E$  and  $\Delta T_D$  are expressed as following equation;

$$\Delta T_E = \sin(2\pi \times f \times t), \quad \Delta T_D = \sin(2\pi \times (2f) \times t - \Delta\theta).$$

The material under test is JIS type 316L austenitic stainless steel. The cyclic axis loading with a frequency of 5 Hz was applied to the specimen. In the staircase-like stress level test [1], stress amplitude was changed from 200MPa to 280MPa. Dissipated energy on the specimen surface was measured by infrared thermography with a MCT array detector. In the constant stress tests, the change of dissipated energy and phase difference was measured during fatigue test. The stress ratio  $R$  was set to be -1, -0.8 and -0.5 in both fatigue tests.

Dissipated energy at  $R=-1$  increased significantly from  $\sigma_a=255\text{MPa}$  and phase difference  $\Delta\theta$  converge to around 60 degree for the stress levels where dissipated energy shows increase. The experiments were carried out at least four times and the results showed good repeatability. The estimated fatigue limit based on dissipated energy coincided with the fatigue limit obtained by  $S-N$  curve ( $\sigma_w=250\text{MPa}$ ). The results at  $R=-0.8$  and  $-0.5$  are similar to that at  $R=-1$ . Change of dissipated energy shows increase from  $\sigma_a=250\text{MPa}$  at  $R=-0.8$ , and  $\sigma_a=240\text{MPa}$  at  $R=-0.5$ . The value of phase difference  $\Delta\theta$  shows constant values of 40 degree at  $R=-0.8$ , and 20 degree at  $R=-0.5$ .

Dissipated energy is small when the applied stress is below the fatigue limit, and then phase difference shows unstable value. On the other hand, phase difference show a certain value when the applied stress is above the fatigue limit and the value of dissipated energy show increasing. Unstable value of phase difference indicates that no slip occurs and measured dissipated energy is in the noise level. The phase information includes the behavior of slip and dislocation. Therefore, phase information can be used as a filtering at dissipated energy measurement.

## Reference

Rosa, G. La, and Risitano, A. (2000): Thermographic methodology for rapid determination of the fatigue limit of materials and mechanical components, *International Journal of Fatigue*, Vol.22, pp.65-73.

## Fatigue damage evaluation of polycrystalline alloy by diffraction contrast tomography using ultra-bright synchrotron radiation

YOSHIKAZU NAKAI, DAIKI SHIOZAWA, SHOICHI KIKUCHI, SHOTA MATSUDA, RYOTA NAKAO

Department of Mechanical Engineering, Kobe University, Kobe, Japan

A data acquisition technique, aiming at simultaneous reconstruction of three dimensional shape of grains in a bulk polycrystalline material, has been proposed by Ludwig et al. [1]. The procedure is termed X-ray diffraction contrast tomography (DCT), which is similar to the conventional X-ray absorption contrast tomography. Projected images of grains are obtained using the occasionally occurring diffraction contribution to the X-ray attenuation coefficient for a grain which fulfills Bragg's diffraction condition. The three-dimensional grain shapes are reconstructed from these projections. The DCT can provide simultaneous access to the sample's three dimensional grain arrangement such as shapes, locations and crystallographic orientations, together with microstructural features visible in X-ray absorption contrast such as cracks, porosity, inclusions, etc.

The authors apply DCT to evaluate dislocation structures in tensile test and low-cycle fatigue test by using SPring-8 (Super Photon ring – 8 GeV), which is the brightest synchrotron radiation facility in Japan [2]. The diffraction spot image spread over a range of successive rotation angle, and only part of the shape of diffracting grain appeared in each projection image. Diffraction spot extend angularly over which individual diffraction spots are visible, and the spread angle must give some measure of the orientation spread within each grain. This spread could be caused by the mosaicity (i.e. sub-grain misorientation) or the curvature of grain caused by the misorientation, which is related to a dislocation structure in each grain. We found that the rotation angle spread for each diffraction/extinc-

tion spot was related to the plastic strain of each grain. In the present study, the developed DCT technique is applied to the change of total misorientation of an individual crystallographic plane of a specific grain during fatigue test of a stainless steel sample or a commercially pure iron sample, where the former is a representative of f.c.c. material, and the latter, b.c.c. material. In high cycle fatigue test of the stainless steel, the misorientation of {111} planes increased with number of cycles. Among {111} planes, the amount of change depended on Schmid factor, i.e., the change was higher for larger Schmid factor.

In low cycle fatigue of the commercially pure iron, the misorientation also increased only for {110} planes. Among {110} planes, however, the amount of change was not affected by Schmid factor. It indicates that multiple slip should be considered for low cycle fatigue of b.c.c. materials.

We can discuss about the fatigue crack initiation condition by considering the change of total misorientation of individual crystallographic plane, size of grain where crack initiate, and difference of grain orientation between neighbor grains.

### References

1. W. Ludwig, S. Schmidt, E. M. Lauridsen and H. F. Poulsen, Journal of Applied Crystallography, 2008, 41, 302-309.
2. D. Shiozawa, Y. Nakai, R. Miura, and S. Matsuda, Materials Science Forum Vols. 783-786, pp.2359-2364 (2014).

## Dislocation-based modelling of low cycle fatigue in FCC single and polycrystals

NICOLÒ GRILLI<sup>1,2</sup>, KOENRAAD G. F. JANSSENS<sup>1</sup>, HELENA VAN SWYGENHOVEN<sup>2,3</sup>

<sup>1</sup>Laboratory for Nuclear Materials, Nuclear Energy and Safety, Paul Scherrer Institut, Villigen, Switzerland

<sup>2</sup>NXMM laboratory, IMX, École Polytechnique Fédérale de Lausanne, Lausanne, Switzerland

<sup>3</sup>Material Science and Simulations, NUM/ASQ, Paul Scherrer Institut, Villigen, Switzerland

Numerical modelling of cyclic plastic deformation behaviour of FCC metals is a currently unsolved problem which involves knowledge of the mechanisms of dislocation motion. Material damage is determined by microstructural features such as dislocation structures.

Therefore, a multiscale approach is necessary, which considers the single dislocation properties, such as mobility and short-range interactions, but is concurrently capable to describe the collective behaviour occurring on a micrometre length scale. We have implemented

specific dislocation-based constitutive equations for cyclic fatigue at room temperature, in which several dislocation density classes are used as state variables, in a crystal plasticity finite element (CPFE) solver. This computational method is suitable for introducing arbitrary geometries, boundary conditions and grain orientations. Real single crystal specimens and polycrystals can thus be modelled. One main novelty we have introduced is a dislocation multiplication law based on the observation that dislocation segments forming locks have no curvature while this property does not apply for dislocations with other orientations (Hochrainer, 2014). A new continuum formulation for cross slip is introduced to take the creation of new Frank-Read sources and secondary dislocations into account. The approach used for short-range interactions relies on a Gaussian distribution of interaction strengths to determine the fraction of mobile dislocations (Catalao, 2005). We present results from single crystal and polycrystal simulations. Dislocation structures in single slip

(vein-channel structures) and multiple slip deformation (labyrinth and cell structures) are found after 100 deformation cycles. The new model is capable to predict the volume fraction, the characteristic length scale and the orientations of dislocation structures, which is not predicted correctly by existing models (Pontes, 2006). Mechanical properties are also shown: cyclic hardening-softening behaviour has been demonstrated, together with the strain amplitude dependence of the model. In this work the DAMASK CPFE code (Roters, 2010) developed at the Max Planck Institute for Iron Research has been used.

#### References

- S. Catalao et al. *Mater. Sci. Eng. A* 400-401 (2005) 349-352.  
 J. Pontes et al. *Int. J. Plast.* 22 (2006) 1486-1505.  
 T. Hochrainer et al. *J. Mech. Phys. Solids* 63 (2014) 167-178.  
 F. Roters et al. *Acta Mater.* 58 (2010) 1152-1211.

## 3D dislocation dynamics simulation of crack shielding and blunting in FCC metals

LAURENT KORZECZEK<sup>1,2</sup>, BENOIT DEVINCRE<sup>1</sup>, RICCARDO GATTI<sup>1</sup>, ARJEN ROOS<sup>3</sup>

<sup>1</sup> ONERA/CNRS, Laboratoire d'Etude des Microstructures, Châtillon, France

<sup>2</sup> ONERA – The French Aerospace Lab, Châtillon, France

<sup>3</sup> Safran Tech Paris-Saclay, France

Subjected to low-amplitude cyclic loading, ductile crystalline solids like FCC metals endorse undergo plastic strain localisations, which may lead to the formation of cracks and subsequent fracture. Experimental evidence shows that crack growth and propagation mainly occurs at low stress intensity strongly depends on the microstructural behavior and characteristics of the material. Among the mechanisms involved, the interactions of the dislocations with the stress concentration ahead of the crack-tip (plastic zone) seem to play a decisive role. Two main phenomena are of interest:

- The shielding effect due to the increase or decrease of the stress acting on the crack surfaces due to the dislocation microstructure developing around the crack tip.
- The blunting effect induced by the emission or absorption of dislocation loops at the crack tip

Modeling these phenomena is a long-standing and complex problem. So far, existing models are essentially 2D [1] and only few attempts in 3D have been made. 3D dislocation dynamics (DD) simulations are then needed to quantitatively investigate the plastic deformation restraining crack propagation through shielding and blunting mechanisms. Only in 3D the influence of crystal symmetry, exact slip system activity and ther-

mally activated processes like dislocation cross-slip can be precisely taken into account.

To model this complex boundary value problem, the Discrete-Continuous Model (DCM) [2] is used to reproduce the interactions of realistic dislocation microstructures with a short sharp initial crack. Several crack orientations have been studied in a monocrystal and detailed analyses of the slip system activity in the plastic zone and the evolution of the shielding and blunting mechanisms at the crack tip are presented. These results are of particular interest for the development of dislocation density based models of crystal plasticity devoted to the complex problem of crack growth in fatigue. To evaluate the strain energy release around the crack tip and to quantify the fracture energy for the crack to propagate, a G-theta integral method is tested on the MDC calculations [3].

Results using the MDC methodology are then compared to Crystal Plasticity Finite Element (CPFEM) simulations using a Meric-Cailletaud law [4] for a copper monocrystal. Strengths and weaknesses of both approaches are discussed.

#### References

- [1] W. A. Curtin, V. S. Deshpande, A. Needleman, E. Van der Giessen, and M. Wallin. Hybrid discrete

- dislocation models for fatigue crack growth. International journal of fatigue, 32(9) :1511–1520, Sep 2010.
- [2] A. Vattré, B. Devincré, F. Feyel, R. Gatti, S. Groh, O. Jamond, and A. Roos. Modelling crystal plasticity by 3d dislocation dynamics and the finite element method: The discrete-continuous model revisited. Journal of the Mechanics and Physics of Solids, 63(0):491–505, 2014.
- [3] Destuynder, Ph, M. Djaoua, and S. Lescure. *Some remarks on elastic fracture mechanics*. Electricite des France, 92-Clamart, 1981.
- [4] L. Méric, P. Poubanne, and G. Cailletaud. Single crystal modeling for structural calculations : Part 1— model presentation. Journal of Engineering Materials and Technology , 113(1) :162–170, 01 1991.

## Analysis of the cyclic plastic response of materials based on the hysteresis loop shape

ROMAN PETRÁŠ<sup>1,2</sup>, JIŘÍ TOBIÁŠ<sup>2</sup>, JAROSLAV POLÁK<sup>1,2</sup>

<sup>1</sup>Institute of Physics of Materials, ASCR, Brno, Czech Republic

<sup>2</sup>CEITEC, Institute of Physics of Materials, ASCR, Brno, Czech Republic

Cyclic plastic response of polycrystalline materials is standardly analyzed using cyclic hardening/ softening curves and cyclic stress-strain curve. More information is however hidden in the hysteresis loop shape. Standard strain controlled low cycle fatigue test program can store the selected hysteresis loops during the fatigue life and hysteresis loop shapes could be analysed later. In low cycle fatigue testing of two polycrystalline materials, austenitic stainless steel and nickel base superalloy in addition to the stress and strain amplitudes also full hysteresis loops were recorded. The first and the second derivatives of the hysteresis half-loops were evaluated using digital smoothing procedures. According to the general statistical theory of the hysteresis loop (Polák 1991) the plot of the second derivative vs. relative strain can be used for the evaluation of the effective stress component and the probability density function of the internal critical stresses. The second derivative of the hysteresis half-loop of a single phase polycrystalline material contains initial drop followed by a single peak of the second derivative. The drop corresponds to the relaxation of the effective stress during unloading. The effective stress changes only slightly during cyclic plastic straining but the probability density function exhibits substantial changes, preferably in the early stage of the fatigue life, i.e. during fatigue hardening/softening. These changes (the height and the position of the peak) were evaluated and discussed in comparison with the observed localization of the

cyclic strain. The more detailed information about the sources of hardening/ softening of the material could be derived.

In two-phase material the initial drop is followed by two peaks provided both phases are deformed during cyclic loading. Each peak corresponds to the cyclic plastic deformation of the individual phase. The effective stress of the harder phase and the probability density function of the internal critical stresses in both phases can be estimated.

Cyclic loading was performed at room temperature and at elevated temperature with two strain rates. The temperature and strain rate dependence of the plastic stress-strain response has been studied and a more detailed information both on the effective stress and the distribution of the internal critical stresses in individual materials was established.

The plot of the second derivative corresponding to the probability density has been approximated by the Weibull distribution. The parameters of this distribution characterize the plastic stress-strain response in saturated state. In two phase material both peaks of the second derivative could be approximated by Weibull distribution provided the volume fractions of the phases are approximately the same.

### Reference

Polák, J. (1991): Cyclic plasticity and low cycle fatigue life of metals. Elsevier; Amsterdam.

Talks Topic C 9:

***Cyclic deformation behavior, crack initiation & crack growth of metals***

---

# The role of graphite in fatigue crack growth of ductile cast iron under the presence of internal and external hydrogen

TAKASHI MATSUO<sup>1</sup>, KOSEI YAMADA<sup>2</sup>, HISAO MATSUNAGA<sup>3,4,5</sup>, MASAHIRO ENDO<sup>1</sup>, SABURO MATSUOKA<sup>4</sup>

<sup>1</sup>Department of Mechanical Engineering, Fukuoka University, Japan

<sup>2</sup> Graduate school of Kyushu University, Japan

<sup>3</sup> Department of Mechanical Engineering, Kyushu University, Japan

<sup>4</sup> Research Center for Hydrogen Industrial Use and Storage (HYDROGENIUS), Kyushu University, Japan

<sup>5</sup> International Institute for Carbon-Neutral Energy Research (I2CNER), Kyushu University, Japan

Two types of fatigue crack growth (FCG) tests of ferritic-pearlitic ductile cast iron were carried out: (i) FCG test in air using hydrogen-charged specimen to clarify the effect of internal hydrogen and (ii) FCG test in 0.7 MPa hydrogen gas using non-charged specimen to clarify the effect of external hydrogen. FCG tests were performed at a stress ratio of 0.1 and a test frequency  $f$  ranged from 0.001 Hz to 5 Hz. The hydrogen-charged specimens were prepared by exposing the specimens to 100 MPa hydrogen gas at 358 K for 200 hours. The ratio of crack growth acceleration due to hydrogen,  $(da/dN)_H / (da/dN)_{H-Free}$  was obtained at the stress intensity factor range  $\Delta K$  of 20 MPa·m<sup>1/2</sup>.

Generally, in BCC steels with a high hydrogen diffusion coefficient, hydrogen-charged specimen is not adequate for investigation of an effect of internal hydrogen at very low frequencies (e.g. 0.001 Hz), since internal hydrogen rapidly outgases from the specimen during the test in air. In contrast, in ductile cast iron, the rate of outgassing is much lower than that of BCC steels owing to the existence of graphites that can store a large amount of hydrogen for a long time (Matsunaga *et al.* 2013). Therefore, we tested the hydrogen-charged ductile cast iron in air to investigate the effect of internal hydrogen on FCG in a wide range of frequencies.

In the hydrogen-charged specimen, an accelerated crack growth did not occur at 5 Hz. In the frequency range from 1 to 0.01 Hz, the acceleration ratio increased with a decrease in  $f$  and reached  $(da/dN)_H / (da/dN)_{H-Free} \approx 17$ . At a lower frequency (e.g.  $f = 0.001$  Hz), the ratio was slightly decreased.

On the other hand, in the tests in hydrogen gas, the acceleration ratio increased with a decrease in  $f$  in the range from 5 to 0.1 Hz, and reached  $(da/dN)_H / (da/dN)$

$\approx 7$ . At a lower frequency (e.g.  $f = 0.01$  Hz), the ratio was drastically decreased and became nearly equivalent to that in air.

The above peculiar frequency dependence of hydrogen-induced FCG acceleration is explained by the difference in hydrogen distribution ahead of crack tip that influences the degree of slip localization (Matsuo *et al.* 2010). In the hydrogen-charged specimen, internal hydrogen is attracted to the vicinity of crack tip owing to the stress-induced hydrogen diffusion. On the other hand, in the test of non-charged specimen in hydrogen gas, external hydrogen penetrates through surface near crack tip. Consequently, internal hydrogen requires longer time to be concentrated to crack tip zone than external hydrogen. As a result, the frequency at which acceleration ratio peaked out is lower for internal hydrogen than external hydrogen. Further, in the case of external hydrogen at very low frequencies (e.g.  $f \leq 0.01$  Hz), hydrogen can be extensively distributed over the plastic zone ahead of crack tip. In this situation, slip localization can hardly occur and thereby the crack tip would be blunted in a similar way to the non-charged specimen tested in air.

## References

- Matsunaga, H., Usuda, T., Yanase, K. and Endo, M. (2013): Ductility Loss in Ductile Cast Iron with Internal Hydrogen – Metallurgical and Materials Transactions A, Vol. 45: 1315-1326.
- Matsuo, T., Matsuoka, S. and Murakami, Y. (2010): Fatigue Crack Growth Properties of Quenched and Tempered Cr-Mo Steel in 0.7 MPa Hydrogen Gas. – Proceedings of 18th European Conference on Fracture, Dresden, Germany.

## Shear mode crack propagation along with plastic flow of small area

SHUTO FUKUDOME<sup>1</sup>, SIGERU HAMADA<sup>2</sup>, MASAHARU UEDA<sup>3</sup>, HIROSHI NOGUCHI<sup>2</sup>

<sup>1</sup>Graduate school of Engineering, Kyushu University, Fukuoka, Japan

<sup>2</sup>Faculty of Engineering, Kyushu University, Fukuoka, Japan

<sup>3</sup>Yawata R&D Lab., Nippon Steel & Sumitomo Metal Corporation, Kitakyushu, Japan

In order to achieve shear mode crack propagation which is appeared around the surface of rolling/sliding contact machine elements along with the plastic flow, a test method was developed and the test results are presented.

Rolling contact fatigue is the damage of rolling/sliding contact machine elements and the crack exist along with the plastic flow. For the applied stress around the crack, shear stress is considered to be dominant caused by the rolling/sliding contact. Therefore, the author considered that the crack propagated along with the plastic flow by shear mode. Usually the shear mode crack is easy to branch to the tensile mode without compression load on the crack surface. Therefore the author considered that the plastic flow acts as a guide to shear mode crack propagation and prevents the branching.

Some studies were conducted about the shear mode crack growth and some test methods were proposed. However, all of the test method needs large (mm scale) specimen. The size of the plastic flow layer on the rolling/sliding contact machine element surface is a few hundred of microns. Therefore, in this study, in order to achieve shear mode crack growth test of such small area, a test method was developed.

Ferritic stainless steel (JIS-SUS430) was adopted in this study. Rolled thin film was used as a specimen. The authors assumed the plastic flow of the rolling/sliding

contact machine element and rolled thin film is the same in terms of plastic flow. The film was cut to disk shape, the thickness of the film was 30 microns and the diameter was three mm in this experiment. For the crack starter, a 600 micron length precrack was introduced on the specimen by FIB (focused ion beam) process. By the FIB process, very thin crack can be introduced on the specimen and the stress intensity factor at the crack tip expected to be large.

Round bar jig and the thin film specimen was bonded by quick-drying glue. To make sure that the glue works properly, flat area was made on the round bar jig. By applying torque on the round bar jig, shear stress was loaded in the precracked thin film indirectly. Rolling direction, precrack direction, and shear loading direction were all arranged to be parallel. Stress intensity factor of the crack tip was roughly calculated considering the glue layer and the restraint crack deformation by the glue. A commercial FEM software was used, and the value is confirmed to be enough to the crack propagation.

After the cyclic loading, long shear mode crack has appeared on edge of precrack and propagated along with the plastic flow direction of the thin film. Therefore, the shear mode crack propagation for thin film without compression load on the crack surface was succeeded. The authors concluded that crack growth direction was guided by plastic flow.

## A Continuum Damage Mechanics Approach For Prediction of Fatigue Crack Initiation Life

SHIVA KUMAR CHITTA, M.M.MAYURAM

Machine Design Section, Department of Mechanical Engineering, Indian Institute of Technology Madras, India

Fracture process of ductile materials is still only partly unravelled and void growth may well represents the whole ductile fracture process (under different combinations of load, time and environment). Fatigue is responsible for up to 80% of the in-service parts failure, which occurs in industry. The effective fatigue design, under ultra-high cycle fatigue is one of the more difficult tasks an engineer faces due to involvement of many factors. In total fatigue life, crack initiation phase can have significant percentage, ca 80% or more in defect-free components and in case of long life fatigue

regime(HCF,UHCF) as summarized by Hael Mughrabi (2013) and it is advantageous to have high crack initiation life. Hence it is important to predict the crack initiation life as accurately as possible.

The present work is to predict the fatigue crack initiation life of Low alloy, SAE 4340 steel, using damage models based on Continuum damage mechanics (CDM). Continuum damage mechanics models proposed by S.Dhar et al.(1996) for the ductile damage evolution and for the micro crack initiation are considered for the simulation of ductile damage and failure.

The work includes both experimental and simulation aspects. The experimental phase includes monotonic tensile test and strain controlled fatigue test on cylindrical specimens of dimensions as per ASTM E606 standard. In the simulation phase, large deformation finite element analysis is carried out using commercial software Abaqus along with its user material subroutine UMAT, on cylindrical tensile test specimen. In The UMAT, an explicit scheme with Continuum Jacobian is used for the integration of constitutive models for the material behavior in elasto-plastic regime and damage evolution law, which are developed based on  $J_2$ -Incremental flow theory along with the concepts of effective stress and hypothesis of strain equivalence.

Salient aspects of the analysis covering the stress and plastic strain for micro crack initiation, the critical damage value and estimation of the fatigue crack initiation life are presented in this paper

#### References

- Hael Mughrabi(2013): Micro structural fatigue mechanisms: Cyclic slip irreversibility, crack initiation, non-linear elastic damage analysis, *Int. J. of Fatigue*, 57, 2-8.
- Dhar S, Raju Sethuraman and Dixit P.M.(1996): A Continuum damage mechanics model for void growth and micro crack initiation, *Engg. Fracture mechanics*, 53(6), 917-928.

## Generalized critical fatigue crack length for transition from microstructure-driven to mechanics-driven propagation

YASUAKI HAMANO, MOTOMICHI KOYAMA, KANEAKI TSUZAKI, HIROSHI NOGUCHI

Department of Mechanical Engineering, Faculty of Engineering, Kyushu University, Fukuoka, Japan

The fatigue life is the sum of fatigue crack initiation life and fatigue crack propagation life. Actually, it is known that the fatigue life is mainly dominated by the fatigue crack propagation life. Crack growth behavior is divided into 3 stages: 1) microstructure-driven small crack growth 2) mechanics-driven small crack growth 3) large crack growth. It has been reported that microstructure-driven small crack growth rate is distinctly scattered. In contrast, the mechanics-driven small crack which does not follow the Paris Law has less scatter. The long crack which follows the Paris Law propagates without scatter, in which the crack growth rate and its associated fatigue crack growth life are predicted precisely. We name the transition crack length where the scatter of  $da/dN$  disappears as  $l_0$ . The length  $l_0$  may be related to mechanical and microstructural factors, e.g. average grain size, mean stress, inclusions, crystal orientations, and grain boundary characteristics. Despite of the importance of  $l_0$ , even engineering definition of  $l_0$  is still unclear. In order to determine  $l_0$  quantitatively,

we propose a new statistical method. Although  $l_0$  depends on many factors as mentioned above, the proposed method can give a statistical result without any considerations of the complicated phenomena. The method consists of two steps: I) measuring of crack propagating speed, II) statistically analyzing the data by using coefficient of variation (CV). The CV value decreases with crack growth. A specified crack length at which the CV value saturates is defined to be  $l_0$ . In this work, strain-controlled tension/compression fatigue testing was conducted at  $\Delta\varepsilon = 2\%$  and the frequency of 1Hz in air. The surface crack length required for determination of  $l_0$  was obtained through replica technique in certain number of cycles.

#### References

- Y. Zhao, Q. Gao, J. Wang: *Fatigue Fract. Engng. Mater. Struct.*, 22, (1999), 459-467.
- M. Goto: *Fatigue Fract. Engng. Mater. Struct.*, Vol.17, No. 6, (1994), 635-649.

## Fatigue crack growth characteristic under hydrogen atmosphere in an ultra-low frequency region in Low Carbon and Interstitial Free Steels

YOUSUKE ONISHI, MOTOMICHI KOYAMA, ATSUSHI NISHIMOTO, DAISUKE SASAKI, YASUJI ODA, HIROSHI NOGUCHI

Department of Mechanical Engineering, Faculty of Engineering, Kyushu University, Fukuoka, Japan

Hydrogen has been known to deteriorate mechanical properties in steels. The understanding mechanical

characteristics under the hydrogen environment is essential in practical uses. In this study, we paid attention

to frequency dependence of the fatigue crack propagation rate under hydrogen environment in low carbon and interstitial free steels. More specifically, the fatigue behavior in an ultra-low frequency region was focused.

At first, we observed the surface fatigue crack propagation in the bending fatigue tests of the ultra-low frequency under the hydrogen environment by optical microscopy to measure the fatigue crack propagation rate. The fatigue testing was conducted at a 0.7% total strain and at hydrogen or nitrogen pressures of 0.18 MPa at 40°C. Next we observed fracture surfaces using a scanning electron microscope.

The hydrogen atmosphere was clarified to accelerate fatigue crack growth rate compared to that in nitrogen atmosphere at a frequency of 6 Hz. However, fatigue crack propagation rate in nitrogen and hydrogen environments did not have a significant difference at frequency of 0.001Hz. In order to investigate the disappearance of the hydrogen effect, we performed the detailed observation of a surface crack and the fracture surface. In the hydrogen atmosphere, a brittle fracture feature including brittle striation was observed partially. An important factor suppressing the hydrogen effect in the low frequency is hydrogen distribution. Namely, a homogenization of hydrogen would diminish the hydrogen effect in terms of hydrogen-enhanced localized

plasticity. However, also note that the “disappearance” of the hydrogen effect cannot be interpreted by only the influence of hydrogen distribution. In this work, we suggest that an influence of carbon diffusion to understand this problem. The hydrogen effects associated with site competition or a reduction in trap energy of hydrogen by carbon is considered to suppress the HELP effect. Moreover, strain age-hardening by carbon at a crack tip also would decrease in the ultra-low frequency which can provide a sufficient time for the carbon diffusion. In this report, we discuss the interactions between hydrogen and carbon and its associated effects on fatigue crack propagation rates by using low carbon and IF steels which do not have a significant carbon and no solute carbon, respectively to confirm the influences of the site competition and the strain age-hardening.

#### References

- J.P. Hirth: *Metall. Trans. A*, 11A (1980), 861.  
 J.E. Costa and A.W. Thompson: *Metall. Trans. A*, 13A (1982), 1315.  
 M. Koyama, E. Akiyama, K. Tsuzakin and D. Raabe: *Acta Mater.*, 61 (2013), 4607.  
 D.G. Enos and J.R. Scully: *Metall. Mater. Trans. A*, 33A (2002), 1151.

## Short crack growth kinetics in heat resistant austenitic stainless steel Sanicro 25

VERONIKA MAZÁNOVÁ<sup>1</sup>, JAROSLAV POLÁK<sup>1,2</sup>, GUOCAI CHAI<sup>3,4</sup>

<sup>1</sup>Institute of Physics of Materials, Brno, Czech Republic

<sup>2</sup>CEITEC, Institute of Physics of Materials, Brno, Czech Republic

<sup>3</sup>Sandvik Materials Technology, Sandviken, Sweden

<sup>4</sup>Linköping University, Engineering Materials, Sweden

Heat resistant austenitic stainless steel Sanicro 25 has been developed for high temperature applications mostly in power generation industry. Its resistance to monotonic and cyclic loading has been studied using creep and low cycle fatigue tests at ambient and elevated temperatures (Chai et al. 2013, Polák et al. 2014). The preliminary study of the mechanisms of damage in cyclic loading (Polák et al. 2014) has revealed appreciable localization of the cyclic strain in the persistent slip bands and early initiation of fatigue cracks.

The cyclic slip localization plays an important role also in the growth of short cracks that often determines the low cycle fatigue life of materials. We have therefore studied both the evolution of the surface relief, the initiation of fatigue cracks, their evolution and kinetics of short crack growth in Sanicro 25 steel at ambient temperatures. The cylindrical specimens with a shallow notch were cyclically strained in computer controlled fatigue testing system with constant strain rate and

different strain amplitudes. The persistent slip bands and fatigue cracks developed either intergranularly or along the grain boundaries were followed in-situ using optical microscopy and in interrupted tests using scanning electron microscopy.

The cracks initiate on the surface and soon acquired the shape close to a semicircle. Surface crack length projected on the plane perpendicular to the loading axis thus reasonably characterizes the crack topology. Multiple cracks develop in specimens during elasto-plastic cyclic loading. The crack density of the and its evolution during cyclic loading has been evaluated. Individual cracks grow, interact and often link together. The growth rate of the longest cracks is affected by the linking with smaller cracks. The crack length of the three or four of the longest cracks in the area of a small notch was plotted vs. number of cycles for different strain amplitudes. The growth of individual cracks could be reasonably well approximated by an exponential de-

pendence. Exponential dependence correspond to the proportionality of the crack growth rate to the crack length. The parameter of the exponential law, denoted as the crack growth coefficient, depends on the strain amplitude or on the saturated plastic strain amplitude. The dependence of the crack growth coefficient on the plastic strain amplitude has been approximated by the power law. The power law dependence of the crack growth coefficient corresponds to the Manson-Coffin law provided the cycle number to crack initiation could be neglected.

#### References

- Chai G. et al. (2013) Creep and LCF Behaviors of Newly Developed Advanced Heat Resistant Austenitic Stainless Steel for A-USC. *Procedia Engineering*, Vol. 55: 232-239.
- Polák J. et al. (2014) Low cycle fatigue behavior of Sanicro 25 steel at room and at elevated temperature. *Mater. Sci. Eng. A615*:175–182

Talks Topic C 10:

***Cyclic deformation behavior, crack initiation & crack growth of metals***

---

# Application of $\sqrt{area}$ parameter for estimation of threshold stress intensity factor range $\Delta K_{\tau th}$ of small shear-mode cracks

SABURO OKAZAKI<sup>1</sup>, HISAO MATSUNAGA<sup>2,3,4</sup>, MASAHIRO ENDO<sup>4,5</sup>

<sup>1</sup>Graduate School of Kyushu University, Fukuoka, Japan

<sup>2</sup>Department of Mechanical Engineering, Kyushu University, Fukuoka, Japan

<sup>3</sup>International Institute for Carbon-Neutral Energy Research (I2CNER), Kyushu University, Fukuoka, Japan

<sup>4</sup>Institute of Materials Science and Technology, Fukuoka University, Japan

<sup>5</sup>Department of Mechanical Engineering, Fukuoka University, Japan

The flaking strength associated with subsurface cracking is strongly influenced by the defect size at fracture origin (Lewis & Tomkins 2012). Therefore, when performing a fracture mechanics-based evaluation, the fracture process must be addressed as a small crack problem. Recently, Matsunaga et al. performed torsional fatigue tests under static compression to measure the ranges of the threshold stress intensity factor (SIF),  $\Delta K_{\tau th}$  and  $\Delta K_{\tau th}'$ , for the shear-mode growth of small surface cracks between approximately 0.01 and 1 mm in length in a bearing steel (Matsunaga et al 2011). Consequently, these authors noted a crack size dependence for  $\Delta K_{\tau th}$  and  $\Delta K_{\tau th}'$ .

In this study, the ranges of the threshold SIF,  $\Delta K_{\tau th}$  and  $\Delta K_{\tau th}'$ , for small shear-mode cracks in bearing steel are measured using torsional fatigue testing under static compression using aforementioned testing method with a newly developed testing machine. The threshold values are described as a function of the crack size and the crack-face interference. The authors suggest that the effect of crack-face interference could be quantified by the fraction of the interfering crack area,  $f$ , which is defined by the following equation:

$$f = \frac{area_{crack}}{area_{defect} + area_{crack}} \quad (1)$$

where  $area_{crack}$  is the area of the interfering crack face and  $area_{defect}$  is the area of the defect with no interference.

In addition, to simplify the evaluation of the shear-mode threshold, a single parameter,  $K_{\tau}$ , is introduced to represent the SIF of shear-mode crack as following formulae:

$$K_{\tau} = 0.58\tau \sqrt{\pi \sqrt{area_i}} \quad (2)$$

(for an internal crack)

$$K_{\tau} = 0.69\tau \sqrt{\pi \sqrt{area_s}} \quad (3)$$

(for a surface crack)

Where  $\sqrt{area_i}$  and  $\sqrt{area_s}$  are the square root of the area of an internal and a surface crack, respectively. Finally, the threshold SIF range for a shear-mode fatigue crack,  $\Delta K_{\tau th}'$ , can be successfully expressed by using the  $\sqrt{area}$  parameter. The threshold SIF range  $\Delta K_{\tau th}$  was also found to exhibit a crack size dependence similar to that of mode I cracks (Murakami & Endo 1983) in the small crack size regime. The  $\Delta K_{\tau th}$  can be approximated by the following formulae:

$$\Delta K_{\tau th} = 1.12 (f + 1.33) (\sqrt{area_i})^{1/3} \quad (4)$$

(for an internal crack)

$$\Delta K_{\tau th} = 1.26 (f + 1.33) (\sqrt{area_s})^{1/3} \quad (5)$$

(for a surface crack)

## References

- Lewis, M.W.J. Tomkins, B. (2012): A fracture mechanics interpretation of rolling bearing fatigue, proceedings of the institution of mechanical engineers, J. Eng. Tribol. 226, 389–405.
- Matsunaga, H. Shomura, N. Muramoto, S. Endo, M. (2011): Shear mode threshold for a small fatigue crack in a bearing steel, Fatigue. Fract. Eng. M., 34, 72-82.
- Murakami, Y. & Endo, M. (1983): Quantitative evaluation of fatigue strength of metals containing various small defects or cracks, Eng. Fract. Mech. 17, 1–15.

## Fatigue crack initiation near inclusions in Ni superalloys – a SEM based study with high resolution EBSD

JUN JIANG<sup>1</sup>, JIE YANG<sup>2</sup>, TIAN TIAN ZHANG<sup>1</sup>, MAKI KUWABARA<sup>1</sup>, FIONN DUNNE<sup>1</sup>, BEN BRITTON<sup>1</sup>

<sup>1</sup>Department of Materials, Imperial College London, UK

<sup>2</sup>Beijing Institute of Aeronautical Materials (BIAM), People's Republic of China

Fatigue lifeing of aeroalloys is an important part of aircraft fleet management and has significant economical repercussions for all major aerospace manufacturers. In highly engineered jet engine components microstructure plays a very important role in total fatigue life, principally in crack initiation and short crack growth which may involve  $\sim 1/3$  of the life of the component (Sangid 2013, Dunne 2014). Understanding of this domain requires high fidelity and high resolution characterisation techniques that capture dominant damage mechanisms involved in fatigue to inform physically motivated modelling efforts. Movement towards 'sufficient but not excessive' design requires significant improvements with experimentally informed models that can physically capture appropriate deformation mechanisms in a timely, efficient and physically motivated manner.

This talk will outline some recent experimental work principally using slip trace analysis and high angular resolution electron backscatter diffraction (HR-EBSD). HR-EBSD is well suited for characterisation at the microstructural lengthscale, capturing residual elastic strains with a precision of  $1 \times 10^{-4}$  and lattice rotations with a precision of  $1 \times 10^{-4}$  and with high spatial resolution ( $\sim 20 \times 60 \times 20 \text{ nm}^3$ ) For more information on the HR-EBSD technique, please see a recent review (Britton et al 2013).

In this study, a series of interrupted three point bending low cycle fatigue tests were carried out on a powder metallurgy FGH96 nickel superalloy sample contain-

ing non-metallic inclusions. High resolution electron backscatter diffraction (HR-EBSD) was used to characterize the distribution and evolution of geometrically necessary dislocation (GND) density, residual stress and total dislocation density near a non-metallic inclusion. Slip trace analysis has been used to characterise active slip systems and local microstructural sensitivity. This work describes a systematic study of room temperature cyclic deformation processes from cyclic hardening, to stabilised cyclic deformation stage, to crack formation and propagation stage focussing on inclusion-matrix interactions. Rather complex deformation structures were directly observed from the first few cycles and the patterning did not vary significantly with increasing number of cycles. Most noticeable, a clear link was found between crack path and the spatially resolved sites of extreme values of residual stress and GND density.

### References

- Britton, T.B., Jiang, J., Karamched, P.S and Wilkinson A.J. (2013): Probing Deformation and Revealing Microstructural Mechanisms with Cross-Correlation Based, High-Resolution Electron Backscatter Diffraction – in JOM 65:1245-53
- Sangid, M.D. (2013): The physics of fatigue crack initiation – in International Journal of Fatigue 57:58-72
- Dunne, F.P.E. (2014) Fatigue crack nucleation: Mechanistic modelling across the length scales – in Current Opinion in Solid State and Materials Science.

## Non-destructive evaluation of multiple-site small cracks in high-temperature low cycle fatigue of an austenitic stainless steel by using multipoint probe DC potential difference measuring system

SHIO NAKANISHI<sup>1</sup>, TAKAYUKI SUZUKI<sup>2</sup>, YUJI NAKASONE<sup>1</sup>

<sup>1</sup> Tokyo University of Science, Japan

<sup>2</sup> National Institute of Advanced Industrial Science and Technology, Ibaraki, Japan

The development of advanced maintenance technologies is a vital issue for extending the fatigue life of energy conservation facilities. Condition-based maintenance (CBM) is one of the promising technologies for

improving the dependability, i.e., the reliability plus availability of the facilities. Effective monitoring technologies are indispensable for non-destructive evaluation of fatigue damage in the CBM.

In the previous study (Nakanishi 2014), the present authors have applied the 4-point probe DC potential difference method to the non-destructive evaluation of multiple-site small cracks in high-temperature low cycle fatigue of an austenitic stainless steel JIS SUS316L at 873K in air. The statistical analysis of the potential difference distributions obtained revealed that standard deviation of normalized potential difference can evaluate initiation, growth and coalescence behavior of multiple-site small cracks in each stage of the fatigue process.

The present study has constructed a potential difference measuring system which can measure potential difference distributions on the surface of specimens by scanning fully automatically the specimen surface of interest. This system consists of the nugget tester equipped with a multipoint probe (Denshijiki Industry Co., Ltd. 2015), motorized X-Y-θ stages, the 4-axis stage controller and a data-collection PC. The probe has as many as 32 mini-pins arranged in two-line zigzag along the longitudinal direction of specimens to be monitored. Each line of the mini-pins has a length of 15 mm and are placed 1 mm apart from each other. This probe can collect potential difference data on the whole reduced-section surface of each one of the present round-bar type specimens within half an hour, about 5 times faster than the previous 4-point probe measuring system (Nakanishi 2014).

Specimens are round bar type made of an austenitic stainless steel JIS SUS316L equivalent of AISI Type 316L. Low cycle fatigue tests were carried out at six applied strain rate levels of up to 1.8% at 873K in air. Local DC potential difference on each specimen surface was

measured throughout the whole fatigue process at adequate intervals by the present multipoint probe DC potential difference measuring system equipped with 32 mini-pin probe. The 4-point mini-pin probe was also used for a comparison purpose. The intervals between points of measurement are 0.5 mm in the longitudinal direction of the specimen and 1.0 mm in the circumferential direction.

The local potential difference can be regarded to have followed normal distributions throughout the fatigue processes investigated in this study. The standard deviation of the potential difference was increased with increasing number of strain cycles at six strain range levels tested. All the fatigue processes investigated can be divided into four stages according to the behavior of cracks; i.e., (1) incubation stage, (2) initiation stage, (3) growth and coalescence stage, and (4) accelerated growth stage. The detection of the onset of the fourth or final stage by the present multipoint probe DC potential difference method can non-destructively predict the residual life of fatigue in which multiple-site small cracks are involved.

#### References

- Nakanishi, S. Suzuki, T. & Nakasone, Y. (2014): Non-Destructive Evaluation of Multiple-site Small Cracks in Low Cycle Fatigue of Austenitic Stainless Steel by Four-point Probe DC Potential Difference Method – In: Proceedings of The 2nd International Conference on Maintenance Science and Technology: 53-54; Kobe, Japan.
- Denshijiki Industry Co., Ltd. (2015): <http://www.emic-jp.com/english/products/ennt4102/>.

## Crack detection by Sonic-IR method using ultrasonic wave inputted through water

YUI IZUMI<sup>1</sup>, HIROTAKA TANABE<sup>1</sup>, TOHRU TAKMATSU<sup>1</sup>, TAKAHIDE SAKAGAMI<sup>2</sup>

<sup>1</sup>The University of Shiga Prefecture, Development of Mechanical Systems Engineering, Japan

<sup>2</sup>Kobe University, Development of Mechanical Engineering, Japan

Sonic-IR, which is also called vibro-thermography, is one of the active thermographic NDT technique. This method, which is based on the detection of the temperature rise due to frictional heating at the defect faces under ultrasonic excitation, has an advantage in the detection of closed defects. The method was originally developed by Henneke (Henneke 1979) and has been advanced and improved (Gleiter 2006, Shepard 2004, Montanini 2010, Sakagami 2009) more recently.

However, in conventional sonic-IR method, to directly input an acoustic energy from ultrasonic transducer to the test area via ultrasonic horn, which may give scratches and deformation in the test object.

In this study, we develop a new sonic-IR method using ultrasonic wave inputted through water, and practicality

of the proposed method for the detection of fatigue crack is experimentally investigated. Experimental results by the proposed method are compared with conventional sonic-IR technique using ultrasonic horn. As a results, it was found that crack detection can be conducted by proposed technique.

#### References

- E. G. Henneke II, K. L. Reifsnider & W.W. Stinchcomb: Thermography – An NDI Method for Damage Detection, *J.Metal*, Vol. 31(9), pp.11-15
- A. Gleiter, G. Riegert, Th. Zweschper, R. Degenhardt & G. Busse: Advanced Ultrasound Activated Lock-in-Thermography for defect selective depth resolved imaging, *Proceedings of SPIE*, Vol. 6205, 62051F

S. M. Shepard, T. Ahmed & J. R. Lhota: Experimental Considerations in Vibrothermography, Proceedings of SPIE, Vol. 5405, pp.332-335  
 R. Montanini, G. L. Rossi & F. Freni: Ultrasound Lock-in Thermography as a Quantitative Technique for Quality Control Assessment of Cast Iron Turbocharger Components, Proceedings of 10<sup>th</sup> International Conference on Quantitative Infrared Thermography

T. Sakagami, R. Katsumata, K. Kuroki, Y. Harada and S. Kubo: Detection of Stress Corrosion Cracking by Sonic-IR Technique, Proceedings of the Seventh International Conference on NDE in Relation to Structural Integrity for Nuclear and Pressurized Components, pp.1087-1093

## Low-cycle fatigue Simulation in micro-scale to obtain fatigue behavior of bimodal AL alloys

H. HOSSEINI-TOUDESHPY, M. JAMALIAN

Department of Aerospace Engineering, Amirkabir University of Technology, Tehran, Iran

Fatigue crack initiation and propagation patterns play an important role in failures. More than 80% of failures are caused by fatigue while purely static loading rarely occurs. Grain refinement, significantly influences the resistance of metals and alloys to fatigue crack initiation and propagation and generally leads to an increased failure resistance, whereas a deleterious effect can be observed on the resistance to fatigue crack growth.

In this study, cryomilled ultra-fine-crystalline Al–Mg alloy is considered as the material for case study. Elastic-plastic analyses including crack initiation and propagation in low-cycle fatigue regime are performed for dual phase microscale models to obtain the damage pattern and damage growth versus number of load cycles. For this purpose, several RVEs are extracted from the available optical microscopy (OM) images of the real material. Then, XFEM is applied to the bimodal material and the brittle and ductile phases are distinguished using real values of parameters in fracture criteria. In the next step, Paris equation coefficients are obtained from the available  $da/dN-\Delta K$  curves for different phases and fatigue simulations are performed for different RVEs by means of XFEM code in ABAQUS.

Finally, the Low-cycle fatigue analysis is applied to the models through the direct cyclic approach. As a result, the crack initiation and propagation pattern in micro-scale are predicted and crack growth variation versus cycle numbers are also obtained. It is shown that the predicted results are in good agreement with the available experimental pattern results. More details will be presented in the full paper.

### References

- Z. Lee, V. Radmilovic, B. Ahn, E. J. Lavernia, and S. R. Nutt, (2009) "Tensile Deformation and Fracture Mechanism of Bulk Bimodal Ultrafine-Grained Al-Mg Alloy," *Metallurgical and Materials Transactions A*, vol. 41, no. 4, pp. 795–801.
- R. Huang, N. Sukumar, and J.-H. Prévost, (2003) "Modeling quasi-static crack growth with the extended finite element method Part II: Numerical applications," *International Journal of Solids and Structures*, vol. 40, no. 26, pp. 7539–7552.
- B. O. Han, E. J. Lavernia, Z. Lee, S. Nutt, and D. Witkin, (2005) "Deformation behavior of bimodal nanostructured 5083 Al alloys," *Metallurgical and Materials Transactions A*, vol. 36, no. 4, pp. 957–965.

## Fatigue of automotive engine cylinder heads – A new model based on crack propagation and microstructure interaction

GUILLAUME MORIN, ROMAIN DEJEAN, JEAN-MICHEL FIARD, MATHIEU BERANGER

Renault, Guyancourt, France

Design of modern automotive internal combustion engines has become an increasing challenging task in the past years due to increasing constraints in terms of performance, fuel economy and emissions. Mechanical and thermal loads increase on high specific power output engines, mainly turbocharged direct injection

Diesel and gasoline engines, has made more and more difficult to reach reliability targets. In parallel, development costs reduction makes it necessary to raise simulation model accuracy in order to get directly the optimized design with reduced physical validation tests. Cylinder head is a critical part in an internal combus-

tion engine. It has a great impact on performance via intake and exhaust aerodynamic optimization and it undergoes high mechanical and thermal loads directly linked to combustion process. Without efficient and dedicated CAE tools, its development can quickly become a blocking point.

The main reliability problem encountered during cylinder head development is the appearance of fatigue cracks during severe endurance tests. These cracks can in particular initiate in the coolant water jacket and lead to the complete part failure. Classically these cracks are associated mainly with combustion pressure alternate stresses and high cycle fatigue in infinite life domain. To prevent their appearance, mechanical simulation results are checked with a Haigh or Dang Van criteria. But the comparison of predictions based on these models with experimental results on engine reveals several difficulties: crack initiation spots are not correctly located, scatter of crack sizes are not predicted, and higher critical results on tests with thermal cyclic loads are not taken into account.

To overcome these difficulties, a new fatigue model dedicated to cylinder heads in aluminum alloy has been developed in Renault powertrain engineering. The main characteristics are the followings. The model is based on a propagation approach in order to take account typical characteristics of foundry alloy microstructure such as porosities which act as initial defects. Statistical distribution of these characteristics is included, which allows to explain and tackle experimental results scatter. Low cycle fatigue effect related to cyclic thermal loads and high cycle fatigue effect related to combustion pressure are combined. The model is fitted thanks to an extensive crack propagation tests database. Consistency with classical high cycle fatigue test results is checked.

This paper will present the theoretical basis of this new model and the correlation with experimental results. Benefit for cylinder head development based on real examples will also be discussed.

Talks Topic D 1:

***In-situ microscopy and diffraction***

## In-situ TEM deformation of lightweight alloys and local strain measurements with diffraction imaging

ANDREW M. MINOR<sup>1,2</sup>

<sup>1</sup>Department of Materials Science & Engineering, University of California, Berkeley, USA

<sup>2</sup>National Center for Electron Microscopy, Molecular Foundry, Lawrence Berkeley National Laboratory, USA

Besides the important results related to the effect of size on the strength of individual nanostructures, the ability to systematically measure the mechanical properties of small volumes through nanoscale mechanical testing allows us to test samples that cannot easily be processed in bulk form, such as a ion-irradiated materials or single crystals of very specific alloys. This talk will highlight recent advances with in situ Transmission Electron Microscopy (TEM) nanomechanical testing techniques that provide insight into small-scale plasticity and the evolution of defect structures in lightweight alloys such as Mg, Al and Ti. In addition to measuring the strength of small-volumes, measuring

the evolution of strain during plastic deformation is of great importance for correlating the defect structure with material properties. Here we demonstrate that strain mapping can be carried out during in-situ deformation in a TEM with the precision of a few nanometers without stopping the experiment. Our method of local strain mapping consists of recording large multi-dimensional data sets of nanodiffraction patterns using a new high-speed direct electron detector. This dataset can then be reconstructed to form a time-dependent local strain-map with sufficient resolution to measure the transient strains occurring around individual moving dislocations.

## CSL $\Sigma 3$ and $\Sigma 9$ activity as a deformation pathway in nanocrystalline Pd and AuPd

AARON KOBLER<sup>1,2</sup>, CHRISTIAN KÜBEL<sup>1</sup>, HORST HAHN<sup>1,2</sup>

<sup>1</sup>Karlsruhe Institute of Technology (KIT), Germany

<sup>2</sup>Technische Universität Darmstadt (TUD), Germany

Most of our current understanding of the deformation mechanisms active in nanocrystalline (nc) metals stems from *in-situ* deformation experiments on bulk materials using x-ray diffraction (XRD). However, XRD cannot directly resolve the local deformation processes, e.g. grain growth or twinning. For a local analysis, these processes are traditionally investigated using BF/DF-TEM. Though, varying contrast due to local orientation changes, bending and defects during *in-situ* BF-TEM straining experiments make an accurate interpretation for nanometer sized grains difficult. On the other hand, the relatively new technique Automated Crystal Orientation Mapping (ACOM-TEM) allows for the identification of crystallographic orientation of all crystallites with crystal sizes <100 nm where EBSD reaches its limitation.

Recently, we combined ACOM imaging in STEM modus with in-situ straining inside a TEM [1], [2]. This combination was the key to new data evaluation based on orientation maps. By tracking individual crystallites through a straining series the change of their orientation can be evaluated in order to distinguish between an overall crystallite rotation and sample bending. In addition, twinning/detwinning and grain growth can be directly followed and the automatic data evaluation

leads to user independent quantitative statistical information such as grain size.

This measurement and evaluation routine was applied to magnetron sputtered Pd<sub>x</sub>Au<sub>1-x</sub> thin film samples of about 50 nm supported by an additional carbon film, which reduces strain localization during tensile tests. Grain growth and grain fragmentation as well as twinning and detwinning have been observed to take place simultaneously at different locations. In addition, the crystallite tracking revealed 40° and 60° orientation changes of individual crystallites indication a CSL relation of the crystallite before and after the deformation. CSL-lattice flips are possible if multiple dislocations are activated from different directions along the grain boundaries, or generally, if pre-existing CSL boundaries are moved by dislocations. This investigation shows that dislocation mediated deformation mechanisms are still very active in nanocrystalline material, even though it was expected that grain boundary mediated processes would become more dominant.

### Acknowledgement

This work was supported by the DFG under grant FOR714.

## References

- [1] A. Kobler, A. Kashiwar, H. Hahn, and C. Kübel, "Combination of in situ straining and ACOM TEM: A novel method for analysis of plastic deformation of nanocrystalline metals," *Ultramicroscopy*, vol. 128, pp. 68–81, Jan. 2013.
- [2] A. Kobler and C. Kübel, "In Situ Straining Analysis with ACOM-TEM," *Imaging Microsc.*, no. 1, 2014.

## In-situ characterization of martensite plasticity by high resolution microstructure and strain mapping

C. C. TASAN<sup>1</sup>, L. MORSDFORF<sup>1</sup>, M-M. WANG<sup>1</sup>, D. BARBIER<sup>2</sup>, O. JEANNIN<sup>1</sup>, D. RAABE<sup>1</sup>

<sup>1</sup>Max-Planck-Institut für Eisenforschung GmbH, Duesseldorf, Germany

<sup>2</sup>Arcelor Mittal Research, Voie Romaine, Maizières-lès-Metz, France

Mechanical behavior of martensite plays the most critical role in many commercial steels used in strength requiring applications. Thus, there is an everlasting interest in identifying alloy design and thermo-mechanical processing strategies to enhance martensite ductility and toughness. In this regard ferrous martensite, although typically considered to fully lack plastic deformation capacity, can accommodate significant amount of micro- or even macro-plasticity prior to micro-cracking. However, a deeper understanding of the governing factors in martensite plasticity is not yet fully available. To improve the fundamental understanding of the multi-scale characteristics of martensitic microstructures and their micro-mechanical properties, first, a multi-probe methodology is developed and applied to low-carbon lath martensitic model alloys. The approach is based on the joint employment of electron channeling contrast imaging (ECCI), electron backscatter diffraction (EBSD), transmission electron microscopy (TEM), atom probe tomography (APT) and nanoindentation, in conjunction with high precision and large field-of-view 3D serial sectioning. This methodology enabled us to resolve (i) size variations of martensite sub-units, (ii) associated dislocation sub-structures, (iii) chemical heterogeneities, and (iv) the resulting local mechanical properties. The identified interrelated microstructure heterogeneity is related to the martensitic transformation sequence, which is proposed to intrinsically lead to formation of a nano-composite structure

in low-carbon martensitic steels [1].

Then, employing in-situ deformation experiments and high spatial resolution microstructure and strain mapping, plasticity is investigated in different model martensitic microstructures. Results of the experiments clearly demonstrate the heterogeneity of plasticity in all investigated materials. Coupling of the EBSD based microstructure maps to the full-field strain measurements reveal that the local differences in crystallography, parent austenite grain size, defect density and boundary character play important roles in the resulting heterogeneity in martensite plasticity. Finally, we also provide direct evidence on the key role of introducing thin films of austenite in enhancing martensite plasticity [2, 3].

## References

- Morsdorf, L., Tasan, C.C., Ponge, D., Raabe, D., 3D structural and atomic-scale analysis of lath martensite: effect of the transformation sequence, (submitted, 2015)
- Wang, M-M, Tasan, C.C., Ponge, D., Dippel, A-C., Raabe, D., Nano-laminate TRIP-TWIP steel with dynamic strain partitioning and enhanced damage resistance, *Acta Materialia*, 85 (2015) 216-228.
- Wang, M-M, Tasan, C.C., Ponge, D., Kostka, A., Raabe, D., Smaller is less stable: size effects on twinning vs. transformation of reverted austenite in TRIP maraging steels, *Acta Materialia*, 79 (2014), 268-281.

## Complex analyses of mechanical and electrical performance of metallic thin films on flexible substrates combined with in-situ Reflectance Anisotropy Spectroscopy

ANDREAS WYSS<sup>1</sup>, MATTHIAS SCHAMEL<sup>1</sup>, RICHARD DENK<sup>2</sup>, MICHAEL HOHAGE<sup>2</sup>, ALLA S. SOLOGUBENKO<sup>1</sup>, RALPH SPOLENAK<sup>1</sup>

<sup>1</sup>Laboratory for Nanometallurgy, Department of Materials, ETH Zurich, Switzerland

<sup>2</sup>Atomic Physics and Surface Science, Institute of Experimental Physics, Johannes Kepler Universität Linz, Austria

For optimal electric performance, a flexible electronic device has to sustain large mechanical stresses without losing its structural integrity. An effect of the mechanical behavior of the whole system (substrate and thin metallic film) on electrical properties of the metallic subsystem is very important and subject of extensive studies. The thin film geometry exerts hard constraints or even excludes a number of conventional techniques for mechanical testing. For the determination of yield strength, synchrotron x-ray diffraction is commonly applied. However, it is restricted by beam time availability and new characterization techniques are desired.

In our study we present complex in-situ characterization of electrical and mechanical behavior of fcc metal thin films, Cu and Cu-Zn, on insulating polyimide substrates. The change in the electrical resistance of the thin metallic films upon uniaxial tensile loading was monitored by a concurrent acquisition of reflectance anisotropy spectra. The latter technique is sensitive to changes in the strain state of the specimen, its phase and microstructural configurations. Since the mechanical behavior of thin metallic film is known to be thickness dependent, the experiments were performed on

films of different thicknesses: 50, 100, 200, 500 and 1000 nm.

Our study reveals that upon straining, the RA spectra of both systems exhibit two main features. The first feature grows linearly with strain and the second feature appears in later stages of straining. The saturation of the linear growth of the first feature indicates yielding and can therefore be used as yield point estimation. These findings were proven by high resolution SEM micrographs. The second feature and its evolution are associated with irreversible deformation in the material as well as material properties for example absorption edges of segregated layers. Upon unloading, the first feature changes sign and gradually reduces, whereas the second feature remains unchanged. The RA features are shifted depending on the chemical composition as seen from Zn additions within the solubility limit of the Cu phase.

Our results show that reflectance anisotropy spectroscopy is a suitable and reliable tool that allows dynamic monitoring of thin film strain states during deformation. Therefore, it can be employed to register microstructural changes in the film upon straining.

## Crystallographic and mechanical characterization of micro-bicrystal cantilevers

S. ZAEFFERER<sup>1</sup>, N. BOZZOLO<sup>2</sup>, S. KLEINDIEK<sup>3</sup>, A. J. SMITH<sup>3</sup>

<sup>1</sup>Max-Planck-Institut für Eisenforschung, Düsseldorf, Germany

<sup>2</sup>Ecole De Mines, Sofia-Antipolis

<sup>3</sup>Kleindiek Nanotechnik, Reutlingen, Germany

The influence on the mechanical behaviour of grain boundaries in crystalline materials depends on the crystallographic character of these boundaries. Grain boundaries are characterized by 5 rotational crystallographic parameters, including 3 for the misorientation across the boundary and 2 for the grain boundary normal. All 5 parameters influence properties like dislocation transmission strength or fracture propagation resistance.

We have developed a method, which allows characterization, in a non-destructive manner, all 5 grain boundary parameters by a pseudo-3D-EBSD approach. Sub-

sequently, grain boundaries with interesting misorientations or grain boundary plane are prepared, using focussed ion beam milling, to form a micro-cantilever bicrystal. These bicrystals are mechanically tested by bending them inside of the SEM using a bending device and micromanipulator developed by Kleindiek Nanotechnik. Finally, the deformed structure of the two grains and the grain boundary is characterized using 2D or 3D EBSD. Geometrically necessary dislocation densities and grain boundary damage are observed.

The described approach is applied to polycrystalline 710 superalloys.

Talks Topic D 2:

***In-situ microscopy and diffraction***

## In-situ micro-mechanical testing at the synchrotron

STEVEN VAN PETGEM

Neutrons and Xrays for Mechanics of Materials, Paul Scherrer Institut, Villigen, Switzerland

A major challenge in metallurgy is to understand the relation between the microstructure of a metal and its behaviour under an applied load or temperature. This requires a detailed characterization of the evolution of the microstructure at different length scales through the determination of the crystal structure, defect density, grain size distribution, texture etc.

During last decade in-situ mechanical testing at the synchrotron has become a widespread tool to investigate the evolution of the microstructure of single and polycrystals during deformation (Van Swygenhoven 2013). Many such in-situ deformation tests are performed during continuous or interrupted uniaxial tensile and/or compression tests of bulk materials and thin films. Several microstructural properties such as the development of intergranular elastic strains and texture evolution can be directly compared with results from, for instance, molecular dynamics simulations or crystal plasticity modeling. While such tests have proven to be very useful, for further refinement of the existing models it is crucial to obtain information from other, more complex deformation tests.

In this work we highlight three such tests recently performed at the Swiss Light Source: (1) in-situ cyclic fatigue of Cu single crystals under shear conditions, (2) stress reduction tests on nanocrystalline Ni and (3) the deformation behaviour of porous silver films.

(1) It is well known that under cyclic fatigue of metals dislocation patterning occurs. The nature of the resulting dislocation structure depends on several parameters, including stacking fault energy, dislocation mobility and loading conditions. To obtain a better understanding of how these structures form a new continuum dislocation-based constitutive model in the crystal plasticity finite element framework is currently under development. In order to validate this new model

in-situ Laue experiments during cyclic shear loading of Cu single crystals have been performed. Laue diffraction is very sensitive to crystal orientation and therefore allows tracking with high resolution the evolution of the misorientation angles between the various dislocation-poor regions that appear under cyclic deformation.

(2) Transient testing is a well recognized technique to capture rate limiting deformation mechanisms. Most popular methods are strain rate jump and stress relaxation tests. Stress reduction tests are maybe less well known, they have however shown to be a suitable technique to determine the full transient response (Mekala 2011). In this work we report on stress reduction tests performed on electrodeposited nanocrystalline Ni. Depending on the magnitude of the stress reduction we observe different regimes, revealing the presence of various deformation mechanisms. The results are interpreted in terms of a competition between plasticity based on dislocation nucleation/glide and recovery mechanisms at grain boundaries.

(3) Sintered nanoporous silver is currently considered as an alternative bonding material in the electronic packaging industry. For the development of lifetime prediction models of components that include such silver layers it is crucial to understand its thermomechanical behaviour. In this work we focus on some key in-situ experiments that highlight the importance of the porous microstructure on the overall mechanical behaviour.

### Reference

- Mekala, S. et al (2011) *Philos. Mag.* 91: 908-931  
Van Swygenhoven, H. & Van Petegem, S. (2013) *Mater. Charact.* 78: 47-59.

## Optimizing Single Crystal Growth for Detector Applications using Energy-dispersive Neutron Imaging

H. MATTHIAS REICHE<sup>1</sup>, SVEN C. VOGEL<sup>1</sup>, EDITH D. BOURRET<sup>2</sup>, ADRIAN LOSKO<sup>3</sup>, ANTON TREMSIN<sup>3</sup>, GREGORY A. BIZARRI<sup>2</sup>, MARTIN M. GASCON<sup>2</sup>, DIDIER PERRODIN<sup>2</sup>, ERIC C. SAMULON<sup>2</sup>

<sup>1</sup>Los Alamos National Laboratory, Los Alamos, U.S.A.

<sup>2</sup>Lawrence Berkeley National Laboratory, Berkeley, U.S.A.

<sup>3</sup>University of California Berkeley, Berkeley, U.S.A.

Advances in neutron flux, neutron instrumentation, and sample environments over the past years allowed the development of unique techniques to characterize

material synthesis and processing. Here, we present capabilities and results using recently developed energy-dispersive neutron imaging and tomography ap-

plied to optimizing single crystal growth. Energy-dispersive neutron imaging and tomography utilize isotope-specific neutron absorption resonances to visualize the distribution of elements in the bulk (Tremisn 2013a & 2013b). Furthermore, so-called Bragg-edges (Vogel 2000) allow measurements of lattice strains and thus imaging of e.g. the stresses in a sample. Beam spots and penetration are both of the order of centimeters, allowing characterization of large single crystals grown e.g. for gamma particle detection. Homogeneous distribution of dopants, such as europium, is essential for the performance in the detector application while controlling and minimizing the stresses reduces mechanical failures. As with many other neutron techniques, sample environments (Reiche 2012) to e.g. study crystal growth by the Bridgman technique in-situ are possible. Such in-situ capabilities provide direct feedback on how processing parameters such as temperature, temperature gradient or growth speed affect material properties such as the dopant distribution, mosaicity, or stresses.

We show examples of the ex-situ characterization of single crystals grown with different processing parameters as well as our capability to study solidification and crystallization processes in-situ with energy-dispersive neutron imaging.

#### References

- Reiche, H. M., Vogel, S. C., et al. (2012): A furnace with rotating load frame for in situ high temperature deformation and creep experiments in a neutron diffraction beam line. *Rev. Sci. Instr.* **83** 053901.
- Tremisn, A.S., Vogel, S.C., et al. (2013a): Non-destructive studies of fuel pellets by neutron resonance absorption radiography and thermal neutron radiography, *J. Nucl. Materials* **440** 633–646.
- Tremisn, A.S., Vogel, S.C., et al. (2013b): Energy resolved neutron radiography at LANSCE pulsed neutron facility, *Neutron News* **24** 28-32.
- Vogel, S.C. (2000): A Rietveld-approach for the analysis of neutron time-of-flight transmission data, PhD thesis, Christian-Albrechts-University Kiel, Germany.

## Time-resolved (4D) in situ x-ray tomographic microscopy at TOMCAT: Understanding the dynamics of materials

J.L.FIFE<sup>1</sup>, F. MARONE<sup>1</sup>, R. MOKSO<sup>1</sup>, M. STAMPANONI<sup>1,2</sup>

<sup>1</sup>Swiss Light Source, Paul Scherrer Institut, Villigen PSI, Switzerland

<sup>2</sup>Institute for Biomedical Engineering, Swiss Federal Institute of Technology and University of Zurich, Switzerland

Non-destructive synchrotron-based x-ray tomographic microscopy is ideal for studying various materials systems in three and four dimensions (3D and 4D, respectively), and the TOMCAT beamline<sup>1</sup> at the Swiss Light Source is one of the premier beamlines in the world for such experiments. Spatial resolution ranges from 1-10 $\mu$ m with fields-of-view from 1-22mm, and temporal resolution is as fast as 0.1s for a full 3D data acquisition<sup>2</sup>. Contrast varies from standard absorption, typically used in metal and composite systems, to propagation- and grating-based phase contrast, predominantly used for biological and other traditionally low-contrast materials. The efficient image processing pipeline provides a full 3D reconstruction within seconds<sup>3</sup>, making visualization close to real time. To exploit these state-of-the-art capabilities and to explore the dynamics of materials at elevated temperatures, a dedicated laser-based heating system has been developed<sup>4</sup> and a mechanical testing device is being commissioned. This talk will highlight the capabilities available at TOMCAT as well as focus on recent achievements in dynamic, time-resolved experimentation. For example, the behavior of geological materials at high temperatures under simple dead-weight compression, 4D self-healing of ceramics and 4D intergranular cracking

of semi-solid grains in Al-Cu microstructures will be discussed. Such studies generate large amounts of data, typically on the order of terabytes, that then require *automated* tools for visualizing and characterizing the resulting phenomena. This talk will also underscore these developments and summarize the future of mechanical testing at TOMCAT.

#### References

- <sup>1</sup>Stamparoni, M, Groso, A, Isenegger, A, et. al. (2006): Trends in synchrotron-based tomographic imaging: the SLS experience.—*Proceedings of the SPIE*, 6318: 63180M-1—63180M-14.
- <sup>2</sup>Mokso, R, Marone, F, Stamparoni, M, et. al. (2010): Real time tomography at the Swiss Light Source.—*AIP Conference Proceedings*, 1234: 87-90.
- <sup>3</sup>Marone, F, Stamparoni, M. (2012): Regridding reconstruction algorithm for real-time tomographic imaging.—*Journal of Synchrotron Radiation*, 19: 1029-1037.
- <sup>4</sup>Fife, JL, Rappaz, M, Pistone, M, et. al. (2012): Development of a laser-based heating system for in situ synchrotron-based x-ray tomographic microscopy.—*Journal of Synchrotron Radiation*, 19: 352-358.

# Grain and subgrain high resolution diffraction from polycrystalline bulk materials

ULRICH LIENERT<sup>1</sup>, WOLFGANG PANTLEON<sup>2</sup>, GÁBOR RIBÁRIK<sup>3</sup>, TAMÁS UNGÁR<sup>3</sup>

<sup>1</sup>Deutsches Elektronen-Synchrotron, Photon Science, Hamburg, Germany

<sup>2</sup>Technical University of Denmark, Dept. of Mechanical Engineering, Lyngby, Denmark

<sup>3</sup>Eötvös University Budapest, Dept. of Materials Physics, Budapest, Hungary

The penetration power of high energy X-rays enables the investigation of polycrystalline bulk materials by diffraction techniques. In the conventional powder diffraction mode, the observable intensities are averages over all grains that are oriented such that their selected reciprocal lattice vectors are sufficiently close to the scattering vector. This mode is suitable for the characterization of parameters describing grain ensembles such as the orientation distribution function. By polfigure inversion techniques average orientation dependent properties can be recovered such as the strain distribution function, and average dislocation densities have been determined through fitting routines to radial line profiles. However, structural properties of individual grains such as the formation and evolution of subgrains and their dislocation densities are not accessible.

With the advent of 3<sup>rd</sup> generation high energy facilities, high energy x-rays became available with unprecedented brilliance and efficient area detectors have been developed. Exploiting these advances, the three dimensional X-ray diffraction (3DXRD) methodology has been developed that enables the identification of diffraction peaks from individual grains within polycrystalline bulk materials (Poulsen 2004). It has been demonstrated that the technique is sufficiently fast for in situ measurements during thermo-mechanical processing.

We demonstrate that by extending the 3DXRD methodology to high reciprocal space resolution intrinsic reciprocal space maps of reflections from individual deformed grains can be recorded and interpreted in terms of (i) subgrain formation and evolution (Pantleon et al. 2014), and (ii) dislocation characters and densities (Ungár et al. 2014). The experimental configurations and selected case studies will be presented.

The formation of subgrains and their evolution was studied within copper samples during tensile deformation. High resolution three-dimensional reciprocal space maps revealed a sub-structure of sharp peaks on

top of a diffuse intensity distribution. These features could be assigned to diffraction from almost dislocation free subgrains and dislocation wall regions, respectively. Based on the observation that the individual subgrains experience different elastic stresses, a refinement of the classical composite model of the radial peak broadening is proposed which resolves an overestimation of the dislocation density within the subgrains by the original model. Subgrain dynamics is followed in situ during uninterrupted tensile deformation, formation of subgrains is observed concurrently with broadening of Bragg reflections shortly after onset of plastic deformation. When the traction is terminated, stress relaxation occurs, but no changes in number, size and orientation of the subgrains are observed.

Grain-by-grain dislocation densities were obtained for tensile pre-deformed CoTi and CoZr intermetallics. A Monte-Carlo-type algorithm has been developed for the fitting of sets of radial peak profiles of individual grains. The technique discriminates dislocation densities of different slip modes, slip systems, and dislocation character. The results confirm that the anomalous ductility of the polycrystals as compared to single crystals is at least in part due to the existence of hard slip modes in the polycrystal which are only rarely observed in deformation experiments of single crystals.

## References

- Poulsen, H.F. (2004): Three-Dimensional X-ray Diffraction Microscopy, Springer, Berlin.
- Pantleon, W., Wejdemann, C., Jakobsen, B., Poulsen, H.F., Lienert, U. (2014) – In: Strain and dislocation gradients from diffraction (Imperial College Press, London), Barabash, R. & Ice, G. (eds.): 322-357.
- Ungár, T., Ribárik, G., Zilahi, G., Mulay, R., Lienert, U., Balogh, L., Agnew, S. (2014): Slip systems and dislocation densities in individual grains of polycrystalline aggregates of plastically deformed CoTi and CoZr alloys, – *Acta Mater.*, 71: 264-282.

## Advanced Laboratory X-ray Microscopy : In Situ Materials Characterization and Diffraction Contrast Tomography

ARNO MERKLE<sup>1</sup>, CHRISTIAN HOLZNER<sup>1</sup>, BENJAMIN HORNBERGER<sup>1</sup>, HRISHIKESH BALE<sup>1</sup>, WILLIAM HARRIS<sup>1</sup>, LEAH LAVERY<sup>1</sup>

<sup>1</sup>Carl Zeiss X-ray Microscopy, Pleasanton, CA, USA

This work presents new capabilities in X-ray Microscopy (XRM) for 3D materials characterization. As a nondestructive technique, XRM presents some unique opportunities for understanding material structure, deformation, and performance. The non-destructive nature of X-rays has made the technique widely appealing, with potential for “4D” characterization, delivering 3D microstructural information on the same sample as a function of time or imposed conditions. The first section of this work will explore advancements in XRM *in situ* material testing spanning a range of length scales from the micron to nanoscale. Incorporating specialized *in situ* stages into the laboratory X-ray microscopes enables control of material stimuli such as temperature, flow, and mechanical load during simultaneous imaging. Several examples will be presented that illustrate the improved insight gained from observing the resultant volumetric changes, on multiple length scales, and the fundamental links to understanding how materials perform and deform in their local mesoscale architecture.

In the second section, new development of a 3D grain mapping technique will be discussed. Traditional X-ray tomography operates mainly based on absorption con-

trast, relying on spatially varying density within the sample to create local variations in the attenuation of the incident x-ray beam. Reconstruction of the data yields a 3D map of sample density but cannot provide crystallographic information since even a polycrystalline structure of a single phase exhibits uniform density. In this work, a laboratory-based solution is presented, termed diffraction contrast tomography (DCT). This imaging modality is implemented on a laboratory X-ray microscope utilizing a polychromatic divergent beam. The sample is incrementally rotated, creating a series of diffraction patterns generated by the sample crystallites each time the Bragg condition is locally satisfied. The patterns are then reconstructed to yield crystallographic information including grain orientation, center of mass, and size for a large number of grains. This is used to complement structural data obtained by traditional absorption-based tomography. This work will present results on laboratory DCT along with discussion and comparison to alternative techniques. Merits of the lab DCT method will be highlighted, particularly its non-destructive operation, leading again to potential 4D evolutionary studies by repeating the imaging procedure numerous times on the same sample.

Talks Topic E 1:

***Size effects and small-scale mechanical behavior of materials***

---

# Size dependent strength and its exploitation for length-scale engineered material systems

ANDY BUSHBY, DAVID DUNSTAN

Queen Mary University of London, London, UK

Over the past 15 years experiments in micro-mechanical testing have shown that smaller structures or smaller stressed volumes are stronger than the bulk properties of the same material (Artz 1998). These 'size effects' are often regarded as being due to different phenomena, for instance depending on the crystal lattice type, bonding type and internal microstructure. They are observed in nanoindentation, micro-pillar compression, micro-tension and torsion and thin foil flexure, and as a function of microstructural features such as grains, sub-grains and twins (Kraft *et al.* 2010), implying that length-scale itself is a strengthening mechanism.

For metallic materials that deform by dislocation multiplication and flow, observable plastic deformation depends on dislocation generation by the operation of sources. The minimum shear stress required depends on the radius of curvature of dislocations in a given space expressed by an equation of the form,

$$\tau = \tau_0 + \frac{A}{L} \left( \frac{h L}{B} + C \right) \quad (1)$$

where  $\tau_0$  is the bulk or size-independent shear strength, the constants A, B & C are well-known material or numerical constants.  $L$  is an effective length-scale which may be a combination of structure size, grain size and deformation length-scale (plastic zone size). This shows that the underlying size dependence has the form  $1/L$  and adds to the bulk strength,  $\tau_0$ , to give the size effects observed in different experiments.

Potentially, all the size dependent strength phenomena associated with dislocation plasticity can be interpreted using Equ 1, including structure size (Dunstan & Bushby 2013), grain size (Dunstan & Bushby 2014) and combinations of these (Dunstan *et al.* 2009).

The important considerations are which material length-scales should be associated with  $L$  and which

with the bulk or size independent term,  $\tau_0$ . Furthermore, how these parameters may change as a function of continued deformation also needs careful consideration, since either hardening or softening can occur depending on the destination of dislocations that have been generated.

The corollary of this approach is that a pure metal, such as gold, may take any strength up the theoretical limit depending on the size  $L$ , and that the minimum strength of a material can be predicted from only 2 parameters,  $L$  and  $\tau_0$ . Understanding how to manipulate these parameters opens the possibility to achieving strength through 'length-scale engineering'. The implications for exploiting size effects in engineering are clear, particularly using production methodologies such as multilayer deposition processes and repeated roll bonding to create simple materials systems with 'engineered' microstructures to control strength through size alone.

## References

- Artz, E. (1998): Size effects in materials due to microstructural and dimensional constraints: a comparative review, *Acta Mater*, 46, 5611 – 5626.
- Kraft, O., Gruber, P., Monig, R. and D. Weygand, D. (2010): Plasticity in confined dimensions, *Annu. Rev. Mater. Res.*, 40 293 - 317.
- Dunstan, D.J. and Bushby, A.J. (2013): The scaling exponent in the size effect of small scale plastic deformation, *Int. J. Plasticity* 40 (2013) 152.
- Dunstan, D.J. and Bushby, A.J. (2014): Grain size dependence of the strength of metals: The Hall-Petch effect does not scale as the inverse square root of grain size, *Int. J. Plasticity* 53 (2014) 56
- D.J. Dunstan, B. Ehrler, R. Bossis, S. Joly, K.M.Y. P'ng and A.J. Bushby (2009): Elastic limit and strain-hardening of thin wires in torsion, *Phys. Rev. Letts*, 103, 155501.

## Three-dimensional modeling of size effects in micromechanical testing

EDGAR HUSSER<sup>1</sup>, ERICA LILLEODDEN<sup>1</sup>, SWANTJE BARGMANN<sup>2</sup>

<sup>1</sup>Institute of Materials Research, Materials Mechanics, Helmholtz-Zentrum Geesthacht, Germany

<sup>2</sup>Institute of Continuum Mechanics and Material Mechanics, Hamburg University of Technology, Germany

A finite-deformation strain gradient crystal plasticity model is developed and implemented in a three-dimensional finite element framework in order to study the influence of dislocation pile-ups in micro-mechanical testing of single crystals, for instance in micro-compression experiments (Husser et al. 2014). The potential-based and thermodynamically consistent material model is formulated in a non-local and non-linear inelastic context in which dislocation densities are introduced via strain gradients. In the 3D context, the model predicts both, the distribution of edge and screw type dislocations and accounts for, e.g., size effects due to accumulation of GNDs (geometrically necessary dislocations), dislocation interactions in terms of latent hardening, and the Bauschinger effect. The robust solution algorithm is based on a numerically efficient non-standard finite element strategy to solve the highly coupled and highly nonlinear system of equations and it is suitable for parallelization on two different 'levels'.

Presented numerical examples are directly related to experiments. For instance, it is shown that the inclusion of the strain gradient into the free energy enables

a reasonable prediction of the deformation behavior in the case of micro-pillar compression. Here, a typical distinct slip band formation is successfully reproduced by the presented theory. This is experimentally supported by an EBSD analysis of the thinned cross-section of a deformed sample where the correlation between the obtained lattice rotation and calculated GND distributions showed great accordance.

### References

- E. Husser, E. Lilleodden, S. Bargmann (2014): *Computational modeling of intrinsically induced strain gradients during compression of c-axis-oriented magnesium single crystal*. In: Acta Materialia, 71, 206-219.
- S. Bargmann, B. Svendsen, M. Ekh (2011): *An extended crystal plasticity model for latent hardening in polycrystals*. In: Computational Mechanics, 48, 631-645.
- B. Svendsen, S. Bargmann (2010): *On the continuum thermodynamic rate variational formulation of models for extended crystal plasticity at large deformation*. In: Journal of the Mechanics and Physics of Solids 58, 1253-1271.

## Dislocation grain boundary interaction in bi-crystalline micro pillars studied by in situ SEM and in situ $\mu$ Laue diffraction

NATALIYA MALYAR<sup>1</sup>, CHRISTOPH KIRCHLECHNER<sup>1,2</sup>, GERHARD DEHM<sup>1</sup>

<sup>1</sup>Max-Planck-Institut für Eisenforschung, Düsseldorf, Germany

<sup>2</sup>University of Leoben, Leoben, Austria

Grain boundaries (GB) act as obstacles for dislocation motion, promoting a higher strength in polycrystalline materials compared to the single crystalline counterparts (Hirth 1972). The grain size as a microstructural material length scale thereby inversely scales with the observed strength (Hall 1951, Petch 1953). This can partly be attributed to the pile-up of dislocations on grain boundaries.

Besides piling up at the grain boundary dislocations can also transfer to the adjacent grain and thus lead to slip transfer. This problem had been addressed during several studies in the past (Livingston and Chalmers 1957, Hirth and Balluffi 1973, Bamford, Hardiman et al. 1986, Shen, Wagoner et al. 1988) but the advances in understanding plasticity and its inherently stochastic

nature at the micron-scale (Dehm 2009, Kraft, Gruber et al. 2010) requires a thorough revisit of the published theories on grain-boundary dislocation interaction.

In the present work bi-crystalline copper micro pillars were grown by the Bridgman method in various different orientations. Subsequently, micron sized compression pillars which were single crystalline or possessed a grain boundary were fabricated using FIB milling. The mechanical tests were performed either in situ in the scanning electron microscope (SEM) or at a micro beam Laue ( $\mu$ Laue) diffraction beamline BM32 of the ESRF synchrotron source.

Aim of the experiments was to understand the size dependent dislocation-GB interaction. For this purpose four different grain boundaries had been investigated:

(i) a general grain boundary not allowing for slip transfer in macroscopic models (ii) a general grain boundary with slip transfer (iii) a coherent S3 twin and (iv) a low angle grain boundary.

The mechanical tests show distinct differences between the various grain boundary types: The different size dependent hardening rates, frequency of load drops, formation of slip steps and the possible grain boundary motion will be discussed in the talk.

Furthermore, our Laue data which is still not fully analyzed proves for instance that dislocations are accommodating at the macroscopically impenetrable grain boundary but no slip transfer happens. Based on these findings models for hardening at the micron scale can be discussed and maybe revisited.

#### References

Bamford, T. A., et al. (1986). "Micromechanism of slip propagation through a high angle boundary in alpha brass." *Scripta Metallurgica* 20(2): 253-258.

Dehm, G. (2009). "Miniaturized single-crystalline fcc metals deformed in tension: New insights in size-dependent plasticity." *Progress in Materials Science* 54(6): 664-688.

Hall, E. O. (1951). "The deformation and ageing of mild steel: 3. Discussion of results." *Proceedings of the Physical Society of London Section B* 64(381): 747-753.

Hirth, J. P. (1972). "Influence of grain-boundaries on mechanical properties." *Metallurgical Transactions* 3(12): 3047-3067.

Hirth, J. P. and R. W. Balluffi (1973). "On grain boundary dislocations and ledges." *Acta Metallurgica* 21(7): 929-942.

Kraft, O., et al. (2010). Plasticity in confined dimensions. *Annual Review of Materials Research*. 40: 293-317.

Livingston, J. D. and B. Chalmers (1957). "Multiple slip in bicrystal deformation." *Acta Metallurgica* 5(6): 322-327.

Petch, N. J. (1953). "The cleavage strength of polycrystals." *Journal of the Iron and Steel Institute* 174(1): 25-28.

Shen, Z., et al. (1988). "Dislocation and grain-boundary interactions in metals." *Acta Metallurgica* 36(12): 3231-3242.

## Size effects and dislocation structure under torsion loading of single crystalline wires: a discrete dislocation dynamics study

DANIEL WEYGAND<sup>1</sup>, PETER GUMBSCH<sup>1,2</sup>

<sup>1</sup>Karlsruhe Institute of Technology, IAM, Germany

<sup>2</sup>Fraunhofer Institut für Werkstoffmechanik IWM, Freiburg, Germany

The seminal experiments (Fleck et al. 1994) on the deformation behaviour of metallic wires, where a so called size effect in the mechanical response was observed, is still a matter of debate in the material science community. Only little is known on the true dislocation microstructure caused by torsion loading (Senger et al. 2011).

In the current contribution, the dislocation microstructure, density distribution and the local plastic strains are analysed for different orientations of the torsion axis within a discrete dislocation dynamics framework (Weygand et al. 2002; Senger et al. 2011). Single crystalline Al beams with a square cross section are simulated. First a simple system with one active slip system is studied, to evaluate the role of the slip plane inclination with respect to the torsion axis on the plastic and hardening behaviour. A model is presented which describes the initial yielding and hardening observed in these simulations. Furthermore within this model setup, the role of cross-slip on the dislocation arrangement is illustrated. As a macroscopic measure, the

average plastic strain tensor is calculated locally on a voxel discretization of the simulated volume. It is found that the equivalent plastic strain determined in volume elements comprising the torsion axis is finite, not expected from Fleck's initial analysis. This observation can be rationalized within a pile-up model, quite similar to the observations under bending (Motz et al. 2008). This effect is most pronounced in small samples or for low initial dislocation densities where forest hardening is negligible. It is also observed, that the equivalent plastic strain depends on the voxel volume, used for averaging. Furthermore the radially averaged dislocation density shows a decrease toward the surface, related to dislocation escape. The thickness of this zone is quite similar for the different samples sized studied.

#### References

Fleck, N.A., G.M. Muller, M.F. Ashby, and J.W. Hutchinson. 1994. "Strain Gradient Plasticity: Theory and Experiment." *Acta Metallurgica et Materialia* 42 (2): 475-87.

Motz, C., D. Weygand, J. Senger, and P. Gumbsch. 2008. "Micro-Bending Tests: A Comparison between Three-Dimensional Discrete Dislocation Dynamics Simulations and Experiments." *Acta Materialia* 56: 1942–55.

Senger, J., D. Weygand, O. Kraft, and P. Gumbsch. 2011. "Dislocation Microstructure Evolution in Cyclically Twisted Microsamples: A Discrete Dislocation

Dynamics Simulation." *Modelling and Simulation in Materials Science and Engineering* 19 (7): 74004.

Weygand, D, L H Friedman, E Van der Giessen, and A Needleman. 2002. "Aspects of Boundary-Value Problem Solutions with Three-Dimensional Dislocation Dynamics." *Modelling and Simulation in Materials Science and Engineering*. /10/4/306.

## Investigation of crystal plasticity of single crystal copper by using micro scale torsion test

KOZO KOIWA<sup>1,2</sup>, CHUANTONG CHEN<sup>1</sup>, NOBUYUKI SHISHIDO<sup>1,2</sup>, MASAKI OMIYA<sup>2,3</sup>, SHOJI KAMIYA<sup>1,2</sup>, HISASHI SATO<sup>1,2</sup>, MASAHIRO NISHIDA<sup>1,2</sup>, TAKASHI SUZUKI<sup>4</sup>, TOMOJI NAKAMURA<sup>4</sup>, TOSHIAKI SUZUKI<sup>2,5</sup>, TAKESHI NOKUO<sup>2,5</sup>

<sup>1</sup>Nagoya Institute of Technology, Nagoya, Japan

<sup>2</sup>Japan Science and Technology Agency, Chiyoda, Tokyo, Japan

<sup>3</sup>Keio University, Yokohama, Japan

<sup>4</sup>Fujitsu Laboratories Ltd., Atsugi, Kanagawa, Japan

<sup>5</sup>JEOL Ltd., Akishima, Tokyo, Japan

Recently, deformation of micro scale single crystal was frequently investigated by using miniaturized specimen. It is known that dislocation burst phenomenon occurred in case of conventional technique such as tensile and compression test because stress is homogeneous in specimen. Dislocation burst is the sudden slip deformation of slip system through specimen, it makes deformation discontinuity around initial yielding area, and continuous deformation behavior around dislocation burst cannot be obtained. However, in nano scale structure such as LSI, since it is assumed that dislocation burst does not occur because large deformation is restricted by other structural materials. Then, to obtain continuous deformation characteristics of crystal plasticity around dislocation burst (initial yielding) area is important. New micro-scale torsion test method was developed. In this method, dislocation burst around initial yielding region did not occur because torsion stress field is inhomogeneous in specimen. In this study, crystal plasticity of micro scale copper single crystal was investigated by using this torsion test and finite element analysis. To incorporate crystal plasticity into the simulation, a program that reflects the crystal plasticity constitutive relation of single crystals using the user subroutine UMAT of the finite element code ABAQUS, which was developed by Huang. However, macroscopic constitutive law of crystal plasticity which was used for macro scale specimen may not be applied to micro scale specimen. Therefore, constitutive law of micro scale specimen is discussed.

Torsion test specimen is fabricated by focused ion beam (FIB) using copper single crystal (99.9999% purity). The shape of specimen is half circular arc (with 3  $\mu\text{m}$  radius, 1  $\mu\text{m}$  width and thickness) of cantilever, and torsion test was conducted by indentation load at the end edge of cantilever. Crystal plasticity parameter of

copper was investigated by inverse analysis using the load-displacement curve which was obtained by simulation and actual torsion test.

As a result, dislocation burst did not occur on load-displacement curve which was obtained by torsion test. However, in case that constitutive law which was applied for macro scale specimen is used, load-displacement curve which was obtained by torsion test and simulation did not match even if any parameter was used for crystal plasticity. Then, new constitutive law of micro scale crystal plasticity was developed. Flow stress shows gradual hardening behavior after sudden drop behavior when resolved shear stress of slip system reached initial flow stress. Similar drop behavior (stress-strain curve) was observed in molecular dynamics simulation by G. Sainath. By using the new constitutive law, load-displacement curve of simulation matched that of torsion test, and crystal plasticity parameter was obtained as the result of fitting. It was demonstrated that the constitutive law of micro scale crystal plasticity is different from that of macro scale, and characteristic of the dislocation burst was obtained.

### References

- D. Kiener et al., A further step towards an understanding of size-dependent crystal plasticity: In situ tension experiments of miniaturized single-crystal copper samples, *Acta Materialia*, Vol. 56, (2008), pp. 580-592
- Y. Huang, Harvard University Report, MECH178 (1991).
- G.Sainath et al., Molecular Dynamics Simulations of Tensile Behaviour of Copper, International Congress on Computational Mechanics and Simulation (IC-CMS) IIT Hyderabad, (2012)

Talk Topic E 2:

***Size effects and small-scale mechanical behavior of materials***

---

## Study of fatigue damage evolution in micron sized bending beams by in situ $\mu$ Laue diffraction

C. KIRCHLECHNER<sup>1,2</sup>, P.J. IMRICH<sup>3</sup>, J.-S. MICHA<sup>4,5</sup>, O. ULRICH<sup>4,5</sup>, C. MOTZ<sup>6</sup>

<sup>1</sup>Max-Planck-Institute for Iron Research, Düsseldorf, Germany

<sup>2</sup>University of Leoben, Austria

<sup>3</sup>Erich Schmid Institute, Austrian Academy of Sciences, Leoben, Austria

<sup>4</sup>CEA-Grenoble/ Institut Nanosciences et Cryogénie, France

<sup>5</sup>CRG-IF BM32 at ESRF, France

<sup>6</sup>Saarland University, Saarbrücken, Germany

Size dependent material properties of single crystalline metals have been severely studied over the last decade by performing micro-compression, -tension and -bending experiments. The experiments accompanied by complementary discrete dislocation dynamics (DDD) simulations remarkably showed the stochastic nature of plastic flow at the micron scale.

Besides monotone uniaxial deformation real devices of Micro-Electro-Mechanical- Systems (MEMS) routinely have to withstand cyclic loading, which was also shown to differ at small scales. The fatigue behavior of thin films has extensively been studied in the previous decade. Notable, dislocation patterns observed in bulk materials are not necessarily observed at the micron scale: If the grain size in pure Copper is reduced to less than  $8\mu\text{m}$  persistent slip bands are rarely observed (Kawazoe, Yoshida et al. 1999) but dislocation walls and cell structures still exist (Zhang, Volkert et al. 2006). Dislocation patterns are replaced by individual dislocations as soon as film thicknesses of less than  $1\mu\text{m}$  are reached.

Recently the first micro fatigue experiments on FIB milled micro-cantilevers (Demir and Raabe 2010, Kiener, Motz et al. 2010) were performed. The experiments by Kiener and co-workers were accompanied by DDD simulations showing a successive storage and escape of dislocations with high reversibility. Due to limited computational resources the study of steady state dislocation patterns forming after several cycles had not been possible by 3D-DDD so far. Also, in depth analysis of the dislocation patterns in the deformed bending beams by TEM were not performed in the aforementioned experiments.

Here we present the first in situ  $\mu$ Laue study investigating the low cycle fatigue of micro- bending beams:  $7\mu\text{m}$  sized single and bi-crystalline copper and silver bending-cantilevers were FIB milled and analyzed with a  $500\text{nm}$  sized, polychromatic X-ray beam at BM32 of the ESRF light source. The in situ loading showed the formation and storage of geometrically necessary dislocations, accompanied by the strong formation of dislocation cell structures. During unloading and back-bending, the number of dislocations was dramatically reduced reaching the initial dislocation densities. The stress-strain response of the samples showed cyclic softening reaching a plateau after two cycles and a pronounced Bauschinger effect. This finding was observed for up to 100 cycles in single crystalline Cu and Ag samples. In the talk, the influence of the different stacking fault energy of Cu and Ag as well as the impact of a single grain boundary in Cu will be discussed.

### References

- Demir, E. and D. Raabe (2010). "Mechanical and microstructural single-crystal Bauschinger effects: Observation of reversible plasticity in copper during bending." *Acta Materialia* 58(18): 6055-6063.
- Kawazoe, H., et al. (1999). "Dislocation microstructures in fine-grained Cu polycrystals fatigued at low amplitude." *Scripta Materialia* 40(5): 639-644.
- Kiener, D., et al. (2010). "Cyclic response of copper single crystal micro-beams." *Scripta Materialia* 63(5): 500-503.
- Zhang, G. P., et al. (2006). "Length-scale-controlled fatigue mechanisms in thin copper films." *Acta Materialia* 54(11): 3127-3139.

# A comparative study of fatigue properties of nanoscale Cu films on a flexible substrate

BIN ZHANG<sup>1</sup>, YING ZHANG<sup>1</sup>, XIAO-FEI ZHU<sup>2</sup>, XUE-MEI LUO<sup>2</sup>, GUANG-PING ZHANG<sup>2</sup>

<sup>1</sup>Key Laboratory for Anisotropy and Texture of Materials (Ministry of Education), Northeastern University, Shenyang, P. R. China

<sup>2</sup>Shenyang National Laboratory for Materials Science, Institute of Metal Research, Chinese Academy of Sciences, Shenyang, P. R. China

Fatigue at small scales is a key issue for the long-term reliability of micro/nano-devices. Recent investigations on fatigue behaviour of thin metal films have shown a strong dependence of fatigue properties on length scales (Kraft et al., 2001; Schwaiger et al., 2003; Schwaiger and Kraft, 2003; Wang et al., 2008). The physical origin for fatigue size effects was attributed to the suppression of cyclic strain localization, leading to the gradual disappearance of typical bulk-like fatigue extrusions/intrusions (Zhang et al., 2006; Zhang et al., 2010). Although these investigations provide a deep insight into the fatigue mechanism of thin metal films with micron or submicron-scale grains, less work on fatigue properties of nanocrystalline metal films has been conducted (Zhang et al., 2008; Luo et al., 2014). In this study, nanocrystalline Cu films with different thicknesses ranging from 25 nm to 250 nm were deposited on a 125  $\mu\text{m}$ -thick polyimide substrate by a magnetron sputtering system. A comparative investigation of fatigue properties of the Cu films as-deposited and annealed were conducted under total strain control at room temperature. Variation in microstructures of the fatigued samples and fatigue damage behavior were characterized by transmission electron microscope (TEM) and high-resolution electron microscope.

Experimental results show that the fatigue strength of the nanocrystalline Cu films as-deposited and annealed increases with decreasing the film thickness, which reveals a similar trend to that found in the Cu and Ag films with grain size about micron or submicron-scales (Kraft et al., 2001; Schwaiger and Kraft, 2003; Wang et al., 2008). Furthermore, TEM observations reveal that grain growth occurred in the as-deposited films after fatigue. For comparison, the grain sizes in the annealed films and the annealed films subjected to fatigue loading were also examined. Evidently different extent

of grain growth in the films were found. In addition, the size of the grains containing twins in the as-deposited and annealed films, and that after fatigue loading was also characterized. The variations in fatigue strength and grain growth behavior with film thickness are discussed. The results may provide a further understanding of fatigue behavior of nanocrystalline metal films.

## References

- Kraft, O., Schwaiger, R., Wellner, P., 2001: Fatigue in thin films: lifetime and damage formation. *Mater Sci Eng A* 319, 919-923.
- Luo, X.M., Zhu, X.F., Zhang, G.P., 2014: Nanotwin-assisted grain growth in nanocrystalline gold films under cyclic loading. *Nat Commun* 5, 3021.
- Schwaiger, R., Dehm, G., Kraft, O., 2003: Cyclic deformation of polycrystalline Cu films. *Philos Mag* 83, 693-710.
- Schwaiger, R., Kraft, O., 2003: Size effects in the fatigue behavior of thin Ag films. *Acta Mater* 51, 195-206.
- Wang, D., Volkert, C.A., Kraft, O., 2008: Effect of length scale on fatigue life and damage formation in thin Cu films. *Mater Sci Eng A* 493, 267-273.
- Zhang, B., Sun, K.H., Liu, Y., Zhang, G.P., 2010: On the length scale of cyclic strain localization in fine-grained copper films. *Philos Mag Letts* 90, 69-76.
- Zhang, G.P., Sun, K.H., Zhang, B., Gong, J., Sun, C., Wang, Z.G., 2008: Tensile and fatigue strength of ultrathin copper films. *Mater Sci Eng A* 483-84, 387-390.
- Zhang, G.P., Volkert, C.A., Schwaiger, R., Wellner, P., Arzt, E., Kraft, O., 2006: Length-scale-controlled fatigue mechanisms in thin copper films. *Acta Mater* 54, 3127-3139.

# Strain-dependent fatigue damage of nanocrystalline 930-nm-thick Au films

XUE-MEI LUO, GUANG-PING ZHANG

Shenyang National Laboratory for Materials Science, Institute of Metal Research, Chinese Academy of Sciences, Shenyang, PR China

Quantitative studies have shown that fatigue behaviors in the thin metal films constrained by a substrate are different from that of their bulk counterparts (Schwaiger, *et al.* 2003, Schwaiger & Kraft 2003, Zhang, *et al.* 2006, Zhang & Wang 2008). Especially when the film thickness or the grain size decreases below micrometer scale, it is hard for the typical micron-scale dislocation structures to form in the film, like persistent slip bands, etc. In addition, GBs in nanocrystalline metals usually become so unstable that grain growth always occurs at room and even low temperatures under various loading modes (Cheng, *et al.* 2010, Fang, *et al.* 2011, Gianola, *et al.* 2008, Luo, *et al.* 2014, Pan, *et al.* 2007, Soer, *et al.* 2004, Zhang, *et al.* 2005). However, the fatigue behaviors of metal films with length scale ranging from micron to nanometer scales are not yet completely understood.

In this study, we investigated grain growth and fatigue damage behaviors of nanocrystalline Au films constrained by a polyimide substrate with the film thickness of 930 nm, in which fatigue damage happened within  $2.6 \times 10^4$  cycles under a total strain range of 1.25% and  $1.8 \times 10^6$  cycles under a total strain range of 0.4%. Features of fatigue damage in the Au films mainly exhibited multiple cracks. Under both strain amplitudes, abnormal grain and normal grain growth happened. There was similar extent of the normal grain growth under both strain amplitudes. Most abnormal grain growth happened along the fully developed cracks due to the stress concentration in front of the crack tip under 0.4% strain range. However, apart from the grain growth due to the crack propagation, much more grains could grow to micron scale before cracks initiated inside the grains under 1.25% strain range.

In addition, the fatigue damage behavior strongly depended on the applied strain amplitude. Under the 1.25% strain range, the films showed a bulk-like damage behavior, i.e. the crack mainly initiated from the places with typical fatigue extrusions/intrusions in the coarsened grains with micron-scale grain size. Under the 0.4% strain range, there were two main crack initiation sites. One is the abnormally-grown grains along the fully-developed cracks where the bulk-like fatigue extrusions/intrusions formed. Another is the grain boundaries and quantitative intergranular cracks were found. The mechanisms for grain growth and fatigue damage were discussed. It is concluded that different grain growth behaviors and damage behaviors are found in the 930 nm thick nanocrystalline Au films under cyclic loading.

## References

- Cheng, S. *et al.* (2010): Phys. Rev. Lett. **104**, 255501  
 Fang, T. H. *et al.* (2011): Science **331**, 1587  
 Gianola, D. S. *et al.* (2008): Adv. Mater. **20**, 303  
 Luo, X. M. *et al.* (2014): Nat. Commun. **5**, 3021  
 Pan, D. *et al.* (2007): Nano Lett. **7**, 2108  
 Schwaiger, R. *et al.* (2003): Philos. Mag. **83**, 693  
 Schwaiger, R. & Kraft, O. (2003): Acta Mater. **51**, 195  
 Soer, W. A. *et al.* (2004): Acta Mater. **52**, 5783  
 Zhang, G. P. *et al.* (2006): Acta Mater. **54**, 3127  
 Zhang, G. P. & Wang, Z. G. (2008): in *Multiscale fatigue crack initiation and propagation of engineering materials: Structural integrity and microstructural workability*, edited by G. C. Sih (Springer Netherlands, pp. 275.  
 Zhang, K. *et al.* (2005): Appl. Phys. Lett. **87**, 061921

# Influence of surface energy and dislocation pile-up on the size dependent strength of single-crystalline micro-pillars

BO PAN, YOJI SHIBUTANI

Dept. of Mechanical Eng., Osaka Univ., Japan

Recent investigations show that the micro-mechanical responses of single-crystals (SC) present strong size dependent plastic yield strength by reducing dimensions of micron- or nanopillars under uniaxial deformation (Uchic, 2004; Dimiduk, 2005; Greer, 2005). The simulating and theoretical researches show their explanations from the boundary, source truncation and dislocation starvation, respectively (Fan, 2012). But few researches focus on describing the dislocation pile-up effect and the surface energy effect on the boundary in SC on size effect.

In this work, the understanding of the size effect dominantly derives from the dimensional grain size and physical interface, besides the inner defect microstructures. At present, discrete dislocation simulation results show that the boundary condition affects the strength by wall thickness (Fan, 2012). The wall thickness has the physical nature of surface effect, and the surface energy can affect on the surface stress  $\sigma^{surface}$ . Thus, the plastic strength can be written as

$$\sigma = \sigma_0 + \sigma^{surface} = \sigma^{inner} + \sigma^{surface}, \quad (1)$$

where  $\sigma_0$  is the conventional plastic strength which is not affected by surface geometrics, and it can also be represented as  $\sigma^{inner}$ . Based on the principle of minimum potential energy, the surface stress  $\sigma^{surface}$  can be derived as

$$\sigma^{surface} = \gamma O_0 (1 - \nu) / A, \quad (2)$$

where  $\gamma$  is the surface energy density,  $O_0$ ,  $A$  are the perimeter and area of the initial cross section and  $\nu$  is the Poisson's ratio. According to the dislocation pile-up configuration, the inner strength  $\sigma^{inner}$  can be obtained by considering the effect of microstructures, such as effective length of dislocation source  $\bar{\lambda}_{max}$ , dislocation pile-up length  $L$ , dislocation density  $\rho_0$ , the number of dislocation sources and so on. It can be expressed as

$$\sigma^{inner} = (\alpha \mu b / \sqrt{L \bar{\lambda}_{max}} + \tau_0 + 0.5 \mu b \sqrt{\rho_0}) / SF, \quad (3)$$

where  $\tau_0$  is Peierls-Nabarro force,  $\alpha$  is the geometric parameter,  $SF$  is the Schmidt factor, also  $\mu$  and  $b$  are the shear modulus, and the Burgers vector, respectively. In this case, the stress of the filed can be finally obtained as

$$\sigma = \left( \frac{\alpha \mu b}{\sqrt{L \bar{\lambda}_{max}}} + \tau_0 + 0.5 \mu b \sqrt{\rho_0} \right) / SF + \frac{\gamma O_0 (1 - \nu)}{A}. \quad (4)$$

It is shown that the "Hall-Petch relation" holds even in SC. The process of simulations indicated that the starvation of dislocation sources is one reason for the observed size effect. Furthermore, it can be found that the surface effect from the geometries and the inner strength from the inner microstructures interplay each other, and both influence on the yielding strength, which has the size-dependent characteristic.

## References

- Uchic, M.D. Dimiduk, D.M. Florando, J. Nix, W.D. (2004): Sample Dimensions Influence Strength and Crystal Plasticity. *Science*, 305: 986-989.
- Dimiduk, D.M. Uchic, M.D. Parthasarathy T.A. (2005): Size-affected single-slip behavior of pure nickel microcrystals. *Acta Mater.* 53: 4065-4077.
- Greer J.R., Oliver W.C., Nix W.D. (2005): Size dependence of mechanical properties of gold at the micron scale in the absence of strain gradients. *Acta Mater.* 53: 1821-1830.
- Fan, H. Li, Z. Huang, M. (2012): Size effect on the compressive strength of hollow micropillars governed by wall thickness. *Scripta Materialia.* 67: 225-228.

## In situ fracture tests of brittle materials at the microscale

GIORGIO SERNICOLA, TOMMASO GIOVANNINI, RUI HAO, T. BEN BRITTON, FINN GIULIANI

Imperial College London, Department of Materials, London, United Kingdom

Understanding fracture behaviour especially at the grain boundaries is of vital importance to extend the life of structural ceramics. Currently the processing parameters of many commercial composite ceramic products are largely empirically derived and therefore result in a large number of different microstructures and properties. Development of new materials and controlled processing routes will greatly benefit from knowledge of the fracture energy of phase and interface present. This requires development of new fracture testing methods capable of granting high spatial resolution and high control over the area to test. Further benefits of these ‘small scale’ approaches will enable testing of specimens for which big volumes are not available (e.g. thin films, coating, or simply samples of dimensions limited by production process). Historically indentation has been largely employed to determine the fracture toughness of brittle materials. However, its spatial resolution is limited by the cracking threshold (Pharr 1998), namely the load at which a crack is initiated, being the size of the impression proportional to the load applied. Moreover, several studies (Anstis, Chantikul et al. 1981, Quinn and Bradt 2007) discourage the use of indentation induced cracks to measure fracture toughness.

Recently, several techniques have been developed using small scaled mechanical testing, based within a nanoindenter, changing tip and sample geometries, including: micropillar compression (Östlund, Howie et al. 2011); microcantilever bending (Di Maio and Roberts 2005, Armstrong, Wilkinson et al. 2011); and double-cantilever compression (Liu, Wheeler et al. 2013). However, the majority of the published works utilises complex geometries resulting into complex analysis of force distribution and stress intensity factor.

Our approach builds upon the work of Lawn (Lawn 1993), who showed that a practical test geometry to calculate the fracture energy  $G$  is that of a double-cantilever beam under constant wedging displacement. We use this geometry at the small scale to directly measure fracture energy in brittle materials and small volumes.

Using Lawn’s analysis,  $G$  is given by:

$$G = 3Eh^2d^3/4c^4$$

where  $E$  is the elastic modulus,  $c$  the crack length and  $d$  and  $h$  the half-width of the beam and the wedging displacement respectively.

We replicate this configuration in our tests fabricating double-cantilever beams of micrometric dimensions by

focused ion beam (FIB) milling and loading them *in-situ* in an SEM using a nanoindenter with a wedge-shaped tip. This has two benefits: the sample is well aligned for a controlled test; images are recorded during the test for later analysis.

This testing approach produces data that can be analysed to directly measure the geometrical parameters required to solve the equation.

Our tests have proved it is possible to initiate and stably grow a crack in a controlled manner in ceramic materials and our fracture energy results have been validated against prior macro-scale fracture data. This approach is being extended to multi-phase materials with unknown materials properties and extends our arsenal of small-scale characterisation techniques required to generate new processing strategies for the next generation of materials design.

### References

- Anstis, G. R., P. Chantikul, B. R. Lawn and D. B. Marshall (1981). “A Critical Evaluation of Indentation Techniques for Measuring Fracture Toughness: I, Direct Crack Measurements.” *Journal of the American Ceramic Society* 64(9): 533-538.
- Armstrong, D. E. J., A. J. Wilkinson and S. G. Roberts (2011). “Micro-mechanical measurements of fracture toughness of bismuth embrittled copper grain boundaries.” *Philosophical Magazine Letters* 91(6): 394-400.
- Di Maio, D. and S. G. Roberts (2005). “Measuring fracture toughness of coatings using focused-ion-beam-machined microbeams.” *Journal of Materials Research* 20(02): 299-302.
- Lawn, B. R. (1993). *Fracture of brittle solids*. Cambridge, Cambridge University Press.
- Liu, S., J. M. Wheeler, P. R. Howie, X. T. Zeng, J. Michler and W. J. Clegg (2013). “Measuring the fracture resistance of hard coatings.” *Applied Physics Letters* 102(17): 171907.
- Östlund, F., P. R. Howie, R. Ghisleni, S. Korte, K. Leifer, W. J. Clegg and J. Michler (2011). “Ductile–brittle transition in micropillar compression of GaAs at room temperature.” *Philosophical Magazine* 91(7-9): 1190-1199.
- Pharr, G. M. (1998). “Measurement of mechanical properties by ultra-low load indentation.” *Materials Science and Engineering: A* 253(1–2): 151-159.
- Quinn, G. D. and R. C. Bradt (2007). “On the Vickers Indentation Fracture Toughness Test.” *Journal of the American Ceramic Society* 90(3): 673-680.

Talks Topic E 3:

***Size effects and small-scale mechanical behavior of materials***

---

## Smaller is not always stronger – inverse scale effect on metal-ceramics interface strength observed in LSI interconnect structures

SHOJI KAMIYA<sup>1,2</sup>, NOBUYUKI SHISHIDO<sup>1,2</sup>, KOZO KOIWA<sup>1,2</sup>, MASAKI OMIYA<sup>2,3</sup>, HISASHI SATO<sup>1,2</sup>, MASAHIRO NISHIDA<sup>1,2</sup>, TAKASHI SUZUKI<sup>4</sup>, TOMOJI NAKAMURA<sup>4</sup>, TOSHIAKI SUZUKI<sup>2,5</sup>, TAKESHI NOKUO<sup>2,5</sup>

<sup>1</sup>Nagoya Institute of Technology, Nagoya, Japan

<sup>2</sup>Japan Science and Technology Agency, Chiyoda, Tokyo, Japan

<sup>3</sup>Keio University, Yokohama, Japan

<sup>4</sup>Fujitsu Laboratories Ltd., Atsugi, Kanagawa, Japan

<sup>5</sup>JEOL Ltd., Akishima, Tokyo, Japan

Smaller is stronger. It is so frequently mentioned since the beginning of nano-technology era, and even today (Kunz et al. 2011, Kraft et al. 2010), in the context that smaller volume of materials has less defects leading to higher apparent strength. However, it may not always be true, especially for the complicated mechanical structures in microscale devices, as explained in the following.

Large scale integrated circuits (LSI) typically have sub-micron mechanical structures, which are interconnect wiring systems fabricated on top of silicon chips for current supply and signal readout. They consist of a layer of insulator with trenches filled with electroplated copper as narrow metal wires and another capping insulation layer on top to seal the wires. A number of these layers are usually stacked alternately to compose multi-layered 3D interconnect structures. Therefore LSI has many weak interfaces, which occasionally causes serious reliability issues even today (Kengeri 2014). Although the strength properties of such interfaces are well surveyed, commonly with four-point bending interface fracture test performed with lab-scale testing machines (Charalambides et al. 1989) and the interconnect structures are designed accordingly, crack propagation to destroy them occasionally takes place especially when LSI chips are packaged and mounted on board causing the extra stress application. Is the strength of four-point bending specimens different from that of the actual sub-micron scale interfaces?

We have measured the strength in life size. Insulation layer on top of copper line was machined by focused ion beam (FIB) into specimens of square brick-like shape. They were prepared in different scales ranging from 10  $\mu\text{m}$  down to 200 nm. Interface strength was evaluated in terms of energy release rate ( $\text{J}/\text{m}^2$ ) by pushing their sidewalls with a diamond stylus to extend interface cracks. As the result, the average strength levels drastically decreased from 11  $\text{J}/\text{m}^2$  to 2  $\text{J}/\text{m}^2$  with the size of specimens decreasing from 10  $\mu\text{m}$  to 200 nm. Finite element simulation of interface

crack extension suggested the reasons, where larger structure needs longer distance of crack extension to completely debond larger area of the interface leading to larger volume of plastic deformation with severer strain level at the crack tip. Smaller was not stronger in such a case.

Smaller specimens had not only smaller average strength. Relative standard deviation (standard deviation divided by average) of the strength distribution also increased sharply with smaller ones, which was due to different crystal orientations of grains and grain boundaries underneath the specimens. In contrast to macro-scale structures where such intrinsic structures of materials are smeared out to yield a homogenized properties, characteristics of individual grains and their combinations far more directly influence the strength. Therefore extremely weak ones also come out far more likely.

These trends newly found as explained above could be a kind of nano-tech syndrome, possibly being a common risk to the reliability of small scale structures. More detailed pathology of such a syndrome and possible diagnosis to evaluate the risk for the reliability of LSI interconnect structures will be discussed in the presentation.

### References

- Kunz, A. et al. (2011): Size effects in Al nanopillars: Single crystalline vs. bicrystalline – *Acta Mater.*, 59:4416-4424.
- Kraft, O. et al. (2010): Plasticity in confined dimensions – *Annu. Rev. Mater. Res.* 40:293-317.
- Kengeri, S. (2014): The critical need for innovations in advanced packaging to drive semiconductor growth in the FinFET era – <http://www.semiconsingapore.org/node/2466>.
- Charalambides, P.G. et al. (1989): A test specimen for determining the fracture resistance of bimaterial interfaces – *J. Appl. Mech.* 56: 77-82.

## Characterisation and Mechanical Properties of the Boundary Layers of Soft Magnetic Composites

TABEA SCHWARK, RUTH SCHWAIGER, OLIVER KRAFT

Karlsruhe Institute of Technology, Germany

are then further processed by a powder metallurgical route. The insulating coating reduces losses related to eddy currents. In comparison to traditional laminated steels, the SMC offers several advantages. For instance, the combination of their isotropic nature and new shaping possibilities opens up the possibility to design new 3D components. Those new designs, however, may demand besides the magnetic properties of the SMC more and more a certain mechanical robustness of the material.

The mechanical properties of the SMC are determined by the combination of the soft matrix and the brittle boundaries between the particles. First characterisation of the boundaries of SMC was reported in [1] and [2]. However, this was a former generation of SMC with a simpler boundary structure. The SMC investigated in this work contains additional iron oxide layers at the particle boundaries changing their characteristics with respect to the mechanical properties. The latter type of SMC was studied in terms of the transverse rupture strength as a function of particle size and pressure as well as in terms of the magnetic properties [3].

In this presentation, we are addressing the micro-mechanical behaviour of the boundaries and the resulting relationship to the overall mechanical and magnetic properties.

The SMC consists of pure iron particles coated by a thin inorganic, phosphorous layer and iron oxide layers at the boundaries. Processing includes after compaction an annealing during which the strength-enhancing oxide layers are formed. Transmission electron microscopy was used to determine the structure of the boundaries. Three types of boundaries were identified: boundaries that grow within pores, boundaries which had several 100 nm space to grow and boundaries which had significantly less space to grow. Nanoindentation

into the boundaries and the interior of the particles do not show a significant difference regarding Young's Modulus and hardness. Also, crack formation in the boundaries was not detected. These results indicate that on a short length scale the layers provide good adhesion between the particles. In order to elucidate this aspect further, beam bending experiments are currently underway. Using focused ion beam preparation, micro-scale beams containing boundaries are produced for characterizing their fracture behaviour.

In summary, it was possible to identify in the SMC different types of boundaries with transmission electron microscopy. On a short scale, the boundaries do not show the expected very brittle behaviour as illustrated by the nanoindentation tests. This finding indicates that the lacking robustness of the material might be rather related to large defects remaining in the material after preparation than to intrinsically brittle boundaries.

### References

- [1] Shin Tajima, T. H., Mikio Kondoh, Masaki Sugiyama, Kiyoshi Higashiyama, Hidefumi Kishimoto and Tadayoshi Kikko (2004). "Properties of High Density Magnetic Composite (HDMC) by Warm Compaction Using Die Wall Lubrication" *Materials Transactions* **45**(6): 1891-1894.
- [2] Oikonomou, C., E. Hryha, et al. (2012). "Development of methodology for surface analysis of soft magnetic composite powders." *Surface and Interface Analysis* **44**(8): 1166-1170.
- [3] H. G. Nguyen, G. D., A. Hartmaier (2013). Grenze der Einsetzbarkeit eines weich-magnetischen Pulververbundwerkstoffes aus Sicht der Mechanik. 19. Symposium Verbundwerkstoffe und Werkstoffverbunde. Karlsruhe.

## Multiscale Modelling of Damage and Failure in a Biological Hierarchical Material

INGO SCHEIDER<sup>1</sup>, SONGYUN MA<sup>2</sup>, EZGI YILMAZ<sup>3</sup>, SWANTJE BARGMANN<sup>1,2</sup>

<sup>1</sup>Institute of Materials Research, Materials Mechanics/ACE-Centre, Helmholtz-Zentrum Geesthacht, Germany

<sup>2</sup>Institute of Continuum and Material Mechanics, Hamburg University of Technology (TUHH), Germany

<sup>3</sup>Institute of Advances Ceramics, Hamburg University of Technology (TUHH), Germany

Dental enamel is a heterogeneous anisotropic material, showing an optimal reliability with respect to the various loads occurring over years. This study aims to

explore the structure-property relationship of dental enamel and discover how the material achieves its structural functions through hierarchical design, ex-

tending the study presented in Bargmann et al., (2013). To this end, the microstructure of enamel at two hierarchical levels, namely parallel rods consisting of bundles of mineral fibres, was modelled and mechanical properties were evaluated in terms of strength and toughness with the help of a multiscale modelling method. The technique used here consists of two steps for each hierarchy level; that is (a) the simulation of a representative unit cell including the material models for the participating microstructural elements and (b) the homogenization with respect to deformation and failure in order to retrieve the material model for the next hierarchy level. For part (a) the representative unit cell contains appropriate hyperelastic material models for the constituents and also damage models for several types of damage. Three kinds of damage are included: Breaking of the fibres, debonding of the fibres from the matrix and matrix damage. All damage models are realized by cohesive interface elements with respective model parameters. The interface elements are placed such that various crack paths and failure mechanisms may occur. The parameters identified during the homogenization phase (b) are strongly dependent on the geometry of the microstructure and thus the failure mechanism.

The established models were validated by comparing with the measured stress-strain curves on two hierarchical levels, see Scheider et al. (2014). The results lead to a close agreement between experiment and simulation, which gives further evidence for some of the

microstructural parameters that cannot be measured experimentally; for example: The interface damage properties between the nano-sized mineral fibres and the thin protein matrix can be estimated by enforcing the interface toughness to be low enough such that debonding occurs but as high as possible to achieve the highest possible strength.

Another case which illustrates the usefulness of microstructural modelling: In order to state a reason for the damage-tolerance behaviour of enamel in relation with the nano-sized crystallites and multiple hierarchies, the size of crystallites below which the structure becomes insensitive to flaws were studied by the representative unit cell. The results reveal that the flaw tolerance size of enamel is about 50 nm, the same size as the mineral fibres appear in dental enamel.

#### References

- S. Bargmann, I. Scheider, T. Xiao, E. Yilmaz, G. Schneider, N. Huber (2013) Towards bio-inspired engineering materials: Modeling and simulation of the mechanical behavior of hierarchical bovine dental structure. *Computational Material Science*, 79, 390-401.
- I. Scheider, T. Xiao, E. Yilmaz, G. Schneider, N. Huber, S. Bargmann (2014) Damage modeling of small scale experiments on dental enamel with hierarchical microstructure. *Acta Biomaterialia*, accepted manuscript

## Surface properties of biopolymer films - Morphology, adhesion and friction

MAURICE BROGLY, AHMAD FAHS, SOPHIE BISTAC

Université de Haute Alsace, LPIM, Mulhouse, France

For pharmaceutical applications, cellulose derivatives are promising raw materials for coatings or films obtained from aqueous systems. A case study is presented on hydrophilic biopolymer for the preparation of oral controlled drug delivery systems. Additives such as plasticizers, surfactants, lipids, colorants or other film-forming polymers are frequently incorporated into biopolymer matrices to produce high quality drug protective films. The matrix used is Hydroxypropyl methylcellulose (HPMC). Additives such as stearic acid and polyethylene glycol (PEG) are added to improve some specific film surface properties such as adhesion and friction. The study investigates then the influence of such hydrophilic plasticizer (polyol) and hydrophobic excipient (fatty acid) on the surface properties of free HPMC films.

The aim of this work is to formulate HPMC films by introducing additives, to explore their surface properties and to investigate the adhesive and frictional properties

at nanoscopic and macroscopic scales. Our expertise in contact mode Atomic Force Microscopy (AFM) allows us to quantify the mechanical behaviors at nanoscale. The influence of additives on HPMC structuration and morphology, permeation, hydrophilic/hydrophobic character as well as surface mechanical characteristics such as adhesion and friction are evaluated. The results clearly underline the strong dependence of film properties on additive nature, concentration or water sensitivity and the interplay with additive-biopolymer matrix compatibility.

Stearic acid additive has a strong influence on HPMC surface properties and morphology. The surface structure of HPMC films shows the presence of granular nano-domains, which disappear with fatty acid content. A sharp variation of nano-adhesion and nano-friction forces is observed with addition of fatty acid. The results show that the addition of only 1% (w/w HPMC) of stearic acid induces a strong decrease (25%) of the

surface free energy. The hydrophobic character becomes predominant and the non-dispersive component to the surface energy tends towards zero. Tapping mode topographic images show that the surface mean roughness of the formulated films decreases with the introduction of stearic acid. These results suggest that stearic acid molecules can migrate at the film surface. As a consequence the torsional forces measured on the basis of AFM nano-friction experiments decrease. Nano adhesion results confirm this tendency and suggest the presence of a weak boundary layer at the film surface, the formation of which is driven by a phase separation process.

PEG additives induce an increase of the surface hydrophilicity and affect HPMC morphology by insertion mechanisms. Swelling of HPMC clusters is observed as PEG content increases

PEG additives also induce an increase of the surface free energy. At the nano scale, the increase of PEG content causes an increase of friction and adhesion forces. Good correlation is obtained at macro scale. Experimental results underline the major role of capillary forces at the nano scale and evidence that PEG behave as a lubricant at macro scale.

The present study underlines the strong dependence of surface film properties on additive concentration and/or water sensitivity. Formulation appears then as an original and simple way to tune surface morphology and surface properties of bio-based polymer films. Finally the present study also shows that AFM is a powerful tool for studying surface adhesion and sliding properties of cellulose based formulated films for pharmaceutical applications such as coatings and films.

#### References

- Brogly, M., Awada, H., Noel O. (2009), in *Nanosciences and Technology, Applied Scanning Probe Methods XI*, B.Bhushan & H. Fuchs Eds., Springer, 73-93; Berlin Heidelberg.
- Fahs A., Brogly M., Bistac S., Schmitt M. (2010), *Carbohydrate Polymers*, 1: 105;
- Brogly M., Fahs A., Bistac S. (2011), In *Nanoscience and Technology, Scanning Probe Microscopy in Nanoscience and Nanotechnology*, B.Bhushan Ed., Springer, 473-504; Berlin Heidelberg.

## Microstructure evolution of Cu/Au and Cu/Cr multilayers under cyclic sliding

ZHAO-PING LUO<sup>1</sup>, GUANG-PING ZHANG<sup>2</sup>, RUTH SCHWAIGER<sup>1</sup>

<sup>1</sup>Karlsruhe Institute of Technology, Institute for Applied Materials, Germany

<sup>2</sup>Institute of Metal Research, Chinese Academy of Sciences, Shenyang, P. R. China

Nanoscale metallic multilayers exhibit high strength, good fatigue properties and wear resistance, high thermal stability, as well as excellent irradiation tolerance (Clemens et al. 1999; Beyerlein et al. 2014). Previous investigations have illustrated that the strength and plastic deformation are length scale dependent but also strongly controlled by the interface structure, which determines the interface barrier strength and slip transmission (Li & Zhang 2010; Wang & Misra 2011). However, a more detailed description of deformation behaviors and the predominant mechanisms are still needed for our understanding of these superior properties.

In this study, two types of nanoscale multilayers, Cu/Au (which is a miscible semi-coherent fcc/fcc structure) and Cu/Cr (which is an immiscible incoherent fcc/bcc structure), were studied. Cyclic sliding experiments which induce large strains in the samples were conducted using a nanoindenter. The microstructures underneath the sliding tracks subjected to 1-1000 cycles of sliding were investigated by scanning electron microscopy (SEM), transmission electron microscopy

(TEM) and scanning TEM with high-angle annular dark-field (HAADF-STEM) imaging on cross-sections prepared by focused ion beam (FIB).

For the Cu/Au multilayers, grain growth and a reduction of the individual layer thickness were observed in both the Cu and Au layers at the early stage of deformation (1-50 cycles). For sliding cycle numbers between 50 and 100, the deformed layers started to curve and formed a vortex structure. In the next stage of deformation (500-1000 cycles), nanostructures were formed in the sliding track. For the Cu/Cr multilayers, plastic deformation and microstructural changes were mainly concentrated on the Cu layers at the early stage of deformation. Then, fracture of the Cr layers whereas the vortex formation did not occur. In the range between 500 and 1000 cycles, a mixed nanostructure was formed in the worn zone. The differences in the deformation microstructures between Cu/Au and Cu/Cr multilayers indicate that different deformation mechanisms are active. The deformation behavior of the two different material systems will be discussed with respect to the interface effect and resulting microstructural changes.

## References

Beyerlein, I. J., Mayeur, J. R., Zheng, S., Mara, N. A., Wang, J. & Misra, A. (2014): Emergence of stable interfaces under extreme plastic deformation. *PNAS*; 111: 4386-4390.

Clemens, B. M., Kung, H. & Barnett, S. A. (1999): Structure and strength of multilayers. *MRS Bulletin*; 24: 20-26.

Li, Y. P. & Zhang, G. P. (2010): On plasticity and fracture of nanostructured Cu/X (X=Au, Cr) multilayers: The effects of length scale and interface/boundary. *Acta Materialia*; 58: 3877-3887.

Wang, J. & Misra, A. (2011): An overview of interface-dominated deformation mechanisms in metallic multilayers. *Current Opinion in Solid State and Materials Science*; 15: 20-28.

# Toward the modulation of interface barrier strength of Cu/Au nanolayered composites

XI LI<sup>1</sup>, GUANG-PING ZHANG<sup>1</sup>,

<sup>1</sup>Shenyang National Laboratory for Materials Science, Institute of Metal Research, Chinese Academy of Sciences, Shenyang, P. R. China

<sup>2</sup>Karlsruhe Institute of Technology, Institute for Applied Materials, Germany

The Interface barrier strength (IBS), which describes the resistance for dislocations to cross an interface, is a key factor that controls the ultrahigh strength of metallic nanolayered composites (Koehler, 1970; Hoagland et al. 2002; Li, et al. 2007; Yan, et al. 2013). Several theory models have been proposed to describe the strengthening mechanisms in multilayered composites and primary contributions to IBS, such as modulus modulation and lattice parameter mismatches et al. (Koehler, 1970; Hoagland et al. 2002; Li, et al. 2007; Yan, et al. 2013). However, the variation of interface microstructure induced by element interdiffusion and its influence on the IBS in metallic nanolayered composites are still not clearly understood (Chu and Barnett, 1995).

In this study, Cu/Au nanolayered composites with individual layer thickness ranging from 25 nm to 250 nm were prepared by DC magnetron sputtering (Zhang, et al. 2006). The Cu/Au nanolayered composites were annealed at 100, 200 and 300 °C for 30 minutes, respectively. Mechanical properties of the nanolayered composites were investigated using a nanoindenter. The microstructures of the nanolayered composites were characterized by transmission electron microscopy (TEM) and high-resolution electron microscopy (HRTEM). The degree of mutual diffusion at the layer interfaces in the Cu/Au nanolayered composites under different heat treatment conditions was characterized by energy-dispersive X-ray analysis (EDX) and HRTEM imaging. Experimental results from nanoindentation show that the Hall-Petch (H-P) slope in the relation between the strength and the individual layer thickness of the nanolayered composites gradually decreases with increasing annealing temperature, indicating a decrease in the IBS. TEM examination of the

microstructures indicates that the change in grain sizes and the amount of twinning in both Cu and Au layers induced by annealing did not significantly affect the H-P slope of the material. The HRTEM characterization reveals that element interdiffusion between the Cu layer and the adjacent Au layer leads to a compositional gradient at the interface. A detailed analysis for effects of the compositional gradient on the resistance to dislocation crossing the interface was conducted. Thus, it is concluded that the interface structure of the Cu/Au nanolayered composites has become the most important factor in governing the IBS. These results provide important guidelines for the interface design of high performance nanolayered composites.

## References

Koehler, J.S., 1970: Attempt to Design a Strong Solid. *Phys Rev B* 2, 547.

Hoagland, R.G., Mitchell, T.E., Hirth, J.P., Kung, H., 2002: On the strengthening effects of interfaces in multilayer fcc metallic composites. *Philos Mag* 82, 643 - 664.

Li, Y., Zhang, G.P., Wang, W., Tan, J., Zhu, S., 2007: On interface strengthening ability in metallic multilayers. *Scripta mater* 57, 117-120.

Yan, J., Zhang, G.P., Zhu, X., Liu, H., Yan, C., 2013: Microstructures and strengthening mechanisms of Cu/Ni/W nanolayered composites. *Philos Mag* 93, 434-448.

Zhang, G.P., Liu, Y., Wang, W., Tan, J., 2006: Experimental evidence of plastic deformation instability in nanoscale Au/Cu multilayers. *Appl Phys Lett* 88, 013105.

Chu, X., Barnett, S.A., 1995: Model of Superlattice Yield Stress and Hardness Enhancements. *J Appl Phys* 77, 4403-4411.

Talks Topic E 4:

***Size effects and small-scale mechanical behavior of materials***

---

## Probing thermally activated properties on a local scale

DANIEL KIENER<sup>1</sup>, ALEXANDER LEITNER<sup>1</sup>, VERENA MAIER<sup>2</sup>

<sup>1</sup>Montanuniversität Leoben, Department Materials Physics, Austria

<sup>2</sup>Erich-Schmid Institut for Materials Science, Austrian Academy of Sciences, Leoben, Austria

On a macroscopic scale, it is well known that face centered cubic (fcc) metals can be considered in their athermal limit. However, once the grain size or sample size is refined into the sub-micron range, significant rate dependent material strength is observed. While there is a body of work focussing on these fcc materials, little effort was spent on studying thermally activated mechanisms for body centered cubic (bcc) metals, which is surprising considering the fact that single crystal samples show a rate dependent behavior already on the macroscopic scale.

In this work, we aimed to investigate both, the influence of crystal structure and microstructure, respectively, on the thermally activated deformation processes in fcc and bcc metals on a local scale. Therefore, we investigated nanocrystalline, ultra-fine grained, and ultra-fine porous Au as representative fcc material, as well as single crystal and ultra-fine grained Cr as typical bcc metal, respectively. All fine grained materials were produced by severe plastic deformation, in detail high pressure torsion, from their bulk counterparts, or pure powders for the foams, respectively.

The local thermally activated deformation behavior was studied using advanced nanoindentation testing techniques at ambient and elevated temperatures using either a Micro Materials or a Keysight system, respectively, where the latter was equipped with a continuous stiffness module. Complementary to these nanoindentation experiments, the bulk material properties were examined. Miniaturized in-situ SEM mi-

cro-compression and in-situ TEM indentation experiments were performed to get a better understanding of the underlying deformation mechanisms.

For the fcc Au tested up to 300 °C, we observe that the strain rate sensitivity increases with reduced grain size and increasing testing temperature. Interestingly, this is true for the ultra-fine grained as well as the ultra-fine porous material, indicating that the rate determining deformation step is the thermally activated nucleation and motion of dislocations from grain boundaries, as recently already suggested for Cu by Kreuzeder et al.. In case of the bcc Cr, a change in the governing deformation behavior is observed. First, the presence of grain boundaries leads to a reduction in strain rate sensitivity for the ufg material compared to the single crystal counterpart, which is due to the increased athermal strength related to the Hall-Petch effect. When increasing the testing temperature and finally exceeding the critical temperature of Cr (~180 °C), the strain rate sensitivity of the ufg material increases, while that of the single crystal Cr is linearly reduced with testing temperature. Thus, above the critical temperature no thermal activation is required for dislocation motion and the bcc Cr essentially behaves fcc-like.

### Reference

Kreuzeder, M. et al. (2015): Fabrication and thermo-mechanical behavior of ultra-fine porous copper. *JMS*, 50: 634643.

## Micro- and Macro-mechanical Testing of Grain Boundary Sliding (GBS)

JUNNAN JIANG, ANGUS WILKINSON, RICAHRD TODD

Department of Materials, University of Oxford, United Kindom

This project aims to explore the fundamental mechanism(s) of grain boundary sliding (GBS) with an emphasis on its role in superplasticity, using both micro- and macro-mechanical testing methods.

Classical models for GBS (Rachinger sliding and Lifshitz sliding) assume that all grains and grain boundaries undergo the same process, but recent results from research in the group show that this is not true. Individual grain boundaries differ in their ability to participate in sliding and diffusion (Rust and Todd, 2011). Therefore, it is important to investigate the response of indi-

vidual grain boundaries to stress by micromechanical tests. Thus, this project is focused on micromechanical tests on microcantilevers and micropillars containing individual grain boundaries. The response of individual grain boundaries will be correlated with grain boundary characterisation by using electron backscattered diffraction (EBSD) to measure the misorientation of the grains on either side of the grain boundary. This will link the crystallography of grains to the tendency for GBS. Furthermore, results of micromechanical tests will be correlated with patterns of GBS seen in poly-

crystals during macromechanical shear tests. Finally, all the experimental results will be used to develop models to be implemented in constitutive equations for numerical modelling techniques on GBS.

The material chosen was Sn-1%Bi alloy, which is expected to exhibit GBS at room temperature. This is because the melting temperature of Sn-1%Bi is around 504K, while room temperature (298K) is almost 60% of its melting point. Furthermore, it is a single-phase alloy, which simplifies the microstructure. The material was cold extruded at liquid nitrogen temperature to an average grain size of 8.5  $\mu\text{m}$ . Polished samples with this fine grain size were used in macro-shear tests. Fine, straight surface marker lines were put on the sample before the test. Surface grids with submicron and coarser pitches were milled by FIB to make quantitative measurements of grain boundary sliding. Macro shear tests were carried out under displacement control at room temperature. GBS was revealed by the offsets of surface marker lines at the grain boundaries. A stress – strain rate curve was plotted from a few shear tests with various strain rates on the same batch of material

with a relatively consistent microstructure. The strain rate sensitivity is of great importance to the mechanism of superplasticity and hence grain boundary sliding.

Micro-cantilevers containing individual grain boundaries have been manufactured for micro-mechanical tests by nanoindenter. Grain boundaries are characterised using EBSD analysis. A few cantilevers have shown grain boundary sliding along the grain boundary plane which is parallel to the displacement direction of the nanoindenter (i.e. normal to the sample surface). When the grain boundary plane is not parallel to the displacement direction or the grain boundary plane is not flat, sliding is inhibited.

#### Reference

RUST, M. A. & TODD, R. I. 2011. Surface studies of Region II superplasticity of AA5083 in shear: Confirmation of diffusion creep, grain neighbour switching and absence of dislocation activity. *Acta Materialia*, 59, 5159-5170.

## Nanoindentation at Room and Elevated Temperatures of Au/Cu-Multilayers

THOMAS KREUTER<sup>1</sup>, GUANG-PING ZHANG<sup>2</sup>, OLIVER KRAFT<sup>1</sup>, RUTH SCHWAIGER<sup>1</sup>

<sup>1</sup>Karlsruhe Institute of Technology, Institute for Applied Materials, Germany

<sup>2</sup>Shenyang National Laboratory for Materials Science, Institute of Metal Research, Chinese Academy of Sciences, Shenyang, People's Republic of China

Thin films and multilayers exhibit strong size effects in their mechanical behavior such as increasing yield strength or hardness with decreasing film or layer thickness. When the film and layer thicknesses approach the nanometer scale, the interfaces and grain boundaries dominate the deformation behavior. Different deformation mechanisms have been suggested for different layer thicknesses and types of interfaces such as dislocation pile-up, confined layer slip or dislocation transmission across the interfaces (Misra 2002).

In this study, Au/Cu-multilayers with individual layer thicknesses in the range from 25 to 250 nm were investigated at room and elevated temperatures using nanoindentation. The samples with a total film thickness of 1  $\mu\text{m}$  were prepared using radio frequency (RF) magnetron sputtering and had a (111) texture in both Au and Cu layers (Zhang 2006). As expected, the hardness and the strain rate sensitivity of the multilayers increased with decreasing layer thickness. With increasing temperature the hardness decreased while only small changes in the strain rate sensitivity were observed for temperatures up to 93°C.

The deformation microstructures were carefully investigated by focused ion beam cross-sectioning. The pile-up of material at the sample surface, the indenta-

tion depth, and the thickness changes of the individual layers were determined. For larger layer thicknesses (100 and 250 nm) the thinning of individual layers was quantified for the measurements at room temperature and at 93°C. A more pronounced layer thinning of the individual layers was identified for the nanoindents at 93°C. For the 100 nm layer thicknesses, the top layers experienced more deformation at both temperatures compared to the 250 nm layers.

Furthermore, shear bands underneath the indents were observed for the thinner layers, as also reported in (Li, 2010). Transmission electron microscopy observation revealed changes of the grain size after the indentation experiments.

In this presentation, the differences in deformation microstructures for the different layer thicknesses will be illustrated and discussed in the context of the active deformation processes. Understanding deformation and failure of nanoscale multilayers will contribute to their future applicability in small-scale mechanical and functional devices.

#### References

Misra, A., Hirth, J.P. & Kung, H. (2002): Single-dislocation-based strengthening mechanisms in nanoscale

metallic multilayers, Philosophical Magazine A, Vol. 82, No. 16, 2935-2951.  
Zhang, G.P. et al. (2006): Experimental evidence of plastic deformation instability in nanoscale Au/Cu

multilayers, Applied Physics Letters, Vol. 88, 013105.  
Li, Y.P. et al. (2010): Investigation of deformation instability of Au/Cu multilayers by indentation, Philosophical Magazine, Vol. 90, No. 22, 3049-3067.

## Mechanical behavior of the MAX-phase Nb<sub>2</sub>AlC at the nanometer and micrometer scale by means of *in situ* indentation

NADINE SCHRENKER<sup>1</sup>, YONNES KABIRI<sup>1</sup>, MIRZA MAČKOVIĆ<sup>1</sup>, JULIAN MÜLLER<sup>1</sup>, PETER SCHWEIZER<sup>1</sup>, FLORIAN NIEKIEL<sup>1</sup>, BJÖRN HOFFMANN<sup>2</sup>, SILKE CHRISTIANSEN<sup>2,3</sup>, ERDMANN SPIECKER<sup>1</sup>

<sup>1</sup>Center for Nanoanalysis and Electron Microscopy (CENEM), Friedrich-Alexander Universität Erlangen-Nürnberg, Erlangen, Germany

<sup>2</sup>Max Planck Institute for the Science of Light, Erlangen, Germany

<sup>3</sup>Helmholtz Centre Berlin for Materials and Energy, Berlin, Germany

MAX phases are layered crystals with ternary or quaternary chemical composition. Due to their unique set of properties, which is a combination of metallic and ceramic attributes, they are in focus of intense research activities. They are excellent electric and thermal conductors, oxidation resistant as well as machinable and damage tolerant [1]. As a result of the layered nature of MAX phases, they behave plastically anisotropic. Depending on the orientation the deformation occurs by a combination of delamination of individual grains, formation of shear and kink bands. The deformation by dislocation glide is assumed to be restricted to the basal planes. According to Frank and Stroh et al. [2] kink bands are initiated by elastic buckling. Above a critical shear stress pairs of dislocations of opposite sign form and move in opposite direction. By extending to the free surface the attraction forces between the dislocation walls are eliminated and a kink band is formed. However, the precise nucleation mechanism of kink bands is not yet known.

By means of *in situ* indentation experiments in the electron microscope we investigate the mechanical behavior of the MAX-phase Nb<sub>2</sub>AlC. The preparation of pillars was performed with a Focus Ion Beam (FIB). In the transmission electron microscope pillar compression tests revealed nucleation and propagation of dislocations on the basal planes with 1/3<11-20> type Burgers vector. Deformation by basal slip was possible, as the basal planes were inclined to the pillar axis. Furthermore, the anisotropic behavior was studied by compression tests of submicron pillars in the scanning electron microscope. According to EBSD measurements pillars with different orientations were chosen. In the case of single crystal pillars where the basal planes are parallel to the compression axis, the layers are constrained and forced to delaminate and bend. Post mortem images reveal that the curvature of bending is high as well as slip traces along the basal planes. In addition, pillars containing a grain boundary revealed the incompatibility of deformation of grains

with different orientations, which is a result of the lack of five independent slip systems. In pillars with a grain boundary between grains oriented close to the [0001] and the [10-10] direction final failure occurred by delamination of the basal planes lying parallel to the surface, which required high stresses. Bending of the basal planes oriented edge-on was impeded in this case by the other grain. Moreover, the compressive strength measured of the submicron pillars exceeds the strength of a bulk material. As the average diameter of the pillars at the free end is 0.67 μm, it is possible that dislocation sources get pinned at the surface and become single arm sources. The critical resolved shear stress is expected to increase with decreasing source length (source truncation) [3]. Dislocation escape at the free surface was observed in other *in situ* studies [4] and could also be an explanation. Furthermore, reaction of nucleated dislocations with preexisting dislocations or FIB induced dislocations can cause paucity of available dislocation sources (exhaustion hardening) [3].

### References

- [1] M.W. Barsoum and M. Radovic, Annu. Rev. Mater. Res., 41(1):195-227, 2011.
- [2] F.C. Frank and A.N. Stroh, Proc. Phys. Soc. B, 65(10):811-821, 1952.
- [3] S.I. Rao, D.M. Dimiduk, T.A. Parthasarathy, M.D. Uchic, M. Tang, and C. Woodward, Acta Mater., 56(13):3245-3259, 2008.
- [4] S. Ho Oh, M. Legros, D. Kiener, and G. Dehm, Nat. Mater., 8:95-100, 2009.

### Acknowledgements

Financial support by the DFG via research training group GRK 1896 "In situ microscopy with electrons, X-rays and scanning probes" is gratefully acknowledged. The authors further thank Prof. Dr. Peter Greil for providing the Nb<sub>2</sub>AlC samples used in this study.

# Deformation behavior of copper thin films indented with patterned nanoindenter tips

ANKE SCHACHTSIEK, OLIVER KRAFT, RUTH SCHWAIGER

Institute for Applied Materials , Karlsruhe Institute of Technology (KIT), Germany

Imprinting or mechanical forming potentially represents a low-cost and high throughput method to produce high resolution patterns at the micro- and the sub-micrometer scales. Typically the mold is brought into contact with the sample and is then loaded with a compressive force for a certain period. In principle, the mold can be used numerous times, ideally without degradation of the imprint quality. While early research in this field focused mainly on patterning of soft polymers, more recent studies investigated the patterning of metals (Lister 2004). However, a standard procedure for metal nanoimprinting has not been established yet. Finding the suitable mold material and sample mount, choosing load, time and temperature represent the main challenges. Recently, focused ion beam and lithographic methods have been adapted successfully for mold fabrication (Lister 2004, Böhm 2001). Furthermore, the hardness of a metal depends on its microstructure affecting the pattern formation. For imprint dimensions comparable to the grain size, the local flow behavior is poor, limiting the achievable pattern dimensions (Durst 2010).

In this study, the deformation behavior of copper was investigated. Using a nanoindenter equipped with a patterned flat punch tip, a cross-shaped groove was created in bulk copper and copper thin films of 800 nm and 1600 nm thickness on Silicon substrates. The deformation pattern shape was analyzed using atomic force microscopy along with scanning electron and focused ion beam microscopy techniques.

With respect to the stress-strain relationship, the thin films exhibit deformation behavior which is apparently

independent of the microstructure. However, the substrate very clearly influences the imprint patterns and may lead to delamination, which typically corresponds to “underfilling conditions” or a high filling factor (Cross 2006). The pile-up flows into single peak or dual peak shapes, depending on the cavity width as described for polymer flow (Rowland 2005).

In this presentation, the applicability of the imprinting method for the direct mechanical forming of micro- and nanoscale metallic structures together with drawbacks and limitations will be discussed.

## References

- Böhm, J., Schubert, A., Otto, T. & Burkhardt, T. (2001); Micro-metalforming with silicon dies *Microsyst. Technol.* 7, 191-195
- Cross, G.L.W. (2006): The production of nanostructures by mechanical forming *J. Phys. D: Appl. Phys.* 39, 363-386
- Durst, K., Hofmann, S., Backes, B., Mueller, J. & Göken, M. (2010): Microimprinting of nanocrystalline metals - Influence of microstructure and work hardening *J. Mater. Process. Technol.* 210, 1787-1793
- Lister, K.A., Thoms, S., Macintyre, D.S., Wilkinson, C.D.W. & Weaver, J.M.R. (2004): Direct imprint of sub-10 nm features into metal using diamond and SiC stamps *J. Vac. Sci. Technol. B* 22 3257–3259
- Rowland H.D., Sun A.C., Schunk P.R. & King W.P. (2005): Impact of polymer film thickness and cavity size on polymer flow during embossing: toward process design rules for nanoimprint lithography *J. Micromech. Microeng.* 15 2414–2425

Talks Topic E 5:

***Size effects and small-scale mechanical behavior of materials***

---

## Using high temperature micromechanical testing to inform microstructure based models: application to IN718

J. MOLINA-ALDAREGUIA<sup>1</sup>, B. GAN<sup>1</sup>, A. CRUZADO<sup>1</sup>, M. JIMÉNEZ<sup>1</sup>, J. SEGURADO<sup>1,2</sup>, J. LLORCA<sup>1,2</sup>

<sup>1</sup>IMDEA Materials Institute, Getafe, Madrid, Spain

<sup>2</sup>UPM- Universidad Politécnica de Madrid, Madrid, Spain

IN718 is widely used in structural applications requiring high strength and toughness [1, 2]. To elucidate the underlying mechanisms responsible for the superior mechanical properties, a polycrystalline sample of IN718 with an average grain size of 150  $\mu\text{m}$  was selected for the present investigation.

The grain orientations were analyzed by Electron BackScatter Diffraction (EBSD) and site-specific micropillars with sizes varying from 1  $\mu\text{m}$  to 18  $\mu\text{m}$  were machined out by Focused Ion Beam (FIB) milling [3, 4]. The micropillars when then tested in compression inside an instrumented nanoindentation system equipped with a flat punch [5] and the effects of pillar size, pillar orientation, strain rate and temperature on the micro-compression behavior were quantitatively assessed.

The results were used to determine the parameters of a single-crystal plasticity (SCP) model of IN718, by comparing the experimental results with finite element (FE) simulations [5]. The calibration of the CP model was done by considering only the plastic contribution of the experimental stress-strain curves. The CP model

developed was then evaluated by comparing the simulation of other independent micro-compression tests with the corresponding experimental results.

Finally, the extracted plasticity parameters were then used in the numerical simulation of the compression behavior of the macroscopic polycrystalline sample. The agreement was remarkable in all the cases [5].

### References

- [1] R Schafrik and R Sprague, *Advanced Mater. & Processes* 162 (2004) 27–30.
- [2] T M Pollock and S Tin, *J. Propulsion & Power* 22 (2006) 361.
- [3] M D Uchic, D M Dimiduk, J N Florando, WD Nix, *Science* 305 (2004) 986.
- [4] P A Shade, M D Uchic, D M Dimiduk, G B Viswanathan, R Wheeler, H L Fraser, *Mater. Sci. and Eng.*, 535 (2011) 53-61.
- [5] A. Cruzado, B. Gan, H. Chang, K. Ostolaza, A. Linaza, S. Milenkovic, J. M. Molina-Aldareguia, J. Llorca and J. Segurado, *Int. J. Plast.*, submitted.

## Multi-scale Fracture Behaviour of Tungsten Alloys for Nuclear Fusion

BO-SHIUAN LI, DAVID ARMSTRONG, JAMES MARROW, STEVE ROBERTS

Department of Materials, University of Oxford, United Kingdom

The plasma facing components (PFCs) of the International Thermonuclear Experimental Reactor (ITER) divertor will require materials exposed to high heat flux, neutron damage, and plasma erosion. Tungsten-based alloys are currently the most promising materials for the PFCs, due to its superior high temperature strength, good thermal conductivity, and high recrystallisation temperature. However, the intrinsic low fracture toughness ( $K_{IC}$ ) and the high ductile-to-brittle-transition temperature (DBTT) limit the structural applications of tungsten. Crystalline defects from fusion neutrons and transmutational helium induces significant hardening/embrittlement and shift the DBTT to the low temperature regime. Therefore, multiscale understandings of the fracture behaviour of tungsten are required before applying it to fusion applications. The macroscopic fracture toughness of polycrystalline

tungsten has been investigated by Gludovatz et al. [1], reporting a strong dependence on the temperature, microstructures, and alloying elements. To gain a deeper insight into the fracture behaviour of tungsten on a micromechanical basis, the effect of microstructure to fracture toughness has to be understood. Micro-fracture experiments become possible by the combination of focused ion beam (FIB) and nanoindentation. They allowed the fracture toughness of single microstructural constituents, such as single grains, grain boundaries, or shallow irradiated layer to be measured. Tested on very brittle materials, the linear elastic fracture mechanics (LEFM) approach yields reasonable fracture toughness value because the plastic zone under the crack tip is small in relation to the specimen size.

Wurster et al. [2] studied the micro-fracture behaviours of single-crystal tungsten using FIB-fabricated micro-

cantilevers. The semi-brittle tungsten yields a larger plastic zone, therefore the LEFM approach is no longer valid, and elastic-plastic fracture mechanics (EPFM) has to be applied. In contrast to the brittle fracture behaviour seen in macro-sized single-crystal tungsten, the single-crystal tungsten microcantilevers behave more ductile and exhibit higher fracture toughness. The current consensus is smaller is stronger, however does this also mean smaller is tougher?

In this research, both microcantilevers and macro-scale four point bending bars with chevron-notches will be used for fracture tests. By virtue of the chevron geometry, crack will form during the early portion of loading and arrests immediately after its formation. Through a cyclic loading-unloading method, crack is able to propagate stably until reaching a critical crack length. Finite element analysis (FEA) is used to select an effective chevron geometry that maximizes the stable crack region, and accurately calculates the stress intensity factor (SIF) along the crack. The EPFM approach requires detailed information of the crack extension.

Through extensive FEA and cyclic loading-unloading, crack length at each loading/unloading segment is obtained. Therefore, fracture toughness can be calculated through the EPFM approach.

Our state-of-the-art hot-stage nanoindenter allows micro-fracture tests to be conducted over a wide range of temperatures (up to 750 °C). For the first time, the fracture behaviour of polycrystalline tungsten can be characterised at different lengthscale and temperatures. Through systematic comparisons of results, the mechanical size effects of polycrystalline tungsten to fracture toughness can be better understood.

#### References

- [1] E. Gaganidze, D. Rupp, and J. Aktaa, "Fracture behaviour of polycrystalline tungsten," *J. Nucl. Mater.*, vol. 446, no. 1–3, pp. 240–245, Mar. 2014.
- [2] S. Wurster, C. Motz, and R. Pippan, "Characterization of the fracture toughness of micro-sized tungsten single crystal notched specimens," *Philos. Mag.*, vol. 92, no. 14, pp. 1803–1825, May 2012

## Effect of composition and morphology on the mechanical and electrical behavior of Cu-Cr thin films

ALLA. S. SOLOGUBENKO<sup>1,2</sup>, WILHELM HÜTTENES<sup>1</sup>, HUAN MA<sup>1</sup>, RALPH SPOLENAK<sup>1</sup>

<sup>1</sup>Laboratory for Nanometallurgy (LNM), ETH Zürich, Switzerland

<sup>2</sup>Scientific Center for Optical and Electron Microscopy (ScopeM), ETH Zürich, Switzerland

Structural integrity, thermo-mechanical stability and electrical performance of Cu-Cr thin films on a polymer substrate are studied in this work in uniaxial loading as a function of temperature, phase state and grain morphology. Cu and Cr, which are immiscible in thermodynamic equilibrium were magnetron co-sputtered as thin films of Cu - X at.% Cr (X=5, 10, 20) compositions onto a Kapton substrate. The metastable solid solution state was aimed in the as-deposited alloys of all three compositions. Thermal annealing at 300°C for 5h prior to straining was performed on films of all compositions to reveal an effect of phase decomposition on the microstructure. The films were produced in continuous and interruptive sputtering modes, to yield the "columnar" and "brick-wall" grain morphologies. The "brick-wall"-morphology was achieved by a periodic introduction of very thin, less than 2 nm, layers of either W or Ag into the body of the film during sputtering. The "columnar", tungsten-modified and silver-modified

films in both, as-deposited and annealed states, were strained with simultaneous monitoring of the change in film electrical resistance. Tensile tests were carried out at room temperature and 100°C.

Our studies show a considerably improved electro-mechanical performance of "columnar" films in comparison to the "brick-walled", W- and Ag-modified ones. We relate this behavior of continuously sputtered films to dense, fine-grained, and in reality non-columnar microstructure. The additional electron scattering in the "brick-wall" films is considered to be due to the presence of the additional scatter centers, such as Ag- and W-interfaces. The exceptionally good behavior of the Cu-5at.% Cr "columnar" films is related to the truly solid solution state of the metastable alloy. The film resistivity increases with Cr and the presence of interlayers with Ag being the worst interlayer material. The 100°C-straining increases the plastic range of all films.

# Thermomechanical influence grinding of electrodeposited chrome coated on a 300M substrate

BENJAMIN WEISS<sup>1</sup>, ANDRÉ LEFEBVRE<sup>2</sup>, OLIVIER SINOT<sup>2</sup>, ALBERT TIDU<sup>1</sup>

<sup>1</sup>LEM3 - Laboratoire d'Etude des Microstructures et de Mécanique des Matériaux, Metz, France

<sup>2</sup>LABPS, Laboratoire de mécanique Biomecanique Polymère et Structure, Metz, France

Hard chromium coating is a commonly used material for industrial application. It is obtained by the well-established electrodeposition technique. These coatings are mainly applied for the production of functional coatings on engineering components in view to enhance their wear, hardness and corrosion resistance properties.

Grinding is a material removal operation widely used in manufacturing industry. It's well known that grinding generates significant deformation and friction compared to other machining processes. The combination of material removal, elastoplastic deformation and friction can transform the surface workpiece. There may be the creation of cracks, the occurrence of burning traces on the workpiece or hardness and stress variation (Papatheodorou 2005), (Lescalier 2002), (Sorsa et al, 2011).

The present study reports results obtained in grinding of electroplated chromium coatings on a steel substrate 300M (a high strength steel substrate obtained after thermal treatment). Although the grinding concerns only the chromium coating.

Several tests were performed to achieve various levels of heat transfer across the coating. The main operating parameters are the wheel speed, the workpiece speed and the depth of cut. After each test, chromium coating and substrate have been characterized using mechanical analysis and microstructural analysis or observations : optical microscopy coupled with hardness measurement, SEM for the observation of crack and grain morphology, XRD for residual stresses and crystallographic texture analysis, Nital etching and Barkhausen noise for metallurgical transformation). Some of these analysis are applied to the substrate and/or to the coating, depending on the measured property.

For the chromium coating, the main result is a clear description of a chromium burned surface. High stresses and crystallographic texture gradient are observed depending on the grinding conditions. Supported by

microstructural observations, thermally and mechanically sub-surface are observed.

For the 300M steel substrate, damage were observed even in the substrate according to the grinding condition. The various characterization tools have been used to characterize the damage of the substrate. Transverse microscopy observation shows the influence of the heat flux through the coating : mainly reduction or increase in hardness or over-tempering of the material and metallurgical change such martensitic transformation.

To support these tests and to explain the observed variation both in metallurgical changes and hardness values, finite element simulations were conducted to understand the spread of the heat flux and the to correlate temperature variations with the observed states of the material. These simulation are conducted using FEM analysis and are based on the moving heat source (Lefebvre, 2012).

## References

- Lescalier, C., Arzur, J., Martin, P. & Bomont, O. (2002). Interactions pièce–outil–machine en rectification. Détermination rationnelle du domaine de fonctionnement. *Mécanique & Industries*, 3(4), 351–360.
- Papatheodorou, T. & Hannifin, P. (2005). Influence of hard chrome plated rod surface treatments on sealing behavior of hydraulic rod seals, *Sealing Technology* (April), 5–10.
- Sorsa, A., Leiviskä, K., Santa-aho, S. & Lepistö, T. (2012). Quantitative prediction of residual stress and hardness in case-hardened steel based on the Barkhausen noise measurement, *NDT & E International*, Vol 46, 100-106.
- Lefebvre, A., Lanzetta, F., Lipinski, P., Torrance, A.A. (2012) Measurement of grinding temperatures using a foil/workpiece thermocouple, *International Journal of Machine Tools and Manufacture*, Vol 58 (July), 1-10.

## Orthogonal machining of a Cu-1.8wt%Be-0.1wt%Co alloy: influence of the microstructure

ALBAN DE SAEVER, ALBERT TIDU

LEM3 - Laboratoire d'Etude des Microstructures et de Mécanique des Matériaux, Metz, France

Elucidating the effect of microstructure is one of the main challenge in the field of material machining removal (Leopold, 2014). For this purpose, copper-beryllium samples with different microstructures has been submitted to orthogonal cutting. The results show the microstructure impact on the mechanical behaviors during the cutting process.

Studies on the mechanisms that rule the age-hardening of a C17300 (Cu-1.8wt%Be-0.1wt%Co) alloy using cold-working and/or specific heat treatments highlighted the sequence of precipitation. Earliest developments showed equivalent sequences (G.P. zones  $\rightarrow \gamma'' \rightarrow \gamma' \rightarrow \gamma$ ) for many authors (Geisler, 1952 - Bonfields, 1974) but reported distinct crystallographic structures. Latest developments (Monzen, 2012) clarified those observations and described the accurate following sequence (G.P. zones  $\rightarrow \gamma'' \rightarrow \gamma'_1 \rightarrow \gamma_1 + \gamma' \rightarrow \gamma$ ) by combining results from heat treatments and stress-assisted nucleation.

Strength hardening of C17300 alloys is mainly dependent on the ageing time and cold-working. By adjusting the couple cold-working (cold-rolling from 0 up to 1.61 true strain)/duration of heat treatment (0 up to 1 hour at constant temperature 573K), 5 samples with different microstructures with equivalent hardness (350 HV20) have been manufactured. A very detailed multi-scale analysis (SEM-TEM-XRD) on those samples showed that various microstructures were present in terms of phases, grain size and particles or plate-like topology. SEM observations revealed that the domain size of inter-granular  $\gamma$ -phase decrease drastically respect to the increase of initial deformation. Even if morphologies of intra-granular phases are always coherent plate-like precipitates, TEM observations showed their distribution, length and width were variable with different thermo-mechanical treatments. Phases quantification were done through X-Ray Diffraction and crystallographic texture of the solid solution  $\alpha$ -CuBe were obtained by EBSD analysis.

Using homemade carbide tools with cutting edge radius under 2  $\mu\text{m}$ , true orthogonal machining on samples with equivalent hardness and different microstructures has been achieved for a unique cutting geometry and

cutting speed (1  $\text{m}\cdot\text{s}^{-1}$ ), but for multiple depths of cut in a range from 2 to 40  $\mu\text{m}$ . A Kistler dynamometer table was used to measure cutting forces. The friction coefficient (Tangent Force / Normal Force) was deduced for each material. As a result, for an increase of prior deformation, the friction coefficient decrease until a minimum value. This trend is clearly noticeable for micro-cutting, and is stronger for an increase of depth of cut. Orthogonal cutting produced serrated continuous chips for each material. SEM observations of the serrated chips show adiabatic shear bands, cracks and drastic changes of the phases composition (confirmed by TEM observations), these observations are clearly dependent on the cutting conditions.

Temperature measurement using a special device including intrinsic thermocouple has shown that temperature rise near the cutting edge tool is about 1050K.

The results highlight that the observed differences during orthogonal cutting are directly correlated to the initial microstructure and its evolution during cutting. A model including the mechanical behavior of the initial strengthened material and the topology of the platelets, in conjunction with thermal reversion is proposed in view to explain the observed trend.

### References

- Leopold, J. (2014): Approaches for modelling and simulation of metal machining – a critical review, *Manufacturing Rev.* 2014, 1, 7
- Geisler, A. H., Mallery, J. H. & Steigert, F. E. (1952): On the Mechanism of Precipitation In Copper-Beryllium Alloys - *Journal of Metals*, March 1952, 307-316; *Transaction AIME*.
- Bonfields, B. & Edwards, B. C. (1974): Precipitation hardening in Cu 1.81 wt% Be 0.28 wt% Co - *Journal of Materials Science* 9, 1974, 398-408; Chapman and Hall Ltd.
- Monzen, R., Okawara, S. & Watanabe, C. (2012): Stress-assisted nucleation and growth of  $\gamma''$  and  $\gamma'$  precipitates in a Cu-1.2 wt% Be-0.1 wt% Co alloy aged at 320°C - *Philosophical Magazine*, Vol. 92, No.14, 11 May 2012, 1826-1843; Taylor&Francis.

Talks Topic E 6:

***Size effects and small-scale mechanical behavior of materials***

---

## Grain size gradient-induced work hardening and extraordinary ductilization

XIAOLEI WU <sup>1</sup>, YUNTIAN ZHU <sup>2</sup>

<sup>1</sup>State Key laboratory of Nonlinear Mechanics, Institute of Mechanics, Chinese Academy of Sciences, Beijing, China

<sup>2</sup>Department of Materials Science and Engineering, North Carolina State University, Raleigh, USA

Strain hardening is critical for structural materials to secure desired ductility, especially for high-strength metals that often suffer from poor ductility. Here we report that the gradient nano-grained (GNG) surface layers sandwiching a coarse-grained core render an extra strain hardening. The grain size gradient in the nano-micro-scale induced a notable strain gradient under tension that converts the applied uniaxial stress to multi-axial stresses. Thereby the accumulation and interaction of dislocations are promoted in the GNG layers, resulting in an extra hardening and an obvi-

ous strain hardening rate up-turn. Such a unique extra strain hardening inherent to the GNG structures, which does not exist in homogeneously-structured materials, provides a novel strategy to develop strong-and-ductile materials by architecting heterogeneous nanostructures. The work uncovers the intrinsic large uniform tensile elongation of the nanostructures and paves the way toward a combination of high strength and good ductility for their structural application.

## Mechanical properties and microstructural changes of high strength AA7075 alloy during low temperature ECAP

SEBASTIAN FRITSCH, MARIO SCHOLZE, MARTIN F.-X. WAGNER

TU Chemnitz, Institute of Materials Science and Engineering, Germany

High strength aluminum alloys are generally hard to deform. Therefore, the application of conventional severe plastic deformation methods to generate ultrafine-grained microstructures and to further increase strength is considerably limited. In this study, we explore cryogenic deformation in a custom-built, cooled equal channel angular pressing (ECAP) tool (internal angle 90°) as an alternative approach to severely plastically deform a 7075 aluminum alloy. We characterize the mechanical behavior and the microstructure of the coarse grained base material at different low temperatures, and we analyze how a tendency for the PLC-effect and the strain hardening rate affect the formability during subsequent severe plastic deformation at low temperatures. We also demonstrate that low-temperature ECAP followed by suitable heat treatments results in increases of the attainable degree of deformation, strength and ductility. We show how pre-aging treatments at room temperature prior to ECAP can be used to influence the grain refinement process. Finally we

demonstrate how these thermo-mechanical processes affect the microstructure and the mechanical behavior of the resulting materials under high strain rates. Our results highlight the potential of forming at low temperatures to produce high-strength aluminum alloys with improved properties after severe plastic deformation.

### References

- Fritsch, S., Hunger, S., Scholze, M., Hockauf, M. & Wagner, M. F.-X. (2011): Optimisation of thermo mechanical treatments using cryogenic rolling and aging of the high strength aluminum alloy AlZn5.5MgCu (AA7075). – In: *Materialwissenschaft und Werkstofftechnik*, 42: 573-579, Weinheim
- Fritsch, S., Scholze, M. & Wagner, M. F.-X. (2012): Cryogenic forming of AA7075 by Equal-Channel Angular pressing. – In: *Materialwissenschaft und Werkstofftechnik*, 43: 561-566, Weinheim

## Effect of creep and aging on the precipitation kinetics of an Al-Cu-Alloy after ECAP

MARKUS HÄRTEL<sup>1</sup>, KEVIN G. ABSTOSS<sup>2</sup>, SWETLANA WAGNER<sup>1</sup>, PHILIPP FRINT<sup>1</sup>, PETER MAYR<sup>2</sup>, MARTIN F.-X. WAGNER<sup>1</sup>

<sup>1</sup>TU Chemnitz, Institute of Materials Science and Engineering, Germany

<sup>2</sup>Professorship of Welding Engineering, TU Chemnitz, Germany

Recent work has shown that severe plastic deformation processes such as equal-channel angular pressing (ECAP) or high pressure torsion accelerate the precipitation kinetics of Al-Cu-alloys. In this study, we analyze how a combination of mechanical load, aging time and aging temperature affects the precipitation kinetics of an AA2017 alloy after ECAP. After solution annealing, the material is deformed in one pass in a 120° ECAP tool at 140°C. Compressive creep tests (which represent a combination of mechanical load, aging time and aging temperature) are performed on the initial (pre-ECAP) condition and on the ECAP-deformed material, and the resulting microstructures are compared using electron microscopy. To differentiate between the effects of mechanical loads, (aging) temperatures and times, the experimental parameters are selected carefully: To investigate the influence of the mechanical load, stopped compressive creep tests are performed and compared with aging conditions (without any mechanical load) at the same temperature and after the same amount of time. By keeping, in another set of stopped compressive creep tests, time and load

constant, the influence of temperature is investigated. Special care is taken to characterize the types and morphologies of precipitates in the aged or crept samples using transmission electron microscopy. Our study shows that increasing mechanical loads accelerate the precipitation kinetics by increasing dislocation density (and thus providing more opportunities for nucleation of the precipitates). Temperature accelerates the precipitation kinetics as well and results in coarser precipitates. Different creep times can lead to the formation of two different regions in the microstructure: regions with only few coarsened S-phase precipitates, and regions with many, fine S-phase precipitates. This evolution into different microstructural zones can be directly related to the heterogeneity of ECAP deformation produced in a single pass. Our study provides important information on how creep and aging of SPD-deformed, thermodynamically instable Al-Cu-alloys affects their precipitation kinetics, and it indicates that applications of ultra-fine grained materials need to be limited to relatively narrow temperature windows.

## On shear localization in an SPD-processed Aluminum Alloy – Part 1: Microstructures and local mechanical properties

PHILIPP FRINT, STEFFEN PFEIFFER, MARTIN F.-X. WAGNER

TU Chemnitz, Professur Werkstofftechnik, Chemnitz, Germany

In this study, we report on the observation of heterogeneous microstructures after processing of the aluminum alloy 6060 by extrusion and subsequent equal-channel angular pressing (ECAP) at room temperature. A macroscopic, alternating structure of two types of bands is observed: shear bands carrying large amounts of deformation are located next to matrix bands that contain significantly less deformation. Scanning (SEM) and transmission (TEM) electron microscopy reveal an ultrafine-grained microstructure in the shear bands, while the microstructure of the matrix bands is characterized by a high fraction of low angle grain boundaries and dislocation cells. These characteristic microstructural features affect the local mechanical properties, which are found to be distinctly different for the two types of bands. Micro-hardness

measurements and nanoindentation jump-tests are performed to explore the characteristics of the deformation bands. In addition to different hardness values, caused by the different deformation induced strain hardening, the ultrafine-grained shear bands exhibit a considerably increased strain rate sensitivity (by a factor of more than 2) compared to the matrix bands. A comparison of the initial extruded microstructure with the ECAP-processed material reveals that simple shear deformation exclusively takes place within the shear bands while the matrix bands pass through the ECAP-die without getting sheared. This observation contradicts the simple theory of homogeneous simple shear during ECAP-processing; we propose a simple mechanical model describing the evolution of the band-structure, based on an alternating interplay of elastic and

plastic deformation inside the shear zone driven by local microstructure-dependent softening of the mate-

rial. In a companion presentation at this conference, we analyze this mechanical model in detail using nu-

## On shear localization in an SPD-processed Aluminum Alloy— Part 2: A simple model concept and FE simulation of the formation of alternating bands

STEFFEN PFEIFFER, PHILIPP FRINT, MARTIN F.-X. WAGNER

TU Chemnitz, Professur Werkstofftechnik, Germany

Equal-channel angular pressing (ECAP) is a method of severe plastic deformation that typically leads to a homogeneous simple shear deformation and that is used to produce ultrafine-grained microstructures. In some special cases, however, single ECAP passes result in the formation of heterogeneous microstructures; this was, for example, observed in a companion study where the formation of alternating types of shear and matrix bands were observed after ECAP of an aluminum alloy 6060. Both microstructural features and mechanical properties (determined by micro- and nanoindentation) demonstrate that the ECAP shear deformation is concentrated in shear bands, whereas the adjacent matrix band regions are hardly deformed. In this contribution, we present a simple mechanical model to rationalize how a discreet material volume can pass the shear zone of the ECAP die without accumulating significant amounts of plastic shear deformation, and how this process results in the alternating formation of matrix and shear band regions. Using 2D finite element

(FE) simulations with an elasto-plastic material model, we identify engineering factors that directly influence the local deformation behavior. Our model predicts that, prior to reaching the yield stress, a well-defined material volume passes through the shear zone simply by elastic deformation – and this process results in the formation of matrix bands adjacent to the shear bands. We analyze how varying inner channel radii and cross sectional areas of the ECAP billet affect displacement-, strain-, strain-rate- and stress-fields in the shear zone. Our results show that the largest equivalent stresses arise at the inner-channel corner, where consequently the formation of shear bands is triggered. Increasing inner-channel radii lead to larger elastic displacements and to wider matrix bands, and the predictions on shear band morphologies and dimensions are in good agreement with our experimental observations. These results contribute to a more detailed understanding of the locally heterogeneous deformation of pre-extruded or heavily work hardened materials during ECAP.

Talks Topic E 7:

***Size effects and small-scale mechanical behavior of materials***

---

## Bio-inspired, self-assembled functionalized Fe<sub>3</sub>O<sub>4</sub> nanoparticles with tunable mechanical properties

GEROLD A. SCHNEIDER<sup>1</sup>, AXEL DREYER<sup>1</sup>, ARTUR FELD<sup>2</sup>, EZGI YILMAZ<sup>1</sup>, ANDREAS KORNOWSKI<sup>2</sup>, TOBIAS KREKELER<sup>3</sup>, HESHMAT NOEI<sup>4</sup>, MARTIN RITTER<sup>3</sup>, ANDREAS STIERLE<sup>4</sup>, HOSRT WELLER<sup>2</sup>

<sup>1</sup>Institute of Advanced Ceramics, Hamburg University of Technology, Germany

<sup>2</sup>Institute of Physical Chemistry, University of Hamburg, Germany

<sup>3</sup>Electron Microscopy Unit, Hamburg University of Technology, Germany

<sup>4</sup>Research Group X-ray Physics and Nanoscience, Deutsches Elektronen-Synchrotron DESY and Physics Department, University of Hamburg, Germany

Nature's hard tissues are typically hierarchical materials with a brick and mortar like structure consisting of hard minerals surrounded by soft organic matter. In nature or enamel the organic content is as low as 15 Vol.% or even less, which makes these biological materials very hard and stiff while retaining an amazing toughness. It seems that one of the keys of this design concept is based on nature's ability to build up its materials from nanometer sized minerals. We therefore applied

this principle to self-assembled 10-20nm – sized Fe<sub>3</sub>O<sub>4</sub> particles functionalized with short ligands. By changing the organic ligands it is possible to tune the strength and elasticity of these hybrid-materials in ranges where they compete with metals and polymers. The cross-linking and grafting of the molecules was evaluated by XPS and FTIR measurements. The arrangement of the particles in grain-like superstructures was investigated by SAXS and TEM measurements.

## *In situ* SEM compression tests of layered crystals

PETER SCHWEIZER, FLORIAN NIEKIEL, ERDMANN SPIECKER

Center for Nanoanalysis and Electron Microscopy (CENEM), University of Erlangen-Nürnberg, Erlangen, Germany

Layered crystals have gained a lot of attention in materials science in the recent years due to their quasi two-dimensional structure which gives rise to a plethora of outstanding properties. Certainly the most well-known example for such a material is graphite which can be broken up into its single layers known as graphene<sup>1</sup>. Another class of materials that is similar in structure and can also be exfoliated into single layers are the transition metal dichalcogenides, which show many extraordinary properties such as semiconductivity, superconductivity or the formation of charge density waves<sup>2</sup>. Besides the electronic properties, the mechanical properties of layered crystals are highly intriguing because they show an extreme case of anisotropy. The strong inner-layer bonds are in stark contrast with the weak van-der-Waals type interlayer bonds. This results in extreme strength for single layers, as it was shown for graphene with a Young's modulus of up to 1 TPa<sup>3</sup>, while at the same time making a bulk sample comprised of many layers very deformable through the mechanism of basal slip. One technological application that arises due to these properties is solid lubrication<sup>4</sup>. A deeper understanding of the exact mechanisms of basal slip and the quantification of the forces necessary to induce slip is required for future applications of layered crystals in advanced mechanical devices.

In this work we present a method to test the slip of basal planes in layered crystals on the example of graphite and vanadium diselenide (VSe<sub>2</sub>). A modified version of the established micro-pillar compression test introduced by Uchic et al.<sup>5</sup> was established that uses the inclination angle of the pillars to achieve the desired crystallographic orientation of the material relative to the compression axis. An FEI Helios Nanolab 660 DualBeam has been used for both sample preparation and *in situ* compression of the studied pillars. The indentations were performed *in situ* enabling a deeper analysis of the deformation process. Force and displacement data was recorded using a combination of a spring table system and digital image correlation. During indentation slip along a single atomic interface was achieved consistently. TEM lamellas of deformed pillars have been prepared in cross-section and plan view of the slip interface to obtain further insights into the deformation behavior and characterize the damage induced into the material by the preparation with the focused ion beam. The presented method enables the quantification of the friction forces at a single atomic interface within a layered crystal. Further experiments will deal with more complex materials like the misfit layer compounds to also investigate the elusive effect of superlubricity at incommensurate interfaces.

## References

1. Novoselov, K. S. et al. Electric Field Effect in Atomically Thin Carbon Films, *Science* 306, 666–669 (2004).
2. Wang, Q. H. Kalantar-Zadeh, K. Kis, A. Coleman, J. N. & Strano, M. S. Electronics and optoelectronics of two-dimensional transition metal dichalcogenides, *Nature Nanotech* 7, 699–712 (2012).
3. Lee, C. Wei, X. Kysar, J. W. & Hone, J. Measurement of the Elastic Properties and Intrinsic Strength of Monolayer Graphene, *Science* 321, 385–388 (2008).
4. Winer, W. O. Molybdenum disulfide as a lubricant: A review of the fundamental knowledge, *Wear* 10, 422–452 (1967).
5. Uchic, M. D. Sample Dimensions Influence Strength and Crystal Plasticity, *Science* 305, 986–989 (2004).

## Acknowledgements

Financial support by the DFG via the research training group GRK 1896 “In situ microscopy with electrons, X-rays and scanning probes” is gratefully acknowledged.

## Material development for high-strength nanocomposites

ALMUT SCHROER, JENS BAUER, OLIVER KRAFT

Institute for Applied Materials, Karlsruhe Institute of Technology, Germany

Further development of materials with low density and high strength is of great interest for lightweight applications. Technical foams are highly porous materials which possess a very low density but at the same time only a low strength due to their random architecture. The macroscopic material properties of cellular materials are strongly influenced by the characteristics of their architecture. Moreover, if the dimensions of the cellular materials reach the nanoscale, the materials benefit of the mechanical size effect with an improved strength and should become less sensitive to flaws (Gao 2003).

Using 3D direct laser writing in combination with atomic layer deposition (ALD), the fabrication of alumina-polymer composites with 3D microarchitecture has been demonstrated (Bauer 2014). The composites are constructed as polymer microstructures with diameters of 0.5-1.0  $\mu\text{m}$ , coated with thin layers of aluminum oxide within the range of 10 to 100 nm. In this way, it was possible to exploit both the structural advantage of ordered frameworks with optimized architecture and the size-dependent strengthening effect. As a result, the nanocomposites exceed the strength-to-weight ratio of other engineering foams. However, the potential for improving the strength of such structures by using different coating materials and coating techniques as well as by further treatments of the polymeric microstructures after the laser writing step, has not been examined.

It is the aim of the work to improve the strength of the nanocomposites due to further development of the used materials. Nanoindentation measurements on thin films of different ceramic ALD coatings on Si

substrates have been performed in order to determine Young's modulus and hardness of the ALD coatings. For instance, the Young's modulus of a 100 nm thick alumina film was determined to be 171 GPa with a standard deviation of 12 GPa, and the hardness to be 12.2 GPa with a standard deviation of 1.5 GPa, respectively. Obviously, the measured modulus is well below that of bulk alumina but in line with earlier measurements of ALD coatings (Tripp 2006). Promising coating materials are further examined using a novel technique based on push-to-pull structures, which are fabricated in the same manner as the composites themselves. The test structures allow for tensile tests of the nanocomposites. The whole specimens are manufactured in one direct laser writing step. First results show increasing strength for decreasing alumina layer thickness between 10 and 100 nm. Also, the role of the thermal treatment of the polymeric microstructures during ALD is examined.

## References

- Gao, H. et al. (2003): Materials become insensitive to flaws at nanoscale: Lessons from nature. – *Proc. Natl. Acad. Sci.* 100 (10): 5597-5600; USA
- Bauer, J. et al. (2014): High-strength cellular ceramic composites with 3D microarchitecture. – *Proc. Natl. Acad. Sci.* 111 (7): 2453-2458; USA
- Tripp, M. K. et al. (2006): The mechanical properties of atomic layer deposited alumina for use in micro- and nano-electromechanical systems. – *Sensors and Actuators A* 130-131: 419-429

# Mechanical behavior of ultrathin aluminum oxide films: Influence of open or closed porosity

A. VAN DER REST, F. HENRY, A. FAVACHE, J. PROOST, Q. VAN OVERMEERE, T. PARDOEN

Institute of Mechanics Material and Civil Engineering, Université Catholique de Louvain, Belgium

Native Al<sub>2</sub>O<sub>3</sub> affects the mechanical response of metallic Al thin films. However, the lack of knowledge regarding the dependence of intrinsic stiffness, strength and ductility of Al<sub>2</sub>O<sub>3</sub> on its microstructure and of the complex mechanical behavior of the Al/Al<sub>2</sub>O<sub>3</sub> interface limits the understanding and control of the mechanical reliability of Al thin films. [1]

In this research, we first explore the dependence of the mechanical properties of Al<sub>2</sub>O<sub>3</sub> films on its microstructure, focusing on the effect of porosity. Ultrathin Al<sub>2</sub>O<sub>3</sub> films encompassing a range of characteristic porosities were produced by reactive magnetron sputtering (random closed porosities) and anodic oxidation (ordered porosities) as illustrated in figure 1.

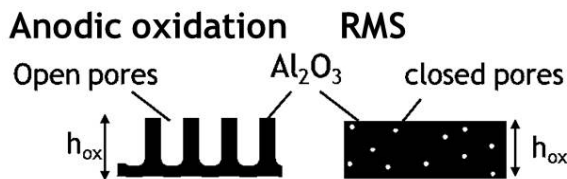


**Fig. 1:** Two processes are used to produce ultrathin Al<sub>2</sub>O<sub>3</sub> thin films: the anodic oxidation produces films with open ordered porosities and the reactive magnetron sputtering produces films having random closed porosities.

The Young's modulus of the films was determined by nano-indentation and compared to the stress strain response characterized with "on-chip" uniaxial nanomechanical testing [2] (see figure 2), providing additional insights on fracture. The Young's modulus measured by on-chip testing are in good agreement with the values obtained by nano-indentation. Considering for instance films with random closed porosities, the Young's modulus decrease with increasing deposition pressure

correlates with the increasing porosity of the films. The stress to failure also decreases with increasing porosity. The precise influence of open porosity fraction and pore dimensions on the Young's modulus and stress to failure will be presented. Differences between open and closed porosities will be highlighted.

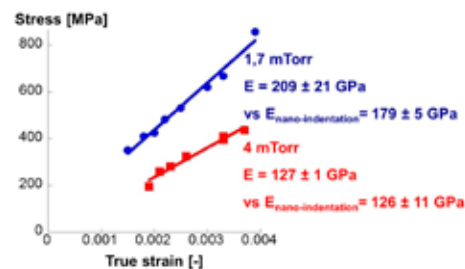


**Fig. 2:** Stress-strain response of the Al<sub>2</sub>O<sub>3</sub> thin films produced by reactive magnetron sputtering at different deposition pressures, characterized with the "on-chip" uniaxial nanomechanical testing.

We will further consider how controlling the porosity allows to design mechanically robust multilayered Al/Al<sub>2</sub>O<sub>3</sub> applications. The first investigations, using nano-indentation, regarding the strength and ductility of Al/Al<sub>2</sub>O<sub>3</sub> thin multilayers with various thickness ratios will be presented and compared to thin films of Al and Al<sub>2</sub>O<sub>3</sub>.

## References

- [1] A. T. Alpas, J. D. Embury, D. A. Hardwick, R. W. Springer, *J. Mater. Sci.* 25, 1603 (1990).
- [2] S. Gravier, M. Coulombier, A. Safi, N. André, A. Boe, J.-P. Raskin, T. Pardoën, *J. Microelectromech. Syst.* 18, 555 (2009).

# Influences of vacancy defects on compressive behaviors of open-tip carbon nanocones

MING-LIANG LIAO

Department of Aircraft Engineering, Air Force Institute of Technology, Taiwan

Since carbon nanocones (CNCs) have similar structures and properties to those of carbon nanotubes (CNTs), applications of such nanomaterial have developed considerably in recent years (Tagmatarchis 2012). While there is considerable achievement in studies of mechanical behaviors of CNCs, studies on mechanical behaviors of CNCs with defects (such as vacancy defects) are deficient. This topic is very important as the practical applications of CNCs are explored largely. Moreover, defects in CNCs can appear at the stage of their growth/purification as well as during their device production, and can be created deliberately by chemical treatments or by irradiation to achieve desired functionalities, as those occurring in CNTs (Andrews et al. 2001; Ni and Sinnott 2000). Therefore, it is worthy to understand influences of defects on mechanical behaviors of CNCs. In contrast to the plentiful studies on mechanical behaviors of CNTs with defects, investigations into this topic for CNCs are rare in the available literature. To fill in this deficiency and provide some information for the practical applications of CNCs, this paper extended the author's previous studies (Liao et al. 2011; Liao 2014) to examine influences of vacancy defects on compressive behaviors of open-tip CNCs. Effects of vacancy location and temperature on the compressive behaviors were inspected in this study. This study investigated influences of vacancy defects on compressive behaviors of open-tip carbon nanocones (CNCs) by molecular dynamics simulations. Effects of vacancy location and temperature on the compressive behaviors were examined in the study. Some interesting findings were attained from the investigations. It was noticed that the CNC with an upper vacancy has comparable degradation in the critical

strain and in the critical load with the CNC with a middle vacancy, whereas the CNC with a lower vacancy has lower degradation in the anti-buckling ability than the above two CNCs. The anti-buckling ability of the CNCs reduces with the growth of the temperature. This temperature effect is much apparent in the perfect CNC than in the vacancy-defect CNCs. It was also observed that the degradation in the anti-buckling ability is obvious at a lower temperature, but it decreases as the temperature grows. Besides, all the CNCs (including the perfect and the vacancy-defect CNCs) exhibited a shrinking/swelling buckling mode shape at the studied temperatures. Existence of the vacancies did not alter the buckling mode shape of the CNCs.

## References

- Andrews, R., Jacques, D., Qian, D., and Dickey, E. C. (2001): Purification and structural annealing of multiwalled carbon nanotubes at graphitization temperatures. *Carbon*, 39: 1681-1387.
- Liao, M. L., Cheng, C. H., and Lin, Y. P. (2011): Tensile and compressive behaviors of open-tip carbon nanocones under axial strains. *J. Mater. Res.*, 26: 1577-1584.
- Liao, M. L. (2014): Buckling behaviors of open-tip carbon nanocones at elevated temperatures. *Appl. Phys. A*, 117: 1109-1118.
- Ni, B. and Sinnott, S. B. (2000): Chemical functionalization of carbon nanotubes through energetic radical collisions. *Phys. Rev. B*, 61: R16343.
- Tagmatarchis, N. (editor) (2012): *Advances in Carbon Nanomaterials: Science and Applications*. Pan Stanford Publishing.

TalksTopic E 8:

***Size effects and small-scale mechanical behavior of materials***

---

## Size Effect of Single Crystalline Noble FCC Metal Nanowires

IN-SUK CHOI

Thigh Temperature Energy Materials Research Center, Korea Institute of Science and Technology, Seoul, Republic of Korea

Researchers have known for some time that smaller is stronger for both nanocrystalline materials, and more recently one-dimensional (1D) nanostructures such as nanowires. However, an elusive but fundamentally important goal is to find 1D nanostructures that are both strong and ductile. In this work, we demonstrate how surface effects enable this important combination of properties by experimentally applying tensile deformation to rhombic cross section Au, Pd and AuPd nanowires that have a  $\langle 110 \rangle$  orientation and four bounding  $\{111\}$  transverse surfaces. We show that high ductility, and fracture strains of about 50% are obtained through a geometric reorientation of the cross section from

rhombic to square through long-ranged, coherent twin propagation, which occurs by a concurrent reorientation of the bounding surfaces from  $\{111\}$  to  $\{100\}$ . Importantly, the ductility is not reduced with an increase in strength, where both the nanowire yield and twin propagation stresses increase with decreasing nanowire diameter. A simple surface energy differential model is found to capture the inverse diameter-dependence of the twin propagation stress, further highlighting the importance of surface effects in enhancing the size-dependent mechanical behavior and properties of metal nanowires.

## Mechanical Behavior of Fivefold Twinned Nanowires understood from Anisotropic Elasticity

FLORIAN NIEKIEL<sup>1</sup>, ERDMANN SPIECKER<sup>1</sup>, ERIK BITZEK<sup>2</sup>

<sup>1</sup>Center for Nanoanalysis and Electron Microscopy (CENEM), Friedrich-Alexander-Universität Erlangen-Nürnberg, Erlangen, Germany

<sup>2</sup>Department of Material Science and Engineering, Friedrich-Alexander-Universität Erlangen-Nürnberg, Erlangen, Germany

Metallic nanowires are currently attracting a lot of interest. On the one hand they show promising electrical, optical and mechanical properties for applications in transparent electrodes and flexible electronics, on the other hand they represent an ideal model system to challenge our understanding of the relation between microstructure and mechanical properties. Most metallic nanowires grown from wet chemical synthesis exhibit a distinctive fivefold twinned microstructure consisting of five segments sharing a common  $[110]$  direction along the nanowire axis and joined by twin boundaries in cross sectional direction. The remaining gap of  $7.35^\circ$  is closed by strain corresponding to a central positive partial wedge disclination.

In this work atomistic simulations and finite element analysis are employed to elucidate the fundamental difference in the mechanical properties of fivefold twinned nanowires compared to their single crystalline counterparts. To achieve this, size effects due to surface stresses and different surface stiffness are carefully analyzed and discriminated from the size-independent elastic response.

Our main result is that the microstructural constraint of the fivefold twinned microstructure leads to an elastic response of these nanowires that is fundamentally different from the elasticity of single crystalline nanowires.

This size-independent effect can be readily understood from theoretical considerations based on anisotropic elasticity. We develop a simple analytical model which correctly describes the systematic trend seen in the change of elastic modulus of fivefold twinned nanowires simulated for different materials (Al, Au, Ni, Ag, Cu).

Moreover, our results show that also the plastic deformation of fivefold twinned nanowires is to a large degree influenced by anisotropic elasticity. Depending on the material, the fivefold twinned microstructure can lead either to an increase or decrease of the yield stress compared to single crystalline nanowires. In simulations of tensile tests a change of the failure mechanism to void formation instead of necking can be observed depending on the anisotropy factor of the material. In compression tests structural dislocations are found to relieve the intensifying stress state due to the disclination. The different deformation mechanisms and yield stresses can be readily explained using the developed analytical model.

### Acknowledgments

Financial support by the DFG via research training group GRK 1896 is gratefully acknowledged.

## Mechanical properties of nano-twinned Ag wires

AARON KOBLER<sup>1,2</sup>, THORSTEN BEUTH<sup>3</sup>, TOBIAS KLÖFFEL<sup>4,5</sup>, MARKUS MOOSMANN<sup>1,6</sup>, HORST HAHN<sup>1,2</sup>, CHRISTIAN KÜBEL<sup>1,7</sup>, BERND MEYER<sup>4</sup>, ERIK BITZEK<sup>5</sup>, THOMAS SCHIMMEL<sup>1,6</sup>

<sup>1</sup>Institute of Nanotechnology (INT), Karlsruhe Institute of Technology (KIT), Germany

<sup>2</sup>Joint Research Laboratory Nanomaterials (KIT and TUD), Technische Universität Darmstadt (TUD), Germany

<sup>3</sup>Institute for Information Processing Technologies, Karlsruhe Institute of Technology (KIT), Germany

<sup>4</sup>Interdisciplinary Center for Molecular Materials (ICMM) and Computer-Chemistry-Center (CCC), Friedrich-Alexander-Universität Erlangen-Nürnberg (FAU), Erlangen, Germany

<sup>5</sup>Materials Science & Engineering, Institute I, Friedrich-Alexander-Universität Erlangen-Nürnberg (FAU), Erlangen, Germany

<sup>6</sup>Institute for Applied Physics, Karlsruhe Institute of Technology (KIT), Germany

<sup>7</sup>Karlsruhe Nano Micro Facility (KNMF), Karlsruhe Institute of Technology (KIT), Germany

The production and investigation of nano wires is a vivid topic, as nano wires exhibit superior mechanical properties such as high tensile strength<sup>1</sup>. These properties make them a perfect candidate for applications in micro-mechanical systems (MEMS). For bulk materials, it is well known that a decreased grain size results in an increased material's strength (Hall-Petch relation (HP))<sup>2</sup>. Introducing nanotwins into a material can increase the ductility while maintaining a high strength<sup>3</sup>. On the other hand, little is known about tuning the microstructure of nanowires (NW). Calculations on twinned Cu NWs showed that the strengthening effects seen in bulk materials can be transferred to NWs. However, the strengthening effect is highly shape and microstructure dependent<sup>4</sup>.

Here, we present Ag NWs with twin planes parallel to the wire long  $\langle 112 \rangle$  axis. A model for the growth mechanism is suggested to explain the observed  $\langle 112 \rangle$  growth direction. The mechanical properties of individual NWs are investigated using tensile, bending and indentation experiments. The tensile experiments revealed increased yield strength in comparison to the bulk. The plastic deformation behavior in indentation tests is highly orientation dependent due to the twin boundaries. The interaction differences between the

glide systems active in fcc metals and the stress direction are discussed to explain indentations orthogonal ( $\langle 111 \rangle$  direction) or parallel ( $\langle 110 \rangle$  direction) to the twin boundaries. Furthermore, density functional theory and atomistic calculations were performed as a reference for the NWs and showed no influence of the twin boundaries on the Yong's modulus in direction of the wires axis.

### References

1. Weinberger, C. R. & Cai, W. Plasticity of metal nanowires. *J. Mater. Chem.* 22, 3277 (2012).
2. Meyers, M. A., Mishra, A. & Benson, D. J. Mechanical properties of nanocrystalline materials. *Prog. Mater. Sci.* 51, 427–556 (2006).
3. Stukowski, A., Albe, K. & Farkas, D. Nanotwinned fcc metals: Strengthening versus softening mechanisms. *Phys. Rev. B* 82, 1–9 (2010).
4. Zhang, Y. & Huang, H. Do Twin Boundaries Always Strengthen Metal Nanowires? *Nanoscale Res. Lett.* 4, 34–38 (2009).

## Influence of artificial defects on the mechanical behavior of Au nanowires

CHARLOTTE ENSSLEN<sup>1</sup>, CHRISTIAN BRANDL<sup>1</sup>, GUNTHER RICHTER<sup>2</sup>, OLIVER KRAFT<sup>1</sup>

<sup>1</sup>Karlsruhe Institute of Technology, Germany

<sup>2</sup>Max Planck Institute for Intelligent Systems, Stuttgart, Germany

Nanostructured materials are of interest for both fundamental scientific and applied research which can be ascribed to their outstanding mechanical properties, e.g. Au nanowires can exhibit high strength (of the order of the ideal strength) and ductility (Sedlmayr et al. 2012). In general, it can be observed that a decrease in the sample dimension results in an increase in strength known as mechanical size effect (see for review, e.g., Kraft et al. 2010). However, data considering the mechanical properties of nanostructures with dimensions smaller than 100 nm are still rare and the corresponding deformation mechanisms and the influence of the microstructure, e.g. inherent defects, on the strength has not been studied comprehensively. In order to develop a profound understanding of the role of defects for the deformation mechanisms of single crystalline Au nanowires, we make use of a helium ion microscope. It offers the possibility to modify nanostructures by altering the surface characteristics or creating nanopores in the nanowire prior to mechanical testing. In-situ tensile tests of modified Au nanowires containing nanopores were performed in an SEM chamber. The simultaneous observation of the specimens upon testing allows an image-based strain measurement and the characterization of the fracture sites after testing.

The deformation behavior and microstructural evolution was further investigated by post-mortem TEM analysis. Additionally, the experimental work is supported by molecular dynamics (MD) simulations. The data indicate that the measured strength of the nanowires is not changed for pore sizes in the range of 25 nm and below. Plastic deformation takes place by the nucleation of partial dislocations and the formation of nanotwins and stacking faults. The plastic deformation zone extends over the whole length of the nanowire and is not localized at the nanopore. Nevertheless, final fracture of all nanowires occurred next to the nanopores. These experimental findings are consistent with the MD simulations.

### References

- Andreas Sedlmayr, Erik Bitzek, Daniel S. Gianola, Gunther Richter, Reiner Mönig, Oliver Kraft (2012): Existence of two twinning-mediated plastic deformation modes in Au nanowhiskers – *Acta Mater.* 60: 3985-3993.
- Oliver Kraft, Patric A. Gruber, Reiner Mönig, and Daniel Weygand (2010): Plasticity in confined dimensions. – *Annu. Rev. Mater. Res.* 40: 293-317.

## In-Situ Electromechanical Properties of ZnO Nanowires

SANJIT BHOWMICK, UDE HANGEN, DOUGLAS STAUFFER, SYED ASIF

Hysitron, Inc., Minneapolis, USA

One-dimensional structures such as nanowires and nanotubes are potential materials for future nanoelectronics, optoelectronics, piezoelectric devices, sensors, and actuators. Due to length scale effects and higher surface-to-volume ratios, nanostructures can exhibit superior mechanical and electrical, as well as other length scale dependent properties. In this work, strain-rate controlled tensile experiments were conducted on zinc oxide nanowires using an electrical push-to-pull (EPTP) device in the SEM and TEM. A source/measurement unit was used for DC current sourcing and voltage measurements in four-point probe mode. Voltage

sweeps at constant strain were performed to obtain I-V curves in order to extract electrical properties. Periodic stress or strain from the nanowires was generated by periodic variation of the applied voltage or current. The EPTP device is a MEMS-based uniaxial nanotensile test platform that has been designed for electromechanical characterization of one-dimension structures. In this presentation, strain-induced electronic mobility and piezoelectric response of ZnO will be addressed. The electronic properties of such nanowires and how these properties can be tailored by applying strain will also be discussed.

Talks Topic F 1:

# ***Advanced steels and steel composite materials***

---

## Mechanical Properties of a 0.2%C–1.5%Si–5%Mn TRIP-aided Annealed Martensitic Steels

KOHICHI SUGIMOTO, HIKARU TANINO

Shinshu University, Nagano, Japan

Impact toughness of a 0.2%C–1.5%Si–(1.5–5.0)%Mn transformation-induced plasticity (TRIP)-aided steels which were subjected to intercritical annealing and then isothermal transformation process after quenching was investigated for automotive applications. The microstructure of these steels composed of annealed martensite structure matrix and retained austenite of 10–40 vol%. The retained austenite fraction increased with increasing Mn content. 5%Mn steel possessed the

highest tensile strength and the largest total elongation by a TRIP effect of metastable retained austenite. However, the Charpy impact absorbed value was lower and ductile-brittle transition temperature was higher than those of 1.5%Mn steel. This was caused by lower retained austenite stability and easy grain boundary fracture by an addition of high Mn content, despite of a larger amount of metastable retained austenite of 40 vol%.

## Nano-laminate TRIP-TWIP steel with dynamic strain partitioning and enhanced damage resistance

C. C. TASAN, M-M. WANG, D. PONGE, D. RAABE

Max-Planck-Institut für Eisenforschung GmbH, Duesseldorf, Germany

Conventional martensitic steels have limited ductility due to insufficient microstructural strain hardening and damage resistance mechanisms. It was recently demonstrated that the ductility and toughness of martensitic steels can be improved without sacrificing the strength, via partial reversion of the martensite back to austenite [1].

These improvements were attributed to the presence of transformation-induced plasticity (TRIP) effect of the austenite phase, and the precipitation hardening (maraging) effect in the martensitic matrix. However, a full micro-mechanical understanding of this ductilizing effect requires a systematic investigation of the interplay between the two phases, with regards to the underlying deformation and damage micro-mechanisms.

For this purpose, in this work, a Fe-9Mn-3Ni-1.4Al-0.01C (mass %) medium-Mn TRIP maraging steel is produced and heat treated under different reversion conditions to introduce well-controlled variations in the austenite-martensite nano-laminate microstructure. Uniaxial tension and impact tests are carried out and the microstructure is characterized using scanning and transmission electron microscopy based techniques and post-mortem synchrotron X-ray diffraction analysis.

The results reveal that (i) the strain partitioning between austenite and martensite is governed by a highly dynamical interplay of dislocation slip, deformation-induced phase transformation (i.e. causing TRIP effect) and mechanical twinning (i.e. causing twinning-induced plasticity (TWIP) effect); and (ii) the nano-laminate microstructure morphology leads to enhanced damage resistance [2]. The presence of both effects results in enhanced strain hardening capacity and damage resistance, hence, the enhanced ductility.

The mechanical properties of the system is then further optimized by a cold rolling treatment which introduces austenitic zones of different stability, and hence, further enhanced strain hardening capacity.

### References

- [1] Wang, M-M, Tasan, C.C., Ponge, D., Kostka, A., Raabe, D., Smaller is less stable: size effects on twinning vs. transformation of reverted austenite in TRIP maraging steels, *Acta Materialia*, 79 (2014), 268-281.
- [2] Wang, M-M, Tasan, C.C., Ponge, D., Dippel, A-C., Raabe, D., Nano-laminate TRIP-TWIP steel with dynamic strain partitioning and enhanced damage resistance, *Acta Materialia*, 85 (2015) 216-228.

## Characterization of strain localizations during plastic deformation of TRIP/TWIP steels

ANJA WEIDNER, CHRISTIAN SEGEL, HORST BIERMANN

TU Bergakademie Freiberg, Institut für Werkstofftechnik, Germany

Modern high-alloy CrMnNi TRIP/TWIP steels exhibit either a deformation-induced martensitic phase transformation or mechanical twinning depending on the austenite stability and the stacking fault energy, which are influenced both by the chemical composition as well as by the deformation temperature. In the past, the individual deformation mechanisms were studied already intensively by comprehensive microstructural investigations using electron microscopy [1] or X-ray diffraction [2]. In addition, studies on the kinetics of these deformation processes were performed applying acoustic emission measurements [3]. Although, the mechanisms of the formation of  $\alpha'$ -martensite as well as the variant selection of  $\alpha'$ -martensite were investigated by numerous authors even by molecular dynamics simulations and the magnitude of shear for  $\epsilon$ -martensite/stacking faults and twins are known from theoretical considerations. Up to now the experimental determination of the individual local shear strain values associated with different mechanisms like  $\alpha'$ -nuclei or mechanical twins is still missing. An excellent method for the experimental determination of these individual strain levels is the performance of quasi *in situ* deformation experiments in a scanning electron microscope complemented by the application of the digital image correlation (DIC) technique on high-resolution SEM images of etched specimen surfaces giving perfect contrast conditions for an excellent pattern recognition. Tensile deformation experiments were performed at room and elevated temperature using a push-pull loading stage inside a field-emission SEM. The DIC-technique was used to evaluate local strain fields in the microstructure developing in dependence on the applied global strain. The areas of interest were analyzed after the tensile tests by electron backscattered-diffraction (EBSD) in order to characterize the developed

microstructure ( $\epsilon$ -martensite,  $\alpha'$ -martensite, twins etc.). The results of the image correlations show a significant difference in the formation of local strain fields depending on the primary deformation mechanism influenced by the chemical composition and the deformation temperature. Moreover, the magnitude of shear for individual constituents of the microstructure like deformation bands with stacking faults ( $\epsilon$ -martensite),  $\alpha'$ -martensite or mechanical twins were calculated. Furthermore, it is shown that the magnitude of shear of  $\alpha'$ -martensite islands depends significantly on their crystallographic orientation [4].

### References

- Biermann, H., Solarek, J. Weidner, A. (2012): SEM Investigation of high-alloyed austenitic stainless cast steels with varying austenite stability at room temperature and 100°C, *Steel research international* 83 (6) 512-520.
- Rafaja, D., Krbetschek, C., Ullrich, C., Martin, S. (2014): Stacking fault energy in austenitic steels determined by using in situ X-ray diffraction during bending, *J. Appl. Cryst.* 47 936-947.
- Vinogradov, A., Lazarev, A., Linderov, M., Weidner, A., Biermann, H. (2013): Kinetics of deformation processes in high-alloyed cast transformation-induced plasticity/twinning induced plasticity steels determined by acoustic emission and scanning electron microscopy: Influence of austenite stability on deformation mechanisms, *Acta Mater.* 61 2434-2449.
- Weidner, A., Segel, C., Biermann, H. (2015): Magnitude of shear of deformation-induced  $\alpha'$ -martensite in high-alloy metastable steel, *Mater. Lett.*, accepted.

## Temperature evolution during tensile straining of high Mn twinning induced plasticity (TWIP) steels

JEEHYUN KANG, TOBIAS INGENDAHL, WOLFGANG BLECK

Steel Institute, RWTH Aachen University, Germany

It is well known that the mechanical properties of high Mn austenitic steels are influenced by their stacking fault energy (SFE) which depends on the temperature as well as composition (Saeed-Akbari 2009 and 2012),

and determines the predominant deformation mechanisms such as TWinning Induced Plasticity (TWIP) and TRansformation Induced Plasticity (TRIP) (Saeed-Akbari 2012). During the deformation of a metal, 70-95%

of mechanical energy is dissipated as heat and the temperature increases accordingly (Zehnder 1990). Especially for high Mn austenitic steels where inhomogeneous deformation occurs at room temperature (Chen 2009), it is likely that the generated heat accumulates in a local region. It is expected that such temperature rise would influence SFE and may affect the deformation behaviour.

In this study, three high Mn austenitic TWIP steels (Fe29Mn0.4C, Fe22Mn0.5C, Fe24Mn0.7C, numbers in wt%) are uniaxially deformed by employing quasistatic tensile tests with infrared thermography at room temperature. When inhomogeneous deformation takes place, both global and local temperature evolutions are acquired and plotted with respect to the applied mechanical energy. The temperature evolution is compared with a Fe18Cr10Ni0.05C austenitic stainless steel, which shows homogeneous deformation behaviour. Finally, their SFEs were estimated according to the observed temperature change.

The investigated high Mn steels show different strength and ductility as well as the onset point of the inhomogeneous flow. During elastic deformation, a small decrease in temperature ( $\sim 0.1\text{--}0.2^\circ\text{C}$ ) is observed due to thermoelastic coupling. The decrement is inversely related to heat capacity of the steels. During plastic deformation, the global temperature is described as a function of the mechanical energy and does not depend on the composition among the high Mn steels. It gradually increases to  $\sim 40\text{--}45^\circ\text{C}$  during deformation. Once inhomogeneous deformation takes place, it is clearly detected in temperature profiles. The difference between local and global temperatures increases with the mechanical energy up to  $\sim 10^\circ\text{C}$  and does not depend on the composition. Comparing it with a

Fe18Cr10Ni0.05C steel, such temperature change is smaller in high Mn steels, possibly due to its higher heat capacity. The corresponding SFE change of the high Mn steels depends on the composition. The global and local temperature rise would result in a SFE change of only  $1\text{ mJm}^{-2}$  and  $2\text{ mJm}^{-2}$ , respectively, which is too small to influence the deformation mechanism.

In conclusion, temperature rises up to  $\sim 40\text{--}45^\circ\text{C}$  during the tensile deformation of high Mn steels. The temperature increase does not depend on the high Mn steel composition, while that of a Fe18Cr10Ni0.05C steel is higher, reaching up to  $\sim 65^\circ\text{C}$  due to necking. When inhomogeneous deformation occurs in high Mn steels, local temperature can reach up to  $55^\circ\text{C}$ . However, such increase results in  $1\text{--}2\text{ mJm}^{-2}$  increase in stacking fault energy, which is unlikely to affect the deformation mechanism.

#### References

- Saeed-Akbari, A. & Mosecker, L. & Bleck, W. (2012): Characterization and prediction of flow behaviour in high-manganese twinning induced plasticity steels: part I. mechanism maps and work-hardening behavior – In: *Metall. Mater. Trans. A*, 43A: 1688-1704.
- Saeed-Akbari, A. & Imlau, U. & Bleck, W. (2009): Derivation and variation in composition-dependent stacking fault energy maps based on subregular solution model in high-Mn steels – In: *Metall. Mater. Trans. A*, 40A: 3076-3090.
- Zehnder, A.T. (1991): A model for the heating due to plastic work – In: *Mech. Res. Comm.* 16, 23-28.
- Chen, L. & Kim, H.-S. & Kim, S.-K. & De Cooman B.C. (2009): Localized deformation due to Portevin-LeChatelier effect in 18Mn-0.6C TWIP austenitic steel – In: *ISIJ Inter.*, 47:1804-1812.

## Microstructure as well as mechanical and magnetic properties of Fe-based alloys with different contents of metastable austenite

MAREK SMAGA, DIETMAR EIFLER, TILMANN BECK

Institut of Materials Science and Engineering, University Kaiserslautern, Germany

Metastable austenitic microstructures can be achieved in steels due to alloying elements like Cr, Ni, Mn, Si and Al. Dependent on the amount of these elements and special heat treatments, advanced steels with a low content of retained metastable austenite ( $< 15\text{ vol.-%}$ ) - so called low alloyed TRIP steels, or fully austenitic steels - so called high alloyed TRIP/TWIP steels can be produced. Some low alloyed TRIP steels were included in the new German/European standard DIN-EN 10346.

The initial microstructure after heat treatment is mainly a ferritic-bainitic matrix with dispersed retained metastable austenite islands. The fully austenitic TRIP/TWIP steels are produced generally based on two alloying concepts: 1st: Cr-Ni-concept for corrosion resistant stainless steels (18 % Cr / 10 % Ni) and 2nd: Mn-Si-Al-concept for new, advanced austenitic steels, where a large variance in chemical composition exists and sometimes an addition of Cr and Ni is used. Depending

on the chemical composition and consequently varying stacking fault energy in the metastable fully austenitic steels the TWIP-effect occurs along or instead of the TRIP-effect. In this contribution the microstructure as well as mechanical and magnetic properties of three types of metastable austenitic steels: (1) low alloyed, (2) Cr-Ni and (3) Mn-Al-Si are presented and discussed. The monotonic deformation behavior and magnetic properties of all investigated materials were characterized by stress-strain-measurements as well as in-situ-measurements of magnetic data using a Feritscope® and Hall-Probe during tensile tests. Additionally stress controlled fatigue tests specimens with measurements of stress and magnetic data were performed on Cr-Ni steel. The monotonic and cyclic plastic deformation of metastable austenite leads to a phase transformation from paramagnetic austenite into ferromagnetic  $\alpha'$ -martensite. Furthermore, according to the Villari effect (Villari 1865) the change in the magnetic induction due to deformation of ferromagnetic phases was measured. Both results, the martensite fraction and the change in the magnetic induction can be used for the estimation of the actual fatigue state using magnetic measurements (Smaga, M., Eifler, D. 2009). Figure 1 shows the change in the magnetic induction during random fatigue loading of AISI 321 with a maximum stress of 450 MPa at ambient temperature. It can be clearly seen, that besides an increase of mean value (blue points), which correlates with the ferromagnetic  $\alpha'$ -martensite, a change in the magnetic induction at each load time can be detected (lines).

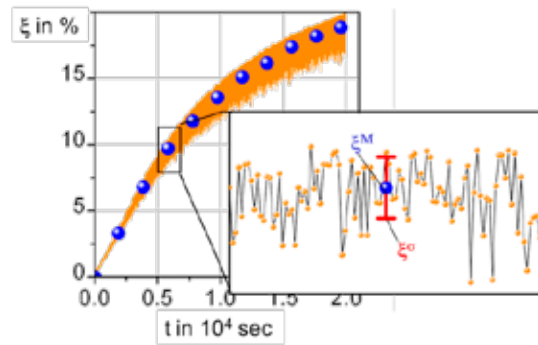


**Fig. 1:** Development of ferromagnetic  $\alpha'$ -martensite content and change in the magnetic induction during random loading of AISI 321.

After comprehensive analyses of the magnetic data, a constant ratio between standard deviation ( $x\sigma$ ) and mean value ( $\xi M$ ) of measured Feritscope® data ( $\xi$ ) was observed. This ratio directly correlates with fatigue and increases with a decrease of fatigue life. By this means magnetic properties offer a possibility for the characterization of microstructure, stress-strain-state and fatigue in advanced metastable austenitic steels.

#### References

- Villari, E. (1865): Ueber die Aenderungen des magnetischen Moments, Bericht d. Berliner Akad., 87-122.  
 Smaga, M., Eifler, D. (2009): Fatigue life calculation of metastable austenitic steels on the basis of magnetic measurements, MP Materials Testing, vol. 51, pp 370-375.

## Microstructural Evolution of TRIP-aided Medium Mn Steel During Warm Deformation

YONGMOON LEE<sup>1</sup>, CHONG SOO LEE<sup>1,2</sup>

<sup>1</sup> Graduate Institute of Ferrous Technology, Pohang University of Science and Technology, Republic of Korea

<sup>2</sup> Department of Materials Science and Engineering, Pohang University of Science and Technology, Republic of Korea

Medium Mn steels, classified as one of third generation advanced high strength steels, are widely studied for its reasonable combination of strength and ductility. To enhance the mechanical properties further, many investigations have attempted to achieve grain refinement in various ways. The aim of this work was to establish more efficient process for grain refinement of medium Mn steels. Uniaxial compression tests were carried out in the temperature range of 773-973K. Re-

sulting microstructures were investigated paying attention to two phenomena (dynamic strain-induced transformation and dynamic recrystallization), which varied with temperature. Variation of texture and crystallographic orientation relationship were analyzed by use of electron backscatter diffraction. Finally, a new process for fabricating ultrafine-grained alloy by warm deformation was suggested.

Talks Topic F 2:

## ***Advanced steels and steel composite materials***

---

## Influence of temperature on fatigue-induced martensitic phase transformation in a metastable CrMnNi-steel

HORST BIERMANN, MATTHIAS DROSTE, ALEXANDER GLAGE

Technical University Bergakademie Freiberg, Institute of Materials Engineering, Germany

An interesting field for current research are metastable austenitic steels showing the TRIP (transformation induced plasticity) effect based on deformation-induced martensitic transformation. This results in higher strength and superior ductility at the same time. Besides monotonic loading martensitic transformation can be observed during cycling loading as well. In this regard, it is generally agreed that a certain strain amplitude and a threshold of the cumulated plastic strain have to be exceeded to trigger the martensitic transformation.

Two of the major variables for the deformation-induced martensitic transformation are the austenite stability and the stacking fault energy (SFE) which both depend on the temperature. As the temperature rises, the austenite stability and the SFE increase, leading to a suppression of the martensite transformation and a fluent transition to other deformation mechanisms like twinning and finally dislocation glide (Martin et al. 2011). Accordingly, in case of monotonic loading there is the so called  $M_d$ -temperature representing the highest temperature at which martensitic transformation can take place. Analogue, this study presents a  $M_{d,c}$ -temperature for cyclic loading as a function of the total strain amplitude for the investigated high-alloy CrMnNi steel (16.3Cr-7.2Mn-6.6Ni-0.03C-0.09N-1.0Si). For this purpose, total strain controlled fatigue tests were performed at temperatures ranging from 10°C to 200°C. The  $\alpha'$ -martensite fraction was determined *in situ* by a feritscope. Furthermore, the *post mortem* microstructure was examined using back-scattered electron contrast (BSE), electron channelling contrast imaging (ECCI) and electron backscatter diffraction

(EBSD) to study the temperature-dependent deformation mechanisms and phase transformations. Subsidiary to these findings this study deals with the accordant cyclic deformation curves as well as fatigue lifetime estimation using the plastic stress-strain product  $SSP_{pl}$  (Glage 2014).

The study shows that decreasing temperatures as well as increasing strain amplitudes result in a shift of the onset of the martensitic transformation to a lower threshold of the cumulated plastic strain, and the maximum transformed amount of  $\alpha'$ -martensite increases. Thus, the  $M_{d,c}$ -temperature increases with increasing total strain amplitudes and finally is approaching a maximum value.

Furthermore increasing temperatures lead to a fatigue-lifetime improvement at high strain amplitudes, whereas decreasing temperatures result in a fatigue lifetime enhancement at low strain amplitudes which could be explained with different operating deformation mechanisms. Nevertheless, the  $SSP_{pl}$  is able to give a reliable fatigue lifetime estimation for the whole range of temperatures.

### References

- Glage, A. (2014): Zyklisches Verformungsverhalten von partikelverstärkten Verbundwerkstoffen mit metastabiler austenitischer Matrix – Doctoral thesis, Freiberg.
- Martin S. et al. (2011): Influence of temperature on phase transformation and deformation mechanisms of cast CrMnNi-TRIP/TWIP steel – In: Solid State Phenomena, Vols. 172-174, pp. 172-177.

## Importance of $\epsilon$ -martensite on embrittlement and fatigue crack growth in Fe-Mn-based austenitic steels

MOTOMICHI KOYAMA<sup>1</sup>, HUICHAO LI<sup>1</sup>, TAKAHIRO SAWAGUCHI<sup>2</sup>, KANEAKI TSUZAKI<sup>1</sup>, HIROSHI NOGUCHI<sup>1</sup>

<sup>1</sup>Department of Mechanical Engineering, Faculty of Engineering, Kyushu University, Fukuoka, Japan

<sup>2</sup>National Institute for Materials Science, Ibaraki, Japan

High Mn austenitic steels with low stacking fault energy have been known to show deformation twinning and  $\epsilon$ -martensitic transformation. Since these characteristic deformation modes have positive influences on mechanical properties, these steels are expected to be used for practical automobile and damping materials.

The former one, deformation twinning, enhances work hardening capacity, improving a balance of strength and ductility owing to twinning-induced plasticity (TWIP) effect. On the other hand, the latter one,  $\epsilon$ -martensitic transformation, has both negative and positive effects on mechanical damage evolution.

As the negative effect,  $\epsilon$ -martensitic transformation causes embrittlement associated with  $\gamma/\epsilon$  interface or intersections of  $\epsilon$ -martensite and annealing twin boundaries. Since even TWIP steels show  $\epsilon$ -martensitic transformation at a slightly lower temperature than room temperature, understanding  $\epsilon$ -martensite-related embrittlement mechanism in Fe-Mn austenitic steels is crucially important to practically use Fe-Mn austenitic steels.

As the positive effect, fatigue crack growth in a strain-controlled low cycle fatigue testing was clarified to be decelerated by  $\epsilon$ -martensitic transformation via deformation-induced reversible transformation, providing a new material design strategy to break Manson-Coffin's law.

In this report, we show some important aspects on embrittlement and fatigue damage evolution associated

with  $\epsilon$ -martensitic transformation in Fe-Mn-C and Fe-Mn-Si-Al austenitic steels. More specifically, we focus on two points: 1)  $\epsilon$ -martensite/annealing twin boundary intersection cracking in a tensile deformation and 2) importance of fatigue crack-propagation-induced  $\epsilon$ -martensite in a strain-controlled low cycle fatigue, which were clarified by EBSD/ECCI microstructure observations and plastic replica method.

#### References

- M. Koyama, T. Sawaguchi and K. Tsuzaki: ISIJ Int. 52 (2012), 161.  
 M. Koyama, T. Sawaguchi and K. Tsuzaki: Metall. Trans. A 43A (2012), 4063.  
 T. Sawaguchi, L.G. Bujoreanu, T. Kikuchi, K. Ogawa, M. Koyama and M. Murakami: Scripta Mater. 59 (2008), 826.

## Importance of strain aging on fatigue limit in austenitic TWIP steels

YUUSUKE YAMAMURA<sup>1</sup>, MOTOMICHI KOYAMA<sup>1</sup>, RENQING CHE<sup>1</sup>, TAKAHIRO SAWAGUCHI<sup>2</sup>, KANEAKI TSUZAKI<sup>1</sup>, HIROSHI NOGUCHI<sup>1</sup>

<sup>1</sup> Department of Mechanical Engineering, Faculty of Engineering, Kyushu University, Fukuoka, Japan

<sup>2</sup> National Institute for Materials Science, Ibaraki, Japan

Strain aging is an important factor enhancing fatigue strength. Fatigue limit of steels are determined by critical conditions associated with two cracking behavior critical stresses for crack initiation and propagation. The latter one is so called non-propagation fatigue crack. The non-propagating fatigue crack phenomenon is dominated by strain aging of carbon in steels. In case of major steels, carbon brings about dynamic strain aging, preventing fatigue crack growth. However, non-propagating fatigue crack phenomenon in austenitic steels has not clarified yet, and is expected to be observed when strain aging occurs also in austenite.

In recent years, twinning-induced plasticity (TWIP) steels have been drawn attention as automobile materials because the steels show an exceptional balance of strength and ductility. Here note that there are two typical types of TWIP steel: carbon-added and carbon-free TWIP steels. The carbon-added TWIP steels are known to show dynamic strain aging, while the carbon-free TWIP steels do not. Because of the strain aging effect, the two types of TWIP steels are speculated to show a clear difference in fatigue limit. Therefore, we studied influences of dynamic strain aging on fatigue properties through a comparative study between the austenitic TWIP steels.

In this study, rotary bending testing was conducted at a frequency of 30 Hz and room temperature. The fatigue crack growth behavior was observed by replica technique and optical microscopy.

Now, it was confirmed that fatigue crack stopped in a stress amplitude of about 350MPa in the TWIP steel including carbon in smooth specimens. In contrast, the fatigue crack in the carbon-free TWIP steel does not stop in a stress amplitude of about 180MPa in smooth specimens. Namely, as we expected, strain aging was elucidated to enhance non-propagating crack phenomenon even in austenitic TWIP steels.

Additionally, in this article, we introduced a notch which is regarded as pre-crack through a combined use of Focusing Ion Beam (FIB) and micro hole drilling to investigate short fatigue crack propagation properties more clearly. The sharp notch consists of a drill hole with dimensions of 100 $\mu$ m in diameter and 100 $\mu$ m in depth, and two FIB-notch with dimensions of 50 $\mu$ m in length, 6 $\mu$ m in width, and 33 $\mu$ m in depth. This notch is placed on the specimen surface and along the transverse direction against the loading direction. In this report, we will discuss the results obtained in the FIB-notched specimen as well as those in smooth specimens.

# Influence of Si addition on deformation and fracture behaviors of aging treated cast Fe-Mn-Al-C lightweight steel

SOON IL KWON<sup>1</sup>, JE HYUN LEE<sup>1</sup>, SEONG JUN PARK<sup>2</sup>, HYUN UK HONG<sup>1\*</sup>

<sup>1</sup>Departement of Materials Science and Engineering, Changwon National University, Gyeongnam, Korea

<sup>2</sup>Ferrous Alloy Department, Korea Institute of Materials Science, Gyeongnam, Korea

Considering environmental, economical requirements and outstanding mobility is becoming more important in these days when we design and develop reduction weight steels that are targeting at the army vehicles application. Thus, there are many studies to investigate the high specific steels that use the aging hardenable Fe-Mn-Al-C system. These steels are almost 15% less dense than traditional steels and are completely austenitic when solution treated above 950°C. The concept of the lightweight steel is high amount of Mn and Al contents (respectively about 30% and 10% contents) [1]. High Mn contents led to fully austenitic matrix. In addition, high Al contents could be lighter weight than the other conventional steels about 15% and it caused  $\kappa$ -carbide precipitation with a chemical formula  $(\text{Fe,Mn})_3\text{AlC}$  in the austenitic matrix by spinodal decomposition during aging treatment.  $\kappa$ -carbide is a f.c.c.-based phase of  $L'1_2$  ordered crystal structures, which resemble that of perovskite oxide [2]. The ordered  $L'1_2$  structure which is similar to that of  $L1_2$  in Ni-base superalloy. Hence, lightweight steel has strong precipitation hardening effect by  $\kappa$ -carbide precipitation. It means that studying about aging response in focused  $\kappa$ -carbide precipitation is essential to understand mechanical properties in this steel. Furthermore, adding Si contents was known to prevent precipitation of harmful phases like  $\beta$ -Mn at grain boundaries. And it is determined that silicon additions lowered liquidus dendrite coherency point (DCP), and solidus temperatures by approximately 30°C [3]. However, the effect of Si upon the mechanical behaviors has not been sufficiently reported. It means that there are not enough reference for relationship of  $\kappa$ -carbide precipitation with Si addition. Especially, the investigation of deformation mechanism and dislocation behaviors is needed to understand Si addition effect. Therefore, the aged cast Fe-Mn-Al-C lightweight steel has been investigated with or without 1%Si addition in the present study.

First, 550 and 530°C aging treatments have been taken to determine peak aging condition. After 550°C aging response, the peak aging hardness (407Hv) of 1%Si specimen is higher than that of no Si specimen (369Hv) and 530°C peak aging hardness is 430Hv and 385Hv for 1%Si specimen and no Si specimen, respectively. However, 530°C peak aging condition required too much longer time than 550°C aging treatment. It should be noted that age hardening kinetics is similar regardless of 1%Si addition. And then, 550°C peak aged 1%Si specimen showing tensile strength up to 1000 MPa with an excellent 26.3% elongation could be obtained at room temperature. One interesting point is that 1%Si specimen has better strength properties than no Si specimen. After tensile test, fractured surface and tensile deformation were observed by SEM and TEM analysis. 1%Si specimen was observed to have cleavage fractures on fractured surface in some area unlikely no Si specimen. In addition, persistent slip band was clearly revealed under fractured surface. The investigation of the relationship between Si addition and tensile deformation was discussed in this paper.

## References

- [1] R. Howell, L. Bartlett, A. Schulte, D. Van Aken and K. Peaslee. A Review of the Physical and Mechanical Properties of a Cast High strength and Lightweight Fe-Mn-Al-C Steel. MS&T, 2010, October, 17-21.
- [2] W. K. CHOO, J. H. KIM and J. C. YOON. Microstructural change in austenitic Fe-30.0wt%Mn-7.8wt%Al-1.3wt%C initiated by spinodal decomposition and its influence on mechanical properties. Acta mater, 1997, No 12, 45, 4877-4885.
- [3] R. Howell, S. N. Lekakh, D.C. Van Aken and V.L. Richards. The effect of silicon content on the fluidity and microstructure of Fe-Mn-Al-C alloys. Transactions of the American Foundry Society, 2008.

## Effect of shot peening on microstructure of steels exhibiting a TRIP effect – Experimental and modeling approaches

ROMAIN GUIHEUX<sup>1,2,3</sup>, SOPHIE BERVEILLER<sup>2</sup>, DENIS BOUSCAUD<sup>2</sup>, RÉGIS KUBLER<sup>3</sup>, ETIENNE PATOOR<sup>2</sup>, QUENTIN PUYDT<sup>1</sup>

<sup>1</sup>IRT M2P, Metz, France

<sup>2</sup>LEM3, Arts et Métiers ParisTech, Metz, France

<sup>3</sup>MSMP, Arts et Métiers ParisTech, Aix-en-Provence, France

Shot peening process is commonly used in mechanical industries to increase life duration of mechanical and structural parts, as automotive gears for instance. It is based on the development of residual compressive stresses at the surface of the component as the surface is hardened by the impact of steel shot. The stress magnitude and the affected depth depend on the process parameters, such as the shot velocity and diameter, their incidence angle with respect to the surface, the coverage... In the case of TRIP-effect steels, the metastable austenite can transform into martensite during shot peening. The final stress state is then more complex as it results from mechanical strain imposed by the process and the martensitic transformation that leads to stress redistribution between austenite and martensite. The aim of this work is to study the behaviour of TRIP-effect steels submitted to shot peening by taking into account martensitic transformation.

There are several existing models of shot peening giving the resulting stress field in the material as a function of parameters process; however, to our knowledge, none of these integrates the phase transformation. Therefore we have performed experimental characterizations and developed a specific model for shot peening using a AISI 301LN stainless austenitic steel.

Residual stresses are determined by X-ray diffraction in both phases, austenite (with Mn radiation) and martensite (with Cr radiation), using the classical  $\sin^2\psi$  law. The martensite volume fraction is also measured by X-ray diffraction taking into account crystallographic textures.

The mechanical behavior was characterized by tensile tests at different strain rates. Shot peening was per-

formed on 60\*60\*8 mm<sup>3</sup> samples using cut wire steel shots (700HV); the turbine rotational speed was varied between 500 and 2000 rpm. An augmentation of this speed increased the maximum residual stress in both phases. Moreover, the higher the turbine rate was, the higher the martensite volume fraction and the affected depth were.

In parallel, finite element simulations of shot peening are performed taking into account residual stresses, plastic strains and hardening parameters for each phase. It is based on the shot peening model with stress and microstructure gradients developed previously by Renaud (Renaud 2011); a semi-phenomenological transformation behaviour law for unstable austenite (Kubler 2011) has been implemented to consider microstructure phase evolution. Model parameters are calibrated from tensile tests and from single-shot impact experiments on AISI 301LN. Output data are the martensite volume fraction, the residual stress and strain fields in each phase, as a function of the depth from the surface. Numerical results are compared to experimental ones on shot peened surfaces.

### References

- Renaud P. (2011) : PhD Thesis - Arts et Métiers ParisTech ; Aix en Provence, France.  
 Kubler R., Berveiller M., Buessler P. (2011): Semi phenomenological modelling of the behavior of TRIP steels. International Journal of Plasticity, 27, 299-327.

# Study of Lüders band propagation using IR thermography and DIC method in the wide range of strain rates

MICHAL MAJ

Institute of Fundamental Technological Research, Polish Academy of Sciences, Warsaw, Poland

The present paper is devoted to the experimental analysis of the Lüders band propagation in C45 steel during uniaxial tension using infrared thermography (IRT) and digital image correlation (DIC) method. The analysis was performed in wide range of strain rates ( $10^{-3} s^{-1} \div 10^1 s^{-1}$ ). Used high speed IR camera gives possibility of studying the thermal effects accompanying Lüders band propagation close to the adiabatic conditions when the heat transfer within the specimen and between specimen and the surroundings can be neglected (Maj 2012). Use of such equipment allowed us to study not only the speed of front propagation but also the initiation and morphology of the front. It has been shown that both the front speed and the band morphology evolve with changing the displacement rate.

It was found that the Lüders plateau is observed at all considered displacement rates. Nevertheless, the significant force fluctuations are observed above the strain rate equal to  $1 \cdot 10^0 s^{-1}$ . The increase in displacement rate results in both the lengthening of Lüders plateau and the increasing level of external force. In other words, after the band passage the higher elongation and hardening of the specimen are observed.

The analysis of thermal images has shown that due to increase of the displacement rate not only the front speed but also the band morphology are changed. Up to strain rate  $5 \cdot 10^{-1} s^{-1}$  the stable front propagation is

observed. For higher strain rates the additional differently oriented narrow bands are present. Presence of such bands at high strain rates can be a result of necessity of accommodation of internal stresses generated due to mounting of the specimen in grips of testing machine. At lower deformation rates such accommodation is probably possible within the band by an evolution of dislocation structure.

It has been shown that the dependence between displacement rate and the Lüders front speed calculated on the basis of thermal images is not linear unlike the results known from the literature (Louche & Chrysochoos 2001). Observed non-linear dependence between front speed and displacement rate may indicate that there can be the limit value of front speed for higher deformation rates.

The results obtained using IRT technique will be verified using analysis of coupled displacement field obtained using DIC method.

## References

- Maj, M. (2012): Analysis of plastic strain localization on the basis of strain and temperature fields. – Arch. Metall. Mater., 57(4): 1111-1116.
- Louche, H. & Chrysochoos, A. (2001): Thermal and dissipative effects accompanying Lüders band propagation. – Mater. Sci. Eng., A307: 15-22.

Talks Topic F 3:

***Advanced steels and steel composite materials***

---

## Homogenization of TRIP steel behaviour using a strain gradient plasticity model

M.K. HATAMI<sup>1</sup>, T. PARDOEN<sup>2</sup>, P. BERKE<sup>1</sup>, P.J. JACQUES<sup>2</sup>, T.J. MASSART<sup>1</sup>

<sup>1</sup>Université Libre de Bruxelles (U.L.B.), Belgium

<sup>2</sup>Université catholique de Louvain, Louvain-la-Neuve, Belgium

An averaging procedure is developed for the simulation of the mechanical behaviour of TRIP steels.

This work further extends previous efforts to model the macroscopic material behavior of TRIP steels which have been based, among others, on the use of mean-field Mori-Tanaka approaches (Delannay, et al 2008). Comparison of their results to experiments motivated the introduction of size effects by means of strain gradient plasticity (Mazzoni, et al 2008). This contribution, based on a simplified representation of a periodic microstructure, focused on the investigation of the effect of size dependent behaviour and higher order boundary conditions combined with the local parameters of the transformation such as the fraction of transforming austenite, the transformation strain, or the strain at which transformation occurs. Due to the associated computational effort, such models were however restricted to the analysis of the local effects within a single RVE, interpreting a single transforming austenite inclusion.

In order to bridging the gap towards macroscopic behaviour, allowing direct comparisons with experiments, homogenizing this strain gradient plasticity description is proposed. The model, in which the local transformation size effect is presented (Mazzoni, et al 2008), is replicated in a high number of different unit cells, each of them being attributed a different strain at which the transformation initiates, based on experimental data. The response of each unit cell is evaluated by homogenizing the results of strain gradient plasticity simulation on all these cells.

The global behavior of a corresponding TRIP steel is subsequently obtained by recombining the unit cell responses by an averaging scheme based on weighting

factors associated to each cell. Such averaging method was originally proposed in (Ognedal, et al 2014).

The averaged response obtained is subsequently fitted to allow comparison with experimental stress strain curves corresponding to a certain grade of TRIP steel with an experimentally obtained transformation kinetics, in terms of strain hardening evolution and necking considere criterion.

The level of strain at which transformation initiates in each cell and the corresponding value of the associated weighting factor are adjusted to match the different transformation rate evolution extracted from experimental data available in (Delannay, et al 2008) already mentioned.

Results show that based on calibrating the strain gradient plasticity behaviour for the internal length scale value, the homogenized response allows to successfully reproducing the evolution of the stress-strain behaviour and of the strain at necking as a function of the transformation rate at various temperatures.

The model subsequently can be used to conduct parametric studies to identify optimal transformation evolutions and to analyse how the ductility varies with local material properties.

### References

- Delannay, L. & Jacques, P. & Pardoën, T. (2008): *Int. J. Solids and Structures*, 45: 1825-43.
- Mazzoni-Leduc, L. & Pardoën, T. & Massart, T.J. (2008): *Int. J. Solids and Structures* 45: 5397-418.
- Ognedal, A.S. & Clausen, A.H. & Berstad, T. & Seelig, T. & Hopperstad, O.S. (2014): *Int. J. Solids and Structures*, 51: 1494-506.

## A crystal plasticity model for advanced high strength steels including both TRIP and TWIP effect

FRANZ ROTERS, SU LEEN WONG

MPI für Eisenforschung, Düsseldorf, Germany

Advanced high strength steels, such as high manganese steels, show an extraordinary combination of strength and ductility. While this provides a tremendous potential for many applications due to a number

reasons these materials are not yet widely used in industry. One of the reasons is a lack of suitable material models. Besides the conventional deformation by slip these materials activate additional deformation mech-

anisms, namely twinning (Twinning Induced Plasticity, TWIP) and phase transformation (Transformation Induced Plasticity, TRIP). This is the reason why conventional models used for the simulation of steels cannot fully describe the mechanical behavior of this material class. As simulation is, however, nowadays an integral part of component layout e.g. in automotive industry, without suitable material models new materials will not be introduced into the production process.

In our contribution we, therefore, present a crystal plasticity formulation that includes both twinning and transformation as additional deformation mechanisms besides the conventional dislocation slip. The twinning model is a crystal plasticity adaption of an analytical model by Steinmetz et al. (2013). The TRIP model considers both stress and strain induced transformation. As depending on material parameters (e.g. stacking

fault energy) and loading conditions (strain rate, temperature) both mechanisms can be triggered and one material and can even be active at the same time, it is of great importance that both effects are taken into account in the constitutive description. The combined model allows us to systematically study under which conditions either one or both mechanisms together can be triggered during deformation.

#### Reference

D. R. Steinmetz, T. Jäpel, B. Wietbrock, P. Eisenlohr, I. Gutierrez-Urrutia, A. Saeed-Akbari, T. Hickel, F. Roters, D. Raabe (2013): Revealing the strain-hardening behavior of twinning-induced plasticity steels: Theory, simulations, experiments, *Acta Materialia* 61: 494 - 510

## Multiscale Modelling of Damage and Fracture in High Mn TWIP Steels

MANJUNATHA MADIVALA<sup>1</sup>, CHRISTIAN SEGEL<sup>2</sup>, ANJA WEIDNER<sup>2</sup>, HORST BIERMANN<sup>2</sup>, WOLFGANG BLECK<sup>1</sup>, ULRICH PRAHL<sup>1</sup>

<sup>1</sup>Steel Institute, RWTH Aachen University, Germany

<sup>2</sup>Institute for Materials Technology, Technical University Bergakademie Freiberg, Germany

The automobile industry has an increasing demand for lightweight components, improved product performance, efficiency and increased safety. High manganese TWIP steels have superior mechanical properties and excellent strength to weight ratio, making them ideal for the development of lightweight vehicles. Achieved high strength and ductility rely on the optimization of the stacking fault energy, which governs mechanical twinning as the primary deformation mechanism in addition to dislocation glide and TRIP. Numerical prediction of damage in Advanced High Strength Steel (AHSS) sheets is of great interest, as it is an effective way to optimize the design of parts and to reduce the product development cycle time.

In order to predict the damage and fracture mechanisms in TWIP steels subjected to uniaxial loading, a Representative Volume Element (RVE) approach is applied to create the virtual polycrystalline microstructure taking into account, the aspects of real microstructure such as grain size, phases, grain size distribution and grain orientations. The uniaxial tensile test is simulated by applying periodic boundary conditions and tensile load to an RVE. Crystal Plasticity (CP) based model is used for predicting the plastic localization in a material. A CZ damage model is also implemented to predict the sudden drop of load carrying capacity

and to reflect void nucleation and growth of the highly deformed regions. From the analysis of the numerical tensile test, the damage initiation and flow behaviour can be well predicted.

Thus in this current work, to predict the material behaviour an evaluation chain including material characterization, numerical simulation with a crystal plasticity based material model for TWIP steels and verification by In-situ tensile tests was established. Digital Image Correlation (DIC) technique was used to identify the local failure strains.

#### References

- F. Roters, Advanced material models for the crystal plasticity finite element method - development of a general CPFEM framework, Habilitationsschrift RWTH Aachen (2011), Fakultät für Georessourcen und Materialtechnik, RWTH Aachen University
- R. Quoy, P.R. Dawson and F. Barbe, Large-scale 3D random polycrystals for the finite element method: Generation, meshing and remeshing, *Computer Methods in Applied Mechanics and Engineering*, vol. 200, pp. 1729-1745, 2011
- F. Roters, P. Eisenlohr, T.R. Bieler, D. Raabe, *Crystal Plasticity Finite Element Methods in Materials Science and Engineering*, Wiley-VCH, 2010

## Artificial microstructure model and its applications on plasticity and damage of the dual phase steels

NAPAT VAJRAGUPTA, MOHAMED SHARAF, JUNHE LIAN, SEBASTIAN MÜNSTERMANN, WOLFGANG BLECK

Department of ferrous metallurgy, RWTH Aachen University, Germany

Heterogeneous alloy systems that contain multiple phases possess the potential of reducing structural component weight, energy consumption as well as thermo-mechanical reliability improvement. This is due to the fact that the matrix of these materials consists of constituents with strong distinction in mechanical properties. For this reason, their industrial utilization has significantly increased in the last few decades. The application of such a material includes implementation of the dual phase steel in the automotive industry. However, the existence of these constituents in the microstructure also results in the highly heterogeneous finite stress distribution along with the high temperature gradients which are presented even within the large components. Furthermore, the constituents in these material systems also affect the failure behaviour in which several competing damage mechanisms can be observed. Therefore, a reliable microstructure-based simulation approach for describing these deformations and damage mechanisms is needed. Furthermore, the developed approach must be able to reflect the influence of microstructure morphologies on the deformation behaviour of the microstructure. Under the framework of microstructure-based simulation approach, the universal platform to generate the artificial microstructure model has been developed and shall be discussed in this study. The ultimate goal for the development of this platform is to generate the most sophisticated representative microstructure model with as least input parameters as possible. For the principle of this platform, the statistical description of the necessary microstructure features such as grain size, aspect ratio etc. is used as input parameters for the weighted Voronoi tessellation based algorithm. Additionally, both 2D and 3D artificial microstructure model can be generated with this proposed platform under the framework of this study.

With the generated artificial microstructure model, material's model definition and parameters calibration are also required. For plasticity description of the constituents, modified phenomenological based crystal plasticity model taking the influence of the grain size into account is applied to ferrite and parameters are calibrated by series of nanoindentation tests while the empirical approach based on the measured local chemical composition is used to approximate the strain hardening behaviour of martensite. To characterize the criteria that trigger the onset of microcrack, the hybrid approach combining the in-situ bending test in the large chamber SEM with the micromechanical-based simulation discipline is conducted. Finally, the applications of this introduced platform such as the strain hardening behaviour prediction, microcrack initiation simulation, shall be discussed in this study.

### References

- Vajragupta, N., Wechsuanmanee, P., Lian, J., Sharaf, M., Münstermann, S., Ma, A., Hartmaier, A., & Bleck, W. (2014): The modelling scheme to evaluate the influence of microstructure features on microcrack formation of DP-steel: The artificial microstructure model and its application to predict the strain hardening behaviour – In: Computational Material Science, Volume 94: 198-213.
- Okabe, A., Boots, B., Sukihara, K., & Chui S.N. (2000): Spatial tessellation: Concepts and applications of Voronoi diagrams, second edition: John Wiley & Son Inc. 1992.
- Roters, F., Eisenlohr, P., Hantcherli, L., Tjahjanto, D.D., Bieler, T.R., & Raabe, D. (2010): Overview of constitutive laws, kinematics, homogenization and multiscale methods in crystal plasticity finite-element modeling: Theory, experiments, applications – In: Acta Materialia, Volume 58: 1152-1211.

# Dislocation plasticity in precipitate hardened advanced austenitic lightweight high-Mn steels by coupled TEM and DDD simulations: Strengthening and dislocation-based mechanisms

E. WELSCH<sup>1</sup>, S.M. HAFEZ HAGHIGHAT<sup>1</sup>, I. GUTIERREZ-URRUTIA<sup>2</sup>, D. RAABE<sup>1</sup>

<sup>1</sup>Max-Planck-Institut für Eisenforschung, Düsseldorf, Germany

<sup>2</sup>National Institute for Materials Science (NIMS), Tsukuba-city Ibaraki, Japan

High performance austenitic lightweight steels with up to 15% density reduction are currently of high interest for the automotive industry. The development of such weight reduced and highly formable steel grades for structural applications includes a range of material systems. One of the most promising alloy systems are low density steels based on the FeMnAlC system [1,2]. This quaternary system offers a combination of excellent mechanical properties, characterized by elongations of up to 70 % at stresses above 1.5 GPa, and specific weight reduction of up to 15%. Al addition promotes the precipitation of L<sub>1</sub><sub>2</sub> ordered (Fe, Mn)<sub>3</sub>AlC carbides, also referred to as κ-carbides. The austenitic matrix of the FeMnAlC steels contains nano-sized cuboidal κ-carbide precipitates that control the dislocation assisted plasticity of these materials. Here we present new insights into κ-carbide strengthened high-Mn steels by using both, transmission electron microscopy (TEM) observations and the simulation of comparable deformed microstructures using discrete dislocation dynamics (DDD) simulations. In the DDD simulations the model previously developed by Hafez Haghighat et al. [3] was used. Precipitates are treated here as impenetrable obstacles to the motion of dislocations. As the model originally was developed for cuboidal γ' strengthened Ni base superalloys it had to be modified to fulfil the requirements of the present study.

The κ-carbide morphology was investigated using similar particle arrangements as observed by TEM probing.

In particular the particle size and position with respect to each other were deduced from TEM observations. In the simulation the particle size and geometry at a fixed particle fraction was varied in order to elucidate the role of penetrating dislocations into the channels between the particles on the mechanical response. DDD simulations in connection with TEM observations elucidate the character of how the geometrical arrangement of these particles governs and influences the plastic deformation.

These investigations provide new guidelines to alloy design of advanced lightweight steels based on the underlying dislocation mechanisms at different κ-carbide geometrical arrangements.

## References

- [1] D. Raabe, H. Springer, I. Gutierrez-Urrutia, F. Roters, M. Bausch, J.-B. Seol, M. Koyama, P.-P. Choi, K. Tsuzaki, Alloy Design, Combinatorial Synthesis, and Microstructure–Property Relations for Low-Density Fe-Mn-Al-C Austenitic Steels, JOM, 2014, Volume 66, pp 1845-1856
- [2] Springer, H., and D. Raabe, 2012, Rapid alloy prototyping: Compositional and thermo-mechanical high throughput bulk combinatorial design of structural materials based on the example of 30Mn-1.2C-xAl triplex steels: Acta Materialia, v. 60, p. 4950-4959.
- [3] S.M. Hafez Haghighat, G. Eggeler, D. Raabe, Acta Materialia 61 (2013).

## Phase-field modeling of solid-solid phase transformations

DANIEL SCHNEIDER<sup>1</sup>, OLEG TSCHUKIN<sup>2</sup>, MICHAEL SELZER<sup>1,2</sup>, BRITTA NESTLER<sup>1,2</sup>

KIT, Institute of Applied Materials -Computational Materials Science, Karlsruhe, Germany

<sup>2</sup> Karlsruhe University of Applied Science, Institute of Materials and Processes, Germany

Computational models based on the phase-field method have become an indispensable tool in material science and physics in order to investigate materials with complex microstructures. The models typically operate on a mesoscopic length scale resolving structural changes of the material and provide valuable information about evolution of microstructure and microstructure mechanical property relations.

For many interesting and important phenomena, such as martensitic phase transformation, mechanical configurational forces play an important role in the evolution of microstructure. In order to investigate such phenomena a calculation of the stresses and strain energy at the transition region is indispensable. We derive a phase-field elasticity model based on force balance and Hadamard jump condition at the interface (Schneider et al. 2015). We show the quantitative characteristics of the model, by comparing the simulated stress profiles in a plate with a round inclusion under hydrostatic tension with the theoretical predicted stress fields and stress field calculated with Voigt/Taylor and Reuss/Sachs approximation. In order to validate the elastic contribution to the driving force of the phase transition, we compare the resulted stress, strain and strain energy profiles, in one dimensional equilibrium condition of serial and parallel material chain as well as in two dimensional systems through

the Gibbs-Thomson condition. Additionally we demonstrate that the formulated driving force is equivalent to the mechanical configurational forces.

In order to calculate the plastic strain, the Prandtl-Reuss model for the particular phase is implemented consisting of an associated flow rule in combination with the von Mises yield criterion and a linear isotropic hardening approximation (Schneider et al. 2014). Simulations are performed illustrating the evolution of the stress and plastic strain using a radial return mapping algorithm for single phase system and heterogeneous microstructures.

Finally we show simulations in polycrystalline systems to martensitic phase transformation in one grain as well as in multigrain systems and simulations to Greenwood-Johnson effect.

### References

- Schneider et al. (2014): Small strain elasto-plastic multiphase-field model: Schneider, D., Schmid, S., Selzer, M., Böhlke, T., Nestler, B.: Computational Mechanics
- Schneider et al. (2015): Phase-field elasticity model based on mechanical jump conditions: Schneider, D., Tschukin, O., Choudhury, A., Selzer, M., Böhlke, T., Nestler, B.: submitted to Computational Mechanics

Talks Topic F 4:

***Advanced steels and steel composite materials***

---

## Z phase strengthened steels for ultra-supercritical power plants

DANIEL F. URBAN, CHRISTIAN ELSÄSSER, HERMANN RIEDEL

Fraunhofer Institute for Mechanics of Material IWM, Freiburg, Germany

To minimize fuel consumption and CO<sub>2</sub> emission of fossil fired power plants, the thermal efficiency, and therefore the steam inlet temperatures, must be as high as possible. In the past 20-30 years sufficiently creep resistant 9% chromium steels were developed, which allowed to increase the steam temperature up to 615 °C. The increased creep resistance was mainly obtained by controlled precipitation of fine (V,Nb)N particles in the steels. Further raise of the steam temperature calls for chromium contents higher than 9% to achieve better corrosion and oxidation resistance. However, it has been found that in 11-12% chromium ferritic-martensitic steels strengthened by fine (V,Nb)N particles, precipitation of the thermodynamically stable Z-phase, Cr(V,Nb,Ta)N, in long-time service is unavoidable and detrimental. Usually, the Z-phase particles are coarse and brittle and grow at the expense of the desired fine (V,Nb)N particles.

A possible solution to this problem is provided by the idea to exploit the Z-phase as a thermodynamically stable strengthening agent in martensitic creep resistant steels. Hence the challenge is to control the precipitation of the Z-phase in 12% Cr steels such that fine Z particles are formed, which are stable for long times. We present atomistic simulations, using density function theory, which reveal the essential mechanisms underlying Z-phase formation. The picture that evolves consists of the diffusion of chromium atoms into nitride particles and their subsequent clustering in a layered arrangement which finally yields the transformation of the nitride particles to Z-phase particles. We study the thermodynamic stability of Z-phase and related structures and predecessors as well as the basic diffusion mechanisms.

This work is part of the Z-Ultra-Project within the EC 7<sup>th</sup> framework program.

## Different mechanical behavior of MA957 ODS and Eurofer'97 steels exposed to flowing helium of 720°C

ANNA HOJNA<sup>1</sup>, HYNEK HADRABA<sup>2</sup>, JANA KALIVODOVA<sup>1</sup>, ROMAN HUSAK<sup>2</sup>

<sup>1</sup>Centrum Vyzkumu Rez s.r.o., UJV Group, Rez, Czech Republic

<sup>2</sup>Institute of Physics of Materials, Academy of Sciences of the Czech Republic, Brno, Czech Republic

Since ODS steels have been developed for the use of high temperature applications in the range from 400 to 700°C, thermal aging related problems at prolonged service times need to be intensively studied. The aim of the work was to describe fracture behaviour of MA957 ODS steel (14%Cr, 0,3Mo, 0,9Ti, 0,25%Y2O3 produced by mechanical alloying process) after high temperature exposure in comparison to the Eurofer'97 plate steel (9%Cr, 1%W) behavior. The both materials are considered for future nuclear energy systems.

Due to microstructural characteristics, the MA957 steel embodies excellent combination of high-temperature strength and oxidation resistance. The fine oxide dispersion also serves as trapping sites for point defects induced by radiation displacement and thus reduces remarkably irradiation swelling of the MA957 steel (Hadraba 2011). For space nuclear reactors cooled by a gas mixture of He and Xe at reactor temperatures <1100°C, the MA-ODS steels are particularly very attractive as structure materials (El-Genk 2005).

It is well known that thermal aging of high Cr ferritic

steels can result in the formation of coherent particles of  $\alpha'$  (Cr-rich ferrite) with an increase in yield and tensile strength, and a reduction in ductility associated with embrittlement when exposed at temperatures above 400°C (Lee 2007). The degree of the embrittlement, manifested in lower impact and fracture toughness, increases with Cr content; for 14 Cr ODS it had been indicated already at 440°C after 320 hours of exposure. The main problems of the MA957 type ODS are connected to lower toughness and heterogeneity of behaviour as well as transition temperature behaviour of ferritic matrix of the steel and strengthening by oxide dispersion. Whereas, the long-term exposure of the Eurofer'97 steel at high temperatures leads to different microstructural changes (Hadraba 2009); the coarsening of the M23C6 (Cr rich) precipitates and recrystallization of subgrains were found after ageing at 550°C/5000 h (Stratil 2011).

Small specimens (MicroCharpy, 3x4x27 mm<sup>3</sup> and miniTensile  $\varnothing$ 2 mm) were exposed to helium gas flowing in the High Temperature Furnace at 720°C for 500 hours.

Then, the specimens were tested for the impact and tensile behavior. The test results are compared to the other two sets of specimens of the previous tests, as received and isothermally annealed at 650°C in the case of the ODS steel. The He exposed materials showed positive shift of transition temperature and change of the upper shelf value. While the upper shelf value decreased in the exposed Eurofer'97, it significantly increased in the ODS steel. The difference is discussed in terms of microscopy observation in the paper.

#### References

- Hadraba H. et al. (2011), *Journal of Nuclear Materials* 417, 241–244  
 El-Genk M.S. et al. (2005), *Journal of Nuclear Materials* 340, 93–112  
 Lee J.S. et al. (2007), *Journal of Nuclear Materials* 367–370, 229–233  
 Hadraba H. et al. (2009), *Journal of Nuclear Materials* 386–388, 564–568  
 Stratil L. et al. (2011), *Journal of Nuclear Materials* 416, 311–317

## Characterization of the weldability of different AHS steel and aluminium alloy grades using thermo-mechanical physical simulation

JÁNOS LUKÁCS, LÁSZLÓ KUZSELLA, ZSUZSANNA KONCSIK, ÁDÁM DOBOSSY, DÓRA PÓSZALAKY

Institute of Materials Science and Technology, University of Miskolc, Miskolc, Hungary

The technological examinations and probes regarding the weldability date back to the development of different welding technologies. Not only the various qualities of materials, but the different welding processes have resulted the elaboration of additional tests (Pohle 1990). They are specified by their variety, applicability within limits, as well as their limited comparability. Considering the complex issue of weldability, such as materials, welding technology and welded structure (Easterling 1983, Boese et al. 1984), there is not one single test which would allow evaluating the problem, it is not and would not be sensible either, consequently weldability cannot be determined with a single characteristic. The underlying reasons are to be examined separately under specific conditions, which then will enable us to rank the different materials based on the given results. The order of ranking depends on the requirements, which means that it is not considered constant. The complex correlations between the factors do not allow defining other properties (e. g. mechanical properties) through characteristics. Besides the experiments, tests and probes, semi-empirical and empirical investigations are given an ever increasing emphasis in order to avoid limitations (Buchmayr 1991).

There is at least double contradiction in the examinations and probes. On the one hand, the actual processes can only be performed on small parts and in small volumes, which means that there are only small-size specimens available to define the data belonging to the materials and/or technologies (Yuan & Sharpe 1996). This fact, due to the aspect of size effect, will decrease the reliability of the results. On the other hand, the technological investigations are reflected within limits as regards the real processes.

The mathematical (computational) simulation may contribute to cancelling the limitations of examinations and probes, as well as those of the different approaches, which are not to be considered in the current study. However, the other consideration is the physical simulation. The basic aim of the first physical simulators (mid-20th century) was to provide reproducibility for the welding, especially for the Heat Affected Zone (HAZ).

Nowadays, the physical simulation is an ultimate innovative way to develop the welding processes. The paper introduces the connection between the weldability and the physical simulation, based on our investigations using Gleeble 3500 thermo-mechanical physical simulator. Four kinds of materials, two advanced high strength steels (S690QL and S960QL) and two aluminium alloys (5754-H22 and 6082-T6) were investigated. Different types of physical simulation test methods (Mandziej 2010) were made, such as identification of the Nil-Strength Temperature (NST), on heating and on cooling Hot Tensile Tests (HTT), as well as HAZ-tests, to characterise the weldability of the investigated materials. The results of the AHS steel grades and the aluminium alloy grades were compared with each other and with the results can be found in the literature.

#### References

- Pohle, C. (1990): *Zerstörende Werkstoffprüfung in der Schweißtechnik*, Deutscher Verlag für Schweißtechnik DVS-Verlag GmbH, Düsseldorf.  
 Easterling, K. E. (1983): *Introduction to the Physical Metallurgy of Welding*, Butterworths Monographs in Materials (BMM), Butterworths & Co (Publishers) Ltd.

Boese, U., Werner, D. & Wirtz, H. (1984): Das Verhalten der Stähle beim Schweißen, Teil II: Anwendung. Deutscher Verlag für Schweißtechnik (DVS) GmbH, Düsseldorf.

Buchmayr, B. (1991): Computer in der Werstoff- und Schweisstechnik: Anwendung von mathematischen Modellen, Deutscher Verlag für Schweißtechnik DVS-Verlag GmbH, Düsseldorf.

Yuan, B. & Sharpe, W. N. (1996): Fatigue testing of microspecimens. – In: Lütjering, G. & Nowack, H. (eds.): Proceedings of the Sixth International Fatigue Congress (FATIGUE'96), Pergamon, Vol. III: 1943-1948.

Mandziej, S. T. (2010): Physical Simulation of Metallurgical Processes. – *Materials in technology / Materials and technology*, 44, Issue 3: 105-119.

## The microstructure characterization of the HAZ and welding CCT diagram of API X100 steel

CHUNLIN QIU<sup>1</sup>, LIANGYUN LAN<sup>2</sup>, XIANGWEI KONG<sup>2</sup>

<sup>1</sup> State Key of Laboratory of Rolling Technology and Automation, Northeastern University, Shenyang, China

<sup>2</sup> School of Mechanical Engineering and Automation, Northeastern University, Shenyang, China

The growing energy demand in different areas of the world and the distance between gas reservoirs and consumers has increased the need to transport gas from far away regions to the final market. The requirements for pipe line steel both quality and quantity is also increased strongly. Welding process is a very important aspect because the steel pipe usually was made by welding method. This work focus on a kind of high strength pipeline steel (API X100) in oil and gas transportation industry.

The chemical composition of X100 steel is(mass%): 0.04% C, 2.0% Mn, 0.29% Si, 0.23% Cu, 0.275%Cr, 0.006% P, 0.0015% S, 0.55% (Ni + Nb + Mo), the balance is Fe. The weld cracking sensitivity index Pcm is 0.21, the hot-rolled plate of 20mm thickness was rolled into hot simulation processing sample, welding thermal cycle simulation test was conducted on the thermal simulation machine MMS300, the different  $t_{8/5}$  cooling time was adopted from 3 to 600s, both microstructure (optical, SEM and TEM) and hardness testing were used to analyzed welding simulation samples, then the CGHAZ-CCT and FGHAZ-CCT was plotted.

The results show that for either CGHAZ or FGHAZ, the granular bainite(GB) was obtained under low cooling rate, after the  $t_{8/5}$  time reached 600s, MA island emerges, with characterization contained degenerate pearlite. when the cooling rate reached to 10~20°C/s( $t_{8/5}$  is 15~30s correspondingly), Microstructure mainly include ferrite and bainite which due to the Mo and Nb put off the transformation form austenite to ferrite and promote the bainite transformation. as further increasing of cooling rate, the volume of martensite in microstructures is increasing gradually, and  $t_{8/5}$  cooling

time is 5s, the lath martensite volume achieved to as much as 50%.

Through the analysis and compare the transformation regulation both CGHAZ and FGHAZ, the started temperature of transformation has same tendency, that is varied from low to high follow the decreasing of cooling rate, whereas the finished temperature of transformation varied from low to high with the decreasing of cooling rate when it is relatively higher, and then turn to decreasing follow the cooling rate decline. Compared with FGHAZ, the started temperature is high in FGHAZ, meanwhile the transformation region is enlarged.

In the low range of cooling rates, with the increasing of cooling rate, the microhardness values are increased in both CGHAZ and FGHAZ, but when a certain cooling rate ( $t_{8/5}$  cooling time is about 30s) is reached, its hardness value tend to a stability and maintained at around 325HV.

### References

- Wang, P. Y., & Mou, Z. Y. (2013). Study on the Weldability of X100 Pipeline Steel on Scene. *Advanced Materials Research*, 753:343-352.
- Amaro, R. L., Rustagi, N., Findley, K. O., Drexler, E. S., & Slifka, A. J. (2014). Modeling the fatigue crack growth of X100 pipeline steel in gaseous hydrogen. *International Journal of Fatigue*, 59: 262-271.
- Zhang, M., & Yang, L. (2013). Microstructure and Mechanical Properties of Joints of X100 Line Pipe by Submerged Arc Welding. *Applied Mechanics and Materials*, 310:139-144.

## Weldability of modern high strength bainitic steel

LIANGYUN LAN<sup>1,2</sup>, XIANGWEI KONG<sup>1</sup>, CHUNLIN QIU<sup>2</sup>

<sup>1</sup>School of Mechanical Engineering and Automation, Northeastern University, Shenyang, China

<sup>2</sup>State Key of Laboratory of Rolling Technology and Automation, Northeastern University, Shenyang, China

With the development of thermo-mechanically controlled process and microalloying technique, hot rolled steel plates always have a good balance of high strength and good toughness. However, this excellent combined mechanical properties can be upset by the thermal cycles experienced during welding, producing regions of poor toughness known as local brittle zones. Although the weldability of modern high strength steels is improved through the composition design of low carbon equivalent, their welding system design is still a difficult issue, which impedes the actual application of the new steels. As Bhadeshia (2013) said: "Super-high strength nanobainitic steel has not been achieved commercial application mainly due to immature welding system". Therefore, to protect the welded joint from property deterioration, e.g., cleavage cracking, the effect of weld process on the microstructure evolution should be further investigated for the modern high strength steels.

In this work, the submerged arc welding technique was employed to weld the high strength bainitic steel using various welding parameters. The main parameters include current, voltage and welding speed, which determines the welding heat input from 1.4 to 4.5 kJ/mm. The microstructure characteristics of welded joints was studied in detail by means of optical microscope, scanning electron microscope equipped with electron backscattering diffraction technique, as well as transmission electron microscope. The relationship between microstructure evolution and mechanical

properties was also discussed to optimize the welding process.

The results showed that the strength of welded joint decreases with the increase in heat input and the fracture region always occurs at the weld metal, which means that this is under matching welded joint. The impact toughness of the weld metal does not change with the heat input, but the HAZ toughness gradually decreases with increasing heat input. Microstructure observation reveals that the weld metal has predominantly acicular ferrite irrespective of heat input, which is the main reason to keep good toughness for the weld metal. However, at the HAZ, the fracture mode changes from quasi-cleavage fracture to complete cleavage fracture with the heat input, which is attributed to the coarse bainite formed in this region.

Compared with the results proposed by Thewlis (2000), who also studied the weldability of X100 pipeline steel by using submerged arc welding, the minimum heat input adopted in our research can optimize the mechanical properties of welded joint.

### References

- Bhadeshia, H.K.D.H. (2013): The first bulk nanostructured metal, *Science and Technology of Advanced Materials*, 14: 1-8.
- Thewlis, G. (2000): Weldability of X100 pipeline, *Science and Technology of Welding and Joining*, 5: 365-377.

Talks Topic G 1:

## *Fracture mechanics*

---

# Numerical Simulation of ZrO<sub>2</sub>(Y<sub>2</sub>O<sub>3</sub>) Ceramic Plate Penetration by Cylindrical Plunger

VLADIMIR BRATOV, NIKITA KAZAIRNOV, YURI PETROV

Saint Petersburg State University, Faculty of Mathematics and Mechanics, Saint Petersburg, Russia

Fracture of ceramics, multi-layered ceramics and ceramic composites is of a great importance in connection with numerous theoretical and practical problems. Theoretical problems primarily include understanding the mechanisms driving static and dynamic fracture of this special class of materials (extremely brittle, very high strength and low toughness) and elaboration of criteria capable of accurate prediction of fracture initiation, development in arrest in quasi-static and dynamic conditions. While the majority of theoretical problems connected with quasi-static ruptures of ceramic materials are solved, mechanisms underlying dynamic fracture of these materials are not clear and generally recognised criteria for fracture are not formed yet. Practical importance of these problems is evident due to wide usability of ceramic-based materials owing to unique physical and mechanical properties and the possibilities of industrial production.

Dynamic fracture properties of ceramic materials are primarily studied due to applications where ceramic/multi-layered ceramics or ceramic composites serve as a protection against mechanical and thermal impacts on an object. Thermal effects are not considered in this work. As regards performance of ceramic materials against high rate mechanical loads, then the function of ceramic protection normally consists in a) absorption of impact energy for deformation and fracture of ceramics b) redistribution of impact energy over a bigger area of the surface underlying protective layer c) weight reduction of the protection system.

In this paper an approach that was previously successfully applied to simulate dynamic fracture in other classes of quasi-brittle materials was applied to study

penetration of ceramic plate by a cylindrical plunger. The focus is primarily on energetic peculiarities of the process, including investigations of histories of fracture surface evolution in fractured ceramic material, calculations of specific fracture energy at dynamic rupture initiation and studies of correlation between new fracture surface within ceramic material created as a result of a plunger impact and initial plunger energy (velocity) as well as the properties of the ceramic material. Visualization and statistical analysis of target fragmentation was used as a supplementary tool for fracture process investigation.

This study is deliberately restricted to the simplest possible geometry and contact problem formulation. In the considered case, an elastic cylindrical plunger with properties typical for steel normally hits circular homogenous ceramic plate, behaving as linear elastic material up to the moment of fracture initiation. Due to obvious axial symmetry of the problem, two-dimensional problem can be formulated. Such a simplicity in formulation provides a possibility to concentrate on key features controlling and driving fracture of penetrated ceramic plate.

## References

- Freund L.B. (1998): *Dynamic Fracture Mechanics*. Cambridge University Press, 584.
- Bratov V. (2011): Incubation time fracture criterion for FEM simulations. – In: *Acta Mechanica Sinica*, 27(4): 541-549
- Bratov V.A., Morozov N.F., Petrov Yu.V. (2009): *Dynamic Strength of Continuum*. St. Petersburg University Press, 224.

# Temporal Peculiarities of Fracture Caused by Threshold Pulses in Spallation

GRIGORY VOLKOV<sup>1,2</sup>, YURI PETROV<sup>1,2</sup>, YURI MESCHERYAKOV<sup>2</sup>, NATALIA MIHAYLOVA<sup>1</sup>

<sup>1</sup>St. Petersburg State University, St. Petersburg, Russia

<sup>2</sup>Institut for Problem of Mechanical Engineering RAS, St. Petersburg, Russia

Spallation test is one of the basic mechanical tests for determining the dynamic properties of materials. This experimental scheme allows studying the strength properties of the material under dynamic tension. Tensile stress originates in the specimen when the compression wave reflects from the free surface. The wave

problem solution within the elastic approach shows that the time profile of the tensile stress pulse coincides with the time profile of the free surface velocity, which can be directly measured by laser interferometry [Zlatin et al. 1974, Bloberg 1970]. This pilot scheme have been used for a long time, but this original meth-

od of determining the tensile stress time profile was reduced to more simple scheme. Usually in most tests, the suprathreshold load pulses were implemented. In this case, the dynamic strength of material can be characterized by the value of the tensile stress corresponding to the time when the fracture occurs. Most researchers estimate this critical value of the tensile stress by a simple formula and interpret it as a spallation strength of material whatever experiments performed.

If the compressive wave initiates the threshold fracture pulse, spallation occurs at the moment of time when the tensile stress in the spall cross-section is decreasing and even can vanish. This effect is referred to as the fracture delay. In this case, the critical tensile stress given by the simple formula cannot be considered as the only characteristic of the spallation strength. The fracture delay effect was experimentally observed by Berezkin who studied fracture of notched specimens under dynamic tension.

In the present work, new experimental data on spallation in nitrogen steel are obtained and analyzed with the use of the original methodic of Zlatin and Pugachev. In the tests when the fracture delay took

place, only initial manifestations of fracture in the form of small cracks are observed. In the specimens destroyed without fracture delay, a main crack expands across the total specimen width. The fracture delay effect is explained in the frames of the structure-temporal approach. The fracture incubation time for the studied steel is determined. This allows predicting the spallation phenomenon and the stress level at the time moment of fracture for given time profile of stress.

#### References

- Broberg, K. (1999): *Cracks and Fracture* – Cambridge University Press; Cambridge.
- Zlatin, N.A., et. al (1986) On brittle solid delay fracture. – *Journal Tech. Phys.* 56 (2), 403-406.
- Berezkin, A.N. et. al (2000) Effect of Delayed Crack Nucleation – *Doklady Physics*, Vol. 45, No. 11, 2000, pp. 617–619
- Petrov, Y.V. & Sitnikova, E.V. (2004) Dynamic Cracking Resistance of Structural Materials Predicted from Impact Fracture of an Aircraft Alloy - *Technical Physics*, Vol. 49, No. 1, pp. 57–60.

## Dynamic fracture of concrete: Experimental and numerical studies on compact tension and L- specimen

JOŠKO OŽBOLT<sup>1</sup>, UWE MAYER<sup>2</sup>, NATALIJA BEDE<sup>3</sup>, AKANSHU SHARMA<sup>1</sup>

<sup>1</sup>IWB, University of Stuttgart, Germany

<sup>2</sup>MPA, University of Stuttgart, Germany

<sup>3</sup>Faculty of Civil Engineering, University of Rijeka, Croatia

It is well known that in concrete structures the resistance, failure mode, crack pattern and crack velocity are strongly influenced by loading rate. The rate dependent response of concrete is controlled through three different effects: (i) through the rate dependency of the growing micro-cracks (influence of inertia at the micro- crack level), (ii) through the viscous behaviour of the bulk material between the cracks (viscosity due to the water content) and (iii) through the influence of inertia of different kind, e.g. structural inertia, inertia due to the softening or hardening of the material or inertia related to the crack propagation.

From the numerical point of view, assuming macro or meso scale analysis, the first two effects can be accounted for by the rate dependent constitutive law. Assuming that the resolution of underlying spatial discretization is fine enough, the third effect should be automatically accounted for through dynamic analysis where the constitutive law interacts with inertia forces.

Recent numerical simulations performed on plain concrete specimens showed very interesting and

complex fracture behavior of concrete under high loading rates. The simulations performed on compact tension (CT) specimen (Ožbolt et al., 2011) highlighted the phenomenon of crack branching at high loading speeds, while the simulations on L-specimen (Ožbolt and Sharma, 2012) brought out the influence of loading rate on direction of crack propagation.

In order to confirm the findings of numerical study and to obtain the experimental evidence on dynamic fracture of concrete, experiments were performed on both CT-specimen and L-specimen. The experiments confirm the results of previously performed numerical predictions.

The phenomenon of crack branching, as predicted by numerical studies, was reproduced experimentally for CT-specimen. The evaluation of test and numerical results show that for strain rates of approximately above 50/s, crack branching occurs. This phenomenon is related directly to the sudden and progressive increase of resistance and is controlled primarily by inertia.

For L-specimen, the experiments confirm the influence of loading rate on the direction of crack propagation

as numerically predicted. For quasi-static load, the crack tends to propagate horizontally, perpendicular to the loading direction. However, with increase of the loading rate the crack propagation tends to get vertical, parallel to the loading direction.

The comparison between numerical and experimental results proves that relatively simple modeling approach based on continuum mechanics, rate dependent microplane model and standard finite elements is capable to realistically predict complex phenomena related to dynamic fracture of concrete and no special criterion is required to capture crack branching, change in crack propagation or progressive increase of apparent strength. The presented, relatively simple,

tests can be used to check whether the numerical model is able to realistically predict complex phenomena related to dynamic fracture of concrete.

#### References

- Ožbolt, J., Sharma, A. and Reinhardt, H.-W. (2011): Dynamic fracture of concrete-compact tension specimen, *International Journal of Solids and Structures*, 48(10), 1534–1543.
- Ožbolt, J. and Sharma, A. (2012): Numerical simulation of dynamic fracture of concrete through uniaxial tension and L-specimen, *Engineering Fracture Mechanics*, 85, 88–102.

## Multiscale model of the dynamic tensile fracture of solid and molten metals: molecular dynamics and continuum mechanics

ALEXANDER MAYER, VASILIJ KRASNIKOV, POLINA MAYER

Chelyabinsk State University, Chelyabinsk, Russia

We report our progress in development of a multiscale theoretical model of fracture of solid metals and metal melts at the high-rate tension. The model is based on our previous works (Mayer & Krasnikov, 2011; Mayer et al. 2013; Mayer et al. 2014). It describes the dynamic deformation of the material on the macrolevel with the use of the mechanics of continua; meanwhile, the evolution of ensembles of microdamages (cavities, cracks) is described on the microlevel with the use of the equations of nucleation, growth and interaction of damages; these equations supplement the macroscopic description. Equations for evolution and nucleation of microdamages and parameters of these equations are obtained from the results of simulations on the basis of the molecular dynamics (MD) and continuum mechanics.

We present the results of MD simulations and continuous modeling of the voids growth in solid metals at tension. Mechanism of growth consists in the plastic deformation in the void vicinity. At the high strain rates ( $>10\text{-}100/\mu\text{s}$ ), the plastic flow starts from the nucleation of dislocations near the void surface. At the moderate strain rates ( $<10/\mu\text{s}$ ), the initially existing dislocations in the material are enough for providing of the required rate of the plastic deformation; the dislocation density are increasing due to multiplication of the existing dislocations. For description of the voids dynamics, we propose the dislocation model, which is based on our previous results (Krasnikov et al. 2011, Mayer et al. 2013). The model is verified and the model parameters are fitted on the basis of the MD and continuum simulation results. We present a multilevel

model of fracture of the uniform solid metal, which includes the model of voids growth and the equation of the voids nucleation (due to the thermal fluctuations). The fracture of uniform metals (homogeneous mode of fracture) makes sense only for the ultrahigh strain rates—more than  $100/\mu\text{s}$ . At the lower strain rates, the initial defects of the material microstructure play a dominant role and decrease the material strength (transition to the heterogeneous mode of fracture).

For melts, the multiscale model is the most simple and allows us to understand more clearly the processes in solids as well. Using of the literature data on the surface tension and viscosity of melts allows us to get a correspondence between the continuum description and MD. With the use of the model, we calculated the strength of the uniform melts of Al, Cu, Fe and Pb within a wide range of strain rates (from  $1\text{-}10/\text{ms}$  to  $1\text{-}100/\text{ns}$ ) and temperatures (from melting temperature to  $70\text{-}80\%$  of critical temperature). Within the range of the strain rates of  $1\text{-}100/\mu\text{s}$ , a homogeneous nucleation mode can be realized, in which the dynamic strength of a melt can be comparable or even higher than the strength of the same solid metal at room temperature. We proposed a schema of experiment for measurement of the tensile strength of uniform metal melts.

The work is supported by the grant from the Russian Science Foundation (Project No. 14-11-00538).

#### References

- Mayer, A.E. & Krasnikov, V.S. (2011): Copper spall fracture under sub-nanosecond electron irradiation. –

Engng Fract. Mech., 78: 1306–1316.  
Mayer, A.E., Khishchenko, K.V., Levashov P.R. & Mayer, P.N. (2013): Modeling of plasticity and fracture of metals at shock loading. – J. Appl. Phys, 113: 193508.  
Mayer, A.E., Mayer, P.N. & Krasnikov, V.S. (2014): Dynamic fracture of metals in solid and liquid states

under ultrashort intensive electron or laser irradiation. – Procedia Mat. Science, 3: 1890–1895.  
Krasnikov, V.S., Mayer, A.E. & Yalovets, A.P. 2011: Dislocation based high-rate plasticity model and its application to plate-impact and ultra short electron irradiation simulations. – Int. J. Plast., 27: 1294–1308.

## Stage I fatigue crack studies in order to validate the dislocation-free zone model of fracture for bulk materials

FLORIAN SCHÄFER, MICHAEL MARX, HORST VEHOFF

Saarland University, Dep. Materials Sciences and Engineering, Saarbrücken, Germany

Stage I fatigue cracks are commonly described by the model of Bilby, Cottrell and Swinden (BCS-model). However, since several experimental investigations have shown a dislocation-free zone (DFZ) in front of crack tips, it is necessary to validate the new DFZ-model and to examine the deviations to the BCS-model. Therefore the dislocation density distribution is derived from height profiles of slip lines in front of stage I fatigue cracks in CMSX4<sup>®</sup> single-crystals measured by contact mode atomic force microscopy. This is possible, because the cracks are initiated at notches milled by focused ion beam technique directly on slip planes with a high Schmid factor. Consequently, the directions of the Burgers vectors are well known and it is possible to calculate the dislocation density distributions from the height profiles. The measured distributions are

compared to the calculated distribution function of the DFZ-model proposed by Chang et al. The additionally measured microscopic friction stress of the dislocations is then used to calculate the influence of grain boundaries on the dislocation density distribution in front of stage I cracks. The calculation is done by the extended DFZ-model of Shiue et al. and compared with the measured distribution function in polycrystalline specimens. Finally the crack tip sliding displacement as a measure for the crack propagation rate is compared for the DFZ-model and the BCS-model with the experimentally revealed values. The important result: The often used BCS-model does not reflect the experimental measurements. On the contrary, the DFZ-model reflects the measurements at stage-I-cracks qualitatively and quantitatively.

Talks Topic G 2:

## ***Fracture mechanics***

---

## The Mechanics of Bridged Fatigue Cracks

JAMIE J. KRUZIC

School of Mechanical, Industrial, and Manufacturing Engineering, Oregon State University, Corvallis, USA

Crack bridging is an effective mechanism for achieving high toughness and strength in many ceramics and composites [1]. However, this mechanism results in a crack size dependence for the fracture properties ( $R$ -curve effect) and fatigue properties (small crack effect) when the crack size is on the order of the bridging zone size [2]. Since brittle materials can only tolerate small crack sizes, making accurate fatigue failure predictions requires approaches that account for crack size effects. In this presentation, it will be described how fatigue threshold  $R$ -curves may be used to understand and predict the fatigue behavior of bridging toughened materials. In this study, fatigue threshold  $R$ -curves are determined for bridging toughened  $\text{Al}_2\text{O}_3$  and  $\text{Si}_3\text{N}_4$  ceramics and then are used to make fatigue endurance strength predictions for realistic semi-elliptical surface cracks [3,4]. Furthermore, it is shown that the fatigue threshold  $R$ -curve can be determined by quantifying the bridging stress distribution for conventional long crack compact tension specimens without the need for difficult small crack experiments [3,4]. Also, different

methods for determining bridging stress distributions are compared [5]. Finally, it is shown how experimentally measured fatigue data for realistic semi-elliptical surface cracks agrees well with predictions based on quantitative bridging zone characterization [3,4]. Overall, it is expected that this methodology can be extendable to cover a wide range of materials toughened by crack bridging, including ceramics, intermetallics, composites, and biological materials.

### References

- [1] P.F. Becher, *J. Am. Ceram. Soc.*, **74** 255 (1991).
- [2] J.J. Kruzic, R.M. Cannon, R.O. Ritchie, *J. Am. Ceram. Soc.*, **87** 93 (2004).
- [3] S. Gallops, T. Fett, J.W. Ager III, J.J. Kruzic, *Acta Mater.*, **59** 7654 (2011).
- [4] R.B. Greene, S. Fünfschilling, T. Fett, M.J. Hoffmann, J.J. Kruzic, *J. Am. Ceram. Soc.*, **97** 577 (2014).
- [5] R.B. Greene, S. Gallops, S. Fünfschilling, T. Fett, M.J. Hoffmann, J.W. Ager III, J.J. Kruzic, *J. Mech. Phys. Solids*, **60** 1462 (2012).

## On the need to reconsider fatigue crack growth at negative stress ratios

CHRISTOPHER BENZ, MANUELA SANDER

University of Rostock, Institute of Structural Mechanics, Germany

It is common practice that negative stress ratio loadings of fatigue cracks are defined by  $K$  ( $\Delta K$  or  $K_{\max}$ ) and  $R < 0$ . But, this does not assure comparability of the loading conditions at the crack tip. There are several indications and even evidence in different literature works. Therefore, within this contribution well known facts, selected literature results and additional results are combined to illustrate the necessity to use a separate crack tip loading parameter for the minimum load at negative stress ratios.

There is a contradiction in literature regarding fatigue crack growth at negative stress ratios. On the one hand there are a lot of results for negative stress ratio loading conditions. The results comprise numerous  $da/dN$ - $\Delta K$ -curve for negative stress ratios and several variable amplitude loading investigations. On the other hand, there are neither basic information regarding the crack tip loading condition at tension-compression loading in textbooks nor detailed information regarding testing procedures in the standards. Therefore, it is estab-

lished to use  $K$  ( $\Delta K$  or  $K_{\max}$ ) and a constant value of  $R$  to define the loading conditions for both positive and negative stress ratios. However, some works claimed that  $K$  ( $\Delta K$  or  $K_{\max}$ ) and  $R$  are not suitable to define the crack tip loading at negative stress ratios and did provide alternatives. Yu, Topper and Au [Yu & Topper & Au 1984] stated already in 1984 "When compressive stress is present in the load cycle the crack growth rate depends on the maximum stress intensity and minimum stress rather than on maximum stress intensity and stress ratio." Zhang et. al performed several finite element analysis [Zhang et al. 2008] and they showed that  $K_{\max}$  and  $R$  does not correlate with the local crack tip loading at negative stress ratios. They also suggested to use a stress based parameter instead. More recently Benz and Sander [Benz & Sander 2014] suggested to use the parameter  $\sigma_{\text{tip}}$  to describe the minimum crack tip loading at negative stress ratios. However, the situation is quite difficult since there are so many data based on the established way and the literature infor-

mation on the alternatives is quite hidden. Therefore, the different contributions on this topic are intensively discussed, interpreted and complemented by additional considerations and results.

An analysis of the proposed concepts to describe the minimum crack tip loading at negative stress ratios reveals that they are quite similar in the basic idea. However, it is shown that  $\sigma_{\text{tip}}$  can be interpreted as a generalization of the former concepts. It will be shown that this concept is not in conflict with the crack closure concept. A discussion on the consequences for fracture mechanical analyses reveals the need to reconsider negative stress ratios in order to assure the reliability of fracture mechanical predictions.

## References

- Yu, M.T., Topper T.H., Au P. (1984): The effects of stress ratio, compressive load and underload on the threshold behavior of a 2024-T351 aluminum alloy? – In: Fatigue 84: proceedings of the 2nd International Conference on Fatigue: 179-90
- Zhang J. et al. (2008): Elastic-plastic finite element analysis of the effect of compressive loading on crack tip parameters and its impact on fatigue crack propagation rate. – In: Engineering fracture mechanics 75(18):5217–28.
- Benz C., Sander M. (2014): Fatigue crack growth testing at negative stress ratios: Discussion on the comparability of testing results. – In: Fatigue & fracture of engineering materials & structures 37(1 ): 62–71.

## Effect of adjacent small defects on fatigue limit of steels

MARI ÅMAN<sup>1</sup>, SABURO OKAZAKI<sup>2</sup>, HISAO MATSUNAGA<sup>3,4</sup>, GARY MARQUIS<sup>1</sup>

<sup>1</sup>Department of Applied Mechanics, Aalto University, Finland

<sup>2</sup>Graduate school of Kyushu University, Fukuoka, Japan

<sup>3</sup>Department of Mechanical Engineering, Kyushu University, Fukuoka, Japan

<sup>4</sup>International Institute for Carbon-Neutral Energy Research (I2CNER), Kyushu University, Fukuoka, Japan

The fatigue strength of a loaded component containing multiple material defects is significantly influenced by the proximity of the defects. In the most simple case of two adjacent defects, the stress concentration is enhanced depending on the distance between the defects. Once cracks emanate from interacting defects, stress intensity factors of the cracks also interact and increase depending on the crack lengths and space between the defects. In order to investigate the interaction effect of defects on the fatigue limit of annealed medium carbon steel JIS-S45C, two adjacent holes were drilled into the surface of round specimens prior to tension-compression fatigue testing. The diameter ( $d$ ) and depth ( $h$ ) of the holes varied from 100  $\mu\text{m}$  to 200  $\mu\text{m}$  while the spacing ( $s$ ) between the two holes ranged from  $0.5d$  to  $1.5d$ . Fatigue limits obtained for various combinations of  $d$ ,  $h$  and  $s$  were compared with the predicted values obtained by the parameter model (Murakami & Endo 1983). In all the cases, fatigue limits were determined by the non-propagation condition of cracks emanating from the holes. The concept of a critical spacing between the defects,  $s_{cr}$ , at which the interaction effect can be ignored has been studied. Murakami *et al.* determined analytically that if the spacing between two defects is larger than the diameter of the smaller of the defects, the interaction effect is negligible (Murakami & Nemat-Nasser, 1982, Murakami 2002). The experimental results from this study are in good agreement with this proposal. For example, in the combination of  $(d_1, h_1, s) = (d_2, h_2, s) = (100, 100, 100) \mu\text{m}$ , the non-propagating cracks did not coalesce at the fatigue limit, *i.e.*, each defect behaved as an individual defect. On the other hand, in the com-

ination of  $(d_1, h_1, s) = (200, 200, 50) \mu\text{m}$  and  $(d_2, h_2, s) = (100, 100, 50) \mu\text{m}$ , the defects coalesced and the crack became non-propagating at the fatigue limit, *i.e.*, two defects together behaved as a single defect in view of the fatigue crack threshold. It has been suggested that, in such a case, the fatigue limit should be evaluated by the *effective defect size* estimated by a contour that envelopes the two defects (Murakami 2002). In accordance with the aforementioned considerations, the fatigue limits for various combinations of  $d$ ,  $h$  and  $s$  were in good agreement with the prediction by the parameter model. A successive observation by the plastic replica method manifested that fatigue crack growth suddenly accelerated soon after coalescence. In our presentation, in addition to the results of JIS-S45C, similar results for the other type of steel with higher strength level will also be shown. The series of experimental findings obtained in this study are necessary to improve the accuracy of the fatigue limit evaluation for various materials, such as cast irons, cast steels and cast aluminium alloys, that contain naturally occurring defects which are detrimental to fatigue strength.

## References

- Murakami, Y. & Endo, M. (1983): Quantitative evaluation of fatigue strength of metals containing various small defects or cracks. Eng. Fract. Mech. 17, 1-15.
- Murakami, Y. (2002): Metal Fatigue: Effects of Small Defects and Nonmetallic Inclusions, Elsevier, UK, ISBN: 0-08-044064-9, p.17-22.
- Murakami, Y. & Nemat-Nasser, S. (1982): Interacting dissimilar semi-elliptical surface flaws under tension and bending. Eng. Fract. Mech 16(3), 373-386.

# Comparison between three fatigue damage models and experimental results for composite materials submitted to spectrum loading

MOHAMMED BOUSFIA, M. ABOUSSALEH<sup>1</sup>, B. OUHBI<sup>2</sup>, R. BOUKHILI<sup>3</sup>

<sup>1</sup>Equipe Mécanique et Ingénierie Intégrée (MII), ENSAM Meknès, Morocco.

<sup>2</sup>Equipe d'Analyse Mathématique et Simulation Numérique des problèmes en mécanique. ENSAM. Morocco.

<sup>3</sup>Centre of Applied Research on Polymers Mechanical Engineering Department Polytechnique de Montreal.

- The theme that we have treated here is about phenomenon of random fatigue of composite structures.
- The failure mode on which we focused in our work is that of inter-laminar fracture delamination.
- Next to experimental results, we have presented three models for predicting damage of structures in order to compare them to test results.
- The effect of the standard deviation of the predictions of the life of composites is also highlighted in the last part of the paper.

Thanks to their excellent fatigue resistance and low weight ratio, today; composite materials are of great importance in humanity life, either in civil or military fields such as aerospace, automotive, marine ... and as is usual, each material reaches failure towards the end of his life which is manifested by the occurrence of fractures. Until now, researchers put their efforts into service in order to achieve accurate and general models for predicting damage of this mysterious material. On our side, we compared three fatigue damage models in order to see the most accurate and consistent with our experimental results. Throughout the work, we adopted a stationary ergodic Gaussian random loading. First, we conducted a thorough study of the inter-laminar fracture of composite laminates subjected to stochastic loads. The choice of this failure mode was inspired by the fact that this failure mode is most predominant among others; moreover, it is more dangerous because it's invisible and undetectable and occurs suddenly between the layers of material. The results of the experiments carried out with graphite epoxy composite laminates [ $\pm 45/0/90$ ]<sub>3s</sub>, were compared to the predictions of three models namely:

- Linear damage model based on the law of Miner,
- Damage mathematical expectancy  $E(t)$ ,
- Stiffness degradation model,

Second time, following an analysis of the results, we found that the three models mentioned above are close to the experimental results. We see that the correlation is the best for the stiffness degradation model. On the other hand, the effects of load sequence and interaction are not taken into account in linear damage model, which can lead to some difference between the model predictions and experimental results.

Finally, we had to study the effect of standard deviation on the life of composite laminates. For this we calculated the lifetime for various values of sigma and various average amplitudes of the applied load. Interpolating the data obtained led us to an equation linking lifetime of structures to standard deviation.

## References

- M. Aboussaleh and R. Boukhili. "Life Prediction for Composite Laminates Submitted to Service Loading Spectra". June 1998; Vol. 19; pp 241-245.
- Adden S, Horst P. "Stiffness degradation under fatigue in multiaxially loaded non-crimped-fabrics". Int J Fatigue 2010; 32:108–22.
- Yung-Li Lee, Tana Tjhung. "Chapter 3 - Rainflow Cycle Counting Techniques". Metal Fatigue Analysis Handbook 2012, pp 89-114.
- SR. Reid and G. Zho. "Impact behaviour of fibre-reinforced composite materials and structures". CRC Press; 2000

## Experimental and numerical analysis of damage in random fibrous networks

E. SOZUMERT<sup>1</sup>, E. DEMIRCI<sup>1</sup>, M. ACAR<sup>1</sup>, B. POURDEYHIMI<sup>2</sup>, V. V. SILBERSCHMIDT<sup>1</sup>

<sup>1</sup>Wolfson School of Mechanical and Manufacturing Engineering, Loughborough University, Leicestershire, UK

<sup>2</sup>Nonwovens Cooperative Research Center, North Carolina State University, Raleigh, NC, USA

Fibrous networks are ubiquitous: they can be found in various engineering applications as well as in biological tissues. Due to complexity of their random microstructures, anisotropic properties and a high extent of stretching, their deformation and damage behaviours are rather cumbersome and need proper analysis and simulations. Though, in the literature, there are numerous studies focusing either on numerical simulations of fibrous networks or explaining their damage mechanisms at micro- or meso-scale, the used models usually do not incorporate actual random material's microstructure and failure mechanisms.

The microstructure of fibrous networks – together with usually highly non-linear mechanical behaviour of their single fibres – is responsible for specific features of initiation of damage, its spatial localization and ultimate failure. Complex scenarios of realisation of damage processes at large extensions are defined by these features but they are not studied sufficiently.

An experimental programme of this study included tensional tests of notched and non-notched specimens of nonwoven fabrics were experimentally tested at different strain rates. To study anisotropy of the deformation and damage properties (linked to a specific type of an orientation distribution function of fibres), five types of specimens, cut at 0°, 30°, 45°, 60° and 90° to a machine direction, were investigated.

To emulate the real-life microstructure in a finite-element model, curled fibres were introduced to capture geometric nonlinearity. The orientation distribution function for fibres obtained from X-ray micro computed-tomography images was considered to introduce

their actual alignment. The new developed model also incorporates fibre-to-fibre interactions. A good correlation between the obtained experimental data and simulations results was observed, and this work revealed a significant effect of fibre interactions on damage evolution (together with their orientation).

### References

- Hou, X., Acar, M. & Silberschmidt, V.V. (2009) 2D finite element analysis of thermally bonded nonwoven materials: Continuous and discontinuous models, *Comput. Mater. Sci.* 46: 700–707.
- Hou, X., Acar, M. & Silberschmidt, V.V. (2011) Non-uniformity of deformation in low-density thermally point bonded nonwoven material: effect of microstructure. *J. Mater. Sci.* 46: 307–315.
- Sabuncuoglu, B., Acar, M. & Silberschmidt, V.V. (2011) Parametric code for generation of finite-element model of nonwovens accounting for orientation distribution of fibres. *Int. J. Numer. Meth. Engng.* 94: 441–453.
- Farukh, F., Demirci, E., Sabuncuoglu, B., Acar, M., Pourdeyhimi, B. & Silberschmidt, V.V. (2014) Numerical analysis of progressive damage in nonwoven fibrous networks under tension. *Int. J. Solids Struct.* 51: 1670-1685.
- Farukh, F., Demirci, E., Acar, M., Pourdeyhimi, B. & Silberschmidt, V.V. (2014) Large deformation of thermally bonded random fibrous networks: microstructural changes and damage, *J. Mater. Sci.* 49: 4081-4092.

Talks Topic G 3:

## *Fracture mechanics*

---

# A boundary finite element for anisotropic/piezoelectric materials containing multiple cracks

CHYANBIN HWU, SHAO-TZU HUANG

National Cheng Kung University, Tainan, Taiwan, R.O.C.

The Green's function for the problem of a two-dimensional linear anisotropic elastic solid containing a straight crack has been obtained analytically by using Stroh's complex variable formalism (Hwu, 2010). Using the Green's function expressed in terms of Stroh's formalism, same mathematical equations can be employed to the piezoelectric materials by just expanding the dimension of corresponding matrix to include the piezoelectric effects (Hwu and Ikeda, 2008). The use of this Green's function leads to a boundary element for a two-dimensional anisotropic or piezoelectric solid containing a single straight crack. The main feature of this special boundary element is that no meshes are needed along the boundary of cracks since the traction-free boundary conditions are satisfied exactly.

In this paper, in order to extend this boundary element to treat the problems with multiple cracks, the element is transformed into an equivalent finite element by using the relation between element nodal force of finite element and surface traction of boundary element (Hwu, et al., 2014). After the transformation, all the elements are assembled together by following the rule of finite element method, and the compatibility and equilibrium considered in the conventional subregion technique can then be satisfied automatically. Note that like the combination employed in the subregion technique, to be compatible with the fundamental solution the system of equations for each subregion is obtained based upon the local coordinate with the origin located at the crack center and the coordinate axes parallel and normal to the crack surface. In order to combine the system of equations for the whole region, a commonly-based global coordinate should be used, and to save computational time the transformation of matrices are suggested to be performed at the nodal level, instead of the subregion level.

After getting the nodal displacements and nodal forces by the system of equations of finite element, the

nodal tractions on the boundary are calculated from the original system of equations of boundary element. Like the calculation of conventional boundary element, if all the values of tractions and displacements on the boundary are determined, the values of displacements, strains and stresses at any interior point can be calculated from the boundary integral equation by setting the free term coefficients to be an identity matrix (Brebbia, et al., 1984). Unlike the conventional method which usually needs very fine meshes near the crack tip, in this paper the stress intensity factors of the crack are evaluated by using only the remote boundary displacements and tractions (Hwu and Liang, 2000). To show the accuracy and efficiency of the proposed boundary finite element method, several numerical examples are executed and compared with the solutions obtained by analytical solutions and the commercial finite element software.

## References

- Brebbia, C.A., Telles, J.C.F. and Wrobel, L.C. (1984): *Boundary Element Techniques*, Springer, New York.
- Hwu, C. and Liang, Y.C. (2000): Evaluation of Stress Concentration Factors and Stress Intensity Factors from Remote Boundary Data, *International Journal of Solids and Structures*, 37(41): 5957-5972.
- Hwu, C. and Ikeda, T. (2008): Electromechanical Fracture Analysis for Corners and Cracks in Piezoelectric Materials, *International Journal of Solids and Structures*, 45: 5744-5764.
- Hwu, C. (2010): *Anisotropic Elastic Plates*, Springer, New York.
- Hwu, C., Li, C.C. and Huang, S.T. (2014): Coupling of Boundary and Finite Elements for the Problems of Multiple Polygon-like Holes, *Advances in Boundary Elements & Meshless Techniques XV*, 275-280, Florence, Italy.

## Effect of micromorphology on crack growth in cortical bone tissue: X-FEM study

MAYAO WANG<sup>1</sup>, XING GAO<sup>1</sup>, ADEL ABDEL-WAHAB<sup>1</sup>, SIMIN LI<sup>1</sup>, ELIZABETH A. ZIMMERMANN<sup>2</sup>, CHRISTOPH RIEDEL<sup>2</sup>, BJÖRN BUSSE<sup>2</sup>, VADIM V. SILBERSCHMIDT<sup>1</sup>

<sup>1</sup>Wolfson School of Mechanical and Manufacturing Engineering, Loughborough University, Leicestershire, UK,

<sup>2</sup>University Medical Center Hamburg-Eppendorf, Hamburg, Germany

Bones play a key role in supporting a body and protecting internal organs. Obviously, bone fractures can have serious consequences, especially in cases of age-related bone degeneration diseases such as osteoporosis or bone diseases. From a point of view of mechanics of materials, a cortical bone tissue can be treated as a natural multi-constituent composite material. At micro-level, osteons are its main structural unit; they contain central canals known as Haversian canals and are randomly distributed within the surrounding interstitial matrix. A thin layer of cement line separates these two constituents. These randomly distributed microstructural components of cortical bone define its heterogeneity and anisotropy that have a direct impact on crack propagation during dynamic loading regime such as a traumatic fall or an accident.

It is well known that various factors (e.g. age, disease etc.) can lead to a loss of bone mineral density due to unbalanced remodelling process, significantly affecting morphology of the underlying microstructure components. As a result, morphological characteristics of osteons in cortical bone are complicated and varied in different groups, such as young, healthy, aged, osteoporosis and bisphosphonate-treated groups. According to the previous studies mechanical properties of cortical bones in four different groups demonstrate significant difference due to various geometrical factors at the osteonal level. However, there is still no detailed investigation on the effects of morphological character-

istics on crack propagation, especially under dynamic loading conditions.

In this study, random distributions of the microstructure in cortical bone tissue representing four different bone morphology groups were analysed. The obtained data were parameterized based on the obtained images and processes employing a MATLAB programme, considering such features as positions, dimensions, orientations and volume fractions of osteons and Haversian canals. Then, statistically representative models of osteonal morphologies were developed and imported into finite-element software used to simulate crack propagation in microstructured bone tissues; an extended finite-element method X-FEM was employed for this purpose. The results from numerical simulations demonstrated that X-FEM is a powerful tool for investigation of the effect of micro-morphology of osteons and volumetric fraction of various microstructural constituents on crack growth under dynamic loading conditions.

### Reference

Bernhard A, Milovanovic P, Zimmermann EA, Hahn M, Djonic D, Krause M, Breer S, Püschel K, Djuric M, Amling M, Busse B. Micro-morphological properties of osteons reveal changes in cortical bone stability during aging, osteoporosis, and bisphosphonate treatment in women. *Osteoporosis Int* 2013;24(10):2671-2680.

## Extended damage modelling for fracture control in modern line pipe steels

AIDA NONN

OTH Regensburg, Faculty of Mechanical Engineering, Germany

Safety assurance against crack propagation in gas pipelines has been one of the major structural integrity challenges since 1960's. Back then, a standardized Drop Weight Test (DWTT) with pressed notch was developed with the purpose to exclude brittle fracture initiation and propagation by requiring minimum of 85-percent shear area. At the same time the materials should also exhibit a minimum Charpy energy value estimated by Battelle-Two-Curve Method (BTCM) to insure an arrest

of propagating ductile fracture. Both criteria were successfully applied for vintage pipeline material.

However, limitations of both criteria have become evident for modern line pipe steels with improved strength and toughness properties. With respect to brittle fracture control, lower strength steels, such as X65 grade, often exhibit propensity to so called "abnormal fracture appearance" (AFA) or inverse fracture in DWTT characterized by ductile crack initiation at

pressed notch followed by onset of cleavage fracture. In this case the 85-percent shear area criterion cannot be applied and DWTT results are declared invalid. Hence, the utilization of these steels remains significantly restricted as long as no suitable tests and criteria are provided to obviate brittle fracture. Regarding ductile fracture control, it was shown that the minimum Charpy energy predicted by BTCM is not sufficient to guarantee ductile fracture arrest, especially for high strength line pipe material such as X100 grade and correction factors have to be introduced in order to account for these deviations.

To develop a small-scale test representative of pipeline fracture behaviour and derive an adequate fracture control criteria for new line pipe steels, it is desirable to combine both experimental efforts and take advantage of numerical methods in material modelling. This paper shows how to reach these goals by applying an extended damage mechanics approach to describe fracture behaviour of modern steels in transition region. The ductile fracture can be successfully captured for both X65 and X100 grades by modified Gurson-Tvergaard-Needleman (GTN) and Cohesive Zone (CZ) damage models. Based on the simulation results, it is pos-

sible to identify major material, geometry and loading parameters controlling ductile fracture propagation/arrest. On the other hand, two approaches have been considered for the fracture simulation in the transition region. One approach includes a simplified cleavage initiation criterion and another couples a ductile damage model to CZ model with traction-separation law for brittle fracture. The material parameters can be estimated by comparison between experimental and numerical results conducted on deep and shallow notched SENB specimens. Subsequently, the calibrated numerical models have been used for fracture simulation in DWTT and pipe models. The results can also serve to understand mechanisms governing the fracture in modern line pipe steels, e.g. inverse fracture behaviour in DWTT, and how they are reflected in actual pipe behaviour.

#### Reference

Scheider, I.; Nonn, A.; Völling, A.; Mondry, A. & Kalwa, C. (2014): A damage mechanics based evaluation of dynamic fracture resistance in gas pipelines. *Procedia Materials Science*, Vol. 3: 1956-1964, doi:10.1016/j.mspro.2014.06.315.

Talks Topic G 4:

## *Fracture mechanics*

---

# Cleavage Initiation Angle for High Strength Steels under Mixed-Mode Conditions

ZEFENG ZHANG, XUDONG QIAN

Department of Civil and Environmental Engineering, National University of Singapore, Singapore

The expected increasing number of infrastructures near the Arctic, driven largely by the global demand on petroleum resources, anticipates the rising consumption of high-strength ferritic steels as the primary structural material. The cleavage fracture for these high-strength steels under the relatively low ambient temperature near the Arctic imposes a critical threat to the safety of these infrastructures. The fracture toughness, measured using the standard material testing protocol [1], exhibits significantly lower toughness values than those measured at the room temperature. In addition, the large scatter in the measured toughness values drives a statistical approach in assessing the brittle structural failure, in contrast to the conventional, deterministic approach for ductile fracture.

The Weibull type statistical model has evolved over the years as a widely recognized approach in estimating the probability of cleavage fracture for ferritic steels under pure mode I loading. Wallin [2] utilized the Weibull distribution to quantify the macroscopic scatter of fracture toughness. Ruggieri and Dodds [4] employed the maximum principal stress to calculate the effective microscopic driving force for cleavage fracture, namely the Weibull stress  $\sigma_w$ . The Weibull stress  $\sigma_w$  represents a scalar measure of the driving force for the microscopic cracks in the fracture process zone. The use of microscopic Weibull stress allows the development of a uniform approach to predict the probability of fracture under varying levels of crack-front constraints. The Weibull stress approach has demonstrated reasonable success in estimating the probability of fracture for a wide range of materials, reflected most recently by the comparison to the Euro fracture database [4]. However, realistic cracks in engineering structures often experience a mixed-mode condition, which requires further understanding on both the cleavage fracture angle and toughness assessment.

This study aims to extend the probabilistic Weibull stress framework to estimate the cleavage fracture angle for high-strength ferritic steels under the mixed-

mode I and II condition at a low ambient temperature ( $-90^\circ$ ). The effective stress required in computing the Weibull stress, which drives the opening of microcracks under a mixed-mode I and II condition, depends on a well-defined stress-based fracture criterion. This paper examines three different fracture criteria, the maximum principal stress, the coplanar energy release rate, and the modified co-planar energy release rate in computing the microscopic Weibull stresses. The angular Weibull stress density  $\sigma_{w-\theta}$  calculated following the three fracture criteria estimates the range of the cleavage fracture angle anticipated during a mixed-mode fracture test. The numerical study further investigates the effect of the crack-front constraints (quantified by the  $T$ -stress) and the large plastic deformations on the cleavage angle.

This paper also reports an experimental program for single-edge notched specimens made of the high strength steel S550 under a four-point bend and shear mixed-mode condition. The experimental results with different mode-mixity angles support the development of a modified Weibull approach to assess the mixed-mode brittle fracture with an experimentally validated stress criterion.

## References

1. ASTM E1921-13a (2013). Standard test method for determination of reference temperature,  $T_0$ , for ferritic steels in the transition range. ASTM International, West Conshohocken, PA.
2. Wallin, K. (1984): The scatter in  $K_{IC}$ -results. Eng Fract Mech, 19, 1085-1093.
3. Ruggieri, C. and Dodds, R.H.Jr. (1998): Numerical computation of probabilistic fracture parameters with WSTRESS. Engng Comput, 15, 49-73.
4. Wasiluk, B., Petti, J.P. and Dodds, R.H.Jr. (2006). Temperature dependence of Weibull stress parameters: studies using the Euro-materials. Engng Fract Mech, 73:1046-69

# Experimental and numerical investigations on the crack growth stage of crane runway girders subjected to cyclic loading

PHILIPP RETTENMEIER, EBERHARD ROOS, STEFAN WEIHE, XAVER SCHULER

Materialprüfungsanstalt (MPA) Universität Stuttgart, Germany

Numerous engineering components as railway tracks or crane runways are subjected to rolling contact fatigue (RCF) due to travelling wheel loads. RCF causes non-proportional mixed mode crack tip loading (Fletcher2014) and mode II controlled or shear mode crack growth (Bold1991, Otsuka1993, Otsuka1996). Traditional fracture mechanic concepts dealing with mode I or tensile mode crack growth are thus not applicable (Bold1991, Yang2014). One of the reasons is the compressive stress field directly below the wheel load suppressing tensile mode crack growth (Otsuka1996).

The contribution is focused on the crack growth stage of crane runway girders consisting of hot-rolled girders with welded rails. Cyclic tests were conducted on full-scale crane runway girders travelled over by wheel loads. Fatigue crack initiation was identified at the sharply notched weld root. As a consequence, detection of crack initiation lifetime was technically not feasible by non-destructive measurements due to the weld geometry. Therefore, a pressure system was used to detect the lifetimes until first through-thickness crack (Rettenmeier2013). Shear mode fatigue crack growth within the weld metal was observed by fractographic investigations after cyclic tests. Additionally, crack growth rate was evaluated by means of tests with C(T) specimens extracted from the weld metal.

Numerical investigations were performed in Abaqus to calculate the crack growth lifetime of the crane runway girders. Stress intensity factors were evaluated by means of modified virtual crack closure technique. Mixed mode crack tip loading was identified. An initial crack length of 1 mm was assumed for crack growth calculations. Numerical calculations showed a significant influence of mode II stress intensity factor on crack growth. Thus, crack growth lifetime was estimated by shear stress intensity factor  $K_{II}$  introduced by Otsuka et al. (Otsuka1975) and NASGRO equation according to Forman/Mettu (Forman1990).

Subsequently, the calculated total lifetime was separated into crack initiation and crack growth lifetime. The former was estimated by MPA AIM-Life concept

in combination with critical plane approach (Rettenmeier2015). The numerical investigations showed that crack growth stage approximately amounts to one half of the total lifetime. Finally, the calculated total lifetime was compared to experimental results until first through-thickness crack.

## References

- Bold, P.E. & Brown, M.W. & Allen, R.J. (1991): Shear mode crack growth and rolling contact fatigue. – *Wear* 144, 307-317
- Fletcher, D.I. (2014): Numerical simulation of near surface rail cracks subject to thermal contact stress. – *Wear* 314, 96-103
- Forman, R. G. & Mettu, R. M. (1990): Behavior of Surface and Corner Cracks subjected to Tensile and Bending Loads in Ti-6Al-4V Alloy, NASA Technical Memorandum 102165
- Otsuka, A. & Mori, K. & Miyata, T. (1975): The condition of fatigue crack growth in mixed mode condition. – *Engineering Fracture Mechanics* 7, 429-439
- Otsuka, A. & Aoyama, M. (1993): Mode II Fatigue under a Compressive Stress Field: a Simplified Model for Rolling Contact Fatigue. – *Mixed Mode Fatigue and Fracture*, 49-60
- Otsuka, A. & Sugawara, H. & Shomura, M. (1996): A test method for mode II fatigue crack growth relating to a model for rolling contact fatigue. – *Fatigue & Fracture of Engineering Materials and Structures* 19, 1265-1275
- Rettenmeier, P. & Euler, M. & Roos, E. & Kuhlmann, U. (2013): Experimental investigations on the fatigue strength of welded joints on full-scale crane runway girders. – *Proceedings of the 10<sup>th</sup> International Conference on Multiaxial Fatigue & Fracture (ICMFF10)*, Kyoto
- Rettenmeier, P. & Roos, E. (2015): Fatigue assessment of full-scale welded crane runway girders. – to be published in *MP Materials Testing*
- Yang, Y. (2014): Linear elastic fracture mechanics-based simulation of fatigue crack growth under non-proportional mixed-mode loading. – PhD Thesis, University of Darmstadt

## Crack Path in connection with the Two-Parameter Fracture Mechanics Approach on X52 steel pipe repairing

M. HADJ MELIANI<sup>1,2</sup>, G. PLUVINAGE<sup>2</sup>, Y.G. MATVIENKO<sup>3</sup>

<sup>1</sup>LPTPM, TF, Hassiba Benbouali University, Chlef, Algeria

<sup>2</sup>LaBPS-ENIM, Metz, France

<sup>3</sup>Mechanical Eng. Research, Moscow, Russia

The use of a composite patches for the repair of the API 5L X52 steel pipe in connection with the crack path estimation are presented in this study. The finite element method (FEM) is used to analyse the fracture resistance of a pipe repaired by a boron/epoxy bonded composite patch by evaluation of the notch stress intensity factor  $K_p$  and the non-singular T-stress as a constraint parameter. The use of the two parameter fracture mechanics (K-T) given a described information's of the crack path of the defect of a structure with and without a reinforcing patch. The

effects of the notch aspect ratio, the type of laboratory specimens (CT, SENT, DCB and RT) and the repairing method on the variation of the applied notch stress intensity factor and the T-stress at the notch tip are highlighted. The obtained results show a considerable decrease of the applied notch stress intensity factor in the case of the repaired defect in connection with the crack path. The use of the composite patch reduces significantly the risk of fracture and increases the service life of the pipeline.

## A modified Sih criterion for crack deflection in dipolar gradient elasticity

IOANNIS D. GAVARDINAS, ANTONIOS E. GIANNAKOPOULOS

University of Thessaly, Civil Engineering Department, Volos, Greece

In recent years, generalized or higher order (non local) continuum theories have attracted attention due to the fact they inherently predict the so called "size effect" in the mechanical behavior of materials. This is attributed to their "constitutive" incorporation of intrinsic or internal material lengths. On the other hand, there exist cases in which classic (local) theories of mechanics have failed to capture the mechanical behavior of these specific materials. The higher order theories provide enhanced models for materials with microstructure like composites, cellular materials, textiles etc. The dipolar or strain gradient elasticity is one such theory which was set forth by (Aifantis 1992) with the introduction of a single material length, following the more general theory of (Mindlin & Eshel 1968).

Adopting a Fracture Mechanics point of view, the issue of crack deflection plays a significant role. Tackling the crack deflection problem was historically initiated by (Griffith 1920) for materials exhibiting a quasi-brittle type of behavior, upon the hypothesis of an energetic balance regarding the transition from the unbroken state of a solid to the broken one. The years to come, several crack deflection criteria have been stated, mainly: the maximum energy release rate criterion (Hussain et al. 1974), the maximum circumferential stress criterion (Erdogan & Sih 1963) and the strain energy density criterion (Sih 1974).

In an effort to attack crack deflection in the context of dipolar gradient elasticity, an issue not attempted before in the relevant literature, we have revisited the Sih's strain energy density criterion, based upon physical considerations for its prevalence. At the same time, we concluded that other crack deflection criteria may not be relevant. Following an analytical study, we validated its applicability for dipolar gradient elastic materials. We have used a second order asymptotic strain energy density close to the crack tip, using the crack tip fields as obtained from the asymptotic analysis of (Gourgiotis & Georgiadis 2009) and (Aravas & Giannakopoulos 2009). We propose that crack deflection will appear at a direction that maximizes the near-tip strain energy density along a specific line around the crack tip. This line requires the determination of the angular distribution of the radial distance  $r$  around the crack tip, such that the first and the second order strain energy densities become comparable. The central crack problem in an infinite medium is examined, for mode I, mode II and mixed mode (I+II) loading. The acquired results lead to a powerful method for predicting crack deflection trajectories in materials with microstructure that can be adequately modeled by dipolar gradient elasticity.

### Acknowledgements

This project was implemented under the “ARISTEIA II” Action of the “OPERATIONAL PROGRAMME FOR EDUCATION AND LIFELONG LEARNING”, project “Fatigue of Materials used in Vascular Surgery-FaMaVaSu”, and is co-funded by the European Social Fund (ESF) and National Resources.

### References

Aifantis, E.C. (1992): On the role of gradients in the localization of deformation and fracture. – *Int. J. Eng. Sci.*, 30: 1279-1299.

Aravas, N. & Giannakopoulos, A.E. (2009): Plane asymptotic crack-tip solutions in gradient elasticity. – *Int. J. Solids Struct.*, 46: 4478-4503.

Erdogan, F. & Sih, G.C. (1963): On the crack extension in plates under plane loading and transverse shear. – *ASME J. Basic. Eng.*, 85: 519-525.

Gourgiotis, P.A. & Georgiadis, H.G. (2009): Plane-strain crack problems in microstructured solids governed by dipolar gradient elasticity. – *J. Mech. Phys. Solids*, 57: 1898-1920.

Griffith, A.A. (1920): The phenomena of rupture and flow in solids. – *Philos. Trans. R. Soc. Lond. A.*, 221: 163-198.

Hussain, M.A., Pu, S.L. & Underwood, J. (1974): Strain energy release rate for a crack under combined mode I and mode II. – *Fract. Anal., ASTM STP 560*, Am. Soc. Test. Mat., 2-28.

Mindlin, R.D. & Eshel, N.N. (1968): On first strain-gradient theories in linear elasticity. – *Int. J. Solids Struct.*, 4: 109-124.

Sih, G.C. (1974): Strain-energy-density factor applied to mixed mode crack problems. – *Int. J. Fract.*, 10: 305-321.

## Cohesive laws for adhesive layers loaded in a state close to pure shear

ULF STIGH<sup>1</sup>, ANDERS BIEL<sup>2</sup>

<sup>1</sup>University of Skövde, Skövde, Sweden

<sup>2</sup>Technical University of Denmark, Risø, Denmark

By representing a thin adhesive layer with a cohesive zone, analysis of fracture of bonded structures is greatly simplified while providing high qualitative predictive capability (Carlberger et al. 2008). With this model, only homogenized stress, deformation and damage measures are used to represent the state of the adhesive. The stress variables are denoted the peel stress  $s$  acting in the normal direction of the surface and the shear stresses  $\tau_1$  and  $\tau_2$  acting in the plane of the surface. The work per unit surface performed by these stresses during a deformation process is given by

$$W = \int_0^w \sigma dw + \int_0^{v_1} \tau_1 dv_1 + \int_0^{v_2} \tau_2 dv_2, \quad (1)$$

where  $w$ ,  $v_1$ , and  $v_2$  denote the deformation components of the adhesive layer measured in the directions of the corresponding stress components. With monotonically increasing deformation, a pseudopotential is associated to the state of the adhesive layer. In this case an evaluation of the path independent J-integral at the edge of an adhesive layer reveals that  $W = J$ . That is, if  $J$  is measured during an experiment, the evolution of  $W$  is also measured. If, at the same time,  $w$ ,  $v_1$ , and  $v_2$  are measured, the gradient of  $W$  provides  $\sigma$ ,  $\tau_1$  and  $\tau_2$ . Thus, the corresponding cohesive law is measured. A number of test specimens and procedures have been developed (Stigh et al. 2010).

In shear loading, the end notched flexure specimen is used. This is a three-point bending test rig where the centrally applied load  $F$  is measured. In one method to evaluate the experiments, only  $F$  and  $v$  at the start of the adhesive layer are measured (Alfredsson 2004); in the alternative method, also the rotations,  $\theta_A$ ,  $\theta_B$  and  $\theta_C$ , of the loading and supporting points are measured (Stigh et al. 2009). The alternative expressions read

$$J_s = \frac{9 F^2 a^2}{16 E B^2 H^2} + \frac{3 F v}{8 B H} \quad (2)$$

$$J_R = \frac{F}{2B} (\sin \theta_A - 2 \sin \theta_B + \sin \theta_C)$$

Evaluations of the same experiments using these two equations show good agreement.

However, during the final stage of the fracture process, the adhesive layer swells, i.e.  $w > 0$  (Stigh and Biel 2014). This swelling is confined to the end of an adhesive layer and it is constrained by the flexural stiffness of the adherends. This shows that a compressive stress develops during shear.

### References

Alfredsson, K.S. (2004): On the instantaneous energy release rate of the end-notch flexure adhesive joint specimen. *Int. J. Sol. & Str.*, 41: 4787–807.

Biel, A., & Stigh, U. (2014): Shear properties of an ad-

- hesive layer exposed to a compressive load. *Proc. Mat. Sci.*, 3: 1626-1631.
- Carlberger, T., Alfredsson, K.S. & Stigh, U. (2008): FE-formulation of Interphase Elements for Adhesive Joints. *Int. J. Comp. Meth. Engin. Sci. & Mech.*, 9: 288-99.
- Stigh, U., Alfredsson, K.S., Andersson, T., Biel, A., Carlberger, T., & Salomonsson, K. (2010): Some aspects of cohesive models and modelling with special application to strength of adhesive layers. *Int. J. Fract.*, 165: 149-62.
- Stigh, U., Alfredsson, K.S. & Biel, A. (2009): Measurement of cohesive laws and related problems. *Proc. ASME IMECE-10474*, USA

## The role of Geometrically Necessary Dislocations in the fracture process of metallic materials

EMILIO MARTÍNEZ-PAÑEDA<sup>1</sup>, CHRISTIAN NIORDSON<sup>2</sup>

<sup>1</sup>University of Oviedo, Spain

<sup>2</sup>Technical University of Denmark, Denmark

Experiments and direct dislocation simulations have shown that metallic materials display strong size effect at the micron and sub-micron scales. Attributed to geometrically necessary dislocations (GNDs) associated with non-uniform plastic deformation, this size effect is especially significant in fracture problems as the plastic zone adjacent to the crack tip may be physically small and contains large spatial gradients of deformation. Since conventional plasticity possesses no intrinsic material length, several continuum strain gradient plasticity (SGP) theories have been developed through the years in order to model observed size effects. Most of them can be classified as a function of their approach: phenomenological (Fleck and Hutchinson, 2001) or mechanism-based (Gao et al., 1999).

The experimental observation of cleavage fracture in the presence of significant plastic flow (Elssner et al., 1994) has encouraged significant interest in the influence of plastic strain gradient effects on crack tip stresses and many authors have shown that GNDs near the crack tip promote local strain hardening and lead to a much higher stress level in the vicinity of the crack as compared with classical plasticity predictions. However, although large deformations take place in the vicinity of the crack, very little work has been done to investigate crack tip fields under SGP accounting for finite strains.

Very recently Martínez-Pañeda and Betegón (2015), in the framework of a mechanism-based approach and within the finite deformation theory, quantified the magnitude and the extension of the differences between classical plasticity and SGP stress distribution predictions ahead of the crack tip. Their numerical results revealed a significant increase in both the magnitude and the domain where GNDs significantly influence the crack-tip fields when finite strains are considered. This is due to the strain gradient contribution to the work hardening of the material, that lowers crack tip blunting and thereby avoids the local stress triaxiality reduction characteristic of conventional plasticity predictions.

In the present work, a comprehensive study of crack-tip fields is performed for both phenomenological and mechanism-based SGP theories with the aim of gaining insight into the role of the increased dislocation density associated with large gradients in plastic strain near the crack. Following the work of Niordson and Redanz (2004), a finite strain generalization is implemented in a general purpose finite element code by means of an updated Lagrangian configuration and physical implications of the results are thoroughly discussed, providing an appropriate framework for damage and fracture assessment within SGP theories.

Results obtained reveal the important influence of strain gradients on a wide range of fracture problems, being particularly relevant in hydrogen embrittlement models, due to the central role that the stress field close to the crack-tip plays on both hydrogen concentration and interface decohesion (Gangloff et al., 2014).

### References

- Elssner, G., Korn, D., Rühle, M. (1994): The influence of interface impurities on fracture energy of UHV diffusion-bonded metal-ceramic bicrystals. *Scr. Metall. Mater.*, 31: 1037-1042.
- Fleck, N.A., Hutchinson, J.W. (2001): A reformulation of strain gradient plasticity. *J. Mech. Phys. Solids*, 41: 1825-1857.
- Gao, H., Huang, Y., Nix, W.D., Hutchinson, J.W. (1999): Mechanism-based strain gradient plasticity I. Theory. *J. Mech. Phys. Solids*, 48: 99-128.
- Martínez-Pañeda, E., Betegón, C. (2015): Modeling damage and fracture within strain gradient plasticity. *Int. J. Solids Struct.* [in press]
- Niordson, C.F., Redanz, P. (2004): Size-effects in plane strain sheet-necking. *J. Mech. Phys. Solids*, 52: 2431-2454.
- Gangloff, R.P., Ha, H.M., Burns, J.T., Scully, J.R. (2014): Measurement and modeling of hydrogen environment-assisted cracking in Monel K-500. *Metall. Mater. Trans. A*, 45: 3814-3834.

Talk Topic G 5:

## ***Fracture mechanics***

---

## On the fracture toughness of bulk-metallic glasses

BERND GLUDOVATZ<sup>1</sup>, JAMIE J. KRUZIC<sup>2</sup>, MARIOS D. DEMETRIOU<sup>3</sup>, WILLIAM L. JOHNSON<sup>3</sup>, ROBERT O. RITCHIE<sup>1,4</sup>

<sup>1</sup>Lawrence Berkeley National Laboratory, Materials Sciences Division, Berkeley, CA, USA

<sup>2</sup>Oregon State University, School of Mechanical, Industrial, and Manufacturing Engineering, Materials Science, Corvallis, OR, USA

<sup>3</sup>California Institute of Technology, Keck Laboratory of Engineering Materials, Pasadena, CA, USA

<sup>4</sup>University of California, Department of Materials Science and Engineering, Berkeley, CA, USA

The excellent combination of properties like high strength, low stiffness and high hardness together with the ease of processing and near net-shape castability make bulk-metallic glasses (BMGs) candidate materials for many structural applications. Their fracture toughness, however, can vary over a wide range (generally between 10 and 200 MPa.m<sup>1/2</sup>) and in terms of ductility, BMGs behave entirely different whether they are loaded in tension, compression or bending. Whereas ductility is rather limited in tension/compression, BMGs can be quite ductile in bending. Standard fracture-toughness tests are normally done on “bending” geometries (three-point bending, compact-tension specimens) but it is not clear how the behavior in BMGs under these constrained stress-states relates to that in tension; as such, the extent of validity of non-linear-elastic fracture mechanics to characterize their toughness is in question.

Here, we report on a systematic study to compare the toughness of three different, Zr-based glasses – one low toughness (< 50 MPa.m<sup>1/2</sup>), one medium and one high toughness (>150 MPa.m<sup>1/2</sup>) – tested under differ-

ent loading conditions, specifically deep-cracked bending vs. edge-cracked tension, to understand influences of sample size and stress-state on the measured fracture toughness of BMGs, as well as to determine the origin of the large variations in toughness often found for these materials.

### References

Demetriou, Marios D., Maximilien E. Launey, Glenn Garrett, Joseph P. Schramm, Douglas C. Hofmann, William L. Johnson, and Robert O. Ritchie. “A Damage-Tolerant Glass.” *Nature Materials* 10, no. 2 (January 9, 2011): 123–28.

Gludovatz, Bernd, Steven E. Naleway, Robert O. Ritchie, and Jamie J. Kruzic. “Size-Dependent Fracture Toughness of Bulk Metallic Glasses.” *Acta Materialia* 70 (May 15, 2014): 198–207.

He, Qiang, and Jian Xu. “Locating Malleable Bulk Metallic Glasses in Zr–Ti–Cu–Al Alloys with Calorimetric Glass Transition Temperature as an Indicator.” *Journal of Materials Science & Technology* 28, no. 12 (December 2012): 1109–22.

## Damage & Fracture Toughness of Fibrous Dual-Phase Steels for Automotive Applications

KARIM ISMAIL<sup>1</sup>, THOMAS PARDOEN<sup>1</sup>, PASCAL J. JACQUES<sup>1</sup>, LAURENCE BRASSART<sup>1</sup>, ASTRID PERLADE<sup>2</sup>

<sup>1</sup>UCL, iMMC, Louvain-la-Neuve, Belgium

<sup>2</sup>ArcelorMittal, Maizières-lès-Metz, France

Dual-Phase steels have long been used in the automotive industry due to their excellent mechanical properties in terms of strength and ductility, as well as their low processing cost. The good compromise between strength and ductility results from the very different properties of the constituent phases comprising ductile ferrite and hard martensite.

In contrast with their plastic flow properties, the fracture toughness of Dual-Phase steels (quantified by  $K_{Ic}$  or  $J_{Ic}$ ) has been far less investigated. Common values of the fracture toughness are around 100[kJ.m<sup>-2</sup>] or even lower; but seldom exceed the 200[kJ.m<sup>-2</sup>]. However, a minimum level of fracture toughness is required to prevent the propagation of small edge damage or cracked zones induced by cutting. Therefore, unravelling the relationship between fracture toughness, microstruc-

ture and damage mechanisms is essential to develop advanced steels with superior forming ability.

Dual-Phase steels are usually processed following an intercritical annealing which generally leads to equiaxed martensite inclusions. An alternative heat treatment, consisting of a double annealing first proposed N.J. Kim and G. Thomas [1] brings about fibrous martensite inclusions. A very recent study on such steels shows that this fibrous microstructure can potentially lead to a very high fracture toughness, while retaining good properties in terms of strength and ductility [2].

The general objective of this research is to investigate the fundamental damage mechanisms that govern the fracture toughness of Dual-Phase steels. Our approach is based on the processing of microstructures in which parameters are varied one by one. In particular, both

equiaxed and fibrous microstructures were investigated in the form of thin sheets.

The Essential Work of Fracture (EWF) method [3] was used to quantify the work per unit area needed at the crack tip for material failure separating it from the total work expended for material failure. An extension of the EWF method also allows us to separate the work of necking from the work of damage [4]. In addition, tomography experiments were conducted in order to study the nucleation and growth of cavities within the sheets. These preliminary measurements constitut-

ed the basis for the development of a micromechanics-based predictive model of the toughness of Dual-Phase steels.

#### References

- [1] N.J. Kim, G. Thomas (1981): Met. Trans A , 12: 483-489.
- [2] A.-P. Pierman (2013): Doctoral Thesis.
- [3] B. Cotterell, J.K. Reddell (1977): Int. J. Fracture, 13: 267-277.
- [4] T. Pardoen, F. Hachez, B. Marchioni, P.H. Blyth, A.G. Atkins (2004): J. Mech. Phys. Solids 52: 423-452.

## New insights on the physically correct application of the $J$ -integral for characterizing fatigue crack growth in elastic-plastic materials

WALTER OCHENSBERGER<sup>1,2</sup>, OTMAR KOLEDNIK<sup>1</sup>

<sup>1</sup>Erich Schmid Institute of Materials Science, Austrian Academy of Sciences, Leoben, Austria

<sup>2</sup>Materials Center Leoben Forschung GmbH, Austria

The majority of failures in technical applications can be attributed to fatigue crack propagation. Cracks under low-cycle fatigue conditions and short fatigue cracks cannot be assessed with the conventional stress intensity range  $\Delta K$ -concept, since linear elastic fracture mechanics is not valid. For such cases, Dowling and Begley (1976) proposed the experimental cyclic  $J$ -integral  $\Delta J^{\text{exp}}$  for the characterization of the fatigue crack growth rate. However, severe doubts exist concerning the application of  $\Delta J^{\text{exp}}$ . The reason is that  $\Delta J^{\text{exp}}$  relies, like the conventional  $J$ -integral, on deformation theory of plasticity, which idealizes the elastic-plastic material to be nonlinear elastic. Therefore, fundamental problems appear due to the strongly non-proportional loading conditions during fatigue crack propagation.

The configurational force concept provides a possible solution to this problem, since it enables the derivation of the  $J$ -integral for elastic-plastic materials with incremental theory of plasticity, called  $J^{\text{ep}}$  (Simha et al. 2008). This  $J^{\text{ep}}$  overcomes the theoretical restrictions of the conventional  $J$ -integral and is physically appropriate to characterize fatigue crack propagation, however, it is, in general, path dependent. In two recent papers, we studied the possible application of this  $J^{\text{ep}}$ -integral for the assessment of the driving force for fatigue crack growth (see Ochensberger and Kolednik 2014, 2015). A driving force term in fatigue should allow the prediction of the crack propagation rate of a fatigue crack. The purpose of the current presentation is to show how  $J^{\text{ep}}$  shall be used to evaluate correctly the driving force for fatigue crack growth, in order to characterize the crack growth rate during fatigue. Therefore, the path dependence of  $J^{\text{ep}}$  is studied in numerical investigations conducted on two-dimensional C(T)-specimens with long cracks subjected to cyclic Mode I loading. Crack

extension occurs by an increment after each load cycle. The maximum load is varied so that small- and large-scale yielding conditions prevail in the specimen. Three different load ratios, for zero-tension, pure tension and tension-compression loading, are investigated.

Theoretical considerations and comparisons with the cyclic crack tip opening displacement  $\Delta \delta_t$  show that the cyclic, incremental plasticity  $J$ -integral for a contour enclosing the active plastic zone of the moving crack tip, DJepactPZ, reflects the magnitude of the “driving force” for fatigue crack propagation. The results show that the parameter DJepactPZ is also able to reflect crack growth retardation after application of a single tensile overload. The validity of the experimental cyclic  $J$ -integral DJexp is also clarified: DJexp is, in principle, correct for stationary fatigue cracks, but does not exactly quantify the “driving force” during fatigue if crack extension occurs.

#### References

- Dowling, N.E. & Begley, J.A. (1976): Fatigue crack growth during gross plasticity and the  $J$ -integral. – ASTM STP 590:82–103.
- Simha, N.K., Fischer, F.D., Shan, G.X., Chen, C.R., Kolednik, O. (2008):  $J$ -integral and crack driving force in elastic-plastic materials. – J. Mech. Phys. Solids 56:2876–2895.
- Ochensberger, W. & Kolednik, O. (2014): A new basis for the application of the  $J$ -integral for cyclically loaded cracks in elastic-plastic materials. Int. J. Fracture 189:77–101.
- Ochensberger, W. & Kolednik, O. (2015): Physically appropriate characterization of fatigue crack propagation rate in elastic-plastic materials using the  $J$ -integral concept. Int. J. Fracture (in press).

## Grain Boundary Precipitation and Creep Crack Growth in polycrystalline Ni-base superalloys

H. SOMMER<sup>1</sup>, C. SOMSEN<sup>1</sup>, F. MUELLER<sup>2</sup>, V. KNEZEVIC<sup>3</sup>, N. DE BOER<sup>4</sup>, J. KLÖWER<sup>4</sup>, G. EGGELER<sup>1</sup>

<sup>1</sup>Institut für Werkstoffe, Ruhr-Universität Bochum, Bochum, Germany

<sup>2</sup>Chair and Institute for Materials Technology, Darmstadt University of Technology, Darmstadt, Germany

<sup>3</sup>Vallourec Research Center, Düsseldorf, Germany

<sup>4</sup>VDM Metals GmbH, Altena, Germany

In the present work the creep crack growth (CCG) behavior of two polycrystalline Ni-base superalloys, A617B and C263, is studied. In the microstructure of C263 a large volume fraction of intermetallic  $\gamma'$  phase and a high density of grain boundary (GB) precipitates are observed. Significantly smaller amounts of  $\gamma'$  phase, as well as a lower density of GB precipitates characterize the solution annealed alloy A617B. Thus, alloy C263 exhibits better creep resistance than alloy A617B. However, alloy C263 shows a higher sensitivity to creep crack propagation. The objective of the present work is to identify the microstructural parameters which govern CCG. For this purpose, compact tension CCG tests were performed according to ASTM E 1457. A preliminary scanning electron microscopy investigation showed that CCG occurred along high angle GBs. Using

focused ion beam micromachining (FIB), thin foils were cut out from the material close to the creep crack. This allowed to study the microstructure which governed CCG. The thin foils were studied using transmission electron microscopy (TEM). GB particles were characterized using energy dispersive X-ray (EDX) analysis and selected area electron diffraction. The density of particles at the GBs was characterized by the ratio between the sum of the projected areas of GBs carbides and the area of the GB region which was affected by carbides. The results of the mechanical and microstructural investigations suggest that the alloy with the higher density of GB carbides is less resistant against CCG. These results are discussed in the light of previous findings and areas in need of further work are highlighted.

## Examination of Evaluation Method for Static Strength of Casting Materials by Regarding Shrinkage Porosity as Cracks: Example of AZX912 Mg Cast Alloy

YU-KI HIGUCHI<sup>1</sup>, NAOYA OCHI<sup>2</sup>, HIROSHI NOGUCHI<sup>1</sup>

<sup>1</sup>Department of Mechanical Engineering, Faculty of Engineering, Kyushu University, Fukuoka, Japan

<sup>2</sup>Department of Materials Science and Engineering, Faculty of Engineering, Kyushu University, Fukuoka, Japan

With respect to a fracture originating any defect, breaking strength is determined sometimes by crack initiation stress and sometimes by crack propagation limit stress. The crack behavior in the process of static fracture is controlled by mechanical conditions and material structures. Incidentally, all casting materials have shrinkage porosity which decreases static strength. Since shrinkage porosity has micron order tip radius, shrinkage porosity is most likely to behave as cracks in the static fracture. Therefore the authors consider that static strength of casting materials can be evaluated from computer simulation regarding shrinkage porosity as cracks whose area is equal to projected area of shrinkage porosity on the plane perpendicular to the principal stress. However, there's no reproducibility of the shrinkage porosity for its shape and arrangements. Therefore, in static fracture it should be considered that behavior of the shrinkage porosity is possibly dif-

ferent from that of cracks.

As for a circumferential notch, it is reported that tensile strength of notched specimens is equal to that of specimens which has a crack of the same size of the notch when notch tip radius is smaller than certain value. Meanwhile, when tip radius is dull, the tensile strength depends on the tip radius. Whether tensile strength depends on tip radius or not can be explained by a magnitude relationship of crack initiation stress and crack propagation limit stress. The crack initiation stress depends on the notch tip radius. In contrast, the crack propagation limit stress doesn't depend on because when a crack exists at the notch tip, stress state is dominated almost only by the crack. When a notch tip is sufficiently sharp to crack initiation stress doesn't exceed crack propagation limit stress, initiated crack at the notch tip can propagate stably with the load increment. Subsequently, if applied tensile stress exceeds

crack propagation limit stress, the crack propagates unstably in another moment. The authors believe that the notch can be regarded as a simple crack in this case. On the other hand, when a notch tip is sufficiently dull to crack initiation stress exceed crack propagation limit stress, fracture from the notch doesn't have a stable crack propagation step. In short, specimens break immediately after the crack initiation. Therefore, tensile strength depends on notch tip radius with a sharp notch, and doesn't with a dull notch. The authors believe that the magnitude relationship of crack initiation stress and crack propagation limit stress decides existence of stable crack propagation in

any defect including shrinkage porosity. The shrinkage porosity as mentioned before, it appears to be needed that clarifying relation between defect shapes and crack behavior such as crack initiation, stable propagation and unstable propagation.

In this study, tensile tests were performed to circumferential notched specimens with variant notch size and tip radius. AZX912 non-combustible Mg cast alloy is adopted. In this paper, we will discuss crack behavior in static fracture considering material structure. Finally we will examine possibility of the method that regarding shrinkage porosity as cracks in strength evaluation of casting materials.

## Insight into MAG welding under constructive constraint conditions by means of high energy synchrotron X-ray diffraction

FLORIAN VOLLERT<sup>1</sup>, JENS GIBMEIER<sup>1</sup>, JONNY DIXNEIT<sup>2</sup>, THORBEN FISCHER<sup>3</sup>, P.STARON<sup>3</sup>, ARNE KROMM<sup>2</sup>, THOMAS KANNENGIESSER<sup>2</sup>

<sup>1</sup>Karlsruhe Institute of Technology (KIT), Institute of Applied Materials (IAM), Karlsruhe, Germany

<sup>2</sup>BAM Federal Institute for Materials Research and Testing, Berlin, Germany

<sup>3</sup>Helmholtz-Zentrum Geesthacht, Institute of Materials Research Hamburg, Germany

Welding using low transformation temperature (LTT) filler materials is an innovative method to mitigate welding residual stresses. In particular due to the selective producing of compressive residual stresses in the weld and in the heat affected zone (HAZ) a significant enhancement of the cold cracking resistance of highly stressed welded components can be expected. For the effective usage of these materials an in-depth comprehension of the microstructural developments during welding is necessary to determine the complex processes that occur during residual stress formation. Solid-state phase transformation kinetics and the evolution of thermal and elastic strains in two different modern LTT weld filler materials (one Ni- and one Mn-containing alloy) are monitored in-situ at the HEMS (High Energy Materials Science) beamline at the synchrotron light source PETRA III in Hamburg. The transferability to real components is ensured by using a realistic MAG welding process under consideration of constructive constraint conditions. Here, two different constraint conditions are considered. During welding of multilayer joints, the local phase transformation and strain evolution of each individual layer is investigated in transmission geometry using a photon energy of 100 keV. Further, the changes in already welded layers are studied, when further layer are welded on top. Debye rings are recorded by means of an area detector at a counting rate of 2 Hz. Evaluation of complete Debye rings in the diffraction images provides local information about phase fraction and transformation kinetics. 15° 'cake pieces' of the Debye rings are defined and integrated to investigate the phase specific strain

in longitudinal and in normal direction to the weld line in the (partially) coexisting martensite and austenite phases. The measurement results are compared to in-situ diffraction experiments using a conventional high strength weld filler material.

Due to the reduced temperature of martensite start (MS), crucial differences in the transformation behavior are observed. In contrast to the LTT weld filler materials the conventional filler material shows higher values of MS and faster martensite transformation kinetics.

Regarding the LTT alloys the martensite formation counteracts the thermal contraction strains, which leads to a significant decrease of the tensile strain distribution during cooling down. Therefore, in contrast to the conventional filler material the LTT alloys are found to exhibit relatively low residual strain, which is attributed to the low martensite transformation temperature. Moreover, the LTT strain distributions, as well as the directional evaluation of phase transformation, show periodical oscillations, attended by defined alteration of the interference peak intensity. This transient effect can be attributed to local changes in crystal-orientation (grain rotation) and is differently pronounced for the different alloys.

Results show that the transformation kinetic is dependent on the position of the welded layer. Furthermore, the strain evolution for each layer differs. This can be attributed to both, the local chemical mixing between weld filler and base material which affects the martensite formation and the constraint condition applied.

Talks Topic G 6:

## ***Fracture mechanics***

---

## Testing fracture toughness of brittle materials via chevron-notched bend bars of microscopic length-scale

GORAN ZAGAR<sup>1</sup>, MARTIN MUELLER<sup>1</sup>, VACLAV PEJCHAL<sup>1</sup>, LIONEL MICHELET<sup>1</sup>, MARCO CANTONI<sup>2</sup>, ANDREAS MORTENSEN<sup>1</sup>

<sup>1</sup>Laboratory of Mechanical Metallurgy, Institute of Materials, EPFL, Switzerland

<sup>2</sup> Interdisciplinary Centre for Electron Microscopy, EPFL, Switzerland

Modern “small scale” technologies are in need of methods for the testing of materials for mechanical properties at microscopic length scales. In particular, fracture toughness at the micron scale has been recently probed using samples machined by the focused ion beam (FIB) method. FIB micromachining technique allows a rather good degree of flexibility in shaping the specimens, thus microscopic beams with straight single-edge notches have been produced and tested mainly as cantilevers or in a 3 point bending-like setup. The main concern associated to the FIB milled specimens, however, is that FIB-based machining is damaging and modifies the specimen surface; FIB milled surfaces can become amorphous due to ion implantation and irradiation and/or they can be contaminated by redeposition. Moreover, and this is particularly important for fracture toughness tests, FIB milled straight-through notches always have a finite tip radius. These features have been documented to potentially cause errors in fracture toughness measurements at the microscale.

To circumvent the main problems associated with FIB-milled specimens used for fracture toughness testing, we explore the testing of microscopic chevron-notched cantilever beams. Two simple, brittle and isotropic model materials are used to probe the technique; namely, nanocrystalline alumina with a grain size ~65nm, and amorphous fused quartz. Microscopic chevron-notched cantilever beams of rectangular cross-section are machined using standard FIB milling. The beams contain a thin triangular ligament (the chevron notch), which is placed near the beam end at

which the cantilever is attached to the bulk material. Cantilevers are deflected up to the point of fracture using a nanoindentation apparatus. We find that for sufficiently thin chevron notches, the crack is regularly initiated at the apex of the triangular ligament under a load that is lower than that corresponding to the onset of crack instability. Subsequent increase in load therefore at first drives the crack thus created to propagate within the plane of a chevron notch in a stable manner, before instability and final fracture of the specimen take place. Test data are interpreted using compliance calibration curves calculated by three-dimensional finite element simulation of each beam individually, after measurement of its dimensions from SEM images. Data obtained are consistent with what one would expect for the material at hand, suggesting that the technique is reliable despite the small specimen size, and that it can therefore be transposed to other materials. Advantages of the method are that the obtained toughness values are not affected by the finite radius of a FIB milled notch since the instability is developed from a real (sharp) crack. In addition, at the onset of unstable growth, the majority of the crack front is situated away from the FIB-machined surface. Thus, the measurements should be minimally influenced by milling-induced defects. The influence of environment-assisted slow crack growth on the test data, which are well known to be operative with alumina and fused quartz in air, is also examined in terms of various specimen geometries and shown to be negligible in the present tests; there lies a third advantage of the method.

## Micro-fracture testing of tungsten single crystals

CHRISTOPH BOHNERT<sup>1</sup>, NICOLA SCHMITT<sup>2</sup>, SABINE M. WEYGAND<sup>1</sup>, RUTH SCHWAIGER<sup>2</sup>, OLIVER KRAFT<sup>2</sup>

<sup>1</sup>Karlsruhe University of Applied Sciences, Faculty of Mechanical Engineering and Mechatronics (MMT), Karlsruhe, Germany

<sup>2</sup>Karlsruhe Institute of Technology (KIT), Institute for Applied Materials (IAM), Eggenstein-Leopoldshafen, Germany

To be able to use tungsten as a structural material in power generation, the characterization of its mechanical properties, in particular with respect to fracture, is essential. Previous studies on polycrystalline tungsten already showed that the microstructure has an im-

mense influence on the fracture toughness. However, these studies have been mainly carried out at the macro-scale. To gain insight into the mechanical response of individual grains, an experimental programme with small scale fracture specimens was set up. Since the

standard procedure for fracture toughness testing is not valid on this size scale, the experimental studies were closely accompanied by finite element simulations.

The aim of the present work is to find a procedure to determine the fracture toughness of such small non standard specimen. The tested free-standing micro-bending beams have a typical dimension of 30  $\mu\text{m}$  in width and thickness and 160  $\mu\text{m}$  in length. They were fabricated by micro-electro-discharging machining followed by surface cleaning and notching by focused ion beam. A Charpy notch was chosen as it leads to a more controlled crack initiation as the resistance against crack propagation increases with increasing crack length. The single crystalline beams starting with an orientation of the  $\{001\}\langle 100\rangle$ -crack system along the loading direction were loaded using a nanoindenter.

Related to this experimental program a finite element (FE) study was performed. The FE model of the notched microbeam was created taking into account plastic deformation at the crack tip. Plastic deformation is implemented using a crystal plasticity (CP) approach (formulated by [1] and written by [2]) which allows for specifying the crystal orientation. Furthermore, the fracture process with crack propagation is

described by using a cohesive zone model (CZM). A distinction between brittle or ductile fracture can be realized with parameter variations of the constitutive traction separation law [3].

The developed crack model was applied to simulate microbending. The simulations of microbending allow for evaluating the details of the fracture process. The results reveal details of the developing plastic zone and which slip systems are active as well as the current crack growth rate. Furthermore, the computed load displacement curves are compared to the measured one. By this comparison, it has been confirmed that this procedure is suitable to determine values for the fracture toughness from experimental force-displacement curves for small-scale specimen. For the single crystals investigated, the obtained values agree well with the ones from macroscopic tests for the same crystal orientation.

#### References

- R.J. Asaro. *Advances in Applied Mechanics* 23 (1983), 1–115.
- Y. Huang. Division of Applied Sciences, Harvard University, Mech. Report No. 178, 1991.
- Ingo Scheider. 2006. *The Cohesive Model Foundations and Implementation*. GKSS Research Centre Geestacht

## An Improved Micromechanical Method for Investigating the Statistical Strength of Poly-Silicon Membranes

JOHN BRÜCKNER<sup>1</sup>, HOLGER PFAFF<sup>2</sup>, ALFONS DEHÉ<sup>3</sup>, SVEN RZEPKA<sup>1</sup>

<sup>1</sup> Fraunhofer ENAS, Chemnitz, Germany

<sup>2</sup> Keysight Technologies, Frankfurt, Germany

<sup>3</sup> Infineon Technologies AG, Munich, Germany

Freestanding poly-silicon membranes are of increasing importance for designing MEMS devices such as pressure sensors, microphones and gyroscopes. It is crucial to accurately determine the mechanical properties of such membranes not only to access parameters for designing new devices but also for assuring proper performance and quality in service. Classically, microscopic tensile tests [1-3] or bulge tests [4] were conducted to obtain Young's modulus and strength of the membrane material. These methods however are prone to artifacts due to crack initiation at edge defects (e.g. predefined notches in tensile specimens [3] or slits in bulge test samples [4]). In search of a method more sensitive to the membrane surface rather than specimen geometries, a novel approach has been introduced more recently. By loading the center region of a circumferentially clamped membrane with a spherical probe, the membrane is stretched all the way up to rupture while precisely recording the load-deflection data. Complementary FEA simulations allow for deter-

mining the failure stresses of individual membranes, based on the mechanical test data. In a subsequent step the tests are analyzed via a two-parameter Weibull approach to statistically evaluate the characteristic fracture strength.

The membranes tested in the given project had a thickness of only 330 nm over a diameter of 1 mm. The necessity to apply minute forces while testing the compliant membranes at quite large deflections with high precision proves to be challenging. Additionally the need for statistical verification requires conducting multiple tests in a reasonable time frame. In the presented work a commercial nanoindenter has been used to match the aforementioned requirements. Lately some methodological improvements have been implemented to maximize throughput by automation and improve accuracy by refining the data analysis to capture the experimental conditions most realistically. Some of these approaches will be illustrated by recent data and explained in detail.

## References

- [1] Sharpe, W. N., Yuan, B., Vaidyanathan, R. and Edwards, R. L.: 1997, Measurements of Young's modulus, Poisson's ratio, and Tensile strength of Polysilicon, IEEE The Tenth Annual International Workshop on Micro Electro Mechanical Systems. An Investigation of Micro Structures, Sensors, Actuators, Machines and Robots, pp. 424-429.
- [2] T. Tsuchiya et al, "Cross Comparison of Thin-Film Tensile-Testing Methods Examined Using Single-Crystal Silicon, Polysilicon, Nickel and Titanium Films", in Journal Of Microelectromechanical Systems, Vol. 14 No. 5, pp. 1178-1186, October, 2005.
- [3] H. D. Espinosa, B. Peng, "A New Methodology to Investigate Fracture Toughness of Freestanding MEMS and Advanced Materials in Thin Film Form", in Journal Of Microelectromechanical Systems, Vol. 14 No. 1, pp. 153-159, February, 2005.
- [4] B. Merle, M. Göken, "Fracture toughness of silicon nitride thin films of different thicknesses as measured by bulge tests", in Acta Materialia Volume 59, Issue 4, Pages 1772-1779, February, 2011.

# How Crystals Break – Crack speed dependent environmental effect and surface instabilities

ANNA GLEIZER, LIRON BEN-BASHAT BERGMAN, DOV SHERMAN

Dept. of Materials science and engineering, Technion, Haifa, Israel

A common wisdom is that cracks in brittle crystals such as diamond, silicon, or sapphire need excessive energy to initiate and 'bursting' at high speed. Atomistic based theoretical studies and atomistic simulations, confirmed by fracture experiments, have been in accord with the common intuition of speed ( $V > 2,000$  m/sec in silicon) and energy ( $G_0 > 1.6 \cdot 2g_s$ ). Contrary, continuum mechanics based theory predicts that cracks can be slow and initiate at  $2g_s$ . Our high-resolution fracture experiments confirm the continuum mechanics theory. In this talk, we will introduce our experimental method. The method consists of gluing a rectangular and thin precracked brittle crystal specimen inside a rectangular hole in an aluminum loading-frame by two 300 mm thick epoxy resin layers. Crack initiation and propagation takes place upon heating the assembly on top of an electrical heating stage by few centigrade, sufficient to initiate and propagate a crack. A relatively long ( $> 10$  mm) precracks were introduced in the specimens (Sherman & Gleizer 2014; Gleizer & Sherman 2014). The strain energy release rate,  $G_0$ , was calculated by quasi-static finite element analysis, and crack speed evaluated by Wallner-lines technique. With this method, we are able to manipulate the energy flux to the crack tip to be low, responsible for low speed cracks. We will introduce two governing parameters,  $dG_0/da$  and  $dV/da$  ( $a$ -the crack length), and the way to control them.

We will show two important phenomena associated with low speed cracks in silicon crystal. The first is crack speed *dependent* stress corrosion cracking, or subcritical crack growth, for cracks propagating on the (110)  $[1\bar{1}0]$  low energy cleavage system of silicon and crack speed *independent* stress corrosion cracking on the (111) $[11\bar{2}]$  crack system. For the (110) plane, full SCC occurs at cleavage energy of  $2.2$  J/m<sup>2</sup> up to crack speed of  $\sim 500$  m/sec, and terminates at crack speed of  $\sim 1200$

m/sec where the cleavage energy is  $3.5$  J/m<sup>2</sup> (Gleizer & Sherman 2014; Gleizer et al. 2014). For the (111) cleavage plane, SCC at energy of  $2.2$  J/m<sup>2</sup> takes place up to the maximum measured speed of  $1200$  m/sec.

The second phenomenon is micron scale surface ridges generated when a slow crack is propagating on the (111) $[11\bar{2}]$  cleavage system of silicon (Kermode et al. 2008) under bending. The ridges initiate at atomistic scale jogs generated when the running crack interact with individual dopants. The jogs generate pile-ups that terminate at micron scale ridges (Ben-Basat Bergman & Sherman 2014; Kermode et al. 2013).

## References

- Ben-Basat Bergman, L. & Sherman, D. (2014): Dynamic crack surface instabilities initiated at dopants. Scripta Materialia 75, 14-17.
- Gleizer, A. & Sherman, D. (2014): The cleavage energy at initiation of (110) silicon. Int. J. Fracture 187, 1-14.
- Gleizer, A., Peralta, G., Kermode, J. R., de-Vita, A. & Sherman, D. (2014): Dissociative chemisorption of O<sub>2</sub> inducing stress corrosion cracking in silicon crystals. Phys. Rev. Lett. 112 115501.
- Kermode, J.R., Albaret, T., Sherman, D., Bernstein, N., Gumbsch, P., Payne, M.C., Csányi, G. & De Vita, A. (2008) Low Speed Fracture Instabilities in a Brittle Crystal. Nature 455 1224-1227.
- Kermode, J. R., Ben-Basat Bergman, L., Atrash, F., Cilliers, J. J., Sherman, D. & de Vita, A. (2013): Macroscopic scattering of cracks initiated at single impurity atoms. Nature Communication 4, 2441.
- Sherman, D. & Gleizer, A. (2014): Evaluating the cleavage energy of brittle single crystals. Performance and Characterization. Mater. Perfor. and Charact. 3, 1- 25.

Talks Topic G 7:

## ***Fracture mechanics***

---

# Influences of hydrogen-affected yielding and work hardening on plastic zone evolution studied by Finite Element Method

DAISUKE SASAKI, MOTOMICHI KOYAMA, KENJI HIGASHIDA, KANEAKI TSUZAKI, HIROSHI NOGUCHI

Department of Mechanical Engineering, Faculty of Engineering, Kyushu University, Fukuoka, Japan

Hydrogen uptake is well known to accelerate fatigue crack propagation rate due to a change in a crack propagation mode, deteriorating fatigue life drastically. From the view point of the propagation mode transition of fatigue crack under hydrogen environment, formation of brittle striation through transgranular crack propagation has been reported in Fe-Si single crystalline and commercial polycrystalline ferritic steels. Additionally, the crack path was independent of any identical crystallographic planes. This brittle striation was explained in terms of micro-void formations and their coalescence associated with hydrogen-enhanced localized plasticity (HELP). The proposed model could explain the brittle-like fractographic feature as well as the acceleration of crack propagation rate. This model has enabled us to estimate the transition condition by simulation. The estimate has an important role on prediction of fatigue life under hydrogen environment. In this study, the hydrogen effect on plastic deformation and hydrogen distribution at the crack tip have been analyzed by finite element method (FEM), since the propagation mode transition noted in this study has required the FEM-scale analysis which would elucidate hydrogen-related factors with a scale ranging from 30.0  $\mu\text{m}$  (plastic zone size on steels at  $K_I = 40.0 \text{ MPa}\sqrt{\text{m}}$ ) to 150 mm (the distance where the displacement is not affected by plastic zone at a crack tip): hydrogen distribution, plastic zone size, plastic strain distribution, and coordination state of hydrogen such as dislocations. The FEM has been successfully applied to the plastic zone analysis with hydrogen diffusion near a crack tip. Here, we noticed a remaining issue in terms of the plastic zone analysis, namely, simulating hydrogen-localized plastic zone which is needed to determine the

transition condition under hydrogen atmosphere. The solution of the remaining issue enables us to estimate precisely the condition.

We have focused on the influences of hydrogen-affected plastic deformation and a comparison parameter for solving the remaining issue of plastic zone size. Mechanical factors dominating plastic zone evolution are considered to be yield strength and work hardening coefficient. In particular, the influence of work hardening coefficient has never been introduced to simulation of the HELP phenomenon. Additionally, expanded plastic zone was observed when compared using the stress intensity factor  $K_I$  in a previous study. Based on the crack-propagation mode transition mechanism, we have compared the plastic zone size by using the new parameter, crack-tip plastic strain.

This study has shown that hydrogen-reduced work hardening coefficient and the crack-tip plastic strain play important roles on simulating localization in plastic zone near the crack tip. Namely, special emphasis of this study was placed on the dependence of yield strength and work hardening coefficient in hydrogen-affected plastic zone evolution clarified through FEM and the influence of the new parameter.

## References

- H. Nishikawa, Y. Oda, Y. Takahashi, H. Noguchi: *J. Solid Mech. Mater. Eng.*, 5, (2011), 179.
- P.J. Ferreira, I.M. Robertson, H.K. Birnbaum: *Acta Mater.*, 47, (1999), 2991.
- P. Sofronis, R.M. McMeeking: *J. Mech. Phys. Solid.*, 37, (1989), 317.

## On the fracture toughness of fcc medium- and high-entropy alloys at ambient to cryogenic temperatures

BERND GLUDOVATZ<sup>1</sup>, KELI V. S. THURSTON<sup>1</sup>, ANTON HOHENWARTER<sup>2</sup>, DHIRAJ CATOOR<sup>3</sup>, HAO BEI<sup>3</sup>, EASO P. GEORGE<sup>3,4</sup>, ROBERT O. RITCHIE<sup>1,5</sup>

<sup>1</sup>Lawrence Berkeley National Laboratory, Materials Sciences Division, Berkeley, CA, USA

<sup>2</sup>Montanuniversität Leoben, Department of Materials Physics, and Erich Schmid Institute of Materials Science, Austrian Academy of Sciences, Leoben, Austria

<sup>3</sup>Oak Ridge National Laboratory, Materials Sciences and Technology Division, Oak Ridge, TN, USA

<sup>4</sup>University of Tennessee, Materials Sciences and Engineering Department, Knoxville, TN, USA

<sup>5</sup>University of California, Department of Materials Science and Engineering, Berkeley, CA, USA

Medium- to high-entropy alloys are an intriguing new class of materials in which three, four, five, or more elements are present in equiatomic concentrations, with the striking characteristic that they often crystallize as single-phase solid solutions with simple crystal structures, despite containing high concentrations of multiple elements with very different crystal structures. Although these alloys are interesting from a fundamental scientific viewpoint, they can have unusual mechanical properties, which make them attractive for a wide range of applications.

Here we examine equiatomic medium- and high-entropy, face-centered-cubic alloys, which exhibit a remarkable combination of strengths above 1 GPa, tensile ductilities of more than 50% and fracture toughness values exceeding 200 MPa√m at crack initiation and more than 300 MPa√m ( $J > 500 \text{ kJ/m}^2$ ) during stable crack growth, properties which actually improve from ambient to cryogenic temperatures. This appears to result from continuous steady strain hardening, which acts to suppress instability, consistent with planar dislocation slip at ambient temperatures which transi-

tions into deformation-induced nano-twinning at lower temperatures. We also report initial results of the fatigue-crack propagation behavior of these materials in the same temperature range.

Research sponsored by the US Department of Energy, Office of Science, Basic Energy Sciences, Materials Sciences and Engineering Division.

### References

- Gali, A., and E.P. George. "Tensile Properties of High- and Medium-Entropy Alloys." *Intermetallics* 39 (August 2013): 74–78.
- Otto, F., A. Dlouhý, Ch. Somsen, H. Bei, G. Eggeler, and E. P. George. "The Influences of Temperature and Microstructure on the Tensile Properties of a CoCrFeMnNi High-Entropy Alloy." *Acta Materialia* 61, no. 15 (September 2013): 5743–55.
- Gludovatz, Bernd, Anton Hohenwarter, Dhiraj Catoor, Edwin H. Chang, Easo P. George, and Robert O. Ritchie. "A Fracture-Resistant High-Entropy Alloy for Cryogenic Applications." *Science* 345, no. 6201 (September 5, 2014): 1153–58.

## Stress corrosion cracking in sensitized austenitic stainless steel type 304 under tetrathionate solution environment

TOMOYUKI FUJII, KEIICHIRO TOHGO, YUTARO MIURA, YOSHINOBU SHIMAMURA<sup>1</sup>

Department of Mechanical Engineering, Shizuoka University, Japan

Stress corrosion cracking (SCC) is a degradation phenomenon caused by specific combinations of stress, environment and material. In nuclear industries and chemical industries, much attention has been paid to SCC as a degradation phenomenon of materials and structures under corrosive environment. SCC life is estimated by crack growth from the millimeter-sized crack detected in periodic inspection to final failure. The process of micro crack formation is major part of SCC life. To predict SCC remaining life, it is necessary to consider SCC process of crack initiation. Tohgo et al. developed a Monte Carlo simulation of the SCC

processes from micro crack initiation to macro crack growth on a smooth surface based on stochastic properties for micro crack initiation and concepts in fracture mechanics for crack coalescence and growth. A number of studies about crack initiation on the basis of crystallographic investigation have been conducted. Gertsman et al. measured misorientation of cracked grain boundaries of polycrystalline materials, and reported that twin ( $\Sigma 3$ ) boundaries were immune to IG-SCC. PAN et al. reported that general low-angle grain boundaries and  $\Sigma 3$  boundaries were immune to IGSCC in alloy X-750 but then some coincidence site lattice

(CSL) grain boundaries lying in the range  $\Sigma 5$ - $\Sigma 49$  were found to be cracked. However, the influence of misorientation of grain boundary on IGSCC behavior remains to be clarified.

In this study, to make clear micro crack initiation behavior by SCC in sensitized austenitic stainless steel 304, a constant load tests was carried out under 1% tetrathionate solution environment. Before the tests, the crystal orientation of specimen surface was measured by a scanning electron microscope (SEM) with an electron back scattered diffraction (EBSD). Tensile load corresponding to tensile strain of 1% or 2% was applied under the corrosive environment, and then the applied load was fixed using compressive spring. During the test, the SCC behavior, such as crack initiation and growth, was observed by a video microscope every five minutes. After the tests, the crack length and number of cracks were measured and the crack formation process was discussed.

As a result of the in-situ observation, initiation of many cracks, crack coalescence and growth were observed. Most of the cracks are perpendicular to the loading

direction. The number of cracks and crack length increase with increasing loading time after incubation period, and then, the number of cracks becomes constant. All cracks initiated in grain boundaries, and the grain boundaries with the misorientation ranging from 20° to 60° seem to be susceptible to crack initiation.

#### References

- Tohgo K., Suzuki H., Shimamura Y., Nakayama G. & Hirano T. (2009); Monte Carlo simulation of stress corrosion cracking on a smooth surface of sensitized stainless steel type 304, *Corrosi. Sci.*, 51, 9, 2208-2217.
- Gersman V.Y. & Bruemmer S. M. (2001); Study of grain boundary character along intergranular stress corrosion crack paths in austenitic alloys; *Acta Materialia*, 49: 1589-1598.
- Pan Y., Adams B.L., Olson T. & Panayotou N. (1996); Grain-boundary structure effects on intergranular stress corrosion cracking of alloy X-750; *Acta Mater.*, 44, 4685-4695.

## Effect of post weld heat treatment on the long-term reliability of austenitic stainless steel 347H

JINE-SUNG JUNG, HAN-SANG LEE, DOO-SOO KIM, KEUN-BONG YOO

Power Generation Lab., Research Institute of Korea Electric Power Corporation, Korea

An austenitic stainless steel 347H is widely used in high temperature components due to the excellent creep strength and oxidation resistance. In the case of power plants, the metal is used in heat exchanger as re-heater and super-heater tubes. These tubes are joined by welding for connecting each other.

So, high residual stresses were existed on the welded joints due to no post weld heat treatment for austenitic materials following some codes. Consequently, potential degradation on the joints could be preceded by high residual stresses during operation on a condition of high-temperature and -pressure.

In these days, some failures on the welded joints of austenitic 347H boiler tubes were happened in thermal power plants. There were some common features in the failures. Firstly, the cracks on the joints were found at the heat affected zone within two years since installation. Secondly, the hardness values were shown near the HAZ as compared to the bare metal. Also, the cracks were propagated along the grain boundaries showing the inter-granular fracture appearance. According to the previous studies, these phenomenons are assigned to the 'relaxation cracking' [1] or 'reheat cracking' based on microstructure analysis. Also, high density of dislocations was observed on the HAZ using a transmission electron microscopy. Generally, defects

in the material such as dislocation and planar fault act as favorable nucleation sites for precipitation [2].

Therefore, in order to decrease or prevent a welded joint of austenitic metals from relaxation cracking damage, there is a need to alleviate the residual stress through the post weld heat treatment together with an avoidance of grain boundary sensitization through a carbide formation on grain boundaries.

In this study, the effect of PWHT on long-term reliability of a welded boiler tube 347H was investigated. The PWHT was conducted using a thermal pad at 900°C for 2 hours.

Prior to the long-term test, creep-rupture tests were performed on the condition of 650°C-176MPa and 600°C-265MPa. The time to rupture was significantly increased upto four times as compared with the as-weld condition.

In order to apply a PWHT to a field, there is a need to checking the long-term effect on a weld joints of boiler tubes 347H. So both as-weld and PWHT tubes were aged in a furnace at 600°C upto 1000 hours. And then a series of hardness, high-temperature tensile and creep-rupture tests mechanical tests were conducted. Also microstructure features such as dislocation density, precipitation fraction and size were analyzed using SEM and TEM.

In the case of 100 hours aging, the ultimate tensile strength (UTS) of the PWHT sample showed a similar level with that of as-weld sample in a high-temperature tensile test, while the elongation was significantly increased. Also, the decrease of dislocation density in the PWHT joint was observed.

Consequently, the beneficial effect of PWHT on the weld joint during the short-term was clearly confirmed. The long-term effect are focusing on an increase of ductility through the control of precipitation behavior.

## References

- H. van Wortel; Control of Relaxation Cracking in Austenitic High Temperature Components; In: Proceedings of the NACE International Conference on Corrosion 2007, Paper No. 07423.
- Dutta B, Valdes E, Sellars CM. Mechanism and Kinetics of Strain Induced Precipitation of Nb(C,N) in Austenite, *Acta Metall Mater*, 1992, Vol. 40, pp.653-662.

## Interaction between torsion damage and toughness anisotropy in a drawn pearlitic steel wire

AURÉLIE JAMONEAU<sup>1</sup>, JEAN-HUBERT SCHMITT<sup>1</sup>, DENIS SOLAS<sup>2,3</sup>

<sup>1</sup>Ecole Centrale Paris, Laboratoire MSSMat, Châtenay-Malabry Cedex, France

<sup>2</sup>Univ Paris Sud, ICCMO, Orsay, France

<sup>3</sup>CNRS, Orsay, France

Pearlitic steel wires drawn under large strains experience a high strength hardening, a microstructure refinement, and a morphological anisotropy. The strengthening mechanisms in tension have been widely studied accounting for the fine structure of the pearlite and the arrangement of lamellae [1, 2]. The mechanical behavior is strongly dependent on the loading conditions: along the longitudinal direction, the maximum tensile strength is significantly high while the total elongation is low, whereas in torsion lower maximum shear strength and high ductility are observed [3]. Moreover, a strong toughness anisotropy, linked to the morphological texture [4], contributes to the development of a specific damage mechanism and rupture mode in torsion [5].

The present work focuses on the mechanical behavior of a drawn wire under sequential loadings, specifically torsion followed by inverse torsion. Mechanical testing, SEM observation as well as X-Ray diffraction are used to characterise the material from the macro to the nano scale.

When the torque vs. angle curves present a smooth behavior leading to a ductile flat rupture in torsion, strong irregularities appear on the shear curve during inverse torsion after a given amount of torsion. These mechanical irregularities are linked to the propagation of a delamination crack along the radial {001} cleavage planes of the wire.

First results allow to partly explain the different behaviors in torsion and inverse torsion:

- Circumferential residual stresses, resulting from drawing, influence the damage initiation: when

stress level is high, delamination starts at the first steps of the torsion. Comparisons between different initial load states lead to quantitative evaluation of toughness.

- Inverse torsion can also reveal the surface defect intensity. In fact, the main stress component applied on the wire surface in torsion is shear stress, which contributes to crack opening in mode III. However, at the beginning of the inverse torsion, due to the inclination of defects with respect to the torsion axis, tension applies normally to the defect plane. If the defect is deep enough after pre-torsion, this could activate longitudinal cracks opening in mode I.
- Electropolishing after pre-torsion reduces the depth of the initial defects. It is shown that it prevents delamination during inverse torsion.

These results have to be completed in order to obtain quantitative predictions of the rupture mechanisms as a function of drawing and pre-deformation in torsion. Further studies of the crystallographic texture of the wire as well as EBSD maps of the structure along the cracks could help resolving this issue.

## References

- [1] J.D. Embury and R.M. Fisher, *Acta Met.* 1966, 14:147
- [2] G. Langford, *Metall. Trans.* 1970, 1:465
- [3] T. Zhao et Al., *Materials design* 2014, 59:397
- [4] A. Hohenwarter et Al., *Metal. Mater. Trans.* 2011, 42A:1609
- [5] B. Goes et Al., *Eng. Fract. Mech.* 1998, 60:255

Talks Topic H 1:

# ***Materials for fission and fusion***

---

# Effects of helium and irradiation damage on microstructure and mechanical properties of Fe base alloys for fusion applications

RICHARD KURTZ

Pacific Northwest National Laboratory, Richland, Washington, USA

The products of a fusion nuclear reaction are a He nucleus and a 14 MeV neutron. The neutrons carry most of the fusion energy that is ultimately dissipated in the materials, components and structures surrounding the plasma. About 10% of the incident neutron energy is deposited in the first-wall, while the balance is transferred to the much larger volume blanket behind the first-wall. The neutrons are slowed by nuclear collisions and reactions as they penetrate the reactor structure. The energetic neutrons interact with the atoms of the structural materials in two ways. One involves transmutation or conversion of one chemical element into another. In Fe base alloys the transmutation reactions of greatest concern introduce copious quantities of He and H by end-of-life. The other mechanism involves elastic and inelastic scattering collisions that generate a cascade of atoms displaced from their equilibrium lattice sites. The vast majority of the displaced atoms recombine with a vacant site, but a small fraction do not. The surviving vacancy and interstitial defect clusters can lead to significant changes in mechanical and physical properties.

Neutron irradiation at temperatures below about 35% of the absolute melting temperature results in accumulation of point defect clusters to high levels, which causes the yield and tensile strength to increase and ductility to decrease. The resistance to crack propagation is also reduced. The effects of displacement damage saturates at relatively low neutron dose, but He can cause increased levels of hardening and embrittlement beyond displacement damage alone. At intermediate irradiation temperatures Fe base alloys are susceptible to dimensional instabilities such as volumetric swell-

ing and irradiation creep. Again He can play a role in exacerbating these degradation mechanisms. Toward the upper operating temperature regime the effects of displacement damage are not the primary concern, but He may significantly impact service life by promoting grain boundary creep cavitation. Consequently development and qualification of structural materials for fusion nuclear service requires knowledge of the effects of neutron damage and He over the entire temperature range.

Reduced activation ferritic/martensitic (RAF/M) steels and nanostructured ferritic alloys (NFA) are attractive materials for first-wall/blanket structural applications in advanced plasma devices and future fusion power plants. RAF/M steels are much more technologically mature than other candidate low-activation structural materials such as vanadium alloys and silicon carbide composites. While NFAs do not enjoy the same level of technological maturity as RAF/M steels this new class of material offers possible significant advantages such as the potential for higher temperature operation and perhaps much greater radiation tolerance. The precise operating temperature and neutron dose limits for these materials remains to be fully established because neutron-induced displacement damage coupled with transmutation produced helium can lead to significant degradation of mechanical properties and dimensional instabilities over the entire range of operating conditions. In this paper we highlight recent experiments and modeling to characterize the effects of He and irradiation damage on RAF/M steels and NFAs for fusion applications.

## New Material Developments for Applications in Fusion Reactors

J.W.COENEN<sup>1</sup>, J.ENGELS<sup>1</sup>, S.HEUER<sup>1</sup>, A.HOUBEN<sup>1</sup>, B.JASPER<sup>1</sup>, A.LITNOVSKY<sup>1</sup>, TH.WEBER<sup>3</sup>, T.WEGENER<sup>1</sup>, W. BIEL<sup>1</sup>, T.HOESCHEN<sup>2</sup>, F.KOCH<sup>2</sup>, R.NEU<sup>2</sup>, J.RIESCH<sup>2</sup>, M.RASINSKI<sup>1</sup>, B.UNTERBERG<sup>1</sup>, CH.LINSMEIER<sup>1</sup>

<sup>1</sup>Forschungszentrum Jülich GmbH, Institut für Energie- und Klimaforschung – Plasmaphysik, Germany

<sup>2</sup>Max-Planck-Institut für Plasmaphysik, Garching, Germany

<sup>3</sup>Forschungszentrum Jülich GmbH, Institut für Energie- und Klimaforschung – Werkstoffstruktur und -eigenschaften, Germany

Materials for application in extreme environments have to show advanced properties in most areas ranging from mechanical strength to thermal properties and in

many ways do fulfill a functional role as well. Materials for the first wall of a fusion reactor have to face unique challenges in many of these areas. The main challenges

include wall lifetime, fuel management and safety of operation. For the lifetime of the wall material, considerations of thermal fatigue as well as transient heat loading are crucial as typical  $10^9$  (30Hz) thermal events during one year of operation are to be expected. Tungsten (W) is the main candidate material for the first wall of a fusion reactor as it is resilient against erosion, shows the highest melting point of any available material and show rather benign behavior under neutron irradiation.

To overcome the brittleness issue when using W, a W-fiber enhanced W-composite material ( $W_f/W$ ) incorporating extrinsic toughening mechanisms can be used. The extrinsic toughening allows for a certain tolerance towards cracking and damage in general. The tension can be released at the crack tip and thus cracks can be stopped where brittle, unenhanced tungsten would fail immediately. First samples have been produced, showing extrinsic toughening mechanisms similar to ceramic materials [1]. Overcoming the brittleness problem will also mitigate effects of operational embrittlement due to neutrons and high operational temperatures. A component based on  $W_f/W$  shall be developed with both a chemical infiltration (CVI), utilizing a newly installed CVI-setup as well as a powder metallurgical path through hot-isostatic-pressing. Mechanical qualification and subsequent testing will be used for qualifying the material options.

A potential problem with the use of pure W in a fusion reactor is the formation of radioactive and highly volatile  $WO_3$  compounds and their potential release under accidental conditions. A loss-of-coolant accident (LOCA) in a He-cooled reactor would lead to a temperature rise to 1400 K after ~10–30 days due to the nuclear decay heat of the in-vessel components [2]. A future application of binary or ternary tungsten-based alloys in a fusion reactor appears feasible, since these compounds can also be processed to thick protective coatings with reasonable thermal conductivity, e.g. by plasma spraying with subsequent densification. Enhanced sputter erosion during normal reactor operation is not a concern, since preferential sputtering of alloying elements will lead to rapid depletion of the first atomic layers and leave a pure W-surface in contact with the plasma [5]. W-Cr-Y with up to 80% of W content already shows  $10^5$ -fold suppression of tungsten oxidation due to self passivation. Rigorous testing of oxidation behavior as well as mass production for candidate materials will be performed.

Developments joining W as PFM with the structural material EUROFER are also ongoing. To mitigate the effect of mismatch in the thermo-mechanical properties functionally graded materials (FGM) are considered and shall be benchmarked with common joining techniques.

In addition the issue of tritium management is an issue for future devices. In order to prevent tritium loss and radiological hazards it is important to suppress tritium permeation through reactor walls [4]. The requirements on barrier layers are high permeation reduction factors, high thermal stability and corrosion resistivity as well as similar thermal expansion coefficients compared to the substrate. In Juelich a new deuterium gas-driven permeation setup is used to investigate the deuterium permeation through different ceramic coatings on EUROFER97 for example  $Er_2O_3$ . Such oxide layers significantly reduce the deuterium permeation compared to bare EUROFER97 substrates [5].

For the development of components including plasma facing materials, functional layers and cooling structures the issue of power exhaust needs to be considered. This might require replacing copper by steel to avoid irradiation induced deterioration, e.g. swelling [6]. Using interface materials such as oxides in composites and as permeation barriers may also decrease the thermal properties and worsen the activation behavior of the components [7]. Therefore all of the above mentioned issues have to be tackled through an integral approach.

#### References

- [1] Riesch, J. et al., Physica Scripta, PFMC-14, 2014
- [2] D. Maisonnier, et al. Conceptual Study of Commercial Fusion Power Plants, Final Report, EFDA-RP-RE-5.0, 13 April 2005
- [3] W. Eckstein et al., Atomic and Plasma-Material Interaction Data for Fusion, 7b, IAEA, Vienna, 2001. pp. 76.
- [4] Levchuck et al., Journal of Nuclear Materials 442 (2013) S592–S596
- [5] Chikada et al. Journal of Nuclear Materials 442 (2013) S592–S596
- [6] S. A. Fabritsiev, S. J. Zinkle and B. Singh J. Nucl. Mat. (1996)
- [7] Forrest, R.; Handbook of Activation Data Calculated Using EASY-2007 EURATOM/UKAEA Fusion Association, 2009

## Functional graded tungsten/EUROFER coating systems for First Wall application

D. D. QU<sup>1</sup>, W.W. BASUKI<sup>1</sup>, J. GIBMEIER<sup>1</sup>, R. VASSEN<sup>2</sup>, J. AKTAA<sup>1</sup>

<sup>1</sup>Karlsruhe Institute of Technology, Institute for Applied Materials, Germany

<sup>2</sup>Forschungszentrum Jülich, Institute of Energy and Climate Research (IEK-1), Germany

Reduced activation Ferritic/Martensitic (RAFM) steels, e.g. EUROFER are primary structural material candidates for the First Wall of DEMO, a demonstration reactor towards future fusion power plants (Kohyama et al. 1996). The interaction between plasma and FW, especially physical and chemical sputtering will limit the FW lifetime under normal operation (Ehrlich 1999). Therefore tungsten coating is selected to protect the FW due to its very low sputtering yield and low activation. However, the mismatch in thermo-physical properties between tungsten and EUROFER can lead to large residual thermal stresses and even failure. The application of functional graded material (FGM) is considered to be a good solution for the thermal mismatch problem (Weber & Aktaa 2011). The erosion protective tungsten coatings with tungsten/EUROFER functional graded (FG) interlayers on EUROFER substrate will be developed and optimized. The coating as well as the FG interlayer will be produced by Vacuum Plasma Spraying (VPS) with parameters optimized by modelling and evaluated by means of microstructural and micromechanical investigations.

To predict optimal parameters of the coating system non-linear finite element simulations are performed

assuming proper behavior for the different materials. Thereby the potential of the FG interlayer in reducing stresses and inelastic strains and hence improving lifetime is demonstrated. Based on the simulation results samples are fabricated by VPS with three different FG interlayers' thicknesses. The samples are comprehensively characterized performing measurements of residual stresses on the surface and among global depth direction, microstructural investigations including porosity et al., and micro and nano-indentation tests identifying basic properties of the different layers. The status of development will be reported presenting and discussing the main results collected so far as well as future theoretical and experimental work planned for the qualification of the developed coatings for FW application.

### References

- A. Kohyama, A. Hishinuma, D.S. Gelles, R.L. Klueh, W. Dietz, K. Ehrlich, *Journal of Nuclear Materials* 233-237 (1996) 138-147  
 K. Ehrlich, *Phil. Trans. R. Soc. Lond. A* 357 (1999) 595-623T. Weber, J. Aktaa, *Fusion Engineering and Design* 86 (2011) 220-226

## CuCrZr alloys reinforced by Tungsten as structural Divertor applications for DEMO

JAN HOFFMANN<sup>1</sup>, STEFFEN ANTUSCH<sup>1</sup>, JENS REISER<sup>1</sup>, MICHAEL RIETH<sup>1</sup>, VERENA WIDAK<sup>1</sup>, SOEREN MUELLER<sup>2</sup>, HOHE JOERG<sup>3</sup>

<sup>1</sup>Karlsruhe Institute of Technology (KIT), Institute for Applied Materials, Germany

<sup>2</sup>TU Berlin, Forschungszentrum Strangpressen, Germany

<sup>3</sup>Fraunhofer-Institut für Werkstoffmechanik (IWM), Freiburg, Germany

One of the crucial points for future fusion reactors like the DEMO powerplant are the high heat flux components of the divertor. Due to the excellent thermal conductivity, copper alloys are considered as a candidate material for these applications in the fusion energy production. While conventional copper alloys have a limited operating window due to the low mechanical strength [Reiser, 2012], reinforcement strategies for copper-based composites may extend this [Commin, 2013]. The already superior mechanical performance of the precipitation hardened CuCrZr compared to conventional alloys can be further improved by the addi-

tion of tungsten particles.

The present study shows the effect of (a) tungsten particles, (b) tungsten fibers and (c) tungsten foils on the mechanical and microstructural properties of the CuCrZr. The focus of the work was the feasibility of industrial production for the composites in large quantities.

The correct heat-treatment processes were experimentally evaluated to reach the desired mechanical and microstructural properties of the CuCrZr base material. Material of the same specifications was gas-atomized into fine powders and mixed with smaller tung-

sten powder to reach a homogeneous distribution of the two materials. The materials were characterized before and after pre-sintering. The Pre-sintering of the powder-mixtures was followed by a hot extrusion at TU Berlin. The resulting products were rod of diameter of 15 mm with a length of more than 2000 mm.

Characterizations were performed by Charpy impact and tensile tests. The microstructure was analyzed by scanning electron microscopy combined with EDS and EBSD maps.

In this presentation the authors give an overview of the concepts of CuCrZr reinforcements by tungsten. These concepts include particle and tungsten wire additions

to a copper matrix. Effects of the production routes on the resulting microstructure are discussed. The possibilities for mass fabrication and large scale processing of pipes by hot extrusion are also addressed.

#### References

- Reiser J, Rieth M., Optimization and limitations of known DEMO divertor concepts, *Fus Eng Des* 2012; 87
- Commin L. et al., Assessment of copper based materials for the Water-Cooled Divertor concept of the DEMO European Fusion reactor, *Conf Fus Eng (SOFE)* 2013

## Lithium evaporation and redeposition experiments under high density linear plasma dumping

X. CAO, W. OU, Z. CAO, Y. XIA, W. ZHANG, X. XUE, C. WANG, J. WANG, D. YANG, S. CHEN, F. GOU

Liquid Metals Research Group, Institute of Nuclear Science and Technology, Sichuan University, Chengdu, P. R. China

With many feasibilities of withstanding high heat flux, absorbing impinging species, compatibility with back wall and recovery of lithium surfaces continuously, the prospect of using liquid lithium as first wall or liquid divertor target plate has been the ongoing object [1-2]. However, due to the high evaporation rate, low ionization energy and splashing under the Lorentz forces at ELMS activities contrasted with conventional solid plasma-facing component (PFC) materials [3], the interactions of core plasma and a large amount of evaporated lithium, splashed lithium, redeposition-induced self-sputtering atom would reduce the temperature of core plasma, which may terminate the fusion ignition[4].

Lithium evaporation and redeposition with capillary pore systems (CPS) have been measured in one cathode linear plasma device. As a candidate plasma-facing material, a lithium sample with 1.2 cm in diameter with different layers of meshes was fixed on the target plate. Langmuir probe is used to monitor the lithium evaporation process near the specimen surface with adjustable plasma parameters of electron temperature ranging from 0.4 to 0.9 eV and electron density from 0.8 to  $3.2 \times 10^{19} \text{ m}^{-3}$ . The line intensity of lithium line 670.78 nm is detected by multi-channel optical emission spectroscopy (OES). The experimental results show that a reduction in lithium evaporation by a factor of 0.2–0.7 is found with increasing the layers of mesh, which is relevant to the binding energy  $E_b$  increase with layers of meshes. And the evaporated lithium vapor cloud plays

shielding role from the incident heat flux dumping. Meanwhile, a semi-empirical temperature-dependent model has been developed to simulate lithium evaporation physics based on several assumptions. The model is consistent well with experimental measurement result, which indicates high redeposition existence in the experiment, and the redeposition rate increases with the applied discharge current.

#### References

- [1] S.V. Mirnov, V.A. Evtikhin, The tests of liquid metals (Ga, Li) as plasma facing components in T-3M and T-11M tokamaks, *Fusion Engineering and Design*, 81 (2006) 113-119.
- [2] R. Bastasz, J.A. Whaley, Surface composition of liquid metals and alloys, *Fusion Engineering and Design*, 72 (2004) 111-119.
- [3] Deng B Q, Huang J H, Yan J C, et al. Study of the effects of liquid lithium curtain as first wall on plasma[J]. *Journal of nuclear materials*, 2003, 313: 630-635..
- [4] R. Majeski, R. Kaita, M. Boaz, P. Efthimion, T. Gray, B. Jones, D. Hoffman, H. Kugel, J. Menard, T. Munsat, A. Post-Zwicker, J. Spaleta, G. Taylor, J. Timberlake, R. Woolley, L. Zakharov, M. Finkenthal, D. Stutman, G. Antar, R. Doerner, S. Luckhardt, R. Seraydarian, R. Maingi, M. Maiorano, S. Smith, D. Rodgers, V. Soukhanovskii, Testing of liquid lithium limiters in CDX-U, *Fusion Engineering and Design*, 72 (2004) 121-132.

Talks Topic H 2:

## ***Materials for fission and fusion***

---

## Analyzing the ions radiation-induced defects and cavity swelling evolution in representative PWR internal austenitic steels

BERTRAND MICHAUT<sup>1</sup>, JOËL MALAPLATE<sup>1</sup>, ALEXANDRA RENAULT LABORNE<sup>1</sup>, FAIZA SEFTA<sup>2</sup>, DANIEL BRIMBAL<sup>3</sup>, LIONEL FOURNIER<sup>3</sup>, BRIGITTE DÉCAMPS<sup>4</sup>

<sup>1</sup>CEA, DEN/DANS/DMN/SRMA/LA2M, 91191 Gif-sur-Yvette, France

<sup>2</sup>EDF R&D, MMC, Site des Renardières, Môtret-sur-Loing, France

<sup>3</sup>AREVA NP, Paris La Défense, France

<sup>4</sup>CSNSM-IN2P3, Paris-Sud University, Orsay, France

The French nuclear industry is looking into the extension of the operation time of pressurized water reactors (PWR) up to 60 years. The nuclear reaction occurs in a vessel which contains the core internals supporting the fuel assemblies. The lower parts of the internals are composed of Solution Annealed (SA) 304 austenitic stainless steel plates and Cold Worked (CW) 316 stainless steel bolts. Due to their high exposition to irradiation (< 10<sup>-7</sup>dpa/s) it is expected to reach doses as high as 120 dpa after 60 years, at a temperature close to 300-370°C.

Irradiation leads to microstructural and microchemical changes such as apparition of black dots, dislocation loops, voids, bubbles, segregation and precipitation. These modifications may result in evolutions of the macroscopic behavior (swelling, irradiation creep, hardening, and corrosion resistance).

Swelling is a macroscopic dimensional modification. In Fast Breeder Reactors, it has been associated to the formation and growth of cavities. It is a threshold phenomenon which can be described by an incubation period (void/bubble nucleation) followed by a macroscopic swelling (cavity growth). Recently bubbles have been observed in PWR irradiated materials, but without macroscopic swelling. With the aim of an extension of the operation time, the evolution of the microstructure at high doses is a matter of concern.

Heavy ion irradiations are a fast and relatively easy way to reach high doses and to avoid drawbacks of neutron

irradiations such as activation. Such experiments are performed to simulate PWR microstructural evolutions under neutron irradiations. Two SA 304 and two CW 316 both containing different amounts of carbon are investigated.

The objective of this work is to study the microstructural and microchemical modifications, induced by ion irradiation in PWR conditions and to determine if swelling occurs or not.

Characterization of the virgin materials is performed (composition, grain size, dislocation network...). Irradiations at low (5 dpa) and moderate (40 dpa) doses with energetic iron ions (10 MeV, ~2x10<sup>12</sup> ions.cm<sup>-2</sup>.s<sup>-1</sup>) were carried out at JANNuS-Saclay facility (higher dose – 100 dpa in the same conditions is also expected). To counterbalance the flux effect, irradiation temperature was set to 450°C. Radiation-induced microstructures are investigated by Transmission Electron Microscopy (TEM). The evolution of radiation-induced defects as cavities, Frank loops and precipitates with the dose are studied as well as the influence of carbon.

Among the results, observations on SA 304L show an increase in the dislocation network. Faceted cavities formed at low dose and do not grow from 5 to 40 dpa. Simultaneously a saturation of the faulted Frank loops is already noticed at 5 dpa. Densities and sizes of frank loops and voids have been estimated, as well as microscopic void swelling values. All results will be discussed with the literature.

## Insights in microstructure of austenitic ods steels

TIM GRAENING, MICHAEL RIETH, ANTON MOESLANG

KIT, Institute for Applied Materials, Karlsruhe, Germany

Several years ago, the development of high performance austenitic steels in Germany started with the goal to produce fuel rod cladding tubes for the application in fission power plants. The aim was to enhance the oxidation, corrosion and creep resistance. Also some special phenomena such as swelling and irradiation assisted stress corrosion cracking occur in ma-

terials under irradiation, which decreases lifespan of structural materials dramatically. The solution to these draw-back was to introduce nanoscale particles in the surrounding matrix. They serve as traps for irradiation induced vacancies which are produced by the collision cascade and reduce swelling due to irradiation. Hence, the mechanical properties can maintain over a long pe-

riod at high temperatures in hazardous environment. [1–3]

Ferritic ods steels have been well researched in last decades in contrast to austenitic steels in irradiated environment, because of their enhanced swelling resistance and only use of low activation elements. Nowadays ods steels are also promising candidates for other high temperature applications, for instance in solar power plants. Whereby the austenitic matrix has the potential to sustain temperatures up to 700 °C and will surpass the limit of 550 °C for recent ferritic ods steels. [4]

To achieve homogeneously distributed precipitates the process of mechanical alloying is essential and followed by hot rolling or extrusion. To modify and affect the mechanical properties, it is important to acquire a thorough understanding of the evolution of microstructure with respect to the production process. Therefore the investigation of powder in different states and its influence on the properties of semi-finished products is inevitable knowledge to optimize the production process with an attritor mill. Due to this background, studies about different states

of powder with the help of TEM, SEM and XRD were performed to make a comparison to the microstructure of rods and hot-rolled sheets. In ferritic steels many studies about the nanostructure of Y have been performed, to get a thorough understanding about the evolution of complex Y-Ti-O precipitates. We want to acquire novel knowledge about the chemical structure of these clusters in each milling step and of the austenitic matrix.

Thus it is possible to bring the production of austenitic ods steel with a attritor mill to the next level up to industrial scale.

#### References

- [1] H. Oka, M. Watanabe, H. Kinoshita, T. Shibayama, N. Hashimoto, S. Ohnuki, S. Yamashita, S. Ohtsuka, J. Nucl. Mater. 417 (2011) 279.
- [2] K. Yabuuchi, Y. Kuribayashi, S. Nogami, R. Kasada, A. Hasegawa, J. Nucl. Mater. 446 (2014) 142.
- [3] A. Hirata, T. Fujita, Y.R. Wen, J.H. Schneibel, C.T. Liu, M.W. Chen, Nat. Mater. 10 (2011) 922.
- [4] P. Susila, D. Sturm, M. Heilmaier, B.S. Murty, V. Subramanya Sarma, J. Mater. Sci. 45 (2010) 4858.

## Studies of high dpa ion beam irradiation effects on fcc AA-6061 and fcc-bcc duplex steel 2205: micromechanical modelling and nano-indentation examination of hardness variations

MICHAEL SALEH<sup>1,2\*</sup>, PAUL MUNROE<sup>2</sup>, LYNDON EDWARDS<sup>1</sup>

<sup>1</sup> Institute of Materials Engineering, Australian Nuclear Science and Technology Organisation. Kirrawee DC, NSW, Australia

<sup>2</sup> School of Material Science and Engineering, University of NSW, Sydney, Australia

The irradiation effects of high dpa and the ramifications on the engineering assessment of reactor components in GEN IV systems is of considerable interest. Most polycrystalline metallic materials derive their strengths from the interactions of dislocations with defects such as solid solution alloying elements, interstitial elements, other dislocations, grain boundaries and sub-microscopic precipitates. Irradiation of metals and alloys at temperatures below those that anneal their defects typically produces pronounced radiation hardening, this is investigated herein to better understand the application of complex alloys in future reactor systems.

The current study focuses on ion beam irradiation of AA6061 and Duplex steel 2205, utilising the ANATRES Accelerator at ANSTO with 12 MeV Au<sup>+5</sup> ions used as the irradiating ions. To induce a 100 dpa damage, often cited as the operating level of GEN IV reactor, heavy Au<sup>+5</sup> ions are necessary as self-ion irradiation would

fail to induce the required damage. The main attribute of ion irradiation is the rapid accumulation of end of life doses over a short duration.. Conversely, neutron irradiation experiments in thermal test reactors may accumulate damage at a rate of 3–5 dpa year, e.g. the ANSTO OPAL reactor with 20 MW is capable of 100 MeV with reactor face neutron thermal flux of 4.0E10 n/cm<sup>2</sup>/s thus resulting in a less than optimal 2 dpa per year.

A key question still exists between the complementarity of neutron and ion irradiation with respect to the nature of damage, size, density and distribution of dislocation loops; black dots; and the extent of the dislocation networks. Although the same number of displacements can be produced using ion irradiation, there are differences in spatial defect distribution between the two. The post-irradiation measurements in effect quantify the final state of damage and the neutron-ion equivalence without an evaluation of

the damage path.

The simulation code Stopping and Range of Ions in Materials (SRIM) is used to model the irradiation process and compute the initial required experimental flux. Post irradiation studies of the micromechanical behaviour are done through nano-indentation (to a depth of 300 nm) using a diamond Berkovich tip. This allows for estimates of moduli and relative estimates of the strengths and hardening of individual phases and in-

dividual grains within a multiphase alloy. The results show a marked increase in the hardening of AA 6061 with a more modest increase in the Duplex steel 2205. Coupling these results to micromechanical FEA and crystal plasticity modelling, the authors hope to better describe the role of multi-scale modelling in complementing micromechanical testing and the extrapolation of results for engineering assessment.

## Mechanical Behavior of Unalloyed Plutonium

ADAM FARROW, TARIK SALEH, DENIECE KORZEKWA, JEREMY MITCHELL

Nuclear Materials Science, Los Alamos National Laboratory, USA

Plutonium possesses six solid allotropes between room temperature and its melting point at 640 Centigrade, displaying many unusual behaviors. The least dense phase (~15.9 g/cc) is a face-centered cubic, which also displays negative thermal expansion. The highest density phase (~19.9g/cc) is a simple monoclinic.

The mechanical behavior of plutonium is widely varied throughout these phases, displaying a broad range of behaviors, many of which are linked to the theoretical melting temperatures of different allotropes. The majority of phases only exist at temperatures above half of their homologous temperatures, as calculated against the theoretical melting temperatures for each phase (Nelson, 1965). This leads to unusual behaviors such as the observation that the beta phase, possessing a monoclinic unit cell of 34 atoms, can be pulled to 600% elongation.

Use of a videoextensometer and backlight in the plutonium facility at Los Alamos National Laboratory has resulted in new data sets with improved strain measurements over existing data sets. New results on the compressive behaviors of alpha (monoclinic), beta

(monoclinic), and gamma (orthorhombic) plutonium will be presented at different temperatures and strain rates, along with a brief review of the literature pertaining to the complex deformation behaviors of various phases of unalloyed plutonium.

As plutonium is extremely sensitive to processing history and microstructure, these will be discussed in the current work, with particular attention paid to bulk densities, microcracking issues during casting, and the effects of retained phases on the measurements of density and other parameters. Thermal expansion will also be discussed in reference to material processing and testing and as a indication of preferred orientation in the specimen stock produced in support of this study.

### References

Nelson, RD, Bierlien, TK, and Bowman, FE (1965): The Steady-State Creep of High-Purity Plutonium. Technical Report BNWL-32, UC-25, Metals, Ceramics and Materials, Pacific Northwest National Laboratory, Richland, WA, January 1965.

## Temperature dependent X-ray adsorption spectroscopy studies of Fe, Cr, and Ni local atomic structure for ferritic and austenitic ODS steels

ANDRIS ANSPOKS<sup>1</sup>, JURIS PURĀNS<sup>1</sup>, ALEKSEJS KUZMINS<sup>1</sup>, PAVEL VLADIMIROV<sup>2</sup>, TIM GRÄNING<sup>2</sup>, JAN HOFFMANN<sup>2</sup>, KĀRLIS LAZDIŅŠ<sup>1</sup>, ARTURS CINTIŅŠ<sup>1</sup>, ANTON MÖSLANG<sup>2</sup>, MICHAEL RIETH<sup>2</sup>

<sup>1</sup>EXAFS Spectroscopy Laboratory, Institute of Solid State Physics University of Latvia, Riga, Latvia

<sup>2</sup>Institute for Applied Materials-Applied Materials Physics, Karlsruhe Institute of Technology, Germany

Oxide dispersion strengthened (ODS) steels have exceptional thermal conductivity and low thermal expansion demonstrating high-temperature creep, corrosion and irradiation resistance. Therefore, they have a great

potential for use as structural materials for concentrated solar power plants, jet engines, chemical reactors as well as for hydrogen production from thermolysis of water. Previous developments are focused mainly

on the nanostructured ferritic (Fe-Cr alloys) ODS steels with very promising applications in, e.g., fusion power reactors up to about 650 °C [1].

Researchers from Karlsruhe Institute of Technology (KIT) suggested recently to employ the outstanding perspectives of austenitic (Fe-Cr-Ni alloys) ODS steels for high temperature fusion applications and solar power plants. It is expected that dispersion of nano-sized oxides particles with still unknown structure ( $x$ )  $Y_2O_3-(1-x)Ti(Fe)O_2$  will suppress the gas bubble growth and related void swelling under neutron irradiation and should reduce irradiation hardening, and increase high temperature resistance up to 800 °C. Moreover, austenitic steels are non-magnetic and do not suffer from a ductile-brittle-transition, which are typical drawbacks of ferritic-martensitic steels.

We used X-ray absorption near edge structure (XANES) and extended X-ray absorption fine structure (EXAFS) spectra to reveal phase and local structure of the absorbing atoms. These analysis revealed the phase and local structure evolution of the Ti and Y in ODS steel matrix during mechanical alloying and thermal treatment.

We found that the increase of the milling time to 80 h reduces the crystallinity of the sample with a transition point between 20 h and 40 h from bcc to fcc phase.

We can clearly distinguish Ti and Y atoms in metallic and oxide states. XAS proved to be excellent tool for answering question – when and how oxide nanoparticles are formed?

Using our recently developed method combining reverse Monte-Carlo and evolutionary algorithms for EXAFS spectra analysis (RMC/EA-EXAFS) [2] we reconstructed local structure of Y in  $Y_2O_3$  and Y containing nanoparticles in ODS steels.

We applied our methodology combining classical molecular dynamics with ab initio EXAFS calculations (MD-EXAFS) [3] to validate existing MD models for  $Y_2O_3$ . Samples were prepared by Karlsruhe Institute of Technology, and XAS analysis was performed by Institute of Solid State Physics.

XAS has proved to be excellent tool for atomic structure analysis.

#### References

- [1] Baluc, N., Boutard, J.L., Dudarev, S.L., Rieth, M., Brito Correia, J., Fournier, B., Henry, J., Legendre, F., Leguey, T., Lewandowska, M., Lindau, R., Marquis, E., Mucoz, A., Radiguet, B., Oksiuta, Z. (2011) Review on the EFDA work programme on nano-structured ODS RAF steels, *J. Nucl. Mater.* 417: 149-153.
- [2] Timoshenko, J., Kuzmin, A., Purans, J. (2014) EXAFS study of hydrogen intercalation into  $ReO_3$  using the evolutionary algorithm. *J. Phys.: Condens. Matter* 26: 055401.
- [3] Kuzmin, A., Evarestov, R.A. (2009) Quantum mechanics-molecular dynamics approach to the interpretation of X-ray absorption spectra. *J. Phys.: Condens. Matter* 21: 055401.

Talks Topic H 3:

## ***Materials for fission and fusion***

---

## Mechanical Properties of a PM2000 ODS alloy tested at temperatures up to 700°C

UDE D. HANGEN<sup>1</sup>, ASTA RICHTER<sup>2</sup>

<sup>1</sup>Hysitron, Inc., Aachen, Germany

<sup>2</sup>Asta Richter, Technische Hochschule Wildau, Germany

Mechanical materials properties at elevated temperatures are of general interest because temperature plays a key role in the making and forming of materials. For materials used in hot environments the long term stability of these properties plays an important role. In the recent years nanoindentation has become a technique that enables for testing at high temperatures and is now reaching levels of 700°C and beyond. These are relevant for many applications in tooling industry, metal processing and for structural materials used at elevated temperatures.

In the present work a PM 2000 FeCrAl alloy with small nanodisperse particles has been investigated for its hardness and modulus as well as for the indentation creep behavior up to 700°C. The methodology of indentation and the considerations taken for the high temperature testing will be discussed. The experiments show that the ODS strengthening mechanism is found to work up to a temperature of 400°C resulting in low creep rates and a stress exponent of  $n=80$  which is typ-

ical for the ODS strengthening mechanism. At 500°C up to 700°C an increase in the creep strain rate is found with a stress exponent of  $n=8.2$ . When returning to room temperature the mechanical behavior found before the heating experiment can be reproduced showing that the microstructure remains mostly unchanged by the heating experiment.

These findings by nanoindentation will be discussed – they are in good agreement with literature data obtained by tensile testing.

### References

C.-L. Chen, A. Richter, L.-T. Wu and Y.-M. Dong, *Materials Transactions*, Vol. 54, (2013) 215-221.

D.G. Morris, M.A. Munoz-Morris, *Acta Materialia* 61 (2013) 4636–4647.

J.H. Schneibel, M. Heilmaier, W. Blum, G. Hasemann, T. Shanmugasundaram, *Acta Materialia* 59 (2011) 1300–1308.

## High temperature investigation of the fusion relevant material EUROFER by instrumented indentation

JULIAN BREDL, MANUEL DANY, HANS-CHRISTIAN SCHNEIDER, OLIVER KRAFT

Karlsruhe Institute of Technology, Institute for Applied Materials, Germany

The prediction of the mechanical behavior of structural materials assigned for future fusion application at their operating conditions is a very important part of the current fusion research. In this regard, the instrumented indentation is an effective method of characterizing even small neutron-irradiated samples. The determination of material parameters e.g. hardness, Young's modulus and yield stress is possible by using the continuous recording of the indentation depth and indentation force, and appropriate analysis procedures.

With the high-temperature indentation device, developed at KIT, it is possible to test materials at temperatures up to 650 °C under remote-handling conditions. Former investigations with a test temperature up to 500°C have shown the functionality of the device and the thermal stability of the heating system. (Bredl, Dany, Schneider & Kraft 2014)

The focus of the investigations of this study lies on the material EUROFER, a reduced-activation ferritic-mar-

tensitic steel. It is characterized at elevated temperatures up to 500 °C for different heat treatments. A decreasing deformation resistance with an increasing temperature, a highly temperature depending hardness and an almost constant Young's modulus of the material is observed.

Besides conventional testing, indentation tests with multiple loading-unloading cycles were performed at elevated temperatures. The results of these multi-cyclic tests can be used for determining material parameter based on a neural network method (Tyulyukovskiy & Huber 2006). For such analysis, however, the quality of the load-depth-time data is crucial and small variations, e.g. related to fluctuations in the cooling system of the device, have a strong impact on the results. Thus, it has turned out that further improvements on the stability of the measurements are required to make full use of this powerful method. Additionally to the spherical indenter tests, measurements with Vickers tips are

carried out with the high temperature indentation device. As indenter tip materials, diamond and sapphire are used for both tip shapes. The latter is used since diamond will react with steels at temperatures of 400 to 500°C. However, sapphire is much more compliant than diamond and the influence of the tip material can be seen in differences in load-displacement-curves. An improved understanding of the mechanical behavior of the tip materials and their influence on the indentation procedure at high temperatures and high loads is an important result of this study.

Another important issue is to establish a routine for frequent inspections of the indenter tip to ensure valid results for every indentation test. This is discussed in this study with respect to the remote handled operation of the device in a Hot Cell.

In summary, the presented results can be considered as the final validation of the high temperature indentation device, which can thus be transferred to a Hot Cell of the Fusion Material Laboratory. Hence, a secure and valid characterization of small volumes of irradiated materials at elevated temperatures has been made possible.

#### References

- Bredl, J.; Dany, M.; Schneider, H.-C. & Kraft, O. (2014): Determination of RAFM steel properties at high temperatures by instrumented indentation – In: Conference SOFT 2014.
- Tyulyukovskiy, E. & Huber, N. (2006): Identification of viscoplastic material parameters from spherical indentation data: Part I. Neural networks – In: Journal of Materials Research 21 (3) 664-676.

## Study of irradiation creep based on nanomechanical lab-on-chip testing

PIERRE LAPOUGE<sup>1</sup>, FABIEN ONIMUS<sup>1</sup>, YVES BRÉCHET<sup>2</sup>, THOMAS PARDOEN<sup>3</sup>, JEAN-PIERRE RASKIN<sup>4</sup>, RENAUD VAYRETTE<sup>3-4</sup>

<sup>1</sup>CEA, DEN, Service de Recherches Métallurgiques Appliquées, Gif-Sur-Yvette, France

<sup>2</sup>INPG, Laboratoire de Science et Ingénierie des Matériaux et Procédés, St Martin D'Hères, France

<sup>3</sup>UCL, Institute of Mechanics, Materials and Civil Engineering, Louvain-la-neuve, Belgique

<sup>4</sup>UCL, Institute for Information and Communication Technologies, Electronics and Applied Mathematics, Louvain-la-neuve, Belgique

Metals and alloys (stainless steels, zirconium alloys, Inconel alloys) used as structural materials in the nuclear core of pressurized water reactor undergo irradiation creep deformation (Morize and Baicry 1985, Rogerson 1988, Scholtz and Matera 2000). A good understanding of the mechanisms that control the deformation is essential in order to predict the dimensional changes under irradiation. At the macroscopic scale, many experimental data are available. However, the microscopic mechanisms are still not yet fully understood (Onimus and Béchade 2012).

Many different mechanisms are proposed in the literature (Matthews and Finnis 1988), involving for instance dislocation climb under irradiation, but only few experimental results have revealed which mechanism is the most likely to control deformation creep. New experiments allowing the characterization of these various mechanisms are therefore needed.

In this study, a novel approach based on lab-on-chip thin freestanding test structures is evaluated. This on chip test method has been developed and optimized at Catholic University of Louvain but not yet used in the context of irradiation studies (Gravier et al 2009, Coulombier et al. 2012). An elementary test structure is composed of three main elements: (i) a thin specimen layer of the material of interest, (ii) an actuator layer

of silicon nitride with strong internal stresses to pull the specimen layer and (iii) a sacrificial layer of silicon dioxide to release the test structure from the underlying substrate. The small thickness of the material below few hundreds nanometers allow full irradiation by heavy ions with a kinetic energy of a few hundreds keV. The equilibrium of the freestanding structure is determined by the intersection between the elastic behaviour of the silicon nitride and the mechanical behaviour of the specimen. Hence one test structure gives one point in the tensile response of the specimen. By modifying the length of the actuator, different points of equilibrium can be reached and the specimen response in tension can be evaluated.

As a first step, test structures were irradiated to assess the mechanical behaviour of the irradiated copper specimen. The as irradiated microstructure was also characterized after Focus Ion Beam milling.

The results are compared with other results obtained on a bulk OFHC copper.

#### References

- Coulombier M., Guisbiers G., M-S. Colla, Vayrette R., Raskin J-P. (2012), Rev. Sci. instrum., Vol 83(10), pp. 105004.
- Gravier S., Coulombier M., Safi A., Andre N., Boe A.,

- Raskin J-P., Pardoën T. (2009), *Journal of MEMS* 18 (3), pp 555-569R
- Matthews J.R., Finnis M.W. (1988), *JNM* 19 pp 257-285
- Morize P., Baicry J., Mardon J.P. (1985) Zirconium in the Nuclear Industry, Seventh International Symposium, ASTM STP 939, pp. 101-119
- Onimus F., Béchade J.L. (2012), *Comprehensive Nuclear Materials*, Vol. 4, pp. 1-31
- Rogerson A. (1988), *JNM* 159, pp 43-61
- Scholz R., Matera R. (2000), *JNM* 283-287 pp 414-417

## Atom probe tomography of nanoscale precipitates in 13% Cr ODS steels with Ti variation

S. ROGOZHNIK<sup>1,2</sup>, N. ORLOV<sup>1,2</sup>, A. ALEEV<sup>1,2</sup>, A. BOGACHEV<sup>1,2</sup>, A. NIKITIN<sup>1,2</sup>, A. ZALUZHNYI<sup>1,2</sup>, R. LINDAU<sup>3</sup>, A. MÖSLANG<sup>3</sup>, P. VLADIMIROV<sup>3</sup>

<sup>1</sup> SSC RF Institute for Theoretical and Experimental Physics, Moscow, Russia

<sup>2</sup> National Research Nuclear University "MEPhI", Moscow, Russia

<sup>3</sup> Karlsruhe Institute of Technology, Institute for Applied Materials – Applied Materials Physics, (IAM-AWP), Germany

Oxide dispersion strengthened steels are promising materials for a variety of applications. First, they obey superior creep resistance at high operational temperature compared to ferritic-martensitic steels. These materials also demonstrate an increased radiation resistance.

It is commonly assumed that excellent mechanical properties of ODS steels are directly related to the high density of well-formed oxide particles (such as Y<sub>2</sub>O<sub>3</sub> or Y-Ti-O) (Klimenkov 2009). However, our previous APT study of EUROFER ODS (Alev 2011) revealed even one order of magnitude higher amount of nanometer size clusters enriched by Y, O, V. The effect of these clusters on the mechanical and irradiation resistance properties of ODS steels and, especially, evolution of their chemical composition under irradiation was not investigated in detail.

One of the current focus in development of ODS steels is set on higher chromium concentration (more than 12%) which originates from corrosion resistance deficiency of ferritic steels and controlled substructure. Addition of Ti in range of 0 to 0.5% leads to better mechanical properties increasing number density of precipitates and decreasing their sizes. In the work presented a model 13.5% ODS steel (He 2012) with variation of titan concentration in range of 0 to 0.5% was investigated by means of atom probe tomography technique. Analysis of spatial distribution of alloying elements in the investigated volumes revealed Clusters

(areas containing not only yttrium and oxygen but also titanium and chromium). Moreover, concentration of titanium in clusters was found to be higher than that of yttrium, which indicates the importance of these elements in cluster formation. The analysis allowed to study matrix composition, size and number density of oxide clusters. It is showed that the number density of clusters grows from  $\sim 1 \times 10^{23} \text{ m}^{-3}$  (for 0 wt.% Ti steel) up to  $\sim 1.5 \times 10^{24} \text{ m}^{-3}$  (for 0.4 wt.% Ti steel) yet the mean size of these clusters remains stable (about  $\sim 3 \text{ nm}$ ). There are considerable evidences showing an important role of titanium in fine cluster formation in 13.5%Cr ODS alloys.

### References

- Klimenkov, M. (2009): Klimenkov M., Lindau R., Möslang A. New insights into the structure of ODS particles in the ODS-Eurofer alloy, *Journal of Nuclear Materials*, 386–388 (2009) 553–556.
- Alev, A. (2011): Alev A.A., Iskandarov N.A., Klimenkov M., Lindau R., Möslang A., Nikitin A.A., Rogozhkin S.V., Vladimirov P., Zaluzhnyi A.G., Investigation of oxide particles in unirradiated ODS Eurofer by tomographic atom probe, *Journal of Nuclear Materials*, 409 (2011) 65–71.
- He, P. (2012): He P., Klimenkov M., Lindau R., Moslang A. Characterization of precipitates in nano structured 14% Cr ODS alloys for fusion application, *Journal of Nuclear Materials*, 428 (2012) 131–138.

## Identification of Cr-Y-O Nano-Cluster in a 14Cr Oxide Dispersion Strengthened Steel

XUE HU<sup>1,2</sup>, WEI YAN<sup>1</sup>, WEI WANG<sup>1</sup>, YIYIN SHAN<sup>1</sup>, KE YANG<sup>1</sup>

<sup>1</sup> Institute of Metal Research, Chinese Academy of Sciences, Shenyang, China

<sup>2</sup> University of Chinese Academy of Sciences, Beijing, China

Oxide Dispersion Strengthened (ODS) steels are being developed as the most promising structural material for the next-generation nuclear energy systems in Japan, Europe, and the United States, due to its excellent resistance to irradiation damage and high-temperature creep.

In this work, the preparation processing and microstructure of the Cr-Y-O nano-cluster dispersion strengthened steel were mainly studied. The preparation processing of Cr-Y-O nanocluster ODS steel is different from that of other ODS steels. The Cr and Y pure metal powders were ball-milled for 4h firstly, and then the mechanical alloying Cr-Y powders were added in the base alloying powders, i.e. China Low Activation Martensitic (CLAM) steel powder. After long-term mechanical alloying (MA) and spark plasma sintering (SPS), the mixed powders were sintered to block-shaped ODS steel, with a high relative density of 98.8%.

The microstructure of the Cr-Y-O nano-cluster ODS steel is full martensite structure with highly dispersed nano-precipitates, including Y<sub>2</sub>O<sub>3</sub> particles (with the size of 20-30nm) and YCrO<sub>3</sub> particles (with the size of 5-30nm). In addition, the orientation relationship between YCrO<sub>3</sub> and the steel matrix have also been investigated, with the zone axis relationship of  $[110]_{\text{BCC-Fe}} // [011]_{\text{YCrO}_3}$ .

### References

- Degueldre, C., et al. (2005). "Characterisation of oxide dispersion-strengthened steel by extended X-ray absorption spectroscopy for its use under irradiation." *Computational Materials Science* 33(1-3): 3-12.
- Ehrlich, K. (2001). "Materials research towards a fusion reactor." *Fusion Engineering and Design* 56-57: 71-82.
- Miller, M. K., et al. (2006). "Characterization of precipitates in MA/ODS ferritic alloys." *Journal of Nuclear Materials* 351(1-3): 261-268.
- Odette, G. R., et al. (2008). "Recent Developments in Irradiation-Resistant Steels." *Annual Review of Materials Research* 38(1): 471-503.
- Hirata, A., et al. (2012). "Characterization of oxide nanoprecipitates in an oxide dispersion strengthened 14YWT steel using aberration-corrected STEM." *Acta Materialia* 60(16): 5686-5696.
- Hirata, A., et al. (2011). "Atomic structure of nanoclusters in oxide dispersion strengthened steels." *Nature Materials* 10: 922-926.
- Hu, X., et al. (2013). "Evolution of microstructure and changes of mechanical properties of CLAM steel after long-term aging." *Materials Science and Engineering: A* 586: 253-258.
- Huang, Q., et al. (2011). "Progress in development of CLAM steel and fabrication of small TBM in China." *Journal of Nuclear Materials* 417(1-3): 85-88.

## Deuterium retention in reduced-activation ODS steels irradiated with 20 MeV W ions

O.V. OGORODNIKOVA<sup>1,2\*</sup>, K. SUGIYAMA<sup>2</sup>, Z. ZHOU<sup>3</sup>, YU. GASPARYAN<sup>1</sup>, V. EFIMOV<sup>1</sup>

<sup>1</sup> National Research Nuclear University "MEPHI", Moscow, Russia

<sup>2</sup> Max-Planck-Institut für Plasmaphysik, Garching, Germany

<sup>3</sup> University of Science and Technology Beijing, China

Ferritic/martensitic steels are one of the candidate materials for the vessel of the spallation target, and reduced-activation ferritic/martensitic (RAFMs) steels are first priority materials of structure for fusion nuclear reactors. These systems are desired to operate at relatively high temperatures. RAFM steels (e.g. Eurofer) possess exceptional thermal conductivity and low thermal expansion while being strongly resistant to void

swelling. Oxide dispersion strengthening (ODS) by the addition of Y<sub>2</sub>O<sub>3</sub> particles has been successfully applied to improve high-temperature strength of of RAFMs. Dispersion of a high number density of nano-size yttria particles is also effective to reduce radiation-induced microstructural change.

In the present work, RAFMs steels including Eurofer (9% of Cr) and ODS steels produced in China with dif-

ferent amount of Cr, namely, 9%, 12% and 16% were exposed to low energy ( $\sim 20$ - $200$  eV per D) deuterium plasma up to a fluence of  $2 \times 10^{25}$  D/m<sup>2</sup> in the temperature range from 290 K to 700 K. The depth profile of deuterium (D) in steels was measured up to 8  $\mu$ m depth by Nuclear Reaction Analysis (NRA) and the total retained amount of D in those materials was determined by thermal desorption spectroscopy (TDS). It was found that D retention in ODS steels is higher compared to Eurofer steel. The D retention in undamaged ODS steels strongly depends on the Cr content: minimum for 12%Cr and highest D retention for 16%Cr were found which can be associated with a change from Ferritic/Martensitic to pure Ferritic structure. High temperature tail was observed in TDS for ODS steels which was not observed for Eurofer. The presence of this tail is, probably, connected with D bound with precipitates.

Pre-irradiation with 20 MeV W ions produces radiation-induced defects which act as trapping sites for

D. Therefore, the D concentration in damaged steels increases. No pronounced effect of Cr on the D retention at radiation-induced traps under exposure at room temperature was observed. The D concentration at radiation-induced defects in ODS and Eurofer steels irradiated at room temperature is similar. Strong influence of D ion energy on both the D retention and surface modification was observed. Lower D retention near the surface in the case of irradiation with 200 eV D compared to 20 eV was found for both undamaged and damaged steels. Surface morphology alters due to preferential sputtering of light elements. The D plasma exposure at high sample temperature of 700 K results in more pronounced nano-structured surface modification which can be connected with migration of precipitates at 700 K. No visible difference in the surface modification for different RAMF steels and for pre-damaged samples was observed.

Talks Topic H 4:

## ***Materials for fission and fusion***

---

## Combined effect of radiation damage and helium on the hardening and embrittlement of ferritic / martensitic steels

YONG DAI, KUN WANG, CHRISTIANE VIEH, VLADIMIR KRSJAK

Laboratory for Nuclear Materials, Paul Scherrer Institut, Villigen, Switzerland

Ferritic / martensitic (FM) steels have been widely studied in various fission, fusion and spallation materials R&D programs. The understanding of irradiation – induced embrittlement effect has been one of most important research topics because it is well known that the ductile-to-brittle transition temperature (DBTT) of FM steels can be greatly increased by irradiation even at a relatively low dose level of few dpa. Furthermore, many observations also indicate that helium can greatly influence the DBTT shift. It is, therefore, important to understand the combined embrittlement effect of radiation damage and helium for fusion and spallation applications due to high helium production rate of FM steels in fusion reactor and spallation target irradiation environments.

In order to support the R&D of high power spallation targets materials, irradiation experiments have been performed in the targets of the Swiss spallation neutron source (SINQ) at the Paul Scherrer Institute (PSI) since 1998. In FM steels irradiated at SINQ under a mixed spectrum of high energy protons and spallation neutrons, accompanied with relatively high radiation damage rate up to 12 dpa per year, helium/dpa ratio ranges from a few appm He per dpa to about 90 appm He per dpa. Various mechanical tests such as tensile, 3-point bend, Charpy impact, small punch and hardness tests have been applied to investigate the irradiation effect on the mechanical properties of FM steels. The important finding is the additional hardening and embrittlement, compared with that induced by fission

neutron irradiation, induced by combined effect of radiation damage and helium in different FM steels at doses above about 10 dpa and helium concentrations above about 700 appm.

It is of essential importance to understand the mechanical behaviors of FM steels irradiated above 10 dpa and 700 appm He because of the additional hardening and embrittlement observed. Great efforts have been devoted to microstructural investigations including TEM observations, positron annihilation and atom probe tomography analyses to obtain rather complete information of irradiation-induced microstructural changes, both visible and invisible on TEM. Two novel observations are: (1) Helium bubbles of 1-2 nm sizes are weak obstacles with barrier strength of 0.1 – 0.15. The great additional hardening can be attributed to the high density,  $\sim 10^{24}/\text{m}^3$  of helium bubbles. While sub-nanometer sized vacancy-helium clusters detected by positron annihilation spectrometry analysis are even much weaker. (2) With the transition from ductile fracture mode to brittle (intergranular and cleavage) fracture mode, defect-free dislocation channels disappeared, instead, mechanical twins (never observed in FM steels) were produced. The formation of mechanical twins should be associated with the additional hardening. These findings will be described in detail and the combined effect of radiation damage and helium on the deformation mechanism of FM steels will be discussed.

## Mechanical Properties of Irradiated Ferritic/Martensitic Steels

TARIK A. SALEH, STUART A. MALOY, TOBIAS ROMERO, MATTHEW E. QUINTANA

Los Alamos National Laboratory, Los Alamos, New Mexico, USA

The US Department of Energy Fuel Cycle Research and Development Campaign supports research into extending the life of cladding material in high burn up, fast spectrum reactor environments. Doses of up to 400 dpa and irradiation temperatures of 300-550°C are expected. Ferritic/martensitic (F/M) steels are candidates for cladding and core materials under these conditions due to their excellent resistance to void swelling and their relatively good ductility in the irradiated

condition at most irradiation temperatures, especially temperatures below 400°C.

This talk will present the mechanical behavior of F/M steels from a number of irradiation experiments, concentrating on two alloys: HT-9 (nominal 12Cr, 1Mo steel) and T91 (nominal 9Cr, 1Mo steel). An overview of various irradiation experiments will be presented, including from spallation environments (STIPV, STIPV and MEGAPIE irradiations), thermal neutron environ-

ments (the UCSB ATR-NSUF irradiation) and fast neutron environments (FFTF reactor). As well as information on handling and testing materials at the Wing 9 hotcells in the CMR facility at the Los Alamos National Laboratory.

Comparison of HT9 and T91 will be made at similar

conditions from a the aforementioned neutron irradiations, ranging in dose from 6-20 dpa at irradiation temperatures ranging from 300-500°C, as well as some higher dose data out to 150 dpa from the FFTF reactor. Mechanical test data from different lots of HT9 material will be compared as well.

## Influence of neutron irradiation on precipitate microstructure in EUROFER97

CHRISTIAN DETHLOFF, ERMILE GAGANIDZE, JARIR AKTAA

KIT - Karlsruhe Institute of Technology, Institute for Applied Materials (IAM-WBM), Germany

Utilization of fusion as a future energy source, besides other sophisticated technologies, demands high performance structural materials. Reduced activation ferritic / martensitic (RAFM) steels like the European type EUROFER97 are primary candidate materials for this purpose, and provide good irradiation resistance at temperatures above 350°C and low activation. However, low temperature neutron irradiation still causes defect formation in the steel microstructure. As a serious consequence mechanical properties are affected leading to hardening and low temperature embrittlement. In this work the influence of neutron irradiation on the precipitate microstructure of EUROFER97 is addressed by performing transmission electron microscopy (TEM) investigations. For this purpose unirradiated samples are compared to specimens which were irradiated to a damage dose of 32 displacements per atom (dpa) at 330°C in the BOR-60 fast breeder reactor in Dimitrograd, Russia [Petersen 2002]. The preparation of TEM specimens out of undefomed parts of unirradiated and irradiated impact specimens involved cutting of slices of 3x4x0.15 mm<sup>3</sup> sizes, mechanical polishing and final thinning to electron transparency by electrolytic polishing (solution of 20% sulfuric acid, 80% methanol) [Dethloff 2014]. TEM investigations were performed at 200 kV with a high resolution FEI Tecnai G<sup>2</sup> F20 microscope located in the Hot Cells of Fusion Materials Laboratory at KIT. Scanning TEM (STEM) is used for a high Z-contrast in combination with energy dispersive x-ray spectroscopy (EDX) for element analysis.

TEM investigations on both unirradiated and irradiated samples show two basic different precipitate types. Large, for the most part elongated precipitates are located mainly along grain or lath boundaries, while small spherical ones are distributed randomly in the matrix. EDX analysis shows them to be M<sub>23</sub>C<sub>6</sub> and mainly Ta enriched MX carbonitrides, respectively. Detrimental composition changes of precipitates due to irradiation as well as irradiation induced new precipitate types like Cr rich  $\alpha'$  are not detected.

Precipitate size distributions are determined in two areas of both unirradiated and irradiated samples. By using EDX we show that the total precipitate size distribution can be easily separated for M<sub>23</sub>C<sub>6</sub> and MX by two log-normal distributions. The mean diameter of precipitates grows for MX from 21.1 nm to 29.0 nm by 37% and for M<sub>23</sub>C<sub>6</sub> from 82.0 nm to 100.0 nm by 22% after irradiation. Precipitate densities for M<sub>23</sub>C<sub>6</sub> are at about 5.7x10<sup>19</sup> m<sup>-3</sup> in 3 of 4 samples, while MX density varies between 2.4x10<sup>19</sup> and 4.2x10<sup>19</sup> m<sup>-3</sup>. Due to irradiation induced precipitate growth the precipitate volume fraction is increased from 0.97% to 1.44% after 32 dpa.

An estimation of hardening caused by irradiation induced precipitate growth after 32 dpa is presented. Application of the dispersed barrier hardening model shows that the effect of precipitate growth on hardening is negligible when compared to other irradiation phenomena like dislocation loop or helium bubble / void formation [Weiß 2012]. Nonetheless, an increase of the precipitate volume fraction leads to a shift of steel matrix elements which could affect hardening and embrittlement. Further investigations concerning irradiation defects formation are in progress.

### References

- Dethloff, C. *et al.* (2014): Quantitative TEM analysis of precipitation and grain boundary segregation in neutron irradiated EUROFER97 – Journal of Nuclear Materials 454: 323-331.
- Petersen, C. *et al.* (2002): The ARBOR irradiation project – Journal of Nuclear Materials 307-311: 1655-1659.
- Weiß, O. J. *et al.* (2012): Quantitative characterization of microstructural defects in up to 32 dpa neutron irradiated EUROFER97 – Journal of Nuclear Materials 426: 52-58.

## Atomic scale investigation of phase decomposition of Fe-22%Cr during thermal aging and subsequent heavy ion irradiation

O. KORCUGANOVA<sup>1,2</sup>, A. ALEEV<sup>1,2</sup>, S. ROGOZHKIN<sup>1,2</sup>

<sup>1</sup> National research nuclear university «MEPhI», Moscow, Russia

<sup>2</sup> SSC RF Institute for Theoretical and Experimental Physics, Moscow, Russia

Understanding of damaging and degradation processes along with correlation between atom-scale alteration and macroscopic properties of solid state materials is of very importance being a key topic in modern material science. One of the focuses in this field is binary systems based on iron, namely Fe-Cr alloy (Dudarev 2009). Its phase diagram is still a field of ongoing debates, which originates from the affinity of iron and chromium and magnetic nature of both of them (Xiong 2011). In case of Cr concentration higher than 10% decomposition of solid solution occurs.

This work is devoted to understanding of the kinetics of such a process in a Fe-22%wt.Cr alloy by means of atom probe tomography. The latter was used to quantitatively describe the nucleation and growth processes at atomic scale as well as stability of formed phases under cascade forming irradiation. Material was heat

treated up to 1200 h at 500 °C and the samples aged up to 50 and 200 hours were afterwards irradiated by heavy Fe ions up to 1 dpa. It was shown that the formation of  $\alpha'$  phase as well as behavior of oversaturated solid solution defies the classical law of coalescence theory of Lifshitz-Slezov and clusters behavior under irradiation depends on their sizes.

### References

Dudarev, S. (2009): The EU programme for modelling radiation effects in fusion reactor materials: An overview of recent advances and future goals. – *J. Nucl. Mater.*, 386–388:1-7.

Xiong, W. (2011): An improved thermodynamic modeling of the Fe-Cr system down to zero kelvin coupled with key experiments. – *Calphad*, 35: 3: 355–366.

## Comparison of mechanical properties between the HT9 and Gr.92 steel with various heat treatment conditions in a viewpoint of microstructure

SANGGYU PARK, HYEONGMIN HEO, JUNHWAN KIM, SUNGHO KIM

Korea Atomic Energy Research Institute, Korea

A Sodium-cooled Fast Reactor (SFR) is a reactor operated by high-energy neutrons that enables it to recycle the spent fuel from a conventional light water reactor. Because of its superior dimensional stability against fast neutron irradiation, Ferritic-martensitic steel (FMS) of 9Cr and 12Cr steels, such as HT9 and Gr.92 are preferable to utilize in the fuel cladding of an SFR in Korea. The objective of this study is to compare the effect of the heat treatment process on the mechanical properties of an HT9 and Gr.92 steel in the viewpoint of microstructure. Both HT9 and Gr.92 steel were normalized and tempered with various temperature settings and the vickers hardness test and tensile test were carried out to find the optimized heat treatment range. The microstructures observations were conducted using OM, and the grain boundary structures were observed by Electron Back-Scattered Diffraction (EBSD). Based on the mechanical properties obtained from the ex-

perimental studies, as well as from correlations with detailed information on boundary characteristics, the heat treatment effects between HT9 and Gr.92 steel are discussed.

To find the optimized heat treatment conditions of the HT9 and Gr.92 steel, it was normalized in a range of 950°C to 1100°C for 30 minutes, and tempered in the range of 700°C to 800°C for 1 hour to change the microstructures. A tension test was carried out in accordance with the ASTM E8 specification. The strain rate was 0.005/min, and tests were performed from room temperature to 650°C.

The microstructure of the HT9 and Gr.92 showed typical tempered martensite structure. As the temperature of the normalizing increases, the sizes of the prior austenite increase. The Vickers hardness was linearly decreased with an increasing tempering temperature and it show higher values with an increasing normal-

izing temperature. Similar tendency were observed in yield strengths obtained from the room temperature test results. Both the yield stress and ultimate tensile stress decreased with an increasing tempering temperature. However, In the case of the samples normalized at 950°C, the strengths tested at 650°C show linear behavior in spite of increasing tempering temperature. The effective grain size were measured by EBSD with considering the misorientations over 15°. Both the HT9 and Gr.92 steel show significant decrease of effective grain size after 950°C normalizing condition. This could be explained the enhancement of high temperature strength in HT9 and Gr.92 steel, and these results will be quantitatively discussed with an EBSD analysis results in detail.

## Creep rupture behavior of the China Low Activation Martensitic steel at 600°C

XUE HU <sup>1,2</sup>, LIXIN HUANG<sup>3</sup>, WEI YAN <sup>1</sup>, WEI WANG <sup>1</sup>, YIYIN SHAN <sup>1</sup>, KE YANG <sup>1</sup>

<sup>1</sup> Institute of Metal Research, Chinese Academy of Sciences, Shenyang, China

<sup>2</sup> University of Chinese Academy of Sciences, Beijing, China

<sup>3</sup> State Key Laboratory of Metastable Materials Science and Technology, Yanshan University, Qinhuangdao, China

Reduced Activation Ferritic/Martensitic (RAFM) steels have been considered as candidate structural materials for future fusion nuclear reactors. As the primary candidate structural material for the Li-Pb blanket, the China Low Activation Martensitic (CLAM) steel was designed and developed in China.

In this work, the creep rupture behavior of the CLAM steel at 600°C was investigated under the load of 130, 140, 150, 170 and 200MPa. It was worth noticing that the creep-rupture life of CLAM steel under 130MPa (about 7914h) is much longer than that under 140MPa (about 969h), although the load was only decreased by 10MPa. This led to that the long-term creep-rupture life of CLAM steel under the load of 130Mpa was much longer than the extended extrapolation of short-term stress/creep-rupture life. The 130MPa seemed to indicate a kind of threshold stress at 600 °C, lower than which, the creep-rupture life could be significantly elongated. In addition, during long-term creep exposure, the martensitic laths and the precipitate distribution changed significantly. Especially, the Laves phase precipitated on the grain boundaries or lath boundaries. The potential mechanisms controlling the excellent creep properties, the creep damage behavior and the microstructure degradation of the CLAM steel have also been studied.

### References

- [1] ] Y. I. Chang, Technical rationale for metal fuel in fast reactor, Nuclear Engineering and Technology, vol. 39, no.3, 2007.
- [2] J. H. Kim, H. M. Heo, J. H. Baek, and S. H. Kim, Evaluation of the Mechanical properties of a HT9 fuel cladding tube for a Sodium-cooled fast reactor, Journal of the Korean Institute of Metal and Materials, vo. 51, no. 25, 2013
- [3] R. L. Klueh and A. T. Nelson, J. Nucl. Mater., vol.371, no. 37, 2007

### References

- Eggeler, G. (1989). "The effect of long-term creep on particle coarsening in tempered martensite ferritic steels." *Acta Metallurgica* 37(12): 3225-3234.
- Fernández, P., et al. (2005). "Creep strength of reduced activation ferritic/martensitic steel Eurofer'97." *Fusion Engineering and Design* 75–79(0): 1003-1008.
- Hald, J. and L. Korcakova (2003). "Precipitate Stability in Creep Resistant Ferritic Steels-Experimental Investigations and Modelling." *ISIJ International* 43(3): 420-427.
- Hu, X., et al. (2013). "Evolution of microstructure and changes of mechanical properties of CLAM steel after long-term aging." *Materials Science and Engineering: A* 586: 253-258.
- Kimura, K., et al. (2009). "Long-term creep deformation property of modified 9Cr–1Mo steel." *Materials Science and Engineering: A* 510–511(0): 58-63.
- Klueh, R. L. (2008). "Reduced-activation steels: Future development for improved creep strength." *Journal of Nuclear Materials* 378(2): 159-166.
- Kostka, A., et al. (2007). "On the contribution of carbides and micrograin boundaries to the creep strength of tempered martensite ferritic steels." *Acta Materialia* 55(2): 539-550.
- Lee, J. S., et al. (2006). "Causes of breakdown of creep strength in 9Cr–1.8W–0.5Mo–VNb steel." *Materials Science and Engineering: A* 428(1–2): 270-275.

Talks Topic H 5:

***Materials for fission and fusion***

---

## Positron annihilation research on ferritic/martensitic steels irradiated under mixed spectrum of high energy protons and spallation neutrons

VLADIMIR KRSJAK, YONG DAI

Paul Scherrer Institut, Villigen, Switzerland

The investigation of the helium-filled nano-scale defects, particularly for those invisible by TEM, in irradiated materials is a significant challenge for both nuclear and material researchers. The behavior and thermal evolution of these defects have an intrinsic effect on the material performance under irradiation. A number of positron annihilation spectroscopy (PAS) experiments was performed recently on various steels irradiated in the SINQ (the Swiss spallation neutron source) targets at PSI to 5-20dpa at the corresponding irradiation temperatures between 100 and 480°C. New methodology based on internal positron source was developed in order to investigate a wide range of sample designs and providing more reliable bulk information. The internal positron source utilized in the experiments is based on the <sup>44</sup>Ti/<sup>44</sup>Sc isotope, which is a typical product of spallation reaction in Fe-based materials and, with the half-life of nearly 60years, a convenient radioisotope source.

The positron lifetime spectra obtained on various ferritic/martensitic (F/M) steels show two defect components having a lifetime 190–250ps and 350-500ps respectively. According to published theoretical data, the first component was attributed to small vacancy clusters up to about 12 vacancies, having a high helium-to-vacancy ratio around 1. The later component

describes larger clusters with low helium content, which are considered to be eventually precursors for helium bubbles.

With increasing irradiation dose and irradiation temperature the helium-to-vacancy increases, which reduce the positron mean lifetime. At about 10-12 dpa/100 appm He, corresponding to irradiation temperature ~150-170°C, a local minimum of positron mean-lifetime was observed in investigated F/M steels. At higher irradiation temperatures - up to 480°C, increase of positron mean-lifetime indicates the coarsening of vacancy clusters along the formation of small helium bubbles. The results also show, that the maximum capability of small vacancy clusters to accommodate the transmutation helium increases with the irradiation temperature, which is in a good agreement with the theoretical modeling data [1]. It seems that the process of accommodation of helium by existing or newly radiation-induced vacancy clusters plays an essential role in the formation and growing of helium bubbles.

### Reference

[1] R.E. Stoller, Yu. N. Osetsky, Journal of Nuclear Materials 455 (2014) 258–262

## Loss of strength and embrittlement of neutron irradiated beryllium

V. CHAKIN, A. MOESLANG

Institute for Applied Materials, Karlsruhe Institute of Technology, Germany

Beryllium is essential as reflector and moderator for material testing nuclear reactors (SM, BR2, etc.), as plasma facing material and neutron multiplier for fusion reactor designs (ITER, DEMO) (Poitevin 2014), and as reflector material for the recently approved European Spallation Source (ESS) in Sweden. In these machines, beryllium is subjected to neutron irradiation resulting in degradation of physical-mechanical properties. Under neutron irradiation, beryllium can be damaged in different degree depending on irradiation parameters (temperature, neutron spectrum and flux, damage dose and helium accumulation). In particular, loss of strength and embrittlement of neutron-irradi-

ated beryllium occur. This degradation of mechanical properties facilitates to formation and propagation of brittle cracks in beryllium (Chakin 2011). In the worst case, the neutron irradiation can lead to loss of integrity of beryllium components what is essential for safety reason.

There is a set of results on dose dependence of mechanical properties of beryllium samples irradiated at temperatures of 343-873 K up to neutron fluences  $(0.04-1.4) \cdot 10^{23} \text{ cm}^{-2}$  ( $E > 0.1 \text{ MeV}$ ) in different material testing nuclear reactors. Analysis of the data was performed that allowed to determine the temperature-dose intervals where irradiation damage of mi-

microstructure and, accordingly, degradation of mechanical properties of beryllium samples were significantly manifested. It was found that the brittle fracture of beryllium samples accompanied by loss of strength started at the lowest temperature of 343 K after irradiation up to neutron fluence of  $0.04 \cdot 10^{23} \text{ cm}^{-2}$  ( $E > 0.1 \text{ MeV}$ ). Increasing the irradiation temperature leads to less degradation of beryllium mechanical properties. Evolution of beryllium microstructure under neutron irradiation is discussed. The irradiation-induced helium accumulation in beryllium takes place resulting in formation of small helium-vacancy clusters, voids and bubbles. These irradiation defects cause swelling. As a rule, the beryllium material is produced by powder metallurgy methods such as hot extrusion, high isostatic pressing, etc. Therefore, the beryllium material has weakened grain boundaries. Under irradiation, anisotropic swelling of grains results in brittle crack forma-

tion on boundaries that leads to loss of strength and embrittlement of the irradiated beryllium samples under mechanical tests.

#### References

- Y. Poitevin, I. Ricapito, M. Zmitko, F. Tavassoli, N. Thomas, G. De Dinechin, Ph. Bucci, J. Rey, A. Ibarra, D. Panayotov, L. Giancarli, P. Calderoni, J. Galabert, J. Vallory, A. Aiello: Progresses and challenges in supporting activities toward a license to operate European TBM systems in ITER. – In: *Fusion Engineering and Design*, Volume 89, Issues 7–8, October 2014: 1113-1118.
- V. Chakin, R. Rolli, H.-C. Schneider, A. Moeslang, P. Kurinskiy, W. Van Renterghem: Pores and cracks in highly neutron irradiated beryllium. – In: *Journal of Nuclear Materials*, Volume 416, Issues 1-2, 1 September 2011: 3-8.

## Modeling Hydrogen Ad- and Desorption on Beryllium-(0001)-Surface

CHRISTOPHER STIHL, DMITRY BACHURIN, PAVEL VLADIMIROV

Karlsruhe Institute of Technology, Institute for Applied Materials - Applied Materials Physics (IAM-AWP), Germany

The proposed application of beryllium in future fusion devices like ITER and DEMO (Vladimirov, P.V. et al. (2014)) as a neutron multiplier and plasma facing material entails the necessity to deal with the production of radioactive tritium as a result of transmutation processes. As tritium retention and release is substantially altered on whether beryllium is deformed severely by creep as in some blanket designs, it is crucial to acquire a thorough understanding of the mechanisms of tritium accumulation and release which is relevant for the evaluation of total tritium inventory. As a first step we perform calculations using the VASP code for basal (0001) surface which is known to be the most energetically favorable among other hexagonal close packed surfaces in beryllium. Significant interlayer distance relaxation of the outermost surface layers is observed in both pure and fully covered with hydrogen basal surface. It is found that the presence of hydrogen on beryllium surfaces leads to a noticeable reduction of surface energy and sometime to surface reconstruction. Activation energy profile for hydrogen diffusion within the outermost surface layers is calculated. Adsorption of hydrogen molecule is simulated with the help of ab initio molecular dynamics.

Further we develop a multiscale modeling approach to hydrogen adsorption and desorption on beryllium surface consisting of (i) ab initio calculations of total energies for particular configurations of hydrogen on the surface (ii) a suitable cluster expansion (Sanchez, J.M. et al. 1984) which approximates the energies of arbitrary configurations, and (iii) a kinetic Monte Carlo method for dynamic simulations of adsorption and desorption.

Our model is based on a set of ab initio total energies for numerous hydrogen adsorption patterns on the beryllium (0001) surface and includes two non-equivalent hydrogen adsorption positions, the hcp and the fcc hollow sites. A suitable cluster expansion enabling total system energy predictions both for low and high hydrogen coverages was found using the MIT Ab initio Phase Stability (MAPS) code. This expansion was used in our Monte Carlo code which is able to run Metropolis or kinetic Monte Carlo (kMC) simulations to model concurrent de- and adsorption processes. The hydrogen desorption, adsorption and surface diffusion processes implemented in the kMC code were first modelled using VASP ab initio molecular dynamics runs. In this work, we present the first results of the application of our multiscale model. Specifically, conditions necessary for the occurrence of adsorption and desorption processes, the equilibrium hydrogen coverages, resulting from concurrent desorption, adsorption, and surface diffusion processes are discussed.

#### References

- Vladimirov, P.V. et al. (2014): Current Status of Beryllium Materials for Fusion Blanket Applications, *Fus. Sci. Tech.* 66: 28-37
- Sanchez, J.M. et al. (1984): Generalized cluster description of multicomponent systems, *Physica A: Statistical Mechanics and its Applications*, 128: 334-350
- van de Walle, A. & Ceder, G. 2002: Automating first-principles phase diagram calculations, *Journal of Phase Equilibria*, 23: 1054-9714

## Dislocation microstructure evolution in tungsten due to indentation loading simulated by discrete dislocation dynamics

KINSHUK SRIVASTAVA<sup>1</sup>, DANIEL WEYGAND<sup>1</sup>, PETER GUMBSCH<sup>1,2</sup>

<sup>1</sup>IAM-ZBS, Institut für Angewandte Materialien-Zuverlässigkeit von Bauteilen und Systemen, Karlsruher Institut für Technologie (KIT), Germany

<sup>2</sup>Fraunhofer IWM, Freiburg, Germany

Tungsten, owing to its material properties is a promising candidate for plasma-facing materials in nuclear fusion reactors. Therefore to understand the plasticity in irradiated samples, it is first necessary to understand the evolution of plasticity based on the activated slip systems in single crystals.

Screw dislocations have a much lower mobility compared to mixed dislocations. Therefore they govern the plasticity in body-centered cubic metals. Screw dislocations glide by the thermally-activated kink-pair mechanism [1] which is controlled by a stress-dependent activation enthalpy. This activation enthalpy not only depends on the resolved shear stresses but also on the so-called non-Schmid stresses.

A computational framework for three-dimensional discrete dislocation dynamics (DDD), incorporating atomistic simulation results on the activation enthalpy of screw dislocations in tungsten is presented [2]. For

loading along the [-149] and [011] directions, the microstructure evolution under spherical indentation in micrometer sized tungsten single crystals is examined. The primary mechanism of dislocation multiplication in the sample is cross-slip which leads to generation of very large density of dislocations and accommodation of the plastic strain-gradients under the indenter. The simulated slip system activity can also be used to interpret the plasticity mechanisms in experiments.

### References

- 1.) Dorn E, Rajnak S. 1964. Nucleation of kink pairs and the peierls' mechanism of plastic deformation. *Trans.AIME*. 230: 1052–64
- 2.) K. Srivastava, R. Gröger, D. Weygand, P. Gumbsch, Dislocation motion in tungsten: Atomistic Input to Discrete Dislocation Simulations, *International Journal of Plasticity* 47 (2013) 126-142

## Characterization and modelling of the mechanical behaviour of Nb<sub>3</sub>Sn

GILLES LENOIR, VERONIQUE AUBIN

Laboratoire MSSMat (UMR CNRS 8579), Ecole Centrale Paris, France

Materials without electrical resistance and a perfect expulsion of magnetic fields, so called superconductors, are important in fusion reactor components (tokamaks, stellarators), magnetic resonance imaging (MRI) and in electricity transport. The materials currently used in high field magnets limit the intensity of the produced magnetic field to 12 Tesla. The use of niobium-tin (Nb<sub>3</sub>Sn) is essential to surpass this limit [Todesco 2011].

The superconducting domain, defined by the critical temperature, the critical field and the critical current density in the superconducting material, is also dependent on the applied strain [Ekin 1980]. Nb<sub>3</sub>Sn is a brittle material and beyond a certain deformation, the damage of the strands prevents the crossing of the current [Miyoschi 2009]. Under this critical value of deformation, some materials show a reversible limitation of the critical current. This dependency is well known for Nb<sub>3</sub>Sn strands [Nijhuis 2009], whereas the mechanical response is not. In fact, mechanical-electrical couplings require a corresponding knowledge of the strand's

response to thermo-mechanical loading due to the manufacturing process, the cabling process and during service. Furthermore, degradation of the electrical performance of the strands under cyclic loading was observed [Bruzonne 2002].

In order to predict the electrical behaviour of the strand, its accurate mechanical behaviour is necessary. It will be done by the characterization and modelling of superconducting strands under monotonous and cyclic loadings. Monotonous tensile tests with unloadings and cyclic tensile tests at various mean stresses were used to identify the constitutive equation. The model will then be validated on more complex tests corresponding to the loadings to which the strands are subjected throughout the manufacturing process and usage. In a second step, observations and analyses will be performed to understand the origins of the degradation of the electrical performance.

In this paper, the characterized mechanical behaviour of Nb<sub>3</sub>Sn superconducting strands is presented in two parts. The first one is devoted to the mechanical re-

sponse of the strands under monotonous and cyclic loading. The second step is the analysis of their local properties. These steps are required to build an accurate model adapted to the complex structure of the superconducting composite.

#### References

Bruzzone P., Fuchs A. M., Stepanov B., Vecsey G. (2002): Performance evolution of Nb3Sn cable-in-conduit conductors under cyclic load [for Tokamaks] – In: *Applied Superconductivity, IEEE Transactions on* 12, 516–519.

Ekin J. W., Suenaga M., Clark M. (1980): Strain scaling law and the prediction of uniaxial and bending strain effects in multi-filamentary superconductors –

In: *Filamentary A15 Superconductors* Plenum Press, New York, USA, 187-203.

Miyoshi Y., van Lanen E. P. A., Dhallé M. M. J., Nijhuis A. (2009): Distinct voltage–current characteristics of Nb3Sn strands with dispersed and collective crack distributions – In: *Supercond. Sci. Technol.*, vol. 22 no. 8.

Nijhuis A., Ilyin Y., Wessel S., Krooshoop E., Feng L., Miyoshi Y. (2009): Summary of ITER TF Strand Testing Under Axial Strain, Spatial Periodic Bending and Contact Stress – In: *IEEE Transactions on Applied Superconductivity* 19, 1516–1520.

Todesco E., Zimmermann F. (2011): The high energy LHC – In: *CERN Yellow Report*, talk at the 2<sup>nd</sup> EuCard meeting, Paris.

## Characterisation and modelling of nuclear graphite : from micrometres to metres

DONG LIU<sup>1</sup>, PETER HEARD<sup>1</sup>, GILLIAN SMITH<sup>1</sup>, BRANKO SAVIJA<sup>2</sup> ERICK SCHELANGEN<sup>2</sup>, PETER FLEWITT<sup>1</sup>

<sup>1</sup>Interface Analysis Centre, HH Wills Physics Laboratory, School of Physics, University of Bristol, UK

<sup>2</sup>Civil Engineering & Geosciences, Delft University of Technology, NL

Graphite is used in UK gas-cooled reactors as a moderator, a reflector and a structural component. The integrity of the graphite bricks making up the reactor core are of major importance for the safe operation and shut-down of the reactor. Specifically, an a nearly isotropic (ratio of about 1.1) Gilsocarbon graphite is used in the operating advanced gas-cooled reactors (AGRs) in the UK and life extension is planned. Gilsocarbon graphite is a multi-phased, polygranular material containing pitch, Gilsonite filler particles and pores and are produced by pressing or moulding. When loaded in bending, non-linear deformation occurs prior to failure. No evidence of plasticity has been observed in these graphites hence the deviation from linear-elastic behavior is attributed to localised micro-cracking (Moskovic et al 2013). It was found that the microstructure in the Gilsocarbon graphite has multi-scale physical and mechanical characteristics. There is also mass loss due to radiolytic oxidation during exposure to the reactor environment. Therefore, understanding the multi-scale mechanical properties and establish a full range of characterisation of the Gilsocarbon graphite is essential to extrapolate the measured properties to the metre-length bricks.

In the present work, the microstructure and mechanical properties of Gilsocarbon graphite have been characterised over a range of length-scales. A range of small-scale mechanical testing approaches are described including a novel in situ micro-cantilever technique based in a dualbeam workstation (Liu et al 2014). It was found that pores ranging from nanometre to tens of micrometre in diameter are present

which modify the deformation and fracture characteristics of the material. These approaches have revealed, for the first time, the significant change of mechanical properties, for example flexural strength, over the length-scale from a micrometre to tens of centimetres. A synthetic multi-scale model of the microstructure is input to a finite element model to predict properties for various amounts of porosity at the tens of centimeter length-scale. It is emphasized that input parameters to these computer models have to be undertaken at the appropriate length-scale to allow predictions with required confidence. When the necessary input parameters are included in the microstructure-based multi-scale numerical model it is possible to describe the deformation, fracture strength and the stochastic features of the strength of the graphite.

#### References

Liu, D., Nakhodchi, S., Heard, P.J., Flewitt, P. E. J.

(2014): Small-Scale Approaches to Evaluate the Mechanical Properties of Quasi-Brittle Reactor Core Graphite,” *Graphite Testing for Nuclear Applications: The Significance of Test Specimen Volume and Geometry and the Statistical Significance of Test Specimen Population*, STP 1578, Nassia Tzelepi and Mark Carroll, Eds., pp. 1-21, doi:10.1520/STP157820130127, ASTM International, West Conshohocken, PA 2014.

Moskovic, R., Heard, P. J., Flewitt, P. E. J., Wootton, M. R. (2013): Overview of strength, crack propagation and fracture of nuclear reactor moderator graphite. *Nuclear Engineering and Design*. Vol 263, 431-442.

Talks Topic I 1:

## ***High temperature materials***

---

# Development of a novel microstructure highly resistant to grain boundary damage during creep at 950°C in Alloy 617

Ji-Won Lee<sup>1</sup>, Hyun-Hwa Park<sup>1</sup>, Tae-Ho Lee<sup>2</sup>, Hyun-Uk Hong<sup>1</sup>

<sup>1</sup>Department of Materials Science and Engineering, Changwon National University, Republic of Korea

<sup>2</sup>Department of Ferrous Alloy Research Group, Korea Institute of Materials Science, Korea

The Ni-based superalloy Alloy 617 is considered as a primary candidate material for the intermediate heat exchanger (IHx) between the primary and the secondary helium coolant circuits in the very high temperature gas reactor (VHTR)[1]. The operation condition of IHx requires the alloy to withstand mechanical degradation at 950 °C and 3~8 MPa in He impurities. The reason of the requirement of the Alloy 617 as candidate material for VHTR is due to its high-temperature mechanical properties. Recently, however, there are some results that this alloy's mechanical properties are unstable during creep at very high temperature[1]. The degradation of its properties resulted from the surface oxidation and decarburization along the grain boundaries (GBs), the dissolution and redistribution of grain boundary (GB) carbides, GB migration and recrystallization. Hence, the great concerns could be given to the GB character for better performance of this superalloy. Therefore, in this paper, the heat-treatment for grain boundary serration in Alloy 617 was introduced as one of the effective method to strengthen the GBs. Actually, Hong et al. [2-4] conducted the specialized heat-treatment to induce the serrated GBs in Alloy 263 and the serrated GBs enhanced creep properties due to their low interfacial free energy. The proprietary direct aging combined with controlled cooling rate led successfully to the transition of serrated GBs in Alloy 617. The lower final aging temperature produced higher amplitude and higher fraction of serrated GBs. The micro structural observation revealed the serrated GBs with stable planar  $M_{23}C_6$  carbides and angulated MC carbides in grain interior. After the creep test under 950°C/30MPa condition, the serrated specimen had about 2 times longer creep life than standard specimen. Moreover, when the serrated specimen was subjected to 5% cold deformation before creep (referred to as 'pre-strained/serrated specimen', hereinafter),

the creep life could be extended to be 2.8 times longer as compared with standard specimen. The longitudinal section of the standard specimen after creep rupture showed a typical sharp crack running and propagating along GB perpendicular to the loading axis in standard specimen. However, the serrated GBs (both serrated and pre-strained/serrated specimens) were highly resistant to GB cracking, resulting in an isolated GB crack with low frequency. It should be also noted that the pre-strained/serrated specimen contained not only coarsened primary carbides but also fine secondary carbides distributed uniformly in  $\gamma$ (FCC) matrix. The transmission electron microscopy indicated that the coarsened intragranular carbides without any interaction with dislocations in the standard specimen. It indicated that initial fine carbides coarsened rapidly with creep test. So, dislocation could slip well and reached to fracture in short time. In the case of the serrated specimen, there were a little intragranular carbides without any interaction with dislocations. However, this specimen had the strengthened GBs, as the result, it had 2 times longer creep life. Finally in the pre-strained/serrated specimen, the fine and stable carbides which precipitated substantially through preliminary 5% cold work treatment, impeded effectively dislocation movement. Thus a correlation between metallurgical factors and optimal microstructures has been proposed in this work.

## References

- [1] S. Kihara, J.B. Newkirk, A. Ohtomo, Y. Saiga, Metall. Trans. A 11 (1980) 1019.
- [2] H.U. Hong, I.S. Kim, B.G. Choi, M.Y. Kim, C.Y. Jo, Mater. Sci. Eng. A 517 (2009) 125.
- [3] H.U. Hong, H.W. Jeong, I.S. Kim, B.G. Choi, Y.S. Yoo, C.Y. Jo, Phil. Mag. 92 (2012) 2809.

## Numerical multi-criterion optimization method for developing Ni-based superalloys: Development of a software tool and experimental validation

RALF RETTIG<sup>1</sup>, NILSS C. RITTER<sup>1</sup>, ALEXANDER MÜLLER, HARALD E. HELMER<sup>1</sup>, ROBERT F. SINGER<sup>1</sup>

<sup>1</sup>Friedrich-Alexander-Universität Erlangen-Nürnberg, Institute for Science and Technology of Metals, Erlangen, Germany

Traditionally alloy development is still dominated by extensive experimental research programs. However, today sophisticated numerical tools are available for calculating many alloy properties in dependency of the composition. In this respect especially the CALPHAD-method shall be mentioned, which allows the prediction of phase fractions and compositions of realistic alloys containing even ten elements or more (Rettig et al. 2009). Further properties, for example density or  $\gamma/\gamma'$ -precipitate misfit are available via semi-empirical models. Despite this high potential, the true computational design of nickel-based superalloys is still in the early stages (Egorov-Yegorov et al. 2005, Reed et al. 2009). This is mainly due to the many requirements for this class of alloys, for example certain  $\gamma'$ -phase fraction, misfit, low content of brittle TCP-phases, high creep strength and low density simultaneously. It is not possible to maximize each of these properties and therefore trade-offs, so called Pareto-optimum compositions have to be found.

In the present work, a new approach based on the mathematical method of multi-criterion global optimization is presented which can easily manage the billions of potentially optimum alloy compositions. It has been implemented with a deterministic Sequential Quadratic Programming solver. In order to reduce calculation times, all properties were calculated from the compositions via pre-calculated metamodels with the Kriging-method. With this method a rhenium-free sin-

gle crystal alloy with nearly the same creep strength as the well-established rhenium-containing alloy CMSX-4 has been computationally developed.

It has been found that the success of the optimization is mostly related to the maximization of the concentrations of the solid solution strengthening elements (i.e. Re, W, Mo) in the  $\gamma$ -matrix phase by optimization of the partitioning ratio of those elements between  $\gamma$  and  $\gamma'$ -phase. This is especially influenced by the  $\gamma'$ -phase forming elements Al, Ta and Ti but also depends on the concentration of all other elements in the alloy. The approach and the actual optimization procedure as well as the verification of the calculations based on creep experiments and further property measurements of the cast optimum alloy are presented.

### References

- Rettig R., Heckl A., Neumeier S., Pyczak F., Göken M., Singer R.F. (2009): Verification of a commercial CALPHAD database for Re and Ru containing nickel-base superalloys. – Defect Diff. Forum, 289-292: 101-108.
- Egorov-Yegorov I.N., Dulikravich G.S. (2005): Chemical composition design of superalloys for maximum stress, temperature, and time-to-rupture using self-adapting Response Surface optimization. – Mater. Manufact. Proc., 20: 569-50
- Reed R.C., Tao T., Warnken N. (2009): Alloys-By-Design: Application to nickel-based single crystal superalloys. – Acta Mater., 57: 5898-5913.

## On the importance of the matrix for the creep properties of single crystal nickel based superalloys

R. VÖLKL<sup>1</sup>, E. FLEISCHMANN<sup>1</sup>, E. AFFELDT<sup>2</sup>, U. GLATZEL<sup>1</sup>

<sup>1</sup>Metals and Alloys, University Bayreuth, Germany

<sup>2</sup>Rabe MTU Aero Engines GmbH, Munich, Germany

The creep properties of single crystal nickel based superalloys, consisting of a two phase  $\gamma/\gamma'$ -microstructure, strongly depend on the size and volume content of the  $\gamma'$ -phase and on the misfit between gamma and  $\gamma'$ . They can be influenced by heat treatment or the composition of the alloy. In the past a lot of work has been done to determine the ideal values of these mi-

crostructural parameters. Due to the high strength of the  $\gamma'$ -particles creep deformation is strongly restricted to the  $\gamma$ -matrix. Thus the mechanical properties of the solid solution hardened matrix may become of high importance.

In this study, nickel based superalloy single crystals with different contents of matrix solid solution strengthen-

ers were cast, heat treated and creep tested at 980°C and different stresses. The influence of the strength of the matrix on the creep properties of the superalloy as well as the solid solution hardening efficiency of Re, W and Mo in the matrix is determined.

#### Reference

Fleischmann, E. (2013): Einfluss der Mischkristallhärtung der Matrix auf die Kriechbeständigkeit einkristalliner Nickelbasis-Superlegierungen – Dissertation, University Bayreuth 2013, ISBN 978-8440-2329-9.

## Influence of misfit stresses on dislocation glide in single crystal superalloys: A three-dimensional discrete dislocation dynamics study

SIWEN GAO<sup>1</sup>, MARC FIVEL<sup>2</sup>, ANXIN MA<sup>1</sup>, ALEXANDER HARTMAIER<sup>1</sup>

<sup>1</sup>Interdisciplinary Centre for Advanced Materials Simulation (ICAMS), Ruhr-Universität Bochum, Germany

<sup>2</sup>University Grenoble Alpes/CNRS, SIMaP-GPM2, Grenoble, France

Ni-base (or Co-base) single crystal superalloys are mainly applied as turbine blades in the hottest regions of gas turbines, due to their outstanding creep deformation resistance. In the characteristic  $\gamma/\gamma'$  microstructure of single crystal superalloys, the lattice mismatch of these two phases results in a significant misfit stress field, which plays a decisive role for the micromechanical processes which lead to the observed macroscopic athermal deformation behavior of these high-temperature alloys. The sign and magnitude of this lattice mismatch depend on the chemical composition of materials as well as on the temperature. All currently used Ni-base superalloys possess a negative lattice misfit that becomes more negative with increasing temperature, while recently developed Co-base superalloys with a similar  $\gamma/\gamma'$  microstructure have a positive lattice mismatch that decreases at higher temperatures (Mughrabi, H. 2014).

Three-dimensional discrete dislocation dynamics (DDD) simulations are applied to investigate dislocation glide in  $\gamma$  matrix channels and shearing of  $\gamma'$  precipitates by superdislocations under external uniaxial stresses, by

fully taking into account internal misfit stresses. Misfit stress fields are calculated by the fast Fourier transformation (FFT) method and hybridized with DDD simulations. For external loading along the crystallographic [001] direction of the single crystal, it was found that the different internal stress states for negative and positive lattice mismatch result in non-uniform dislocation movement and different dislocation patterns in horizontal and vertical  $\gamma$  matrix channels. Furthermore, positive lattice mismatch produces a lower deformation rate than negative lattice mismatch under the same tensile loading, but for an increasing magnitude of lattice mismatch, the deformation resistance always diminishes. Hence, the best deformation performance is expected to result from alloys with either small positive, or even better, vanishing  $\gamma/\gamma'$  lattice mismatch.

#### Reference

Mughrabi, H. 2014: The importance of sign and magnitude of  $\gamma/\gamma'$  lattice misfit in superalloys---with special reference to the new  $\gamma'$ -hardened cobalt-base superalloys. *Acta Mater.*, 81:21-29, 2014.

## TEM analysis of localized, planar deformation events which govern creep of single crystalline CoNi-super alloys with $\gamma/\gamma'$ -microstructures

YOLITA M. EGGELER<sup>1</sup>, JULIAN MÜLLER<sup>1</sup>, MICHAEL S. TITUS<sup>2</sup>, AKANE SUZUKI<sup>3</sup>, TRESA M. POLLOCK<sup>2</sup>, ERDMANN SPIECKER<sup>1</sup>

<sup>1</sup> Center for Nanoanalysis and Electron Microscopy (CENEM), University of Erlangen-Nürnberg, Germany

<sup>2</sup> Materials Department, University of California Santa Barbara, USA

<sup>3</sup> GE Global Research Center, One Research Circle, Niskayuna, USA

In the present study we use transmission electron microscopy (TEM) to study the effect of creep on the microstructures of a novel CoNi-based single crystal su-

peralloy with  $\gamma$  (fcc) -  $\gamma'$  ( $L1_2$ ) microstructure after [001] tensile creep testing at stresses close to 300 MPa and a temperature of 900 °C. The alloy investigated contains

28 at.% Ni, which was added to the Co-Al-W ternary system to expand the  $\gamma$ - $\gamma'$  phase field and to increase the  $\gamma'$ -solvus temperature [1].

Conventional transmission electron microscopy (CTEM) using two beam conditions with fundamental and superlattice reflections was performed for fault characterization by applying the invisibility criterion. TEM samples cut perpendicular to the tensile axis show a high density of antiphase boundaries (APB) in the ordered  $\gamma'$  precipitates produced by unit dislocations of type  $a/2[011]$  and  $a/2[01-1]$  which cut the  $\gamma'$  phase [2]. Samples cut parallel to the tensile axis reveal the presence of extended ribbons of faults in the  $\gamma/\gamma'$  microstructure. Along these defects, each  $\gamma'$  precipitate exhibits a characteristic APB/SISF/APB configuration whereby a superlattice intrinsic stacking fault (SISF) is fully embedded in an antiphase boundary (APB). While the SISF is confined to the (111) plane the surrounding APB shows migration towards energetically favorable {100} orientations. The two types of planar defects are separated by a Shockley partial dislocation loop with Burgers vector  $1/6[-211]$  as explicitly shown by large angle convergent beam electron diffraction (LACBED). Using CTEM, the translation vector of the APB was identified to be  $a/2[01-1]$ , which is perpendicular to the Burgers vector of the dislocation loop. The intrinsic nature of the SISF was confirmed by high resolution transmission electron microscopy (HRTEM) combined with geometric phase analysis (GPA).

Possible energetic and kinetic reasons for the nucleation of a SISF loop inside an APB and the relationship to a similar mechanism in Ni-based superalloys [3] which has been controversially discussed in the literature are addressed.

An in-situ TEM heating analysis of an APB originally lying on a {111} plane confirms the migration to {100}

planes which are associated with a lower planar fault energy. Further increase of the temperature results in coarsening of the APB and lateral expansion of a disordered ( $\gamma$ ) region originating from the APB. Upon slow cooling the  $\gamma'$  phase nucleates in the form of small precipitates at the position of the former APB. ChemiSTEM reveals significant segregation at APBs corroborating the importance of atomic diffusion and reordering during creep, which can locally lower the planar fault energy. Furthermore, the in-situ TEM heating experiments confirm that tertiary  $\gamma'$  precipitates do not act as obstacles for dislocations at temperatures above 850 °C, and that the  $\gamma'$  volume fraction decreases with increasing temperatures.

The present analysis contributes to a better understanding of cutting events in CoNi-based Superalloys. In particular, the importance of local diffusion, as evident from the APB migration, will be discussed, and the need for accurate predictions and assessments of fault energies and kinetics of the fault transformation process will be emphasized.

#### References

- [1] K. Shinagawa, T. Omori, J. Sato, K. Oikawa, I. Ohnuma, R. Kainuma, and K. Ishida, "Phase Equilibria and Microstructure on  $\gamma'$  Phase in Co-Ni-Al-W System," *Mater. Trans.*, vol. 49, no. 6, pp. 1474–1479, 2008.
- [2] Y. M. Eggeler, M. S. Titus, A. Suzuki, and T. M. Pollock, "Creep deformation-induced antiphase boundaries in L12-containing single-crystal cobalt-base superalloys," *Acta Mater.*, vol. 77, pp. 352–359, Sep. 2014
- [3] M. Condat and B. Décamps, "Shearing of  $\gamma'$  precipitates by single  $a/2 \langle 110 \rangle$  matrix dislocations in a  $\gamma/\gamma'$  Ni-based superalloy," *Scr. Metall.*, vol. 21, no. 5, pp. 607–612, May 1987.

Talks Topic I 2:

## ***High temperature materials***

---

## On the Formation of Ledges and Grooves at $\gamma/\gamma'$ Interfaces of Single Crystal Superalloys

ALIREZA B. PARSA<sup>1</sup>, PHILIP WOLLGRAMM<sup>1</sup>, HINRICH BUCK<sup>1</sup>, ALEKSANDER KOSTKA<sup>1</sup>, CHRISTOPH SOMSEN<sup>1</sup>, ANTONIN DLOUHY<sup>2</sup>, GUNTHER EGGELER<sup>1</sup>

<sup>1</sup>Institut für Werkstoffe, Ruhr-Universität Bochum, Germany

<sup>2</sup>Institute of Physics of Materials, Brno, Czech Republic

Ni-base superalloys are material of choice for high temperature applications. Single crystal Ni-base superalloys are mainly used in gas turbine blades for energy conversion and aero engines, where they are exposed to elevated temperatures close to their melting point in a highly corrosive environment. The microstructure consists of two phases,  $\gamma$  and  $\gamma'$ , with coherent interface where the  $\gamma'$  cuboidal precipitates are in a  $\gamma$  matrix. In this study formations of grooves and ledges have been investigated. Previous studies indicate that during high temperature low stress creep of Ni-base superalloys the interface irregularities increase and show that their size and number increases. Diffraction contrast scanning transmission electron microscopy (STEM) is used as well as stereo microscopy to provide new evidence for the existence of ledges and grooves. These features are usually accompanied with a dislocation nearby at the  $\gamma/\gamma'$  interface. A small 2D model is implemented

that illustrates how stress field of a dislocation changes the local chemical potential and provide driving force for diffusional fluxes that result in the formation of a groove. The results in this study hint that the formation of grooves and ledges investigated represent an elementary process which, should be accounted for when rationalizing the kinetics of rafting i.e. the directional coarsening of  $\gamma'$  cubes during high temperature deformation.

### References

- Kolbe M, Dlouhy A, Eggeler G. *Mater Sci Eng A* 1998; 246:133.  
Epishin A, Link T, Nolze G. *Journal of Microscopy* 2007; 228:110.  
Link T, Epishin A, Paulisch M, May T. *Mater Sci Eng A* 2011; 528:6225.

## The influence of Re and Ru on the high-temperature creep strength and phase stability of Ni-based superalloys

KAMIL MATUSZEWSKI, RALF RETTIG, ROBERT F. SINGER

Institute of Science and Technology of Metals WTM, University of Erlangen-Nuremberg, Erlangen, Germany

There is no doubt that the efficiency of gas turbines is relying upon the temperature of the combustion process and, in turn, on the high temperature strength of applied materials. Hence the increasing demand for more efficient stationary gas turbines for energy production drives the development in the field of Ni-based superalloys. Over the last decades the effort was successfully put into the improvement of manufacturing process, eventually leading to obtain single-crystal castings. Nowadays even more effort is put into the optimization of the chemical composition of Ni-based superalloys in respect to both high-temperature creep strength and long-term phase stability maintaining relatively low costs of material.

The very high solid solution strengthening effect of Re [1-3] and its very low diffusion coefficient [4, 5] bring the significant improvement in high-temperature strength. The previous results of our group [6] clearly indicate that the maximum application temperature of Ni-based superalloys can be increased by 87 K with

addition of Re from 1 to 2 at.% at the expense of Ni. Further, Ru raises the temperature limit by 38 K when added to low Re-containing superalloys.

Besides the beneficial effect, the addition of Re results in a relatively strong dendritic segregation. This enforces firstly the need of expensive heat-treatments. Secondly, it leads to precipitation of topologically close packed (TCP) phases [7-9].

The effect of TCP phase precipitation is very detrimental due to two main factors. At first, TCP phases are composed from refractory elements and thus they deplete the  $\gamma$ -matrix phase from strengtheners, i.e. the solid solution strengthening effect of expensive refractory elements cannot be fully used and thus creep strength is reduced [7, 8]. Secondly, TCP phases exhibit complex morphology, transforming with time from plate-like into lath-like particles [9]. Their precipitation can thus lead to a reduction of fatigue life-time of the material [8].

In the present study we clarify the effect of Re and Ru on the high-temperature phase stability of Ni-based superalloys in respect to predict their influence on high-temperature creep strength.

The microstructure of experimental Ni-based superalloys with various content of Re and Ru is investigated and studied quantitatively. The results show the huge dependency of TCP phase precipitation on the Re-content. Influence of Ru is especially evident in the early stages of precipitation, i.e. nucleation. CALPHAD calculations are performed to understand the information about Re and Ru influence. The results are complemented with the detailed chemical composition analysis of TCP phases as well as  $\gamma/\gamma'$  microstructure. It is found that addition of Ru increases the solubility limit of Re within the  $\gamma$ -matrix phase. All this results together bring the new insight into the understanding the effect of Re and Ru and optimizing the creep strength and phase stability of Ni-based superalloys.

## References

- A. F. Giamei, D.L. Anton, *Met. Trans. A* 16A, 1997-2005 (1985)
- G. L. Erickson, in *Superalloys 1996* (The Minerals, Metals and Materials Warrendale, PA, USA, 1996), pp. 35-44
- D. Blavette, P. Caron, T. Khan, in *Superalloys 1988* (The Metallurgical Society, Warrendale, PA, USA, 1988), pp. 305-314
- M.S.A. Karunaratne, P. Carter, R.C. Reed, *Mat. Sci. Eng.* A281, 229-233 (2000)
- R.A. Hobbs, M.S.A Karunaratne, S. Tin, R.C. Reed, C.M.F. Rae, *Mat. Sci. Eng.* A460-461, 587-594 (2007)
- A. Heckl, S. Neumeier, M. Göken, R.F. Singer, *Mat. Sci. Eng.* A528, 3435-3444 (2011)
- R.A. Hobbs, L. Zhang, C.M.F. Rae, S. Tin, *Met. Mat. Trans. A* 39A 1014-1025 (2008)
- M. Simonetti, P. Caron, *Mat. Sci. Eng.* A254, 1-12 (1998)
- K. Matuszewski, R. Rettig, R.F. Singer, *Proceedings of 2nd European Symposium on Superalloys and their Applications (Eurosuperalloys 2014)*, MATEC Web of conferences, 14 (09001), 1-6, (2014)

## Super-Solvus Heat Treatments of Ni-Based Superalloys in a Hot Isostatic Press/Quench Unit

LAIS MUJICA RONCERY, INMACULADA LOPEZ-GALILEA, BENJAMIN RUTTERT, WERNER THEISEN

Chair of Materials Technology, Ruhr-Universität Bochum, Germany

In the field superalloys, hot isostatic press have been conventionally used to reduce the porosity generated during the cast and homogenization processes. The integration of the HIP within the steps conventional heat treatment steps of casting  $\rightarrow$  homogenization  $\rightarrow$  precipitation hardening has not a general rule. Some heat treatment schemes prefer the use of HIP after casting, which is not useful since new pores can arise during homogenization due to the Kirkendall effect [Bokstein]. Other schemes prefer the incorporation after homogenization, nevertheless the use of a short annealing and quenching is additionally needed because of the limitations of most HIP units to incorporate quench.

New strategies in the development of the hot isostatic press allow performing quenching during the HIP cycle. In such a way it is possible integrate heat treatments within the HIP process [Åkerberg, Ahlfors, Laker]. In the case of the superalloys, it is possible then to integrate homogenization and HIP in one step, and even more to incorporate precipitation hardening within the HIP cycle.

Previous studies have shown the large influence of the cooling rate, temperature and pressure on the po-

rosity and microstructure of single crystal superalloys [Lopez-Galilea]. In the frame of this work, the combination of different pressures and quench/cooling strategies in a HIP/Quench unit is studied in the second generation ERBO-1 (similar to CMSX-4) single crystal Ni-Based superalloy during super-solvus HIP treatment (1280-1320°C).

From the process point of view, pressures between 25 and 200 MPa are applied, having a direct influence on the physical properties of the gas such as density and viscosity. Additionally, different nozzles are used to influence de gas speed. The combination of these variables influences the heat transfer coefficient and therefore the quenching speed. The extrapolation of these factors for further integrated heat treatments is considered.

From the microstructural point of view, the differences of the relationship between the isostatic pressure and the porosity of the material are analysed. Additionally, the morphology of the  $\gamma/\gamma'$  in dependence on the quenching rates are considered.

## References

- Bokstein B.S., Epishin, A.I., Link, T., Esin, V.A., Rodin A.O., Svetlov, I.L. (2007) Model for the porosity growth in single-crystal nickel-base superalloys during homogenization. *Scripta Materialia* 57 (2007) 801–804
- Åkerberg, A. (2014). The difference between URQ and U2RC. Proceedings of the 11<sup>th</sup> Conference on hot isostatic pressing.
- Ahlfors, M. (2014). The Possibilities and Advantages with Heat Treatments in HIP. Proceedings of the 11<sup>th</sup> Conference on hot isostatic pressing.
- Larker, R. Rubin, P. Uniform Rapid Quenching enables Austempering Heat Treatment in HIP (2012). Proceedings from the 6th International Quenching and Control of Distortion Conference
- Lopez-Galilea I.; Huth, S., Theisen, W. Fockenberger, T., Chakraborty, S (2012) Effect of high pressure and high temperature on the microstructural evolution of a single crystal Ni-based superalloy. *Journal of Materials Science*.
- Lopez-Galilea, I. Huth, S. Theisen, W. (2014) Challenges in Reducing Casting Porosity in Superalloys. HIP'14 pp. 346–358
- Lopez-Galilea, I., Huth, S., Theisen, W. (2014) Effect of the cooling rate during heat treatment and hot isostatic pressing on the microstructure of a SX-Ni Superalloy. Proceedings of Eurosuperalloys. MATEC Web of Conferences 14, 13009.

## Crystal plasticity modeling of porosity reduction in an as-cast Ni-base single crystal superalloy during hot isostatic pressing

SIWEN GAO<sup>1</sup>, INMACULADA LOPEZ-GALILEA<sup>2</sup>, ANXIN MA<sup>1</sup>, STEPHAN HUTH<sup>2</sup>, WERNER THEISEN<sup>2</sup>, ALEXANDER HARTMAIER<sup>1</sup>

<sup>1</sup>Interdisciplinary Centre for Advanced Materials Simulation (ICAMS), Ruhr-Universität Bochum, Germany

<sup>2</sup>Institut für Werkstoffe, Ruhr-Universität Bochum, Germany

Owing to the excellent performance of Ni-base single crystal superalloys to resist extreme working conditions at high temperature, they are the material of choice for application in the hottest regions of modern gas turbine. Although the deformation resistance at the elevated temperature significantly increases by adding a high concentration of refractory elements, a stronger dendritic segregation during solidification and pores accumulation in the interdendritic region during an extensive homogenization heat treatment tend to occur, which deteriorates mechanical properties of materials (Link, T. 2006). In order to heal these micropores, hot isostatic pressing (HIP) as an advanced thermal treatment is utilized, which combines creep deformation and diffusion bonding to homogenize the alloy composition by the appropriate pressure and high temperatures (Kim, M.T. 2006).

According to the experimental observation of HIP on an as-cast Ni-base single crystal superalloy, a quasi-two-dimensional (2D) crystal plasticity finite element model is developed to investigate the influence of different temperatures, isostatic pressures and duration time on the porosity reduction during HIP. In this crystal plasticity based creep model, the internal stress caused by lattice misfit and strain heterogeneity inside the typical  $\gamma/\gamma'$  microstructure have been considered.

The temperature dependency mainly comes from the atoms self-diffusion coefficients and the initial and saturated dislocation slip resistances.

This study aims at determining the relationships between HIP parameters and pore annihilation kinetics. With respect to several quasi-2D pore geometries, we have achieved a good agreement between measured and simulated pore area reduction. It was found that by increasing HIP temperature or by increasing isostatic pressure one can get comparable porosity evolutions. We have also observed some important microstructure geometry influence such as: Under the same conditions, large pore shrinks faster than small one at the beginning; Big  $\gamma'$  phase particles near a pore retard the pore annihilation speed; Pore shape does strongly affect the pore shrinkage.

## References

- Link, T. 2006: Synchrotron tomography of porosity in single-crystal nickel-base superalloys. *Materials Science and Engineering A*, 425:47-54, 2006.
- Kim, M.T. 2006: Effect of HIP process on the microstructural evolution of a nickel-based superalloy. *Materials Science and Engineering A*, 441:126-134, 2006.

## Characterization of $\langle 100 \rangle$ superdislocations and the $\gamma/\gamma'$ interface by an advanced FIB lamella lift out technique

JULIAN MÜLLER<sup>1</sup>, MICHAEL J. MILLS<sup>2</sup>, ERDMANN SPIECKER<sup>1</sup>

<sup>1</sup>Center for Electron Microscopy and Nanoanalysis, University of Erlangen-Nürnberg, Erlangen, Germany

<sup>2</sup>Center for Electron Microscopy and Analysis, Ohio State University, Columbus, USA

Single crystalline Ni-based superalloys exhibit unique properties when it comes to high temperature deformation since they possess an excellent mechanical stability, sufficient oxidation resistance and a good damage tolerance. As the complete deformation mechanism from the as heat treated base alloy to the ruptured creep sample is highly complex, there are still unresolved questions regarding the underlying microscopic mechanisms. Two key factors which influence the creep properties are the structure and local chemistry of the  $\gamma/\gamma'$  interface and the cutting of the  $\gamma'$  phase by superdislocations.

In the present work an advanced FIB lamella lift out technique is employed to study the above mentioned microstructural features of Ni-base superalloys. The lift out technique is based on the preparation of FIB lamellas from conventional TEM samples. This enables characterizing e.g. a superdislocation first in plan-view geometry by conventional TEM techniques and afterwards in cross section geometry by HRSTEM to determine the dislocation core configuration. Hence, it becomes possible to investigate a large number of dislocations in plan-view and categorize them in terms of their appearance, Burgers vector or connection to the channel dislocation network. After selecting a characteristic dislocation and applying the FIB lamella lift out technique cross section HRSTEM can be used to reveal the dislocation core structure and unravel the role the dislocation plays in the creep process. In the present work the core structures of two characteristic  $\langle 100 \rangle$  superdislocations which do not experience any glide or climb force from the external load are studied. Interest-

ingly, also the superpartials in which the superdislocations dissociate do not experience glide or climb forces from the external load. Instead, an osmotic pressure generated by a vacancy supersaturation is proposed to cause the dislocations to climb through the  $\gamma'$  phase.

As a second application of the FIB lamella lift out technique the  $\gamma/\gamma'$  interface width is studied. Even though the preferential orientation of the interface is  $\{100\}$ , locally it exhibits angular deviations of up to several degrees ( $\sim 8^\circ$  for the present sample). Consequently, in a regular TEM sample it is not possible to ensure that the  $\gamma/\gamma'$  interface is in edge on orientation. As result projection effects lead to an overestimation of the actual interface width. To overcome these limitations a  $\gamma/\gamma'$  interface region with in plane orientation very close to  $\langle 100 \rangle$  was selected from a regular plan-view TEM sample. The precise orientation of the interface was determined by means of selected area electron diffraction. Afterwards the FIB lamella lift out technique was employed to prepare a cross section sample from the selected interface region. With this approach it was possible to reduce TEM projection effects to a minimum. Applying HRSTEM imaging under conditions of Z contrast the chemical width of the interface was measured to be  $< 1$  nm. Taking into account geometrical broadening due to atomic scale roughness the actual width of the interface is expected to be even smaller.

### Acknowledgement

The authors gratefully acknowledge financial support by the German Research Foundation (DFG) through the SFB Transregio 103 and the GRK 1229.

## New Experimental Results on Atomistic and Microstructural Aspects of Creep of Ni-Base Single Crystal Superalloys (SXs)

H. BUCK, A. KOSTKA, P. NÖRTERSCHÄUSER, A.B. PARSA, P. WOLLGRAMM, G. EGGELER

Institut für Werkstoffe, Ruhr-Universität Bochum, Germany

*Single crystal Ni-base superalloys (SXs)* are directionally solidified cast materials which are used to fabricate blades for gas turbines [1]. Despite numerous ongoing efforts, there are presently no alternative high temperature materials in sight which can replace SXs. SXs combine good creep strength with reasonable ductility. In SX technology, there is a need to adjust alloy com-

positions with respect to the availability of strategic alloy elements which become scarce. This holds for example for Re. Before such elements can be replaced, however, their role during solidification, post cast heat treatments and high temperature exposure must be fully understood. This is one of the research objectives of the collaborative research center *SFB/TR 103* which

is funded by the German Research Association (DFG). Microstructural heterogeneity on two length scales is a salient feature of SXs. There are dendritic and interdendritic regions which reflect the cast microstructure of the directionally solidified materials. A typical dendrite spacing is 500  $\mu\text{m}$ . And the typical length scale of the  $\gamma/\gamma'$ -microstructure which forms during the post cast heat treatments is thousand times smaller, 0,5  $\mu\text{m}$ . During processing, alloy elements partition on both length scales [1]. Thus, on the large length scale, Al and Re partition to interdendritic and dendritic regions, respectively. In the  $\gamma/\gamma'$ -microstructure, on the other hand, there is more Al in the  $\gamma'$ -phase than in the  $\gamma$ -channels, while the opposite holds for Re. The understanding of the role of these large and small scale heterogeneities is another research objective of SFB/TR 103. SXs have a microstructure which consists of  $\gamma'$ -cubes (edge length: 0,5  $\mu\text{m}$ , volume fraction: 80 %, ordered  $L1_2$  crystal structure) which are separated by thin  $\gamma$ -channels (channel width: 100 nm, volume fraction: 20 %, fcc). When this microstructure is exposed to creep conditions in the 1000°C/100 MPa range, microstructural changes occur.  $\gamma$ -channels fill with dislocations, dislocation networks form around  $\gamma'$ -particles, dislocations cut the  $\gamma'$  phase and directional coarsening of the  $\gamma'$ -phase, known as rafting, occurs. The present contribution presents some new experimental results which were obtained in the first funding period of SFB/TR 103. First, scale bridging microstructural characterization and miniature specimen creep testing was used to characterize the homogeneity of a cast blade

of 140 x 100 x 20 mm<sup>3</sup>. In a collaborative project where several projects work on different aspects of a material from one batch, it is important to know which scatter one has to expect [2]. Then we show how dislocation plasticity and rafting affect high temperature and low stress creep anisotropy [3,4,5]. And finally, an attempt is made to study the interaction of  $\gamma$ -channel dislocations with  $\gamma'$ -particles. The formation of ledges and grooves is documented. It is proposed that grooves form because dislocation stress fields affect local chemical potentials and drive diffusional fluxes. All results are discussed in the light of previous findings which were published in the literature. Areas in need of further work are identified.

#### Acknowledgement

The authors acknowledge funding through projects A1 and A2 of the Collaborative Research Project SFB/TR 103 funded by the German Research Association (DFG).

#### References

- [1] R.C.Reed, The Superalloys: Fundamentals and Applications, Cambridge University Press, Cambridge, UK, 2006.
- [2] Alireza B. Parsa et al., Advanced Engineering Materials, 2014, DOI: 10.1002/adem.201400136
- [3] L.Agudo Jácome et al., Acta Mater., 61 (2013) pp. 2926-2943
- [4] L.Agudo Jácome et al., Acta Mater., 69 (2014) pp. 246-264
- [5] P.Nörtershäuser et al., Mater. Sci. Eng. A, accepted

Talks Topic I 3:

## ***High temperature materials***

---

## Mechanical properties and microstructures of new polycrystalline $\gamma/\gamma'$ Co-base superalloys

STEFFEN NEUMEIER, LISA FREUND<sup>1</sup>, MATHIAS GÖKEN

Friedrich-Alexander-Universität Erlangen-Nürnberg (FAU), Materials Science & Engineering, Institute I, Erlangen, Germany

Polycrystalline  $\gamma'$  precipitation hardened Ni-base superalloys are widely used in aircraft gas turbines for rotating discs and static components due to their outstanding, well-balanced high temperature corrosion resistance and strength. However, to improve the turbine operating efficiency, higher inlet gas temperatures and new materials with enhanced properties are needed. In 2006, Sato et al. [1] discovered a new  $\gamma'$  Co<sub>3</sub>(Al,W) phase with L1<sub>2</sub> crystal structure in the Co-Al-W system. Hence, new Co-base superalloys with similar microstructures compared to Ni-base superalloys comprising of coherently embedded  $\gamma'$  precipitates have been developed [2]. It has been shown, that the yield strength anomaly of Co<sub>3</sub>(Al,W) is shifted towards higher temperatures and that high  $\gamma'$  volume fractions at application temperature can be achieved in Co-base superalloys although the  $\gamma'$  solvus temperature is lower compared to that of Ni-base superalloys. This is beneficial because they can be easily forged at high temperatures above  $\gamma'$  solvus and a high strength can be obtained at application temperature. Therefore, the  $\gamma/\gamma'$  Co-base superalloys have a great potential as a new type of high temperature wrought alloys.

In this work, two newly developed polycrystalline  $\gamma/\gamma'$  Co-base superalloys with high Chromium content will be presented. After casting and hot-rolling the alloys were recrystallised and aged during a three-step heat treatment. Both alloys have a fine-grained microstructure with comparably high  $\gamma'$  volume fraction, as shown

by transmission and scanning electron microscopy. The alloy with higher contents of Ti and Ta possesses cubic  $\gamma'$  precipitates while the other alloy shows globular precipitates. Previous 3D-atom probe tomography investigations could show that Ti and Ta partition preferentially to the  $\gamma'$  phase [3] and thus increase the lattice parameter of  $\gamma'$ . The different precipitate shapes are, accordingly, a result of the different positive lattice misfit which has been determined by high-energy synchrotron X-ray diffraction from room temperature up to 900°C. Compression tests from RT to 850°C show that a similar yield strength below 800 °C could be achieved compared to Ni-base superalloys Waspaloy and Udimet 720Li. At temperatures above 800°C the yield strength is even higher than for the compared Ni-alloys. However, the advantage of both  $\gamma/\gamma'$  Co-base superalloys appears particularly when comparing the creep properties under compression at 700 °C. The investigated Co-base superalloys have a much higher creep strength than comparable Ni-base superalloys.

### References

- [1] Sato J., Omori T., Oikawa K., Ohnuma I., Kainuma R. & Ishida K. – Science 312 (2006) 90
- [2] Bauer A., Neumeier S., Pyczak F. & Göken M. – Scripta Materialia, 63 (2010) 1197
- [3] Povstugar I., Choi P.-P., Neumeier S., Bauer A., Zenk C.H., Göken M. & Raabe D. – Acta Materialia 78 (2014) 78

## Investigation of the quaternary system Co-Al-W-Ta in the range of Co9Al10W2Ta

ALEXANDER EPISHIN<sup>1</sup>, THOMAS LINK<sup>1</sup>, JAN MIDTLYNG<sup>1</sup>, NIKOLAY PETRUSHIN<sup>2</sup>, GERT NOLZE<sup>3</sup>

<sup>1</sup>Technical University of Berlin, Germany

<sup>2</sup>All-Russian Institute of Aviation Materilas, Moscow, Russia

<sup>3</sup>Federal Institute for Materials Research and Testing, Berlin, Germany

Recently a new class of Co-base alloys (Co-Al-W-Ta-X) with  $\gamma/\gamma'$ -microstructure similar to Ni-base superalloys was discovered [1]. Before practical application however many obstacles have to be overcome, e.g. low thermal stability of the microstructure ( $\gamma'$ -solvus  $\leq 1150^\circ\text{C}$  [2] and precipitation of deteriorating phases), element partition between  $\gamma$ - and  $\gamma'$ -phases unfavourable for solid solution hardening, etc. In order to solve these metallurgical problems, a starting composition

of Co9Al10W2Ta was selected, because it provides according to [1,3,4] a relatively stable strengthening  $\gamma'$ -phase. This composition was systematically varied. 2 elements were always kept constant, the other 2 elements varied. Varying the elements Co $\leftrightarrow$ Al, Co $\leftrightarrow$ W, Co $\leftrightarrow$ Ta, Al $\leftrightarrow$ W, Al $\leftrightarrow$ Ta, W $\leftrightarrow$ Ta by  $\pm 2$  at% gives 12 compositions. The as-cast material was investigated by digital scanning calorimetry (DSC), providing the  $\gamma'$ -solvus-, solidus- and liquidus- temperatures. The volume

fraction of the non-equilibrium eutectic was measured metallographically. Al, W and Ta increase the  $\gamma'$ -solvus, whereby Ta is 2 times more effective than Al and W. However, Ta significantly increases the volume fraction of the eutectic, namely up to 30 vol. % at 4 at% Ta.

The 12 alloys were grouped in 6 diffusion couples, each varying in the same two elements. They were welded in vacuum at 1050°C/1 h and then annealed at 1240°C/192 h in order to get broad diffusion zones, then aged for 1000 h/ 900°C to get the equilibrium microstructure at the temperature of interest. The specimens were investigated by scanning electron microscopy (SEM), electron probe microanalysis (EPMA) and electron back scatter diffraction (EBSD). The phase compositions corresponding to different chemical compositions were identified. Increase of W and Ta above (8W+2Ta) results in precipitation of undesirable phases enriched by W/Ta.

Identification of small precipitates was performed in transmission electron microscope (TEM). TEM foils were prepared from the samples of the starting alloy and its 12 variations, all homogenised and aged exactly like the diffusion couples.

Additionally the diffusion mobility of each element of the Co-Al-W-Ta system was determined. Here the homogenised alloy Co9Al8W2Ta could be used, because it is single-phase ( $\gamma$ ) above 1083°C. It was diffusionally welded with pure cobalt and annealed between 1100 and 1250°C. From the measured concentration profiles the temperature dependent diffusion mobilities were calculated.

#### References

- Sato, J. Omori, T. Oikawa, K. Ohnuma, I. Kainuma, R. Ishida, K. (2006): Co-base high temperature alloys. - Science, Vol. 312, 90-91.
- Bauer, A. Neumeier, S. Pyczak, F. Singer, R. F. Görken, M. (2012) Creep properties of different  $\gamma/\gamma'$ -strengthened Co-base superalloys, Mater. Sci. Eng., A 550, 333– 341.
- Pollock, T. M. Dibbern, J. Tsunekante, M. Zhu, J. Suzuki, A. (2010) New Co-based high temperature alloys. – JOM, 62, 58-63.
- Bauer, A. Neumeier, S. Pyczak, F. Görken, M. (2010): Microstructure and creep strength of different  $\gamma/\gamma'$ strengthened superalloy variants. - Scripta Mater., 63, 1197-1200.

## Influence of rhenium on the local mechanical properties of the $\gamma$ and $\gamma'$ phase in cobalt-base superalloys

M. KOLB, C. ZENK, S. NEUMEIER, M. GÖKEN

Friedrich-Alexander-Universität Erlangen-Nürnberg (FAU), Materials Science & Engineering, Institute, Germany

The new class of cobalt-base superalloys with a fcc  $\gamma$  matrix hardened by coherently embedded  $\text{Co}_3(\text{Al,W})\gamma'$  precipitates is very interesting for high temperature applications [1,2]. The melting point of cobalt is about 40 °C higher (1495 °C) than the one from nickel which gives rise to the hope for higher possible service temperatures and good creep properties [3]. However, in cobalt-base superalloys the partitioning behaviour of various elements is different to that one in nickel-base superalloys. The  $\gamma$  matrix in cobalt-base superalloys is not sufficiently hardened since most of the alloying elements partition preferentially to the  $\gamma'$  phase. Also the effective solid solution strengthener tungsten mainly partitions to the  $\gamma'$  phase. As known from nickel-base superalloys rhenium strongly improves the mechanical properties at high temperatures. This is commonly explained by the strong partitioning to the  $\gamma$  matrix, the effectiveness as solid solution hardener and its very small diffusion coefficient [4,5]. To further clarify the role of Re it is important to know, if it shows the same effects in cobalt-base superalloys.

This work aims to study the local mechanical properties of the  $\gamma$  and  $\gamma'$  phase in a rhenium containing and a rhenium-free cobalt-base superalloy by using nanoindentation. This method provides a possibility to char-

acterize the mechanical properties on the scale of the  $\gamma$  and  $\gamma'$  phase. Complementary investigations of the  $\gamma/\gamma'$  partitioning behaviour of all elements by means of various methods are inevitable to interpret the results from nanoindentation. It is shown that the addition of rhenium influences the partitioning behaviour of the other alloying elements. This results in a change of the measured local mechanical properties of the individual phases. Additionally the effect of rhenium in cobalt-base superalloys is compared to the effect of rhenium in nickel-base superalloys which has been addressed previously [4].

#### References

- [1] J. Sato, T. Omori, K. Oikawa, I. Ohnuma, R. Kainuma, K. Ishida, Science 312 (2006), 90
- [2] A. Bauer, S. Neumeier, F. Pyczak, R.F. Singer, M. Göken, MSE A 550 (2012), 333
- [3] A. Bauer, S. Neumeier, F. Pyczak, M. Göken, Scripta Mat. 63 (2010), 1197
- [4] S. Neumeier, F. Pyczak, M. Göken, Phil. Mag. 91 (2011) 4187
- [5] M.S.A. Karunaratne et al., Proc. 9th Int. Sym. on Superalloys (2000) 263

## Radiation stability of ZrSiN system under the Xe ions irradiation

VLADIMIR UGLOV<sup>1,2</sup>, VITALI SHYMANSKI<sup>1</sup>, GREGORY ABADIAS<sup>3</sup>, GENNAGY REMNEV<sup>2</sup>, ANDREY SUVALOV<sup>1</sup>

<sup>1</sup>Belarusian State University, Minsk, Belarus

<sup>2</sup>Tomsk Polytechnic University, Russia

<sup>3</sup>Institut P', Poitiers, France

Active research in recent years in the study of the structure and properties of nanocrystalline materials have shown particular promise of composite coatings on the basis of ZrSiN, which is characterized by the thermal stability of the structure at temperatures up to 1300 °C and high mechanical properties [1]. However, there are no any reliable data on the radiation stability of such structures, which is particularly relevant for their operation in conditions of high radiation exposure. These materials can be considered as protective materials in reactor system of fission. The aim of the present work was to study the radiation stability of the ZrSiN system implanted with Xe ions.

ZrSiN system was formed as a thin film coating on silicon substrate by reactive magnetron sputtering of zirconium and silicon target in Ar+N<sub>2</sub> (p<sub>N</sub> = 8.8 mPa) atmosphere at temperature of 650 °C. The power on the Zr and Si cathodes was 300 and 250 W, respectively. In the formed ZrSiN coating the ions of Xe<sup>+2</sup> with energy of 180 keV and the doses 5·10<sup>16</sup> and 10<sup>17</sup> cm<sup>-2</sup> were implanted. The implantation was carried out at room (T=20 °C) and higher (T=800 °C) temperatures.

The elemental composition of the ZrSiN system was determined on the basis of Rutherford back-scattering (RBS), The phase composition was studied by means of X-ray diffraction (XRD).

The ZrSiN coatings are characterized by uniform distribution of elements across the thickness (600 nm) coating, the concentrations being equal to 34 at. % (Zr), 22 at. % (Si) and 44 at. % (N). The phase composition of the coating represents by the cubic zirconium nitride ZrN, the lattice parameter of which equals to 0.4572 nm. Diffraction reflections, indicating the presence of phases based on silicon have no been identified, however, the relation of the concentrations N/Si, being approximately equal to 2, allows to suppose [1] an amorphous matrix of Si<sub>3</sub>N<sub>4</sub> formation with included therein

nanocrystalline (10 – 30 nm) particles of zirconium nitride ZrN.

RBS results allowed to determine the concentration profiles of the xenon distributed in the ZrSiN coatings, according to which the maximum concentration of xenon increases from 8 to 17 at. % with the dose increasing from 5·10<sup>16</sup> to 10<sup>17</sup> cm<sup>-2</sup> (at T=20 °C). According to the XRD data the lattice parameter of zirconium nitride ZrN is equal to 0.4572 nm, which corresponds to the lattice parameter of ZrN in the unirradiated system. The implantation of xenon ions at T=800 °C results in displacement of the maximum concentration to the depth of about 200 nm that is accompanied by broadening of the concentration profile. The lattice parameter of the zirconium nitride ZrN is not changed after xenon ions implantation that can indicate on the stability of the structure for this type of radiation exposure. The reason for such behavior can be associated with nanocrystalline particles of zirconium nitride, which promotes the migration of radiation-induced defects to the interface [2].

Thus, it was shown that the structure of coatings ZrSiN, formed by reactive magnetron sputtering, characterized by the radiation resistance under the xenon ions (180 keV) irradiation.

### References

1. Musil J., Daniel R., Zeman P., Takai O., Structure and properties of magnetron sputtered Zr-Si-N films with a high  $\geq 25$  at.% Si content // Thin Solid Films. 2005. V.478 P.238
2. V.V. Uglov, G.E. Remnev, N.T. Kvasov, I.V. Safronov. Dynamic processes in metal nanoparticles under irradiation. Journal of surface investigation. X-ray, synchrotron and neutron techniques. – 2014. – Vol. 8, № 4. – P. 703-707.

## Effect of casting defects on high cycle fatigue behavior of nickel-based superalloy MAR-M 247

MIROSLAV ŠMÍD<sup>1</sup>, STANISLAVA FINTOVÁ<sup>1</sup>, LUDVÍK KUNZ<sup>1</sup>, PAVEL HUTAŘ<sup>2</sup>, KAREL HRBÁČEK<sup>3</sup>

<sup>1</sup>Institute of Physics of Materials, AS CR, Brno, Czech Republic

<sup>2</sup>CEITEC IPM, Institute of Physics of Materials, Brno, Czech Republic

<sup>3</sup>PBS Velká Bíteš, a. s., Velká Bíteš, Czech Republic

High-cycle fatigue tests were performed on the cast polycrystalline superalloy MAR-M 247. The alloy underwent hot isostatic pressing treatment and heat treatment in order to minimize inherited porosity and improve mechanical properties. Fatigue life of the alloy was determined at temperatures of 650, 800 and 900 °C under conditions of constant stress amplitude and fully reversed loading regime. After fatigue tests the specimens were subjected to fractographical analysis with the aim to localize fatigue crack initiation sites and to determine main damage mechanisms. Shrinkage pores or their clusters were found to be typical sites of the fatigue crack initiation. Subsequently, metallographic samples prepared from specimen gauge length were thoroughly analysed by optical microscope. The analysis of defect size distribution by extreme value statistics was employed in order to estimate maximum area of a defect likely to occur on the area of gauge length cross section. Estimated defect sizes were matched with obtained fatigue life-times and also with real fatigue crack initiation sites observed on the fracture surfaces. The results showed good agreement for specimens

cycled at 800 and 900 °C and reasonable agreement for temperature of 650 °C. Fatigue lives were in good correlation with estimated defect sizes from metallographical analysis. The results obtained from the fractographical analysis and the metallographic analysis of defect size distribution proved that fatigue behavior of the MAR-M 247 alloy at 650 °C is not determined just by defects but also by different damage mechanisms than at temperatures of 800 °C and 900 °C. Crystallographically dependent crack propagation at 650 °C smoothly transformed into non-crystallographic transgranular crack propagation with typical fatigue fracture surface features at 900 °C.

### Acknowledgement

This research was supported by Technology Agency of the Czech Republic by project no. TA04011525. Research team was also supported by CEITEC – Central European Institute of Technology with research infrastructure supported by the project CZ.1.05/1.1.00/02.0068 financed from European Regional Development Fund.

## Finite Element Simulation of the creep behavior of directionally solidified NiAl-9Mo

JÜRGEN ALBIEZ<sup>1</sup>, IOANNIS SPRENGER<sup>2</sup>, MARTIN HEILMAIER<sup>2</sup>, THOMAS BÖHLKE<sup>1</sup>

<sup>1</sup>Institute of Engineering Mechanics, Karlsruhe Institute of Technology (KIT), Germany

<sup>2</sup>Institute for Applied Materials, Karlsruhe Institute of Technology (KIT), Germany

For high temperature structural applications, the B2-ordered intermetallic phase NiAl has promising material properties, such as high oxidation resistance, high melting temperature, high thermal conductivity and relatively low density (Johnson 1995). However, the use of NiAl for structural applications suffers from its low creep resistance and its weak room temperature fracture toughness (Noebe 1993). To improve these two material properties at the same time, directional solidification of eutectic alloys leads to a formation of stoichiometric NiAl and a reinforcing phase of a refractory metal e.g. Cr, Mo, W, Re (Johnson 1995). A directional solidified NiAl-9Mo (at. %) eutectic consists of well-aligned single-crystal molybdenum-rich fibers embedded in a Ni-50Al matrix. The steady-state creep

rate of the directional solidified NiAl-9Mo can be more than five orders of magnitude lower compared to the intermetallic NiAl (Dudová 2011, Haenschke 2010, Hu 2013, Seemüller 2013). It has been shown that these as-grown molybdenum-rich fibers are dislocation free and plastic flow begins, when the fibers' stress approaches the theoretical strength (Bei 2007, Bei 2008). After start of yielding, the flow stress reduces due to strain softening of the fibers (Bei 2008). An additional advantage of using the directional solidification of eutectic alloys is that the phases are thermodynamically stable even up to the melting point (Johnson 1995). To be able to predict the directional solidified NiAl-9Mo material behavior under several conditions, material models describing each phase are necessary.

Our single crystal plasticity model for large deformation is based on a phenomenological approach with a state variable describing the accumulated slip of the glide systems. We use an overstress type power law flow rule to model the slip in each slip system and to consider the elastic range of the fibers. The two phases are modeled by an elasto-viscoplastic approach with a voce-softening behavior for the fibers and a perfect plasticity behavior for the matrix. The voce-softening behavior is motivated by the observation of the strain softening of the fibers (Bei 2008).

A creep curve simulation of a NiAl-9Mo representative volume element with periodic boundary conditions is compared to experimental results. The simulation results show that the molybdenum-rich fibers carry the load and reduce the stress in the NiAl matrix. This load partitioning leads to a reduction of the steady-state creep rate compared to the NiAl intermetallic phase.

#### References

Johnson, D. R. (1995): Processing and mechanical properties of in-situ composites from the NiAl-Cr

and the NiAl-(Cr,Mo) eutectic systems – *Intermetallics* 3: 99-113.

Noebe, R. D. (1993): Physical and mechanical properties of the B2 compound NiAl – *International Materials Reviews* 38(4): 193-232.

Dudová, M. (2011): Creep in directionally solidified NiAl-Mo eutectics – *Scripta Materialia* 65: 699-702.

Haenschke, T. (2010): Synthesis and characterization of lamellar and fibre-reinforced NiAl-Mo and NiAl-Cr – *Journal of Physics: Conference Series* 240.

Hu, L. (2013): Tensile creep of directionally solidified NiAl-9Mo in situ composites – *Acta Materialia* 61: 7155-7165.

Seemüller, C. (2013): Influence of fiber alignment on creep in directionally solidified NiAl-10Mo in-situ composites – *Intermetallics* 35: 110-115.

Bei, H. (2007): Compressive strengths of molybdenum alloy micro-pillars prepared using a new technique – *Scripta Materialia* 57: 397-400.

Bei, H. (2008): Effects of pre-strain on the compressive stress-strain response of Mo-alloy single-crystal micropillars – *Acta Materialia* 56: 4762-4770.

Talks Topic I 4:

## ***High temperature materials***

---

## On the nucleation of Mo-rich Laves phase particles in 12% Cr tempered martensite ferritic steels

ALEKSANDER KOSTKA<sup>1</sup>, MEHMET IKBAL ISIK<sup>2</sup>, GUNTHER EGGELER<sup>1</sup>

<sup>1</sup>Institute for Materials, Ruhr-University Bochum, Germany

<sup>2</sup>Max-Planck Institute for Iron Research, Düsseldorf, Germany

12% Cr tempered martensite ferritic steels (TMFSs) are used for critical components in fossil-fired power plants where they have to withstand mechanical loads at temperatures up to 650°C. The creep strength of these materials strongly relies on  $M_{23}C_6$  carbides which stabilize the subgrain structure [1]. However, during high temperature exposure Laves phase particles form. Their compositions are close to  $(Fe, Cr)_2Mo$ , and Si plays a key role in their nucleation and growth [2].

The present work focuses on 12 wt.% Cr tempered martensite ferritic steel with 1 wt.% Mo and 0.2 wt.% C (German grade X20CrMoV12-1). High-resolution characterization techniques, such as analytical transmission electron microscopy (TEM) and atom probe tomography (APT), are used to study the combination of elementary processes that lead to the formation of Laves phase particles.

The material was exposed to 550 °C for time intervals between 864 and 81,984 h. For comparison, a few creep tests were carried out at 550 °C and 120 MPa (duration between 864 and 12,456 h). All tests were interrupted after specific time periods and microstructures were investigated.

Laves phase particles were not detected in the initial state. Nucleation begins at micrograin boundaries in the immediate vicinity of micrograin boundary carbides where Si and Mo segregate from the matrix [3]. That segregation is additionally enhanced by the fact, that growing  $M_{23}C_6$  carbides do not dissolve Si and P and thus pushes these elements towards a micrograin boundary [4]. Creep stress and strain have no significant effect on the early stages of Laves phase formation.

### References

- [1] Kostka, A., Tak, K.G., Hellmig, R.J., Estrin, Y., Eggeler G. (2007): ,Acta Mater., 55: 539-550.
- [2] Aghajani, A., Somsen C., Eggeler G. (2009): Acta Mater., 57: 5093–5106.
- [3] Isik, M.I., Kostka, A., Eggeler, G. (2014): Acta Mater., 81: 230-240.
- [4] Isik, M.I., Kostka, A., Yardley, V.A., Pradeep, K.G., Duarte, M.J., Choi, P.P., Raabe, D., Eggeler, G. (2015): Acta Mater., submitted.

## Temperature dependent solid solution strengthening of Nickel by transition metal solutes

HAMAD UR REHMAN<sup>1</sup>, KARSTEN DURST<sup>2</sup>, STEFFEN NEUMEIER<sup>1</sup>, ROGER REED<sup>3</sup>, MATHIAS GÖKEN<sup>1</sup>

<sup>1</sup>Friedrich-Alexander-Universität Erlangen-Nürnberg, Materials Science and Engineering, Institute-I, Germany

<sup>2</sup>Institute of Physical Metallurgy, TU Darmstadt, Germany

<sup>3</sup>Department of Engineering science , University of Oxford, UK

Rhenium (Re) is an important  $\gamma$ -matrix strengthening solute for improving the creep properties of single crystalline nickel based superalloys. It improves the creep life of these alloys due to its slow diffusion coefficient<sup>1</sup>, as the diffusion controlled climb of dislocations at the  $\gamma$ - $\gamma'$  interfaces is the rate controlling step during creep at high temperature and low stress<sup>2</sup>. In the present work, temperature dependent solid solution strengthening of Nickel was studied using strain rate jump tests on (100) oriented single crystalline Ni and binary Ni-2 at. % X (X=Ta,W,Re) alloys at RT and between 800-1200°C. The applied strain rate is varied in the range  $10^{-3}$ - $10^{-5}$ . The results show that at temperatures up to 800°C, Ta is the strongest strengthening sol-

ute followed by W and Re, irrespective of the applied strain rate. At  $T \geq 1000^\circ\text{C}$ , Re becomes a better solid solution strengthener than Ta at a slower strain rate ( $10^{-5}$ ). This effect is further amplified at 1200°C, where Re is a better solute at all the strain rates. This effect is caused by temperature and strain rate dependent strengthening mechanisms. At RT, solutes exert pinning forces on moving dislocations and the strengthening effects could be explained using Labusch theory<sup>3</sup>. At high temperatures ( $T > 0.5T_m$ ) solute atoms create a Cottrell atmosphere<sup>4</sup> by accumulating on moving dislocations that exert a drag force on the dislocations. Mathematical modeling was used to calculate this solute drag. It was shown that Re atoms exert a higher

drag force on the moving dislocations in contrast to W and Ta. Furthermore, Re atoms reduce the diffusion controlled climb of dislocations. This combined effect of reduced diffusion controlled climb and higher solute drag is responsible for Re being a better solute for Nickel at higher temperatures and slow strain rates.

#### References

1. Karunaratne, M. S. ., Carter, P. & Reed, R. . Interdiffusion in the face-centred cubic phase of the Ni–Re,

Ni–Ta and Ni–W systems between 900 and 1300°C. *Mater. Sci. Eng. A* 281, 229–233 (2000).

2. Reed, R. C. *The superalloys fundamentals and applications*. (Cambridge University Press, 2006).

3. Labusch, R. Statistische theorien der mischkristallhärtung. *Acta Metall.* 20, 917–927 (1972).

4. Cottrell, A. H. & Jaswon, M. A. Distribution of Solute Atoms Round a Slow Dislocation. *Proc. R. Soc. A Math. Phys. Eng. Sci.* 199, 104–114 (1949).

## Effect of the Stress Multi-Axiality on the Creep Damage in Fine Grained HAZ of Mod. 9Cr-1Mo Steels

KIMIYAKI YOSHIDA<sup>1</sup>, MASATAKA YATOMI<sup>2</sup>, MASAOKI TABUCHI<sup>3</sup>, KEN-ICHI KOBAYASHI<sup>4</sup>

<sup>1</sup>IHI Corporation, Yokohama, Japan

<sup>2</sup>IHI Asia Pacific, Singapore

<sup>3</sup>National Institute for Materials Science, Tsukuba, Japan

<sup>4</sup>Chiba University, Chiba, Japan

High-chromium ferritic heat resisting steels have been used for structural components at elevated temperature, because of their excellent creep properties. However it is well known that creep strength of the welded joints of these steels is decreased during long-term use at higher temperatures due to Type-IV creep damages formed in the fine grained heat affected zone (HAZ). Fine grained HAZ are subjected to complex multi-axial stress conditions due to constraint effect on the deformation from the base and weld metals. It has been pointed out that the stress multi-axiality has an influence on creep damage evolution. It is, therefore, needed to identify the effect of multi-axial stress condition on creep damage in fine grained HAZ and to predict the creep rupture and the creep damage under multi-axial stress conditions for preventing the type IV fracture precisely.

In this study, circumferentially notched bar creep rupture and interrupted tests have been conducted on simulated HAZ specimens of mod. 9Cr-1Mo Steels. Metallographic examination has been carried out to quantify creep damage accumulation in the specimens. From the experimental results, it has been founded that stress multi-axiality has a significant effect on the creep damage and rupture time of the notched bar specimens. Finite element predictions based on a continuum damage mechanics model with ductility exhaustion approach have been proposed to predict the creep damage and rupture time under multi-axial stress conditions and applied to the notched bar specimens. Compared with the experimental results, it has been concluded that the ductility exhaustion approach provides reasonable life predictability almost in a scatter band of a factor of 2.

## Thermal stability of ferritic and austenitic nanocluster containing ODS steels

SASCHA SEILS<sup>1</sup>, DANIEL SCHLIEPHAKE<sup>1</sup>, DANIEL JANDA<sup>1</sup>, ALEXANDER KAUFFMANN<sup>1</sup>, JULIA N. WAGNER<sup>1,2</sup>, MARTIN HEILMAIER<sup>1</sup>

<sup>1</sup>Karlsruhe Institute of Technology (KIT), Institute for Applied Materials, Germany

<sup>2</sup>Karlsruhe Nano Micro Facility, Germany

Oxide dispersion strengthened (ODS) steels became a promising materials class for applications in future fusion and fission power plants due to their excellent resistance against swelling under radiation. Additionally they show high temperature stability and excellent creep behavior, which opens a field of application to e.

g. advanced steam turbines or solar technology. These superior material properties result most likely from the formation of very fine distributed, nanoscaled (< 4 nm) and thermodynamically stable Y-Ti-O clusters. Although it was shown that the addition of micro alloying elements like titanium can significantly decrease

the size of these clusters in ferritic ODS steels [2], the mechanisms of their formation is not completely understood, yet. As well, detailed knowledge about the development of these clusters at high temperatures is crucial to further improve the microstructural stability during annealing and the creep resistance. While the processing of ferritic ODS steels was established for years, the synthesis of the austenitic counterpart revealed several challenges in the past. However, due to their crystal structure austenitic ODS steels are supposed to have even better high temperature properties regarding creep behavior.

In this contribution, we show results on the thermal stability of two ferritic ODS steels, differing in contents of yttria and titanium in comparison to an austenitic ODS steel with similar composition. The samples were mechanically alloyed by high energy ball milling of elemental or pre-alloyed powders and compacted by field assisted sintering technique (FAST). Electron backscattering diffraction (EBSD) results on the ferritic ODS steels show, that even annealing at 1000 °C for 1000 h

does not result in a significant Ostwald ripening, which might be hindered effectively by nanoclusters pinning the grain boundaries. The grain size was determined to be about 300 nm after consolidation and heat treatment, respectively. Atom probe tomography (APT) technique enables the visualization of Ti-Y-O-rich clusters which have a size of 3 to 4 nm, only. Slightly larger clusters could also be found in austenitic samples, resulting in a comparable thermal stability of the microstructure. Furthermore, the influence of cluster size and distribution on the outstanding creep properties will be presented.

#### References

- [1] Schneibel, J.H. et al., (2009): Ultrafine-grained nanocluster-strengthened alloys with unusually high creep strength – In: *Scripta Mater.* 61; 793-796.
- [2] Ukai, S. & Fujiwara, M. (2002): Perspective of ODS alloys application in nuclear environments – In: *J. Nucl. Mater.* 307-311; 749-757.

## Microstructure and micromechanics of directionally solidified eutectic alloys

AMRITESH KUMAR, RUTH SCHWAIGER, OLIVER KRAFT

Institute for Applied Materials (IAM-WBM), Karlsruhe Institute of Technology (KIT), Germany

The ever increasing demand to improve the efficiency of high temperature structural applications such as gas turbine engines, requires development of materials with better properties such as lower density, higher operating temperature, and higher fracture toughness. Nickel aluminides has gained a lot of attention as a candidate for next generation high temperature structural material, owing to their superior properties such as, high melting point, good oxidation resistance, and low density. While low ductility and fracture toughness at room temperature and insufficient high temperature strength have been identified as major drawbacks of nickel aluminides, alloying with refractory metals has shown to improve their properties. Producing these alloys by directional solidification results in a highly aligned microstructure with the refractory metals to form continuous fibers or laminates. This microstructure enhances creep properties, fracture toughness and microstructural stability. The diameter of the fibers and the spacing between the fibers depend on the speed of directional solidification. Thus, it is important to investigate the mechanical behavior of these materials at varying length scales in order to understand in detail relationships between microstructure, processing parameters and alloying additions on the macroscopic properties of the material. The starting material for this study is NiAl-Cr eutectic alloy, prepared by di-

rectional solidification at three different solidification speeds (20 mm/h, 50 mm/h and 80 mm/h respectively) where NiAl forms the matrix and Cr forms continuous fibers with fiber diameter ranging from about 800 nm for 20 mm/h samples to about 250 nm for 80 mm/h samples.

We have employed different micromechanical techniques to characterize the material at different length scales including nanoindentation, in-situ tensile test of the fibers and micro-pillar compression tests, and first results will be presented in this paper. Hardness and modulus of the overall alloy obtained by nanoindentation appears to be independent of the solidification speeds. The modulus values correspond well with those reported in literature. Micro-pillars containing single Cr fibers surrounded by the matrix were fabricated using Focused Ion Beam milling for compression testing to evaluate the strength of the composite on small scale. The strength of micro-pillars shows a weak dependence on the fiber diameter with smaller diameter pillars showing higher strength. Micro-pillar compression tests also suggest that the interface between fiber and matrix is rather strong as no delamination or fracture at the interface was observed in any of the tests. Currently, micro-pillar testing of the individual phases is being carried out in order to investigate the role of the interface for the deformation behavior.

Moreover, Cr fibers were isolated from the matrix by chemical etching and in-situ SEM tensile tests of these isolated fibers were carried out. It was observed that the single-crystalline fibers deformed to plastic strains of several percent and that for most fibers tested neck

formation preceded the fracture. These investigations demonstrate that the individual phases of the directionally solidified alloy are intrinsically not brittle and, thus, it is conceivable that the highly ordered alloys can reach reasonable toughness at large scale.

Talks Topic I 5:

## ***High temperature materials***

---

## Tungsten (W) laminate pipes made of ultrafine-grained (UFG) W foil

JENS REISER, SIMON BONK, JAN HOFFMANN, MICHAEL RIETH<sup>1</sup>

Karlsruhe Institute of Technology, Institute for Applied Materials, Germany

Tungsten (W) is the metal with the highest melting point of all metals (3422°C) and would therefore be an excellent fit for structural high temperature applications. One disadvantage that impedes the use of tungsten for structural parts is its low room temperature (RT) fracture toughness,  $K_{IC}$ , and its high brittle-to-ductile transition temperature (BDTT). However the situation appears different for tungsten in the shape of a highly cold rolled ultrafine-grained (UFG) foil.

Tungsten foil in the as-rolled (and stress relieved) condition has exceptional mechanical properties in terms of ductility [Wei, 2008], toughness [Pippan, 2011], and brittle-to-ductile transition (BDT) [Németh, 2015]. Wei and Kecskes [Wei, 2008] evaluated the tensile behaviour of commercially pure W as a function of low-temperature rolling. They observed that rolling below the nominal recrystallization temperature of 1523 K (1250°C) concomitantly enhances the strength and ductility of W. Furthermore Pippan [Pippan, 2011] assessed the fracture toughness of pure W foil with a thickness of 160  $\mu\text{m}$  in the as-rolled condition. He determined a RT fracture toughness,  $K_{IC}$ , of 70  $\text{MPa}(\text{m})^{1/2}$  in L-T direction and of 55  $\text{MPa}(\text{m})^{1/2}$  in T-L direction. Finally Németh et al. [Németh, 2015] evaluated the nature of the BDT of annealed coarse-grained and as-received ultrafine-grained (UFG) tungsten foil. For the UFG tungsten foil he determined a BDTT of about 77 K arguing that the BDT in UFG tungsten is controlled by the glide of edge dislocations. These exceptional mechanical properties might be attributed both to the positive response of tungsten to cold rolling and the ultrafine-grained microstructure of the tungsten foil. Our approach to make W ductile makes use of the exceptional properties of UFG W foils. These foils are the

starting point of the synthesis of a W foil laminate, a multi-layer material. Through the synthesis of a tungsten laminate, the properties of the foil can be transferred to the bulk and by rolling up and joining tungsten laminate pipes can be produced [Reiser, 2014]. The technical maturity of these W laminate pipes has been approved by high heat flux tests performed at the Plataforma Solar de Almería, Spain, as well as at the Max Planck Institute of Plasma Physics, Garching, Germany [Reiser, 2014].

Within this presentation we give an overview of W laminate material in general and of W laminate pipes in particular. This includes aspects like (i) the mechanisms of the exceptional mechanical properties of UFG W foil, (ii) the temperature stability of the mechanical properties of the UFG W foil, (iii) the joining techniques used to produce W laminate plates, as well as the evolution of their interfaces during ageing, (iv) the change of the Charpy impact properties of W laminates during ageing and (v) the production of a 1000 mm long W laminate pipes and their possible application for innovative high temperature energy conversion systems.

### References

- Wei Q, Kecskes LJ. *Mat Sci Eng A-Struct* 2008;491:62.
- Pippan R, presented at W conference, organized by Odette GR, UCLA, Santa Barbara, USA, February 2011.
- Németh AAN, Reiser J, Armstrong DEJ, Rieth M. *Int J Refract Met H* 2015;50:9.
- Reiser J, Rieth M, Möslang A, et al. Tungsten (W) laminate pipes for innovative high temperature energy conversion systems, *Adv Eng Mater*, DOI: 10.1002/adem.201400204 (article in press).

## Internal Friction and Shear Modulus Temperature Dependence of 9%Cr Ferritic Steel P92 in 25 ÷ 750°C Temperature Range

ELGUJA KUTELIA<sup>1</sup>, GEORGE DARSVELIDZE<sup>1</sup>, TENGIZ KUKAVA<sup>1</sup>, TEMUR DZIGRASHVILI<sup>1</sup>, IA KURASHVILI<sup>1</sup>, FRANCISCO J. PEREZ TRUJILLO<sup>2</sup>

<sup>1</sup> Georgian Technical University, Tbilisi, Georgia

<sup>2</sup> Universidad Complutense de Madrid, Spain

The creep rate in practical steels, especially in ferritic 9%Cr steels (P92), is controlled by the diffusion of sol-

ute atoms rather than vacancies. Chromium is an exceptional solute because the size difference of Cr ver-

sus  $\alpha$ -Fe is very small. Consequently, its diffusion plays an important role in the formation of precipitates in the steel matrix at early stages as well as in the final formation of stable phases during a long-term thermo-mechanical impact. It is also important that the above steel contains many minor alloying elements, and therefore, actual estimation of the diffusion parameters and mechanical properties at service temperatures is not easy in heat-resistant steels. Development of methods of substructural strengthening of alloys requires a deep insight of the processes of formation and stabilization of substructure. The latter necessitates use of structure-sensitive methods, among which the method of internal friction is most efficient. The temperature dependences of  $Q_1(t)$  and  $f_2(t)$  were measured in the relaxometer with the reverse torsion pendulum at frequencies  $\sim 1$  Hz and amplitudes of deformation  $10^{-5}$ – $10^{-3}$  in the temperature range  $25$ – $750^\circ\text{C}$ , with the rate of heating/cooling  $2^\circ\text{C}/\text{min}$ . For the first measurement the samples were cut and machined to a size  $(1 \times 1 \times 50)$  mm<sup>3</sup> out of bulk coupons, previously normalized at  $1060^\circ\text{C}/20$  min + tempered at

$770^\circ\text{C}/60$  min. Additional heat treatment after the first measurement was conducted directly in the relaxometer via annealing at  $950^\circ\text{C}/20$  min, after which  $Q_1(t)$  and  $f_2(t)$  were measured repeatedly. Two maxima of internal friction were revealed at temperatures  $570^\circ\text{C}$  and  $650^\circ\text{C}$ , accompanied by shear modulus defects. In the temperature range  $300$ – $750^\circ\text{C}$  reduction of shear modulus occur with different rates, depending on previous heat treatment of the sample. The first maximum is determined to be of relaxation nature, and is characterized by the activation energy of  $\sim 52000$  cal/mol and the relaxation time constant equal to  $10$ – $14$  sec. According to its activation features, the maximum at  $570^\circ\text{C}$  may be attributed to the relaxation rearrangement of couples of chromium atoms during diffusion in  $\alpha$ -phase through a Zener mechanism of relaxation in the bcc substitution alloys. The temperature of the second maximum does not depend on the oscillation frequency. Its shape, intensity and temperature considerably changes in accordance to cooling/heating rate, amplitude of deformation and annealing time at temperatures lower than  $\alpha$ - $\gamma$  transformation point.

## Bayesian approach to determine optimum inspection intervals for structural components of high temperature materials subjected to creep

Kyoko Nakamura, YUJI NAKASONE

Tokyo University of Science, Japan

Besides state-of-the-arts materials, the development of advanced maintenance technology is a vital issue for extending the life of energy conservation facilities. Condition-based maintenance (CBM) is one of the promising technologies for improving the dependability, i.e., the reliability plus availability of the facilities. Effective monitoring technologies including maintenance strategies provide the key to success in CBM.

Kitagawa et al. considered an effect of inspections for cracks of pressure vessels and have proposed a probabilistic strategy for determining optimum intervals of in-service inspections (Kitagawa 1977). Many of energy conservation facilities are used at high temperature and their lives are greatly influenced by creep damage. For these facilities, CBM may adopt creep strain as the target parameter to monitor instead of crack size for assessing the actual conditions of structural components of the facilities.

The present paper proposes a Bayesian approach to determine optimum inspection intervals for the structural components of high temperature materials subjected to creep. The Monkman-Grant relation or the omega method is adopted to make the residual life prediction of components in high temperature struc-

tures (Prager 2000). Since predicted residual creep life varies (Nonaka 1997, Nakasone 2015), it is assumed that creep strain to monitor at an arbitrary time is a random variable having the mean obtained by the Monkman-Grant relation and a variance which remains constant with time.

The fracture probability  $P_f$  of a high temperature structural component is formulated based on the Bayes' theorem. The optimum inspection intervals for the structural component is calculated for different types of in-service-inspection (ISI) models with real maintenance operations taken into consideration; i.e., time-based-model (TBM) in which equal interval for ISI is assumed and CBM model in which intervals are varied with the magnitude of creep strain monitored. "Replacement" and "repair" models have been also investigated. The "replacement" model simulates TBM and/or CBM in which a component is found ruptured and is replaced with a new one having zero creep strain. The "repair" model simulates TBM in which creep strain of a component is reduced to a certain extent if the creep strain exceeds a given critical value at a  $k$ -th ISI interval where  $k$  is a natural number. In the case of CBM, however, a creep strain of a component

is relaxed just when the creep strain is found to exceed the critical value.

Variations of the fracture probability of each model with the number of inspections or with time are calculated and compared by using creep data obtained for modified 9Cr-1Mo steel.

#### References

Kitagawa, H. & Hisada, T. (1977): Reliability Analysis of Structures under Periodic Nondestructive Inspection. – In: Proc. of 3rd Int. Conf. on Pressure Vessel Tech., 1: 475-480; Tokyo, Japan.

Prager, M. (2000): The omega method – an engineering approach to life assessment – In: Trans. of ASME, Journal of pressure vessel technology: 122(3): 273-280.

Nonaka, I. et al. (1997): Evaluation of Creep Residual Life for Mod. 9Cr-1Mo Steel Based on Omega Method, J. of the Soc. of Mats. Sci., Japan, 45(4): 438-442 (in Japanese).

Nakasone, Y. & Suzuki, H. (2015): To be presented at Materials and Mechanics Conf., Japan Society of Mechanical Engineers: Kanagawa, Japan.

## Microstructural study on the intermetallic compound NiAl-Cr

ANTJE KRUEGER, MICHAEL KLIMENKOV, ANTON MOESLANG

KIT, Institute for Applied Materials, Eggenstein-Leopoldshafen, Germany

Structural materials for energy efficient applications are developed emphatically over the past decades. Therefore the intermetallic NiAl seems to be a good candidate. It has a low density and good corrosion as well as oxidation resistance, but at temperatures higher than 600 °C the creep resistance gets weak. Refractory elements, e.g. Chromium, Molybdenum and Rhenium, can strengthen the NiAl alloy by forming fibers / lamellae. During the directional solidification the fibers / lamellae are well aligned in the NiAl matrix and can be used for turbine blades, e.g. in gas turbines engines. In our investigation we analyze the creep behavior and microstructure of the intermetallic compound NiAl-Cr. Therefore compressive creep measurements are performed under constant conditions (temperature > 900 °C and applied stress range 100 - 300 MPa). Then the microstructure of the crept specimen is analyzed by means of transmission electron microscopy. We found from selected area diffraction pattern that both phases, the NiAl matrix and the Cr-fibers are oriented in

<100> direction parallel to the growth direction. At the interface of the NiAl and the Cr phase periodic interface dislocation networks exist with an average dislocation spacing of around 96 nm. Cline et al. found 70 nm (Cline et al., 1971). These dislocation networks can hinder the motion of dislocations when applying a certain stress. This is also observed by Chen et al. (Chen et al., 1995). If the stress is high enough dislocations will be able to bridge, cut or surround the fibers.

These results give information about the creep mechanisms responsible for deformation at high temperatures.

#### References

Chen X.F. et al. (1995): Deformation and fracture of a directionally solidified NiAl-28Cr-6Mo eutectic alloy – In: J. Mater. Res., 10: 1159-1170.

Cline et al. (1971): The variation of interface dislocation networks with lattice mismatch in eutectic alloys – In: Acta Metallurgica, 19: 405 – 414.

## The crystallographic template effect preceding the formation of stable $\alpha$ -Al<sub>2</sub>O<sub>3</sub> during low temperature oxidation of Fe-Al alloys

PEDRO BRITO<sup>1</sup>, HAROLDO PINTO<sup>2</sup>, ANKE KAYSSER-PYZALLA<sup>3</sup>

<sup>1</sup>Pontifical Catholic University, Mechanical Engineering, Belo Horizonte, Brazil

<sup>2</sup>University of São Paulo, Materials Engineering, São Carlos, Brazil

<sup>3</sup>Helmholtz Zentrum Berlin for Materials and Energy, Germany

Many materials designed for high temperature applications, such as Fe-Al or Ni-Al alloys, rely upon a stable corundum structured  $\alpha$ -Al<sub>2</sub>O<sub>3</sub> scale for corrosion and oxidation resistance. The formation of this passive

oxide film is generally understood as being preceded by the appearance of less protective metastable Al<sub>2</sub>O<sub>3</sub> polymorphs which usually develop at temperatures below 1000°C in the initial stages of oxidation and only

later transform into the stable  $\alpha$ -Al<sub>2</sub>O<sub>3</sub> modification. The formation of these transient Al<sub>2</sub>O<sub>3</sub> polymorphs has a negative impact on the oxidation resistance of the alloys due to their rapid growth rate and also because their subsequent transformation to  $\alpha$ -Al<sub>2</sub>O<sub>3</sub> induces large tensile stresses in the oxide scale, which may lead to its failure, exposure of the substrate and increase of degradation rates (Grabke, 1999).

While the formation mechanism of stable  $\alpha$ -Al<sub>2</sub>O<sub>3</sub> films has been well established for Ni-Al alloys, less is known regarding the phase formation during oxidation of Fe-Al. Oxidation of Fe based aluminides is significantly different from Ni-Al alloys because at low and intermediate temperatures, Fe (or Cr, which is also commonly present) reacts with O before Al to form a precursor oxide ( $\alpha$ -Fe<sub>2</sub>O<sub>3</sub> or  $\alpha$ -Cr<sub>2</sub>O<sub>3</sub>) with the same crystal structure of  $\alpha$ -Al<sub>2</sub>O<sub>3</sub>. The isostructural oxide, which may also be an Al-containing solid solution, acts as a template for the nucleation of stable  $\alpha$ -Al<sub>2</sub>O<sub>3</sub>, accelerating the formation of the protective layer. In recent investigations, this template effect was shown to be active in thin Fe layers deposited on Fe-Al substrates which were then submitted to isothermal oxidation (Kitajima *et al*, 2011). Upon oxidation of the coated materials, the deposited Fe was oxidized to form  $\alpha$ -Fe<sub>2</sub>O<sub>3</sub>, which served as a site for heterogeneous nucleation of  $\alpha$ -Al<sub>2</sub>O<sub>3</sub> causing either the suppression of metastable Al<sub>2</sub>O<sub>3</sub> formation or the acceleration of the metastable to  $\alpha$ -Al<sub>2</sub>O<sub>3</sub> transformation. Another aspect that follows this template mechanism is that the thermally grown  $\alpha$ -Al<sub>2</sub>O<sub>3</sub> inherits the crystallographic orientation of the precursor oxide (Brito *et al*, 2012).

Hence, the presence of a template oxide may have a significant impact on the oxidation resistance of Fe-Al alloys, since it reduces the possibility of metastable Al<sub>2</sub>O<sub>3</sub> development in the oxide scale. With the objective of further investigating the template effect on the nucleation of stable  $\alpha$ -Al<sub>2</sub>O<sub>3</sub> in thermally grown oxide layers, in the present work the oxidation of binary Fe-Al alloys was analysed in-situ by applying synchrotron X-ray Diffraction (XRD) and also ex-situ by Raman Spectroscopy at different oxidation times. Raman Spectroscopy is interesting in the present case because it allows for estimating the amount of Al<sup>+3</sup> present in the  $\alpha$ -Fe<sub>2</sub>O<sub>3</sub> structure in substitution of Fe<sup>+3</sup> ions (Zoppi *et al*, 2007). The experiments were complemented by texture analysis using synchrotron XRD and by examining the oxidized surfaces via Scanning Electron Microscopy.

#### References

- Grabke, H. J. (1999): Oxidation of NiAl and FeAl. – *Intermetallics*, 7: 1153-115.
- Kitajima, Y., Hayashi, S., Nishimoto, T., Narita, T. & Ukai, S. (2011): Acceleration of Metastable to Alpha Transformation of Al<sub>2</sub>O<sub>3</sub> Scale on Fe–Al Alloy by Pure-Metal Coatings at 900 °C. – *Oxid. Met.* 75: 41-56.
- Brito, P., Pinto, H., Genzel, Ch., Klaus, M. & Kaysser-Pyzalla, A. (2012): Epitaxial stress and texture in thin oxide layers grown on Fe-Al alloys. – *Acta Mat.* 60: 1230-1237.
- Zoppi, A., Lofrumento, C., Castellucci, E. M. & Sciau, Ph. (2007): Al-for-Fe substitution in hematite: the effect of low Al concentrations in the Raman spectrum of Fe<sub>2</sub>O<sub>3</sub>. – *J. Raman Spec.* 39: 40-46..

Talks Topic K 1:

## ***Polymer based composites***

---

# Integrative simulation of short glass fibers reinforced polyamides: methodology followed to identify polymer matrix constitutive models on a wide range of solicitations, temperature, moisture and strain rate

GILLES ROBERT, OLIVIER MOULINJEUNE

Solvay Engineering Plastics, Technyl Innovation Center, Saint Fons, France

Integrative simulation has raised a growing interest recently among glass fibers reinforced users. A number of industrial solutions has appeared recently to perform such simulations, the more widespread being Digimat, edited by e-Xstream.

Integrative simulation allows taking into account injection molding process, which generates glass fiber orientation in Finite Elements Analysis (FEA). Given material anisotropy, this can lead to a spectacular increase in FEA accuracy. However, to take advantage of this technology: (i) glass fiber orientation computed must be accurate enough; (ii) the constitutive model of the matrix must be accurate.

This paper focuses on the methodology followed to identify constitutive models on PA66 matrix optimized for integrative simulation and on the modeling strategies developed to take into account relevant variables: temperature, strain rate, moisture uptake of the material and nature of the solicitation applied (tension, compression, and shear).

Some preliminary points have a strong importance on constitutive models accuracy. Specimen must be machined in molded plaques whose geometry is carefully chosen in order to achieve a good level of microstructure homogeneity. This cannot be achieved with any geometry. A careful choice must be done about plaque geometry and specimen machining positions. Moreover, such choices cannot be considered without a control of glass fiber orientation based on experimental measurements and not on simulations only.

A method of glass fiber orientation measurements through X-ray micro computed tomography has been developed. Orientation tensors were extracted from initial volumes images and have allowed an optimal control of specimen orientation and homogeneity. Measured orientation data has proved much more accurate than any software simulations to characterize microstructure of reinforced PA66.

Mechanical characterizations of reinforced materials have been led on a wide set of materials, temperature, moisture and strain rates, with a videometric control of

volume strain of specimens. Solicitations applied have been static tensile, compressive and shear. Static tests have been completed with dynamic tensile testing.

Many developments have been made on matrix constitutive models identification by reverse engineering. It has been proved that measured orientation data were key to obtain accurate results. The number of tensile curves necessary to achieve reliable results has also been tested.

Modeling strategy of the different parameters of matrix constitutive models is based on time temperature superposition. A method has been found to integrate strain rate, temperature and moisture concentration in a single parameter. Through this approach it becomes very easy to predict matrix behavior in a large domain of environmental conditions, in tension as well as in compression, with some interesting insights about tension-compression asymmetry.

Identifications have proved extremely efficient of specimens, with very small differences between computed and measured data. Moreover constitutive models obtained have been widely tested during FEA of complex structures, implicit as well as explicit and have proved extremely performing.

## References

- Maurel-Pantel A., Baquet E., Bikard J., Billon N. (2011): Coupled Thermo Mechanical Characterization of Polymers Based on Inverse Analyses and IR Measurements - Applied Mechanics and Materials ; 70:393-398.
- Kammoun S., Doghri I., Adam L., Robert G., Delannay L., (2011): First pseudo-grain failure model for inelastic composites with misaligned short fibers - Composites Part A-applied Science and Manufacturing ; 42(12): 1 892-1902.
- Buffière J.Y. , Maire E. , Adrien J. , Masse J.P. , Boller E. (2010): In situ experiments with X-ray tomography: An attractive tool for experimental mechanics - Experimental Mechanics 50, 289-305.

# X-ray microtomography and finite element modelling of the failure mechanism in epoxy syntactic foams under compressive loads

PEIFENG LI, RUOXUAN HUANG

School of Mechanical and Aerospace Engineering, Nanyang Technological University, Singapore

Epoxy syntactic foams containing glass or ceramic microballoons have been increasingly used in transport applications due to their high strength-to-weight ratio and excellent energy dissipation capability (Li 2009). The bulk mechanical behaviour of syntactic foams is intrinsically determined by the properties of various phases in the foam and the unit cell structures such as the geometry and distribution of microballoons. Recent developments in x-ray microtomography (XMT) have allowed 3D characterisation of various microstructural phases in materials including syntactic foams (Awaja 2009, Yu 2012). Finite element modelling (FEM) has been the effective tool to analyse the stress field and to further characterise the constitutive behaviour of materials (Li 2015). This work investigated the failure mechanism in syntactic foams especially in the constituents: the epoxy matrix and cenospheres (ceramic microballoons) using the combined XMT and FEM method.

In-situ compression experiments in the XMT machine were conducted on cenosphere epoxy syntactic foams to track the internal microstructural changes at various deformation stages. A FE model of the full scale foam containing randomly distributed cenospheres were developed to predict the stress and damage evolution of the constituents in the foam. A good agreement was obtained between the FE predictions and the XMT observations of the foam under compressive loads.

It was found that the localised stresses in cenospheres are noticeable higher than those in the matrix, indicating that the main load bearing constituents are the

cenospheres. The stresses of individual cenospheres concentrate in the equator normal to the loading direction and decrease with the distance from the equator. Both XMT and FEM revealed that the large cenospheres crush first in the foam by the longitudinal splitting fracture along the compression direction. Subsequently, the cenospheres nearly in the transverse (cross-sectional) plane progress to crush, leaving the voids in the matrix. Meanwhile, micro-cracks arise in the matrix where the stresses concentrate and then propagate to join the adjacent micro-cracks and voids, thus forming damage bands (macro-cracks) in the transverse plane. The internal failure mechanism of the syntactic foam can be summarised to be the layered crushing mode.

## References

- Li, P., Petrinic, N., Siviour, C.R., Froud, R. & Reed, J.M. (2009): Strain rate dependent compressive properties of glass-microballoon epoxy syntactic foams. – *Mater. Sci. Eng. A*, 515: 19-25.
- Awaja, F. & Arhatari, B.D. (2009): X-ray Micro Computed Tomography investigation of accelerated thermal degradation of epoxy resin/glass microsphere syntactic foam – *Compos. A*, 40: 1217-22.
- Yu, M., Zhu, P. & Ma, Y. (2012): Experimental study and numerical prediction of tensile strength properties and failure modes of hollow spheres filled syntactic foams – *Comput. Mater. Sci.*, 63: 232-43.
- Li, P. (2015): Constitutive and failure behaviour in selective laser melted stainless steel for microlattice structures – *Mater. Sci. Eng. A*, 622: 114-20.

# Mechanical Properties of CFRTP Made from CF/PA Composite Yarn Sutured with PA Fiber

YUJI TAKUBO<sup>1</sup>, HIROAKI KIMURA<sup>1</sup>, TAKASHI MATSUOKA<sup>1</sup>, TOMOKO HIRAYAMA<sup>1</sup>, HIROYUKI FUJITA<sup>2</sup>, YASUJI MIYATA<sup>3</sup>, KUNIO FUJII<sup>4</sup>

<sup>1</sup> Department of Mechanical Engineering, Doshisha University, Japan

<sup>2</sup> Hyogo Prefectural Institute of Technology, Japan

<sup>3</sup> Miyata Fabrics Co., Ltd, Japan

<sup>4</sup> Toho Textile Co., Ltd, Japan

The thermoplastic composite materials is widely used from the standpoint of productivity and recycling. However, it is well known to be difficult to impregnate the thermoplastic resin to reinforcement fiber because

of its high viscosity. In this study, CFRTP was developed with using the composite yarn which sutured reinforcement fiber (carbon fiber) and core matrix fibers (PA6 fiber) by using Mellow Sawing Machine with plat-

ing fibers (PA6 fiber), and it was confirmed that the impregnation state of resin into the carbon fiber bundle was improved. And also, the composite yarn was made by suturing two kinds of yarns which the core matrix fibers were oriented parallel to the reinforcement fiber bundles. So, as a characteristic of this composite yarn, the interfacial adhesion state of the carbon fiber and PA6 resin is expected to improve by the impregnation. In addition, the composite yarn is possible to control the fiber volume content by changing the number of core matrix fibers easily. The treatment of composite yarn is important to get a good interfacial adhesion state on the composite material. The machine oil and contamination adhere to the surface of CF/PA6 composite yarn through manufacturing process, and they are more likely to produce some voids and the non-impregnation region in the composite materials. Therefore, an acetone treatment was performed for the purpose of removing them on the composite yarn. In addition, a good impregnation state can be expected by removing the sizing agent of carbon fiber. The acetone treatment can be performed easily under the state of the composite fabric, even if the sizing agent of carbon fiber is removed. The following results were obtained from this study;

It was confirmed that the fiber volume content of CFRTP could control to about 35%-45% by changing the number of core matrix fibers.

The impregnation state was investigated from the cross-sectional SEM observation. As a result, it was confirmed to have a good impregnation state as increasing the core matrix fibers. And the fiber content rate becomes low in that case.

The three-point bending test was performed in accordance with JIS K7074. As a result, it was clear that the bending strength became higher on the low fiber content type, because the impregnation of resin into the carbon fiber bundle was good.

It was shown that the bending strength of acetone treatment CFRTP have been increasing about 200% in comparison with that of the non-treatment CFRTP. It was confirmed that the acetone treatment was an useful method to obtain a good interfacial adhesion.

The impact absorption energy was evaluated by the penetration impact testing. As a result, it was shown that the impact absorption energy decreased on the low fiber content type because of the brittle material.

## Overall mechanical properties of composites with complex orientationally distributed microstructures

OLESYA I. ZHUPANSKA, PAVLO KROKHMAL

Department of Mechanical and Industrial Engineering, University of Iowa, USA

This study is concerned with development of bounds on the elastic properties of fiber reinforced composites with arbitrary orientational distribution of fibers. The main motivation comes from study of the effects of the orientational distribution of carbon nanotubes (CNTs) in buckypapers on the overall elastic properties of CNT buckypaper polymer matrix composites.

Buckypapers are thin sheets of porous carbon nanotubes networks that are prepared by a multi-step process of dispersion and filtration of nanotube suspension. Bulk buckypaper polymeric composites are obtained by impregnation of nanotube buckypapers into a polymer matrix. Unless a special care is taken, the nanotubes are distributed randomly in buckypaper sheets. To achieve certain alignment, buckypaper sheets are produced by filtrating well-dispersed nanotube suspension through a filter placed in a high strength magnetic field (Liang et al. 2003). A strong magnetic field (5–15 T) substantially improves alignment of CNTs and thereby increases the buckypaper's elastic modulus and strength in the direction of alignment. Moreover, alignment controls the elastic, thermal, and electrical properties of buckypaper nanocomposites. On the other hand, it is virtually impossible

to achieve perfect alignment of individual nanotubes, and, therefore, nanotubes' orientational distribution must be taken into account in determination of effective properties of buckypaper nanocomposites.

In this paper, a generalization of various micromechanical approaches (including the Mori-Tanaka model (Mori & Tanaka 1973) and Hashin-Schtrikman variational bounds (Hashin & Shtrikman 1963) to the cases of non-aligned composite phases will be examined. Orientation distribution function (ODF) is used to describe CNT orientation distributions in buckypaper. Given the stochastic nature of the nanotubes distribution in buckypaper nanocomposites, the ODF defines orientation probability density and must result in a composite with overall isotropic properties, if CNTs are distributed randomly in buckypaper. ODF is derived from the analysis of the SEM images of CNT buckypapers. Analytical ODFs describing various microstructures are also introduced.

It will be shown that the Mori-Tanaka scheme applied to the non-aligned CNT buckypaper polymer matrix composites leads to violation of symmetry of the effective elastic moduli tensor.

The study of the literature also reveals that there are no known bounds derived for the composites with orientational distribution (except for the random uniform distribution) of phases. To overcome this issue a problem of finding tightest bound for the composites with non-aligned phases is formulated as a nonlinear semidefinite optimization problem, i.e., an optimization problem where the optimization variables are represented by symmetric positive semidefinite matrices. Such a formulation guarantees that any solution of the optimization problem represents a valid tensor of elastic material properties. The problem is solved by an interior point method, and an optimal solution produces bounds for the overall elastic properties of the multiphase composites with orientational distribution of phases.

#### References

- Liang, Z., Shankar, K.R., Barefield, K., Zhang, C., Kramer, L., & Wang, B. (2004): Investigation of magnetically aligned carbon nanotube bucky papers/epoxy composites. - In: Proceedings of SAMPE (48th ISSE). Long Beach, CA, May, 2003.
4. Mori, T. & Tanaka, K. (1973): Average stress in matrix and average elastic energy of materials with misfitting inclusions. - *Acta Metall.*, 21: 571-574.
8. Hashin, Z. & Shtrikman, S.A. (1963): Variational approach to the theory of the elastic behaviour of multi-phase materials. - *J. Mech. Phys. Solids*, 11: 127-140.

## Estimation of Dispersion Condition for PP/CNT Nano Composite by Using the New Segments with Extensional Flow for Co-Rotating Twin Screw Extruder

KOKI MATSUMOTO, TAKAYUKI MORITA, YOSHIHIKO ARAO, TATSUYA TANAKA

Mechanical Engineering, Department of Science and Engineering, Doshisha University, Kyoto, Japan

Presently, nano composites, consisting of polymers that are reinforced with nano fillers, have been developed to obtain further mechanical properties and further functionalities. However, intended properties have not been achieved because of nano filler agglomerations in the polymer. Extensional flow has been shown to be more efficient solution for improving the dispersion of nano-composites as compared to shear flow from Grace Curve. One of the production processes of nano-composites is melt extrusion with co-rotating twin screw extruder (TSE) which is superior in terms of productivity and mixing performance. However, it is difficult to disperse the fillers by conventional processing (e.g. shear mixing flow with Kneading Block).

Therefore we attempt to disperse the fillers by using new segments with elongational flow for twin screw extruder. This new segment is called "Blister Disk" and it has many small holes on Disk. However, it was difficult to evaluate the mixing performance of Blister Disk because the flow patterns are complex in TSE and there is some possibility of no flow through the holes of Blister Disk. Then, to evaluate the dispersion effect of only holes, fundamental extrusion equipment was developed. Our objective is estimation the dispersion condition by changing the Blister Disk geometries (e.g. hole numbers, hole diameter and hole width) in the case of polypropylene (PP) and Carbon Nano Tube (CNT) nano composite.

Firstly, the pressure drop at the Blister Disk were measured with fundamental extrusion equipment by changing the geometries and volumetric flow rate. The dispersion is caused by stress magnitude and the extensional stress can be expressed by entrance pressure drop from Cogswell equation. Then, the dispersion degree of extruded specimens was observed by microscopy and TEM. Moreover, as the other evaluation method of dispersibility, the rheology analysis with rotational viscometry and electric conductivity. Finally, these results were validated the tendency. From these results, the critical Pressure value can be estimated and the dispersibility of PP/CNT nano composites were increased dramatically by extensional flow.

#### References

- Tokihisa, M., Yakemoto, K., Sakai, T., Utracki, L.A., Sephehr, M., Li, J. & Simard, Y. (2006): Extensional Flow Mixer for Polymer Nanocomposites - *Polym. Eng. Sci.*, 46: 1040-1050
- Cogswell, F.N. (1972): Convexing Flow of Polymer Melts in Extrusion Dies - *Polym. Eng. Sci.*, 12: 64-73
- Grace, H.P. (1982): Dispersion Phenomena in High Viscosity Immiscible Fluid Systems and Application of Static Mixers as Dispersion Devices in Such Systems - *Chem. Eng. Comm.*, 14: 225-277

## Characterisation of graphene-reinforced nanocomposites: optical-microscopy analysis of spatial non-uniformity

OSMAN BAYRAK<sup>1</sup>, MARIANA IONITA<sup>2</sup>, EMRAH DEMIRCI<sup>1</sup>, VADIM V. SILBERSCHMIDT<sup>1</sup>

<sup>1</sup>Wolfson School of Mechanical and Manufacturing Engineering, Loughborough University, Leicestershire, UK

<sup>2</sup>University Politehnica of Bucharest, Advanced Polymer Materials Group, Romania

In the last decade, graphene has emerged as one of very promising reinforcement materials for nanocomposites. Apparently, it can outperform many other known nano-reinforcements, improving properties and performance of nanocomposites (Rafiee, 2009).

As a field of study that is only a decade old, there are still many features of such nanocomposites that need a thorough analysis. One of them is the effect of their microstructural characteristics and their spatial non-uniformity on deformation processes. To understand their mechanical behaviour, such characterisation is indispensable. Although many studies performed characterisation of graphene-reinforced nanocomposites with transmission or scanning electron microscopy, or atomic force microscopy (Kuilla, 2010), these methods are rather time-consuming and cumbersome in interpretation of their results related to the macroscopic behaviour. Employment of optical microscopy, that is easy to implement compared to TEM, SEM and AFM, could simplify significantly characterization of nanocomposites and, hence, their performance.

In this study, samples of graphene oxide (GO)-alginate composites were studied based on a combination of mechanical tests (tensile loading up to failure) and microstructural characterisation using optical microscopy (supported with TEM studies). Pull-outs of GO flakes were compared quantitatively for nanocomposites with different volume fractions of nano-filler. The images obtained provided information that can contribute to understanding of the mechanical behaviour of the analysed materials. The study will be extended to incorporate the obtained results into finite-element models.

### References

- Rafiee MA, Rafiee J, Wang Z, Song HH, Yu ZZ, Koratkar N. Enhanced Mechanical Properties of Nanocomposites at Low Graphene Content. *ACS Nano* 2009;3(12):3884-3890.
- Kuilla T, Bhadra S, Yao DH, Kim NH, Bose S, Lee JH. Recent advances in graphene based polymer composites. *Progress in Polymer Science* 2010;35(11):1350-1375.

Talks Topic K 2:

## ***Polymer based composites***

---

# Progressive damage evaluation of Glass-Epoxy laminated composites under fatigue loading

SORAN HASSANIFARD, MOHSEN FEYZI

Department of Mechanical Engineering, University of Tabriz, Iran

Polymeric composite materials are widely used in many fields of industry due to the excellent specific strength, good electrical resistance and high speed production. In the past five decades, the researchers have focused on determining the fatigue life of these materials. However, this phenomenon is not known completely. There has been lots of research on the fatigue life estimation that can be classified in some strings.

Some of the works are available that define a damage model in composite materials during fatigue failure process. In these studies, one of the mechanical properties are selected as damage variable and the changes in this parameter are recorded within failure development. Finally, a damage function is fitted on experimental data. Often, the dynamic modulus is chosen as mentioned parameter (Giancane et al 2009).

A number of investigators have proposed a fatigue failure criterion based on components of stress tensor. They have replaced the static strengths in these theories by corresponding fatigue functions and then determined the fatigue cycles to failure. They formulated these criteria according to stresses that affect on the mode of failure (Hashin and Rotem 1973). In the aforementioned model, the effect of stress ratio has not been considered exactly and the model is limited to value of the stress ratio. Many investigations in literature have tried to develop a failure law to solve this challenge. In a composite specimen the value of stress ratio is not equal at different locations. Therefore, it should be applied to the solution. A failure criterion could be obtained based on phenomenological fatigue ratio. If the strength versus life curves at different stress ratios are normalized based on the phenomenological equation, all curves with different stress ratios collapse to a single curve (Kawai 2004).

In the present study, a Finite Element (FE) model based on Hashin's failure criterion was developed to predict fatigue life of (0,90,0,90)s, (90,0,90,0)s E-glass fiber re-

inforced laminates. In addition, this model can predict the modes of fatigue failure. The iterative algorithm was used so that at each step of solution, maximum load was applied to the model and stresses were evaluated. Then the appropriate failure criterion was applied to inspect for possible failure in all layers of all elements. For failed layer in an element, material properties were modified according to the failure mode and progressive damage theory. In other elements that were not failed, the damage parameter was calculated. If the value of the damage in each element exceeds 0.9, the layer of the element was assumed to be failed and the algorithm was continued, then the fiber and matrix failure in tension were analyzed. In addition, a new useful and simple model was presented to assess the changes in residual stiffness during fatigue procedure.

Also, to characterize the effect of stress ratio, the Kawai's failure criterion were applied, however this law cannot recognize the modes of failure. The predicted fatigue life was compared to the experimental results available in the literature and good agreement was observed.

## References

- Giancane, S., Panella, F.W. & Dattoma, V. (2009): Characterization of fatigue damage in long fiber epoxy composite laminates, *International Journal of Fatigue*, No. 32, pp. 46-53.
- Hashin, Z. & Rotem, R. (1973): A Fatigue Failure Criterion for Fiber-Reinforced Materials, *J. Compos. Mater.*, No. 7, pp. 448-464.
- Kawai, M. (2004): A phenomenological model for off-axis fatigue behavior of unidirectional polymer matrix composites under different stress ratios, *Journal of composites (Applied science and manufacturing)*, No. 13, pp. 955-963.

## Experimental Investigation of Cold Forming of PC-Films and tensile bars using Optical Measurements

KAI-UWE WIDANY, CHRISTIAN DAMMANN, ROLF MAHNKEN

Chair of Engineering Mechanics (LTM), University of Paderborn, Germany

The alignment of polymer chains is a well known microstructural evolution effect due to straining of polymers. This has a drastic influence on the macroscopic properties of the initially isotropic material.

In this work, cold forming is performed at room temperature on a tensile testing machine. Polycarbonate films are examined in two loading phases. In the first phase the specimen is loaded to induce anisotropy, and in the second phase it is re-loaded while the material direction is varied. The investigations are supported by an optical measurement system to gain knowledge about the inhomogeneous behavior in the initial loading phase and the about the anisotropic behavior in the re-loading phase. Two-dimensional strain contours are obtained from the test data.

Additionally, we propose a method for approximation of the true stress-strain curves at the local material points. This method is aided by experimental investigations on tensile bars to gain knowledge about the evolution of volumetric strains.

### References

- Arruda, E. M. & Boyce, M. C. & Quintus-Bosz, H. (1993) – Effects of Initial Anisotropy on the Finite Strain Deformation Behavior of Glassy Polymers, *Int. J. Plast.*, 9: 783-811
- Dammann, C. & Caylak, I. & Mahnken, R. (2014) – Experimental Investigation of PC-Films Using Optical Measurements, *Intern. Polymer Processing*, 29 (2): 260-271

## Failure processes of fiber reinforced composites under off-axis loading

CHRISTIAN MAROTZKE, TITUS FELDMANN

BAM (Federal Institute for Materials Research & Testing), Mechanics of Polymers, Berlin, Germany

In structural applications of fiber reinforced materials the composite plies comprising the laminates are loaded by multiaxial stresses. Composite plies are very sensible against the loading angle because of their highly anisotropic mechanical properties. Especially the strength strongly depends on the loading angle because the strength of the fibers is several times higher than the strength of matrix and interface. The elastic properties as well as the failure processes under multiaxial loading can be studied by off-axis tests. However, in off-axis tests two different failure mechanisms occur, this is, fiber fracture or inter fiber failure. Depending on the specimen geometry either one or the other failure process can occur in case of small off-axis angle. Since the ultimate load depends on the geometry the test results have to be split into failure with and failure without fiber fracture.

A series of off-axis tests is performed for a carbon fiber reinforced epoxy resin with a fiber volume fraction of 55%. For the given specimen geometry pure inter fiber failure occurs for off-axis angles larger than 6°. Due to the large fracture surface the strength of the specimens is very high for small angles. The failure stress rapidly decreases with growing off-axis angle. At an

off-axis angle of 30° only 12% of the initial inter fiber failure load is left.

The fracture plane in off-axis tests naturally is loaded by a combination of normal and shear stresses. For off-axis angles below 45° the failure is dominated by shear stresses parallel to the fibers while above 45° it is dominated by stresses normal to the fibers. Fracture surfaces for off-axis angles lower than 45° show the typical shear cusps develop which become more and more pronounced with decreasing off-axis angle. Even in case of epoxy matrices very high deformations occur leading to extremely cliffy fracture surfaces of the matrix zones between the fibers. In contrast, the fracture surfaces are rather flat in case of pure tensile stresses normal to the fibers. In any case the fiber-matrix interface fails because the interface commonly is weaker than the pure matrix.

A fracture mechanical analysis of the inter fiber failure process is performed by finite element simulations. The energy release rate is calculated by using the virtual crack closure method. The model consists of a regular hexagonal 12-fiber array. In order to determine the influence of the distance between the fibers the fiber volume fraction is varied between 5% to 85%. The

analyses reveal a strong influence of the fiber content on the fracture process. The results show that the total energy release rate increases during a large part of the debonding process indicating an unstable crack propagation.

In addition to pure interface cracks the kinking of the cracks from the interface into the matrix at different positions is analysed. The results show a strongly varying energy release rate for the cracks along on their path to the neighbouring fibers.

## References

- Marotzke C. Influence of the interface on the on the strength of fiber reinforced polymers. Proceedings of the ECCM 14, Budapest, Hungary, 2010.
- Correa E, Mantic V, Paris F. Numerical characterisation of the fibre–matrix interface crack growth in composites under transverse
- Hobbiebrunken T., Hojo M., Adachi T., de Jong C., Fiedler B. Evaluation of interfacial strength in CF/epoxies using FEM and in-situ experiments. *Composites Part A* 2006;37:2248–56.
- Marotzke, C. Feldmann, T. Failure of composites under transvers loading - a fracture mechanical approach. Proceedings of ECCM15, Venice, Italy, 2012.

## Analysis and Simulation of the Fatigue Behaviour of CFRP Laminates

JANKO KREIKEMEIER<sup>1</sup>, LUKAS GEIGER<sup>2</sup>

<sup>1</sup>German Aerospace Center, Structural Mechanics, Braunschweig, Germany

<sup>2</sup>Karlsruhe Institute of Technology, Continuum Mechanics, Germany

The simulation of the fatigue behaviour of carbon fibre reinforced plastics (cfrp) is very complex and challenging. Compared to isotropic materials, the experimental characterization of cfrp materials suffers high costs. Additionally, there exist many failure mechanisms which appear in parallel, i.e. fibre failure in tension and compression, matrix failure in tension and compression as well as delamination phenomena.

In the present work the constitutive model of (Govindjee, Kay, & Simo, 1995) is utilized to model the cfrp fatigue behaviour. Originally developed for the description of concrete like structures, the model does not take into account failure mechanism caused by cyclic loading conditions. For this reason, the model is exploited to cycle dependence to capture the fatigue behaviour, as well. Both, the elastic constants as well as the strength values are degraded under cyclic loading conditions. The static strength values used in the failure criterion are replaced by the residual stress counterparts as function of the cycle number and the actual stress state. Thus, the corresponding function of residual stresses is explicitly dependent on the static strength and the number of load cycles and implicitly dependent on the actual stress state. For full description of the function, the Wöhler curve has to be known from experiments. The approximation of the residual stresses is necessary for all strength values, because common failure criteria utilize numerous strength values for failure description. In this work, the non-differentiating Tsai-Wu failure criterion, (Tsai & Wu, 1971), is used for description of the damage onset.

The cyclic loading is taken into account via the cycle jump algorithm available in Abaqus. In this approach, the material degradation of the structural response of a single load cycle is extrapolated over a discrete number of cycles to prevent the computation of every load cycle. For this reason, periodic displacement functions are utilized via Fourier series expansions.

The model is implemented into the finite element system Abaqus via the User Material Subroutine utility (UMAT). In conjunction with the cycle jump algorithm, this methodology is a powerful tool for the fatigue investigation of composite materials.

In addition, the constitutive characterization of the cfrp material under investigation is carried out by means of cyclic tension tests longitudinal as well as transverse to the fibre direction following the standard DIN 527-5.

The verification of the constitutive model via the simulation of the cyclic tension tests and the comparison with the experimental results revealed the suitability of the approach for the fatigue investigation of cfrp materials.

## References

- Govindjee, S., Kay, G., & Simo, J. (1995). Anisotropic modelling and numerical simulation of brittle damage in concrete. *International Journal for Numerical Methods in Engineering* 38 (21), S. 3611-3633.
- Tsai, S., & Wu, E. (1971). A general theory of strength for anisotropic materials. *Journal of Composite Materials* 5 (1), S. 58-80.

# Inline metrology of carbon fiber preforms as an indicator of mechanical properties of consolidated CFRP parts

DANIEL BRABANDT, GISELA LANZA

Karlsruhe Institute of Technology, wbk Institute of Production Science, Germany

The material group of carbon fiber reinforced polymers (CFRP) is getting more important as a construction material. Due to its high mechanical load capacity CFRP can be applied in many applications. The low density in combination with its mechanical properties makes this material predestinated for lightweight design. Due to this CFRP are getting into the focus for the automotive serial production. But to establish them the production costs and the cycle times have to decrease significant (McKinsey & Company 2012).

To facilitate a large-scale use the automated production has to be further developed. Irrespective to the kind of infiltration the forming operation of the semi-finished textiles is a significant process step that has to be controlled. In the so called preforming process the two dimensional semi-finished textiles are laid up in several layers and are transformed into a three dimensional near net shape geometry. Due to the anisotropic properties of carbon fibers this process is crucial for the final mechanical properties of the consolidated part.

The complexity of the process makes it susceptible to defects such as form deviations, folds and misalignment of the textiles (Härtel & Middendorf 2013). These deviations can lead to a significant loss of the mechanical properties of the final part. Currently these kinds of defects are typically detected in an end of line quality inspection by using nondestructive testing (NDT) methods. Thus to get a holistic understanding of the production process it is necessary to measure the preform directly after the preforming process (Lanza & Brabandt 2013).

The objective of the presented approach is to generate a complete surface measurement of the preform. Therefore a triangulation system using laser stripe sensors is implemented on a three-axis-kinematics that moves the sensors over the surface. It will be discussed what kind of specific challenges occur by measuring carbon fiber preforms and how they are solved by the presented setup. As a reference carbon fiber

specimens representing typical geometric features are investigated. Based on the generated data-sets which are represented by a cloud of points further analysis can be performed. The data can help to improve the manufacturing technologies within the preforming process by getting a three dimensional model of the preform. This model offers the opportunity to analyze the macroscopic behavior of the semi-finished textile in the forming operation. Furthermore the three dimensional model of the preform can be used as a validation for draping simulations.

In a direct link to the production process the implementation of an inline metrology system will give the possibility to evaluate deviations from given tolerance limits so that a quality judgment can be made at an early stage. This leads to reduced production costs and scrap rates. The presented metrology system will also give an support to set the right tolerance limits. By digitalizing specimens with known defects a holistic approach for the evaluation of effects of defects (EoD) will be possible by giving essential information to combine them with NTD and destructive end of line tests.

## References

- McKinsey & Company (2012): Lightweight, heavy impact – How carbon fiber and other lightweight materials will develop across industries and specifically in automotive; Advanced Industries.
- Härtel F, Middendorf P. (2013): Preforming parameter studies and comparison of different preform processes with NCF material. 19th International conference on composite materials ICCM19.. p. 7577-7587.
- Lanza G, Brabandt D. (2013): Design of a measurement machine for quality assurance of preforms in the CFRP process chain. Apprimus Verlag, Aachen. ISMTII 2013: Metrology - Master Global Challenges. ISBN 978-3-863-59138-0.

# Characterization of complexly warped components made from locally reinforced UD-tape laminates

BENJAMIN HANGS<sup>1</sup>, TOBIAS LINK<sup>1</sup>, FRANK HENNING<sup>1,2</sup>

<sup>1</sup>Fraunhofer-Institut for Chemical Technology (ICT), Pfinztal, Germany

<sup>2</sup>Karlsruhe Institut of Technology (KIT), Institute for Vehicle System Technology (FAST), Germany

In the past decades significant research has been conducted with regard to efficient processing of thermoplastic advanced composites. One aspect, out of a wide variety, is the formation of thermal stresses in the course of the cooling stage. The main cause for this effect is the highly anisotropic material behavior of continuous fiber-reinforced thermoplastics. In particular, the significantly different coefficients of thermal expansion (CTE) of polymer matrix and reinforcing fibers [1].

From a process perspective, balanced thermal stresses within a symmetric laminate are not necessarily critical. By contrast, unbalanced thermal stresses, especially in thin walled components, result in significant shape deformation leading to difficult or even impossible assembly. Two main aspects exist which create unbalanced thermal stresses across a laminate's cross-section. First are process related disturbance variables such as cooling gradients, tool-part interaction and others. In addition, unsymmetric layup design is a key driver [2]. Although the latter is ultimately avoidable, this kind of layup design is of interest for creating highly tailored components with locally reinforcing material along the main load paths. Automated tape-laying technologies nowadays provide the possibility to create such tailored layups with the required accuracy.

This presentation deals with the layup-induced warpage of tailored laminates made from UD-tape. For this purpose, rectangular CF/PPS laminates (baseplate G) with a centered, longitudinal reinforcement patch (P) are produced with a wide variety of layup combinations for G and P. The baseplate as well as the patch are designed as symmetric layups. In consequence an un-

symmetric layup results for the patched section which causes the coupon to warp. The coupon is illustrated in Figure 1.

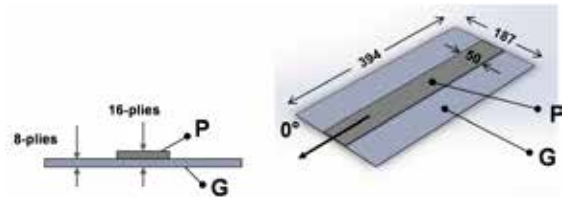


Fig. 1: Illustration of the investigated coupon

To characterize the complex deformation modes which result from the locally unsymmetric layups, it is essential to have an accurate geometric dataset representing the warped coupons. Within this study a hand-operated laser scanner is used to generate precise 3D point clouds of the physical components. This data is then post-processed with the aim to analyze the types of warpage for the different layups and to determine its quantity. Based on these findings, parameters are derived which allow to compare and categorize the different deformation modes observed.

## References

- Nairn J.A., Zoller P.; Matrix solidification and the resulting residual thermal stresses in composites, *Journal of Material Science* 20 (1985) p. 355-367  
 Hyer M.W.; Some Observations on the cured shape of thin unsymmetric laminates, *Journal of Composite Materials* 15 (1981) p. 175-194

Talks Topic K 3:

## ***Polymer based composites***

---

## RVE modeling of fibre-reinforced-polymer curing coupled to visco-elasticity

CHRISTIAN DAMMANN, ROLF MAHNKEN

Chair of Engineering Mechanics (LTM), University of Paderborn, Germany

Our work concentrates on the mesoscopic constitutive model for temperature-dependent visco-elastic effects accompanied by curing, which are important phenomena in production processes of intrinsic hybrids. These integral components are hybridized in a modified resin transfer molding process adding e.g. steel as a second semi-finished product to the textile. During hybridization and later mechanical loading, the periodic microstructure defined by resin and fibers is taken into account as a representative unit cell (RVE) subjected to thermo-mechanical loading.

The polymeric resin component is modeled using an approach from Mahnken (2013), where an additive ternary decomposition of the logarithmic Hencky strain tensor into mechanical, thermal and chemical parts is used. Based on the concept of stoichiometric mass fractions for resin, curing agent and solidified material the bulk compression modulus as well as the bulk heat- and shrinking dilatation coefficients are derived and compared with ad hoc assumptions from the literature Halley & Macackay (1996), Lion & Höfer (2007). Moreover, we use the amount of heat generated during differential scanning calorimetry until completion of the chemical reactions, to define the chemical energy. As a major result, the resulting latent heat of curing occurring in the heat-conduction equation derived in our approach reveals an ad hoc approach from Hilton (2003) as a special case.

Linear elastic fibers in addition with the resin are used to model an RVE on the mesoscale. Periodic boundary conditions for displacements are applied including a macrostrain from the upper scale, to describe mechan-

ical loading, while thermal loading is handled homogeneously on the mesoscale. Homogenization leads to results on the less resolved macroscale.

In the examples we illustrate the characteristic behavior of the model, such as shrinking due to curing and temperature dependence and simulate the hybridization process as well as mechanical loading of the cured part with the finite-element-method. Results from the mesoscale are compared with those of the macroscale.

### Acknowledgements

This work is based on investigations of the „SPP 1712 - Intrinsische Hy-bridverbunde für Leichtbautragstrukturen“, which is kindly supported by the Deutsche Forschungsgemeinschaft (DFG).

### References

- Mahnken, R. (2013): Thermodynamic consistent modeling of polymer curing coupled to visco-elasticity at large strains – International Journal of Solids and Structures, 50: 2003-2021.
- Halley, P.J. & Macackay, M.E. (1996): Chemorheology of thermosets, an overview - Polymer Engineering and Sciences, 36(5): 593-609.
- Lion, A. & Höfer, P. (2007): On the phenomenological representation of curing phenomena in continuum mechanics - Archive of Mechanics, 59: 59-89.
- Hilton, H.H. (2003): Optimum viscoelastic designer materials for minimizing failure probabilities during composite curing - Journal of Thermal Stresses, 26: 547-557.

## Characterization and simulation of the time-dependent anisotropic deformation behaviour of continuously reinforced PA6 material

ANDREAS ROESNER, LUISE KAERGER, FRANK HENNING

Karlsruhe Institute of Technology, Institute for Vehicle System Technology, Germany

The mass production of continuously reinforced composites is a challenge that has not been finally solved. Composites with thermoplastic matrix systems offer relatively short cycle times and easy handling. Due to the capability of thermoplastic matrices to melt again after initial consolidation, the composite material can

be reshaped after manufacturing and can be recycled after lifetime. Because of these positive characteristics continuously reinforced thermoplastics are an attractive alternative for the use in structural applications. However, it is not yet fully understood how the time-dependent viscoelastic-viscoplastic deformation

behaviour of the isotropic thermoplastic matrix is transferred to the orthotropic, continuously reinforced composite. As a consequence, there is still a lack of suitable material models for describing the macroscopic, time-dependent and directional material behaviour of said composites. Considering the carbon fiber reinforced polyamide 6 material presented in this work the aspect of fiber waviness has to be taken into account. Depending on the geometry of the part and the chosen process parameters, fiber waviness may occur in rather large areas of the composite part. The carbon fibre PA6 tapes are processed through heating above melt temperature, shaping and lastly cooling of the shaped part. During cooling the matrix shrinks considerably due to crystallization while the carbon fibers elongate slightly due to a moderately negative thermal expansion coefficient. Hence, the carbon fibres are compressed and wrinkle due to their extreme slenderness. This leads to a significant decrease in axial stiffness depending on the amplitude to wavelength ratio of the wavy fibers (Garnich & Karami 2004).

This work presents a numerical characterization of the time-dependent deformation behavior of the unidirectional carbon fiber PA6 material using representative volume elements (RVE). A material model for the ma-

trix is incorporated that shows viscoelastic, as well as plastic behavior, in order to analyse whether plastic deformation can be neglected or need to be considered in a homogenized, macroscopic material model. As proposed by Garnich & Karami (2004), who assume purely elastic behavior of the constituents, wavy unit cells are used to study the time-dependent behavior under tension and compression depending on the amplitude to wavelength ratio. It is shown that triaxial strain states significantly influence the time dependence and that fibre waviness leads to asymmetric stiffness as well as creep compliance under tension and compression.

Based on the micromechanical unit cell model, a three-dimensional macromechanical model is proposed that adequately represents the time-dependent, directional behavior of the investigated unidirectional carbon fibre PA6 material.

#### Reference

Garnich, M. & Karami, G. (2004): Finite Element Micromechanics for Stiffness and Strength of Wavy Fiber Composites. – In: Journal of Composite Materials, Vol. 38, No.4 2004.

## Topological Interlocking Materials - Towards New Polymeric Hybrid Materials

LEE DJUMAS, ANDREY MOLOTNIKOV, GEORGE P.SIMON, YURI ESTRIN

Department of Materials Engineering, Monash University, Clayton, Australia

Composites play an important role as structural materials in a broad range of fields due to the potential to combine beneficial properties of their constituents. In Nature, composites display fascinating architectures at multiple length scales, each of which can influence different properties. They are increasingly being used as inspiration to develop novel materials. One particular principle of interest is the combination of hard building blocks, that constitute a majority phase, and a soft matrix phase, thus mimicking the microstructure of nacre, with its exceptional fracture toughness (Meyers et al., 2014).

In this work we present a geometrical concept known as *topological interlocking* (Estrin et al., 2011), which can be utilised to vary the geometry of the hard building blocks and potentially produce structures with improved properties compared to traditional platelet-like blocks. The concept of topological interlocking is based on periodic assemblies of identical, discrete elements with specifically designed geometries where each block is held kinematically in place by its neighbours. Our previous investigations have demonstrated that a plate segmented into interlocked ceramic elements

can withstand flexural deflections ten times larger than those of a solid plate of the same thickness from the same material (Krause et al., 2012). It is anticipated that hybrid materials obtained by adding a soft phase to assemblies of topologically interlocked blocks will have superior mechanical properties.

With the aid of additive manufacturing, which has gained much attention due to its broad and far reaching potential applications, we are granted further design freedom allowing fabrication of complex geometries with fine features at micrometre resolutions. Employing the latest state of the art 3D printing technology as a simple and efficient rapid manufacturing technique, we are able to print multiple polymeric materials with intricate inner architectures and widely contrasting mechanical properties within the same build. As a result, the ability to develop and investigate complex polymer composite assemblies, based upon the two design principles - topological interlocking and mimicking nacre - has become highly viable.

In this talk we will present a combination of results detailing the experimental and computational modelling work done to develop and fabricate multi-material

topologically interlocked structures using 3D-printing techniques. Preliminary work on multi-phase assemblies motivated by nacre structures will also be presented.

#### References

Meyers, M. A., and Chen, P.-Y. (2014), *Biological Materials Science: Biological Materials, Bioinspired Materials, and Biomaterials*, Cambridge University Press.

Estrin, Y., A.V. Dyskin, and E. Pasternak (2011), Topological interlocking as a material design concept. *Materials Science and Engineering C*, **31**, pp. 1189-1194.

Krause, T., Molotnikov, A., Carlesso, M., Rente, J., Rezwani, K., Estrin, Y., Koch, D. (2012), Mechanical Properties of Topologically Interlocked Structures with Elements Produced by Freeze Gelation of Ceramic Slurries, *Advanced Engineering Materials* **14**, pp. 335-341.

## Homogenisation of thermoelastic properties of short-fibre reinforced polymers and validation based on experimental characterisation

L. KEHRER, V. MÜLLER, B. BRYLKA, T. BÖHLKE

Chair for Continuum Mechanics, Institute of Engineering Mechanics, Karlsruhe Institute of Technology (KIT), Germany

Polymer based composites are increasingly applied as lightweight material in various fields due to their advantageous material properties. Short-fibre reinforced thermoplastics provide additionally advantages concerning fabrication by injection moulding and recycling. The fabrication process, however, influences the properties of the microstructure. Introduced local fibre orientation distribution, spatial distribution, and variation in geometry of the fibres, e.g., cause inhomogeneous and anisotropic mechanical material behaviour. During the injection moulding process, cooling rates lead to effects on the microstructure of the composite, cf., e.g., McGonigle et al. (1999) and Meister et al. (2012). These structures are not balanced and exhibit post-crystallisation effects. The original amorphous structures can be restored by an increase of temperature. Especially in case of semi-crystalline thermoplastics, the stiffness depends on the degree of crystallisation, which is linked to temperature and time. Thus, the degree of crystallisation affects the mechanical properties. In addition to the anisotropic and inhomogeneous material behaviour, the effective stiffness properties depend further on temperature and strain-rate and are coupled to temperature history.

By means of dynamic mechanical analysis (DMA), material properties of polypropylene as well as fibre reinforced polypropylene are investigated by tensile tests under thermal loading. The impact of crystallinity on viscoelasticity of the matrix material is analysed. The thermal loading is varied in a range of -50°C and 120°C. Changes of mechanical material properties of the experimental data by thermal loading history are discussed.

The effective thermoelastic material behaviour of the fibre reinforced composite is modelled by use of the

interaction direct derivative (IDD) estimate developed by Zheng and Du (2001). Based on the three-phase model, cf., e.g., Christensen and Lo (1979), the IDD estimate considers interaction between fibres and the surrounding matrix material and the fibre distribution. The mean field homogenisation with the IDD approach is performed by means of micro-computed tomography data describing the microstructure of the composite, cf., Müller et al. (2014). For the application of the homogenisation scheme, experimental data of the polypropylene matrix obtained by the DMA are used as input parameters. The effective properties of the composite, resulting from numerical homogenisation with the IDD scheme, are compared to experimental results for various time-temperature loading histories as well as to homogenisation results by means of the self-consistent method. The results of both homogenisation methods qualitatively represent the temperature-dependent material behaviour. However, the IDD estimate is closer to the experimental results than the self-consistent approximation.

#### References

Müller, V., Brylka, B., Dillenberg, F., Glöckner, R., Kolling, S., Böhlke, T. (submitted 2014): Homogenization of Elastic Properties of Short Fiber-reinforced Composites Based on Measured Microstructure Data.

McGonigle, E. A., Daly, J. H., Gallagher, S., Jenkins, S. D., Liggat, J. J., Olsson, I., Pethrick, R. A. (1999): Physical Ageing in Poly(ethylene terephthalate) - its Influence on cold Crystallization. – In: *Polymer*, **40**: 4977-4982.

Meister, S., Jungmeier, A., Drummer, D. (2012): Long-Term Properties of Injection-Molded Micro-Parts:

- Influence of Part Dimensions and Cooling Conditions on Ageing Behavior. – In: *Macromolecular Materials and Engineering*, 297: 994-1004.
- Zheng, Q.-S., Du, D.-X. (2001): An explicit and universally applicable estimate for the effective properties of multiphase composites which accounts for inclusion distribution. – In: *Journal of the Mechanics and Physics of Solids*, 49: 2765-2788.
- Christensen, R. M., Lo, K. H., (1979): Solutions for effective shear properties in three phase sphere and cylinder models. – In: *Journal of the Mechanics and Physics of Solids*, 27: 315-330.

## Phenomenological characterization and macromechanical modeling of anisotropic, non-linear behavior of sheet molding compounds (SMC)

MARINA MRKONJIĆ<sup>1</sup>, UTE RAYLING<sup>2</sup>, KAY ANDRÉ WEIDENMANN<sup>3</sup>, LUISE KÄRGER<sup>4</sup>, FRANK HENNING<sup>5</sup>

<sup>1,2,4</sup> Karlsruhe Institute of Technology (KIT), Institute of Vehicle System Technology (FAST), Department of Lightweight Technology (LBT), Germany

<sup>2</sup>now: French-German Research Institute of Saint-Louis, Advanced Materials Technologies, Saint-Louis, France

<sup>3</sup>Karlsruhe Institute of Technology (KIT), Institute for Applied Materials IAM-WK, Germany

<sup>5</sup>Fraunhofer Institute for Chemical Technology (ICT), Polymer Engineering (PE), Pfinztal, Germany

The present work deals with anisotropic and non-linear effects in the mechanical behavior of sheet molding compounds (SMC) as a viscoelastic damageable material.

SMC, as a long fiber reinforced thermoset primarily produced by compression molding, is considerably affected by the processing parameters resulting in anisotropic material properties. Local inhomogeneities may also occur.

Different macroscopic measurements have been employed to determine the material parameters needed for modeling. For the characterization of non-linear effects, cyclic test procedures are developed. In the early stages of the SMC deformation, damage mechanisms and viscoelasticity occur simultaneously.

A constitutive model for the macromechanical simulation of anisotropic SMC is implemented in the FE software ABAQUS. Assuming that damage mechanisms and viscoelastic effects can be decoupled (Oldenbo 2004), the two effects are analyzed individually. The damage evolution is

considered to be time-independent, irreversible and dependent on the maximum stress state, causing stiffness degradation with increasing strain. The anisotropic elastic damage theory by Chow and Wang is used (Chow & Wang, 1987). Material failure can be predicted by one of the tensor-polynomial failure theories that are implemented in the FE-code.

Finally, a comparison of simulation and experimental results is presented, showing good accordance between the stress-strain-curves, thus validating the model.

### References

- Oldenbo, M. (2004): Anisotropy and non-linear effects in SMC composites from material data to FE-simulation of structures, Lulea University of Technology, Diss.
- Chow, C.L. & Wang, J. (1987): An anisotropic theory of elasticity for continuum damage mechanics, *International Journal of fracture* 33:3-16; Dordrecht.

Talks Topic L 1:

## ***Lightweight alloys and structures***

---

# Mechanical properties and microstructure of Ti6Al4V fabricated by selective laser melting

RADOMILA KONECNA<sup>1</sup>, GIANNI NICOLETTO<sup>2</sup>, ADRIAN BACA<sup>1</sup>, LUDVIK KUNZ<sup>3</sup>

<sup>1</sup>University of Zilina, Zilina, Slovakia

<sup>2</sup>University of Parma, Parma, Italy

<sup>3</sup>Institute of Physics of Materials, Brno, Czech Republic

Selective Laser Melting (SLM) is one of the emerging technologies in the broad area of Additive Manufacturing (AM). In SLM method the metal powder is selectively melted layer-by-layer by a computer driven concentrated laser beam (Levy 2010). The solidified material progressively generates a part of any complex 3D shape thus minimizing the need for material removal, (e.g. by means of milling and drilling) (Kahlen & Kar 2011).

The SLM process is characterized by the generation of complex microstructure and a residual stress system, which depend on the laser path, laser energy and speed, solidification rate and the other parameters of this advanced technology. The process is capable of producing an almost fully dense material, although hot isostatic pressing at high temperature is often used to further improve the ductility and toughness. However, the relative novelty and the complexity of the processing/ microstructure and properties relationships make SLM a manufacturing technology requiring further detailed investigation, focussed on relations among microstructure, mechanical properties and the parameters of the manufacturing process.

This study is aimed on an examination of relationships among mechanical properties and microstructure of Ti6Al4V alloy produced by SLM and the fabrication parameters. SLM process was followed by a hot isostatic pressing (HIP) treatment of the final product to obtain fully dense material of high quality.

Flat specimens with cross-section 6.25 x 4 mm for tensile tests were manufactured using a Renishaw A250 system which operates with an Ytterbium fiber laser with a wavelength of 1075 nm. The source material for SLM procedure was in the form of atomized titanium powder with a granulometry in the range 15-45  $\mu\text{m}$ . Tensile specimens with two different orientations of layer-by-layer building were prepared. Displacement controlled tensile tests with the rate of 0.001 mm/s were conducted. An analysis of microstructure was performed on metallographic specimens extracted from the gauge length of the tensile bars after testing.

Light and scanning electron microscopy were applied to reveal the microstructure.

It has been found that the ultimate tensile strength and elongation depends on the layer-by-layer building orientation of the specimen gauge length. The studied alloy Ti6Al4V prepared by SLM is a typical two phase  $\alpha+\beta$  structure containing  $\alpha$  and  $\beta$  phases which are stabilized by alloying elements. The HIP process improved porosity and density of the specimens and affected the structure, too. The microstructure consists of a lamellar structure of  $\alpha+\beta$  phases. During the SLM process  $\alpha'$  martensite is formed. The subsequent HIP process converted the original structure into a lamellar  $\alpha+\beta$  structure.

During the tensile tests the digital image correlation (DIC) technique was used to determine and monitor the full field strain distributions. The heterogeneous nature of the strain and damage accumulation within the material microstructure was observed and discussed. The severe strain gradients determined by DIC were then verified by micro hardness mapping of the microstructure.

The applied DIC technique enables to determine the degree of material anisotropy in tensile specimens fabricated from Ti6Al4V alloy. The strain heterogeneity is an index of expected scatter in microstructure-sensitive mechanical properties, which are crucial for the safe application of this manufacturing technology in view of the ready-to-use characteristics of the SLM parts e.g. in the demanding aerospace and biomedical fields (Hollander et al 2006).

## References

- Levy, G.V. (2010): The role and future of the Laser Technology in the Additive Manufacturing environment. *Physics Procedia* 5, 65-80.
- Kahlen, F. J. & Kar, A. (2011): *J. Manuf. Sci. Eng.* 123, 38.
- Hollander, D. A., von Walter, M., Wirtz, T., Sellei, R. Schmidt-Rohlfing, B., Paar, O., Erli, H.-J. (2006): *Bio-materials* 27, 955.

## Formation of Twin Bands and Inhomogeneous Deformation in Mg-wrought Alloy AZ31 During Tension-Compression or Bending Loading

K. ANTEN, A. LIEHR, B. SCHOLTES

University of Kassel, Institute of Materials Engineering – Metallic Materials, Germany

Sheets of wrought Mg-alloy AZ31 exhibit a pronounced rolling texture with basal planes preferably oriented parallel to the sheet plane. Due to this preferred orientation of the hexagonal elementary cells, the dominant deformation mechanism – twinning or dislocation glide – depends on the loading direction regarding the crystallite orientation. This results in a pronounced asymmetry of the deformation behavior under tension or compression loading of AZ31 sheet material. In addition the formation of individual deformation bands with a higher twinning density compared to adjacent areas has been observed, leading to a pronounced inhomogeneity of deformation (Hazeli et al. 2013; Liehr et al. 2014). In this paper the formation and propagation of deformation bands and their microstructure is studied in detail for tension-compression loading as well as for bending loading. Optical as well as X-ray methods

have been applied. In particular the development and disappearance of bands is investigated in case of cyclic plastic deformation. The studies have shown that even within the bands, a characteristic inhomogeneity of deformation exists and that, depending on the loading condition, in the low cycle fatigue regime, inhomogeneous deformation persists until fracture.

### References

- Hazeli, K.; Cuadra, J.; Vanniamparambil, P.A.; Kotsos, A. (2013), *Scripta Materialia* 68, S. 83–86.
- Liehr, Alexander; Anten, K.; Scholtes, B. (2014), In: Fortschritte in der Werkstoffprüfung für Forschung und Praxis: Werkstoffeinsatz, Qualitätssicherung und Schadensanalyse, Hrsg. Wolfgang Grellmann und Holger Frenz. Deutscher Verband für Materialforschung und -prüfung e.V. Berlin

## Electrochemical-based characterization of the corrosion fatigue behavior of creep-resistant magnesium alloy DieMag422

MARTIN KLEIN, PHILIPP WITTKÉ, FRANK WALTHER

TU Dortmund University, Department of Materials Test Engineering (WPT), Germany

Magnesium alloys offer a high potential for lightweight construction, e.g. in automotive applications. However their application range is limited due to their low corrosion resistance.

In the present study the influence of corrosion on the microstructure and the depending mechanical properties under cyclic loading of the newly developed, creep resistant magnesium alloy DieMag422 (Mg-4Al-2Ba-2Ca) was investigated. The corrosion fatigue behavior was characterized in distilled water and sodium chloride solutions as well as under simultaneous anodic polarization. In this context, fatigue properties were estimated in load increase tests, using plastic strain and electrochemical measurements, and afterwards validated in constant amplitude tests. These results

were correlated with corrosion properties of the alloy, which were evaluated in potentiodynamic polarization measurements and instrumented immersion tests. Concurrently, corrosion- and deformation-induced microstructural changes were observed by light and scanning electron microscopy, yielding at a mathematical description of structure-property relationship.

In the corrosion fatigue tests a significant reduction of the corrosion fatigue strength with increasing corrosion impact of the environments was determined, which could be quantitatively correlated with the respective corrosion rates. Plastic strain amplitude and deformation-induced changes in electrochemical measurands could be equivalently applied for a precise corrosion fatigue assessment.

## Very High Cycle Fatigue (VHCF) Assessment of Selective Laser Melted (SLMed) AlSi12 Alloy

SHAFQAAT SIDDIQUE, FRANK WALTHER

Department of Materials Test Engineering (WPT) TU Dortmund University, Germany

Selective laser melting (SLM) is a novel technique in additive manufacturing which uses laser energy to melt the powder material according to the geometry of the computer aided design (CAD) model provided to the SLM system. The manufacturing process employs layer-wise build-up of the part by melting powder material. The process is specifically suitable for complex geometries and customized parts which otherwise would be costly and, even, impossible to be manufactured using conventional manufacturing processes. This study aims at determining the high cycle fatigue (HCF) as well as very high cycle fatigue (VHCF) behavior of AlSi alloy manufactured by the SLM process. Different sets of process parameters, along with post-build heat treatment, have been analyzed and fatigue characterization has been carried out to determine the effect of SLM process parameters on HCF and VHCF behavior of AlSi alloy. Fatigue assessment has been carried out using an

economical test procedure to determine the optimized set of process parameters on the basis of combined multiple step tests and constant amplitude tests. HCF tests were carried out employing servohydraulic test system, and the VHCF investigations were performed using an ultrasonic fatigue (USF) testing system. Besides, optical and scanning electron microscopes were used for microstructural and fracture analysis. The results show that there is a considerable influence of process parameters and post-build heat treatment on the fatigue performance. HCF and VHCF performance of SLM manufactured parts is, at least, comparable to that of conventionally manufactured alloys, and can be further improved by carefully selecting the set of process and post-process parameters. A microstructure- and mechanism-based analysis has been carried out for property-optimized manufacturing.

## Formability Enhancement of 7075 Al Sheet with Two Step Forming

YONG-NAM KWON, YOUNG SEON LEE

Korea Institute of Materials Science, Changwon, Korea

As the automotive industry has kept seeking the lighter car body, Al alloys became the most practical solution for weight reduction of automotive components. It has become very easy to find various Al parts in every section of car body, such as hoods, doors, and chassis. However, Al alloys did not replace every steel part currently in use. This comes not only from higher cost of Al compared to steel but also from a relatively inferior formability especially in sheet. Usually, it has been known that Al sheet formability reached only 2/3 of steel sheet at room temperature. Even though development of new Al alloys with higher formability would be the most desirable goal to expand Al alloy application for lighter weight car, the new forming process to best use of Al formability now available would be another way to increase Al usage for weight reduction. In the present study, two step forming comprised of mechanical and gas blow forming was investigated to fabricate automotive part having a complicated shape using Al 7075 alloy with a conventional formability which has been known to be quite lower compared to deep drawing steels. Usual Al sheet forming consists of several steps of forming, sometimes with the use of heated dies. Also, superplastic gas blow form-

ing has been applied to form complicated shape with fine grained sheet. However, superplastic blow forming with slow production cycle cannot be an adequate solution for large volume productions like automotive industry. Also, conventional Al alloy sheets with large and pan-caked grain structure cannot be a solution for gas blow forming that requires low flow stress level at the elevated temperatures. We have designed the two step forming in which Al sheet was drawn to a kind of preform step following gas blow forming for accurate geometry. In order to judge a formability enhancement of Al sheet in terms of forming process, model geometry came from a practical automotive part which had quite depth with complicated curvatures. The optimum forming conditions for respective forming steps were considered most important technical features of this process and would be discussed in details. Also, the effort to avoid detrimental microstructure evolutions was given and discussed for a practical application.

### Reference

Blair Carlson, etc. Challenges and opportunities relative to increased usage of aluminum within the automotive industry, TMS2010 meeting, TMS.

Talks Topic L 2:

## ***Lightweight alloys and structures***

---

# Effect of Missing Cells on the Initial Stiffness and Plastic Yielding Surface of Three-Dimensional Micro-Lattice Structures

KUNIHARU USHIJIMA<sup>1</sup>, DAI-HENG CHEN<sup>2</sup>, WESLEY JAMES CANTWELL<sup>3</sup>

<sup>1</sup>Tokyo University of Science, Tokyo, Japan

<sup>2</sup>Jiantsu University, Zhenjiang, China

<sup>3</sup>Khalifa University of Science, Abu Dhabi, UAE

Over the decades, cellular materials such as two-dimensional honeycombs, three-dimensional foams and lattice materials have been investigated and developed as load-carrying by many researchers owing to their superior mechanical properties per unit volume (Gibson & Ashby, 1997).

The authors have been also studied on the mechanical behaviour of three-dimensional lattice blocks which can be manufactured by selective laser metal sintering technique under uniaxial compression and shear loadings (Ushijima et al., 2013). One of co-authors have developed the selective laser melting (SLM) technique for manufacturing micro-lattice structures at length scales of microns (Tsupanos et al. 2010).

The wide variety of mechanical response can be achieved by changing the geometry of micro-architecture.

The behaviour of intact and damaged cellular materials have been also investigated by some researchers up to now. It can be anticipated that the behaviour is different from that for conventional continuum materials. For example, Guo and Gibson have investigated the Young's moduli, elastic buckling strength and plastic yield strength of regular honeycombs with defects consisting of missing cells based on finite element analysis. Also, Chen et al. have studied the effect of geometrical imperfection on the plastic yielding of two-dimensional foams subjected to biaxial loading.

In this study, the effects of cell geometry on the initial stiffness and plastic yielding surface of three-dimensional lattice materials with defect have been studied by using finite element method. In particular, emphasis is placed on predicting the yielding surface of lattice materials subjected to biaxial loading.

This study can be a foundation for detecting the fractured cell walls in a lattice plate from the stiffness. Also, the effectiveness and ineffectiveness of introducing the missing cell region on the mechanical properties per unit mass for lattice structures can be clarified.

## References

- Gibson L.J. & Ashby, M.F. (1997): Material properties in "Cellular Solids: Structure and Properties", 2nd ed. Cambridge, Cambridge Press: 52-92.
- Ushijima, K., Cantwell W.J, Chen, D.H. (2013): Prediction of the Mechanical Properties of Micro-Lattice Structures Subjected to Multi-Axial Loading, International Journal of Mechanical Science, 68: 47-55.
- Tsupanos S., Mines, R.A.W., McKown, S., Shen, Y., Cantwell, W.J., Brooks, W., & Sutcliffe, C.J. (2010): The Influence of Processing Parameters on the Mechanical Properties of Selectively Laser Melted Micro-Lattice Structures, Journal of manufacturing Science Engineering (ASME) 32: DOI:10.1115/1.4001743

# High-strength microarchitected cellular materials: The interplay of design and size-dependent strengthening

JENS BAUER, OLIVER KRAFT<sup>1</sup>

Karlsruhe Institute of Technology, Germany

Light materials are weak and strong materials are heavy, strength and density are generally considered as strongly coupled. However, microarchitected cellular materials offer the opportunity to overcome that long standing barrier on the search for light yet strong materials. The lightest bulk materials have a density

in the range of 1 g/cm<sup>3</sup>, only porous materials such as technical foams may reach considerably lower values (Gibson & Ashby 1997). Although successfully used in various lightweight components the mechanical properties of such cellular solids are limited by their characteristic stochastic architecture (Fleck et al.

2010). Certain natural cellular materials such as bone, on the other hand, remain strong since they have an optimized architecture and their basic material is hierarchically structured, actually consisting of nanometer-size building blocks, providing enhanced material strength because of mechanical size-effects (Gao et al. 2003).

It has been shown that high-strength cellular materials with specifically designed micro-architecture can be fabricated artificially, applying 3D direct laser writing and atomic layer deposition. The resulting truss structures consist of polymer beams with a typical diameter of 0.5-1.0  $\mu\text{m}$  coated with thin alumina layers. The conjunction of both structural design and size dependent material strengthening effects enables outstanding ratios of strength to weight. (Bauer et al. 2014)

In this paper we present an overview of the mechanical properties of such micro-structured cellular materials. The interplay of size-dependent strengthening effects

with different topological designs under several load cases is shown. Optimization approaches of topology and shape with the aim to further enhance strength-to-weight ratios are discussed.

#### References

- Gibson, L. J. & Ashby, M. F. (1997) Cellular Solids: Structure and properties..
- Fleck, N. A., Deshpande, V. S. & Ashby, M. F. (2010) Micro-architected materials: past, present and future. Proc. R. Soc. A Math. Phys. Eng. Sci. 466, 2495–2516.
- Gao, H., Ji, B., Jaeger, I. L., Arzt, E. & Fratzl, P. (2003) Materials become insensitive to flaws at nanoscale: Lesson from nature. Proc Natl Acad Sci USA 100, 5597–5600.
- Bauer, J., Hengsbach, S., Tesari, I., Schwaiger, R. & Kraft, O. (2014) High-strength cellular ceramic composites with 3D microarchitecture. Proc Natl Acad Sci USA 111, 2453–2458.

## Self-assembled ultra high strength, ultra stiff mechanical metamaterials based on inverse opals

GEROLD A. SCHNEIDER<sup>1</sup>, JEFFERSON J. DO ROSÁRIO<sup>1</sup>, ERICA T. LILLEODDEN<sup>1,2</sup>, MARTIN WALECZEK<sup>3</sup>, ROMAN KUBRIN<sup>1</sup>, ALEXANDER YU. PETROV<sup>4</sup>, PAVEL N. DYACHENKO<sup>4</sup>, JULIAN E.C. SABISCH<sup>2</sup>, KORNELIUS NIELSCH<sup>3</sup>, NORBERT HUBER<sup>2</sup>, MANFRED EICH<sup>3</sup>

<sup>1</sup>Institute of Advanced Ceramics, Hamburg University of Technology, Hamburg, Germany

<sup>2</sup>Institute of Materials Research, Materials Mechanics, Helmholtz-Zentrum Geesthacht, Geesthacht, Germany

<sup>3</sup>Institute of Nanostructure and Solid State Physics, Universität Hamburg, Jungiusstrasse 11, 20355, Hamburg, Germany

<sup>4</sup>Institute of Optical and Electronic Materials, Hamburg University of Technology, Hamburg, Germany

Inverse opals are known metamaterials in the field of photonics, being able to effect the propagation of light. In this work, we present the inverse opal structure not as a photonic metamaterial but explore its design as a mechanical metamaterial. Silica and titania coated silica structures with densities in the range of 330-910 kg/m<sup>3</sup> resulted in unexpected strengths of 48 to 336 MPa

and elastic modulus of 1.7 to 7.5 GPa as measured by uniaxial compression of micro-pillars. Simulations have shown that these properties arise from a nearly homogeneous distribution of stresses in the structure. The results suggest that inverse opals open new possibilities of design for lightweight structures with enhanced mechanical properties.

## An efficient analysis model for the stresses in arbitrary adhesive lap joints with flat laminated adherends

NICOLAS STEIN, PHILIPP WEISSGRAEBER, WILFRIED BECKER

Institute of Structural Mechanics, TU Darmstadt, Germany

With the growing demand for lightweight constructions adhesive joints are increasingly used in industrial applications. One of the major advantages of adhesive bonding is that it enables to join thin-walled compo-

nents with dissimilar materials. This is of special interest with regard to the widespread use of fibre reinforced plastics (FRP). However, the knowledge of the load transfer and stress distribution in the adhesive

joint is crucial for the design of engineering structures. Moreover, efficient analysis methods are required for pre-dimensioning or optimization processes.

Most of the proposed models in literature addressing the analysis of stresses in adhesive joints (Volkersen, 1938, Goland & Reissner, 1944, Hart-Smith, 1981, Renton & Vinson, 1975, Tsai et.al., 1998) are joint specific. They focus on only one type of joint design but in practice adhesive joints may occur in many different joint configurations. A first generalization of these models regarding the joint geometry was proposed by Bigwood and Crocombe (Bigwood & Crocombe, 1989). Their model is often referred to as general sandwich-type model since it considers only the overlap region. The model allows for a stress analysis of various joint designs with isotropic adherends, such as single lap joints, L-joints and T-joints. When FRP adherends are used it is important to take shear deformations into account. This has been done in joint specific approaches (das Neves et. al., 2009, Tsai et.al., 1998) by employing the First Order Shear Deformation Theory (FSDT). In this work an efficient general sandwich-type model for adhesive joints with shear flexible composite adherends including bending-extension coupling (Weißgraeber et.al., 2014) is presented which allows for the analysis of several joint designs, such as single lap joints, balanced double lap joints, L-joints, reinforcement patches, T-joints and peel joints. For the case of symmetric joints with isotropic adherends a closed-form analytical solution for the stresses can be obtained. For the general case a system of ordinary differential equations with constant coefficients of seventh order has to be solved. The corresponding solution procedure can be implemented very efficiently.

In a comprehensive study the solution of the stress distributions in the adhesive layer for several joint designs with isotropic and laminated adherends with different

stacking sequences and bending-extension coupling are compared to numerical results of a detailed Finite Element Analysis. It is shown that a good agreement is obtained for all observed configurations. Further, the effect of the shear deformation of the adherends on the stress distribution in the adhesive is discussed.

#### References

- Bigwood D.A. & Crocombe A.D. (1989): Elastic analysis and engineering design formulae for bonded joints – In: International Journal of Adhesion and Adhesives 1989, Vol.9, 229-242.
- das Neves P.J.C., da Silva L.F.M., Adams R.D. (2009): Analysis of Mixed Adhesive Bonded Joints Part I: Theoretical Formulation – In: Journal of Adhesion Science and Technology 2009, Vol.23, 1-34.
- Goland M. & Reissner E. (1944): The stresses in cemented joints – In: Journal of Applied Mechanics 1944, Vol.1, 17-27
- Hart-Smith L. (1981): Stress analysis – A continuum mechanics approach (in adhesive bonded joints) – In: Developments in adhesives 1981, Vol.2, 1-44
- Renton W.J. & Vinson J.R. (1975): The efficient design of adhesive bonded joints – In: The Journal of Adhesion 1975, Vol. 7, 175-193
- Tsai M., Oplinger D.W., Morton J. (1998): Improved theoretical solutions for adhesive lap joints – In: International Journal of Solids and Structures 1998, Vol.35, 1163-1185
- Volkersen O. (1938): Die Nietkraftverteilung in zugbeanspruchten Nietverbindungen mit konstanten Lastenquerschnitten – In: Luftfahrtforschung 1938, Vol.15, 41-47
- Weißgraeber P., Stein N., Becker W. (2014): A general sandwich-type model for adhesive joints with composite adherends – In: International Journal of Adhesion and Adhesives 2014, Vol. 55, 56-63

## Optimization of fatigue behaviour of metallic shear joints

TAHA BENHADDOU<sup>1,2</sup>, ALAIN DAIDIE<sup>1</sup>, PIERRE STEPHAN<sup>1</sup>, CLEMENT CHIROL<sup>2</sup>, JEAN-BAPTISTE TUERY<sup>2</sup>

<sup>1</sup>Institut Clément Ader - Insa de Toulouse, France

<sup>2</sup>Airbus Operations SAS, Toulouse, France

Mechanical fastening is the most widely used technique for assembling aerostructural elements thanks to several advantages concerning the performance and the cost of the process. However, it presents one major drawback, linked to the stress concentration area created during hole drilling, which may lead to structural fatigue issues.

In the case of shear joints, an emerging opportunity to optimize structural joints involves applying the preload more accurately. Currently, the clamping force (or preload) applied to join the parts together is achieved

by applying torque to the bolt head or to the nut. In fact, torque specifications can be considered as unreliable because they can often lead to high uncertainties in the amount of preload that has actually been achieved, and yet preload is the only parameter that can define the joint behaviour under thermo-mechanical loads.

In order to demonstrate the beneficial effect of preload on the durability of metallic shear joints, the experimental means used, either for installing or for monitoring, are preload- oriented ones. This means that

the scatter on the preload value is reduced from about 30% (typical torque tightening scatter) to about 10%. The influence of preload on the fatigue life of metallic shear joints is thus demonstrated through the use of experimental and numerical methods and a positive correlation is established between the two approaches. The effect of some preload-related parameters such as interfacial sealant, radial adjustment and size effect will also be covered.

Finally, an industrial application case is presented: continuous monitoring of the preload generated by the use of ultrasonic fasteners allows us to perform a global analysis of the joint performance throughout its fatigue life. It also permits fatigue crack initiation to be detected and the effect of preload on its creation to be understood.

#### References

- Bickford, J. H. (1997). *An Introduction to the Design and Analysis of Bolted Joints*, 3rd ed., Marcel Dekker.
- Chakherlou, T. N., & Abazadeh, B. (2012). Experimental and numerical investigations about the combined effect of interference fit and bolt clamping on the fatigue behavior of Al 2024-T3 double shear lap joints. *Materials & Design*, 33, 425–435.
- Boni, L. and Lanciotti, A. (2011), Fatigue behaviour of double lap riveted joints assembled with and without interfacial sealant. *Fatigue & Fracture of Engineering Materials & Structures*, 34: 60–71.

## Microstructure evolution and deformation texture during rolling of TIMETAL407

GAURAV SINGH, J. QUINTA DA FONSECACA<sup>1</sup>, M. THOMAS<sup>2</sup>, M. PREUSS<sup>1</sup>

<sup>1</sup>The University of Manchester, School of Materials, Manchester, UK

<sup>2</sup>TIMET UK, Witton, Birmingham, UK

TIMETAL407 is a new titanium alloy primarily developed for increased ductility enabling a higher degree of energy absorption. In this study, the evolution of microstructure and crystallographic texture during rolling of TIMETAL407 is examined. For this purpose, TIMETAL407 was first  $\beta$  heat treated before rolling in the upper or lower  $\alpha + \beta$  phase region to 60% reduction in thickness followed by a recrystallisation heat treatment. Detailed texture analysis was carried out using electron back scattered diffraction, while microstructural characterization was performed using optical and scanning electron microscopy. The material rolled

in the lower temperature band displays strong basal pole concentrations inclined about 30 degree towards rolling direction (RD) together with a weak transverse texture component. When the material was rolled in the high temperature band, the texture reversed showing a strong transverse type of texture and with a relatively weak 30 degree texture component towards RD. The  $\alpha$  texture evolution will be discussed in terms of slip and twinning modes as well as possibilities of  $\beta$  rolling texture affecting  $\alpha$  texture formation. Further, the effect of those two different textures on formability of TIMETAL407 are investigated.

Talks Topic X 1:

## ***General mechanical behavior***

---

## Wedge indentation studies of Zr-Cu-based bulk metallic glass

V. NEKOUIE, A. ROY, V.V. SILBERSCHMIDT

Wolfson School of Mechanical and Manufacturing Engineering, Loughborough University, Leicestershire, UK

Bulk metallic glasses (BMGs) are a relatively new type of materials, which are poised for widespread use in the industry thanks to their unique mechanical properties. Such mechanical performance is primarily due to the absence of a long-range order in atomic structure and a lack of defects such as dislocations, which control ductility in traditional metallic materials. Typically, inorganic glasses are brittle at room temperature, showing a smooth fracture surface as a result of mode-I brittle fracture. In BMGs, formation and evolution of localised shear bands is a primary deformation mechanism, resulting in a significant level of plasticity at small scale with a brittle response in the macroscale.

In this study, a Zr-Cu-based BMG is characterised using a relatively new technique, namely wedge indentation.

This technique was employed to apply incremental loading on the BMG to study systematically and elucidate the processes of formation and evolution of shear bands. Digital image correlation was used to measure local strains during incremental loading of specimens. A thorough structural characterisation of shear bands around the indented region was carried out to understand the nature of shear banding.

### Reference

Nekouie, V., Abeygunawardane-arachchige, G., Kühn, U., Roy, A. & Silberschmidt, V.V. (2014) Indentation-induced deformation localisation in Zr-Cu-based metallic glass, *J. Alloys Comp.* 615: 93-97.

## Mechanics Behavior of Protein Material

INCHUL BAEK, MYEONGSANG LEE, HYUN JOON CHANG, JAE IN KIM, SUNGSOO NA

Department of Mechanical Engineering, Korea University, Seoul, S. Korea

One of the known pathogenesis of several degenerative and neuro-degenerative diseases, e.g. type II diabetes, dialysis-related diseases, Creutzfeldt-Jakob disease, Alzheimer's disease, Huntington's disease, Parkinson's disease, etc., is concerned with misfolded, denatured proteins called amyloids. The chief reason behind such amyloidosis lies on the amyloid self-assembly process, related to the repeated fracture of an immature amyloid fibril. In order to figure out the disease mechanism, establishing the mechanical stability of such amyloids therefore takes an essential role, substantiating the path for treatment. Meanwhile, several researchers also claim that amyloid proteins can be recognized as a functional biological materials that can be used in nano sensor, bacterial biofilms, coatings, and so on. Due to these reasons, there have been many *in vitro* methods to determine the material characteristics via force spectroscopy methods: Atomic Force Microscopy and Optical Tweezers to exemplify. While such methods reveal the quantitative structure stability, mechanical properties, and functional mechanisms, they yield to *in silico* methods, such as Molecular Dynamics (MD), Discrete Molecular Dynamics (DMD) and Elastic Network Model (ENM) for example, due to the fact that they additionally provide a more in-depth information in atomic scale about amyloids by visualizing the conformation. In this research, we have unraveled the structure characteristics and mechanical properties of two different polymorphic structures, i.e. two differ-

ent phenotypes based on stacking directions such as parallel and anti-parallel composition, of Human Islet Amyloid Polypeptide (hIAPP) by using MD simulations under tensile Steered Molecular Dynamics (SMD) conditions. Here, we investigated the polymorphic characteristics, which are caused by physiological conditions such as thermal fluctuations. From our results, we have verified the distinct characteristic differences according to the structural array through hydrogen bond fracture analysis, and elucidated the relationship between sequence-structure-property. This study will hopefully serve as a template for degenerative disease treatment and also constitute a foundation for the functional biological materials.

### Acknowledgements

S.N gratefully acknowledges the Basic Science Research Program through the National Research Foundation of Korea (NRF) funded by the Ministry of Science, ICT & Future Planning (MSIP) (No. 2007-0056094, 2014R1A2A1A11052389).

H.J.C is grateful to the financial support from the Global Ph.D Fellowship Program through the National Research Foundation of Korea (NRF) funded by the Ministry of Education (No. 2014H1A2A1021042)

### References

Pepys MB (2006) Amyloidosis. *Annual Review of Medicine* 57: 223-241.

Merlini G, Bellotti V (2003) Molecular Mechanisms of Amyloidosis. *New England Journal of Medicine* 349: 583-596.

Sawaya MR, Sambashivan S, Nelson R, Ivanova MI, Sievers SA, et al. (2007) Atomic structures of amyloid cross-[bgr] spines reveal varied steric zippers. *Nature* 447: 453-457.

## Rigidity characterization and fracture analysis of the solar-grade multi-crystalline silicon plates at low temperature

LV ZHAO, ANNE MAYNADIER, DANIEL NELIAS

Université de Lyon, INSA Lyon, France

The rigidity and the fracture behavior of the multi-crystalline silicon plates integrated in the solar panels are of great importance in the fabrication, transportation and service of the latter.

In our study, we carry out both experimental and numerical investigations on the multi-crystalline plates that come from classical ingot growth process (MCSI) (Chung et al. 2014) and the Ribbon on Sacrificial Template process (RST) (De Moro et al. 2012). Both types of plates are laser cut from wafers to obtain 50x50 mm<sup>2</sup> specimens. The RST plates are thinner (around 90µm) than the MCSI plates (170µm). This work aims to characterize the elastic behavior as well as the fracture mode and source of these structures. These informations are of great importance to improve the strength during production, reduce the waste during handling and lengthen the lifetime during service.

Rigidity is characterized by performing 4-point bending tests. The Young's moduli are calculated using the beam deflection theory (Bruneau & Pratt 1962). In order to verify the experimental assessments, a finite element parametric model is carried out with the commercial FE software Abaqus 6.13. The latter models the grain morphologies using the Voronoi tessellation. The crystallographic orientations are distributed in an aleatory manner. The grain boundaries are considered as perfect interfaces between the grains. Thus, we assigned the same anisotropic elastic behavior given by [Hall 1967] to all the grains.

Using the beam theory, the Young's modulus for the MCSI plates is assessed at 160±8 MPa without distinction in the surface directions. Meanwhile, that for the RST plates is estimated at 200±20MPa in the drawing direction and at 210±10MPa in the perpendicular direction. The FE analysis reveals that the rigidity for MCSI plates is reasonable, while that for RST plates is over-estimated. The main contribution to the over-estimation stems from the important variation of the thickness for the RST plates.

Regarding the fracture aspect, we investigate how the two types of solar-grade multi-crystalline silicon plates

fracture (intra/intergranulaire manner?) and which source initiates the fracture. During 4-point bending tests, the tensile side of the specimen is imaged with a high speed camera. The crack pattern is observed over the microstructure. The fracture source investigation relies on the fractography analysis. The micrographies are referred to Sherman's work (Sherman 2009) on the single crystals under 3-point bending.

As regards the experimental observations, we found that the MCSI plates break with multiple cracks-cracks are intragranular and straight over one grain. Crack direction changes at grain boundaries. The fracture facies analysis indicates that the cracks initiate always from the edges for both types of plates. Further microscope observations reveal some pre-cracks on the specimens' edges, which are likely due to the laser cutting.

Acknowledgment: The authors would like to thank Elsa Tupin, Fabrice de Moro and Christian Bellouet from Solarforce for precious exchange about this work, carried out in the frame work of DEMOS FUI project.

### References

- Chung W.L.; Chuck, H. & Kazuo, N. (2014): Chapter 10: Multicrystalline silicon crystal growth for photovoltaic application. *Handbook of crystal growth: Bulk crystal growth*, 2nd edition.
- De Moro F.; Focsa A.; Derbouz K.; Slaoui A.; Auriac N.; Lignier H. & Keller, P. (2012) : Multicrystalline silicon solar cells from RST ribbon process. *Phys. Status Solidi C* 9, 2092-2096.
- Bruneau, A. & Pratt, P. (1962): The bending deformation of magnesium oxide. *Philosophical Magazine* 7, 1871-1885.
- Hall, J.J. (1967): Electronic Effects in the Elastic Constants of n-Type Silicon. *Physical Review* 161, 756-761.
- Sherman, D. (2009): Fractography of Dynamic crack propagation in Silicon Crystal. *Key Engineering Materials* 409, 55-64

# Quantum field theory approach in mechanics of polycrystalline materials

VYACHESLAV SHAVSHUKOV, ANATOLY TASHKINOV

Perm National Research Polytechnic University, Russia

Most of inorganic structural materials (metallic alloys, ceramics, minerals etc.) are polycrystalline aggregates, consisted of macroscopically large quantity of single-crystal grains (crystallites). The mechanical behavior of the specimen of polycrystalline material is governed by the physical and mechanical processes in the grains and interaction of the grains. Thus the deformation of polycrystalline material is a cooperative phenomenon typical for condensed matter physics and mechanics of heterogeneous materials. The passing of these processes depend on many parameters, including stress states of individual grains and its evolution during macrodeformation.

Complex structure of polycrystals makes impossible the exact solution even the simplest elastic problems, for instance calculating strains in grains under homogeneous macro deformation. So many approximate methods were developed. In this paper we present new method based on a mathematical analogy between the equations of the mechanics of heterogeneous polycrystalline materials and the equations of quantum theory of particles scattering. This analogy allows to apply the methods of quantum field theory to solution of the equations of solid mechanics for heterogeneous media.

The equilibrium equation of boundary value problem for inhomogeneous strains in polycrystals, written in integral form with kernel as Kelvin-Somigliana tensor for homogenized medium, is mathematically identical to the Schrödinger equation (written in integral form) for wave function of particle scattered with many external potentials. The typical example of the latter equation is Korringa-Kohn-Rostocker (KKR) equation for wave function of conductance electron in crystal lattice of two-component disordered alloy. The crystal lattice of alloy is regarded as perfect lattice of one component disturbed by atoms of another component. The KKR method gives the solution for wave function as perturbation series upon this disturbance.

Integral equation for strains in polycrystals reads that inhomogeneous strain can be treated as a result of

multiple scattering of macroscopic coarse-grained homogeneous strain upon elastic heterogeneities caused by grains disorientation. The solution of the equation is represented as perturbation series upon these heterogeneities. The zero-order solution corresponds to absence of scattering and yields well known Voigt approximation. The exact value of strain in any given separate grain is defined by multiple scattering on the heterogeneity of this grain and on all others. The latter terms describe elastic interaction of grains.

This approach allowed, for instance, to calculate probability density function for stresses in grains under arbitrary macrodeformation of polycrystal [2]. Application of the method to classical problem of homogenization gives new formulae for the effective moduli of disordered polycrystalline medium [3].

The mechanical behavior of polycrystals strongly affected by their microstructure. The offered approach allows to take into account the influence of grain shape and size on stress and strain state of the grain, the elastic interaction of adjacent and more remote grains, and other effects. It is shown that influence of elastic interaction of grains falls rather fast with distance between grains.

## Acknowledgements

This work was supported by the Russian Foundation for Basic Researches grant 13-01-96052.

## References

- Ziman, J.M. (1972): Principles of the Theory of Solids, 2nd Edition; Cambridge University Press.
- Shavshukov, V.E.(2012): Stress field distribution in polycrystalline materials. - Physical Mesomechanics. Vol. 15, pp. 85-91.
- Tashkinov, A.A. & Shavshukov, V.E. (2013): Field theory approach for describing the deformation of multicomponent polycrystalline materials. - Vestnik SamGTU: phys.-math. No. 4(32), pp. 87-97.

## Axial Crash and Crush Response of Novel Nested Tubes

ZANA EREN<sup>1</sup>, FATİH USTA<sup>1</sup>, ZAFER KAZANCI<sup>2</sup>, HALİT S. TÜRKMEN<sup>1</sup>, ZAHİT MECİTOĞLU<sup>1</sup>

<sup>1</sup>Istanbul Technical University, Turkey

<sup>2</sup>Turkish Air Force Academy, İstanbul, Turkey

This paper presents a novel nested design of crash tubes with different cross sections which are subjected to axial crashing and crushing. Tubular thin-walled structures with different shapes are widely used in various transportation systems as energy absorbing components of which dissipation of kinetic energy is the most important parameter during violent collisions and crashes.

The effect of the nested design shows that when a tube fails under progressive buckling, the initial peak force is much greater than the subsequent peak. In many instances, these tubes are used to absorb energy in cars and the high force peaks lead to high acceleration on the vehicle occupants during an accident/impact event. An ideal energy-absorbing device should therefore cause a uniform deceleration during the entire stroke. This ideal structure would absorb the shock first and then deform under progressive buckling to absorb the

energy. Thus we consider a new geometric crash tube model which would be nested with different lengths. The longest tube would absorb the kinetic energy first, and they could act together with the other tube(s) after strongest impact effect. This new tube would be lighter than bi tubular crash tubes and alignment of the tubes, geometric parameters would be important. In this study, explicit nonlinear analysis of the tubes which are made from Dual-Phase steel 600 and Aluminum 6063 are done in ABAQUS and Ls-DYNA programs. The virtual crush and crash test data are used to aid the entire development of a new design. The objective is to show that, nested tube design provides decreasing peak forces gradually while increasing absorbed energy. Also, the mesh efficiency is measured by changing element lengths in both ABAQUS and Ls-DYNA.

## Neutron diffraction and imaging for industrial and engineering applications

ANNA PARADOWSKA

<sup>1</sup>Bragg Institute, Australian Nuclear Science and Technology Organisation, Lucas Heights, NSW, Australia

The OPAL research reactor at ANSTO has a number of neutron instruments available for science and engineering applications. The instruments have a unique non-destructive ability to determine critical aspects of a wide variety of material systems. This includes surfaces, defects, fine scale dispersions, texture and residual stresses. This information can provide a direct impact into optimization of modern manufacturing processes,

improved product reliability, enhanced design performance, reduced production cost, and extended life prediction on significant engineering assets (e.g. power-station utilities, gas pipelines, aircrafts, trains, etc.). This presentation will focus on two instruments in particular: Kowari, the strain scanner and crystallographic texture measurement system and Dingo the radiography/tomography instrument.

Talks Topic X 2:

## ***General mechanical behavior***

---

# Preparation and Characterization of Neat and Thermally-treated Silicon Carbide Fibers-reinforced Gypsum Cements

Y. E. GREISH<sup>1</sup>, H. F. EL MAGHRABY<sup>2</sup>, O. GEDEON<sup>3</sup>, O. ALNUAIMI, M. S. KATSIOTIS, K. POLYCHRONOPOULOU<sup>4</sup>

<sup>1</sup>Department of Chemistry, College of Science, UAE University, UAE

<sup>2</sup>Department of Ceramics, National Research Centre, Egypt

<sup>3</sup>Department of Glass and Ceramics, Institute of Chemical Technology, Czech Republic

<sup>4</sup>Department of Mechanical Engineering, Khalifa University of Science and Technology, UAE

Synthetic biomaterials that are intended to partially or totally replace defective hard tissues are strongly recommended to have matching composition and properties to those of natural hard tissues. Two main components make up the construction of hard tissues; namely hydroxyapatite (HAp), and collagen. In nature, HAp nanocrystals deposit along and onto the surfaces of nanofibrous collagen fibers, making a mechanically interlocked assembly that provides hard tissues with their unique mechanical properties (Buckwalter 1996). Upon formation of defects, bone cavities are usually treated with cements. However, a major drawback of most currently existing cements is their low mechanical stability and to some extent their limited bioactivity. In the current research, a calcium sulfate-based bone cement has been studied after incorporating neat and thermally treated SiC fibers. Calcium sulfate cement is one of the early known bone cements and is a known bioresorbable material. On the other hand, SiC is a structural ceramic material that has been also recognized as a bioinert material (Zhang 2009). Upon thermal treatment in air, partial oxidation of the SiC fiber's surface takes place leading to the formation of a silica (SiO<sub>2</sub>) layer. Materials containing SiO<sub>2</sub> have potential bioactivity where hydration of SiO<sub>2</sub> yields hydrated silica layer which has been long shown to nucleate HAp after implantation or when soaked in simulated body fluid (Li 1992). Therefore, the rationale of incorporating SiC fibers is to work on improving the mechanical performance of the cement and introduce bioactivity by virtue of the SiC oxidized fibers.

In the current study, the formation of a novel cement of gypsum reinforced with up to 25 wt% SiC fibers has been investigated. Setting times of the prepared composites were recorded until complete solidification, phase composition of the composites was studied using XRD, FTIR, DTA and TGA techniques. In addition, in-

ternal morphology of the cement composites was evaluated using SEM-EDX technique. Cement composites containing neat and thermally treated SiC fibers were also subjected to tensile strength measurement as a function of the concentration of SiC. Cement composites were further soaked in protein-free SBF media for up to 14 days to evaluate their preliminary bioactivity. SBF-treated samples were investigated by SEM-EDX, while aliquotes were analyzed every 2 days for changes in the concentrations of Ca<sup>2+</sup>, SO<sub>4</sub><sup>2-</sup>, and SiO<sub>4</sub><sup>4-</sup> ions with time.

Results showed no chemical interaction between the components of the cement during their solidification. A homogeneous distribution of the SiC fibers within the gypsum set cement was reflected on stable mechanical performance of the composites, with an overall improvement in the tensile strength by addition of 10% SiC fibers. Moreover, SEM observations showed growth of HAp-like spherulites onto the SiC fibers, especially those thermally pre-treated. The advantages of the currently studied composites are, therefore, the enhancement of the bioactivity, the ability to control the biodegradation of the composite by controlling the proportion of POP in the original powder mixture of the reactants, as well as the slight improvement in the mechanical properties by the addition of 10 wt% SiC fibers.

## References

- Buckwalter JA, Glimcher MJ, Cooper RR, Recker R. Instr Course Lect. 1996;45:371-86.
- Zhang Lei-Lei, Li He-Jun, Li Ke-Zhi, Lu Jin-Hua, Shen Xue-Tao, Lan Feng-Tao. Surf. Rev. Lett. 2009; 16, 683
- Li P, Ohtsuki C, Kokubo T, Nakanishi K, Soga N, Nakamura T, Yamamuro T. J Amer Ceram Soc. 1992; 75: 2094-2097

## Phase-field modeling for microstructure formation of metal foam materials

TAKUYA UEHARA

Yamagata University, Yonezawa, Japan

Metal foam materials have been developed and utilized in a wide variety of fields owing to their remarkable advantages. Characteristics of these materials depend strongly on the microstructure as well as the properties of base metal, and hence the control of the microstructure, i.e. shape, size and their distribution of the foam cells, is of great importance. Computer simulation is indispensable for this purpose, since direct observation of the dynamic process of foam formation is difficult. However, the mechanism of the foam structure formation has not been clarified yet, thus a numerical modeling is necessary.

Phase field model is a promising tool; various microstructures, such as dendrite, lamellar, cellular, and polycrystalline structures, are successfully regenerated. Most phase field models describe liquid and solid phases to account for the solidification and in-solid phase transformation. In this paper, the conventional model is modified to simulate foam structure formation.

Foam structure considered in this paper is closed-cell type, in which small vacancies or cells surrounded by thin solid walls are distributed. This structure is similarly found in bubble foam made by soap or froth. These kind of structures have long been studied, and even recently investigations are actively in progress (e.g. Sye & Sethian 2013). Kelvin cell is one of the most sophisticated structures, which had been considered to be the best structure making the total surface area of the cell boundaries smallest in any space-filling structures until alternative structure was found by Weaire and Phelan (Weaire & Phelan 1994). Uehara made an approach to this problem using a two-dimensional phase-field simulation, and proposed an additional term which control the cell volume (Uehara 2014) based on their pre-

vious models (Uehara & Suzuki 2012, Uehara 2012). In this paper, the model is extended to three-dimensional foam structure.

First, Kelvin-cell structure is constructed and the stability is verified by providing various degrees of fluctuation in regularity. A rhombic dodecahedron, which is one of the close-packed space-filling structures, is also tested, and the advantageous stability of Kelvin cell was confirmed. Then, random seeding conditions are introduced assuming realistic process. As a result, distorted cells are formed in the early stage, but they revealed to promptly change the morphology to be stable convex polyhedra. The mechanical properties of the metal foam consisting of the simulated structures will be numerically evaluated in the next stage of our study.

### References

- Sye, R. I. & Sethian, J. A. (2013): Multiscale modeling of membrane rearrangement, drainage, and rupture in evolving foams, *Science* 340, 720-724.
- Weaire, D & Phelan, R. (1994): A counter-example to Kelvin's conjecture on minimal surfaces, *Phil. Mag. Lett.* 69, 107-110.
- Uehara T. & Suzuki H. (2012): Numerical simulation of homogeneous polycrystalline grain formation using multi-phase-field model, *Appl. Mech. Mater.* 197, 2610-2614.
- Uehara T. (2012): Grain-size equalization model using multi-phase-field model, *Proc. 7th Int. Workshop on Modeling Crystal Growth*, 82-83.
- Uehara T. (2014): Numerical simulation of foam structure formation and destruction process using phase-field model, *Adv. Mater. Res.* 1042, 65-69.

## Fiber-reinforced Calcium Sulfate Bone Cement Composites with Enhanced Bioactivity, Mechanical Properties and Controlled Biodegradability

YASER E. GREISH<sup>1</sup>, ABDEL HAMID I. MOURAD<sup>2</sup>, NUHA F. ATTIA<sup>1</sup>

<sup>1</sup>Department of Chemistry, College of Science

<sup>2</sup>Department of Mechanical Engineering, College of Engineering  
United Arab Emirates University, Al Ain, UAE

Hard tissues are natural composites of inorganic (hydroxyapatite-HAP), and organic (collagen) components. The interlocking between the collagen

nanofibers and the HAp nanocrystals growing on them provides the well known unique mechanical stability of hard tissues (Buckwalter 1996). In case of partial

fractures; bone or dental cements are often used. A widely used polymer; polymethyl-methacrylate (PMMA), has been long applied in this regard (Rohmiller 2002). However, this polymer is classified as a bioinert material that can be accepted by the human body without having a positive interaction; bioactivity, with the surrounding tissues. Therefore, attempts have been done to introduce more bioactive bone/dental cements to replace PMMA.

Gypsum has been always considered a bioresorbable material and has wide scope of biomedical applications. In fact, gypsum is one of the first known biomaterials to be introduced to augment broken hard tissues (Orsini 2004). However, gypsum as a calcium sulfate is characterized by its fast resorption after implantation, which may lead to limited stability of the cement after use. In addition, its chemical composition is different from that of the mineral components in hard tissues; HAp. Due to these concerns, a bioactive calcium silicate; known as wollastonite, has been considered to be added to gypsum to improve its bioactivity. Wollastonite is relatively more stable than gypsum in the body and is known to bond to the surrounding bone tissue through the formation of bone apatite-like layers on its surfaces after implantation (Liu 2008).

The current study investigates the formation of a composite of gypsum and wollastonite at weight percentages of 1, 5, and 10%. Three types of wollastonites; varying in their degree of crystallinity were used in the study. Powder mixtures of a gypsum precursor; Plaster of Paris (POP) and wollastonite were well blended prior to reactions with water. The effect of using as-received wollastonite fibers or those treated in acidic media on the setting reactions, phase composition, morphology, mechanical properties and the preliminary *in vitro* performance of the produced

composites were studied. Phase composition and morphology were investigated by XRD, FT-IR, TGA, and SEM techniques. Both tensile and compressive strengths of the composites were measured. Preliminary *in vitro* performance tests were carried out in simulated body fluids and were followed by studying the variations of concentrations of certain ions in the solutions and morphology of the SBF-treated composites after soaking for up to 14 days in these solutions.

Results showed an overall enhancement in the bioactivity of the composites as a result of the addition of wollastonites; both as-received and acid-treated. A slight decrease in the mechanical properties of the composites was observed with the addition of wollastonite fibers. Phase composition of the composites indicated no interference of wollastonite with the formation of gypsum. The advantages of the currently studied composites are, therefore, the enhancement of the bioactivity and the ability to control the biodegradation of the composite by controlling the proportion of POP in the original powder mixture of the reactants.

#### References

- Buckwalter JA, Glimcher MJ, Cooper RR, Recker R. Instr Course Lect. 1996;45:371-86.
- Orsini G, Ricci J, Scarano A, Pecora G, Petrone G, Lezzi G, J. Biomed. Mater. Res. Part B: Appl. Biomater. 199–208, 68B (2004).
- Michael T. Rohmiller, MD\*, Dugan Schwalm, MS, R. Chris Glattes, MD, Tarek G. Elalayli, MD, Dan M. Spengler, MD. The Spine Journal, 255–2602, 2 (2002)
- Xuanyong Liu, Macro Morra, Angelo Carpi, Baoe Li. 526-529, 62 (2008)

## Mixed Elastic Variational Formulation of Composite Plates Based on Dimension Reduction Method

MOHAMMAD JAVAD KHOSHGOFTAR<sup>1</sup>, MOHAMMAD MIRZAALI<sup>2</sup>

<sup>1</sup> Department of Mechanical Engineering, Faculty of Engineering, Arak University, Iran,

<sup>2</sup> Institute for Surgical Technology and Biomechanics, University of Bern, Switzerland

In the present research, a new modeling approach for elastic composite plates is studied. By adopting mixed variational formulation and dimension reduction method along the thickness, a general plate model is derived. Firstly, shape functions weighted with arbitrary coefficients adopted along the thickness of plate for both displacement and stress field and then, partial differential equation system of plate is derived by using

the Hellinger-Reissner principle. Moreover, a comparison between current work and other theories such as Classical and First Order Shear Deformation Theory has been done, and advantages of this method are discussed. Needless of shear correction factor, more accurate results and independent stress from displacement field are some advantages of this approach.

# Effect of Friction on Material Mechanical Behaviour in Non-equal Channel Multi Angular Extrusion (NECMAE)

MOHAMED S. EL-ASFOURY<sup>1</sup>, MOHAMED N. A. NASR<sup>1,2</sup>, AHMED ABDEL-MONEIM<sup>1</sup>

<sup>1</sup>Dept. of Materials Science & Engineering, Egypt-Japan University of Science & Technology, Alexandria, Egypt

<sup>2</sup>Dept. of Mechanical Engineering, Faculty of Engineering, Alexandria University, Egypt

Severe plastic deformation (SPD) is typically used to achieve significant grain refinement, which in turn results in higher mechanical strength and crack resistance, but lower ductility. For bulk ultra-fine grain (UFG) materials, additional requirements - such as, homogeneity and reasonably equi-axed grains with the majority of grain boundaries having high angles of disorientation - are required. Different SPD techniques are currently available, where the equal channel angular pressing (ECAP) and high pressure torsion (HPT) are the most widely used for producing UFG materials.

The ECAP technique was first introduced by (Segal et al., 1981). However, in order to achieve higher degrees of refinement and better degrees of homogeneity, different modifications have been presented; for example, equal channel multi-angular pressing (ECMAP), and non-equal channel angular pressing (NECAP), which impose higher strains compared to ECAP (Hasani et al., 2010). Another example is the twist channel angular pressing (TCAP), where a twist angle is introduced at the die inlet in order to increase the imposed strains and improve homogeneity (Kocich et al., 2013). Even though these modified processes showed better results than ECAP, they are still characterized by irregular shear strain distribution, where the deformation inhomogeneity index increases with corner angle, strain hardening and friction effects.

In an effort to improve the degree of homogeneity and impose higher strains, the current authors have developed a new process, with the aid of finite element modelling (FEM), which combines ECMAP with extrusion (El-Asfoury et al., under review). The new process, named "non-equal channel multi angular extrusion (NECMAE)", uses a die with three channels. The first two represent a standard ECAP process, while the third one experiences a reduction in cross-sectional area. Different percentages of area reduction (10%, 30% and 50%) were examined at well-lubricated conditions. It has been shown that, NECMAE improves the degree of uniformity and imposes higher magnitudes of strains; i.e., more grain refinement. Such results were attributed to back pressure effects, as well as the change in the shear angle during deformation.

The current work represents the second step in developing the NECMAE process, where the effect of friction on process mechanics is examined. FEM was used to model a NECMAE process with 50% area reduction, where different values were assigned to the friction coefficient (0, 0.1 and 0.2). A two-dimensional thermo-mechanical plane strain model was built using the commercial software ABAQUS/Explicit. The workpiece material is pure aluminium. The model was validated by comparing the predicted average strain values to available data in the literature.

The coefficient of friction was found to affect the corner gap size, as friction tends to increase the sticking possibility of the workpiece to the die. Accordingly, this helps in filling up the dead zone, and results in higher temperatures especially near the die surface. However, as expected, the central portion of the workpiece was found to be slightly affected. Finally, cases with higher coefficient of friction were found to have higher and much uniform plastic deformation, as well as higher required punching loads.

## References

- Segal, V. M., V. I. Reznikov, A. E. Drobyshevskii, and V. I. Kopylov. 1981. "Plastic Metal Working by Simple Shear." *Izvestia Akademii nauk SSSR. Metallurgy* 115–23.
- Hasani, Arman, László S. Tóth, and Benoît Beausir. 2010. "Principles of Nonequal Channel Angular Pressing." *Journal of Engineering Materials and Technology* 132(3):031001. Retrieved November 10, 2014
- Kocich, Radim, Lenka Kunčická, Milan Mihola, and Kateřina Skotnicová. 2013. "Numerical and Experimental Analysis of Twist Channel Angular Pressing (TCAP) as a SPD Process." *Materials Science and Engineering A* 563:86–94.
- El-Asfoury M., Nasr M. and Abd Elmoneim A. "Modelling Material Behaviour during Non-equal Channel Multi Angular Extrusion (NECMAE) - A New Process", under review.

# Poster

---

Poster Topic A:

***Multiscale phenomena in plasticity***

# The effect of hydrogen on the macroscopic strain localization of steels

SVETLANA BARANNIKOVA<sup>1,2</sup>, ANATOLY MALINOVSKY<sup>2</sup>, DMITRII PESTSOV<sup>2</sup>

<sup>1</sup>Institute of Strength Physics & Material Science, SB RAS, Tomsk, Russia

<sup>2</sup>Tomsk State University of Architecture & Building, Tomsk, Russia

Embrittlement due to hydrogen (H) involves a vast loss of mechanical properties with the following characteristics such as, for example, decrease of ductility and fracture tension with the increase of H concentration (Sofronis, Liang & Aravas 2001). This phenomenon poses a serious practical problem, the solution of which determines the durability and safety of operation of a steel structure. Previously, we presented experimental data (Zuev & Barannikova 2010) according to which plastic strain development in solids exhibited a localized character over the entire process. This phenomenon is especially clearly manifested on a macroscopic scale, where the patterns of strain localization are related to the deformation hardening operative on the corresponding stages of straining. The main aim of this investigation was to elucidate the effect of dissolved hydrogen on the macroscopic plastic flow localization patterns in tensile strained steels.

The investigations were performed for FCC monocrystals of the austenitic stainless steel (*Fe-18%Cr-12%Ni*) and BCC polycrystals of low-carbon steel (*Fe-0.07%C*). The samples had a working part with dimensions of 25·5·1 mm and were tensile strained at 300 K on an Instron testing machine at a mobile clamp velocity of  $8.3 \cdot 10^{-6}$  m/s. The stress-strain diagram was obtained simultaneously with measuring the fields of the displacement vectors  $r(x, y)$  with the aid of double-exposure speckle photography technique. A special device was also designed (Zuev, Gorbatenko & Pavlichev 2010); it had field of vision  $\sim 100$  mm; spatial resolution comparable to optical microscopy  $\sim 1 \dots 2$   $\mu\text{m}$  and real-time mode of operation. This enabled reconstruction of displacement vector fields  $r(x, y)$  for the sample surface. On the base of this data, the plastic distortion tensor is evaluated for the deforming sample in the coordinates  $x, y$  and  $z$ , i.e. longitudinal ( $\varepsilon_x$ ), transverse ( $\varepsilon_y$ ), shear ( $\varepsilon_{xy} = \varepsilon_{yx}$ ) and rotation ( $\omega_z$ ) components. This technique can visualize localized plastic flow nuclei, using the spatial distributions of

plastic distortion tensor components; the kinetics of nuclei motion can be determined from the temporal evolution of nuclei.

The samples were electrolytically saturated with hydrogen in a thermostatted three-electrode electrochemical cell with graphite anode, operating at a controlled constant cathode potential of  $U = -600$  mV (relative to silver chloride reference electrode) in a 1 N sulfuric acid solution containing 20 mg/l thiourea. The hydrogenation was effected at 323 K for 24 h after preliminary purging the solution with nitrogen. The current-voltage curves were recorded using an IPC-Compact potentiostat.

It has been found that the propagation velocity and wavelength of the localized plasticity waves are affected by the strength characteristics of steels, which are determined by the interstitial impurity content  $H$ . Therefore, the wave patterns of macroscopic localized plasticity appear to be useful for a detailed analysis of plasticity exhibited by real metals and alloys. The use of such patterns can help derive more exhaustive and accurate information about the processing limits of a material relative to conventional characteristics, e.g. elongation and reduction of cross-section.

## References

- Sofronis, P., Liang, Y. & Aravas, N. (2001): Hydrogen induced shear localization of plastic flow in metals and alloys: *European Journal of Mechanics – A: Solids*, Vol. 20: 857-872.
- Zuev, L.B. & Barannikova, S.A. (2010): Evidence for the existence of localized plastic flow auto-waves generated in deforming metals: *Natural Science*, Vol. 2: 476-483.
- Zuev, L.B., Gorbatenko, V.V. & Pavlichev, K.V. (2010): Elaboration of speckle photography techniques for plastic flow analyses: *Measurement Science and Technology*, Vol. 21, 054014: 1-5.

## Atomistic analyses of nucleation and propagation behavior of ridge shaped kink band in long-period-stacking-ordered phase

RYOSUKE MATSUMOTO, MASAYUKI URANAGASE

Kyoto University, Kyoto, Japan

Materials with strong plastic-anisotropy typically show kinking deformation under a compressive deformation. Deformation boundaries of kinking deformation (kink boundary) do not have specific misorientation-angle, and thus it is considered that kinking deformation occurs by unclear mechanisms different from twinning deformation.

Recently developed Mg alloys that contain long period-stacking-ordered (LPSO) phases have attracted considerable attention because they have been reported to exhibit excellent mechanical properties, including high yield stress and reasonable ductility (Kawamura 2001). The LPSO phases deform by generating a lot of ridge-shaped deformation bands (Hagihara 2010). Based on the detailed observation of the kink boundaries, the deformation bands are confirmed special type of kink band. It is also examined that these deformation bands appear with shorter timescale than tens  $\mu$ s (Hagihara 2013). This study aims to reveal the formation mechanisms of ridge shaped kink band in LPSO phases.

In this study, we performed molecular dynamics simulations. The model material employed is LPSO phase with 10H stacking which is composed by single element whose interatomic interaction is described by the Lennard-Jones potential (Matsumoto 2013). Here, we performed two kinds of MD simulations; (1) bending deformation of beams under compressive load parallel to the basal plane, and (2) compressive deformation of square columns including initial dislocations which constitute TB (tilt boundary). Most simulation models are composed by about 1.5 million atoms, and all simulations were performed at 300 K.

(1) From the bending deformation of beams, it is confirmed that, initially, (a) non-basal slips occur, and (b) low angle boundaries are formed through cross-slip mechanism described in Matsumoto 2013. When the misorientation angle reaches about 20°, (c) the boundaries become dislocation source, and (d) the dislocation emission from the boundaries drastically increases the misorientation angle of themselves.

(2) The compressive deformation of square columns with initial TB indicated that once tilt boundary is formed in the LPSO phase through some processes, such boundary emits a lot of dislocations to both sides of the boundary under compressive load and forms ridge shaped kink band.

### References

- Hagihara, K. & Yokotani, N. & Umakoshi, Y. (2010): *Intermetallics*, 18: 267-276.
- Hagihara, K. & Fukusumi, Y. & Yamasaki, M. & Matsumoto, R. & Honnami, M. & Izuno, H. & Nakano, T. & Kawamura, Y. (2013): Deformation behavior of LPSO phase and Zn accompanied by kink band formation, 8th Pacific Rim International Congress on Advanced Materials and Processing 2013; 2: 973-978, Waikoloa.
- Kawamura, Y. & Hayashi, K. & Inoue, A. (2001): *Materials Transaction*, 42: 267-276.
- Matsumoto, R. & Uranagase, M. & Miyazaki, N. (2013): *Materials Transaction*, 54: 686-692.

## Microtension behavior of hydrogen-containing metastable austenitic stainless steel

RYO MATSUOKA, KAORU KOGA, YOJI MINE, KAZUKI TAKASHIMA

Kumamoto University, Kumamoto, Japan

The susceptibility to hydrogen embrittlement of austenitic stainless steels is dependent on their austenite stability. The metastable austenitic stainless steel such as type 304 suffers from severe HE, whereas the type 310S stable austenitic steel exhibits a little degradation

in ductility due to deformation localization in the presence of hydrogen. This difference is related to the intrinsic tendency to the deformation-induced martensitic transformation. On the other hand, fractographic observation often showed a planar fracture feature in HE austenitic stainless steels, and it was presumably formed in

association with annealing twin boundaries (Fukuyama, 1985). However, the role of twin boundary in the HE of metastable austenitic steels has not yet been clarified. The present study applied microtension testing to the analysis of the HE in bicrystals, with particular focus on the effect of twin boundary on the deformation-induced martensite transformation.

The material used in the present study was a solution treated 304 stainless steel with an average grain size of 60  $\mu\text{m}$ . Microtension specimens with  $20\mu\text{m}\times 20\mu\text{m}\times 50\mu\text{m}$  dimensions of the gauge section were fabricated using focused ion beam. Single-crystalline specimens and bicrystalline specimens with a twin boundary were prepared so that the loading direction (LD) is parallel to [111]. For the bicrystalline specimen, the twin boundary is arranged perpendicular to the LD. Hydrogen was cathodically charged at a current density of  $27\text{ A m}^{-2}$  in a  $\text{pH} = 3.5$  aqueous solution of  $\text{H}_2\text{SO}_4$ . Specimens were

hydrogen-charged for 7h at a temperature of 353K. Microtension testing was performed at room temperature in the atmospheric air and at a loading rate of  $0.1\ \mu\text{m s}^{-1}$ . After tensile test, the deformation microstructure was observed by orientation imaging microscopy (OIM).

In the uncharged single-crystalline specimen, after yielding occurred at a stress of 270 MPa, the 910 MPa ultimate tensile strength and the 70% strain-to-failure were attained through a significant strain hardening. The uncharged bicrystalline specimen exhibited a higher yield stress, but lower ultimate tensile strength and strain-to-failure. This is because the deformation was hindered by the twin boundary and was localized at the one grain. In both the single- and bicrystalline specimens, the yield stress was increased but the ductility was drastically decreased by the hydrogen pre-charge. As for the fracture morphology, the hydrogen-charged single- and bicrystalline specimens exhibited a quasi-cleavage and a planar facet fracture, respectively. The OIM observation of the deformation microstructures suggests that hydrogen-induced fractures occurred along the martensite block and austenite twin boundaries.

#### Reference

Fukuyama, S., Yokogawa, K., Kudo, K., & Araki, M. (1985): Fatigue Properties of Type 304 Stainless Steel in High Pressure Hydrogen at Room Temperature, *Trans. Jpn. Inst. Met.*, 26: 325-331.

## Microtension behaviour of dual-phase steel subjected to pre-straining

SHINYA OGATA<sup>1</sup>, YOJI MINE<sup>1</sup>, KAZUKI TAKASHIMA<sup>1</sup>, HIROSHI SHUTO<sup>2</sup>, TATSUO YOKOI<sup>2</sup>

<sup>1</sup>Kumamoto University, Kumamoto, Japan

<sup>2</sup>Nippon Steel & Sumitomo Metal Corporation, Oita, Japan

The dual-phase (DP) steel is a high tensile strength steel consisting of a soft ferrite phase and a hard martensite phase. This steel is widely used for automotive applications because of its enhanced balance between strength and ductility. However, its low hole expandability is often a major drawback. When the DP steel is subjected to deformation, strain partitioning occurs between the ferrite and martensite phases, resulting in the inhomogeneity of the strain distribution (Park, 2014). The local strain, which depends on the constraint conditions, differs from the macroscopic strain. Thus, it is important to comprehend the mechanical characteristics of the microstructures evolved by localized deformation through the stress concentration at the interface between the ferrite and martensite phases. In the present study, we conducted microtension testing on inhomogeneous microstructures evolved by pre-straining with cold rolling, with particular focus on the role of the fine-grained ferrite microstructure in the deformation and fracture process of the DP steel. The material used in the present study was a low carbon steel, composed of 0.14 C, 1.00 Mn (mass%), and the balance Fe. A DP microstructure with a martensite

fraction of 29 vol.% was obtained by heating at a temperature in ( $\alpha+\gamma$ ) two-phase region followed by water cooling. Pre-strains were introduced by cold rolling (CR) at reductions of 60% and 88% in thickness. The deformation microstructure was characterized using electron backscatter diffraction analysis. Microtension specimens with  $20\mu\text{m}\times 20\mu\text{m}\times 50\mu\text{m}$  dimensions of the gauge section, including the ferrite/martensite

interface, were fabricated using focused ion beam. Microtension testing was performed at room temperature in the atmosphere and at a loading rate of  $0.1\ \mu\text{m min}^{-1}$ .

Ferrite grains with continuously gradated crystallographic orientations were observed after 60% CR. By 88% CR, an ultrafine-grained ferrite microstructure was also evolved in the region neighbouring the martensite phase. The grain refinement presumably occurred by severe deformation at the interface between the ferrite and martensite phases. In the 60% CR specimen exhibiting an yield stress of  $\sim 720\text{ MPa}$  and an elongation-to-failure of  $\sim 10\%$ , yielding occurred in the coarse ferrite grain, leading to a chisel-edge failure. By contrast, the 88% CR specimen exhibited high yield

strength but low ductility when compared to the 60% CR specimen. In the 88% CR specimen, a shear type fracture occurred in the ultrafine-grained ferrite without necking. This may be attributed to the strain localization at the ultrafine ferrite grains. In this presentation, we will discuss the plastic deformation transfer at the ferrite/martensite interface.

#### Reference

Park, K., Nishiyama, M., Nakada, N., Tsuchiyama, T. & Takaki, S. (2014): Effect of the martensite distribution on the strain hardening and ductile fracture behaviors in dual-phase steel, Mater. Sci. Eng. A, 604: 135–141.

## Adaptive boost molecular dynamics method for study of rare events in plastic deformation

NAOMCHI TSUJI<sup>1</sup>, AKIO ISHII<sup>1</sup>, JUNPING DU<sup>1</sup>, SHIGENOBU OGATA<sup>1,2</sup>

<sup>1</sup>Osaka University, Japan

<sup>2</sup>Kyoto University, Japan

Molecular dynamics (MD) is a powerful technique to study the plastic deformation of materials under atomic scale. However, because of the limited time-scale (nanoseconds) in regular MD simulation, the strain rate in MD ( $10^6$ – $10^{10}$  s<sup>-1</sup>) is orders of magnitude higher than that in experiment ( $10^{-6}$ – $10^1$  s<sup>-1</sup>). So it is difficult to analyze long time-scale phenomena by combining MD simulations and experiments, such as shear-coupled grain boundary motion and dislocation nucleation from surface or grain boundary.

An accelerated MD simulation method, adaptive boost (AB) MD method [1], have been developed to study the rare events in material science. In this method, the smooth histogram of collective variables (CVs) is firstly evaluated by regular MD simulation. CVs can be used to characterize the accelerated phenomena and have one or more degrees of freedom. Then, a boost potential is determined by  $\Delta G^\ddagger$ , and is added to the original free energy surface. A fictitious force on particle can be evaluated based on boost potential,  $\Delta G^\ddagger$ . Such adaptive and cumulative operations are repeated until state transition occurs. The time acceleration is evaluated by the hyperdynamics theorem [2], the relationship between the transition period  $\tau^*$  and the actual transition period  $\tau$  can be expressed as  $\tau^* = \tau \exp(\beta \Delta G^\ddagger)$ .

The definition of CVs is correlated to the atomic process in the rare events. We define CVs as  $\mathbf{r}_i$ , where  $N$  is total number of atoms,  $\mathbf{r}_i$  is prepared parameter, and  $\mathbf{r}_i$  is coordinate of atoms. By this definition, it is possible to accelerate rare events that can be characterized by linear combination of coordinate of atoms.

In this study, we applied the ABMD method to the shear-coupled grain boundary migration and the dislocation nucleation from a corner of nanopillar and a grain boundary in Cu. First, the behavior of a symmetric tilt grain boundary in Cu crystal is simulated under shear stress along the grain boundary. The grain boundary migration velocity and strain rate consistent with those in experiments are obtained. The results demonstrate a mechanism transition from displacive to diffusive motions with increasing temperature. Next, we applied this method to dislocation nucleation from a corner of nanopillar and a grain boundary of Cu. In the simulation, a half partial dislocation loop is emitted from the corner of nanopillar and grain boundary, and propagates on the boosted {111} planes. The dislocation nucleation rates, which is beyond the ability of regular MD, are obtained under a wide range of temperature and strain. The activation parameters, such as activation enthalpy and activation volume, are evaluated from the simulations.

#### References

- [1] Ishii, A., Ogata, S., Kimizuka, H. & Li, J. (2012): Adaptive boost molecular dynamics simulation of carbon diffusion in iron, Physical Review B, 85-6, 064303.
- [2] Arthur, F. Voter (1997): Hyperdynamics: Accelerated Molecular Dynamics of Infrequent Events, Physical Review B, 78-20, 3908.

# Quantitative evaluation of dislocation nucleation as thermal activation process via atomistic simulations

MASAYUKI URANAGASE, RYOSUKE MATSUMOTO

Kyoto University, Kyoto, Japan

Dislocation nucleation, which is one of the elementary processes of deformation, plays an important role for deformation when there are less pre-existing dislocations, e.g., compression of micro pillar metals. However, deformation due to dislocation nucleation is not confined to the case where the size of the specimen is extremely reduced. For instance, it is proposed that formation of a kink band occurred in recently developed magnesium (Mg) alloy (Kawamura 2001) based on dislocation nucleation (Hagihara 2010). This kink band is contributed to overwhelming strength of this alloy with keeping fair ductility, which extends possibility for application of Mg to various industrial applications. Therefore, it is worth quantitatively evaluating dislocation nucleation for understanding some kinds of macroscopic deformation modes.

In this study, we consider dislocation nucleation in pure Mg via atomistic simulations. Atomistic simulation enables to analyze detailed mechanisms of deformation, though applicable scales of time and space are strictly restricted because of its heavy computational cost. In particular, when one treat elementary process of deformation, one has to overcome the problem comes from restriction of time scale. Here, we adopt metadynamics method (Laio 2008) to solve this problem. In metadynamics method, collective variables, which characterize the phenomenon focused on, are initially set. Then, history dependent bias potential is added to the system to urge the change of collective variables. This bias potential is also used for construction of free energy surface in the space spanned by collective variables. In our work, we construct one dimensional collective variable for dislocation nucle-

ation (Uranagase 2014) and evaluate the activation free energy of nucleation of basal and prismatic dislocations.

Using the method mentioned above, we studied the dependence of the activation free energy of dislocation nucleation on ambient temperature and applied stresses in detail. For instance, it is possible to estimate the shear stress in slip direction necessary for dislocation nucleation in realistic time scale if the activation free energy obtained from atomistic simulations is fitted to analytic expression. We also discuss the linear relation between the enthalpic and the entropic contributions to the activation free energy, which are obtained from temperature dependence of the activation free energy, and the influence of normal stress on degree of nucleation of dislocation.

## References

- Hagihara, K. *et al.* (2010): Plastic deformation behavior of  $Mg_{12}YZn$  with 18R long-period stacking ordered structure. – *Intermetallics*, 18: 267-276.
- Kawamura, Y. *et al.* (2001): Rapidly Solidified Powder Metallurgy  $Mg_{97}Zn_1Y_2$  Alloys with Excellent Tensile Yield Strength above 600 MPa. – *Mater. Trans.*, 42: 1172-1176.
- Laio, A. and Gervasio, F. L. (2008): Metadynamics: a method to simulated rare events and reconstruct the free energy in biophysics, chemistry and material science. – *Rep. Prog. Phys.*, 71: 126601.
- Uranagase, M. and Matsumoto, R. (2014): Thermal activation analysis of enthalpic and entropic contributions to the activation free energy of basal and prismatic slips in Mg. – *Phys. Rev. B*, 89: 224103.

Poster Topic B:

***Mechanical behavior***

---

## Residual stress evaluation of shot peened Ag-based contact materials via diffraction technique

SEUNG-YUB LEE<sup>1</sup>, JINGJING LING<sup>1</sup>, HYO-SOO LEE<sup>2</sup>, MIN-HA LEE<sup>2</sup>

<sup>1</sup>Department of Applied Physics and Applied Mathematics, Columbia University, New York, USA

<sup>2</sup>Korea Institute of Industrial Technology, Incheon, Republic of Korea

Silver cadmium oxide (Ag-CdO) is one of the most popular electrical contact materials due to its high electrical conductivity from Ag, and excellent wear & arc resistance from CdO. For example, the 90% Ag and 10% CdO has been widely used in medium to heavy duty switches and controls, wall switches, motor starters, DC switches and relays, AC and DC circuit breakers, motor protectors, etc, because it has a high current carrying capability, low arc erosion, high conductivity (80% IACS), good hardness (75 in HR-15T), and great sticking resistance (Brainin Company, 2015).

However, due to the imminent environmental regulations, there have been a lot of efforts to replace the toxic cadmium with other alternatives without compromising surface durability and electrical conductivity; the most successful CdO substitution so far is the silver tin oxides (Ag-SnO<sub>2</sub>) with various additives among the many other choices such as Ag-Ni, Ag-Cu, Ag-Pd, Ag-Fe, Ag-Au, etc (Frederic Pons, 2010).

The Korea Institute of Industrial Technology (KITECH) is currently developing a Cd-free (Ag-Cu-Fe)-Sn/Zn alloy system to form SnO<sub>2</sub> or ZnO via internal oxidation process to replace CdO. A minor addition of Cu and/or Fe is designed to reduce Ag for an economical reason. In order to increase surface wear resistance, shot peening process was applied, which is also expected to affect the depth of oxidation layer.

Focusing on characterization of the mechanical property of the electrical contact materials, two kinds of alloy systems have been tested: Ag(88)-Cu(1)-Fe(1)-Zn(10), and Ag(90)-Cd(10) reference. Thermal oxidation and shot peening processes were selectively applied for both alloys, and micro vickers, X-ray diffraction, and

SEM measurement were carried out for the hardness test and phase analysis.

Since surface residual stress is also a critical parameter affecting mechanical stability, Columbia University investigated residual stress under biaxial stress assumption with the traditional  $\sin^2\psi$  technique (Noyan, 1987). Experiments were performed at the synchrotron beam line, X20A, in the National Synchrotron Light Source (NSLS) in Brookhaven National Laboratory.

Residual stress evaluation from the silver phase shows that shot peening was not much effective in terms of stress reinforcement, especially when followed by the thermal oxidation process to form ZnO or CdO. However, it affected internal oxidation behavior differently for each alloy system. This seems to be related to the stress-induced diffusion mechanism as well as interface formation between Ag and ZnO/CdO (Necker, 1988). The quantitative results will be presented along with microstructural analyses.

### References

- Brainin Company (2015): Electrical Contact Materials List in the Technical Resources. <http://www.pepbrainin.com/technical-resources/electrical-contact-materials>.
- Pons, F. (2010): Electrical Contact Materials Arc Erosion: Ph.D. Thesis, Georgia Institute of Technology, p 8-11.
- Noyan, I. C., and Cohen, J. B. (1987): Residual Stress, Springer-Verlag, New York, NY, p 117-125.
- Necker, G. and Mader, W. (1988): Characterization of Ag/CdO interfaces: Philosophical Magazine Letters, 58, 4, p 205-212.

## Structural phase states and residual stresses in the Ta/TiNi surface layers before and after high-current pulsed electron beam impact

L.L.MEISNER<sup>1,2</sup>, M.G.OSTAPENKO<sup>1,3</sup>, M.A.ZAKHAROVA<sup>3</sup>, E.YU.GUDIMOVA<sup>1,2</sup>

<sup>1</sup>Institute of Strength Physics and Materials Science of Siberian Branch Russian Academy of Sciences, Tomsk, Russia

<sup>2</sup>Tomsk State University, Russia

<sup>3</sup>Tomsk Polytechnic University, Russia

It is known that NiTi based alloys are widely used in medicine. There is a problem release of nickel ions, which is potentially dangerous. As barrier coatings can

be used coating of tantalum, which have good biocompatibility. To improve the adhesion strength of the tantalum coating to the NiTi substrate can be used electron beam impacts. Apparently, the surface properties

of NiTi alloy with tantalum coating after electron beam impacts are defined by the structural phase state and residual stress in its modified surface zone.

Therefore, the aim of this work is to study the formation of structural-phase states and residual stresses in the tantalum coatings and based on NiTi, and their changes after impacts with pulsed electron beams.

As the initial samples was used alloy NiTi, which were characterized by a two-phase state (~95 vol.% B2+~5 vol.% Ti<sub>2</sub>Ni). Magnetron sputtering was carried out at the facility KVANT-M. The coating thickness was about 400 nm (hereinafter – Ta/NiTi). The Ta/NiTi specimens were subjected to pulsed surface irradiation by a low-energy high-current electron beam (LEHCPEB). The beam energy density was  $E = 15 \text{ J/cm}^2$ . X-ray diffraction (XRD) analysis was performed at room temperature on a DRON-7 diffractometer.

It was found that after the deposition of Tantalum coating on the X-ray diffraction pattern of samples the absence of peaks of the Ti<sub>2</sub>Ni phase and new reflexes correspond to bcc  $\alpha$ -Ta (space group Im3m) and tetragonal  $\beta$ -Ta (space group P42/mnm) phases are observed, with the prevalence of the  $\alpha$ -Ta phase (~ 65 vol.%). Interpretation of the X-ray pattern of the sam

ple Ta/NiTi after LEHCPEB shows that the new peaks correspond to the B19' martensite phase with monoclinic structure (space group P2<sub>1</sub>/m).

Analysis of the depth distribution of the chemical elements in Ta/NiTi samples, obtained by AES, showed that, between the coating and the substrate, there is a transition layer (~400 nm) containing 8 ÷ 20 at.% Oxygen and ~ 8 at.% Carbon, that can lead to the formation therein of oxide and carbide phases and decrease the adhesive strength of Ta coatings with substrate. The treatment by LEHCPEB led to forming on the surface of NiTi uniform layer consisting mainly of Ta with no clearly defined boundaries between the coating and the NiTi substrate was formed. We can assume that in the surface layer of the samples Ta/TiNi after LEHCPEB as a result of partial dissolution of tantalum atoms in NiTi was formed ternary phase based on (TiNi)–Ta with B19' martensite structure [1].

Comparison of the results of quantitative evaluation of the residual stress in the surface layers Ta/TiNi samples before and after electron-beam impacts showed that after modification, the amount of residual stress in B2 phase in the surface layer of the samples was not significantly increased.

#### Reference

1. Gong C.W., Wang Y.N., Yang D.Z. Phase transformation and second phases in ternary Ni–Ti–Ta shape memory alloys // *Materials Chemistry and Physics*, 2006. – V. 96. – P. 183–187.

## The effect of residual stresses on the change of the B2 phase lattice parameter in the NiTi with Tantalum coating after pulsed electron-beam treatment

M.G. OSTAPENKO<sup>1,2</sup>, L.L. MEISNER<sup>1,3</sup>, M.A. ZAKHAROVA<sup>2</sup>, E.YU. GUDIMOVA<sup>1,3</sup>

<sup>1</sup> Institute of Strength Physics and Materials Science of Siberian Branch Russian Academy of Sciences, Tomsk, Russia

<sup>2</sup> Tomsk Polytechnic University, Russia

<sup>3</sup> Tomsk State University, Russia

Nickel titanium is widely used as material for medical application due to shape memory effect and superelasticity. High requirements were claimed on the alloy in regard to its biocompatibility and corrosion resistance [1]. One of the ways to improve these properties is the biocompatible coatings deposition. Highly attractive metal to apply is tantalum, but coating formation requires taking into account the surface texture of NiTi may change because of martensitic transformation. This can lower the adhesive strength of coating. Adhesion can be improved by low energy high current pulsed electron beam treatment (LEHCPEB).

Residual stresses can be formed as a result of LEHCPEB not only in the area of direct irradiation, but also in the layers below. The presence of residual stresses leads to the significant change of functional properties of NiTi alloys [2].

The aim of this work is to study residual stresses fields' evolution in the near-surface layers of NiTi with tantalum coating, irradiated with electron beam of 15 J/cm<sup>2</sup> energy density.

The investigation of structure-phase states and the estimation of residual stresses were performed using X-ray diffraction analysis, which allows determining lattice and elastic constants both. Symmetric and asymmetric scanning schemes were applied to study the structure in the bulk and near surface layers.

Initial sample was made of alloy, melted from iodide titanium and NO-grade nickel (Ti<sub>49,5</sub>Ni<sub>50,5</sub>), and then coating with thickness of 400 nm was deposited by magnetron sputtering. The sample under study was in three-phase state at room temperature: phase B2 (bcc structure, CsCl ordering) of substrate,  $\alpha$ -Ta (bcc, space group Im3m) and  $\beta$ -Ta (tetragonal, space group P42/

nm) phases of coating. It was revealed phase  $\beta$ -Ta disappeared after LEHCPEB treatment due to rapid quenching ( $\sim 10^9$  K/s) of the near surface layer of the sample. Peaks of martensitic phase B19' was found while analyzing diffraction patterns of irradiated sample.

For sample, treated with LEHCPEB, it was revealed that lattice parameter of B2 phase has changed from 3.0108 up to 3.0247 Å. That might be related to the presence of significant residual stresses.

Quantitative estimation comparison for initial and irradiated samples shown LEHCPEB treatment causes significant change in residual stresses' values from  $\sim 145$  MPa up to  $\sim 540$  MPa for B2 phase in the near-surface layer.

Thus, analysis of obtained results have shown, that LEHCPEB treatment with energy density of 15 J/cm<sup>2</sup> for samples with coatings leads to partial coating retention, B19' martensitic phase and significant residual stress values appearance.

#### References

- [1] Cheng Y., Cai W., Li H.T., Zhao C. (2003): Corrosion property of TiNi shape memory alloys coated with tantalum. – *Journal of Material Science*, 1681-1683; Harbin.
- [2] Meisner L.L., Lotkov A.I., Ostapenk M.G. Gudimova E.Yu. (2012): X-ray diffraction study of residual elastic stress... - *Physical Mesomechanics*, 79-89; Tomsk.

## Laser assisted residual stress determination in ceramic coatings

PETER WEIDMANN<sup>1</sup>, GIANCARLO PEDRINI<sup>2</sup>, VENANCIO MARTÍNEZ-GARCÍA<sup>3</sup>, ULRICH WEBER<sup>1</sup>, ANDREAS KILLINGER<sup>3</sup>, MARTIN WENZELBURGER<sup>3</sup>, SIEGFRIED SCHMAUDER<sup>1</sup>, RAINER GADOW<sup>3</sup>, WOLFGANG OSTEN<sup>2</sup>

<sup>1</sup>University of Stuttgart, IMWF, Germany

<sup>2</sup>University of Stuttgart, ITO, Germany

<sup>3</sup>University of Stuttgart, IFKB, Germany

Technical compounds under high thermal and abrasive loads are often coated to enhance the materials wear resistance and thermal durability. Therefore, ceramic coatings with high hardness and low thermal conductivity are preferable. Such coatings may be produced by i.e. plasma or high velocity oxygen fuel spraying. But due to quenching of splats and differences in the thermal properties of substrate and coating, residual stresses will build up. These stresses can lower the lifetime of the coated product or even enhance it in the case of pressure stresses within brittle ceramic layers.

A convenient way to determine such residual stresses are incremental hole drilling measurements. Hereby, a hole is drilled incrementally into the stress afflicted material. This leads to a relaxation of surrounding material. The hereby occurring surface strains around the hole can be measured with strain gauges and transferred into the depth dependent residual stress. But this method implies direct contact with the specimen and the preparation of strain gauge rosettes which leads to a rather time consuming process especially for incremental drilling procedures. To overcome these constraints a method is wanted where the drilling is done by a laser and the occurring surface deformations are recorded by digital holography measurements. Therefore, new approaches and extension of known procedures are required to determine residual stresses contact-free with the imposed method.

The presented work is related to the underlying assumptions and calculations to determine the depth dependent stress values from extensive displacement

measurements in consideration for the inhomogeneous elastic material properties and deviations from cylindrical hole geometry. To cover all involved fields numerical studies for conventional hole drillings with differential and integral determination schemes were conducted and the ablation process was simulated. As the laser cannot produce ideal cylindrical geometries appropriate mathematical approximations by means of least square optimisation are used to choose a representative hole profile. Furthermore, the calculation of stress based on full field displacement measurements is done with an own developed program in several depth increments. These calculations are based on numerical calibration data for the elastically inhomogeneous compound of coating and substrate. The physical experiments were done on aluminium and steel plates with applied aluminium- or aluminium-titanium-oxide layers. The coatings have been made by atmospheric plasma spraying up to a thickness of 200  $\mu\text{m}$ .

#### References

- Weidmann, P. & Weber, U. & Schmauder, S. & Venancio Martínez-García (2014): Investigation of Influence Factors on Residual Stress Determination within Coated Surfaces in Consideration of the Differential and Integral Method – In: *Advanced Materials Research* 996: 307-312.
- Schajer, G. S. & Steinzig, M. (2005): Full-field calculation of hole drilling residual stresses from electronic speckle pattern interferometry data – In: *Experimental Mechanics* 45-6: 526-532.

Poster Topic C:

***Cyclic deformation behavior, crack initiation & crack growth of metals***

---

## Fatigue crack initiation from notches and mean stress effect in 2024 T351 Al-alloy

MUSTAPHA BENACHOUR<sup>1</sup>, NADJIA BENACHOUR<sup>1,2</sup>, MOHAMED BENGUEDIAB<sup>3</sup>

<sup>1</sup>IS2M Laboratory, Mechanical Engineering Department, University of Tlemcen, Algeria

<sup>2</sup>Physics department, Faculty of Sciences, University of Tlemcen, Algeria

<sup>3</sup>LMSR Laboratory, Mechanical Engineering Department, University of Sidi Bel Abbes, Algeria

Fatigue phenomenon presents an essential failure mode in aircraft structures. The percentage of failure varies from 55 to 61% in Aeronautic components. Crack initiation due to various defects presents the main investigation of aircraft components. The initiation of crack is essentially attributed to machining defects and to the concentration of stress at notch.

The aim of this work is to present mean stress effect on fatigue crack initiation in 2024 T351 Al-alloy used in aircraft components. In this investigation, fourth bending fatigue tests were carried out to evaluate evolution in fatigue initiation life from V-notches. A fatigue criterion was established to predict crack-initiation at the tip of a V-notch. Best correlation of present criterion was given comparatively to others results for same material and stress ratio.

## Resonant acoustic for nondestructive inspection of accumulated damage assessment in austenitic stainless steel subjected to fatigue tests in rotating bending

RICARDO A. CASALI<sup>1</sup>, MARIA A. CARAVACA<sup>2</sup>, CESAR G. VEROLI<sup>3</sup>, GABRIEL VALLEJOS<sup>3</sup>, JORGE FORTE<sup>2</sup>

<sup>1</sup>Departamento de Física. Facultad de Ciencias Exactas, Naturales y Agrimensura, Corrientes, Argentina

<sup>2</sup>Departamento de Físico-Química. Facultad de Ingeniería, Resistencia. Argentina

<sup>3</sup>Departamento de Mecánica. Facultad de Ingeniería, Resistencia, Argentina

In this work we study by resonant inspection the damage that may accrue to the specimens, subjected to fatigue tests using the method of Staircase. The resonant inspection shows enlargements (damping factor) and frequency shifts of resonance peaks of bending and longitudinal modes, indicating greater plasticity with respect to the initial state, without fatiguing. In the failed specimens crack and its position is recognized by identifying bending mode resonances (F1, F2, F3, F4) and longitudinal (L1). Specimens of steel „did not fail“ are tested again with a stress level below the fatigue limit. These are used to study, after further cyclized scheduled, based on applying the theory Miner of cumulative damage. These studies are complemented by metallographic and hardness tests at different points of specimens used in tensile tests, notched fatigued and without fatigue.

### References

- R.A. Casali et al <http://www.ndt.net/article/pan-ndt2007/papers/109.pdf>
- ASTM Standard E2001-08, Standard Guide for Resonant Ultrasonic Spectroscopy for Defect Detection in Both Metallic and Non-metallic Parts.
- G. Stultz, R. Bono and M. Schiefer, “Fundamentals of Resonant Acoustic Method NDT”, [www.modalshop.com](http://www.modalshop.com)
- Suheng-Kuei lin, Yung-Li lee, Ming-Wei Lu, “Evaluation of the staircase and accelerated methods for fatigue limit distributions”, International Journal of fatigue, Vol 23, (2001) 75-83
- Man, X. T. C., Wang, Z., and Finch R. D., “Vibration monitoring of steel beams by evaluation of resonance frequency decay rates”, J. Acoust. Soc. Am. 96 (2), 867-873 (1994).

## Determination of the Critical Resolved Shear Stress in a Ni-Al-Cr composite by Discrete Dislocation Dynamics

HERVE GAKAM<sup>1</sup>, DANIEL WEYGAND<sup>2</sup>

<sup>1</sup>KIT Karlsruhe Institut of Technology, IZBS, Germany

<sup>2</sup>KIT Karlsruhe Institut of Technology, IZBS, Germany

Within the research program IMD ([www.imd.kit.edu](http://www.imd.kit.edu)) a new high temperature superalloy shall be developed. The microstructure consists of a NiAl matrix [1], which alone has poor mechanical properties at high temperatures, and Cr fibers, which block the motion of dislocations within the NiAl matrix and increase the creep resistance significantly. The microstructure is obtained by solidification at the eutectic composition for the ternary system and under ideal conditions long Cr fibers are expected [2, 3]. In a two dimensional Cross-section with the normal parallel to the Cr fibers axis a close to hexagonal arrangement of the fibers cross-sections is observed. In order to determine the Critical Resolved Shear Stress (CRSS) for a dislocation passing through this almost hexagonally arranged obstacle field discrete dislocation dynamics (DDD) simulations are performed [2, 5]. The role of the irregularities in the arrangement and the fibers diameters in the experimentally measured microstructures is explored by a systematical variation of the obstacle distribution in the simulations. The simulations use periodic boundary conditions to eliminate surface effects and the fibers are treated in this first step as non-shearable and those bypassing occurs by the Orowan mechanism. In order to determine the CRSS valid for this superalloy the length L between two centers of Cr fibers is varied. Furthermore several distributions of the Cr precipi-

tates taking in consideration the variation of the length L and Diameter D of the fibers are produced on the basis of the experimental received data and used in the simulation set up [4].

It is observed that, with increasing irregularity the CRSS as their spread in the obtained increases. Furthermore the effect of the elastic interaction between multiple dislocations on parallel planes gliding through this obstacle field shall be addressed. At the end the softening effect at the boundary interface between Cr fibers and NiAl matrix doing to lattice mismatch is investigated and it was found that the CRSS decrease in this case for non shearable fibers of about 20%.

### References

- [1] R. R. Bowman, R. D. Noebe et al., metall. Trans. V23A p.1493, 1992
- [2] Walter, J.L. and Cline, H.E. Metal. trans. volume 1, p. 1221, 05.1970
- [3] M. Heilmaier, T. Haenschke1, A. Gali, M. Krueger, H. Bei, E.P. George, J. Phys.: Conf. Ser. 240 012063, 2010
- [4] Bako, B. and Weygand, D. and Samaras, M. and Hoffelner, W. and Zaiser, M. Phys. Rev. B, v.78 p. 144104, 2008
- [5] D. Weygand, modell. Sim. Mater. Sci. Eng. vol. 10, pp. 437 - 468, 2002

## Cyclic softening in the MA956 ODS steel

IVO KUBENA<sup>1</sup>, JAROSLAV POLÁK<sup>1</sup>, TOMÁŠ KRUML<sup>2</sup>

<sup>1</sup>Institute of Physics of Materials, Brno, Czech Republic

<sup>2</sup>CEITEC IPM, Brno, Czech Republic

High chromium steel (MA956) prepared by mechanical alloying (MA) and strengthened by fine oxide dispersion was investigated. Coarse microstructure with grains larger than 100  $\mu\text{m}$  was revealed. The oxide distribution was analyzed by the means of transmission electron microscopy. Specimens were cycled with constant strain amplitude and strain rate at room temperature. Continuous cyclic softening consisting of three stages was measured. Short initial stage of rapid cyclic softening was followed by relatively long stage where the softening rate is constant and lower than the one measured in the first stage. In last stage, cyclic softening rate again increases, but this rather influenced by the growth of long cracks.

Cyclic softening and role of oxide dispersion was discussed in relation with microstructural observations. Moreover, microstructure and cyclic softening of the MA956 steel is compared with different ODS steels

# Influence of pre-strain on fatigue crack growth behavior in rolled AZ31 magnesium alloy

RYOICHI MOMOE<sup>1</sup>, SHIGEKI MORITA<sup>2</sup>, TSUYOSHI MAYAMA<sup>3</sup>, NOBUSUKE HATTORI<sup>2</sup>

<sup>1</sup>Graduate Student, Department of Science and Engineering, Saga University, Japan

<sup>2</sup>Department of Mechanical Engineering, Saga University, Japan

<sup>3</sup>Organization for Innovation and Excellence, Kumamoto University, Japan

It is well known that the {10-12} deformation twin is occurred as tension is applied parallel to the *c* axis for magnesium alloys [1]. Hong et al. [2] showed that the compressive deformation along the rolling direction yielded at much lower stress as compared to the tensile deformation and the exactly reversed features were observed for the normal direction. Shiozawa et al. [3] claimed that the step-wise *S-N* curve was induced by the crack initiation mechanism changing from the twin deformation in high-stress amplitude level to slip deformation in low-stress amplitudes. Recently, Huang et al. [4] suggested that in rolled AZ31 magnesium alloy by pre-compression deformation, the deformed samples showed much longer fatigue life than the as-rolled sample. The aim of present study is to investigate the influence of twin deformation on fatigue crack growth behavior in rolled AZ31 magnesium alloy.

Material used in the present study is commercial rolled AZ31 magnesium alloy. Basal planes are aligned parallel to rolling direction. A mean grain size of approximately 38  $\mu\text{m}$ . Tensile 0.2% proof stress is 129 MPa parallel to the rolling direction and 53 MPa parallel to the short transverse direction. The fatigue crack propagation (FCP) specimens with width 12 mm, thickness 4 mm, initial slit length 1 mm were machined from the plate. The specimen which loading axis is parallel to the rolling direction; fatigue crack propagated parallel to the transverse direction is defined as the L-T specimen. The specimen which loading axis is parallel to the rolling direction; fatigue crack propagated parallel to the short transverse direction is defined as the L-S specimen. The specimen which loading axis is parallel to the short transverse direction; fatigue crack propagated parallel to the transverse direction is defined as the S-T specimen. In order to introduce {10-12} deformation twin, the S-T specimens were loaded parallel

to the short transverse direction. Pre-tensile plastic strains were generated at 1%, 2%, 3% with a mechanical testing machine. The pre-strained specimens were defined as 1% pre-strained, 2% pre-strained, 3% pre-strained, respectively. FCP tests were performed at a stress ratio of  $R=0.1$  and a frequency of 10 Hz at room temperature. The fracture surfaces were observed by SEM.

The FCP rate of the S-T specimen showed higher than that of the L-T and the L-S specimens. The FCP rate depends on the texture. The FCP rate of the pre-strained specimens showed lower than that of the undeformed S-T specimen. The FCP rate of the 2% pre-strained specimen was lowest in the examined pre-strained specimens. Compared with the fracture surface of the undeformed specimen, much lines and bigger steps were observed in that of the pre-strained specimens. It is suggested that the existence of {10-12} deformation twin at a crack tip might interfere crack propagation and make FCP rate lower.

## References

- [1] Barnett, M. R. (2007): Twinning and the ductility of magnesium alloys Part 1: "Tension" twins – Mater. Sci. Eng. A 464, 1-7.
- [2] Hong, S. G. et al. (2010): Anisotropic fatigue behavior of rolled Mg-3Al-1Zn alloy – J. Mater. Res. 25, 966-971.
- [3] Shiozawa, K. et al. (2010): Fatigue behaviour and fractography of extruded AZ80 magnesium alloys in very high cycle regime – Procedia Engineering 2, 183-191.
- [4] Huang, G. et al. (2014): Improving low-cycle fatigue properties of rolled AZ31 magnesium alloy by pre-compression deformation – Materials and Design 58, 439-444.

## Anisotropy of cyclic deformation and fatigue properties in rolled AZ31 magnesium alloy

SHIGEKI MORITA<sup>1</sup>, RYOTA IKEDA<sup>1</sup>, TSUYOSHI MAYAMA<sup>2</sup>, NOBUSUKE HATTORI<sup>1</sup>

<sup>1</sup>Saga University, Japan

<sup>2</sup>Kumamoto University, Japan

Magnesium alloys are the lightest structural material with a high strength-to-weight ratio. These features make magnesium alloys attractive for applications in the automotive and aircraft industry. Wrought Mg-Al-Zn system alloys are suitable candidates for structural parts. It is important to elucidate the cyclic loading behavior and fatigue properties of the material used for structural parts.

It is well known that wrought magnesium alloys have a hexagonal close-packed (HCP) structure, and strong textures are formed by rolling and extrusion. Basal planes are aligned parallel to the rolling direction by rolling. Depending on their microstructure, magnesium alloys show unique deformation behavior such as mechanical anisotropy (Chino et al. 2008), pseudoelasticity in loading-unloading (Ca'ceres et al. 2003), and asymmetry of stress-strain hysteresis loops in strain controlled low-cycle (Hong et al. 2010) and load controlled high-cycle (Morita et al. 2010) fatigue tests.

To investigate the anisotropy of cyclic deformation and fatigue properties, cyclic compressive and tensile loading-unloading tests were carried out using cylindrical smooth specimens of rolled AZ31 magnesium alloy. Load-controlled axial fatigue tests were also carried out with smooth specimens attached on strain gages at specified stress amplitudes levels. Monotonic tensile and compressive 0.2% proof stresses of the L-specimen (loading axis is parallel to Longitudinal direction) were 129 MPa and 78 MPa, respectively. On the other hand, monotonic tensile and compressive 0.2% proof stresses of the S-specimen (loading axis is parallel to Short-transverse direction) were 53 MPa and 85 MPa, respectively. Pseudoelastic behaviors were observed in compressive and tensile loading-unloading tests for L- and S-specimens. The larger anelastic strains were observed in compressive stress-strain hysteresis loops

for the S-specimen. The fatigue strengths at 10<sup>7</sup> cycles of the L- and S-specimens were 80 MPa and 60 MPa, respectively. The fatigue strengths were similar to the monotonic compressive or tensile 0.2% proof stresses for both specimens. Stress-strain hysteresis loops were linear in tensile and compressive phases at the lower stress amplitude of fatigue strength and the complicated elastic-plastic-pseudoelastic deformations were observed in tensile and compressive phases at the higher stress amplitude of fatigue strength of load-controlled axial fatigue test. Tensile mean strain generated by cyclic elastic-plastic-pseudoelastic deformations at the higher stress amplitude of fatigue strength for the S-specimen. The deformation twins were observed in the specimen subjected to the higher stress amplitude of fatigue strength and free deformation twins were observed in the specimen subjected to the lower stress amplitude of fatigue strength.

### References

- Chino, Y., Kimura, K., Hakamada, M. & Mabuchi, M. (2008): Mechanical anisotropy due to twinning in an extruded AZ31 Mg alloy - *Mater. Sci. and Eng. A*, 485: 311-317.
- Ca'ceres, C. H., Sumitomo T. & Veridit M. (2003): Pseudoelastic behavior of cast magnesium AZ91 alloy under cyclic loading-unloading - *Acta Mater.*, 51: 6211–6218.
- Hong, S.G., Park, S.H., Huh, Y.H. & Lee, C.S. (2010): Anisotropic fatigue behavior of rolled Mg-3Al-1Zn alloy - *J. Mater. Res.*, 25: 966-971.
- Morita, S., Tanaka, S., Ohno, N., Kawakami, Y. & Enjoji, T. (2010): Cyclic Deformation and Fatigue Crack Behavior of Extruded AZ31B Magnesium Alloy – *Mater. Sci. & Forum*, 638-642: 3056-3061.

## Fatigue properties of fine-grained AZ31 magnesium alloy

YUJI OKAMOTO<sup>1</sup>, TAKAHITO HORI<sup>1</sup>, SHIGEKI MORITA<sup>2</sup>, HIDETOSHI SOMEKAWA<sup>3</sup>, TSUYOSHI MAYAMA<sup>4</sup>, NOBUSUKE HATTORI<sup>2</sup>

<sup>1</sup> Graduate student, Department of Mechanical Engineering, Saga University, Japan

<sup>2</sup> Department of Mechanical Engineering, Saga University, Japan

<sup>3</sup> Research Center for Strategic Materials, National Institute for Materials Science, Japan

<sup>4</sup> Organization for Innovation and Excellence, Kumamoto University, Japan

Magnesium alloys are the lightest structural material, and have higher strength-to-weight ratio than steel and aluminium alloy. These features make magnesium alloys attractive for applications in the automotive components, e.g. steering wheel frame and gear box housing<sup>1</sup>. It is important to investigate cyclic loading behavior and fatigue properties of the material used for structural parts.

In the case of magnesium alloys, deformation twins easily form when coarse-grained alloy is subjected to compressive stress in loading direction parallel to extrusion<sup>2,3</sup>. This behavior causes lower compressive yield strength compared with tensile one for extruded alloys<sup>4,5</sup>. It is known that twinning can be essentially reduced by grain refinement. The mechanical property and anisotropy of magnesium alloys were significantly improved by grain refinement<sup>4</sup>. However, the fatigue property in fine-grained magnesium alloy is far from fully understood. This paper presents fatigue strength and fatigue crack initiation and propagation behavior of fine-grained extruded AZ31 magnesium alloy.

AZ31 (Mg-3%Al-1%Zn) magnesium alloy with a thickness of 5 mm was extruded at temperature of 473 K. Subsequently, the alloys were annealed at 423 K for 86.4 ksec. The texture exhibits the combined features of the typical rolling and extrusion textures. The average of the grain size was 2.5  $\mu\text{m}$ . Tensile and compressive specimens were machined from the annealed bar. Loading axis was parallel to the extrusion direction. The tensile and compressive tests were performed on an mechanical testing machine at a crosshead speed of  $8.3 \times 10^{-6}$  m/s in laboratory air at room temperature. Fatigue specimens with gage length of 10 mm, a width ( $W$ ) of 5 mm, a thickness ( $t$ ) of 4 mm were machined from the annealed bar. SENT (Single Edge Notched Tension) specimens with a width ( $W$ ) of 12 mm, a thickness ( $t$ ) of 4 mm, an initial slit length ( $a$ ) of 2 mm, and a length ( $L$ ) of 50 mm were machined from the annealed bar. The axial fatigue tests and fatigue crack propagation tests were performed on an electro-hydraulic test

ing machine (capacity: 9.8 kN) in laboratory air at room temperature, at frequency of 10 Hz and stress ratio of 0.1. Crack initiation and small crack growth were monitored with replication technique.

Mechanical properties of fine-grained alloy, e.g. tensile and compressive strength and fracture strain show superior to the coarser-grained AZ31 magnesium alloys. The ratio of 0.2% proof stress was  $\sigma_{0.2\text{compression}} / \sigma_{0.2\text{tension}} = (193/209) = 0.92$ . Compared with coarser-grained alloys, the mechanical anisotropy of fine-grained alloy was improved. Fatigue strength of fine-grained alloy was  $\sigma_{\text{max}} = 170$  MPa. The fatigue crack initiated at 39% of total fatigue life. The fatigue crack initiated at the interface between the inclusion and the matrix. The fatigue crack propagation rate was similar as the other coarse-grained alloys at stress ratio of 0.1. As the results, fatigue crack initiation can be improved by grain refinement, however, fatigue crack propagation was slightly influenced by grain refinement.

### References

- Mordike, B. L. and Ebert, T. (2001): Magnesium Properties - applications - potential - Mater. Sci. Eng. A, 302 : 37-45.
- Wang, J. T., Yin, D. L., Liu, J. Q., Tao, J., Su Y. L. and Zhao, X. (2008): Effect of grain size on mechanical property of Mg-3Al-1Zn alloy - Scri. Mater, 59: 63-66.
- Barnett, M.R., Keshavarz, Z., Beer, A.G. and Atwell, D. (2004): Influence of grain size on the compressive deformation of wrought Mg-3Al-1Zn - Acta Mater., 52: 5093-5103.
- Chino, Y., Kimura, K., Hakamada, M. and Mabuchi, M. (2008): Mechanical anisotropy due to twinning in an extruded AZ31 Mg alloy - Mater. Sci. and Eng. A, 485: 311-317.
- Somekawa, H., Maruyama, N., Hiromoto, S., Yamamoto, A. and Mukai, T. (2008): Fatigue Behaviors and Microstructures in an Extruded Mg-Al-Zn Alloy - Mater. Trans., 49: 681-684.

## Dwell effects on low cycle fatigue behaviour of diffusion coated nickel base superalloy IN 713LC at temperature of 800 °C

IVO ŠULÁK<sup>1</sup>, KAREL OBRTLÍK<sup>1</sup>, SIMONA HUTAŘOVÁ<sup>2</sup>, MARTIN JULIŠ<sup>2</sup>, TOMÁŠ PODRÁBSKÝ<sup>2</sup>, LADISLAV ČEKLKO<sup>2</sup>

<sup>1</sup>Institute of Physics of Materials, AV CR, Brno, Czech Republic

<sup>2</sup>Brno University of Technology, CEITEC, Czech Republic

Materials used for high temperature applications such as disks, blades and vanes of gas turbine engines require exceptional resistance to mechanical and thermal loading as well as against chemical attacks by oxidation, which significantly increases with operating temperature. First generation Ni-base superalloy IN 713LC developed by the International Nickel Company in the 1950s is the representative of cast materials used for these purposes, especially because of favorable price in conjunction with satisfying high temperature properties. However, the continuous enhancing of operating temperature severely degrades the material surface and adversely affects the strength properties and component life. Protection of the surface and prevention of its degradation is a major goal of today and tomorrow. Diffusion coatings are primarily used to safeguard the material from aggressive environments and to improve corrosion and oxidation stability of surface. Nowadays, superalloy surface is enriched with appropriate oxide formers such as aluminum and other elements (Cr, Si..).

The topic of the present paper is focused on the study of low cycle fatigue with tensile dwells of cast nickel-base superalloy IN 713LC with Al-Cr diffusion coating at 800 °C. Increased attention is paid to the microstructure observation of the substrate material and Al-Cr diffusion layer. Macrostructure of IN 713LC consists of coarse dendritic grains whose average size was determined to 2.4 mm ± 0.5 mm and some shrink

age pores. Microstructure is formed by  $\gamma$  matrix with  $\gamma'$  strengthening precipitates, carbides and eutectics.

Polycrystalline diffusion Al-Cr coating was prepared by a Cr modified aluminizing using the chemical vapor deposition (CVD) out of pack process. The coating was deposited in two-steps: 1050 °C/5h and 950 °C/5h. Microstructure of the Al-Cr layer comprises an outer layer and an inner diffusion layer with dispersion of a large amount of complex particles based on Cr, Mo and Nb. For purpose of this work cylindrical specimens were machined from the rods manufactured using investment castings technique. Low cycle fatigue tests and tests with 10 minute tensile dwells included in each cycle were conducted in strain control mode with constant total strain amplitude and strain rate at 800 °C in air.

The fatigue behaviour was characterized by cyclic hardening/softening curves, cyclic stress-strain curves, Manson-Coffin curves and Basquin curves. The substrate and the Al-Cr coating were examined in as-received conditions and also after cyclic loading by means of optical microscopy, SEM and energy dispersive spectroscopy (EDS). Micro-hardness depth profile was obtained with the Knoop indenter. The fracture surface observation, changes in microstructure and investigation of polished section parallel to the specimen axis help to discuss the mechanisms operating in fatigue degradation of surface treated superalloy in both regimes of cycling.

Poster Topic D:

***In-situ microscopy and diffraction***

## Strain induced martensitic Transformation in Austempered Ductile Iron (ADI)

XIAOHU LI<sup>1</sup>, PATRICK SAAL<sup>2</sup>, MICHAEL HOFMANN<sup>1</sup>, MARKUS HÖLZEL<sup>1</sup>

<sup>1</sup> Forschungs-Neutronenquelle FRM II, Technische Universität München, Germany

<sup>2</sup> Institute of metal forming and casting, Technische Universität München, Germany

Austempered ductile iron (ADI) is a nodular ductile iron which has undergone a special heat treatment to greatly enhance mechanical properties. The heat treatment process of ADI consists of austenitization, quenching to a temperature typically between 250°C and 450°C and isothermal austempering [1]. After such heat treatment the microstructure consists of acicular ferrite and high carbon enriched retained austenite. The microstructure of ADI strongly depends on the austenitization and austempering temperatures. Details on dependence of microstructure and temperature can be found in [1, 2]. In industrial applications alloying elements such as Ni, Mn or Cu are used in order to delay the phase transition kinetics, which improves the austemperability of thicker geometries.

The high carbon enriched retained austenite can transform to martensite during plastic deformation. Four different treatment parameters (austenitization temperature, austempering temperature, austempering time and alloying composition) can influence the retained austenite fraction, grain size and its stabilisation [3],[4], which in turn will influence the following martensitic transformation.

The influence of different treatment and composition parameters on the martensitic transformation have been investigated using in-situ neutron diffraction during applying either tension or compression to different

plastic strains. In addition texture measurements using neutron diffraction have been performed to calculate the texture distribution of ferrite and austenite phases for different strain levels. Combining the detailed information on texture with the in-situ studies is necessary for quantitative phase analysis and extraction of martensite phase fractions.

The results of these experiments allows us to illustrate the martensitic transformation kinetic in ADI with austempering temperature, alloy element Nickel and plastic strains.

### References

- [1] Leopold Meier, Michael Hofmann, Patrick Saal, Wolfram Volk, Hartmut Hoffmann, Materials Characterization 85 (2013) 124-133
- [2] Miguel Angel Yescas-González, Modelling the microstructure and mechanical properties of austempered ductile iron, Dissertation in department of materials science and metallurgy, University of Cambridge, (2001)
- [3] Srinivasmurthy Daber, K. S. Ravishankar and P. Prasad Rao, J.Mater.Sci (2008) 43:4929-4937
- [4] C. Capdevila, F. G. Caballero and C. García de Andrés; Analysis of the effect of alloying elements on the martensite-start temperature of the steels; Department of Physical Metallurgy, CENIM

## An in situ experimental method for evaluating the tensile property of single crystalline gold nanorod

YABIN YAN<sup>1</sup>, XIAOYUAN WANG<sup>1</sup>, TAKASHI SUMIGAWA<sup>2</sup>, TAKUYA NAKANO<sup>2</sup>, TAKAYUKI KITAMURA<sup>2</sup>

<sup>1</sup>Institute of Systems Engineering, China Academy of Engineering Physics, Mianyang, China

<sup>2</sup>Department of Mechanical Engineering and Science, Kyoto University, Kyoto, Japan

The mechanical properties of submicron- or nanoscale materials are of practical importance because they are used in interconnections above semiconductor layers in ultra-large-scale integrated circuits. The mechanical properties of submicron- and nanoscale materials are different from those of the bulk because of the small volumes of the former. Although bending and nano-indentation tests have examined the size effects in plasticity (McElhaney et al. 1998), severe strain gradients exist in the specimens. Micro- or nanoscale pillar compression experiments (Dimiduk et al. 2005, Uchic et al. 2005) where the strain gradients are minimal have

also been performed; however, this method can not yield fracture properties. Thus, tensile experiments are desired, because of the uniform stress distribution as well as the ability to obtain fracture behavior at large strains.

In this work, we develop a new *in situ* experimental method for evaluating tensile properties of nano-materials and apply it to a single crystalline gold nanorod with a square section of 189 nm × 189 nm. The nanorod, which is carved out of a bulk material by focused ion beam processing, is mounted on a lozenge-shaped silicon frame and is pulled by a compressive load ap-

plied onto the top face of the frame. Although the applied load increases linearly in the early stages of deformation, it drops rapidly at a certain displacement. *In-situ* TEM observations indicate that the rapid drop is induced by the crystallographic slip generation within the nanorod. The critical resolved shear stress on the active slip system at yielding is evaluated to be 325.8 MPa, which is almost 600 times larger than that of the bulk counterpart. The high critical resolved shear stress is due to the low dislocation density in the nanorod. When the tensile elongation becomes large, the nanorod shows necking and isotropic plastic behavior independent on the crystalline structure.

#### References

- Dimiduk, D. M., et al. (2005): Size-affected single-slip behavior of pure nickel microcrystals. *Acta Materialia*, 53, 4065-4077.
- McElhaney, K. W., et al. (1998): Determination of indenter tip geometry and indentation contact area for depth-sensing indentation experiments. *Journal of Materials Research*, 13, 1300-1306..
- Uchic, M. D., et al. (2005): A Methodology to Investigate Size Scale Effects in Crystalline Plasticity using Uniaxial Compression Testing. *Materials Science and Engineering A*, 400-401, 268-278.

Poster Topic E:

***Size effects and small-scale mechanical behavior of materials***

---

## Indentation Size Effect of Nanoporous Gold: Correlated by Unique Structure and its Size-Dependent Mechanical Behavior

SEUNG-MIN AHN, YOUNG-CHEON KIM, AND JU-YOUNG KIM

School of Materials Science & Engineering, UNIST (Ulsan National Institute of Science and Technology), Korea

Nanoporous gold (np-Au), a low density open-cell structure material with ligaments and pores, has been studied as attractive candidates in various applications such as sensor, catalyst, and actuator due to high surface-to volume ratio that combined with chemical and electrical properties of gold. In addition, one of the merits on np-Au is simply fabricating using dealloying method that, based on Ostwald ripening, is used to remove a sacrificial element of Ag from a precursor alloy, Au-Ag alloy, which is followed by surface diffusion of Au and aggregation of Au adatoms into clusters that form the interconnected ligaments of the nanoporous structure. For using various application, estimation of mechanical behavior of np-Au is a priority. According to several researches, the mechanical properties of foams were evaluated by nano-indentation with scaling equations basis on the basis of foam relative density. Furthermore, recent experimental results on np-Au have shown a rapid increase in hardness with decreasing indentation depth, so-called indentation size effect (ISE). In the case of fully dense materials, ISE is observed up to  $10^3$  nm of indentation depth, and underlying principle was revealed Nix and Gao that increase in the relative density of geometrically necessary dislocations (GNDs) with decreasing indentation depth. However, in porous materials, for foams with relative density less than 30%, there are a certain limit to explanation of ISE using the principle due to its open-cell structure that pores in np-Au does not carry indentation force, thus GNDs does not affect the plastic deformation regions. Besides, ISE mechanisms for np-Au have not been discussed clearly so far. Furthermore, in case of plastic indentation, it has been known the hardness is nearly

equal to yield strength because of the underneath the indenter is not constrained by the surrounding materials. For this reason, we intended to discuss ISE and to characterize mechanical properties of bulk np-Au specimens. We prepared np-Au specimens with ligament diameters of 20 through 150 nm which was fabricated by free corrosion dealloying process. The ligament diameters are controlled by dealloying conditions such as temperature and concentration of nitric acid solution. We estimated the mechanical properties of np-Au having variable ligament size using nanoindentation and uni-axial compressive test. And then combined it for establish its correlation. To confirm deformation behavior of underneath the indenter we used FIB milling as residual indent marks and observed plastic collapse, densification, using cross-sectional SEM images. This makes it possible to discuss additional factor of ISE in porous materials. We discussed ISE of np-Au in terms of densification of specimen, and suggested optimized modeling of ISE in np-Au excluded of effect of GNDs.

### References

- Gibson, LJ & Ashby, MF. (1997): Cellular Solids: Structures and Properties, 2<sup>nd</sup> ed., Cambridge University Press, Cambridge.
- Oliver, WC & Pharr, GM. (1992): An improved technique for determining hardness and elastic modulus using load and displacement sensing indentation experiments, *J. Mater. Sci.* 7, 1564-1583
- Nix, WD & Gao, H (1998): Indentation size effect in crystalline materials: A law for strain gradient plasticity, *J. Mech. Phys. Solids* 46, 411-425.

## High temperature nanoindentation - Dynamic measurements for thin film analysis

DENNIS BEDORF, MARTIN KNIEPS, WOLFGANG STEIN

SURFACE, Hueckelhoven, Germany

Nanoindentation at non-ambient conditions has become more and more popular. Many users ask for the ability to measure material properties at elevated or lowered temperatures. The materials of interest are metals, semiconductors and polymers. The investigation of polymers and of some metals at elevated temperatures often includes time dependent properties

like creep, frequency depended modulus, or strain rate sensitivity. The study of these properties is depending on temperature stability in a crucial manner. We will present recent progress in the control of temperature stability and homogeneity of the tested volume and give examples in the field of polymer characterization and creep measurements.

# Ductility in cold-rolled ultrafine-grained (UFG) tungsten (W): Correlation between microstructure and mechanical properties

SIMON BONK, JENS REISER, JAN HOFFMANN, MICHAEL RIETH

Karlsruhe Institut of Technology, Institute for Applied Materials – Applied Materials Physics, Karlsruhe, Germany

The progress in energy technologies, be it future processes like fusion or optimizing the efficiency in existing applications by higher temperatures, demands new materials with enhanced thermomechanical and thermophysical properties. From a functional point of view, tungsten has outstanding properties like the highest melting point of all metals, a high recrystallization temperature, good thermal conductivity, as well as high temperature strength and creep resistance. The main problem of tungsten for the application as a structural material is its high brittle to ductile transition temperature (BDTT), resulting in brittle behavior at low temperatures and a difficult manufacturing process. Wei and Kecskes [1, 2] showed the possibility of tailoring tungsten down to the UFG (ultrafine-grained) regime by severe plastic deformation (SPD). This leads to much higher strengths, a reduction in strain rate sensitivity (SRS), an increase in ductility and an elastic, nearly perfectly plastic stress-strain-behavior. Furthermore a significant toughness and a decrease of the BDTT by several 100°C were demonstrated for thin cold-rolled foils [3, 4], validating their potential for the use in structural applications. But despite a few interesting findings, a systematic study of the various aspects of plastic deformation of SPD processed ultrafine grained (UFG) W is still lacking [5].

To shed light on the deformation mechanisms in UFG-W and to access the question if the good properties in tungsten foils result from the ultra-fine grain size or could already be found in cold-rolled foils with coarser grains, a batch of W-sheets with different thicknesses has been produced by subsequent cold-rolling by PLANSEE, Reutte. All plates are rolled out of the same sintered compact of commercially pure tungsten (99,97% W). This unique batch of samples allows investigating the mechanical properties without an influence of the chemical composition or fabrication differences in the production of the sintered compact. The mechanical properties can thereby be correlated directly to the grain size and cold-work induced defects. For

this purpose, three main aims are projected: (1) characterize the microstructure and defect structure of the as-received plates, (2) determine the mechanical properties and access the deformation mechanisms indirectly by mechanical testing as tensile- and indentation-SRS-tests, (3) access the deformation mechanisms directly by high-resolution electron microscopy.

In this poster the actual results of the basis analysis of the microstructure and a first correlation to mechanical properties will be presented. EBSD-studies show the evolution of the microstructure with increased true strain and allow determining the grain size and texture of the samples. A grain refinement from fine grained well down to the UFG regime could be verified. Micro hardness measurements verify a continuous increase of the hardness with decreasing grain size up to 700 HV0.1, demonstrating the positive effect of the grain refinement in the UFG regime of tungsten compared to coarse-grained tungsten which exhibits a degree of hardness under 500 HV0.1.

## References

- [1] Q. Wei, R. Valiev et al., Mechanical behavior and dynamic failure of high-strength ultrafine grained tungsten under uniaxial compression, *Acta Mater.* (2005).
- [2] L.J. Kecskes, Q. Wei et al., Grain size engineering of bcc refractory metals: Top-down and bottom-up—Application to tungsten, *Mat. Sci. Eng. A 1-2* (2007) 33–43.
- [3] J. Reiser, R. Pippan et al., Tungsten (W) Laminate Pipes for Innovative High Temperature Energy Conversion Systems, *Adv. Eng. Mater.* (2014).
- [4] A. Németh, J. Reiser, D. Armstrong, M. Rieth, The nature of brittle-to-ductile transition of ultra fine grained tungsten (w) foil, *Int. J. Refract. Met. H.* 50 (2015) 9-15.
- [5] Q. Wei, L. J. Kecskes, Effect of low-temperature rolling on the tensile behavior of commercially pure tungsten, *Mat. Sci. Eng. A 1-2* (2008) 62–69.

## Fabrication of Al-Cu Composite Reinforced with BN by Powder Liquid-Phase Forging

CUNGUANG CHEN<sup>1</sup>, LEICHEN GUO<sup>2</sup>, WENWEN WANG<sup>1</sup>, JI LUO<sup>1</sup>, ZHIMENG GUO<sup>1</sup>

<sup>1</sup>Institute of Advanced Materials and Technology, University of Science and Technology Beijing, Beijing, China

<sup>2</sup>School of Engineering, Rensselaer Polytechnic Institute, Troy, USA

Semi-solid powder processing (SPP) has attracted increasing interest, which involves compaction of metallic alloy powders or element powders in temperature ranges when both solid and liquid phases coexist (Wu & Kim 2014). Powder liquid-phase forging (PLF) belongs to the category of SPP, which can be successfully applied in processing of alloy materials and composite materials.

Gas atomizing aluminum powder, electrolytic copper powder and hexagonal boron nitride (h-BN) powder were used as raw materials. Al-5.3 wt% Cu composite reinforced with 3.0 wt% h-BN with nearly full densification was fabricated by the process of powder liquid-phase forging with the load pressure 10 MPa. The powder morphology and comparative structural characteristics were analyzed using X-ray diffraction, scanning and transmission electron microscopy, and the composite hardness was measured by Brinell tester. Special attention was paid to the effects of the technique on the densification and the interface bonding of as-forged composites. These revealed the composite densification can be promoted effectively with plenty of embedded liquid phase under pressure. The composites fabricated using aluminium powder with different granularity showed different grain characteristics, and in situ recrystallization occurred inside the original grains with 35  $\mu\text{m}$  aluminium powder. Moreover,

a good interface consisted of Al/Al<sub>2</sub>O<sub>3</sub>/BN was apparent in the composite. However, there are no findings of AlN, AlB<sub>2</sub> and AlB<sub>12</sub> from the interfacial reaction between BN and Al as other research reports (Lee & Sim 2002; Xia & Li 2005). Compared with the basis alloy, the composite hardness was increased nearly by 15%, and the composite with 2  $\mu\text{m}$  aluminium powder showed the better performance. These findings were caused by the compact oxidation film naturally formed on the surface of aluminum powder. It is noteworthy that the film thickness of 2  $\mu\text{m}$  aluminium powder was larger than 35  $\mu\text{m}$  aluminium powder. The former was about 20 nm, while the latter was 2 nm or so observed by high resolution transmission electron microscopy (HRTEM).

### References

- Wu, Y.-F. & Kim, G.-Y. (2014): Compaction Behavior of Al6061 Powder in the Semi-solid State. *Powder Technology*, 214: 252-258; Lausanne.
- Lee, K.-B. & Sim, H.-S. (2002): Tensile Properties and Microstructures of Al Composite Reinforced with BN Particles. *Composites Part A: Applied Science and Manufacturing*, 33: 709-715; Oxford.
- Xia Z. & Li Z. (2005): Structural Evolution of Al/BN Mixture during Mechanical Alloying. *Journal of Alloys and Compounds*, 399: 139-143; Lausanne.

## Mechanical response of nanoporous gold made from Au-Ag precursor alloys with different initial microstructure

EUN-JI GWAK, YOUNG-CHEON KIM, JU-YOUNG KIM

School of Materials Science & Engineering, UNIST (Ulsan National Institute of Science and Technology), Korea

Nanoporous metals have been widely studied for catalyst, sensor, actuator and other applications due to their open cell porous structure with high surface-to-volume ratio. And nanoporous gold (np-Au) has been the subject of extensive research due to their chemical inertness, high electrical and thermal conductivity, and biological compatibility. Nanoporous structure is easily fabricated via dealloying, which use difference in chemical reactivity of elements in precursor alloy. For nanoporous gold, less noble silver of gold-silver alloy is removed chemically in nitric acid (HNO<sub>3</sub>) to make a porous structure with gold. In dealloying process, silver

atoms at the surface of alloy dissolve into nitric acid leaving gold adatoms, and gold adatoms agglomerate into a form of interconnecting ligament. In this process, size of ligaments and pores can be varied by controlling dealloying conditions, such as concentration and temperature of nitric acid, composition of Ag-Au precursor alloy and time of etching (Gwak, E.-J. 2013). The resulting structure consists of open cell porous material where dimension of ligament is from tens of nanometer to hundreds of nanometer.

As new materials such as nanoporous metals are developed, mechanical properties of nanoporous mate-

rials should be investigated for practical use. In bulk materials it has been shown that, at the nanoscale less than 100 nanometer, grain size and sample size affect the overall mechanical strength (Kim, J.-Y. 2010). Similarly, size of ligaments and pores (Biener, J. 2006) and relative density (Gibson, L.J. 1999) affect the strength of nanoporous gold. In bulk material, microstructures such as grain boundary or dislocation density have a strong influence on mechanical property, but effects of grain structure and dislocation density of nanoporous gold have not been investigated. In this research, mechanical property and deformation behavior of nanoporous gold with different microstructure is studied by nanoindentation.

There are some researches that microstructure of precursor survives through dealloying process. Therefore, by controlling microstructure of precursor alloy, nanoporous gold with different microstructure is obtained. In this research, tens of nanometer grain, hundreds of micrometer-sized grain, and micrometer-sized grain with high dislocation density are chosen. Nanocrystalline Ag-Au precursor alloy is fabricated by high energy ball milling using ball mill. After heat treatment at 850°C without ball milling, Ag-Au precursor has several hundreds micrometer-size grain. And annealed

Ag-Au alloy is pressed until thickness decreases to 95% to increase dislocation density without noticeable grain size changes. Sacrificial Ag element is selectively leached in 35% nitric acid at 80°C. Microstructures of precursor and nanoporous gold are observed by scanning electron microscope (SEM), energy-disperse X-ray spectroscopy (EDAX) and electron backscattering diffraction (EBSD). Mechanical property and deformation behavior of nanoporous gold with various microstructures are analyzed by nanoindentation curves.

#### References

- Gwak, E.-J. et al. (2013): Microstructure evolution in nanoporous gold thin films made from sputter-deposited precursors, *Scripta Materialia*, 69, 720-723.
- Kim, J.-Y., et al. (2010): Tensile and compressive behavior of tungsten, molybdenum, tantalum and niobium at the nanoscale. *Acta Materialia*, 58, 2355-2363.
- Biener, J., et al. (2006): Size effects on the mechanical behavior of nanoporous Au. *Nano Letters*, 6, 2379-2382.
- Gibson, L.J., Ashby, M.F. (1999): *Cellular Solids: Structure and Properties*. Cambridge University Press.

## Simulation of mechanical properties of nanotwin-strengthened metals

<sup>1</sup>H. HOSSEINI-TOUDESHPY, <sup>1</sup>M. YADOLLAHPOUR

<sup>1</sup>Department of Aerospace Engineering, Amirkabir University of Technology, Tehran, Iran

The nanotwin-strengthened metals have provided a novel potential for optimizing the strength and ductility of coarse grained materials. In this paper, finite element simulations based on the mechanism-based strain gradient plasticity and the Johnson–Cook failure criterion has been carried out to investigate tensile behavior of the nanotwin-strengthened metals. Constitutive equations of the nanotwin-strengthened metals is employed based on a mechanism-based strain gradient plasticity model to describe the flow stress of these materials by incorporating the competition and transition of different deformation mechanisms as the twin spacing is reduced. Then, a finite element analysis, together with the Johnson–Cook failure criterion, is performed

to characterize the failure process and the numerical results are compared with nanotwin-strengthened copper. The results show that the material strength and ductility strongly depend on the grain size and the distribution of twin lamellae microstructures in these materials. Also, the comparison between the results of numerical calculation and experimental data shows that the proposed model adopted in the present research can well characterize the mechanical properties and size effect of nanotwin-strengthened copper.

**Keyword:** nanotwin-strengthened metal; mechanism-based strain gradient plasticity; Johnson–Cook failure criterion; mechanical properties.

## Nanotubular ZnO for flexible gas sensor

NA-RI KANG, JU-YOUNG KIM

School of Materials Science & Engineering, UNIST (Ulsan National Institute of Science and Technology), Korea

ZnO has been focused on hydrogen sensing material because of its thermal stability and high mechanical strength and mobility. But it has the weakness that it is very brittle. And nowadays, flexible electronics technologies are being driven by trend such as low complexity and high reliability. A high strength-to-weight ratio makes interconnected tubular networks an creative design strategy for reducing the linear decrease in strength and stiffness of low-density materials with increasing porosity. So we synthesized ultralow-density nanotubular structured ZnO with high surface area to volume ratio for flexible hydrogen gas sensor application using the sacrificial template, nanoporous gold. We measured its mechanical properties by tensile test and hydrogen gas sensing sensitivity. Dog-bone shaped nanoporous gold with pore size 1  $\mu\text{m}$ , gauge length 2 mm was prepared by free corrosion dealloying from gold-silver mother alloy. For nanotubular structured ZnO, 50, 100, 150 nm-thick ZnO layer was deposited on nanoporous gold by atomic layered deposition (ALD). After nanoporous gold was selectively etched by gold etchant TFA, nanotubular structured ZnO which have shell thickness of 50, 100, 150 nm were obtained. We synthesized ZnO thin film with 50, 100, 150 nm-thick to compare mechanical properties and hydrogen gas sensing sensitivity with nanotubular structured ZnO. And in previous

studies, tensile properties of ZnO thin film have not been reported, so we tried that. After ZnO was deposited on gold thin film by equal ALD condition, dog-bone shaped pattern prepared by photolithography. Dog-bone shaped ZnO thin film were obtained by reactive-ion etching because dog-bone shaped positive photoresist protected ZnO during etching other region. Tensile testing of ZnO thin film and nanotubular ZnO was performed by using the nano-tensile tester under conditions of a speed of  $2\mu\text{m/s}$  at a distance of 2mm. We discuss flexibility of the nanotubular ZnO based on its nanotubular structure or shell thickness. We also measured hydrogen gas sensing sensitivity, defined as a ratio of change in conductance upon exposure to  $\text{H}_2$  gas to that in vacuum, of the ZnO thin film and nanotubular ZnO. We discuss hydrogen sensor efficiency of the nanotubular ZnO based on its high volume-to-surface area and application of flexible hydrogen gas sensor.

### References

- Hsial, C. (2014) : A Rapid process for Fabricating Gas Sensors., *Sensors* 12219-12232; doi: 10.3390/s140712219
- Biener, M. (2014) : Ultra-strong and Low-Density Nanotubular Bulk Materials with Tunable Feature Sizes., *Adv. Mater.*, 26: 4808-4813

## Improved elasticity of bilayer graphene cantilevers with interlayer shear and in-plane extension effects

ABED MOHEB SHAH DIN, AMIN FARROKHABADI

Aerospace Department, Engineering Faculty, Semnan University, Iran

Graphene is measured to be the strongest and a one atom thick material whose usage has been widely reported in various applications especially in electronic devices. Due to its remarkable electrical, thermal and stable mechanical properties, graphene has become an interesting field of research in scientific communities. As a result of the outstanding properties of graphene, it appears to be one of the best candidates in designing reinforced nanoelectromechanical systems (NEMS) devices such as nano-actuators, resonators and the other possible nano-structures with high stiffness. Graphene layers have been observed to slide over each other within multilayered structures like graphene nanoribbon (GNR) due to the weak interlayer van der

Walls bond when the external force exceeds the forces between graphene layers. Since the classical Euler-Bernoulli beam theory cannot simulate the interlayer shear effect, multi-beam shear model has been conducted in recent years to illustrate the governing equation of graphene multilayer beam.

It is worthy to note that the multi-beam shear model is a reduced form of the model proposed and applied by Newmark in (1952) for composite beams. Newmark's theory includes interlayer shear which involves interlayer shear modulus and interlayer stretching which has been neglected in the past few studies.

In this letter, we are proposing an improved governing elasticity of bilayer graphene cantilever beam sub-

jected to a concentrated load at the beam tip in order to investigate the effect of in-plane extension on the graphene layered beams. The interlayer shear effect and in-plane extension are simulated through minimum energy principle moreover the governing equation and boundary conditions are given consequently. Results indicate that the extension in layers occurs due to the interlayer shear modulus as in zero interlayer shear modulus, i.e. no bond between layers, the effect of extension is practically nil. On the other hand, considering extension in layers, the structure behaves softer compared with the case in which the interlayer extension is neglected. In order to give a proper insight, the behaviour of bilayer beam is discussed and shown in absence and presence of interlayer shear and extension.

#### References

- Rokni, H & Wei, Lu. (2013): Effect of graphene layers on static pull in behaviour of bilayer graphene/substrate electrostatic microactuator. *Journal of Microelectromechanical Systems*, Vol.22, No. 3.
- Liu, D.Y & Chen, W.Q & Zhang, Ch. (2013): Improved beam theory for multilayer graphene nanoribbons with interlayer shear effect. *Physics Letters A* 377, 1297-1300.
- Alfredsson, K.S & Bogetti, T.A & Carlsson, L.A & Gillespie, J.W & Yiourans, A. (2008): Flexure of beam with an interlayer– Symetric beam with orthotropic adherends. *Journal of Mechanics of Materials and Structures*. Vol. 3, No. 1.

## Fracture of brittle spheres in compression: testing microscopic fused quartz

VACLAV PEJCHAL, GORAN ŽAGAR, DENIS LANG, MARTA FORNABAIO, ANDREAS MORTENSEN

Laboratory of Mechanical Metallurgy, Institute of Materials, EPFL, Switzerland

The crushing of particles between two parallel platens is widely used as particle fracture has relevance in many branches of engineering (powder metallurgy, food or pharmaceutical industries and of course materials science). Recent years have seen increased attention to micro and nano-mechanical testing, a combined result of interest in expanding the field of application of the method, and progress in testing methodologies and tooling at the microscale.

Although the implementation of such test is relatively easy, at the microscopic scale it is often realized by crushing a particle between two hard platens, typically of diamond. This often leads to particle failure by the propagation of defects initiated at the particle/platen contact due to the very high local stresses that are reached at this point. Resulting test data therefore do not sample the weakest existing flaws within the particle or along its surface; rather, the failure is induced by microcracks that develop at the contact during the test,

where the particle contacts the hard diamond platens. In this study we explore the use of softer elasto-plastic platens, which reduce the stress concentration at the contact point with hard, brittle particles. We develop the method on a laboratory-built instrumented crushing apparatus, which we use here to crush microscopic fused quartz particles. The use of soft platens leads to the development of a higher contact area over which the load is applied on the particle. The particle partially sinks into the platen leaving an indentation, the size of which is controlled chiefly by the elasto-plastic properties of the platens. The higher area over which the load is applied leads to lower local stresses at the contact compared to the tensile stresses that develop (i) in the center of the sphere and/or (ii) at the equatorial belt of the sphere surface. In combination with extensive FEM analysis we explore how this modification of the particle crushing test can be used as a means of measuring the strength of particles.

## How to optimize the fatigue properties of bimodal microstructures of nanocrystalline (nc) and ultrafine grained (ufg) Nickel?

DOMINIC RATHMANN, MICHAEL MARX, CHRISTIAN MOTZ

Saarland University, Chair of Materials Science and Methods, Saarbrücken, Germany

Nc-materials show very high strength compared to their coarse grained counterparts. On the contrary, they provide only low ductility and an insufficient resistance against fatigue crack growth. An approach to fix this deficit for a single-phase material is to modify the nc-microstructure to a bimodal "composite" consisting of nc- and ufg-grains which has much better fatigue properties than the respective monomodal microstructures. The bigger ufg-grains enable plastic deformation and improve the crack resistance while the nc grains preserve the high toughness.

Starting from pulsed electrodeposited nc-Nickel, bimodal microstructures can be developed by adding special additives to the electrolyte in combination with a following heat-treatment of the material. The underlying effect is the abnormal grain growth of single grains. Thereby, segregation at grain boundaries plays

an important role; however the abnormal behavior has not been investigated satisfactorily so far. Therefore atom probe tomography is used to study the effect of segregation.

To measure the effect of the microstructure's modification concerning the fatigue strength, Wöhler-tests of monomodal nc- and ufg-samples as well as bimodal nc/ufg-samples were performed and evaluated for the LCF and HCF region. Furthermore crack propagation mechanisms have been investigated by in-situ tests in SEM. The monomodal microstructures work as reference.

Goal of the present work is to identify and produce an optimal microstructure concerning the fatigue properties of nc materials without losing the increased strength and toughness. Therefore the ratio and volume fraction of nc- and ufg-grains will be varied by the amount of additives and different heat treatments.

## Surface oxidation of metallic glass surfaces and its effect on nanotribology

K. RITTGEN<sup>1,2</sup>, A. CARON<sup>1</sup>, R. BENNEWITZ<sup>1,2</sup>

<sup>1</sup>INM Leibniz-Institute for New Materials, Saarbrücken, Germany

<sup>2</sup>Department of Experimental Physics, University of Saarbrücken, Germany

Owing to their high strength and hardness metallic glasses have been recognized as potential materials with enhanced wear resistance for tribological applications (A.L. Greer et al. 2002). While metallic glasses are prone to oxidation, the formation of surface oxide and its impact on tribological properties has been scarcely investigated (A. Caron et al. 2011, A. Caron et al. 2011). In this work we use a correlative approach to determine the influence of surface structure and chemistry on the friction and wear of metallic glass surfaces. Surface structural properties are investigated by nc-AFM in ultra-high vacuum after Ar-sputtering and controlled oxidation treatments. Surface oxides are further characterized by TEM and XPS. The tribological behavior of metallic glass surfaces with and without oxide layer is determined by AFM- and nano-scratching.

### References

- A. Caron et al. 2011: Structure and nano-mechanical characteristics of surface oxide layers on a metallic glass; 2011 Nanotechnology 22 095704 (2011); A Caron, C L Qin, L Gu, S Gonzales, A Shluger, H-J Fecht, DV Louzguine-Luzgin, A Inoue
- A. Caron et al. 2011: Effect of surface oxidation on the nm-scale wear behavior of a metallic glass; Journal of applied physics 109, 083515 (2011); A. Caron, P. Sharma, A. Shluger, H-J Fecht, DV Louzguine-Luzgin, A Inoue
- A.L. Greer et al. 2002: A.L. Greer, K.L. Rutherford, and I.M. Hutchings, Inter. Mater. Rev. 47, (2002) 87

# Investigation of mechanical anisotropy in Mg using Berkovich indentation

JULIAN E. C. SABISCH<sup>1,2</sup>, ERICA T. LILLEODDEN<sup>1,3</sup>

<sup>1</sup>Institute of Materials Research, Materials Mechanics, Helmholtz-Zentrum Geesthacht, Germany

<sup>2</sup>University of California, Berkeley. Department of Materials Science and Engineering, USA

<sup>3</sup>Institute of Advanced Ceramics, Hamburg University of Technology, Hamburg, Germany

Berkovich indentation has been shown to be an important method for determining mechanical properties on small length scales. (Oliver, W.C. & Pharr, G.M 2004) While the imposed stress state from axisymmetric indentation leads to largely isotropic measurements, the use of non-axi-symmetric indenters offers possibilities to investigate anisotropy in mechanical behavior, such as the elastic modulus and hardness.

Here, we investigate how the relationship between the crystallographic c-axis direction and the Berkovich tip relate to the modulus and hardness in a Mg-4Gd single crystalline volumes.

A sample of cast Mg-4Gd was selected for the experiments due to its large grains and resistance to the formation of a surface oxide. Electron backscatter diffraction was used to find suitable grains for indentation. Grains with the three distinct orientations were chosen: (i) with the c-axis normal to the surface, (ii) with the c-axis at an  $\sim 45^\circ$  angle to the surface, and (iii) with the c-axis in-plane. All indentations were carried out to a nominal maximum depth of 3000nm, with a 75 $\mu$ m indent spacing. The same sample was used without remounting in order to remove any load frame stiffness changes and to maintain the initial surface to indent alignment for all tests. Initial testing of all grain orientations showed a slight variance in both modulus and hardness. SEM imaging was used to investigate the residual indentation. Again, dependence on orientation was observed. Highly symmetric indents with appreciable pileup in the c-axis normal orientation were observed. Conversely, orientations with the c-axis not aligned with the loading direction displayed considerable sink-in and an elongation of the indent impression along the direction coincident with the projected c-axis.

SEM indent images were further used to create a set of ratios between the actual imaged indent area and the ideal area from a symmetric tip. Ratios were differentiated based on orientation then averaged with grain (i) showing a ratio above one and grains (ii) and (iii) having ratios less than one. A ratio greater than one would correspond to pile up while a ratio less than one would correspond to sink in. The ratios were used to correct the values of modulus. Interestingly, this correction increased the variation between the orientations, with the highest average value of 53.0 GPa for the grain (ii) orientation, and the lowest average value of 47.2 GPa for the grain (i) orientation. These results show that the use of Berkovich indentation can be used to investigate the anisotropic plastic response in hcp systems, such as technological Mg- and Ti-based alloys – materials of critical interest for lightweight structural applications – where bulk single crystals are not readily attainable.

## References

- Oliver, W.C. & Pharr, G.M (2004): Measurement of hardness and elastic modulus by instrumented indentation: Advances in understanding and refinements to methodology; *J. Mater. Res.*, Vol. 19, No. 1, Jan 2004.
- Vlassak, J.J., & Nix, W.D. (1994): Measuring the elastic properties of anisotropic materials by means of indentation experiments; *J. Mater. Res.*, Vol. 27, No. 1, Jan 14, 2012.
- Zambaldi, C., et al. (2012): Orientation informed nanoindentation of  $\alpha$ -titanium: Indentation pileup in hexagonal metals deforming by prismatic slip; *J. Mater. Res.*, Vol. 27, No. 1, Jan 14, 2012.

## Size- and phase-dependent mechanical properties of ultrathin silicon and $\text{Ge}_2\text{Sb}_2\text{Te}_5$ films

FRANZISKA SCHLICH, RALPH SPOLENAK

ETH Zürich, Laboratory for Nanometallurgy, Zürich, Switzerland

Ultrathin semiconductors or phase-change materials (5-30 nm) on metals constitute color filters, which selectively absorb wavelength ranges of the incident light (Kats et al., 2012). Recently, it was demonstrated that these coatings are attractive for tunable color devices (Hosseini et al., 2014; Schlich et al., 2014). Color change of ultrathin Si and  $\text{Ge}_2\text{Sb}_2\text{Te}_5$  was induced by reversible switching between the amorphous and crystalline phase. These structures hold significant promise for optical data storage and for flexible display applications. During operation thermal stress caused by temperature gradients are introduced and could lead to failure of the material. The mechanical properties of Si (Oh et al., 2005) and  $\text{Ge}_2\text{Sb}_2\text{Te}_5$  (Choi et al., 2010) have been investigated before. However, crack formation in ultrathin semiconductors and phase-change materials have yet to be reported.

Here, the mechanical properties of these ultrathin films are determined by uniaxial tensile tests in dependence of the film thickness. Si and  $\text{Ge}_2\text{Sb}_2\text{Te}_5$  films in the thickness range between 10 nm and 50 nm are sputter deposited on polymeric substrates. The onset strain of fragmentation is measured and the crack formation is investigated for amorphous and crystalline films. Different methods like resistance measurements, optical microscopy, Raman spectroscopy and scanning electron microscopy are applied to observe the crack development in the films. Generally, cracks occur later for amorphous films in comparison to crystalline films.

Moreover, the results follow the trend of increasing onset strain of fragmentation with decreasing film thickness.

Besides optical data storage and display applications these results are of great interest for MEMS applications and ultrathin solar cells.

### References

- Kats et al. (2012): Nanometre optical coatings based on strong interference effects in highly absorbing media- In *Nature Materials* 12: Kats, M.A. Blanchard, R., Genevet, P., Capasso, F., 12, (20-24).
- Hosseini et al., (2014): An optoelectronic framework enabled by low-dimensional phase-change films- In *Nature*, Hosseini, P., Wright, C.D., Bhaskaran, H., 511 (206-211).
- Schlich et al., (2014): submitted in *ACS Photonics*, Schlich, F.F., Zalden, P.; Lindenberg, A.M., Spolenak, R.
- Oh et al., (2005): Comparison of the Young's modulus of polysilicon film by tensile testing and nanoindentation- In *Sensors and Actuators A: Physical*, Oh, C.-S., Lee, H.-J., Ko, S.-G., Kim, S.-W., Ahn, H.-G., 117, (151-158).
- Choi et al. (2010): Elastic Modulus of Amorphous  $\text{Ge}_2\text{Sb}_2\text{Te}_5$  Thin Film Measured by uniaxial Microtensile Test- In *Electronic Materials Letters*, Choi, Y., Lee, Y.-K., 6, (23-26).

## Compression-shear behavior of a strongly textured Magnesium alloy AZ31 under different strain rates

SEBASTIAN SEIPP<sup>1</sup>, SHIBAYAN ROY<sup>2</sup>, BENJAMIN ZILLMANN<sup>1</sup>, MARTIN F.-X. WAGNER<sup>1</sup>

<sup>1</sup> TU Chemnitz, Institute of Materials Science and Engineering, Chemnitz, Germany

<sup>2</sup> Materials Science and Technology Division, Oak Ridge National Laboratory, Oak Ridge, USA

Texture plays a key role in determining anisotropy and mechanical properties of magnesium alloys. Here, we study the deformation behavior of a strongly textured AZ31 magnesium alloy processed by Equal-Channel Angular Pressing (ECAP) under compression-shear loading. For compression-shear testing, we use a special sample geometry (tilted cylinder geometry) that leads to super-imposed shear stresses (and a preferred shearing-direction) within the sample under nominally uniaxial compressive loading. After ECAP, compres-

sion-shear specimens are taken from the material oriented such that the preferred shear direction is parallel to the last shear plane induced by the final ECAP pass. The specimens are tested at three different strain rates ( $10^{-3}$ ,  $10^0$ ,  $10^2 \text{ s}^{-1}$ ), ranging from quasi-static to dynamic, and strain fields are evaluated with a digital image correlation (DIC) system. In case of the lower strain rates, texture dominates the material behavior in terms of plastic deformation, crack propagation and fracture behavior even when the super-imposed shear stresses

are supposed to promote deformation along different directions. At high strain rates, however, the material is observed to fail in the direction of the highest shear stresses, and this behavior can be rationalized by considering (quasi) adiabatic processes and the relative-

ly stronger impact of thermo-mechanical conditions during dynamic testing. Our results provide a detailed picture of the interaction between microstructure and texture, complex loading conditions and fracture behavior of AZ31.

## Roughness behaviour of nanomaterials

SAYAH TAHAR, BOUTI SAMIR

USTHB, Faculty of Mechanical Engineering, Algiers, Algeria

We propose an experimental study of the surface to dry and analysis of the evolution parameters roughness. The simplified model was proposed to predict the metrological parameters in the contact area of the deformed surface. The model is based on the analysis of the topography 3D of the deformed surface.

Study aims to characterize the topography of sintered materials obtained by wear tests. Therefore it is interesting initially in the evolution of wear for the loads applied and to characterize the different roughness emerging from 3D AFM observations.

Experimental and theoretical research on the topography changes during dry contact deformation was carried out in [1], [2], [3] and [4], providing results that demonstrate the persistent nature of roughness asperities even under high loading when bulk plastic deformation appears. Most theoretical investigations of the problem have been based on a simplified model neglecting the statistical distribution of asperities on the real surface, [5]. In [6] used test and 3D measurement of surface topography in order to investigate its frictional behaviour. The mechanism of contact of a rigid plane with a rough surface in the presence of a lubricant is different than in the case of dry contact.

The topography of the samples was measured both in initial undeformed and in the deformed state after removal of the load. In these states, however, a change of the shape of the samples when compared to the initial state was observed. Thus, prior to the determination of roughness parameters of the deformed surfaces, their curvature was removed using a filtration procedure.

The essential differences in surface topography of samples loaded in dry condition are confirmed in the analysis of roughness parameter evolution. The following 3D parameters were considered. In the unloaded state, flattened asperities can be observed on the deformed surface Fig 1.a. The real contact area corresponding to the maximal load attained in the surface compression experiment can be identified from measurement of the deformed roughness after unloading.

The identification of the real contact area was carried out using a special algorithm based on single profile analysis. The single, randomly selected profiles were extracted from the measured topography of the deformed surface. It should be noted that the profiles obtained in this way have a common reference level. The selected profiles also have the same direction, which, in the case of anisotropic surfaces (turning, grinding) should be perpendicular to the direction of the movement of the machining tool. The proposed model was applied to analyze a wear of four kinds of rough surfaces. The predicted values were compared with experimental results.

The wear and surface roughness based on the parameters of dry friction tests were measured. This study suggested the optimal parameters of chemical composition, and analysis of the effects alloying elements on surface roughness and wear in the process dry friction tests.

### References

- R. G. Bayer, P. A. Engel, J. L. Sirico, (1972) Impact wear testing machine, *Wear*, 19, pp. 343–354
- S. L. Rice, S. F. Wayne, H. Nowotny, (1980) Material transport phenomena in the impact wear of titanium alloys, *Wear*, 65, pp. 215–226
- S. L. Rice, S. F. Wayne, H. Nowotny, (1981) Characteristics of metallic subsurface zones in sliding and impact wear, *Wear*, 74, pp. 131–142
- A. Bartoszewicz, J. Radziejewska and G. Starzyński, (2004), 3D roughness analysis of deformation of surface at contact loading, *Adv Manuf Sci Technol* 28 (4) pp. 17–30
- Hibi, Y., Miyake, K., Murakami, T., Sasaki, S. (2006) Tribological behavior of SiC-reinforced Ti3SiC2-based composites under dry condition and under lubricated condition with water and ethanol, *J. Am. Ceram. Soc.* 89(9), pp. 2983–2985
- Zhang J J, Zhu J H. (2009) Surface structure evolution and abnormal wear behavior of the TiNiNb alloy under impact load, *Metall MaterTrans A* , 40, pp. 1126–113

## Electronic properties and mechanical stability of ZnO in the bulk and nanowire structures under large uniaxial stresses

LUCY A. VALDEZ, RICARDO A. CASALI

Facultad de Ciencias Exactas y Naturales y Agrimensura, Universidad Nacional del Nordeste, Corrientes, Argentina

ZnO is a semiconductor with a wide range of technological applications due to its physical advantages: direct wide band gap, large excitation binding energy, high thermal conductivity and piezoelectricity.[1] In addition, ZnO is very important in high-pressure physics where it has been probed experimentally that ZnO transforms from hexagonal wurtzite (B4) to rocksalt (B1) under hydrostatic pressures.[1] Some of the ZnO properties are improved in the nanosize scale, specially its piezoelectric and semiconducting properties. For this reason, we have been studying ZnO(B4) nanowire and bulk material in order to compare its properties due to confinement.

In the present work, we have first analyzed ZnO using the SIESTA [2] and ABINIT codes [3] in the bulk material. Our calculations with SIESTA were performed using the generalized gradient approximation (GGA) and the local density approximation (LDA).

Then ZnO was subjected to hydrostatic pressures until 10 GPa. Nearby to 4 GPa, the system has presented an anomalous behavior. The same situation appeared when we employed the ABINIT code and it allowed us to associate such behavior to a possible phase transition. The lattice parameters, equilibrium volumes, bulk modulus and its pressure derivative were close to experimental results and other theoretical assessments. [1] The phonon modes, which were calculated with SIESTA and ABINIT at the center of the Brillouin zone, are in excellent agreement with other theoretical calculations and experiment results [1], specially the when using the LDA-GGA hybrid functional. On the other hand, our calculations with ABINIT code provide a lattice parameters, bulk modulus, elastic and piezoelectric constants close to experiments.[1,4]

In the case of ZnO nanowires using the SIESTA code, we have considered non-interacting hexagonal NWs

composed by cells of 48 atoms with periodicity  $1c$  and  $2c$  along  $[0001]$  direction and 108 atoms, with periodicity  $1c$ . We have chosen the hexagonal shape because it is the most stable in growth ZnO nanowires. [5] Its total energies, solid pressure, stress tensor and residual forces was compared and we choose the most stable cell for our studies. Then, a strain along the  $c$  vector was applied to determine the Young modulus and the break tensile of the nanowire into the cell. The obtained values are in agreement with other DFT calculation.[5,6]

By the application of uniaxial strains until 10 GPa, we have calculated the NW Poisson coefficient, variation of lattice vectors with pressure and changes in a hexagonal area bounded by Zn atoms. The more important changes are seen around 6 GPa and 7 GPa, which correspond to nanowires with 48 and 108 atoms, where layers of atoms move away from each other and we could device a possible phase transition under uniaxial stress. In the NW band structure we found a band gap (1.5 eV) larger than the calculated in bulk material (0.9 eV), which is associated to quantum confinement effects.

### References

- [1] Zinc oxide: Fundamentals, Materials and Device Technology. H.Morkoç, Ü.Özgür. 2009. WILEY
- [2] User's Guide SIESTA 3.1. Emilio Artacho et al. (2011)
- [3] X. Gonze et al., *Comput. Mater. Sci.* 25, 478 (2002); see website: <http://www.abinit.org>
- [4] P. Gopal and A. Spaldin. Polarization, piezoelectric constants and elastic constants of ZnO, MgO and CdO. 2005. arXiv:cond-mat/0507217
- [5] S. Haffad et al. *Energy Procedia* 10 128 (2001)
- [6] R. Agrawal et al. *Nano Lett.* 2010, 10, 3432-3438.

## First-principles study on ferroelectricity and its coupling behavior with mechanical deformation of ultrathin PbTiO<sub>3</sub> nanotube

XIAOYUAN WANG<sup>1</sup>, TAKAHIRO SHIMADA<sup>2</sup>, TAKAYUKI KITAMURA<sup>2</sup>

<sup>1</sup>Institute of Systems Engineering, China Academy of Engineering Physics, Mianyang, China

<sup>2</sup>Department of Mechanical Engineering and Science, Kyoto University, Japan

In this study, the ferroelectric (FE) properties and its coupling behavior with mechanical strain of ultrathin PbTiO<sub>3</sub> nanotubes are investigated by first-principles calculations. Different from the thin films, the spontaneous polarization still exists in the nanotube despite their sidewalls being thinner than the critical thickness at which the thin films lose ferroelectricity (Fong et al 2004), which indicates the absence of an intrinsic critical size of ferroelectricity in the nanotube structure. The total energy of nanotube is lower than that of the thin film. This means that the nanotube structure is energetically more stable than the thin film. Moreover, the ground state of the nanotube is not purely FE since it primary involves antiferrodistortive (AFD) rotation of oxygen atoms due to compression in the inner tube wall. The emergence of the AFD displacement plays a central role in stabilizing both the nanotubular structure and FE distortions due to direct AFD-FE coupling. In addition, the coupling behavior of ferroelectricity

and axial strain has also been studied. The axial polarization of nanotube is enhanced by the tensile strain. On the other hand, with the increase of compressive strain, the axial polarization becomes weak and disappears, and the nanotube structure becomes paraelectric state. With the further increase of compressive strain, a vortex type of polarization emerges along the circumferential direction, and the nanotube structure becomes ferroelectric state again. These rich phase transitions in the nanotube structure are induced by the change of covalent Pb-O bond due to the applied strain. Finally, the mechanical strength of PbTiO<sub>3</sub> nanotube is evaluated, and the critical stresses under the tension and compression states are obtained.

### Reference

Fong, D. D., et al. (2004): Ferroelectricity in ultrathin perovskite films. *Science*, 304, 1650-1653.

## Thickness-dependent tensile properties of PEDOT:PSS

O BAE WOO·JU-YOUNG KIM

School of Materials Science & Engineering, UNIST (Ulsan National Institute of Science and Technology), Korea

Future electronic device will progress being transparent and flexible to apply human body. Accordingly researchs about wearable, stretchable devices are studying actively. This leads increasing interest about PEDOT:PSS. PEDOT:PSS have high conductivity, high transmittancy in visible light range among conducting polymers. So PEDOT:PSS has been researched various area like transparent electrode, solar cell, OLED fields. Especially research about flexible transparent electrode using PEDOT:PSS is promising field. But to use PEDOT:PSS to flexible transparent electrode, reliability test comes to the fore as using PEDOT:PSS on flexible substrates. So in this study, tensile test was conducting for reliablity estimation of PEDOT:PSS. We measured tensile properties of PEDOT:PSS and compared data depending on thickness of PEDOT:PSS.

Copper thin film was deposited polypropylene substrate for spin coating. PMMA fucion as scrifice layer was spin coated on copper thin film. PEDOT:PSS was prepared by two methods. Mico-scale samples were air dried at ambient conditions more than 12 hours after spread on substrate. Nano-scale samples were

spin coated and annealed at 115 °C. Air dried samples were pressed with die-cutting press to dog-bone shape for tensile testing. Spin coated samples were fabricated to dog-bone shape using ion milling system. Samples aligned with polypropylene jigs. PMMA scrifice layer was etched in acetone. Thickness of tensile samples was 6 μm, 600nm, 60nm each. Different stress-strain curve was obtained by tensile tests depending on film thickness. We discuss about tensile properties depending on thickness of PEDOT:PSS.

### References

- Udo L. (2009): Mechanical characterization of PEDOT:PSS thin films, *Synthetic Metals* 159 473-479
- Udo L. (2009): Microscopical investigations of PEDOT:PSS thin films, *Adv. Funct. Mater.* 19, 1215-1220
- Y. Y. Lee. (2013): Stretching-induced growth of PEDOT-rich cores: A new mechanism for strain-dependent resistivity change in PEDOT:PSS, *Adv. Funct. Mater.* 23, 4020-2027

Poster Topic F:

***Advanced steels and steel composite materials***

---

# Effect of filler metal on micro-structural, mechanical and corrosion behavior of austenitic stainless steel weldment 316L

A. SRIBA<sup>1,2</sup>, K. M. REHOUMA<sup>1</sup>, S.E. AMARA<sup>2</sup>, N. MADAOU<sup>3</sup>

<sup>1</sup>Welding And N.D.T. Research Centre, Algiers, Algeria

<sup>2</sup>Laboratoire D'électrochimie-Corrosion Métallurgie et Chimie Minérale, Faculté De Chimie, Université Des Usthb, Alger, Algeria

<sup>3</sup>Division Milieux Ionisés, Centre de Développement des Technologies Avancées, Alger, Algeria

Austenitic stainless steels in this case 316L grade are widely used in fields and varied industrial sectors. They are generally considered weldable if proper precautions are followed, however, they present a number of problems during and after welding: hot cracking during welding, intergranular corrosion and precipitation of embrittling phases during prolonged maintaining in the temperature range from 400°C to 900°C [1]. The remaining deposit (called seam) in these alloys has austeno-ferritic structure. The essential factors governing the metallurgical embrittlement of these deposits are the ferrite[2,3,4] content and the carbon content of the deposited metal. The ferrite within the molten zone plays an important role in the embrittlement of the welded alloys, its content depends mainly on the nature of the filler metal. For this reason, the choice of filler metals is an important element in the manufacture of articles of austenitic stainless steels and ensure good reliability for these welds service [5]. The study reported in this paper brings out and shows the influence of the chemical composition of the filler metal (ER316L and ER308L) on the microstructure resulting after welding by TIG process, mechanical and corrosion behavior of austenitic stainless steel weldment 316L. The mechanical tests are: micro-hardness and Charpy impact strength, corrosion tests is carried out in sodium chloride 3.5%.

## References

Allegro, M. (2006): What does it mean? – In: Turm, P., Bauer, B. & Läufer, R. (eds.): Guess what. Springer, 16-44; Hintertux.

- Rusitzka, E. & Jubitz, K.-B. (1968): Trias. – In: Grundriß der Geologie der DDR, Bd. 1: 268-89; Berlin.
- Wolburg, J. (1969): Die epirogenetischen Phasen der Muschelkalk und KeuperEntwicklung Nordwest-Deutschlands, mit einem Rückblick auf den Buntsandstein. – Geotekt. Forsch., 32: 165; Stuttgart.
- P. Lacombe, G. Beranger. « Structures et diagrammes d'équilibre des diverses nuances des aciers inoxydables. Conséquences sur les traitements thermiques », édition de physique, les Ulis, 1990.
- J.A. Brooks, A.W. Thompson « Microstructural development and solidification cracking susceptibility of austenitic stainless steel welds ». International Materials Reviews. 1991, Vol.36, n°1, pp.16-44.
- Rajasekhar K., Harendranath C. S., Raman R., Kulkarni S. D. « Microstructural evolution during solidification of austenitic stainless steel weld metals: A color metallographic and electron microprobe analysis study ». Materials characterization. 1997, Vol.38 (2), p. 53-65.
- Elmer J.W., Allen S.M., Eagar T.W. « Microstructural Development during Solidification of Stainless Steel Alloys ». Metallurgical and Transactions A. 1989, Vol.20A, p. 2117-2131.
- Rehouma K., Shabadi R.S, Taillard R., Bouabdallah M., Imad A. « Effect of ageing at 700°C on Ferrite Transformation in a 316L/308L weldments ». Materials and Manufacturing Processes. 2012, Vol.27, Issue 12, p.1370-1375.

Poster Topic G:

***Fracture mechanics***

---

## Estimation of Fracture Toughness of Metallic Materials Using Instrumented Indentation Test

JUN-YEONG KIM<sup>1</sup>, WOJOO KIM<sup>1</sup>, SEUNG-HUN CHOI<sup>1</sup>, DONGIL KWON<sup>1</sup>

<sup>1</sup>Department of Materials Science & Engineering, Seoul National University, Seoul

Fracture toughness is one of the most important material properties required for Fitness For Service (FFS). In practice, however, it is usually unavailable for components of structures in the field since its testing can be difficult because of the specific specimen geometry and size requirement, the complex procedure, and the destructiveness of the method. The instrumented indentation test (IIT) has been proposed as a unique solution to overcome these drawbacks and has been developed for nondestructive testing of in-field structures. Previous investigations, however, have encountered a major problem: how to determine the critical fracture point corresponding to crack propagation, since there

is no crack event during indentation for deformable

metallic materials. We develop a simple and realistic approach based on fracture mechanics and contact mechanics to estimate fracture toughness of metallic materials. Models are developed for brittle and ductile fracture. Different criteria are applied to each model to determine the critical fracture point during indentation in terms of critical fracture stress/strain. In this study, fracture toughness was estimated for various metallic materials from each model and compared with that measured from standard fracture-toughness test. In addition, we extend our models to low temperature tests as well.

## The experimental study of stress-strain states in stress concentrators with the use of the method of digital image correlation

ELENA M. SPASKOVA, EVGENIY V. LOMAKIN

Perm National Research Polytechnic University, Perm, Russia

One of the important tasks in the field of solid mechanics is to study the effect of different types of stress concentrators on the behavior of structural elements.

The aim of the work is an experimental study of the stress-strain states in hubs using the method of digital image correlation.

In this work we consider the use of three-dimensional digital optical system, Vic-3D, the mathematical apparatus of which is based on the method of digital image correlation.

The video system is designed for the analysis of displacement fields and strain on the sample surface.

This article describes the technique of the experiment with the use of a digital optical system, its structure and working principle.

The mathematical foundations of the computing device system were formulated, and uniaxial compression „Brazilian test“ were done in order to develop the methodology of the experiment using a digital optical system.

The results of the uniaxial tensile tests on plates made of plexiglass with concentrators of different geometries, as well as the results of tests on a uniaxial tensile carbon plate with a circular hole using a digital optical system, were presented. Mechanical uniaxial tensile test were performed on the test system Instron 5882

and Instron 5989, together with the use of digital optical system Vic-3D.

As a result of the plates tensile test, transverse, longitudinal, shear deformations, as well as the intensity deformation fields were constructed.

The use of video system made it possible to detect not only changes in strain, but also to assess the impact of stress concentrators that implement complex stress-strain state of the material.

The system allowed to record the evolution of the fields of displacements and strains to evaluate the nature of heterogeneity of fields to keep track of the material deformation processes occurring on the surface of the sample. The add-on software video „virtual extensometer“ was used in determining the mechanical properties of the material.

The high efficiency of the method of correlation of digital images in the study the behavior of the material in the event of non-uniform strain fields was shown.

This work was carried out in the PNRPU with support of the Government of Russian Federation (the decree No. 220 on April 9, 2010) under the Contract No. 14.B25.310006, on June 24, 2013, and Russian Fund for Basic Research (grant № 13-08-00304, № 14-08-31387).

## References

Sutton M.A., Orteu J.-J., Schreier H. (2009): Image Correlation for Shape, Motion and Deformation Measurements. – University of South Carolina, Columbia, SC, USA – 364 p.

Tretyakova T.V., Spaskova E.M. (2013): Experimental study of limit stress-strain state quasi-brittle materi-

al using correlation techniques digital images. PNR-PU Mechanics Bulletin, no. 2, pp. 186-198.

Tretyakova T.V., Wildemann V.E. (2014): Study of spatial-time inhomogeneity of serrated plastic flow Al-Mg alloy: using DIC technique. Fracture and Structural Integrity, no. 27, pp. 83-97.

# Methods of Stochastic Mechanics for Characterisation of Microstructural Failure in Heterogeneous Materials

MIKHAIL TASHKINOV, NATALIA MIKHAILOVA

Perm National Research Polytechnic University, Russia

The problem of determination of mechanical and physical properties of heterogeneous materials is highly topical. Replacing experimental testing with multi-scale simulations, when material's properties are obtained by modelling at the smaller scales, can save considerable efforts. One of the major barriers for applications of multi-scale methods is complexity of a micro-scale structure of composites. Computational and experimental research has proved that randomness of the microstructural geometrical and physical parameters plays an important role in behaviour of multicomponent materials (e.g. Kwon 2008, Rasool 2012). Thus, the precision of their behaviour modelling depends on ability to consider the peculiarities of the non-periodic heterogeneous microstructure. This work offers a model, which combine several approaches of stochastic mechanics to create a tool that can assess deformation and fracture processes in heterogeneous materials on a micro-scale basing on the mechanical and morphological properties of the components.

The approach based on correlation functions is used to formalize the heterogeneous materials' microstructure. The set of correlation functions allows to characterize and quantify various microscopic properties of the materials including dispersion, clustering and orientation of inclusions. It is also used for reconstruction of the 3D structure of heterogeneous material in order to avoid repeating costly high resolution imaging techniques during analysis of microstructure (Jiao 2007, Liu 2013).

The suggested methodology implies that mechanical properties of microstructural components are defined with conventional phenomenological equations and criteria while the effective properties of composite and characteristics of microscopic deformation fields are computed using the elastic and elastoplastic solutions of stochastic boundary value problems (SBVPs) with piecewise constant coefficients equations. The multipoint statistical moments and functions of the stochastic stress and strain fields are used as the characteristics of the deformation processes in the components of the material. Their analytical expressions are

obtained by connecting the microstructural correlation functions with the SBVP solution (Tashkinov 2014). The material properties were defined as the constants in the integral-differential equations, while loading on the volume's boundaries was set as the boundary conditions of SBVP.

The case studies of representative volumes of fibre-reinforced composites as well as of multicomponent composites with randomly distributed spherical and ellipsoidal inclusions were investigated. The micro-scale geometry of the samples was obtained both with modelling and experimental analysis. The numerical results were calculated for high order statistical moments and function and were used for characterisation for failure prediction in micro-scale constituents of the materials. The work was carried out at the Perm National Research Polytechnic University with support of the Government of Russian Federation (The decree № 220 on April 9, 2010) under the Contract № 14.B25.310006, on June 24, 2013.

## References

Jiao Y., Stillinger F.H., Torquato S. (2007): Modeling heterogeneous materials via two-point correlation functions: Basic principles. *Physical Review*, 76:031110.

Kwon YW, Allen DH and Talreja R (eds) (2008): *Multi-scale Modeling and Simulation of Composite Materials and Structures*. Springer, New York.

Liu Y., Steven Greene M., Chen W. et al. (2013): Computational microstructure characterization and reconstruction for stochastic multiscale material design. *Computer-Aided Design* 45:65–76

Tashkinov, M. (2014): Statistical characteristics of structural stochastic stress and strain fields in poly-disperse heterogeneous solid media. *Computational Materials Science* 94:44–50

Rasool A, Böhm HJ (2012): Effects of particle shape on the macroscopic and microscopic linear behaviors of particle reinforced composites. *International Journal of Engineering Science* 58:21–34.

## The complex experimental studies of the mechanical properties of reinforcing elements

MARIA S. TEMEROVA, VALERIY E. VILDEMAN, EVGENIY V. LOMAKIN

Perm National Research Polytechnic University, Russia, Perm

Optimization of properties of composite materials and their products has brought about the demand for fundamental studies of properties of filaments and fibres, as well as fabrics, under different active external influences. The complexity of the design of such materials provided the basis for the development of questions about the mechanical behavior of textile structures that characterize the relationship between the structure and properties of materials.

In this paper we propose to study reinforcing materials, namely fibres and fabrics, in a complex test. We have conducted quasi-static tensile tests on strips of fabric and fibres, impact tensile tests on belts, thread-pulling tests on fabric, and breaking tests on fabric.

The aim of this work was to obtain new data reflecting the basic laws of deformation and fracture mechanisms of woven materials.

From these experiments and analysis of the data obtained it can be concluded that the study of woven fabric requires further investigation of additional solutions and methodological issues.

This work was conducted in Perm National Research Polytechnic University, with the financial support of the Russian Foundation for Basic Research (grant № 13-08-96016 r\_ural\_a) and the Government of the Russian Federation (Decree number 220 of April 9, 2010), contract number 14.V25.310006 24 June 2013.

### References

- Scardino F., J. Heerlen., S. Kawabata et al. Woven structural composites: Trans. from English. / Ed. T.-W. And F. Chu Ko. - M.: Mir, 1991.-432 pp., pic.
- Lobanov D.S., Temerova M.S. Features quasi-static test yarns and fabrics // Bulletin of Perm National Research Polytechnic University. Mechanics. 2013 № 2. - P. 96-109.
- Grushetsky I.V., Dimitrienko I.P., Ermolenko A.F. et al. Destruction of structures made of composite materials. Ed. V.P. Tamuzs, V.D. Protasov. - Riga: Zinatne, 1986.-264 with.
- Vildeman V.E., Babushkin A.V., Tretyakov M.P. et al. Mechanics of materials. Methods and means of experimental studies: a tutorial / VE Vildeman [et al.]; Ed. VE Wildemann. - Perm: Publishing House of Perm. nat. issled. Polytechnic. University Press, 2011. - 165 p. - ISBN 978-5-398-00652-0
- Fedorov A.E., Samartsev V.A., Gavrilov V.A., Vildemann V.E., Slovicov S.V. Experimental study of mechanical properties of modern surgical absorbable sutures // Russian Journal of Biomechanics. - T. 13, № 4 (46). - 2009. - S. 78-84.

## Shock loading direction effects on ejection mass and particle sizes of micro-jet from a grooved metal surface

SHI YI-NA, QIN CHENG-SEN

Institute of Applied Physics and Computational Mathematics, Beijing, China

Metals under shock-loaded conditions can lead to complex phenomena depending on the properties of the material and initial shock conditions. It has long been known that the reflection of strong shock waves from metal surface can cause a fine spray of matter particles (ejecta). The phenomenon has attracted much attention since being discovered by Walsh and Asay et al, due to its importance in shock response of material interface, and its application in inertial confinement fusion.

Previous studies have shown that the formation of ejecta is very complicated, and ejecta is often caused by various factors, such as surface microstructure, shock

condition and release melting et al. There inevitably exist many grooves on metal surfaces in the form of pits, scratches and machine marks. The micro-jet from those grooves may become one kind of main ejection modes. Up to now, significant efforts have been dedicated to studying on the micro-jet mechanism by experimentally and theoretically. Experiment techniques include thin-foils, Asay windows, piezoelectric pins and pulsed x-rays. The effects of groove shape, shock wave rise-time and shock pressure on micro-jet are investigated. Theoretical models and numerical simulations on micro-jet have also been carried out, including continuum level and molecular dynamics simulations. Re-

cently, some measured results on ejecta particle sizes are given, which are also predicted by percolation theory. Some MD simulations investigated nano-scale jet breakup and particle size distribution. However, due to the complexities, developing a model that predicts the amount and particle size of ejecta based on the above micromechanical processes is a difficult problem.

In this work, we investigate the dynamic properties of shock-induced surface micro-jet from grooved aluminum as regards shock direction and groove angle effects. The grooves of 20  $\mu\text{m}$  depth are set on metal surface. Different loading directions are discussed in detail, with the same impact velocity. One is the case that shock loading is generated along the direction perpendicular to metal surface, and another is the case of head-on colliding shock loading parallel to the surface. The formation processes of micro-jet from AL surface under the above shock conditions are simulated by using the code MEPH, which is an independent-developed multi-material Eulerian hydrocode with a VOF approach to capture the interface. A new model for the particulate spray is developed to study the instability evolution and fragmentation of micro-jets. Ejecta particle diameter is micron, and the particle size distribution of micro-jet is predicted to exhibit a power-law scaling with exponents, in good agreement with Sorenson experiment. The results indicate that the total ejected mass increases significantly, and the ejecta size is less

for the case of head-on colliding shock loading. The cause may be that the micro-jet have melted or release melted. In addition, we discuss the evolution properties of micro-jet matter with time to different groove angles. It is valuable for the study on the mechanism of metallic surface fragmentation under shock-loaded condition.

#### References

- Asay J.R. (1976): Material ejection from shock-loaded free surfaces of aluminum and lead. -Report No. SAND-76-0542.
- Sorenson D.S., Minich R.W., et al. (2002): Ejecta particle size distributions for shock loaded Sn and Al metals. -J. Appl. Phys., 92(10): 5830.
- Shi Y.N. & Qin C.S. (2009): The instability and breakup of stretching metallic jets. -Chin. J. Theor. Appl. Mech., 41(3): 361-369.
- Durand O. & Soulard, L. (2012): Large-scale molecular dynamics study of jet breakup and ejecta production from shock-loaded copper with a hybrid method. -J.Appl.Phys., 111:044901.
- Dimonte, G. Terrones, G., et al. (2013): Ejecta source model based on the nonlinear Richtmyer-Meshkov instability., -J. Appl. Phys., 113: 024905.
- Li B., Zhao F.P., Wu H.A. & Luo. S.N. (2014): Micro-structure effects on shock-induced surface jetting. -J. Appl. Phys., 115: 073504.

Poster Topic H:

***Materials for fission and fusion***

---

## XRD examination of oxide dispersion strengthened steels irradiated by swift heavy ions

ANDREI BENEDIKTOVITCH<sup>1</sup>, VLADIMIR UGLOV<sup>1</sup>, SVETLANA VLASENKO<sup>1</sup>, TATIANA ULYANENKOVA<sup>2</sup>, ALEXANDER SOHATSKY<sup>3</sup>, JACQUES O'CONNELL<sup>4</sup>, VLADIMIR SKURATOV<sup>4</sup>

<sup>1</sup>Belarusian State University, Minsk, Belarus

<sup>2</sup>Rigaku Europe SE, Ettlingen, Germany

<sup>3</sup>Joint Institute for Nuclear Research, Flerov Laboratory of Nuclear Reactions, Dubna, Moscow region, Russia

<sup>4</sup>Centre for HRTEM, Nelson Mandela Metropolitan University, Port Elizabeth, South Africa

Oxide dispersion strengthened (ODS) steels are promising functional materials for the IV-th generation nuclear reactors. Oxide nanoparticles incorporated into Fe matrix are expected to improve the swelling and high temperature creep resistance of these alloys exposed to high radiation damage doses.

One of the source of radiation, which effects remain much less studied in comparison with others, are fission fragments, because corresponding structural changes can be simulated using dedicated high energy heavy ion accelerators only. In this work we have studied radiation damages in 15Cr-3: Fe-15Cr-2W-0.2Ti-0.35Y<sub>2</sub>O<sub>3</sub> ODS steel irradiated by 700 MeV Bi ions. The room temperature irradiation up to a fluence of  $6.15 \cdot 10^{12}$  cm<sup>-2</sup> was done at U400 FLNR JINR cyclotron, Dubna. Swift heavy ion induced radiation damages were characterized using transmission electron microscopy (TEM) and X-ray diffraction techniques. The XRD examination included the residual stress analysis,

pole figure measurements and  $\theta$ - $2\theta$  scans. The  $\theta$ - $2\theta$  scans were measured with Ge(220)x2 monochromator at diffractometer equipped with 9kW rotating anode source. The aim of the  $\theta$ - $2\theta$  measurement was to collect high quality data for whole profile analysis (Ribarik & Ungar, 2010). The method of convolutive whole profile analysis was extended to account for the peak broadening due to distortions of the Fe matrix caused by oxide nanoparticle.

TEM analysis have revealed that Bi ions induce complete amorphization of Y<sub>2</sub>Ti<sub>2</sub>O<sub>7</sub> pyrochlores composing nanoparticle population in studied ODS material as a result of multiple latent track overlapping.

### Reference

Ribarik, G. & Ungar, T. (2010): Characterization of the microstructure in random and single crystals by diffraction line profile analysis. – Material Science and Engineering A., 528: 112121.

## Creep and anelasticity of ferritic ODS steel MA956

JOSÉ RODOLPHO DE OLIVEIRA LEO<sup>1</sup>, AMIR SHIRZADI<sup>1</sup>, JAN KOWAL<sup>1</sup>, MICHAEL E. FITZPATRICK<sup>2</sup>

<sup>1</sup>Materials Engineering Group, The Open University, Milton Keynes, UK

<sup>2</sup>Faculty of Engineering and Computing, Coventry University, Coventry, UK

ODS steels are still regarded as promising materials for advanced nuclear power plants, given the presence, in the microstructure, of homogeneously distributed oxide nanoparticles, which impart high temperature mechanical strength and resistance against irradiation-induced damage [1]. However, performance of the material is subjacent to the operational conditions as well as to microstructural features, which result from composition and fabrication history.

MA956 is a commercial grade of ferritic ODS steel classified as FeCrAl alloy, due to the 20%Cr and 4.5%Al in its composition. It is known for its excellent corrosion and creep resistance at high temperature and high anisotropy of properties, as a consequence of its strongly textured columnar grains [2], [3]. However, the suitability of this class of steel composites to advanced power plant components and structures would depend on

its ability of resisting the severe operational environment for extended periods of time.

During a plant's lifecycle, variations in demand and stops for maintenance, refuelling or emergencies are expected. These conditions impose transients of load (or load and temperature), which trigger anelasticity in previously crept materials. It was seen before that anelasticity, characterized as time-dependent plastic strain recovery, is beneficial to a material, since it increases the creep-rupture life and decreases the creep ductility [4].

The work being developed aims at studying to what extent anelasticity takes place in a creep-resistant steel, such as the ferritic ODS MA956. Anelastic response of a material is related to intergranular and intragranular back stresses, whose origins are associated with dislocation motion and interactions in grains and grain

boundaries. The natural creep strength of this steel, then, may be enhanced by recovery phenomena during transients.

The characterization of anelastic response was found to be a multidisciplinary approach, involving comprehension of dislocation motion through the lattice system and investigation of microstructural relevant features. For this reason, techniques such as EBSD, TEM and neutron diffraction are employed here, on materials tested for a transient manifested as a full unloading stage during creep deformation.

Preliminary results show that the MA956 is characterized by {111}<110> and {001}<110> texture systems, which appear to exert influence on its room temperature mechanical response, while high temperature behaviour seems less affected by its microstructures. Samples for anelastic response are being tested in the longitudinal direction, that is, parallel to the extrusion direction, along which the columnar grains are elongated, due to its higher strength. Quantitative and qualitative TEM will determine magnitudes of intragranular back stresses, associated with dislocations, while neu-

tron diffraction will study the intergranular stress component between the textured fibres.

#### References

- [1] A. Alamo, V. Lambard, X. Averty, and M. H. Mathon, "Assessment of ODS-14%Cr ferritic alloy for high temperature applications," *J. Nucl. Mater.*, vol. 329–333, pp. 333–337, 2004.
- [2] K. Turba, R. C. Hurst, and P. Hähner, "Anisotropic mechanical properties of the MA956 ODS steel characterized by the small punch testing technique," *J. Nucl. Mater.*, vol. 428, no. 1–3, pp. 76–81, Sep. 2012.
- [3] T. S. Chou and H. K. D. H. Bhadeshia, "Recrystallization temperatures in mechanically alloyed oxide-dispersion-strengthened MA956 and MA957 steels," *Mater. Sci. Eng. A*, vol. 189, no. 1–2, pp. 229–233, Dec. 1994.
- [4] D. G. Morris, "Anelasticity and creep transients in an austenitic steel," *J. Mater. Sci.*, vol. 13, pp. 1849–1854, 1978.

## Application of Automated Ball Indentation Innovative Technique on the Determination of Mechanical Properties of Nuclear Structural Materials

JAN ŠTEFAN<sup>1,2</sup>, RADIM KOPŘIVA<sup>1</sup>, JAN SIEGL<sup>2</sup>

<sup>1</sup>ÚJV Řež, a. s., Husinec, Czech Republic

<sup>2</sup>KMAT-FJFI-ČVUT, Prague, Czech Republic

Nuclear reactor pressure vessel safety assessment and lifetime extension are important topics of nuclear power plant management. Through the operation, the reactor pressure vessel and its inner components are subject to high temperature, high pressure, and mainly the intensive flux of fast neutrons. Microstructural changes, proceeding in neutron-irradiated materials, result in substantial degradation of their mechanical properties, namely the radiation hardening, the radiation embrittlement etc. Therefore, solution of the nuclear power plant safety assessment requires precise information on the degradation of the mechanical properties of the components structural materials.

Mechanical properties of the nuclear power plant components' structural materials are evaluated by testing methods, comprising of surveillance programs. Strength properties are evaluated from tensile tests results, fracture properties are evaluated either from Charpy impact tests, or from fracture toughness tests. However, all the above mentioned methods of mechanical testing are based on the employment of large specimens. This is connected with high consumption of testing material, availability and volume of which is often limited. Therefore, demand arose to develop and

implement innovative testing methods with low requirements on the the necessary volume of the testing material, capable of testing irradiated materials.

Automated Ball Indentation (ABI) test is a fully computer-controlled test based on the indentation of a metallic material of a thickness greater than 0.5 mm. Its purpose is to determine the yield strength and the tensile strength of materials in a non-destructive and localized fashion. ABI is a simple method since it requires no special device (standard tensile testing machine is sufficient). ABI test appears to be a prospective mechanical testing method for the irradiated structural materials' mechanical properties evaluation. Employment of the method would contribute to the improvement of mechanical properties evaluation by enlarging the present data base.

The paper is focused on the description of the employment of the ABI technique in the process of reactor pressure vessel components structural materials testing and evaluation at the accredited semi-hot cell testing laboratory of the Mechanical Testing Department in ÚJV Řež, a. s. The research was done in cooperation with the Department of Materials, Faculty of Nuclear Sciences and Physical Engineering, Czech Technical

University in Prague (KMAT-FJFI-ČVUT). Comparison of the results of the ABI tests with the results, collected by conventional mechanical testing methods, is depicted. The results were created within the project TA03011266: "Development of innovative semi-destructive method of high active material evaluation for nuclear reactor components lifetime assessment". The project is focused on preparation of a certified procedure for quantification of mechanical properties of structural materials of WWER type reactor components using miniaturized specimens. The project start-

ed in 2013, and the completion of the last stage of the project is planned for December 2015 with evaluation of suitability of the method for the quantification of mechanical properties of irradiated materials.

#### Reference

Eliášová, I. – Kopřiva, R. – Falcník, M. (2014): "Hodnocení mechanických vlastností strukturních materiálů komponent JE využitím semidestruktivních metod." (in Czech language) In: All for Power (periodical). 109-110, ISSN: 1802-8535, Czech Republic

## Radiation stability of ZrSiN system under the Xe ions irradiation

VLADIMIR UGLOV<sup>1,2</sup>, VITALI SHYMANSKI<sup>1</sup>, GREGORY ABADIAS<sup>3</sup>, GENNAGY REMNEV<sup>2</sup>, ANDREY SUVALOV<sup>1</sup>

<sup>1</sup>Belarusian State University, Minsk, Belarus

<sup>3</sup>Institut P', Poitiers, France

Active research in recent years in the study of the structure and properties of nanocrystalline materials have shown particular promise of composite coatings on the basis of ZrSiN, which is characterized by the thermal stability of the structure at temperatures up to 1300 °C and high mechanical properties [1]. However, there are no any reliable data on the radiation stability of such structures, which is particularly relevant for their operation in conditions of high radiation exposure. These materials can be considered as protective materials in reactor system of fission. The aim of the present work was to study the radiation stability of the ZrSiN system implanted with Xe ions.

ZrSiN system was formed as a thin film coating on silicon substrate by reactive magnetron sputtering of zirconium and silicon target in Ar+N<sub>2</sub> (p<sub>N</sub> = 8.8 mPa) atmosphere at temperature of 650 °C. The power on the Zr and Si cathodes was 300 and 250 W, respectively. In the formed ZrSiN coating the ions of Xe<sup>+2</sup> with energy of 180 keV and the doses 5·10<sup>16</sup> and 10<sup>17</sup> cm<sup>-2</sup> were implanted. The implantation was carried out at room (T=20 °C) and higher (T=800 °C) temperatures.

The elemental composition of the ZrSiN system was determined on the basis of Rutherford back-scattering (RBS), The phase composition was studied by means of X-ray diffraction (XRD).

The ZrSiN coatings are characterized by uniform distribution of elements across the thickness (600 nm) coating, the concentrations being equal to 34 at. % (Zr), 22 at. % (Si) and 44 at. % (N). The phase composition of the coating represents by the cubic zirconium nitride ZrN, the lattice parameter of which equals to 0.4572 nm. Diffraction reflections, indicating the presence of phases based on silicon have no been identified, however, the relation of the concentrations N/Si, being approximately equal to 2, allows to suppose [1] an amorphous matrix of Si<sub>3</sub>N<sub>4</sub> formation with included therein

nanocrystalline (10 – 30 nm) particles of zirconium nitride ZrN.

RBS results allowed to determine the concentration profiles of the xenon distributed in the ZrSiN coatings, according to which the maximum concentration of xenon increases from 8 to 17 at. % with the dose increasing from 5·10<sup>16</sup> to 10<sup>17</sup> cm<sup>-2</sup> (at T=20 °C). According to the XRD data the lattice parameter of zirconium nitride ZrN is equal to 0.4572 nm, which corresponds to the lattice parameter of ZrN in the unirradiated system. The implantation of xenon ions at T=800 °C results in displacement of the maximum concentration to the depth of about 200 nm that is accompanied by broadening of the concentration profile. The lattice parameter of the zirconium nitride ZrN is not changed after xenon ions implantation that can indicate on the stability of the structure for this type of radiation exposure. The reason for such behavior can be associated with nanocrystalline particles of zirconium nitride, which promotes the migration of radiation-induced defects to the interface [2].

Thus, it was shown that the structure of coatings ZrSiN, formed by reactive magnetron sputtering, characterized by the radiation resistance under the xenon ions (180 keV) irradiation.

#### References

1. Musil J., Daniel R., Zeman P., Takai O., Structure and properties of magnetron sputtered Zr-Si-N films with a high  $\geq 25$  at.% Si content // Thin Solid Films. 2005. V.478 P.238
2. V.V. Uglov, G.E. Remnev, N.T. Kvasov, I.V. Safronov. Dynamic processes in metal nanoparticles under irradiation. Journal of surface investigation. X-ray, synchrotron and neutron techniques. – 2014. – Vol. 8, № 4. – P. 703-707.

Poster Topic I:

***High temperature materials***

---

# Atomistic Simulations of Dislocation-Interface Interactions in the $\gamma/\gamma'$ Microstructure in Ni-base Superalloys

FREDERIC HOULLE, JUAN WANG, JULIEN GUENOLE, JOHANNES J. MÖLLER, ARUNA PRAKASH, ERIK BITZEK

Friedrich-Alexander-Universität Erlangen-Nürnberg (FAU), Department of Materials Science and Engineering, Institute I, Erlangen, Germany

The superior strength of single crystalline Ni-base superalloys is mainly caused by the high volume fraction of the cuboidal  $L1_2$  ordered  $\gamma'$  hardening phase which is precipitated in a disordered face-centered cubic  $\gamma$  matrix. The strengthening effect is rooted in the difficulty of channel dislocations in the  $\gamma$ -phase to cut into the  $\gamma'$ -precipitate. The interaction of dislocations with the  $\gamma/\gamma'$  interphase boundary (IPB) is an inherently atomistic problem related to the dislocation core structure and energy within the different phases. A quantitative determination of the critical resolved shear stress  $\tau_c$  required for dislocations in the  $\gamma$  matrix to penetrate into the  $\gamma'$ -phase is therefore difficult to obtain directly from experiments. Although atomistic simulations are ideally suited to study this process, only very few, qualitative studies exist in the literature (Yashiro et al. 2002, Zhu et al. 2013).

Here we report on a quantitative atomistic study on dislocation cutting into the  $\gamma'$  phase.  $\tau_c$  is determined from quasi-static simulations on infinitely long, straight dislocation lines interacting with a coherent planar (100) IPB in a quasi-2D simulation setup using periodic boundary conditions in line and propagation direction and 2D boundary conditions with applied forces in the direction of the glide plane normal. This setup allows one to incorporate screw dislocations as well as  $60^\circ$  mixed dislocations. The atomic interaction is modeled by two different embedded atom method (EAM) type potentials (Du et al. 2013, Mishin 2004). Studying different types of dislocations and using different potentials allows one to evaluate the influence of lattice misfit on the critical cutting stress, and to correlate  $\tau_c$

with potential properties like the stable and unstable stacking fault energies. In addition to the determination of  $\tau_c$  in a pure Ni/Ni<sub>3</sub>Al system, the influence of Al concentration gradients across the coherent IPB on  $\tau_c$  as well as the role of Re atoms on dislocation-IPB interactions was investigated. These results can be directly used to parameterize e.g. dislocation dynamics (DD) simulations. The simulations are compared to 3D simulations of the deposition of dislocation segments by threading channel dislocations and to the situation in the presence of a misfit dislocation network. The results are discussed in the context of a recent multi scale modeling approach for single crystalline Ni-base superalloys.

## References

- Du, J. P., Wang, C. Y. & Yu, T. (2013): Construction and application of multi-element EAM potential (Ni–Al–Re) in  $\gamma/\gamma'$  Ni-based single crystal superalloys. *Model. Simul. Mater. Sci. Eng.* 21, 015007.
- Mishin, Y. (2004): Atomistic modeling of the gamma and gamma'-phases of the Ni-Al system. *Acta Met.* 52, 1451–1467.
- Yashiro, K., Naito, M. & Tomita, Y. (2002): Molecular dynamics simulation of dislocation nucleation and motion at gamma/gamma' interface in Ni-based superalloy. *Int. J. Mech. Sci.* 44, 1845–1860.
- Zhu, Y., Li, Z. & Huang, M. (2013): Atomistic modeling of the interaction between matrix dislocation and interfacial misfit dislocation networks in Ni-based single crystal superalloy. *Comput. Mater. Sci.* 70, 178–186.

## Internal Friction and Shear Modulus Temperature Dependence of 9%Cr Ferritic Steel P92 in 25 ÷ 750°C Temperature Range

ELGUJA KUTELIA<sup>1</sup>, GEORGE DARSAVELIDZE<sup>1</sup>, TENGIZ KUKAVA<sup>1</sup>, TEMUR DZIGRASHVILI<sup>1</sup>, IA KURASHVILI<sup>1</sup>, FRANCISCO J. PEREZ TRUJILLO<sup>2</sup>

<sup>1</sup>Georgian Technical University, Tbilisi, Georgia

<sup>2</sup>Universidad Complutense de Madrid, Spain

The creep rate in practical steels, especially in ferritic 9%Cr steels (P92), is controlled by the diffusion of solute atoms rather than vacancies. Chromium is an exceptional solute because the size difference of Cr versus  $\alpha$ -Fe is very small. Consequently, its diffusion plays an important role in the formation of precipitates in the steel matrix at early stages as well as in the final formation of stable phases during a long-term thermo-mechanical impact. It is also important that the above steel contains many minor alloying elements, and therefore, actual estimation of the diffusion parameters and mechanical properties at service temperatures is not easy in heat-resistant steels. Development of methods of substructural strengthening of alloys requires a deep insight of the processes of formation and stabilization of substructure. The latter necessitates use of structure-sensitive methods, among which the method of internal friction is most efficient. The temperature dependences of  $Q^{-1}(t)$  and  $f_2(t)$  were measured in the relaxometer with the reverse torsion pendulum at frequencies  $\sim 1$  Hz and amplitudes of deformation  $10^{-5}$  ÷  $10^{-3}$  in the temperature range 25 ÷ 750°C, with the rate of heating/cooling 2°C/min. For the first measurement the samples were cut and

machined to a size (1x1x50)mm<sup>3</sup> out of bulk coupons, previously normalized at 1060°C/20min + tempered at 770°C/60min. Additional heat treatment after the first measurement was conducted directly in the relaxometer via annealing at 950°C/20min, after which  $Q^{-1}(t)$  and  $f_2(t)$  were measured repeatedly. Two maxima of internal friction were revealed at temperatures 570°C and 650°C, accompanied by shear modulus defects. In the temperature range 300-750°C reduction of shear modulus occur with different rates, depending on previous heat treatment of the sample. The first maximum is determined to be of relaxation nature, and is characterized by the activation energy of  $\sim 52000$  cal/mol and the relaxation time constant equal to 10-14sec. According to its activation features, the maximum at 570°C may be attributed to the relaxation rearrangement of couples of chromium atoms during diffusion in  $\alpha$ -phase through a Zenner mechanism of relaxation in the bcc substitution alloys. The temperature of the second maximum does not depend on the oscillation frequency. Its shape, intensity and temperature considerably changes in accordance to cooling/heating rate, amplitude of deformation and annealing time at temperatures lower than  $\alpha$ - $\gamma$  transformation point.

Poster Topic K:

***Polymer based composites***

---

## Research of the Processing Parameters of Three-dimensional Printer and the Product

KUNIHIRO ARAKI, GOSHI HAMABE, TATSUYA TANAKA, YOSHIHIKO ARAO

Applied Materials Engineering Laboratory, Faculty of Engineering, Kyoto, Japan

“Additive Manufacturing (AM)”, which started from the 1980s, is the third manufacturing technology had been gotten by humans, neither the first manufacturing technology: “Removal Processing” nor the second technology: “Forming Processing”, AM is the shaping method of stacking materials in layers. As a result, the product can be made, in this way, even though it has a too difficult shape to be made by the conventional methods such as a porous morphology. “Optical Shaping Method” was the only AM technology when the earliest stage of AM. For the past three decades, the types of AM have dramatically increased. Among them, “Fused Deposition Modelling (FDM)” type has been used by anyone in a general office and at home. The reasons are mainly as follows: first of all, FDM’s basic principles are relatively easy to make; secondly, the FDM’s costs are low because expensive parts aren’t used (e. g. such as laser); and thirdly, the major patents of FDM had been finished. FDM type of printers can easily make a 3D product with thermoplastic resins and the 3D-CAD data. However, mechanical property of the product has a close relationship with process parameters. So, the suitable parameters should be found in order to increase mechanical properties of FDM type products. Therefore, the purpose of this study is researching of the processing parameters to achieve the product with high mechanical properties and less in deformation.

In this study, tensile test specimens were made using

FDM type 3D printer by changing six process parameters. The parameters such as heat cover, layer height, mesh grade, correction of joint, fill density, and speed for print moves were studied. Their influences were investigated by the tensile properties of products and the warpage of products. Five test specimens were made in each condition. The orders of the experimental were random sampling because of reducing a constant error. In order to reduce the amount of experimental conditions, the experiments were carried out using design of experiments. And also, the cross sections of specimen after tests were observed by a light microscope, and their cross section areas were calculated. The investigation material isn’t only poly lactic acid (PLA), but also PLA/cellulose composite.

### References

- Sood, A. K., R. K. Ohdar, R. K., & Mahapatra, S. S. (2010): Parametric Appraisal of Mechanical Property of Fused Deposition Modelling Processed Parts – In: *Materials and Design*, 31: 287-295; Elsevier
- Bagsik, A. & Schoppner, V. (2011): Mechanical Properties of Fused Deposition Modeling Parts Manufactured with Ultem\*9085 – In: ANTEC 2011; Boston
- Huang, B. & Singamneni, S. (2014): Raster Angle Mechanics in Fused Deposition Modelling – In: *Journal of Composite Materials*, 0: 1-21; USA
- Hayano, S. (2014): *Hikari Zoukei kara AM Gijyutsu madeno 25 Nen* – In: *Seikei-Kakou*, 26: 141; Japan

## Supervised Estimation of the Local Glass Fiber Content from 2D X-ray Imaging of Plate-like Parts made from Sheet Molding Compounds

BENJAMIN BERTRAM, KAY ANDRÉ WEIDENMANN

KIT, Institute for Applied Materials - WK, Karlsruhe, Germany

Mechanical Properties of glass fiber reinforced plastics specifically sheet molding compounds (SMC) is largely affected by the local fiber architecture which describes how many fibers occur at some position within the part and their orientations. The SMC process is applied in the automotive industry to form a discontinuous fiber-reinforced polymer. The complex microstructure of SMC encompasses pores, filler particles and fibers, whose random orientation is caused by the disaggrega-

tion of fiber bundles during molding and is likely affected by the large variety of SMC process parameters in use. Therefore the fiber propagation in the flow of the SMC semi-finished material during molding and the mechanical properties of the cured solid parts are hard to predict. Micro computed tomography ( $\mu$ CT) can be applied to recover fiber orientations within discontinuous GFRP (Garesci 2013) but only if there is a good fiber-matrix contrast. Therefore  $Al(OH)_3$  has been used

as the filler material. One further implication of  $\mu$ CT is that samples are restricted to a small subsamples on the millimeter scale that have to be cut out from the part in order to resolve single fibers.

We propose a supervised, X-ray based and non-destructive method to retrieve local fiber volume content from plate-like parts which is the typical geometry for SMC applications. In (Schipp 1992) the absorption of X-rays was measured to determine fiber content but no locally resolved content map was created and no mineral filler deteriorated the fiber-matrix contrast. Unlike in (Schipp 1992) non-linear deviations from Lambert-Beer's law are taken into account by using polynomial regression and by selecting the image features which minimize the test error prediction. It is a two step approach that is very common in the context of machine learning. At the first stage ("learning phase") a stochastic estimator is trained from known data pairs that consist of X-ray image features and some reference or "ground truth" of the value to be predicted i.e. the average fiber content of the specimen. In this case image features are computed from radiographs of flat SMC samples captured with an industry scale cone beam  $\mu$ CT system. The image features depend not only on the local fiber content but also on the part thickness along the X-ray beams that cover one detector pixel. Therefore a map of the local through-thickness of each pixel had to be computed from the part geometry and the camera parameters of the CT setup.

The ground truth is then obtained by incineration of the sample. A prediction model is obtained by linear regression of the known fiber content from image features and local through-thickness. Cross-validation has been used to estimate the prediction error of the model on samples that were unknown in the learning phase.

At the second stage the model can be applied to any field of vision of the SMC part at coarsely the same focus-object-distance as the learning samples as long as the local through-thickness can be provided.

The method has been applied to sections of flat SMC plate samples (800 mm x 250 mm x 3 mm) and inhomogeneities in local fiber content and the influence of the process parameters, i.e. fiber length fiber content and layout of the semi-finished mats within the mold.

#### References

- Schipp, C. & Röber, S. & Zachamann, H. G. & Seferis, J. C. (1992): Determination of the Fiber Content in Polymer Composites by Means of X-Ray Absorption Measurements. – In: *Journal of Applied Polymer Science*, 44 (9): 1631–1634
- Garesci, F. & Fliegner, S. (2013): Young's Modulus Prediction of Long Fiber Reinforced Thermoplastics. – In: *Composites Science and Technology*, 85: 142–147;

## Deformation and fracture of aircraft fibrous polymer composites in external actuating factors and high temperature mechanical tests

DMITRII S. LOBANOV, VALERIY E. WILDEMAN, EVGENIY V. LOMAKIN

The Centre of Experimental Mechanics, Perm National Research Polytechnic University, Perm, Russia

The aim of this work is investigation of mechanical properties of fiberglass and carbon fiber reinforced plastics (CFRP) standard plain specimens under shear and bend loading before and after external actuating factors and high temperatures were applied. Research of physical-mechanical properties of sandwich panels with a tubular filler made from fiberglass and CFRP under tension and compression loading before and after special environments and high temperatures (100°C, 150°C) were applied too.

Groups of fiberglass and CFRP specimens were soaked in water, oil, gas, hydraulic fluid and petroleum solvent. This work contains analysis of impact contaminants environments and high temperatures on the mechanical properties of polymer fiber composite materials and structures. The methodological issues of using modern test equipment for studying the properties of composite materials and structures were considered. Tests

were carried out on the universal electromechanical test system Instron 5882 with temperature chamber (-100°C - +350°C) and advanced video extensometer.

The work presents results of mechanical tests of fiberglass and CFRP specimens: transverse bending and interlaminar shear (short beam method), sandwich panels under tension and compression loading. The effect of external polluting operating and high temperature on mechanical properties of polymer fiber composite materials and structures was estimated. Stress-strain diagrams were obtained in tests.

This work was carried out in the PNRPU with support of the Government of Russian Federation (the decree No. 220 on April 9, 2010) under the Contract No. 14.B25.310006, on June 24, 2013 and Russian Fund for Basic Research (grant No. 13-08-96016 r\_ural\_a).

## References

- Babushkin A.V., Wildemann V.E., Lobanov D.S., Tensile tests of unidirectional high-filled fiberglass composite at normal and high temperatures, *Factory laboratory. Materials' diagnostics*, V.76, №7, pp. 57-59, 2010.
- Babushkin A.V., Lobanov D.S., Kozlova A.V., Morev I.D., Research of the effectiveness of mechanical testing methods with analysis of features of destructions and temperature effects, *Frattura ed Integrità Strutturale*, Vol.24, pp. 89-95, 2013.
- Lobanov D., Vildeman V., Babin A., Grinev M. Impact estimation of external actuating factors and operational contamination on operational capability of polymer fibrous composite materials // Seventeenth international conference «Mechanics of composite materials»: book of abstracts, Riga, 28 May-01 June 2012. — Riga, Latvia, 2012. — P. 139.
- Lobanov D.S., Babushkin A.V. Deformation and fracture of fibrous polymer composites in thermo-mechanical impact conditions // Proc. of ECCM15: European Conference on Composite Materials, Venice, Italy, 24-28 June 2012. — Paper ID: 1224. — ISBN 978-88-88785-33-2.

## Numerical simulation for developing grounds in support of application of fiber optic sensors for monitoring of composite materials

VALERY P. MATVEENKO<sup>1</sup>, GRIGORIY S. SEROVAEV<sup>1,\*</sup>, VALERY, V. KOREPANOV<sup>1</sup>, NATALIYA A. YURLOVA<sup>1</sup>, ALEKSANDR N. ANOSHKIN<sup>2</sup>, ANATOLIY A. TASHKINOV<sup>2</sup>, GLEB S. SHIPUNOV<sup>2</sup>, VALERIY Y. ZUYKO<sup>2</sup>

<sup>1</sup>ICMM UB of RAS, Perm, Russia

<sup>2</sup>PNIPU, Perm, Russia

One of the most promising ways of developing intellectual systems which can provide online monitoring of the mechanical state of structures is application of sensors embedded into the host structural material. Due to several advantages, the most valuable of which is their small size, optical fiber sensors are the most commonly used sensors. In addition, optical fiber sensors are highly sensitive, resistant to vibrations and impacts, and are able to work under high temperatures and interact with other smart materials like piezoelectric ones (Udd 2011).

The small size of optical fibers makes them easy to embed into composite materials at the stage of manufacture. However, differences in their mechanical characteristics and larger sizes compared to reinforcing composite fibers can have a negative effect on the mechanical characteristics of the object and may cause different defects.

Optical fiber is modeled as an inclusion of cylindrical form. The optical fiber cross-sectional distribution corresponds to the real coordinates in the test specimen. The coordinates were obtained by special processing of the photographs. The coordinates of optical fiber through the width of the cross section are distributed randomly during the packaging process. To assess the influence of this random distribution on the mechanical characteristics of the specimen, calculations were performed, in which the coordinates through the width of the model specimen were taken using a random-number generator.

Application of the commercial software ANSYS made

it possible to calculate numerically the stress-strain fields.

Calculations and experiments were conducted on six twelve layered specimens made from glass-reinforced plastic with epoxy matrix. Panda optical fiber with cross-sectional diameter of 0,16 mm was used.

The influence of different distribution patterns of optical fibers through the cross section of specimen and defect known in literature as “resin pocket” was studied (Jensen 1992). “Resin pocket” is a widely spread type of defect in composite materials with inclusions. The technology of optical fiber inclusion into the composite structure consists in successive stacking of layers: an optical fiber is put after each resin impregnated layer. Due to this procedure, composite fibers begin to bend around the optical fiber surrounded by resin

The results of numerical and mechanical experiments have shown that embedded optical fibers do not have a significant influence on stiffness during tensile tests but have a stronger (5 %) effect on stiffness during bending tests. Besides, the stress-strain field distribution around optical fiber in the case of resin pocket was calculated.

Examples of numerical experiments have been presented to illustrate the process of finding the most appropriate schemes for incorporation of fiber optic sensors allowing registration of the required mechanical characteristics under static and dynamic loads.

The reported study was supported by RFBR, research projects (No. 14-01-96003, 14-01-96029).

**References**

Udd, E. & Spillman, W.B., Jr. (2011): Fiber Optic Sensors: An Introduction for Engineers and Scientists – Udd, E. & Spillman, W.B., Jr. (eds) 2nd Edition, Wiley, New York.

Jensen, D.W., Pascual, J., & August, J.A. (1992): Performance of graphite/bismaleimide laminates with embedded optical fibers. I. Uniaxial tension – Smart Materials and Structures, 1. 24-30.

Poster Topic L:

***Lightweight alloys and structures***

# Ab-initio coarse-grained approach for modeling the two-dimensional packing structure of solute nanoclusters in Mg-based LPSO phases

HAJIME KIMIZUKA<sup>1</sup>, SHIGENOBU OGATA<sup>1,2</sup>

<sup>1</sup>Department of Mechanical Science and Bioengineering, Osaka University, Osaka, Japan

<sup>2</sup>Center for Elements Strategy Initiative for Structural Materials, Kyoto University, Kyoto, Japan

Mg-based nanolamellar phases of the  $(h_m c_n)$  type (here,  $h$  and  $c$  represent hexagonal and cubic close-packed motifs, respectively;  $m$ ,  $n$ , and  $k$  are integers) formed in ternary Mg-TM (transition metal)-RE (rare-earth metal) alloys have recently attracted significant attention owing to their use in the strengthening of Mg alloys and as promising components for designing advanced lightweight structural materials. In such phases (often called “long-period stacking ordered (LPSO) phases”), the two-dimensional stacking-fault (SF)-type interfaces containing solute atoms can play a significant role in the formation of a nanostructured state with low-energy boundaries. As a result, the phases are allowed to contain a high density of SFs and exhibit continuously regular nanolamellar structures formed by SF boundaries, which are an inherent part of their crystal lattice. To understand the fundamental mechanism of the formation of Mg-based LPSO phases, it is important to elucidate the essential natures of heterogeneities and medium-range orders in two-dimensional solute-cluster packing at SF-type interfaces. In this study, we proposed and established a coarse-grained (CG) modeling approach based on *ab initio* calculations for predicting the equilibrium superlattice structures of solute nanoclusters confined in an atomically close-packed SF. The approach was used to exploit the intriguing solute-enriched layers observed in Mg-M-Y (M = Al or Zn) LPSO phases as examples of multicomponent SF complexes (i.e., interfacial phases).

We investigated the energetic stability and two-dimensional ordering with varying packing density of  $L1_2$ - and  $E2_1$ -type core-shell-like M-Y clusters in the SF, depending on the temperature and composition, by considering effective intercluster interactions derived

from first-principles calculations based on the density functional theory. Using the results of the *ab-initio* CG Monte Carlo calculations, we characterized the positional and orientational orders of the attractively or repulsively interacting solute clusters in two dimensions, in particular the transformation of the possible local ordering patterns of clusters, considering them analogous to two-dimensional colloidal hard-sphere system. The CG model indicated that the Zn-Y clusters are arranged in multiple (i.e., at least two) kinds of six-fold domain structures with intercluster distances of  $2\sqrt{3}a_{Mg}$  and  $\sqrt{19}\sim\sqrt{21}a_{Mg}$ , respectively, in a manner consistent with recent scanning tunneling microscopy measurements (Kimizuka *et al.* 2014). The increase in volume fraction of solute clusters results in close packing transition of solute clusters, which explains the steady reduction of radial correlation length between clusters that was observed in small-angle X-ray scattering measurements for  $Mg_{85}Zn_6Y_9$  LPSO alloys during the annealing at high temperature (Okuda *et al.* 2013). This study was supported by Grant-in-Aid for Scientific Research on Innovative Area (No. 23109004) and the Elements Strategy Initiative for Structural Materials.

## References

- Kimizuka, H., Kurokawa, S., Yamaguchi, A., Sakai, A. & Ogata, S. (2014): Two-Dimensional Ordering of Solute Nanoclusters at a Close-Packed Stacking Fault: Modeling and Experimental Analysis, *Sci. Rep.* 4: 7318.
- Okuda, H. *et al.* (2013): Evolution of long-period stacking order structures on annealing as-cast  $Mg_{85}Y_9Zn_6$  alloy ingot observed by synchrotron radiation small-angle scattering, *Scr. Mater.* 68:575-578.

## Surface Nitriding of Titanium Using Atmospheric-controlled IH-FPP Treatment

OTA SHUMPEI<sup>1</sup>, MURAI KAZUE<sup>2</sup>, OMIYA MSAKI<sup>2</sup>, KOMOTORI JUN<sup>2</sup>, FUKAZAWA KENGO<sup>3</sup>, MISAKA YOSHITAKA<sup>3</sup>, KAWASAKI KAZUHIRO<sup>3</sup>

<sup>1</sup>Graduate School of Science and Technology, Keio University, Japan

<sup>2</sup>Department of Mechanical Engineering, Keio University, Japan

<sup>3</sup>Technical Headquarters, Neturen Co., Ltd., Japan

Titanium is superior in corrosion resistance and specific strength, but inferior in wear resistance. Surface hardening by nitriding, for example, gas nitriding<sup>1-2)</sup>, plasma nitriding<sup>3-4)</sup>, laser nitriding<sup>5-6)</sup> and surface nitriding using friction stir processing (FSP) method<sup>7)</sup>, is effective to improve wear resistance. The problem of gas nitriding and plasma nitriding is a longer processing time. Surface nitriding using laser or FSP method is possible to form nitrided layer on titanium surface relatively in a short time, however there are limits on shape and size of substrate.

In order to form surface nitrided layer in a short time without limits on shape or size, we tried nitriding by Atmospheric-controlled Induction Heating Fine Particle Peening (IH-FPP) treatment. Atmospheric-controlled IH-FPP treatment system is able to shoot particles at high speed in a controlled atmosphere. In the treatment, the substrate is heated to higher temperature by high frequency induction heating.

In this study, pure titanium was nitrided by Atmospheric-controlled IH-FPP treatment. The treatment was performed under nitrogen atmosphere at 900 °C for 3 minutes. Two types of processes were carried out; one is that nitrogen gas flow rate was set 10, 70 or 130 L/min without supplying particles, the other is that peening time was set 0, 1 or 3min when nitrogen gas flow was 130 L/min. In the latter, high speed steel particles (<45 μm in diameter) was used to FPP. We discussed the effects of nitrogen gas flow rate and IH-FPP treatment on the formation of the surface nitrided layer. The layer was characterized by macroscopic observation, X-ray diffraction analysis (XRD) and Vickers hardness measurement at cross section.

The surface color of the specimen which was treated at nitrogen gas flow rate of 10 L/min was silver, but the color of the specimens treated at 70 or 130 L/min were

gold. The XRD surface analysis of each kind of the treated specimen showed the presence of TiN. TiN peak intensity increased as gas flow rate increased. As a result of Vickers hardness measurement at cross section, the value of highest hardness near the surface and the thickness of hardened layer depended on nitrogen gas flow rate. In the treatment that nitrogen gas flow rate was 130 L/min, the value of highest hardness near the surface was 500HV and the thickness of hardened layer was 100 μm. These results suggest that the formation of nitrided layer on titanium surface is accelerated by nitrogen gas blow. This means that nitrogen gas blow is effective for surface nitriding of titanium.

The surface color of the specimens which were treated by IH-FPP were not gold. As a result of Vickers hardness measurement at cross section, the value of highest hardness near the surface and the thickness of hardened layer decreased as peening time was longer. These results suggest that IH-FPP treatment inhibits formation of nitrided layer on titanium surface.

### References

- 1) A. Zhecheva *et.al.*, Surface & Coating Technology, No.201, (2006), pp.2467-2474.
- 2) Hideki Shibata *et. al.*, Fatigue, Vol.16, (1994), pp.370-376.
- 3) V. Foquet *et.al.*, Applied Surface Science, No.221, (2004), pp.248-258.
- 4) P. Saillard *et.al.*, Surface & Coating Technology, No.45, (1991), pp.201-207.
- 5) H.C.Man *et.al.*, Applied Surface Science, No.258, (2011), pp.436-411.
- 6) Naofumi Ohtu, Surface & Coating Technology, No.244, (2014), pp.57-62.
- 7) Bo Li *et.al.*, Applied Surface Science, No.274, (2013), pp.356-364.

Poster Topic X:

***General mechanical behavior***

---

## Thermal ageing effect on mechanical behavior of polycarbonate

HAMID BBABOU<sup>1</sup>, FERHOUM RABAH<sup>1</sup>, MEZIANE ABERKANE<sup>1</sup>

Laboratory of LEMM, University Mouloud MAMMERRI of Tizi-Ouzou, Algeria

This work is devoted to the experimental study of thermal ageing effects, with different temperature and duration, on microstructure and mechanical properties of amorphous polycarbonate (PC).

The temperature of treatment is fixed at 100 and 150°C, and for three duration 72, 144 and 216 hours; uniaxial-compression tests are conducted at 25 °C, in order to characterize the mechanical behavior of PC before and after ageing; the influence of the thermal ageing on the material microstructure is characterized using spectra IRTF and micro-hardness analyses.

It is found that the thermal annealing causes the increase of all properties of material, including Young Modulus and yield stress, plastic flow stress, etc. Moreover, the superposition of spectra IRTF shows that the material microstructure influenced by increasing of intensity of the bands of vibration of connections C=C, C-O and C-H; in addition, an increase of 30% of micro-hardness was detected after 216 hour of ageing at 100°C.

### References

J Rösler, H Harders, M Bäker (2006): *Mechanical behavior of engineering materials*. German edition published by the Teubner Verlag Wiesbaden, ISBN 978-3-8351-0008-4.

- R. FERHOUM (2012): Etude expérimental et modélisation numérique du comportement mécanique du PEHD à l'état vierge et après vieillissement thermique. Ph.D, UMMTO.
- R. FERHOUM, K. HACHOUR, M. ABERKANE, M. HABAK (2014): ANALYSIS OF ANNEALING EFFECT AND MACROSCOPIC TRIAXIALITY ON HIGH DENSITY POLYETHYLENE. U.P.B. Sci. Bull., Series B, Vol. 76, Iss. 2.
- J. M. Hutchinson (1995): Progress in polymer Science 20, 703-760, 1995.
- B. Fayolle, L. Audouin and J (2000): Verdu, Polymer Degradation and Stability 70, 333-340.
- Steeve COLLIN (2013): Etude du vieillissement des disques optiques numériques recherche de corrélations entre évolution des constituants et perte de l'information. Ph.D, Blaise Pascal, 2013.
- V. A. Soloukhin, J. C. M. Brokken-Zijp; O. L. J. Van Asselen and G. de With (2003): Macromolecules 36, 7585-7597.
- J. Lu, Y. Wang and D. Shen (2000): Polymer Journal 32, 610-615.
- E. L. Cussler (1997): Diffusion Mass Transfer in fluid Systems Second Edition, Cambridge University Press ISBN 0 521 56477 8.
- G. Montaudo, S. Carroccio and C. Puglisi (2002): Journal of Analytical and Applied Pyrolysis 64, 229-247.

## Effect of Ultra-violet radiation on the mechanical behavior of PMMA (polymethyl methacrylate)

AMIRAT BOUKHALFA, FERHOUM RABAH

Department of Mechanical Engineering, Mouloud Mammeri Tizi-Ouzou University, Algeria

The investigation we conducted the profile of the mechanical behavior of polymethyl methacrylate (PMMA) the virgin state and what have you exposed to UV radiation is motivated by what this amorphous polymers in its good mechanical characteristics and appearance exile visual make him one of the most industrialized and plastic used in various application [1], but it has a weakness tends to UV radiation, one of the main factors behind the degradation of the polymer [2].

In this context, our work is based on the validation of accelerated aging tests acute laboratory correlated with the natural exposure to derive the potential of the material in question in terms of the mechanical behavior vis-a-vis UV radiation and characterize the critical

parameters of aging and to provide elements for understanding the mechanism of degradation.

Indeed uniaxial compression tests on specimens practice PMMA has the UV radiation virgin state and after exposure approved the influence of UV irradiation on PMMA, for that there was an evolution of the all mechanical material properties (elastic limit, Young's modulus ...).

IR spectroscopy was our use for diagnosis of microstructural variations; it has revealed that this degradation is caused by damage at the chains cutting effect linkages functions.

## References

- [1] OKHAY Nidhal, « synthèse de réseaux polymères thermoréversibles par Diels-Alder », Thèse de doctorat de l'université Jean Monnet, 2012, p224.
- [2] Mercier Jean Pierre., Maréchal Ernest. *Traité des matériaux. Chimie des polymères. Synthèse Réactions, Dégradation.* Tome 13. Chapitre 10. EPFL-éditeur-Lausane-Suisse. 1996.

## Dynamic Mechanical Properties of Cortical Bone Depend on Bone Mineral Content

ZUDE FENG, TING WANG

College of Materials, Xiamen University, China

Bone is a natural composite material primarily consisting of an organic phase (mostly Type I collagen) as matrix and a mineral phase (hydroxyapatite crystal) as reinforcement. From the theory of composite materials, the mineral phase imparts the strength and stiffness to bone, whereas the organic phase the toughness and viscoelasticity. Therefore, a better understanding of the biomechanical properties of bone and its mechanism will contribute to further development of novel bone substitute. In this study, the effect of mineral content on the viscoelastic behavior, collagen structure, and denaturation temperature of cortical bone was investigated.

Fresh bovine cortical bone was used in this investigation. Forty specimens, 25.0×6.0×0.6 mm (length × width × thickness) in dimensions, were machined from the lateral and medial cortices of the midshaft of fresh bovine femora (within 24 hours after slaughter) under physiological saline irrigation. The specimens were randomly divided into four groups: each containing ten specimens. The specimens in one group served as the control without any treatment. The specimens in the remaining three groups were immersed in a buffered (pH 7.3) 0.2 M EDTA solution at 2 °C for 12 hours, 24 hours, and 48 hours, respectively. The solution was continuously agitated and changed every 24 hours. Among each group three specimens were used to conduct DMT analysis, four specimens for apparent density and mineral content (BMC) measurement, and three specimens for collagen structure characterization and thermal analysis. The dynamic-mechanical-thermal analysis was carried out under a single cantilever load scheme. Temperature was scanned from 20 °C to 300 °C at 2 °C min<sup>-1</sup> under a loading frequency of 1 Hz. The collagen structure was characterized by infrared spectrometer (FTIR). The denaturation temperature of intact and demineralized bone was assessed by a differential scanning calorimeter (DSC).

The statistical analysis revealed that there were statistically significant differences in apparent density and mineral content of bone between the different test groups ( $P < 0.01$ ). The results of FTIR analysis indicat-

ed that EDTA treatment did not induce a significant change to the collagen structure. The results of DSC measurements indicated that the denaturation temperatures of bone were influenced by degree of demineralization. The higher denaturation temperature (239.2 °C) was obtained from the bone specimens in control group. The results of DMTA revealed that storage modulus ( $E'$ ) and loss modulus ( $E''$ ) were strongly influenced by mineral content. Higher values of  $E'$  and  $E''$  were observed in control group compared to that demineralized. However, lower values of  $\tan \delta$  were observed in control group compared to that demineralized groups. The  $\tan \delta$  peak broadened and splitted into two peaks with the decreasing mineral content. A shift of peak temperature of  $\tan \delta$  to lower temperature with decreasing mineral content could be observed. The results were approximately coincidental with that obtained from DSC assessment.

The results of this investigation reveal that the bone mineral content plays an important role on the viscoelastic property of bone (i.e.  $E'$  and  $E''$ ). The structure of Type I collagen in bone is long-chained and cross-linked to neighboring collagen molecules. Type I collagen plays a major role in the viscoelastic nature of bone. In addition, research indicated that the effect of interaction between matrix and reinforcement in composite on its viscoelasticity was significant. Due to the intimate combination and interaction between mineral crystal and collagen fibers in sub-nanometer scale, the mineral crystal has a significant effect on bone's viscoelasticity. The presence of mineral phase will reduce the movability of collagen chains. Besides, since the higher  $E''$  value means improvement of bone's ability to absorb impact energy in accident, the result of this investigation suggests that dynamic mechanical property is the same important parameter as elastic modulus and ultimate strength in evaluating bone's quality. However, the underlying mechanism is not very clear because the complicate interaction between mineral crystal and collagen fibers. Further study will be required to explore this issue.

## Study of concretes and mortars made with metallic fibers

SOUAD KHERBACHE, KARIM MOUSSACEB, NEDJIMA BOUZIDI, A. KADER TAHAKOURT

University A. Mira, Departement of Civil Engineering, Bejaia, Laboratory [of Genius of the Building and of Architecture, Aleria](#)

The use of fibers [in building materials; particularly in mortar and concretes a more and more used technology, for several reasons, is ecological, either economic, or to improve some properties in the hardened or cool state. Indeed, the use of the metallic fibers in substitution of cement allows a reduction of the consumption of the clinker by contributing, in a considerable way, to reduce the energy price and to regulate problems linked to the pollution of environment by the CO<sub>2</sub>.](#)

As generally known, the sector of building materials is the third biggest sector issuing CO<sub>2</sub> in industry, worldwide (Yu, Spiesz & Brouwers 2014). They say that the production of cement represents 7 % of all programs of anthropogenic CO<sub>2</sub> (Capros, Kouvaritakis, Mantzos 2001).

The concrete is a composite material with a low resistance to traction and low tension (Uygunoglu 2008). Generally the addendum of fibers in the concrete mixture can considerably improve the properties of engineering of the concrete such as; inflexion, tiredness and force of abrasion, the capacity of distortion, hardness and capacity holder after cracking (Mohammadi, Singh, Kaushik 2008) & (Yazici, Inan, Tabak V 2007)

Although the concrete is the material of building most used on earth, this material always has some problems; he has a good resistance against efforts of compression, but a resistance to very low traction. Under duress of traction, the concrete cracks easily and almost any ductility. Medium classic to resolve this problem can be the application of strengthening by fibers. The other solution is the application of different types fibers in the concrete, this material is then called «the concrete of fibers».

With the intention of highlighting the influence of the metallic fibers on the properties of concretes and of mortar, cement was substituted by different percentages.

Purpose aimed in the present job is to search optimum in rate of substitution of the cement by the metallic fibers which will give at the same time a good resistance to compression and to inflexion, and acceptable shrinking and inflation.

### References

- R.Yu, P. Spiesz, H.J.H. Brouwers (2014): Mix design and properties assessment of Ultra-High Performance Fiber Reinforced Concrete (UHPFRC), Cement and concrete Research, Volume 56, Pages 29-39.
- P. Capros, N. Kouvaritakis, L. Mantzos (2001): Economic evaluation of sectorial emission reduction objectives for climate change top-down analysis of greenhouse gas emission possibilities in the EU, Contribution to a study for DG environment. European commission.
- Uygunoglu T. (2008): Investigation of microstructure and flexural behavior of steel fiber reinforced concrete. Mater Struct; 41(8):1441–9.
- Mohammadi Y, Singh SP, Kaushik SK. (2008): Properties of steel fibrous concrete containing mixed fibers in fresh and hardened state Construct Build Mater, 22(5):956–65.
- YAZICI S, Inan G, Tabak V. (2007): Effect of aspect ratio and volume fraction of steel fiber on the mechanical properties of SFRC. Construct Build Mater 21(6):1250–3.

## Effect of Strain-Rate on Tensile Properties of Nuclear Piping Materials at RT and 316oC

JIN WEON KIM, [MYUNG RAK CHOI](#)

Dept. of Nuclear Eng., Chosun Univ., Gwangju, Korea

The integrity of piping components in nuclear power plants (NPPs) should be maintained under seismic condition as well as normal operating condition. Thus, it is important to reliably evaluate the integrity of piping components under seismic loading condition. In the existing evaluation procedure, the integrity is evaluated based on the magnitude of seismic load given by linear-elastic analysis and mechanical properties tested

at quasi-static monotonic loading condition (DeGrassi, 2008). However, the seismic loading has random, dynamic, and cyclic characteristics. Some studies reported that the deformation and fracture behaviors of material under dynamic and cyclic loading were much different from those under quasi-static monotonic loading and the dynamic and cyclic loading effects depended on type of materials (Hopper, 1996; Boyce,

2009). Thus, it is necessary to investigate the effects of dynamic and cyclic loads on the mechanical properties of nuclear piping materials to ensure the reliability of integrity evaluation under seismic loading conditions. Therefore, this study conducted a series of tensile tests on SA508 Gr.1a low alloy steel and SA312 TP316 stainless steel piping materials under various strain-rates ranging from  $3.95 \times 10^{-4}$  to  $10 \text{ s}^{-1}$ . The tests were conducted at RT and operating temperature of NPPs ( $316^\circ\text{C}$ ). SA508 Gr.1a low alloy steel and SA312 TP316 stainless steel are materials commonly used in primary piping system of NPPs. From the results of tensile test, the effect of strain-rate on tensile properties of nuclear piping materials was investigated for each pipe material.

The results showed that the tensile properties for both pipe materials were compliant with typical strain-rate dependence at RT; i.e., the strength increased and the ductility decreased as strain-rate increased. At  $316^\circ\text{C}$ , however, the dependence was different from the typical strain-rate dependence. Tensile strength as well as elongation of SA508 Gr.1a low alloy steel decreased as strain-rate increased. Reduction of area was non-linearly varied with strain-rate; it decreased initially and then increased with increase in strain-rate. Thus, reduction of area at  $10 \text{ s}^{-1}$  was almost the same as that at  $3.95 \times 10^{-4} \text{ s}^{-1}$ . These characteristics are associated with dynamic strain aging phenomenon appeared in ferritic steels at  $200\text{--}300^\circ\text{C}$  (Baird, 1971). For SA312 TP316 stainless steel, the variations of strength, elongation, and reduction of area with strain-rate were negligible at  $316^\circ\text{C}$ . Regardless test temperatures, the strain hardening rate was nearly independent of strain-rate for SA508 Gr.1a low alloy steel, while it gradually decreased with increasing strain-rate for SA312 TP316

stainless steel. It is concluded that at operating temperature of NPPs tensile properties of SA508 Gr.1a low alloy steel are sensitive to strain-rate and show abnormal strain-rate dependence. But the tensile properties of SA312 TP316 stainless steel are less sensitive to strain-rate at  $316^\circ\text{C}$ .

#### Acknowledgments

This research was supported by National Research Foundation of Korea(NRF) funded by the Ministry of Science, ICT and Future Planning(NRF-2013M2A8A1040924) and the Nuclear Power Core Technology Development Program of the Korea Institute of Energy Technology Evaluation and Planning (KETEP), granted financial resource from the Ministry of Trade, Industry & Energy, Republic of Korea(20141520100860).

#### References

- DeGrassi, G., Nie, J., Hofmayer, C. (2008): Seismic Analysis of Large-Scale Piping Systems for the JNES-NUPEC Ultimate Strength Piping Test Program, NUREG/CR-6983.
- Hopper, A., Wilkowski, G., Scott, P., Olson, R., Rudland, D., Kilinski, T., Mohan, R., Ghadiali, N., Paul, D. (1996): The Second International Piping Integrity Research Group (IPIRG-2) Program – Final Report, NUREG/CR-6452, BMI-2195.
- Boyce, B.L., Dilmore, M.F. (2009): The dynamic tensile behavior of tough, ultra-strength steels at strain-rates from  $0.0002 \text{ s}^{-1}$  to  $200 \text{ s}^{-1}$ , *Int. J. Impact Eng.*, 36, 263-271.
- Baird, J.D. (1971): The effects of strain aging due to interstitial solutes on the mechanical properties of metals, *Metall. Reviews*, 16, 1-18.

## Variation of Mechanical Properties in the Pipe Bends Fabricated by High-frequency Induction Bending

JIN WEON KIM<sup>1</sup>, MI YEON LEE<sup>1</sup>, YOUNG JIN OH<sup>2</sup>, HEUNG BAE PARK<sup>2</sup>, KYUNG SU KIM<sup>2</sup>, TAE SOON KIM<sup>3</sup>

<sup>1</sup>Dept. of Nuclear Eng., Chosun Univ., Gwangju, Korea

<sup>2</sup>Power Engineering Research Institute, KEPCO E&C, Kyoungki, Korea

<sup>3</sup>Center for Research Institute, KHNP, Daejeon, Korea

The use of pipe bends fabricated by high-frequency induction bending gradually increases in piping systems of power plants and shipbuilding plants because of several advantages such as eliminating welds between elbow and pipes, improving flexibility of pipe routing, and less costs (Lee 2011, Lee 2012). Recently, it is attempted to use the pipe bends for piping systems of nuclear power plants. However, high-frequency induction bending could locally change microstructure of pipe material induced by local heating and rapid cooling (Lee 2012). Thus, the mechanical properties

of the pipe bend would be different from those of original pipe and show spatial variation within pipe bend. Therefore, it is necessary to investigate the local mechanical properties of pipe bend fabricated by high-frequency induction bending. In particular, the investigation is important for piping systems applying leak-before-break (LBB) concept because the lower bound mechanical properties should be used for LBB evaluation (USNRC 1984).

This study carried out a series of tensile tests to investigate the local mechanical properties of SA312 TP316

stainless and SA335 P22 ferritic steel pipe bends fabricated by high-frequency induction bending. The tests were conducted at both ambient temperature and operating temperature of piping systems (316°C for TP316 stainless steel pipe bend and 292°C for P22 ferritic steel pipe bend). The specimens were machined from the various locations in the pipe bend, including intrados, extrados, and crown regions of bend, start and end of bend, and straight pipe. Also, microstructures were observed at different locations for both pipe bends using optical microscope (OM) and scanning electron microscope (SEM).

For both pipe materials, the pipe bends always showed higher strength and lower ductility than original straight pipe. This means that the strength was increased and the ductility was decreased by high-frequency induction bending for both pipe materials. For TP316 stainless pipe bend, the change in the strength and ductility was almost proportional to the degree of strain applied by bending process. Thus, the change of mechanical properties was considerable at center of bend than at start and end of bend region. Within the center of bend region, the highest strength and lowest ductility appeared at intrados region rather than extrados. For P22 ferritic pipe bend, however, the mechanical properties were nearly independent of locations within pipe bend, although the properties were

much different from those of original straight pipe. The observation of microstructures revealed that the mechanical properties of TP316 stainless steel pipe bend were strongly affected by dynamic recrystallization followed by plastic strain. However, the properties of P22 ferritic steel pipe bend were affected by heating and cooling process rather than plastic strain applied by bending process.

#### Acknowledgments

This work was supported by the Nuclear Power Core Technology Development Program of the Korea Institute of Energy Technology Evaluation and Planning (KETEP), granted financial resource from the Ministry of Trade, Industry & Energy, Republic of Korea.

#### References

- Lee, H., Bae, J., Kim, M., and Kim, C., (2011): Optimal Design of Pipe Bending Based on High-Frequency Induction Heating Using Dynamic Reverse Moment, *Int. J. Prec. Eng. & Manuf.*, 12, 1051-1058.
- Lee, Y., Lim, J. & Moon, Y. (2012): Mechanical Characteristics of Low-Carbon-Steel Pipe Bent by Local Induction Heating with Small Bending Radii, *Mat. Trans.*, 53, 847-852.
- USNRC (1984): Evaluation of Potential for Pipe Breaks, NUREG-1061, Vol.3

## Modeling and observation of compressive behaviors of anisotropic aluminum cellular structures based on the Voronoi tessellation concept

SANG-YOUN PARK<sup>1</sup>, BYOUNG-HO CHOI<sup>1</sup> SEUNG KI MOON<sup>2</sup>, IL-HYUK AHN<sup>2</sup>

<sup>1</sup> School of Mechanical Engineering, Korea University, Seoul, Republic of Korea

<sup>2</sup> School of Mechanical and Aerospace Engineering, Nanyang Technological University, Singapore

In these days, foams have been used in many industrial applications due to many mechanical and physical benefits comparing with conventional solid structure. Especially, it has been known that foams have a wide range of applications such as noise and vibration absorption, impact and static energy absorption, thermal insulation and so on. Foams are usually having a high stiffness-weight ratio, so they can be a good alternative for oversized heavy structures. Because of their applications, compressive loads can be a major loading conditions, so the understanding of compressive load-displacement of foams is practically important. Gibson and Ashby insist that foam's compressive behavior is depending on many physical and material factors such as base material, shape and size of their cellular structure, the homogeneity of cells and so on. Depending on the combination of such physical and material

factors, plastic collapse, elastic and/or plastic buckling, brittle fracture can occur as a major failure mechanism. Regarding the cell structure of foams, many artificial shapes, such as hexagon honeycomb, triangle, square and so on., have been introduced and commercially produced. However, these models are usually ideal, so foams with random cellular structures can not analyzed by those models.

In this paper, Voronoi tessellation concept was adapted to make a mathematical model to describe random structures of foams. Originally, Voronoi theory was used to divide the jurisdiction. For engineering researches of random cellular structures, this model can be very useful. Here is the brief description of generating Voronoi cells : First, seeds are randomly scattered. Based on this seeds, perpendicular bisector can be produced. Then Voronoi cell is produced.

However, the method for scattering seed based on conventional Voronoi theory may bring another problems. Seed's distribution is too irregular, the geometric significance of produced cells can be weak. So, in this paper, the concept of centroidal Voronoi tessellation (CVT) is adopted. CVT is a scattering method which uses cell's center of mass. When iterations of generating Voronoi cells is progressed, cell sizes becomes uniform asymptotically. In this paper, the number of iterations are 1,5,10 and 30 to generate the various random cell structures. At the same time, conventional cell structures such as hexagon, square and triangle are also generated.

After making various 2-D cells using a commercial program, i.e. Matlab, the cells are extruded to mimic common Honeycomb-like structures. Elasto-plastic compressive behaviors of various aluminum foams are numerically analyzed by Abaqus, one of popular commercial programs for finite element analysis (FEA). Failure mechanisms as well as load-displacement behaviors of various structures are discussed

and compared. The relationship between key physical properties and relative density is also discussed. In addition, the anisotropy of cellular structures can be an important factor to determine mechanical properties of the cellular structures. So, various anisotropic cell structures are generated, the variation of compressive behaviors is discussed.

Finally, experiments of selected cell structures which are generated by a 3-D printer using alluminum alloy are performed. The experimental results are compared and discussed with the results obtained from numerical analysis.

#### References

- Lorna J. Gibson and Michael F.Ashby. (1997):Celluar solids:structures and properties – second edition, ; CAMBRIDGE.
- Wolburg, J. (1969): Uniaxial stress–strain behavior of aluminium alloy foams. – Acta Materialia 47,8 :2323-2330;Cambridge.

## Influence of the addition of cooked and crushed clay on the mechanical strength of a self-compacting concrete

FATIHA SOUDI, NASSER CHELOUAH, TIZIRI BEZZI

Laboratoire Génie de Construction et Architecture (LGCA)

Self-compacting concrete (SCC) are very fluid concretes that are taking place under the effect of gravity without addition of vibration.

Cement production, essential for the production of concrete in general, is accompanied by a release of a large amount of CO<sub>2</sub> (greenhouse gas). The awareness of the harmful effects of such emissions into the atmosphere favors more new environmental approaches to be taken into account in the formulation of concrete and more of the specifications. Our goal is to make “green” SCC based on mineral additions. For this, we chose to use two mineral additions: the Cooked and Crushed Clay (CCC) and the limestone filler tiles from sanding waste. The CCC is used in substitution for a certain amount of cement. Limestone fillers are used to obtain the required properties of fresh SCC. The choice of CCC as a mineral addition is very interesting because its production emit very little CO<sub>2</sub> in the atmosphere and it has very good pozzolanic properties. The use of limestone fillers as to it leverages an industrial waste. Self-compacting concrete containing varying proportions of CCC (0%, 5%, 10%, 15% and 20%), boiled for 1 hour at 750 ° C and limestone fillers rates were studied. The compressive strength results show that the optimum ratio is 10% CCC. Furthermore, it is found that the use of CCC and limestone fillers reduces shrinkage deformation.

#### References

- R. D. Toledo Filho et al. Potential for use of crushed waste calcined-clay brick as a supplementary cementitious in Brazil. *Cement and Concrete Research*, Vol 37; pp 1357-1365, 2007.
- B.B. Sabir, S. Wild, J. Bai, Metakaolin and calcined clays as pozzolans for concrete: a review, *Cement and Concrete Composites*. Vol 23; pp441-454; 2001.
- R. D. Toledo Filho, B.B. Americano, E.M.R. Fairbairn, J.S Rolim, J. Farias Filho, Potential of crushed waste calcined-clay brick as partial replacement for Portland cement, in : V.M. Malhotra(E.d), Third Intenational Symposium on Sustainable Development of Cement and Concrete, ACI SP-202 (2001) 147-156.
- N. KAIDI et al. Un béton performant et durable a base de la pouzzolane naturelle de Beni Saf. 3 ème séminaire sur les technologies du béton ; 17 et 18 septembre 2006, Alger.
- E. Badogiannis, S. Tsvivilis. Exploitation of poor Greek kaolins : Durability of metakaolin concrete .*Cement and Concrete Composites*. Vol 31; pp128-133; 2009.
- M. ABIB et. al. L'influence du métakaolin sur les propriétés du béton; 3 ème séminaire sur les technologies du béton ; 17 et 18 septembre 2006, Alger.

E. Badogiannis, G. Kakali, G. Dimopoulou, E. Chaniotakis, S. Tsvilis, Metakaolin as a main cement constituent: exploitation of poor Greek kaolins. Cement and Concrete Composites. Vol 27; pp197-203; 2005.

Rafat Siddique, Juvas Klaus. Influence of metakaolin on the properties of mortar and concrete: a review. Applied Clay Science, vol 43; pp 392-400; 2009.

## Retained Austenite: Non Destructive Analysis by using X-Ray according to ASTM 975-03

M. MICHEL VAN DER MEY

Managing Director of Greensilver Germany GMBH

Retained austenite as a crucial parameter that affects the operating performances of mechanical parts, must be under control.

The X-Ray diffraction technique allows to measure it in a non destructive way. Standard practices to measure retained austenite are laid down in ASTM 975-03.

Retained Austenite affects fatigue strength, toughness, hardness, yield strength and machinability. Retained austenite can further transform during the service life of the product into other phases, providing the poten-

tial for changes in the dimension of the part leading to crack initiation.

Physical properties depend on different phases amount, if phase transformation occurs also these physical properties change.

The presentation's aim is to demonstrate how the ARE X can easily determine retained austenite by using X Ray and as a consequence to control and tune the production steps.

